

LOCKHEED MARTIN ENERGY RESEARCH LIBRARIES



3 4456 0515298 2

CENTRAL RESEARCH LIBRARY

ORNL-5137

Cy 21

PHYSICS Division - Annual PROGRESS REPORT

Period Ending December 31, 1975

OAK RIDGE NATIONAL LABORATORY
CENTRAL RESEARCH LIBRARY
DOCUMENT COLLECTION

LIBRARY LOAN COPY

DO NOT TRANSFER TO ANOTHER PERSON

If you wish someone else to see this
document, send in name with document
and the library will arrange a loan.

UNIVERSITY
OF
CHICAGO

OAK RIDGE NATIONAL LABORATORY

OPERATED BY UNION CARBIDE CORPORATION FOR THE ENERGY RESEARCH AND DEVELOPMENT ADMINISTRATION

Printed in the United States of America. Available from
National Technical Information Service
U.S. Department of Commerce
5285 Port Royal Road, Springfield, Virginia 22161
Price: Printed Copy \$8.00; Microfiche \$2.25

This report was prepared as an account of work sponsored by the United States Government. Neither the United States nor the Energy Research and Development Administration/United States Nuclear Regulatory Commission, nor any of their employees, nor any of their contractors, subcontractors, or their employees, makes any warranty, express or implied, or assumes any legal liability or responsibility for the accuracy, completeness or usefulness of any information, apparatus, product or process disclosed, or represents that its use would not infringe privately owned rights.

ORNL-5137
UC-34 — Physics

Contract No. W-7405-eng-26

**PHYSICS DIVISION
ANNUAL PROGRESS REPORT
for Period Ending December 31, 1975**

P. H. Stelson, Director

MAY 1976

OAK RIDGE NATIONAL LABORATORY
Oak Ridge, Tennessee 37830
operated by
UNION CARBIDE CORPORATION
for the
ENERGY RESEARCH AND DEVELOPMENT ADMINISTRATION

LOCKHEED MARTIN ENERGY RESEARCH LIBRARIES



3 4456 0515298 2

Reports previously issued in this series are as follows:

ORNL-2718	Period Ending March 10, 1959
ORNL-2910	Period Ending February 10, 1960
ORNL-3085	Period Ending February 10, 1961
ORNL-3268	Period Ending January 31, 1962
ORNL-3425	Period Ending May 21, 1963
ORNL-3582	Period Ending January 31, 1964
ORNL-3778	Period Ending December 13, 1964
ORNL-3924	Period Ending December 31, 1965
ORNL-4082	Period Ending December 31, 1966
ORNL-4230	Period Ending December 31, 1967
ORNL-4395	Period Ending December 31, 1968
ORNL-4513	Period Ending December 31, 1969
ORNL-4659	Period Ending December 31, 1970
ORNL-4743	Period Ending December 31, 1971
ORNL-4844	Period Ending December 31, 1972
ORNL-4937	Period Ending December 31, 1973
ORNL-5025	Period Ending December 31, 1974

Contents

1. EXPERIMENTAL NUCLEAR PHYSICS	1
Oak Ridge Electron Linear Accelerator Program	1
Introduction – J. A. Harvey	1
(n,α), (n,p), (n,γ), and Total Neutron-Cross-Section Measurements on ^{59}Ni – J. A. Harvey, J. Halperin, N. W. Hill, S. Raman, R. L. Macklin	2
Total Neutron-Cross-Section and Resonance Parameters of ^{249}Bk – J. A. Harvey, R. W. Benjamin, N. W. Hill, S. Raman	3
Fission Cross-Section Measurements on Small Ultrapure Curium Samples – J.W.T. Dabbs, C. E. Bemis, Jr., N. W. Hill, S. Raman	3
Monte Carlo Calculations of Multiple-Pulse Pileup – J.W.T. Dabbs	4
Angular Anisotropy in the $^6\text{Li}(n,\alpha)\text{T}$ Reaction in the eV Energy Region – J. A. Harvey, J. Halperin, N. W. Hill, S. Raman	4
Duration of Stellar Nucleosynthesis – R. L. Macklin, J. Halperin, R. R. Winters	5
Neutron-Capture Mechanism in Light and Closed-Shell Nuclides – R. L. Macklin, J. Halperin, R. R. Winters, B. J. Allen, J. W. Boldeman, M. J. Kenney, A. R. Musgrove, Hla Pe	5
Neutron-Capture Gamma-Ray Studies – S. Raman, R. F. Carlton, G. G. Slaughter, J. C. Wells, Jr., D. A. McClure	5
Neutron Interactions with ^{100}Mo – W. Weigmann, S. Raman, G. G. Slaughter, J. A. Harvey, R. L. Macklin, J. Halperin	6
Measurements on Total Neutron Cross Sections for Understanding Neutron Capture – C. H. Johnson, J. Halperin, R. R. Winters, R. L. Macklin	6
Resonant States of ^{209}Pb from Total Neutron-Cross-Section Measurements – J. L. Fowler, C. H. Johnson, N. W. Hill	7
<i>d</i> -Wave Admixtures in <i>s</i> -Wave, $J = 1$ Resonances in $^{207}\text{Pb} + n$ – D. J. Horen, J. A. Harvey, C. H. Johnson, N. W. Hill	7
Giant Resonances in ^{208}Pb and Neutron Resonances – D. J. Horen, J. A. Harvey, N. W. Hill	7
Oak Ridge Isochronous Cyclotron Program	9
Introduction – E. E. Gross	9
University Isotope Separator at Oak Ridge (UNISOR) Project	9
Spherical and Deformed Bands in ^{186}Hg – J. D. Cole, J. H. Hamilton, A. V. Ramayya, B. van Nooijen, H. Kawakami, L. L. Riedinger, K.S.R. Sastry	9

Structure of the Odd-Mass Gold Isotopes – J. L. Wood, E. F. Zganjar, R. L. Mlekodaj, D. A. McClure, R. W. Fink, A. G. Schmidt, F. T. Avignone III	11
Triaxial Rotor Description of the Odd-Mass Gold Isotopes – J. L. Wood, E. F. Zganjar, R. W. Fink, J. Meyer-ter-Vehn	11
Structure of the Odd-Mass $^{187-197}\text{Hg}$ Levels – G. M. Gowdy, A. G. Schmidt, E. F. Zganjar, J. L. Wood, R. W. Fink, R. L. Mlekodaj	14
Triaxial Bands in $^{193,195}\text{Tl}$ from Lead Decay – L. L. Riedinger, L. L. Collins, A. C. Kahler, C. R. Bingham, G. D. O'Kelley	18
Decay of ^{190}Tl and ^{192}Tl ; Negative-Parity Bands in Mercury – C. R. Bingham, F. E. Turner, L. L. Riedinger	19
Positron Measurements and Mass Differences – J. L. Weil, B. D. Kern	20
On-Line Mass-Separator Studies of Thallium and Mercury Alpha Emitters with $A \leq 186$ – K. S. Toth, M. A. Ijaz, J. Lin, E. L. Robinson	20
Decay of ^{194}Pb – E. L. Robinson, B. H. Ketelle, B. O. Hannah	22
Feasibility Studies of UNISOR Experiments in the $A \approx 60-80$ Region A. C. Rester, H. Kawakami, R. M. Ronningen, H. K. Carter, M. D. Barker, J. Galambos, A. DeLima, J. L. Wood, E. F. Zganjar, J. H. Hamilton	22
Gyromagnetic Ratio of the First Excited 2^+ State in ^{126}Xe – K.S.R. Sastry, R. S. Lee, R. L. Mlekodaj, A. V. Ramayya, J. H. Hamilton, N. R. Johnson	23
UNISOR Development – R. L. Mlekodaj, H. K. Carter, E. L. Robinson, F. T. Avignone III, E. H. Spejewski, A. G. Schmidt, B. O. Hannah, L. L. Collins, G. M. Gowdy	24
Heavy-Ion Macrophysics	26
Strongly Damped Collisions Involving Medium-Mass Targets	26
$^{20}\text{Ne} + \text{Ni}$ – M. L. Halbert, D. C. Hensley, R. G. Stokstad, A. H. Snell, F. Plasil, R. L. Ferguson, F. E. Obenshain, F. Pleasonton	26
$^{16}\text{O} + \text{Ni}$ – R. G. Stokstad, D. C. Hensley	26
$^{12}\text{C} + ^{63}\text{Cu}$ – R. A. Dayras, C. B. Fulmer, M. L. Halbert, D. C. Hensley, R. G. Stokstad	28
Heavy-Ion-Induced Fusion, Fission, and Quasi Fission	31
Competition Between Fission and Particle Emission in the ^{135}Tb Compound Nucleus – F. Plasil, R. L. Ferguson, R. L. Hahn, F. E. Obenshain, F. Pleasonton	31
Neon-Induced Fission of Nickel – F. Pleasonton, R. L. Ferguson, F. E. Obenshain, R. L. Hahn, F. Hubert, A. H. Snell, F. Plasil	32
Argon and Krypton Reactions with Copper and Silver at Energies of 4 to 8 MeV/amu R. L. Ferguson, F. Plasil, H. C. Britt, B. H. Erkilli, R. H. Stokes, H. H. Gutbrod, M. Blann	32
Quasi Fission in Argon and Copper Bombardments of Gold – C. Ngô, J. Péter, F. Plasil, B. Tamain, F. Hanappe, M. Berlinger	33
Fusion of $^{14}\text{N} + ^{12}\text{C}$ at High Energies – R. G. Stokstad, J. Gomez del Campo, J. A. Biggerstaff, A. H. Snell, P. H. Stelson	33
Transfer Reactions That Lead to the Nuclei ^{245}Cf and ^{244}Cf : Interaction of ^{16}O and ^{20}Ne with ^{239}Pu – R. L. Hahn, F. Hubert, P. F. Dittner, K. S. Toth	36

Monte Carlo Hauser-Feshbach Computer Code -- J. Gomez del Campo, R. G. Stokstad	36
Modification of a Proportional Counter to an Ionization Chamber -- A. H. Snell	37
Position-Sensitive Counter Telescope -- R. G. Stokstad, D. C. Hensley, A. H. Snell	37
Gamma-Ray Multiplicities in $^{20}\text{Ne} + ^{150}\text{Nd}$ Bombardments -- D. G. Sarantites, S. A. Gronemeyer, E. Eichler, N. R. Johnson, J. H. Barker, M. L. Halbert, D. C. Hensley, R. A. Dayras	38
Heavy-Ion Microphysics	41
Reaction $^{14}\text{C}(^6\text{Li}, ^6\text{He})^{14}\text{N}$ and Distribution of Gamow-Teller Strength -- C. D. Goodman, D. C. Hensley, W. R. Wharton	41
$^{12}\text{C} + ^{12}\text{C}$ Reactions -- R. M. Wieland, C. B. Fulmer, D. C. Hensley, S. Raman, A. H. Snell, P. H. Stelson, R. G. Stokstad, G. R. Satchler, L. D. Rickertsen	42
Nuclear Reorientation Effect for Inelastic Heavy-Ion Scattering -- F. Todd Baker, D. C. Hensley, Alan Scott, D. L. Hillis, E. E. Gross	45
Inelastic Scattering and Transfer Reactions from ^{12}C Ions on ^{90}Zr -- S. T. Thornton, D. E. Gustafson, J.L.C. Ford, Jr., K. S. Toth, D. C. Hensley	45
Elastic and Inelastic Scattering of 70-MeV ^{12}C Ions from the Even Neodymium Nuclei -- D. L. Hillis, E. E. Gross, D. C. Hensley, L. D. Rickertsen, C. R. Bingham, A. Scott, F. T. Baker	46
Microscopic Description of Inelastic ^{12}C Scattering from ^{208}Pb -- G. R. Satchler, J.L.C. Ford, Jr., K. S. Toth, D. C. Hensley, E. E. Gross, D. E. Gustafson, S. T. Thornton	49
Analysis of the ($^{12}\text{C}, ^{13}\text{C}$) and ($^{12}\text{C}, ^{11}\text{B}$) Reactions Induced by ^{12}C on ^{208}Pb -- K. S. Toth, J.L.C. Ford, Jr., G. R. Satchler, E. E. Gross, D. C. Hensley, S. T. Thornton, T. C. Schweizer	51
Heavy-Ion-Induced Transfer Reactions on ^{148}Nd -- H. Oeschler, M. L. Halbert, G. B. Hagemann, B. Herskind	53
Decay Rates for Even-Even $N = 84$ Alpha Emitters and the Subshell Closure at $Z = 64$ -- W.-D. Schmidt-Ott, K. S. Toth	54
Production and Investigation of Tungsten Alpha Emitters, Including the New Isotopes ^{165}W and ^{166}W -- K. S. Toth, W.-D. Schmidt-Ott, C. R. Bingham, M. A. Ijaz	56
New Information Concerning the Decay of ^{147m}Tb -- K. S. Toth, E. Newman, C. R. Bingham, A. E. Rainis	58
Rotational Bands in Thallium Nuclei by (H.I., xn) -- L. L. Riedinger, P. Hubert, N. R. Johnson, E. Eichler, A. C. Kahler, G. J. Smith, R. L. Robinson, P. H. Stelson	59
Bands in ^{164}Yb from Lutetium Decay -- C. R. Hunter, L. L. Riedinger, D. L. Hillis, C. R. Bingham, K. S. Toth	59
Lifetimes of States in a Decoupled Band in ^{165}Yb -- E. Eichler, P. Hubert, N. R. Johnson, L. L. Riedinger	61
Measurements of Lifetime and Multiple Coulomb Excitation in ^{162}Dy -- P. P. Hubert, N. R. Johnson, E. Eichler	61
High-Spin States in ^{74}Se -- M. L. Halbert, P. O. Tj�om, I. Espe, G. B. Hagemann, B. Herskind, M. Neiman, H. Oeschler	63
Light-Ion Reactions	63

Inelastic Proton Excitation of Giant Resonances in <i>sd</i> -Shell Nuclei – F. E. Bertrand, D. C. Kocher, E. E. Gross, E. Newman	63
Excitation of Giant Resonances in ^{208}Pb and ^{197}Au via Proton Inelastic Scattering – F. E. Bertrand, D. C. Kocher	66
Study of the Structure of the Even-Even Isotopes of Germanium with the (<i>p,t</i>) Reaction – A. C. Rester, R. Auble, J. B. Ball	66
Inelastic Scattering of 30-MeV Polarized Protons from $^{90,92}\text{Zr}$ and ^{92}Mo – R. de Swiniarski, G. Bagieu, M. Bedjiam, C. B. Fulmer, J. Y. Grossiord, M. Gusakow, M. Massaad, J. R. Pizzi	66
Excitation of Neutron-Hole States in the $^{206}\text{Pb}(p,p')$ Reaction at 61 MeV – Alan Scott, F. T. Baker, C. T. Chung, M. Owais, M. L. Whiten	68
^3He and Alpha-Particle Scattering from ^{27}Al and $^{28,29,30}\text{Si}$ – G. Bagieu, A. J. Cole, R. de Swiniarski, C. B. Fulmer, D. H. Koang, G. Mariolopoulos	68
Selective Enhancement of a Probable Particle-Hole State in $^{16}\text{O}(^3\text{He,t})^{16}\text{F}$ – C. D. Goodman, F. E. Bertrand, D. C. Kocher, R. L. Auble	69
Nuclear Chemistry	70
Measurement of the Electron-Capture Branch of the Decay of ^{225}No – R. J. Silva, P. F. Dittner, C. E. Bemis, Jr., D. C. Hensley	70
Decay Properties and <i>L</i> X-Ray Identification of Element $^{260}105$ – P. F. Dittner, C. E. Bemis, Jr., D. C. Hensley, R. J. Silva, R. L. Hahn, J. R. Tarrant, L. D. Hunt	71
Attempted Production of $^{256}104$ – P. F. Dittner, R. J. Silva, C. E. Bemis, Jr., R. L. Hahn, J. R. Tarrant, L. D. Hunt, D. C. Hensley	73
X-Ray Identification and Decay Properties of Isotopes of Lawrencium – C. E. Bemis, Jr., P. F. Dittner, R. J. Silva, D. C. Hensley, R. L. Hahn, J. R. Tarrant, L. D. Hunt	73
Determination of the Half-Wave Amalgamation Potential of Nobelium (Element 102) – R. E. Meyer, W. J. McDowell, P. F. Dittner, R. J. Silva, J. R. Tarrant	74
EN Tandem Program	75
High-Spin States of the $K^\pi = 3/2^+$ and $1/2^+$ Bands of ^{23}Na – D. E. Gustafson, S. T. Thornton, T. C. Schweizer, J.L.C. Ford, Jr., P. D. Miller, R. L. Robinson, P. H. Stelson	75
Study of the Coherence Widths Γ in ^{28}Si Measured by the $^{12}\text{C}(^{16}\text{O},\alpha)$ Reaction – J. Gomez del Campo, M. E. Ortiz, A. Dacal, J.L.C. Ford, Jr., R. L. Robinson, P. H. Stelson, S. T. Thornton	77
Evidence for Rotational Structure in ^{74}Se – R. B. Piercey, A. V. Ramayya, R. M. Ronningen, J. H. Hamilton, R. L. Robinson, H. J. Kim	79
Tests of the Coexistence of Spherical and Deformed Shapes in ^{72}Se – J. H. Hamilton, H. L. Crowell, R. L. Robinson, A. V. Ramayya, W. E. Collins, R. M. Ronningen, V. Maruhn-Rezwani, J. A. Maruhn, N. C. Singhal, H. J. Kim, R. O. Sayer, T. Magee, L. C. Whitlock	81
^{46}Ti High-Spin States – H. J. Kim, R. L. Robinson, R. Ronningen	82
^{50}Cr High-Spin States – H. J. Kim, R. L. Robinson, W. K. Tuttle III, R. Ronningen, R. O. Sayer, J. C. Wells, Jr.	82
High-Spin States in ^{68}Ge – A. P. de Lima, B. van Nooijen, R. M. Ronningen, H. Kawakami, A. V. Ramayya, J. H. Hamilton, R. B. Piercey, R. L. Robinson, H. J. Kim, W. K. Tuttle III	83

In-Beam Gamma Rays from the $^{60}\text{Ni}(^{12}\text{C},2p)^{70}\text{Ge}$ and $^{61}\text{Ni}(^{12}\text{C},2pn)^{70}\text{Ge}$ Reactions -- R. L. Robinson, H. J. Kim, R. M. Ronningen, J. C. Wells, Jr., J. H. Hamilton, G. J. Smith, R. O. Sayer	84
Coulomb Excitation Studies of $^{156,158}\text{Dy}$, $^{162,164}\text{Er}$, and ^{168}Yb via the (α,α') Reaction -- R. M. Ronningen, R. S. Grantham, J. H. Hamilton, R. B. Piercey, A. V. Ramayya, B. van Nooijen, H. Kawakami, C. F. Maguire, R. S. Lee, W. K. Dagenhart, L. L. Riedinger	84
Absolute Cross Sections for the $^{61}\text{Ni}(^{16}\text{O},3n)^{74}\text{Kr}$ Reaction -- J. C. Wells, Jr., R. L. Robinson, H. J. Kim, J.L.C. Ford, Jr.	86
Heavy-Ion Neutron Yields -- J. K. Bair, J. Gomez del Campo, P. D. Miller, P. H. Stelson	87
Interaction Barriers for the $^{16,18}\text{O}$ Plus Nickel, Copper, and Zinc Systems -- R. L. Robinson, J. K. Bair	87
2. NUCLEAR DATA PROJECT -- R. L. Auble, B. Harnatz, F. E. Bertrand, D. J. Horen, Y. A. Ellis, H. J. Kim, W. B. Ewbank, D. C. Kocher, M. J. Martin, F. K. McGowan, M. R. Schmorak	89
3. EXPERIMENTAL ATOMIC PHYSICS	92
Atomic Structure and Collision Experiments -- I. A. Sellin, S. B. Elston, J. P. Forester, K. H. Liao, D. J. Pegg, R. S. Peterson, R. S. Thoe, H. C. Hayden, P. M. Griffin	92
Charge-Transfer Measurements -- D. H. Crandall, D. C. Kocher	96
Electron-Impact Excitation and Ionization Cross Sections -- D. H. Crandall, R. N. Phaneuf, P. O. Taylor	97
Multiple-Electron-Loss Cross Sections for 60-MeV I^{10+} in Single Collisions with Xenon -- L. B. Bridwell, J. A. Biggerstaff, G. D. Alton, C. M. Jones, P. D. Miller, Q. Kessel, B. W. Wehring	97
Screening by Bound K Electrons in Electronic Stopping -- S. Datz, P. F. Dittner, J. Gomez del Campo, P. D. Miller, J. A. Biggerstaff	99
Planar Channeling and Hyperchanneling of Charge-State-Selected 27.5-MeV Oxygen Ions in Silver -- S. Datz, C. D. Moak, B. R. Appleton, J. A. Biggerstaff, T. S. Noggle	100
Electron Emission from Fast Oxygen and Copper Ions Emerging from Thin Gold Crystals in Channeled and Random Directions -- S. Datz, B. R. Appleton, J. A. Biggerstaff, T. S. Noggle, H. Verbeek	100
Spatial Ion Temperature Measurements -- D. P. Hutchinson, K. Vander Sluis, J. Waldman	101
Stark Measurements of Electric Fields in ORMAK -- K. Vander Sluis, P. M. Bakshi	102
Energy-Momentum Neutral-Particle Analyzer -- J. A. Ray, C. F. Barnett	102
Excited Electronic States of Hydrogen Molecules -- C. F. Barnett, T. J. Morgan, J. A. Ray	102
Neutral-Particle Reflection -- E. Ricci	103
Absolute X-Ray-Production Cross Sections for Heavy Ions Incident on a Wide Variety of Targets -- P. D. Miller, G. D. Alton, J. L. Duggan, F. D. McDaniel, R. Mehta, G. Monigold, J. Tricomi, G. Pepper, R. P. Chaturvedi, R. M. Wheeler, F. Elliott, K. A. Kuenhold, J. McCoy, L. A. Rayburn, S. J. Cipolla, A. Zander, J. Lin	103
Controlled Fusion Atomic Data Center -- C. F. Barnett, M. I. Wilker	105

4. ACCELERATORS	106
Heavy-Ion Laboratory	106
Heavy-Ion Facility Project — J. B. Ball, J. A. Martin, J. A. Biggerstaff, R. S. Lord, C. M. Jones, R. L. Robinson, J. K. Bair, R. M. Beckers, E. Eichler, K. N. Fischer, J.L.C. Ford, Jr., C. D. Goodman, E. D. Hudson, J. W. Johnson, R. F. King, J. D. Larson, M. L. Mallory, J. E. Mann, G. S. McNeilly, W. T. Milner, S. W. Mosko, J. A. Murray, J. D. Rylander, R. O. Sayer, J. A. Steed, N. F. Ziegler	106
Heavy-Ion Facility — Phase II Proposal — J. B. Ball, J. A. Martin, J. A. Biggerstaff, E. D. Hudson, R. S. Lord, J. E. Mann, G. S. McNeilly, S. W. Mosko, J. A. Murray, R. L. Robinson	110
Beam-Buncher Test Program — W. T. Milner, S. W. Mosko, N. F. Ziegler, R. F. King	112
Dependence of ^{12}C and ^{16}O Charge-State Yields on Stripper-Gas Flow — R. O. Sayer, E. G. Richardson	113
Magnet-Model Studies for Separated-Sector Heavy-Ion Cyclotrons — E. D. Hudson, R. S. Lord, L. L. Riedinger, J. A. Martin, F. Irwin, G. S. McNeilly, S. W. Mosko, M. A. Barre, M. P. Bourgarel, T. T. Luong, M. Ohayon	113
INGRID Proposal — M. J. Saltmarsh, R. E. Worsham	116
ORIC Operations — C. A. Ludemann, M. B. Marshall, H. L. Dickerson, C. L. Viar, H. D. Hackler, C. L. Haley, G. A. Palmer, J. W. Hale, N. R. Johnson, A. D. Higgins, E. W. Sparks, R. C. Cooper	118
ORIC Development — C. A. Ludemann, S. W. Mosko, E. E. Gross, E. D. Hudson, R. S. Lord, J. E. Mann	119
ORIC Data-Acquisition System Development — D. C. Hensley	121
Development of a Gas-Jet-to-Tape Transport System — H. K. Carter, J. L. Wood, R. L. Mlekodaj, E. H. Spejewski, K. S. Toth, R. J. Silva	121
ORIC Harmonic-Beam Space-Charge Effect — M. L. Mallory, K. N. Fischer, E. D. Hudson	122
Ion-Source-Development Program	124
Negative-Ion-Source Test Facility — G. D. Alton	124
Negative-Ion-Source Development — G. D. Alton	125
Preliminary Evaluation of Mueller-Hortig Geometry Negative-Ion Source — G. D. Alton	126
Van de Graaff Laboratory	128
Tandem Van de Graaff Operations — G. D. Alton, R. P. Cumby, J.L.C. Ford, Jr., J. W. Johnson, E. G. Richardson, N. F. Ziegler	128
CN Van de Graaff Operations — F. K. McGowan, M. B. Lewis, M. J. Saltmarsh, C. H. Johnson, G. F. Wells, F. A. DiCarlo, R. P. Cumby, Martha Inman, N. H. Packan	128
Oak Ridge Electron Linear Accelerator — J. A. Harvey, H. A. Todd, T. A. Lewis, J. G. Craven	131
5. THEORETICAL PHYSICS	133
Introduction — G. R. Satchler	133
Macroscopic Nuclear Dynamics and Heavy-Ion Collisions — J. J. Griffin, J. A. McDonald, T. A. Welton, J. A. Maruhn, C. G. Trahem, C. Y. Wong	133
Basis for a Macroscopic Description — C. Y. Wong, J. A. Maruhn, T. A. Welton, J. A. McDonald	134

Numerical Solution of the Fluid-Dynamical Equations -- J. A. Maruhn, T. A. Welton, C. Y. Wong	134
Spin and Isospin Dynamics of Nuclear Fluid -- C. Y. Wong, T. A. Welton, J. A. Maruhn	137
A Hamiltonian Formulation for Eulerian Hydrodynamics -- T. A. Welton, C. G. Traheru	137
Simple Hydrodynamics in Droplet Collisions -- C. Y. Wong, J. J. Griffin	138
Microscopic Models of Nuclei and Heavy-Ion Collisions -- J. P. Bondorf, R. Y. Cusson, K.T.R. Davies, H. T. Feldmeier, S. Garpman, E. C. Halbert, S. E. Koonin, S. J. Krieger, J. A. Maruhn, V. Maruhn-Rezwani, J. W. Negele, P. J. Siemens	139
Adiabatic Model -- R. Y. Cusson	139
Dynamics and the TDHF Theory -- R. Y. Cusson, K.T.R. Davies, H. T. Feldmeier, S. E. Koonin, S. J. Krieger, J. A. Maruhn, V. Maruhn-Rezwani, J. W. Negele	141
$^{12}\text{C} + ^{12}\text{C}$ and the TDHF Model -- R. Y. Cusson, J. A. Maruhn	141
Two-Dimensional TDHF Calculations -- K.T.R. Davies, H. T. Feldmeier, S. E. Koonin, S. J. Krieger, V. Maruhn-Rezwani	142
Three-Dimensional TDHF Calculations -- J. A. Maruhn, R. Y. Cusson	143
Classical Microscopic Description of Heavy-Ion Collisions -- J. P. Bondorf, H. T. Feldmeier, S. Garpman, E. C. Halbert, P. J. Siemens	144
Nuclear Reaction Theory -- E. C. Halbert, G. R. Satchler, L. D. Rickertsen, L. W. Owen, J. B. McGrory	145
Second-Order DWBA for Heavy-Ion Inelastic Scattering -- L. D. Rickertsen	146
Microscopic Description of Heavy-Ion Scattering -- L. D. Rickertsen, G. R. Satchler	147
Single-Nucleon Transfer Reactions -- G. R. Satchler, L. W. Owen	148
Coupled-Channel Analysis of $^{26}\text{Mg}(^{16}\text{O}, ^{14}\text{C})^{28}\text{Si}$ Using Shell-Model Spectroscopic Amplitudes -- E. C. Halbert	148
Semiclassical Scattering with Complex Trajectories -- L. D. Rickertsen	149
Nuclear Structure Theory -- R. L. Becker, T.T.S. Kuo, N. M. Larson, J. B. McGrory, E. C. Halbert, A. D. MacKellar, J. A. Smith, J. P. Svenne, B. H. Wildenthal	149
Propagator-Renormalized Brueckner Theory -- R. L. Becker, N. M. Larson, A. D. MacKellar, J. A. Smith, J. P. Svenne	150
Nuclear Shell Model -- J. B. McGrory, E. C. Halbert, T.T.S. Kuo, B. H. Wildenthal	152
6. HIGH-ENERGY AND MEDIUM-ENERGY ACTIVITIES -- H. O. Cohn, G. T. Condo, W. M. Bugg, E. L. Hart, H. R. Brashear, T. H. Handler	153
The $\pi^+ + d \rightarrow p + p$ Reaction and the Deuteron D State -- E. E. Gross, C. A. Ludemann, M. J. Saltmarsh, B. M. Preedom, C. W. Darden, R. D. Edge, T. Marks, M. Blecher, K. Gotow, R. L. Burman, R. P. Redwine, W. R. Gibbs, E. L. Lomon, K. Gabathuler, P. Y. Bertin, J. Alster, J. P. Perroud, B. Goplen	154
7. MOLECULAR AND MATERIALS RESEARCH	156
Electron Spectroscopy	156
Introduction -- T. A. Carlson, W. B. Dress	156

Ultrahigh-Vacuum Chamber and Data System for Electron Spectroscopy – T. A. Carlson, W. B. Dress, F. H. Ward	157
Study of Satellite Structure Found in the Photoelectron Spectra of Gaseous Hydrocarbons – T. A. Carlson, W. B. Dress, F. A. Grimm, J. S. Haggerty	158
Hyperfine Interactions in Solids – F. E. Obenshain, P. G. Huray, J. O. Thomson, G. Pettit, C. M. Tung	161
Radio-Frequency Surface Resistance of Lead Near the Critical Temperature – J. R. Thompson, C. M. Jones	163
High-Resolution Microscopy Program – R. E. Worsham, W. W. Harris	165
Infrared Spectra of SO_3F^- and $\text{SO}_3(\text{OH})^-$ in Solid Solution H. W. Morgan, P. A. Staats	165
Helium Implantation in Potential First-Wall CTR Materials – J. A. Horak, M. J. Saltmarsh, R. L. Auble, J. W. Woods, C. K. Thomas	166
8. PUBLICATIONS	168
9. PAPERS PRESENTED AT SCIENTIFIC AND TECHNICAL MEETINGS	184
10. OMNIANA	195

1. Experimental Nuclear Physics

Oak Ridge Electron Linear Accelerator Program

INTRODUCTION

J. A. Harvey

The Oak Ridge Electron Linear Accelerator (ORELA) has continued to excel as a facility for accurate, high-resolution neutron-cross-section measurements. During the past year, neutron-cross-section experiments of many types were continued, and techniques and equipment for making the measurements were improved. In addition, a new type of experiment to measure the (n,α) and (n,p) cross sections of ^{59}Ni was performed. Many of the isotopes and elements studied are selected because of the need for nuclear data on these nuclides in the nuclear power program. A summary of the types of measurements, the nuclides studied, and the energy ranges covered are summarized in Table 4.11 (see Chap. 4). A selected portion of the activities of Physics Division experimenters is discussed briefly below.

One of the more pressing needs with regard to the possibility of recycling actinide wastes is for fission cross-section data on actinide samples that may be highly alpha-active and available only in very small quantities. This year, fission measurements were started on a 10- μg sample of ^{243}Cm giving 10^7 α /sec. A hemispherical-plate fission chamber demonstrated a discrimination against alpha detection of a factor of $>10^{10}$ while still permitting $>95\%$ fission counting efficiency.

Capture cross-section measurements were extended from the earlier low-energy cutoff of ~ 3 keV down to 100 eV to permit a measurement of the capture cross section of ^{59}Ni . The nuclides ^{203}Tl and ^{205}Tl were studied to determine the duration of stellar nucleosynthesis. The result was a probable value for the mean time between neutron captures of only 23 years, with a lower limit of 12 years. In addition to measurements of nuclides applicable to reactor needs, such as ^{58}Ni and ^{60}Ni , other nuclides near closed shells were studied, such as ^{32}S , ^{88}Sr , and ^{100}Mo , which are associated with nonstatistical mechanisms such as channel and valence capture.

Capture gamma-ray spectra measurements continued to be a powerful technique for nuclear spectroscopy. The investigation of the isotopes of tin and lead was rewarding in determining level schemes for the odd isotopes of tin and in providing information on $E2$ radiative strength in ^{208}Pb . A study of the capture gamma rays from neutrons on ^{100}Mo showed that valence capture does not play a dominant role for this nuclide.

A modification to permit the use of unmoderated neutrons from the ORELA tantalum target for total cross-section measurements has greatly improved the quality of the data in the MeV energy region. In addition to the study of nuclides such as ^{208}Pb to determine the fragmentation of the shell-model states, total cross-section measurements were made on several nuclides such as ^{23}Na , ^{233}U , ^{240}Pu , and the isotopes of nickel to obtain data to satisfy nuclear reactor needs. An analysis of the total cross section of ^{207}Pb showed a large d -wave contribution in addition to the s -wave contribution for $1 \sim$

states. This technique appears to provide a unique means to gain information on the d -wave strength function.

A new experiment to measure the (n,α) and (n,p) cross sections of ^{59}Ni from 0.01 eV to ~ 20 keV, using a diffused-junction silicon detector, has produced several unique results. In addition to providing valuable applied information, such as the $^{59}\text{Ni}(n,\alpha)$ thermal cross section and the alpha width of the 203-eV resonance which are important for helium production in nickel alloys in power reactors, alpha and proton widths of many resonances were determined in the keV energy region. Measurements of $^6\text{Li}(n,\alpha)T$ have shown that the alphas and tritons are anisotropic even in the eV energy region, and this must be considered when this cross section is used as a standard for measuring neutron fluxes.

Finally, in the pursuit of accurate cross-section measurements, it has been necessary to develop electronics, equipment, and techniques. One valuable development is that of a new neutron-flux monitor consisting of a thin ^6LiF layer between two 0.1-mm sheets of NE-110 scintillator, producing a fast, good-resolution, $\alpha + T$, 4π detector for the reaction products. The light is detected by two photomultipliers located out of the neutron beam.

(n,α) , (n,p) , (n,γ) , AND TOTAL NEUTRON-CROSS-SECTION MEASUREMENTS ON ^{59}Ni

J. A. Harvey N. W. Hill²
 J. Halperin¹ S. Raman
 R. L. Macklin

In addition to (n,γ) and total neutron-cross-section measurements on ^{59}Ni , we have made (n,α) and (n,p) measurements at ORELA from ~ 0.01 eV to ~ 20 keV. The thermal and resonance (n,α) cross sections of this isotope, which is produced from $^{58}\text{Ni}(n,\gamma)$, are important because of helium embrittlement and swelling of the structural material of power reactors.

The (n,α) and (n,p) measurements were made simultaneously with a diffused-junction silicon detector located 9.03 m from the water-moderated neutron target at ORELA and resulted in a neutron energy resolution of 0.5% (FWHM). A sample of ^{59}Ni (95%, 91 $\mu\text{g}/\text{cm}^2$) was electroplated upon a 1-mil platinum foil. A deposit of ^6Li (95%, 104 $\mu\text{g}/\text{cm}^2$) was evaporated on top of this ^{59}Ni deposit. The triton and alpha groups (2728 and 2056 keV, respectively, for thermal neutrons) from the $^6\text{Li}(n,\alpha)$ reaction were easily resolved from the 4759-keV alpha group released by the $^{59}\text{Ni}(n,\alpha)$ reaction. The $^{59}\text{Ni}(n,p)$ measurements were made with a deposit of ^{59}Ni only, because the 1827-keV protons were difficult to separate from the alphas of ^6Li .

The (n,γ) cross-section measurement was made with a 3.136-g nickel sample of 2.54-cm diam, enriched to 2.96% in ^{59}Ni . The measurements were made from 100 to 12,000 eV, with an energy resolution of 0.15%, using the total-energy detector located at a 40-m flight path. Because the sample contained a small amount of ^{60}Co ,

the bias level on this gamma-ray detector was set at ~ 2 MeV, involving an uncertainty of $10 \pm 5\%$. Another measurement is planned with a "clean" sample to reduce the uncertainty due to this extrapolation.

Total neutron-cross-section measurements were also made with this 3.136-g sample, with an inverse thickness of 5295 b/atom of ^{59}Ni , using an 80-m flight path. The total cross section of the 203.4-eV resonance obtained with this sample was 1.32 times that obtained from earlier measurements using the ~ 9 -mg, 95%-enriched sample reported last year.³ This ~ 9 -mg sample has been emptied, reweighed on a microbalance, and examined for oxygen by measuring the ^{16}N activity produced by the $^{16}\text{O}(n,p)$ reaction with 14-MeV neutrons. These measurements confirmed the neutron analysis that the original sample contained only 7.0 mg of nickel instead of 9.2 mg. This increases the thermal-capture and -absorption cross sections reported last year to 70 ± 5 and 87 ± 6 b respectively.

The measurements on ^{59}Ni in the thermal energy range yield a value of 12 ± 1 b for the (n,α) cross section and 2.0 ± 0.5 b for the (n,p) cross section. This (n,α) result is to be compared with earlier values of 13.7 ± 1.2 , 18.0 ± 1.6 , and 22.3 ± 1.6 b reported by Eiland and Kirouac,⁴ by Werner and Santry,⁵ and by McDonald and Sjöstrand⁶ respectively. The (n,p) result is lower than the value of 4 ± 1 b reported by McDonald and Sjöstrand.⁶ The results of our four experiments have been combined to produce the following parameters for the 203.4-eV resonance: $E_0 = 203.4 \pm 0.2$ eV, $\Gamma = 13.3 \pm 0.2$ eV, $g = \frac{3}{8}$, $J = 1$, $\Gamma_n = 8.50 \pm 0.15$ eV, $\Gamma_\gamma = 4.0 \pm 0.6$ eV, $\Gamma_\alpha = 0.50 \pm 0.03$ eV, and $\Gamma_p = 0.063 \pm 0.006$ eV. Assuming that the thermal cross sections arise mainly from the large

203.4-eV resonance, the (n,p) thermal cross section would be expected to be one-eighth the (n,α) cross section, or 1.5 b.

Fifteen higher energy resonances have been observed in the four types of experiments. The alpha and proton widths of the resonances vary widely because of selection rules and because they are essentially single-channel processes to the ground state. For example, for the 2^- resonance at 3203 eV, Γ_α is $\leq 0.01\Gamma_p$, but for the 1^- resonance at 203.4 eV and the 9103-eV resonance, Γ_α is $\geq 7\Gamma_p$.

-
1. Chemistry Division.
 2. Instrumentation and Controls Division.
 3. S. Raman et al., *Phys. Div. Annu. Prog. Rep. Dec. 31, 1974*, ORNL-5025 (1975), p. 110.
 4. H. M. Eiland and G. J. Kirouac, *Nucl. Sci. Eng.* **53**, 1 (1974).
 5. R. D. Werner and D. C. Santry, *Nucl. Sci. Eng.* **56**, 98 (1975).
 6. J. McDonald and N. G. Sjöstrand, submitted to *Atomkernenergie*.

TOTAL NEUTRON-CROSS SECTION AND RESONANCE PARAMETERS OF ^{249}Bk

J. A. Harvey N. W. Hill²
R. W. Benjamin¹ S. Raman

Several years ago, a cooperative program was initiated between the Oak Ridge National Laboratory and the Savannah River Laboratory to measure the total neutron cross section of the heavy actinides as samples became available. Initially the interest in the cross sections of the transplutonium isotopes was to enable more accurate calculations of ^{252}Cf production. Recently, however, the study of the problem of managing radioactive wastes, particularly the long-lived actinides, and the possibility of recycling these long-lived actinides has emphasized the need for additional and better data on many heavy isotopes. Total neutron-cross-section measurements on small samples (too small and/or radioactive to permit a direct capture cross-section measurement) can readily be interpreted to yield the absorption cross section in the thermal energy range and often up to ~ 100 eV.

This year, a 6-mg sample of ^{249}Bk became available through the cooperation of John Bigelow of the Transuranium Facility (TRU). Two samples were prepared from this material, a "thick" sample containing 5.3 mg ($N = 0.00061$ atom/b) and a "thin" one containing ~ 0.8 mg. The sample holders had inside diameters of 1.6 mm, and the neutron beam was

collimated to a diameter of 1.3 mm. The samples were cooled with liquid nitrogen to reduce the Doppler broadening, which is greater than the neutron energy resolution up to ~ 100 eV. Measurements were made on the samples using an 11.0-cm-diam, 1.3-cm-thick ^6Li -glass scintillator located at a 17.87-m flight path. The measurements covered the energy range from 0.005 to $\sim 10,000$ eV, with an energy resolution of 0.3%.

A total of 47 resonances below ~ 130 eV was observed. A large resonance observed at 0.197 eV is responsible for most of the thermal-absorption cross section, which departs markedly from a $1/v$ energy dependence. The average level spacing based on the resonances up to 20 eV is 1.1 eV. The large resonance in ^{249}Cf at 0.70 eV was also observed, even though there was only $\sim 2\%$ ^{249}Cf in the sample (i.e., ~ 10 μg) at the time of measurement. After about half of the 330-day ^{249}Bk has decayed into ^{249}Cf , additional measurements will be made to obtain parameters for the resonances in ^{249}Cf as well as its thermal-absorption cross section. These measurements will be combined with the fission cross-section measurements of Dabbs et al.³ to obtain a complete set of parameters of the low-energy resonances of ^{249}Cf .

-
1. Savannah River Laboratory, Aiken, S.C.
 2. Instrumentation and Controls Division.
 3. J. W. Dabbs et al., *Phys. Div. Annu. Prog. Rep. Dec. 31, 1973*, ORNL-4937 (1974), p. 181.

FISSION CROSS-SECTION MEASUREMENTS ON SMALL ULTRAPURE CURIUM SAMPLES

J.W.T. Dabbs N. W. Hill²
C. E. Bemis, Jr.¹ S. Raman

Measurements on a 10- μg sample of ^{245}Cm (99.94% purity) were started in February. Some 700 hr of ORELA operation at high power was required. Ten new resonances below 20 eV were observed. The operation of the new hemispherical-plate ionization chamber was satisfactory in suppressing alpha particle pileup; however, the fission pulse spectrum was degraded (because of extraneous material in the deposit) such that the data will require normalization to the well-known thermal fission cross section. Low-repetition-rate runs at ORELA were made for this purpose in March, and the runs were completed in July.

A second chamber containing plates with ^{243}Cm (10 μg , 10^7 α/sec), ^{235}U , ^{239}Pu (decay daughter of ^{243}Cm), and a sample of spontaneously fissioning ^{252}Cf (for testing the chamber and time digitizer) was

prepared and tested extensively at the Transuranium Research Laboratory (TRL). The hemispherical-plate fission chamber has exceeded expectations in suppressing alpha pileup counts relative to fission counts. A factor of $>10^{10}$ reduction was obtained while permitting $>95\%$ fission counting efficiency.

A new neutron-flux monitor has also been developed. Lithium-6 fluoride was vacuum evaporated to a thickness of $96 \mu\text{g}/\text{cm}^2$ onto a 0.1-mm sheet of NE-110 plastic scintillator. Another sheet of NE-110 served to convert this "open-faced sandwich" into a "normal sandwich." This assembly was suspended in a vacuum chamber and inside two truncated cones (back to back) made of 0.0127-cm aluminum sheet. Light produced by the α, t pair in the two NE-110 sheets was reflected by the inner cone surfaces into two 12.7-cm photomultipliers on either side of the neutron beam. The beam passes directly through the cones, the NE-110 sheets, and the ^6LiF deposit. Although it was found necessary to reduce the area of the scintillator to lower the background, a satisfactory situation was finally obtained.

Measurements on ^{243}Cm began in December and will continue at least through March 1976. These measurements are part of a comprehensive program designed to provide accurate fission cross-section data for the higher actinides. Many important decisions regarding use, management, and storage of radioactive wastes depend on the knowledge to be acquired through this and other related measurement programs.

-
1. Chemistry Division.
 2. Instrumentation and Controls Division.

MONTE CARLO CALCULATIONS OF MULTIPLE PULSE PILEUP

J.W.T. Dabbs

In fission cross-section measurements, it is often desired to make measurements in the presence of an intense alpha particle background. It is obvious that with sufficiently fast electronic equipment the alpha pulse pileup can be reduced to unimportance, but quantitative knowledge of the problem is needed to choose the allowable amounts of material with particular ionization chambers, gas scintillator systems, or segmented ionization chambers.

A new method for Monte Carlo calculations, which is applicable to pulse pileup to any desired multiplicity of pileup, has been developed and used with a mini-computer for pileups with as many as 20 pulses.

Previously, closed-form calculations have been presented only for four pulses, except in the trivial case of square pulses. The present calculations are easily adaptable to unusual geometries such as in the hemispherical-plate fission chamber work described elsewhere in this report.

The method consists of setting up a table of 32 values (nominally one value per nanosecond) for the pulse shape in question. A double interval in time, 64 units long, is established. Then, for each multiplicity k (from 1 to some upper limit, say, 20) of pulses in the interval, $2k$ such pulses are distributed, to begin randomly in time over the double interval, and their amplitudes are added in each unit of the second half of the double interval, thus generating 32 values of pulse height for that k . After 250 repetitions of this process for each k value, one has an 8000-member height distribution for that k . The pulse-height distributions are then weighted by the Poisson distribution factor, p_k , for the particular counting rate involved and are summed to give the final pulse-height distribution. Comparison with observed values in a practical case has established the validity of the calculation. Such calculations have been used in designing three experiments so far.

ANGULAR ANISOTROPY IN THE $^6\text{Li}(n,\alpha)\text{T}$ REACTION IN THE eV ENERGY REGION

J. A. Harvey N. W. Hill²
J. Halperin¹ S. Raman

The yield of tritons and alphas in forward and backward directions ($\Omega \approx \pi$) from the interaction of neutrons with ^6Li has been measured from a thin sample of ^6LiF ($101 \mu\text{g}/\text{cm}^2$), from 0.5 to 25,000 eV. The measurements were made with a diffused-junction silicon detector located 9.03 m from the water-moderated tantalum target at ORELA. The alpha and triton groups at 2.06 and 2.73 MeV are well resolved, enabling one to obtain an accurate ratio of their intensity as a function of neutron energy. The intensity of the alpha peak was greater than the intensity of the triton peak in the forward direction but less in the backward direction. This difference is measurable down to 10 eV. An anisotropy has already been reported for 25-keV neutrons by Schroder et al.,³ who made measurements using an iron-filtered neutron beam. In the 10-eV to 10-keV energy region, our results give an energy dependence for the alpha-to-triton ratio at 180° (or triton-to-alpha ratio at 0°) of the form $1 + cE^{0.54}$, where c is ~ 0.005 and E is the neutron energy in eV. At 100 eV, this ratio equals 1.06. It is necessary to

consider this angular anisotropy when the ${}^6\text{Li}(n,\alpha)$ cross section is used as a standard in the low-energy region. This angular anisotropy probably arises from the interference between the large p -wave resonance at 245 keV and many s -wave resonances, which account for the large $1/v$ (n,α) thermal cross section.

-
1. Chemistry Division.
 2. Instrumentation and Controls Division.
 3. I. G. Schroder et al., *Conference on Neutron Cross Sections and Technology*, NBS Special Publication 425, U.S. Government Printing Office, Washington, D.C., 1975, p. 240.

DURATION OF STELLAR NUCLEOSYNTHESIS

R. L. Macklin¹ J. Halperin¹ R. R. Winters²

The elements heavier than iron which are found in the solar system were formed 5 to 10 billion years ago, deep inside stars that subsequently exploded. Most of the heavy material was built up slowly by the capture of one neutron at a time during the slow evolution of red giant stars. The radioactive decay half-lives of certain isotopes in the chain of mostly stable isotopes allow us to set limits to the fast-neutron-flux levels involved and hence the mean time between neutron captures, using the isotopic abundances found on Earth.

A favorable branch in the s process occurs at thallium, and our neutron-capture data for ${}^{203}\text{Tl}$ and ${}^{205}\text{Tl}$ lead to a probable neutron flux (for a temperature near 350 million $^\circ\text{K}$) of 1.0×10^{16} neutrons/cm², with an upper limit of 2.0×10^{16} neutrons/cm². The mean neutron-capture time was found to be only 23 years, with a lower limit of 12 years. The upper limit (~ 150 years) is less reliably established, and a value of 250 years estimated (by others³) from ${}^{151}\text{Sm}$ capture and decay is preferred.

-
1. Chemistry Division.
 2. Denison University, Granville, Ohio.
 3. B. J. Blake and D. N. Schramm, *Astrophys. J.* **197**, 1615 (1975).

NEUTRON-CAPTURE MECHANISM IN LIGHT AND CLOSED-SHELL NUCLIDES

R. L. Macklin¹ J. W. Boldeman³
 J. Halperin¹ M. J. Kenney³
 R. R. Winters² A. R. Musgrove³
 B. J. Allen³ Hla Pe³

The search for evidence of nonstatistical mechanisms in nuclear reactions has been extended to our neutron-capture data on a number of promising nuclides,

including ${}^{28}\text{Si}$, ${}^{32}\text{S}$, ${}^{40}\text{Ca}$, ${}^{88}\text{Sr}$, ${}^{90}\text{Zr}$, ${}^{138}\text{Ba}$, and several of their neighboring, enriched, stable isotopes. The low compound-nucleus cross sections at closed nucleon shells leave the nonstatistical components such as channel and valence capture more prominent in the data.

The ${}^{88}\text{Sr}(n,\gamma)$ reaction, for example, with the 50-neutron closed-shell target, has shown strong evidence of the valence-capture mechanism. This is shown both through correlation of reduced neutron and radiative widths (coefficients of 0.96 for $p_{1/2}$ resonances and 0.77 for $p_{3/2}$ resonances) and optical-model-based calculations of the valence-model widths, agreeing within 25 to 30% with the experimental results. In capture by ${}^{40}\text{Ca}$ and ${}^{138}\text{Ba}$, a further nonstatistical mechanism beyond the valence component seems to be required by the data, and the investigation is continuing, using Ge(Li)-detector data on the partial radiative widths at particular levels.

-
1. Chemistry Division.
 2. Denison University, Granville, Ohio.
 3. Australian Atomic Energy Commission, Lucas Heights, Australia.

NEUTRON-CAPTURE GAMMA-RAY STUDIES

S. Raman G. G. Slaughter
 R. F. Carlton¹ J. C. Wells, Jr.²
 D. A. McClure³

The tin isotopes are well suited to a study of nuclear structure within the framework of the nuclear shell model because the magic number of protons ($Z = 50$) minimizes the need for considering n - p pairing interactions in theoretical calculations and because the large number of stable isotopes makes it possible to study systematic trends in both experimental and shell-model features. The existing experimental data on the odd- A tin isotopes are not as extensive as might be expected on the basis of their theoretical importance. Thermal-neutron-capture studies have not been widely used because of the extremely small capture cross sections for the heavier even- A tin isotopes. Most experimental studies (especially nucleon-transfer studies) are beset with the problem of interference from isotopic impurities. This usually necessitates an extensive study of all tin isotopes before conclusive results can be obtained. Resonance neutron capture offers a powerful technique for studying tin isotopes because interference from unwanted isotopes can be greatly suppressed through the combination of enriched targets and selection of resonances known to be in the nucleus under study. We

have, therefore, undertaken a systematic investigation of the level structure of six odd tin isotopes between $A = 115$ and $A = 125$. Measurements have been completed on all the isotopes except ^{115}Sn and ^{117}Sn , which will be carried out in the near future. In the case of ^{121}Sn , treated here as typical, capture gamma rays (18 primary and 32 secondary) from 16 neutron resonances up to 7 keV, obtained with a Ge(Li) detector, have been used to determine 20 excited levels in ^{122}Sn . Several new levels have been found. Spin and parity assignments have been made to many of the levels. When the present series of studies have been completed, the resulting level schemes for the tin isotopes are expected to significantly increase our understanding of their energy systematics.

We have also begun (n,γ) measurements in the lead region to obtain information on absolute gamma-ray transition widths and on reaction mechanisms. Measurements have been completed on enriched ^{206}Pb and ^{207}Pb targets. Unlike the case of the tin isotopes, the gamma-ray spectra in lead isotopes are strikingly simple, being composed of less than five primary gamma-ray transitions. The idea, then, would be to combine the relative gamma-ray intensities obtained with a Ge(Li) detector (or even an NaI detector) with the total gamma-ray widths obtained with a total-energy detector⁴ to deduce the partial widths. In this manner, we have been able to determine the $E2$ radiation widths for the ground-state transitions in ^{208}Pb from 2^+ neutron resonances at 3.1, 10.2, and 16.2 keV. The observed strengths represent only $\approx 0.3\%$ of the energy-weighted sum-rule (EWSR) strength. By extending the (n,γ) measurements to higher neutron energies, we hope to locate other pieces of the $E2$ strength as well as the $E1$ and $M1$ strengths. Initial results⁵ obtained with a large NaI detector, up to a neutron energy of 200 keV, are encouraging.

1. Middle Tennessee State University, Murfreesboro.
2. Tennessee Technological University, Cookeville.
3. Georgia Institute of Technology, Atlanta.
4. R. L. Macklin and J. H. Gibbons, *Phys. Rev.* **159**, 1007 (1967).
5. In collaboration with G. L. Morgan and G. T. Chapman of the Neutron Physics Division.

NEUTRON INTERACTIONS WITH ^{100}Mo

W. Weigmann ¹	J. A. Harvey
S. Raman	R. L. Macklin
G. G. Slaughter	J. Halperin ²

Neutron capture in the isotopes ^{92}Mo and ^{98}Mo is known to be dominated by the "valence-capture"

mechanism. Among the observations related to valence capture are strong correlations between reduced neutron widths of p -wave resonances and partial radiation widths to final states with large (d,p) spectroscopic factors, such as the ground state. The nucleus ^{100}Mo was considered another candidate for valence capture, particularly because a strong concentration of p -wave strength occurs between 1- and 2.5-keV neutron energy. Therefore, neutron-capture gamma-ray spectra were measured in separated resonances of ^{100}Mo . As neutron widths given in the literature for the resonances in question are strongly discrepant, a transmission measurement was also performed to redetermine neutron widths. Simultaneously, total-capture data, obtained earlier at the ORELA neutron-capture cross-section measurement facility, have been analyzed.

The capture gamma-ray spectra were measured with a 40-cm³ Ge(Li) detector, using a 10.2-m flight path for neutron time-of-flight spectroscopy. Capture gamma-ray spectra have been obtained for individual resonances up to about 5-keV neutron energy. The transmission measurement has been performed at an 80-m flight path, and resonance analysis is being done up to about 25 keV.

Although analysis of the data is still in progress, two main results can be given: (1) The neutron widths of the strong p -wave resonances between 1- and 2.5-keV neutron energy are considerably (up to a factor of 3) smaller than those given in BNL-325.³ This reduces the probability that valence capture dominates and may, in part, explain the second observation. (2) Valence capture does not play a dominant role in these resonances; for instance, a transition to the ground state of ^{101}Mo (spectroscopic factor, 0.42) is not observed in three of the four strongest p -wave resonances.

1. Visiting scientist from Bureau Central de Mesures d'Nucléaires, Geel, Belgium.

2. Chemistry Division.

3. S. F. Mughabghab and D. I. Isaac, *Neutron Cross Sections, Vol. 1, Resonance Parameters*, 3d ed., BNL-325, Brookhaven National Laboratory, Upton, N.Y., 1973.

MEASUREMENTS ON TOTAL NEUTRON CROSS SECTIONS FOR UNDERSTANDING NEUTRON CAPTURE

C. H. Johnson	R. R. Winters ²
J. Halperin ¹	R. L. Macklin

In the valency model for neutron capture, enhanced dipole transitions occur from states with relatively large neutron widths to final states with large neutron

spectroscopic factors. To study this phenomenon, we need to know not only Γ_γ for each resonance but also the neutron widths and J^π values. The observed total cross sections give the neutron width and J values for well-resolved resonances. The parity can also be deduced if the nonresonant phase shift is large enough to give an interference pattern.

We have measured the total neutron cross section of ^{32}S , using the 200-m flight path with 5-nsec pulses at ORELA, to supplement our earlier neutron-capture data obtained at the 40-m station. From these data were determined Γ_n and J^π for 15 of the ~ 60 resonances observed in capture. There is no obvious correlation of Γ_n and Γ_γ , but the radiative widths predicted from the valency model from the observed Γ_n and J^π are large fractions of the observed Γ_γ . Furthermore, resonances predicted to have relatively large valency capture are observed to have relatively intense high-energy gamma rays in the emitted spectra.

-
1. Chemistry Division.
 2. Denison University, Granville, Ohio.

RESONANT STATES OF ^{209}Pb FROM TOTAL NEUTRON-CROSS-SECTION MEASUREMENTS

J. L. Fowler C. H. Johnson
N. W. Hill¹

Using a suitable combination of three natural samples of lead in a transmission experiment, we have measured the total neutron cross section of effectively 99.6% ^{208}Pb . The ORELA time-of-flight facility provided 4- to 5-nsec pulses of neutrons for the 200-m flight path. About 100 resonances between 0.7 and 1.5 MeV were observed, about twice as many as were seen in a previous experiment² carried out with $^7\text{Li}(p,n)$ neutrons. In this energy interval, resolution varied from ~ 0.6 keV at 0.7 MeV to ~ 1.4 keV at 1.5 MeV. The improved energy resolution and statistics from this experiment, together with differential cross sections from the previous experiment,² will enable us to identify the J values, parities, and reduced widths of the resonant states of ^{209}Pb more definitely than was possible earlier. In the case of the other doubly closed-shell nuclei, such data give information on the fragmentation of shell-model states.^{3,4}

-
1. Instrumentation and Controls Division.
 2. J. L. Fowler, *Phys. Rev.* **147**, 870 (1966).
 3. J. L. Fowler, C. H. Johnson, and R. M. Feezel, *Phys. Rev. C* **8**, 545 (1973).
 4. C. H. Johnson, *Phys. Rev. C* **7**, 561 (1973).

d-WAVE ADMIXTURES IN *s*-WAVE, $J = 1$ RESONANCES IN $^{207}\text{Pb} + n$

D. J. Horen C. H. Johnson
J. A. Harvey N. W. Hill¹

Previous analyses of resonances in neutron transmission experiments ($E_n \lesssim 500$ keV) have usually ignored all but the lowest l -wave contribution to the resonance cross section. However, preliminary analysis of the neutron transmission of ^{207}Pb indicates the presence of d -wave admixtures in some of the resonances which are of s -wave, $J = 1$ character. In particular, a two-channel single-level R -matrix analysis of the 256.25-keV resonance ($\Gamma = 3.2$ keV) reproduced the experimental data with a d -wave width of $\Gamma_n^d = 0.71\Gamma_n^s$. A fit to the data assuming only s -wave contribution would require an abnormally high radiative absorption width (i.e., $\Gamma_\gamma \gtrsim 1$ keV). The admixture found here is comparable to that deduced by Holt² from a reanalysis of available angular distribution data from the inverse reaction and from a study of the $^{208}\text{Pb}(\gamma, n_0)$ reaction. From our results, it appears that there is appreciable d -wave admixture in the 181.45-keV resonance ($\Gamma \approx 150$ eV) and probably a small component in the 101.78-keV resonance ($\Gamma \approx 70$ eV) as well.

The high resolution ($\Delta E/E \approx 0.07\%$) attainable at the 200-m flight path at ORELA was instrumental in providing the quality of data required to investigate such admixtures.

The study of d -wave admixtures in s -wave resonances would appear to provide a unique means to gain information on the d -wave strength function. In general, it is difficult to determine the parity of a resonance (except for s waves) and, hence, whether it was formed by an even or an odd l wave. This problem can be resolved when there is admixture (of the d) with an s wave. The determination of d -wave widths in such admixed resonances could be used to derive a lower limit on the d -wave neutron strength function.

-
1. Instrumentation and Controls Division.
 2. R. Holt, private communication, January 1976.

GIANT RESONANCES IN ^{208}Pb AND NEUTRON RESONANCES

D. J. Horen J. A. Harvey
N. W. Hill¹

The investigation of giant resonances in ^{208}Pb continues to be an active area of research which involves

various types of nuclear reactions (e.g., inelastic hadron and electron scattering, photonuclear reaction). Because the giant resonances lie in a region of high density, the "resonances" observed in such experiments usually overlap more than one excited level. Lack of detailed knowledge of the microstructure of the observed "resonance" can sometimes lead to erroneous interpretations of, or conclusions from, the data obtained in such experiments.

High-resolution neutron-transmission experiments can provide unique information to aid in the interpretation of the resonances observed in these reactions in an energy interval up to about 1 MeV (and in some cases higher) above the neutron separation energy. The value of such total cross-section data has been pointed out by Harvey et al.^{2,3} Recently, Morsch, Decowski, and Benenson⁴ reported detection of part of a giant monopole resonance in ^{208}Pb at 9.11 MeV (which corresponds to $E_n \sim 1.74$ MeV in the $^{207}\text{Pb} + n$ system). This work was performed with 45-MeV protons ($\Delta E/E \sim 35$ keV) and 70-MeV ^3He ($\Delta E/E \sim 45$ keV). The contribution to the energy-weighted sum rule for this fragment was calculated to be $\sim 7\%$.

The neutron transmission of ^{207}Pb provides a valuable means for locating 0^+ states in the continuum region of ^{208}Pb . Even though one cannot determine whether such states contribute to the giant monopole resonance, their observation can serve as a guide for investigation (and an independent confirmation of J^π) by experiments of other types which are capable of sampling the monopole transition element to the ground state. Thus far the analysis of the ^{207}Pb data has revealed four 0^+ resonances in the neutron energy region of 80 to 265 keV. These, as well as parameters for some other resonances, are presented in Table 1.1. Analysis of the data both below and above the energy region reported here is in progress.

1. Instrumentation and Controls Division.
2. J. A. Harvey et al., *Phys. Div. Annu. Prog. Rep. Dec. 31, 1973*, ORNL-4937 (1974), p. 194.
3. J. A. Harvey and N. W. Hill, *Phys. Div. Annu. Prog. Rep. Dec. 31, 1974*, ORNL-5025 (1975), p. 126.
4. H. P. Morsch, P. Decowski, and W. Benenson, Report NSUCL-197, University of Michigan, Ann Arbor, December 1975.

Table 1.1. Resonances in $^{207}\text{Pb} + n$

E_n (keV)	l	J^π	Γ_n^l (eV)	$g\Gamma_n^l$
82.07	1	0^+	100 ± 10	
82.97		1, 2, 3		27
87.73		1, 2, 3		16
90.16	2^a	1^{+a}	279 ± 9	
98.37		2	106 ± 4	
101.78	$0 + (2)$	1^-	$74 \pm (1.6)$	
103.54	1	0^+	240 ± 30	
112.08		2, 3		60
115.12	1^a	1^{+a}	854 ± 50	
128. (doublet)				
130.20	1^a	1^{+a}	100 ± 10	
132.16	1, 2	1, 2		53
135.23	1	0^+	127 ± 10	
136.46				20
139.65	1^a	2^{+a}	163 ± 5	
145.38	1^a	1^{+a}	111 ± 8	
148.19		1, 2, 3		18
149.12		1, 2, 3		23
153.74		1, 2, 3		23
155.68	1^a	1^{+a}	112 ± 5	
158.86		1, 2, 3		55
168.47	1^a	1^{+a}	190 ± 6	
171.08	1^a	2^+	156 ± 8	
179. (doublet)				
181. (doublet)				
181.45	$0 + 2$	1^-	$\sim 81 + \sim 69$	30 40
186.24				
207.54	1	0^+	211 ± 20	
209.38	2^a	2^{-a}	521 ± 5	
210.60		1, 2, 3		20
211.69		(1), 2, 3		83
218.35	1^a	1^{+a}	128 ± 5	
220.15		2, (3)		190
223.93		2, 3		103
227.89	0	0^-	9435 ± 200	
229.66	1^a	1^{+a}	659 ± 15	
233.20		1, 2, 3		43
240.60		(1), 2, 3		36
243.44		1, 2, 3		74
249. (doublet)				
254.35	(2^a)	2, 3		185
256.25	$0 + 2$	1^-	$1875 + 1339$	
262.11		1, 2, 3		71
265.33	1^a	1^{+a}	190 ± 20	

^aFrom phase shift.

Oak Ridge Isochronous Cyclotron Program

INTRODUCTION

E. E. Gross

The following summaries show that the research program at the Oak Ridge Isochronous Cyclotron (ORIC) is broad in scope and extensive in participation. It is important to realize that this report represents the efforts of all ORIC participants, thereby cutting across many divisional and institutional lines. Despite the wide variety of results reported here, the program is a cohesive, integrated effort that has been shaped or influenced by ORIC schedule meetings, Program Committee reviews, and frequent informal research seminars. These interactions have provided an atmosphere conducive to new ideas. Conditions have also been favorable for continual regroupings of collaborators as new experiments are proposed.

In this process of continual evolution, we note the many reports from a fully matured UNISOR project. Significant results from this effort include evidence for coexistence of spherical and deformed bands in ^{186}Hg , new mass determinations by positron endpoint energies or alpha-decay energies, and a g -factor measurement for the first 2^+ state in ^{126}Xe , using the separator as an ion implantation device. A combination of in-beam gamma-ray studies and isotope separator measurements has led to a thorough understanding of the roles of the $h_{11/2}$ neutron and $h_{9/2}$ proton orbitals throughout the mercury isotopes. One also notes that the research program has a strong commitment to a systematic investigation of "macroscopic" phenomena in general and to "strongly damped" reaction processes in particular. Interesting details are beginning to appear, such as structure in the "deeply inelastic" yields of $Z \gtrsim 8$ products from 130-MeV ^{12}C bombardment of ^{63}Cu . It will also be noted that the attack on heavy-ion fission, fusion, and "deeply inelastic" phenomena is supplemented by experiments at other accelerators.

The "microscopic" heavy-ion reaction continues to show promise as a spectroscopic tool. Two results are outstanding in this regard. One is a clear demonstration that the ($^6\text{Li}, ^6\text{He}$) charge-exchange reaction is a reliable probe for Gamow-Teller strength in nuclei. The other is an equally clear demonstration that heavy-ion inelastic scattering can be used as a sensitive probe of nuclear shapes. The latter results from a coupled-channels analysis of 2^+ , 4^+ , and 3^- states excited by 70-MeV ^{12}C inelastic scattering from $^{142,144,146,148,150}\text{Nd}$. Other significant contributions from the areas of transfer reactions, giant resonance excitation, Doppler-shift lifetime determinations, and nuclear chemistry can be gleaned from the following reports.

UNIVERSITY ISOTOPE SEPARATOR AT OAK RIDGE (UNISOR) PROJECT

The UNISOR project is a cooperative venture and is organized as a unit of Oak Ridge Associated Universities (ORAU). Participants include the University of Alabama in Birmingham, Georgia Institute of Technology, Emory University, Furman University, the University of Kentucky, Louisiana State University, the University of Massachusetts, Oak Ridge Associated Universities, Oak Ridge National Laboratory, the University of South Carolina, the University of Tennessee, Tennessee Technological University, Vanderbilt University, and Virginia Polytechnic Institute and State University. UNISOR was formed for the

primary purpose of studying nuclei lying far from the region of beta stability by means of an isotope separator installed on-line to ORIC. The following reports describe UNISOR research and development efforts using the ORIC facility.

SPHERICAL AND DEFORMED BANDS IN ^{186}Hg

J. D. Cole ¹	B. van Nooijen ¹
J. H. Hamilton ¹	H. Kawakami ¹
A. V. Ramayya ¹	L. L. Riedinger ²
K.S.R. Sastry ³	

In our UNISOR studies of the decay of ^{188}Tl , we reported last year the first evidence for the existence of

two bands: one band on a spherical and one band on a deformed shape in ^{188}Hg , where low- and high-spin states were seen in both bands (Fig. 1.1). Such coexistence of spherical and deformed states can occur if there is a second minimum in the potential at large deformation. From in-beam gamma-ray studies,⁴⁻⁶ the high-spin deformed states are observed to drop in energy in $^{186,184}\text{Hg}$. Thus, one expects to see a deformed band with its 0^+ band head at lower energies in ^{186}Hg . The existence and position of these 0^+ band heads are essential to visualizing the theoretical picture of the coexistence of spherical and deformed shapes.

We have identified the new isotope ^{186}Tl and have studied its decay to ^{186}Hg to test and to extend our understanding of nuclei in this region. Analysis of the primary features of I_γ and I_e multiscale and $\gamma\text{-}\gamma$ and $e\text{-}\gamma$ coincidence studies of the ^{186}Tl decay now confirms our ^{188}Hg interpretation. A 373.9-keV transition has a $4.5^{+1.0}_{-1.5}$ -sec half-life and is assigned as an isomeric decay in ^{186}Tl (Fig. 1.2).

Our I_e and $e\text{-}\gamma$ data show that an $E0$ transition of 522 ± 1 keV feeds the ground state to establish a 0^+ level at this energy in ^{186}Hg and that a 215.8-keV transition is $E0 + E2(+M1)$ and feeds the first 2^+ state to establish a 2^+ level at 621.0 keV. These two states are interpreted as the band head and first excited state in the strongly deformed band seen at higher spins in the yrast cascade.⁴⁻⁶ Transitions seemingly associated with higher spin states in the band built on a near-spherical ground state are also seen. The levels in the spherical

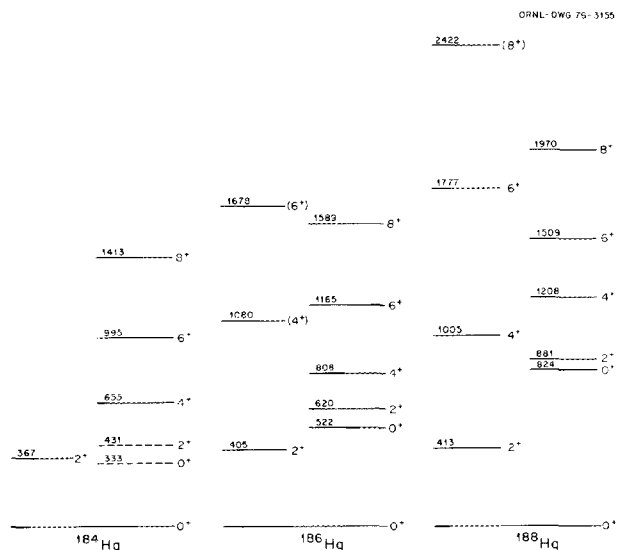


Fig. 1.1. Systematics of spherical and deformed bands in $^{188,186}\text{Hg}$, as determined in UNISOR work, and predictions for ^{184}Hg .

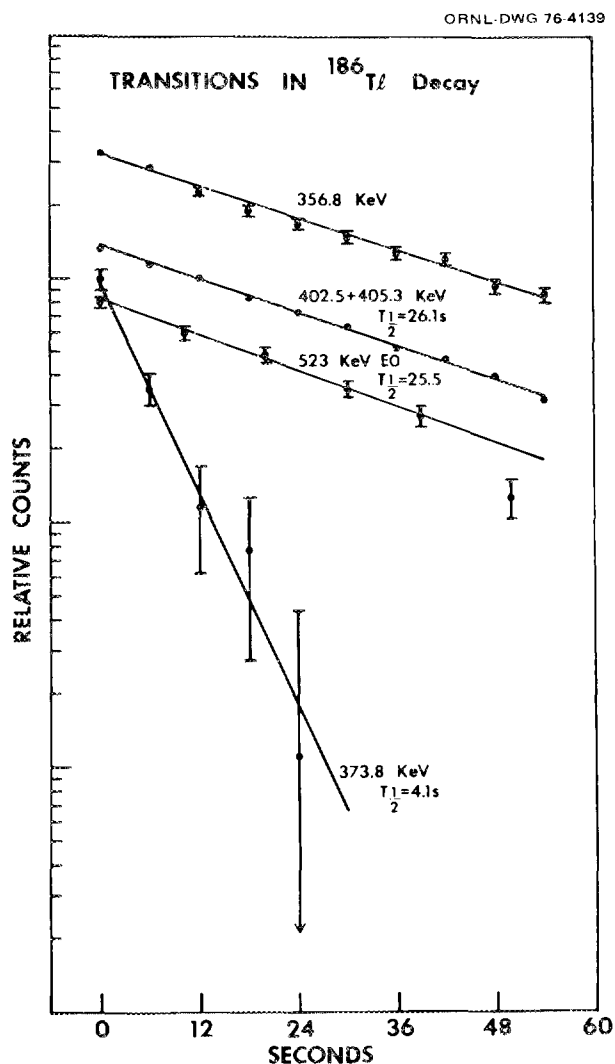


Fig. 1.2. Decay curves for prominent transitions in ^{186}Tl decay.

and deformed bands in ^{186}Hg are shown in Fig. 1.1. These data confirm the same coexistence and crossing of bands built on near-spherical and deformed shapes in ^{186}Hg as seen in ^{188}Hg , except that the deformed band has dropped in energy, as expected from recent theoretical⁷ and experimental^{4,6} studies. These studies used the high-spin yrast states in ^{184}Hg . One may predict that the first excited state in ^{184}Hg is the 0^+ band head of the deformed band, as shown in Fig. 1.1.

1. Vanderbilt University, Nashville, Tenn.
2. University of Tennessee, Knoxville.
3. University of Massachusetts, Amherst.
4. D. Proetel et al., *Phys. Rev. Lett.* 31, 896 (1973).

5. N. Rud et al., *Phys. Rev. Lett.* **31**, 1421 (1973).
 6. D. Proetel, R. M. Diamond, and F. S. Stephens, *Phys. Lett.* **48B**, 102 (1974).
 7. S. Frauendorf and V. V. Pashkevich, *Phys. Lett.* **55B**, 365 (1975); and Joint Institute for Nuclear Research, 1974, Dubna, U.S.S.R., Report E2-8087, to be published.

3. UNISOR, Oak Ridge Associated Universities, Oak Ridge, Tenn.
 4. University of South Carolina, Columbia.
 5. *Phys. Div. Annu. Prog. Rep. Dec. 31, 1974*, ORNL-5025 (1975), p. 72.
 6. E. F. Zganjar et al., *Phys. Lett.* **58B**, 159 (1975).
 7. J. O. Newton et al., *Nucl. Phys.* **A236**, 225 (1974).

STRUCTURE OF THE ODD-MASS GOLD ISOTOPES

J. L. Wood¹ D. A. McClure¹
 E. F. Zganjar² R. W. Fink¹
 R. L. Mlekodaj³ A. G. Schmidt³
 F. T. Avignone III⁴

The early stages of these studies were described in last year's annual report.⁵ Since then, we have reported the systematic features of the $h_{11/2}$ bands and the positive-parity states for $^{189-195}\text{Au}$.⁶ These studies have now been extended to ^{187}Au , and the low-spin levels in ^{193}Au have been investigated through the beta decay of the low-spin ^{193}Hg ground state produced indirectly via the beta decay of ^{193}Tl . The systematics of the positive-parity states of low j are shown in Fig. 1.3; the shell-model states and isomerism are shown in Fig. 1.4. The $h_{11/2}$ systematics are shown in the following section of this report, together with details of the $h_{9/2}$ bands and the interpretation of these high- j orbital bands as the coupling of the odd proton to a triaxial rotor.

It is not easy to explain the intrusion of the $h_{9/2}$ and $i_{13/2}$ proton orbitals across the $Z = 82$ closed shell to appear near the Fermi energy in the odd-mass gold isotopes (and also the odd-mass thallium isotopes -- see article in this section).

The deformation required in the Nilsson model is about twice that reflected by the rotational structure of the bands built on these orbitals. A strong pairing correlation (blocking) effect has been invoked by Newton et al.⁷ to explain the low energy of $h_{9/2}$ (one-particle--two-hole) states relative to $s_{1/2}$, $d_{3/2}$ (one-hole) states in the odd-mass thallium isotopes. It is difficult to understand how such a large pairing effect can arise when going from the $s_{1/2}$, $d_{3/2}$, $d_{5/2}$, $h_{11/2}$ (three-hole) states to the $h_{9/2}$, $i_{13/2}$ (four-hole--one-particle) states in the odd-mass gold isotopes. This problem, which is fundamental to the whole picture of the transition from the spherical shell model to the deformed Nilsson model, is being explored further, particularly with regard to the role of the pairing force.

TRIAxIAL ROTOR DESCRIPTION OF THE ODD-MASS GOLD ISOTOPES

J. L. Wood¹ R. W. Fink¹
 E. F. Zganjar² J. Meyer-ter-Vehn³

Recent work by Meyer-ter-Vehn⁴ has demonstrated the remarkable ability of a triaxial rotor model with Coriolis and pairing forces to describe the coupling of single high- j nucleons to the nuclear core in regions traditionally referred to as transitional (i.e., between spherical and strongly deformed prolate shape). The $h_{11/2}$ band in ^{195}Au has played a distinctive role in this development.⁵ The extension of the model to the systematic behavior of the $h_{11/2}$ bands and the $h_{9/2}$ bands through $^{187-195}\text{Au}$ (Figs. 1.5 and 1.6) strongly suggests an effective core concept, namely, that the $h_{11/2}$ and $h_{9/2}$ bands in the gold isotopes are largely determined by the even-even cores corresponding to an $h_{11/2}$ hole and an $h_{9/2}$ particle, the presence of the odd nucleon having very little effect on the collective parameters of the even-even core treated and a triaxial rotor. Figure 1.7 illustrates this for the unique nucleus ^{189}Au , where the $h_{11/2}$ and $h_{9/2}$ states have the effective cores ^{190}Hg and ^{188}Pt , respectively. The triaxial rotor parameters defined by the energy level spectra of ^{190}Hg and ^{188}Pt are consistent with $\beta = 0.14$, $\gamma = 37^\circ$ and $\beta = 0.18$, $\gamma = 23^\circ$ respectively. (Note that the level spectrum of an even-even nucleus cannot distinguish between prolate and oblate shapes.)

When the $h_{11/2}$ and $h_{9/2}$ bands are scaled in energy by the factors shown in Fig. 1.7, they show a striking similarity. This is in agreement with a particle-hole symmetry predicted to be valid for single- j shell triaxial rotors and in this case is given by

$$\beta h_{9/2}^2 [E_I(\gamma, h_{9/2} \text{ particle})] \\ = \beta h_{11/2}^2 [E_{I+1}(60^\circ - \gamma, h_{11/2} \text{ hole})]$$

The bands in the odd-mass gold isotopes have also been discussed in terms of the cluster-phonon coupling model⁶ and in a microscopic model based on the pseudo-Su(3) coupling scheme;⁷ however, neither of these models can describe a simple particle-prolate,

1. Georgia Institute of Technology, Atlanta.
 2. Louisiana State University, Baton Rouge.

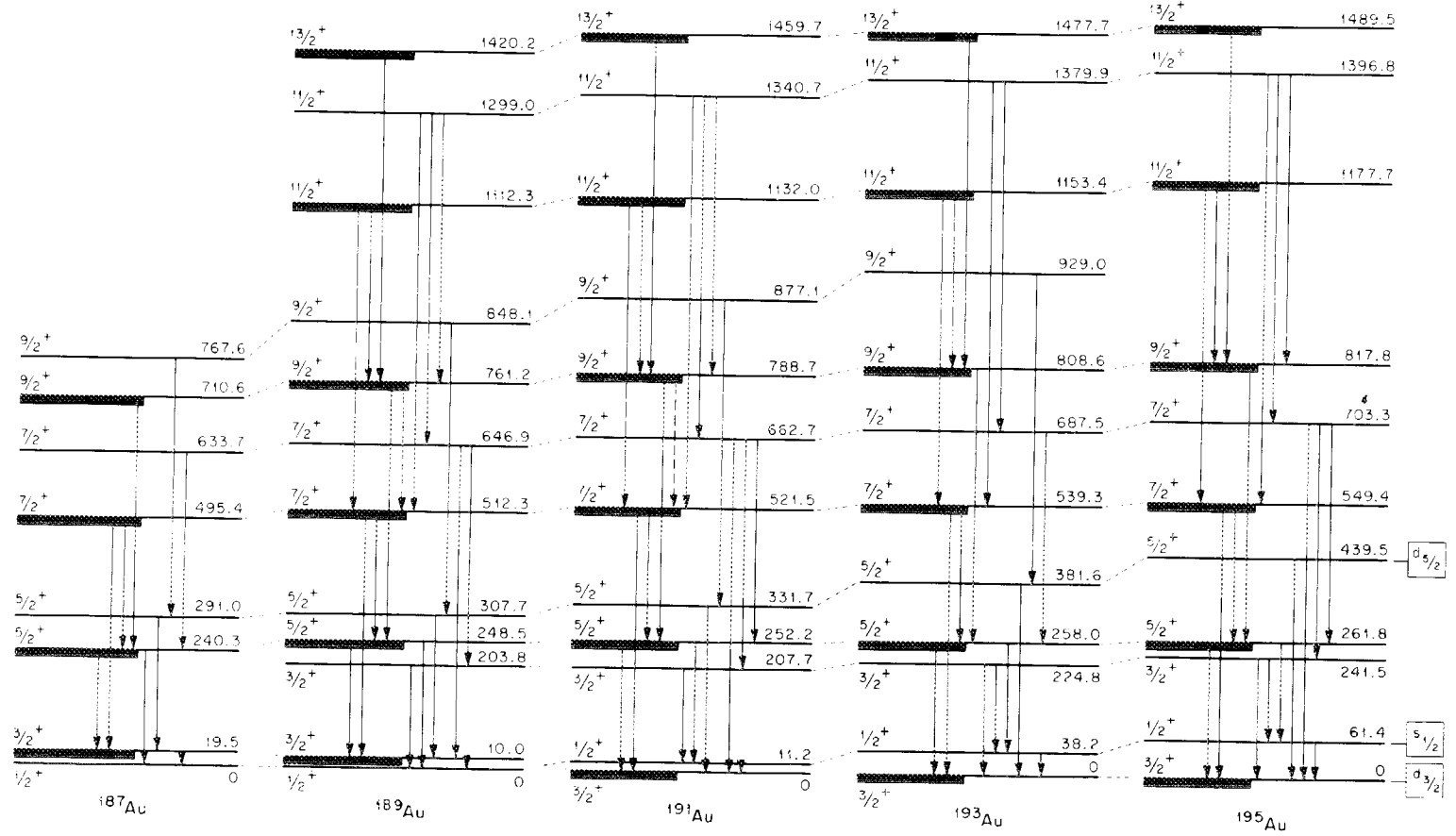


Fig. 1.3. Positive-parity states in odd-A gold nuclei. The states associated with the $d_{3/2}$ orbital are shown as levels with heavy bars.

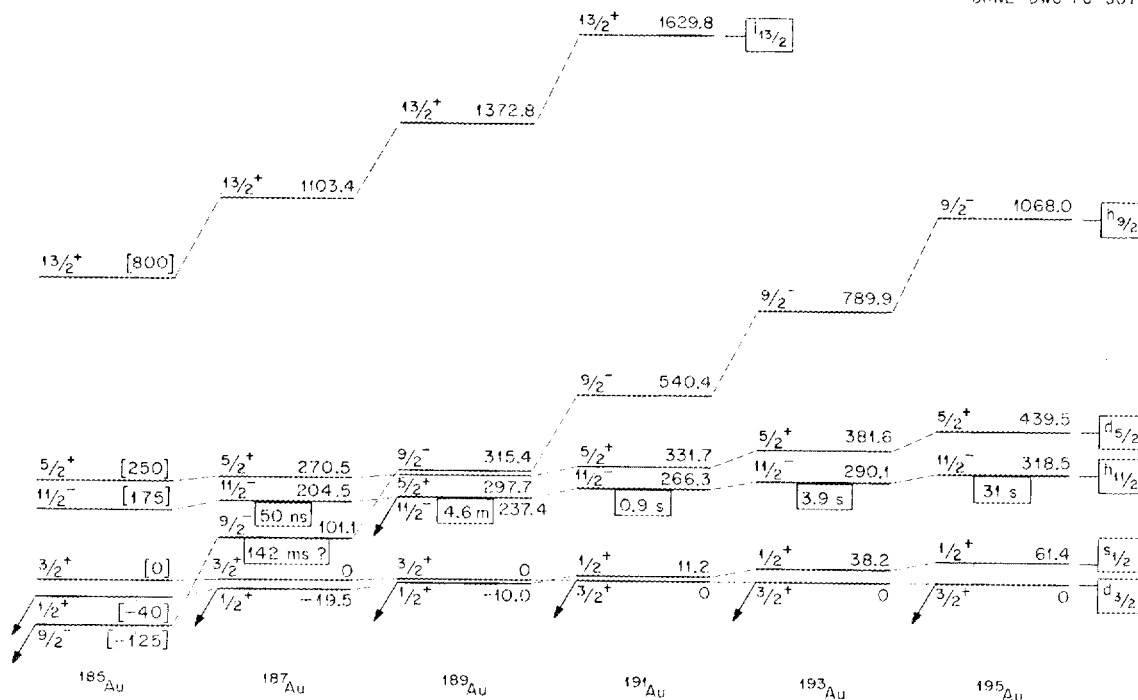


Fig. 1.4. Single-particle states in the light gold isotopes. The levels shown in ^{185}Au are projections from systematics and suggest the 3.9-min and 8.9-min activities observed in ^{185}Au to be the states $s_{1/2}$ and $h_{9/2}$.

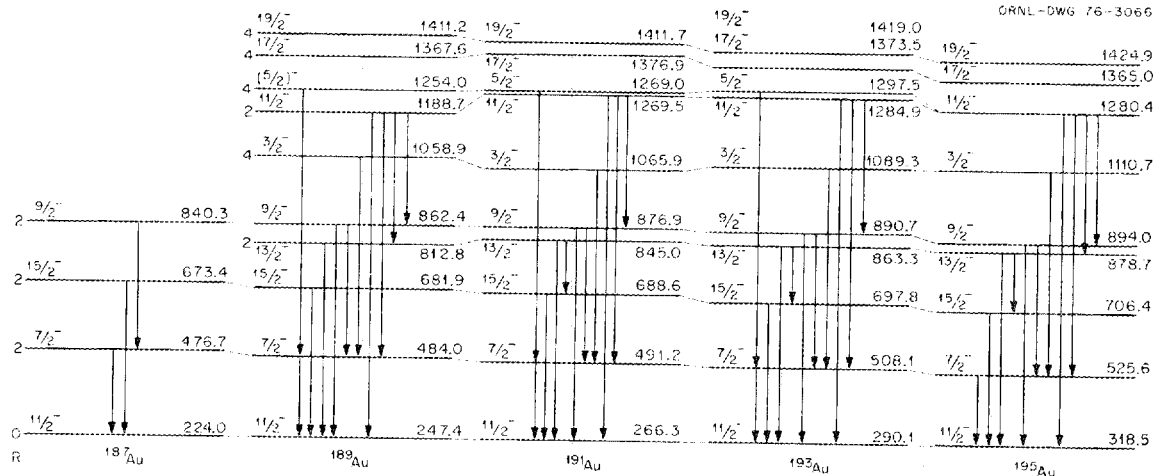


Fig. 1.5. Negative-parity states in odd-A gold nuclei based on the $h_{11/2}$ orbital. The $19/2^-$ states and the $17/2^-$ states in $^{193,195}\text{Au}$ are taken from in-beam reaction studies.

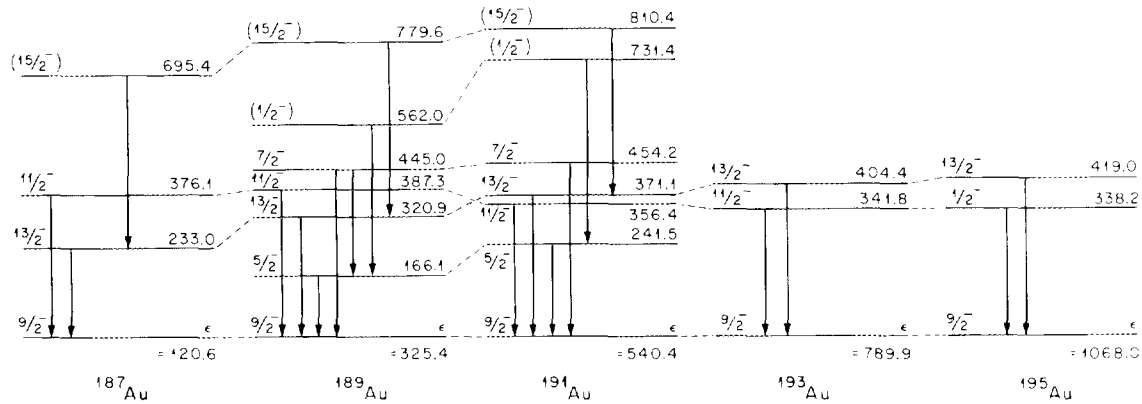


Fig. 1.6. Negative-parity states in odd- A gold nuclei based on the $h_{9/2}$ orbital. The only transitions between these levels and those of the $h_{11/2}$ bands are between the band heads: they are retarded by 1.5×10^4 relative to a Weisskopf single-particle estimate for $M1$.

hole-oblate symmetry. A mixed- j triaxial rotor approach is also being considered for the positive-parity states in $^{178-195}\text{Au}$.

1. Georgia Institute of Technology, Atlanta.
2. Louisiana State University, Baton Rouge.
3. Lawrence Berkeley Laboratory, Berkeley, Calif.
4. J. Meyer-ter-Vehn, *Nucl. Phys.* **A249**, 111 (1975); and *Nucl. Phys.* **A249**, 141 (1975).
5. J. Meyer-ter-Vehn, *Phys. Rev. Lett.* **32**, 1383 (1974).
6. V. Paar et al., preprint, 1975.
7. K. T. Hecht, *Phys. Lett.* **58B**, 253 (1975).

STRUCTURE OF THE ODD-MASS $^{187-197}\text{Hg}$ LEVELS

G. M. Gowdy¹ J. L. Wood⁴
 A. G. Schmidt² R. W. Fink⁴
 E. F. Zganjar³ R. L. Mlekodaj²

The levels in $^{187-197}\text{Hg}$ populated in the decays of $^{187-197}\text{Tl}$ have been investigated both on- and off-line. Gamma-ray and conversion-electron multiscaled singles spectra and γ - γ and conversion-electron-gamma coincidence data have been obtained to study these nuclei. From these data, rather complicated, preliminary level schemes for the mercury isotopes have been constructed. (See Fig. 1.8 for an example.)

Figure 1.9 shows the feeding of the mercury levels from their thallium parents. The heavier thallium isotopes ($A \geq 195$) β^+ decay only from their low-spin

$s_{1/2}$ ground states: ^{189}Tl and ^{191}Tl are observed in UNISOR experiments to β^+ decay from the high-spin $h_{9/2}$ isomer, whereas ^{187}Tl and ^{193}Tl are shown by our data to β^+ decay from both high- and low-spin states. The $^{193g,m}\text{Tl}$ isomers are especially important because of their ease of production and the information they yield concerning both high- and low-spin structure in the mercury isotopes.

The low-spin Hg structure (Fig. 1.10) is being studied and compared with the theoretical predictions available, using quasi-particle-plus-phonon⁵ and mixed- j triaxial rotor⁶ models. The high- j band built on the $i_{13/2}$ mercury isomer is also under study, incorporating the yrast levels reported by other authors⁷ and the non-yrast levels for which a search is being conducted at UNISOR. Detailed comparisons of the experimental results with those from the isotonic platinum isotopes and the single- j triaxial rotor model⁸ are also being undertaken.

1. Oak Ridge Graduate Fellow from the School of Chemistry, Georgia Institute of Technology, Atlanta, under appointment from Oak Ridge Associated Universities.
2. UNISOR, Oak Ridge Associated Universities, Oak Ridge, Tenn.
3. Louisiana State University, Baton Rouge.
4. School of Chemistry, Georgia Institute of Technology, Atlanta.
5. T. Fényes et al., *Nucl. Phys.* **A247**, 103 (1975).
6. H. Toki and A. Faessler, *Nucl. Phys.* **A253**, 231 (1975).
7. R. M. Lieder et al., *Nucl. Phys.* **A248**, 317 (1975).
8. J. Meyer-ter-Vehn, *Nucl. Phys.* **A249**, 111 (1975).

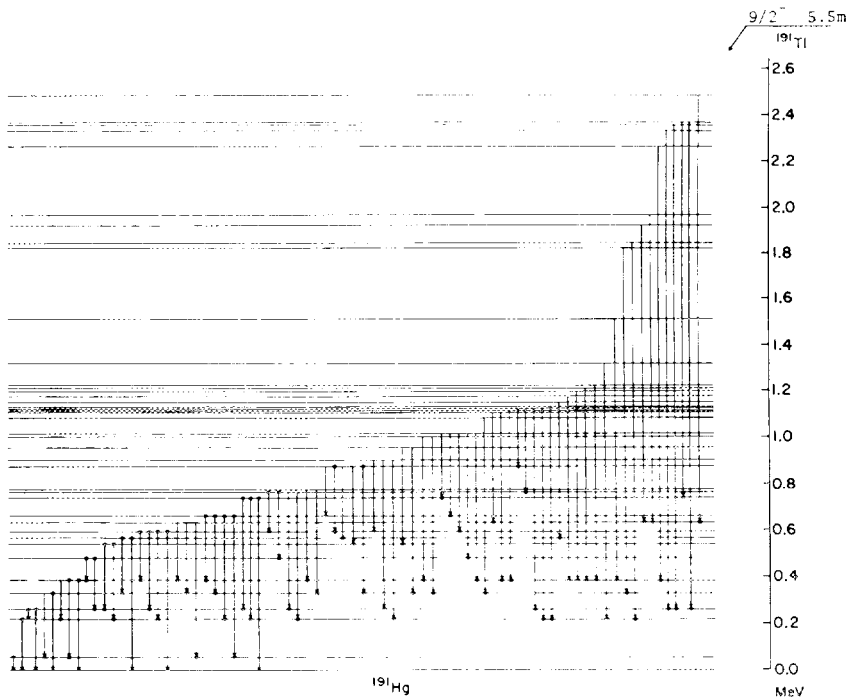


Fig. 1.8. Level scheme for ^{191}Hg shown with a rough energy scale. Other odd-mass mercury isotopes show similar structural complexity in their level schemes.

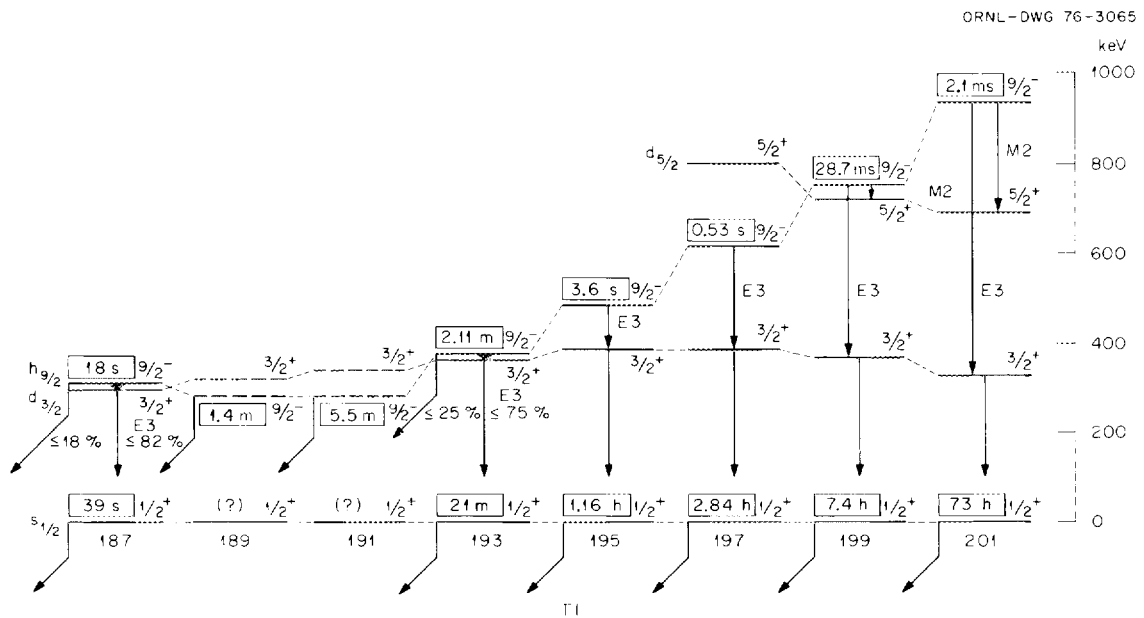


Fig. 1.9. Systematics of the shell-model states in the odd-mass thallium isotopes.

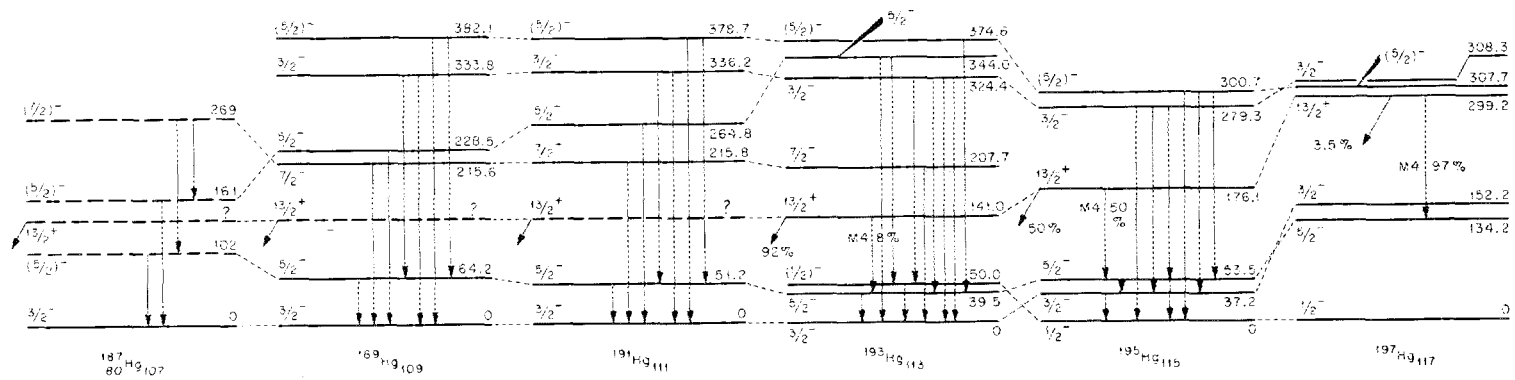


Fig. 1.10. Systematics of the low-lying states in the odd-mass mercury isotopes.

TRIAXIAL BANDS IN $^{193,195}\text{Tl}$ FROM LEAD DECAY

L. L. Riedinger¹ A. C. Kahler¹
L. L. Collins¹ C. R. Bingham¹
G. D. O'Kelley²

In the past year, much has been learned about bands of levels built on proton states in the odd- A gold nuclei (e.g., see the UNISOR contribution to this report). There the particle states are quite representative of a platinum core, whereas the hole states reflect the mercury core. To further test these ideas, we have been performing experiments on levels in thallium nuclei, where mercury and lead are the effective cores of the expected states. Levels in $^{193,195}\text{Tl}$ have been investigated through the radiative decay of $^{193,195}\text{Pb}$, mass-separated at the UNISOR facility. Almost all the observed states are populated in the decays of 16.4-min ^{195}Pb and 5.5-min ^{193}Pb , the $i_{13/2}$ isomer in each case.

The systematics of the single-particle states throughout the light Tl nuclei are shown in Fig. 1.11. The $h_{11/2}$ state is a lower-lying well-known state in gold nuclei but had not been seen before in the Tl nuclei. In contrast to the rather constant energies of this and the low-spin states are the rapidly falling $h_{9/2}$ and $i_{13/2}$

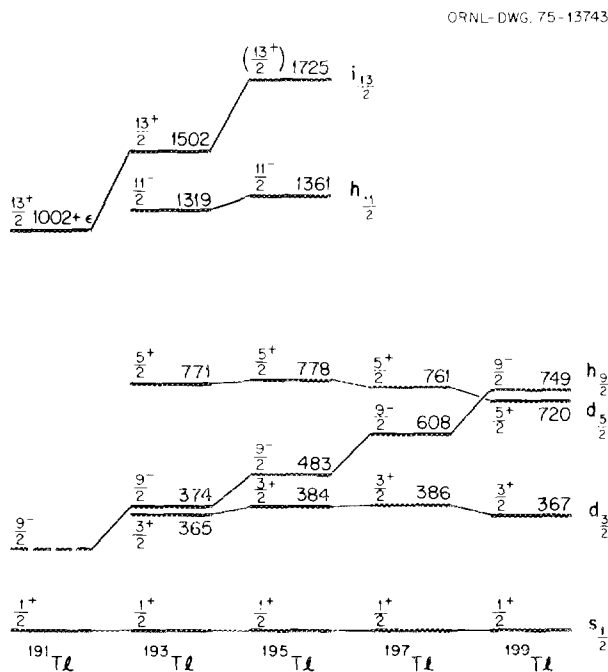
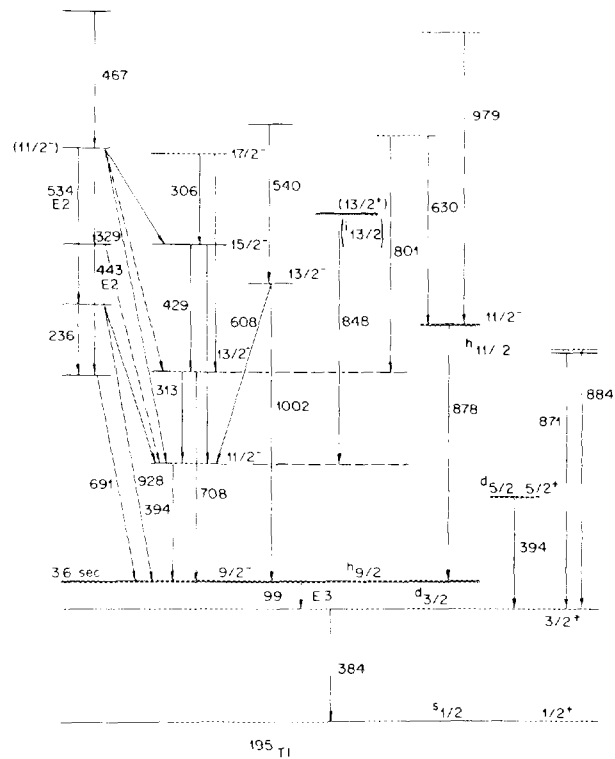


Fig. 1.11. Trends of single-particle states in light thallium nuclei.

levels. These are intruders into the $Z = 81$ nuclei from above the $Z = 82$ gap, lowered partially by a gain in pairing energy and partially by deformation of the core. To test in detail the shape of the nucleus in these high- j shell-model states, we feel that it is important to study structures of levels built on these states. This has been done quite successfully in the case of the $h_{9/2}$ bands in $^{193,195}\text{Tl}$. A preliminary level scheme for ^{195}Tl is shown in Fig. 1.12. Note first the presence of rather high-energy transitions feeding our proposed $h_{11/2}$ state. These spacings seem to reflect the approximately 1-MeV first 2^+ energy of the lead core for this proton-hole state. By contrast, the approximately 400-keV spacings in the $h_{9/2}$ band are quite regular throughout the thallium isotopes [e.g., see the (H.1...vii) contribution to this report]. The sequential ordering of these yrast states indicates an oblate core, as discussed by Newton et al.³ However, to answer the question of core symmetry or asymmetry, one must consider the non-yrast members of this structure. In ^{195}Tl , we have seven such levels which branch to various yrast members. These levels are divided into two cascades, one beginning with spin lower than $7/2$ and consisting of five



levels, the other beginning with spin $1\frac{3}{2}$. The asymmetric rotor model of Meyer-ter-Vehn⁴ predicts such a behavior. Assuming $\beta = 0.15$ and $\gamma = 37^\circ$ (taken from mercury core levels), he has predicted a band in ^{190}Tl beginning with a $5\frac{1}{2}^-$ state immediately below the yrast $1\frac{3}{2}^-$ level and another side band beginning with a second $1\frac{3}{2}^-$ state below the yrast $1\frac{5}{2}^-$. Recently acquired data are being analyzed; thus far we are not certain of the multipolarity of the 691-keV transition. However, it is possible that the calculations for ^{190}Tl can fit the observed levels in ^{195}Tl . More calculations will be performed, but invoking core triaxiality appears essential to explain this $h_{9/2}$ structure. A similar picture results from our ^{193}Pb decay studies. States quite similar to the second $1\frac{3}{2}$ and $1\frac{5}{2}$ are seen, as are three levels analogous to the lower-spin side band. The core thus appears to be rather constant for the light thallium nuclei.

1. University of Tennessee, Knoxville.

2. Chemistry Division.

3. J. O. Newton, F. S. Stephens, and R. M. Diamond, *Nucl. Phys. A*236, 225 (1974).

4. J. Meyer-ter-Vehn, *Nucl. Phys. A*249, U11 (1975).

DECAY OF ^{190}Tl AND ^{192}Tl ; NEGATIVE-PARITY BANDS IN MERCURY

C. R. Bingham¹ F. E. Turner¹
L. L. Riedinger¹

A study of the decay of ^{190}Tl and ^{192}Tl has been made, using mass-separated sources. The data consist of the multiscaled spectra of gamma rays, internal conversion electrons, and β^+ and of γ - γ - t and γ - x - t coincidence data. The results are extensive, and for the case of ^{190}Tl we have prepared a paper for publication. Some of the main results relating to the decay scheme will be discussed here; the β^+ endpoint energies are discussed elsewhere in this report.

The even thallium isotopes are believed to have two isomers with spins of 7^+ and 2^- . The present data are also more consistent with these values than with any other possibility, although a few slight discrepancies in the ^{190}Tl decay are unexplained. The half-lives, which were determined from gamma-ray multiscaled spectra, are 3.7 ± 0.3 min (7^+) and 2.6 ± 0.3 min (2^-) for ^{190}Tl and 10.8 ± 0.3 min (7^+) and 8.6 ± 0.3 min (2^-) for ^{192}Tl .

The ground-state bands of ^{190}Hg and ^{192}Hg were observed up to the 8^+ state, and a number of non-yrast positive-parity levels were observed. These positive-parity levels fit fairly well within the framework of the

vibrational model, particularly if interactions between phonons such as proposed by Iachello and Arima^{2,3} are included. The negative-parity states can also be explained in such a model — they are based on octupole phonons interacting with quadrupole phonons. However, for the present nuclei, a different interpretation of these states, given below, seems preferable.

In ^{190}Hg and ^{192}Hg , we observe negative-parity states (Fig. 1.13.) These negative-parity states are believed to result from the coupling of two neutrons, one in the $i_{13/2}$ orbital and the other in a $p_{3/2}$ or $f_{5/2}$ orbital, to different rotational states of a slightly deformed core.⁴ In the odd mercury isotopes (e.g., ^{191}Hg), the $i_{13/2}$ band appears to exhibit a Coriolis alignment of the $i_{13/2}$ neutron along the rotation axis since the $1\frac{3}{2}^+$, $1\frac{7}{2}^+$, $2\frac{1}{2}^+$, ... members have essentially the same spacings as the 0^+ , 2^+ , 4^+ , ... levels of the even- A core.⁵ The other states of this band, that is, $1\frac{5}{2}^+$, $1\frac{9}{2}^+$, ... , appear at higher energies and again have spacings similar to the spacings of the $1\frac{3}{2}^+$, $1\frac{7}{2}^+$, $2\frac{1}{2}^+$, ... levels. The 5^- , 7^- , 9^- , ... levels of the even mercury nuclei, which have also been populated by (α, xn) reactions,⁵ probably result from the coupling of a $p_{3/2}$ neutron with the core-decoupled $1\frac{3}{2}^+$, $1\frac{7}{2}^+$, $2\frac{1}{2}^+$, ... members of the $1\frac{3}{2}^+$ band. Similarly, one would expect 6^- , 8^- , 10^- , ... states resulting from the less favored $1\frac{5}{2}^+$, $1\frac{9}{2}^+$, $2\frac{3}{2}^+$, ... members. These qualitative arguments are verified by the calculations of Neergard, Vogel, and Padomski,⁶ the results of which are shown in Fig. 1.13.

The lowest 5^- , 7^- , and 9^- states in ^{190}Hg and ^{192}Hg are well established, both by the present experiment

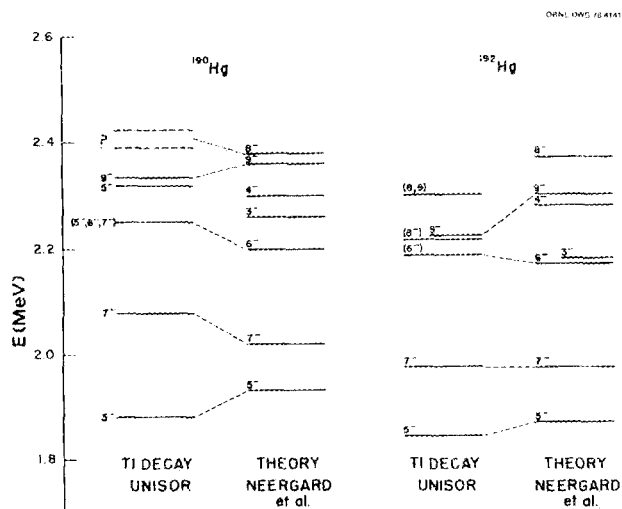


Fig. 1.13. Comparison of negative-parity levels observed in ^{190}Hg and ^{192}Hg with calculations from ref. 6.

and by in-beam work.⁵ These levels fit very well with the predictions of Neergard et al.⁶ The level in ^{190}Hg at 2252 keV must be 5^- , 6^- , or 7^- , based on the $E2$ character of the transition to the first 5^- level and on the presence of a transition to the 6^+ level. This state lies above the 7^- level of the 5^- band and thus is a candidate for the 6^- member by analogy to the fact that the $1^{5/2^+}$ member of the $i_{13/2}$ band lies above the $1^{7/2^+}$ state. Similarly, the 8^- should be at a slightly higher energy than the 9^- band member; levels observed at 2392.1 and 2424.9 keV are candidates for this state. In ^{192}Hg , the probable 6^- state agrees well with the theoretical prediction, but possible 8^- states appear to be somewhat lower than the prediction, though still within 100 to 200 keV. In ^{192}Hg , the odd-spin negative-parity states have been observed up to the 15^- member by the $(\alpha, n\gamma)$ experiment;⁷ these states also agree well with the theory of Neergard, Vogel, and Padomski.⁶ The state immediately below the 9^- state in ^{192}Hg was assigned $I = 8$ in the in-beam work.⁷ A similar state below the 9^- in ^{190}Hg , also assigned $I = 8$ in ref. 7, is within 0.2 keV of the second 5^- state observed in the present work. It is difficult to understand the different assignments in our work and that of Lieder et al.;⁷ possibly, there are two close-lying states near 2318.7 MeV. The second 5^- state could result from the coupling of an $f_{5/2}$ neutron with the $1^{5/2^+}$ state. Neergard, Vogel, and Padomski⁶ published only the lowest state of a given spin and parity; hence, comparison with the theory is not possible.

1. University of Tennessee, Knoxville.
2. F. Iachello and A. Arima, *Phys. Lett.* **53B**, 309 (1974).
3. A. Arima and F. Iachello, *Phys. Lett.* **57B**, 39 (1975).
4. P. J. Daly et al., p. 193 in *Proceedings of the International Conference on Nuclear Physics, Munich, Germany, 1973*, J. de Boer and H. J. Mang, Eds., North-Holland, Amsterdam, 1973.
5. H. Beuscher et al., *Phys. Rev. Lett.* **32**, 843 (1974).
6. K. Neergard, P. Vogel, and M. Padomski, *Nucl. Phys.* **A238**, 199 (1975).
7. R. M. Lieder et al., *Nucl. Phys.* **A248**, 317 (1975).

POSITRON MEASUREMENTS AND MASS DIFFERENCES

J. L. Weil¹ B. D. Kern¹

The positron decay of several proton-rich nuclides in the $A = 116$ and $A = 190$ regions has been studied with the use of plastic scintillators and lithium-drifted germanium detectors. Time-sequential spectra were obtained in the positron singles and in the positron-gamma coincidence modes.

The work on 2.91-sec ^{116}I was completed. It decays to the ground state and to two excited states at 0.697 and 1.219 MeV of ^{116}Te . The ground-state decay produces positrons with $E_{\text{max}} = 6.69$ MeV. A β - γ coincidence establishes the presence of the other two levels. The Q_{β} calculated by several of the mass formulas is in good agreement with the experimental $Q_{\beta} = 7.71$ MeV.

The decay of ^{190}Tl to ^{190}Hg yields two identifiable positron endpoint energies of 5.70 ± 0.04 MeV and 4.18 ± 0.30 MeV. Through selective production of each of the two isomers of ^{190}Tl , their lifetimes have been measured: The 5.70-MeV positron group is assigned to the decay of the 2.6-min 2^- isomer and the 4.18-MeV group to the 3.7-min 7^+ isomer. The precision does not permit the determination of which isomer is the ground state, but their separation appears to be approximately 100 keV. (A report on this is to be published soon.)

In the mass $A = 192$ radioactivity, there has been measured a positron endpoint energy of 4.26 ± 0.30 MeV, belonging to either ^{192}Tl or ^{192}Hg .

A chemically separated ^{194}Pb source was studied, yielding a positron endpoint energy of 3.61 ± 0.20 MeV. Thallium-194 was found to decay with a maximum positron energy of 4.4 ± 0.3 MeV.

1. University of Kentucky, Lexington.

ON-LINE MASS-SEPARATOR STUDIES OF THALLIUM AND MERCURY ALPHA EMITTERS WITH $A \leq 186$

K. S. Toth J. Lin²
M. A. Ijaz¹ E. L. Robinson³

Alpha decay for thallium isotopes ($Z = 81$) has never been clearly established even though a large number of alpha-emitting mercury ($Z = 80$) and lead ($Z = 82$) nuclides are known. The existence of thallium alpha emitters has been indicated in helium gas-jet experiments performed here at ORIC⁴ and in Orsay, France, with the accelerator ALICE.⁵ The ORIC gas-jet results, obtained in ^{16}O bombardments of ^{181}Ta , showed that if thallium alpha emitters did exist, their decay energies were similar to those of mercury isotopes with adjacent mass numbers. The use of the UNISOR mass-separator facility was thus clearly necessary if definitive answers were to be obtained.

The isotope ^{186}Tl was chosen to start the study because, from alpha-decay systematics, one would predict it to be the heaviest (and therefore the easiest to study from the standpoint of a production cross

section) thallium nuclide to have a reasonably large alpha-decay branch. Also, its electron capture (EC)/ β^+ decay had already been investigated by the UNISOR consortium.⁶ A target of 99%-enriched ^{182}W was bombarded with 168-MeV ^{14}N ions to produce ^{186}Tl in the ($^{14}\text{N}, 10n$) reaction. On-line multiscale data were obtained for $A = 186$ isotopes, simultaneously using alpha-particle, gamma-ray, and x-ray detectors. Figure 1.14 shows the measured alpha-particle spectrum. In addition to ^{186}Hg , a close-lying doublet is observed: (1) ^{185}Hg ($E_\alpha = 5.653$ MeV) and (2) a new alpha peak with $E_\alpha = 5.641 \pm 0.010$ MeV. We assign this new group to ^{186}Tl because the peak decayed with about a 30-sec half-life, that is, close to the value of 28 ± 2 sec reported for ^{186}Tl EC/ β^+ decay.⁶ It should be pointed out that the alpha branch of ^{185}Hg is more than 300 times larger than that of ^{186}Hg .⁷ A small amount, $\leq 0.3\%$, of cross contamination thus accounts for its presence in the $A = 186$ spectrum.

The 405.3-keV $2^+ \rightarrow 0^+$ transition in ^{186}Hg is known to encompass essentially all of the EC/ β^+ decay strength of ^{186}Tl .⁶ From its intensity in our gamma-ray spectrum, the alpha-decay branching ratio of ^{186}Tl was then determined to be $(6 \pm 2) \times 10^{-4}$.

Preliminary measurements were also made for $A = 185$ and 184 nuclides. Some weak and previously unobserved alpha groups were seen. The x-ray spectral measurements indicate the ($^{14}\text{N}, xn$) yields to be small. More data are therefore needed before assignments can be made for these new alpha groups.

Significant information, however, was obtained as a result of the $A = 185$ and 184 measurements, namely, the first confirmation of the alpha-decay energies reported by the ISOLDE group for $^{183-186}\text{Hg}$.⁷ This is shown in Fig. 1.15, where we have plotted experimental E_α values for Bi, Pb, Hg, Au, and Pt nuclides as a function of neutron number. Note the abrupt discontinuities that occur for the mercury isotopes 182--186, which are absent for the other nuclides. These anomalies may be related to the sudden changes in the nuclear charge radius observed for ^{183}Hg and ^{185}Hg ,⁸ in contrast to the smoothly varying values seen in the heavier mercury isotopes with $A = 187$ to 204. In our search for thallium alpha emitters with $A < 186$, we also intend to investigate the alpha-decay properties of the mercury isotopes with the same mass numbers. One case in point is ^{185m}Hg , which is reported to have a lower E_α than ^{185g}Hg (ref. 7) (Fig. 1.15).

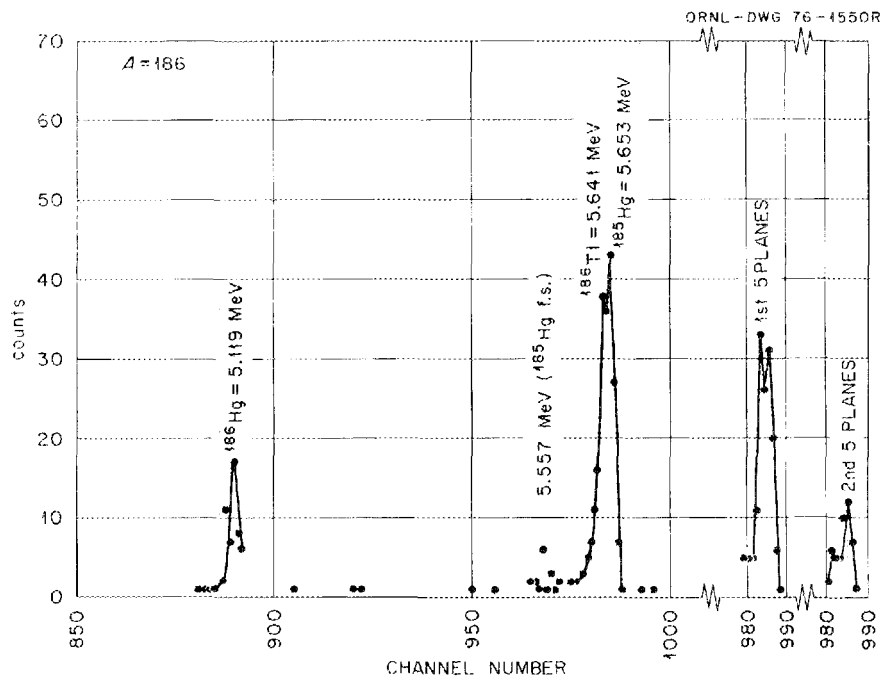


Fig. 1.14. Alpha spectrum measured at $A = 186$ in ^{14}N bombardments of ^{182}W . The new 5.641-MeV alpha group is assigned to the decay of 28-sec ^{186}Tl . These results represent the first clear-cut identification of alpha decay in thallium isotopes.

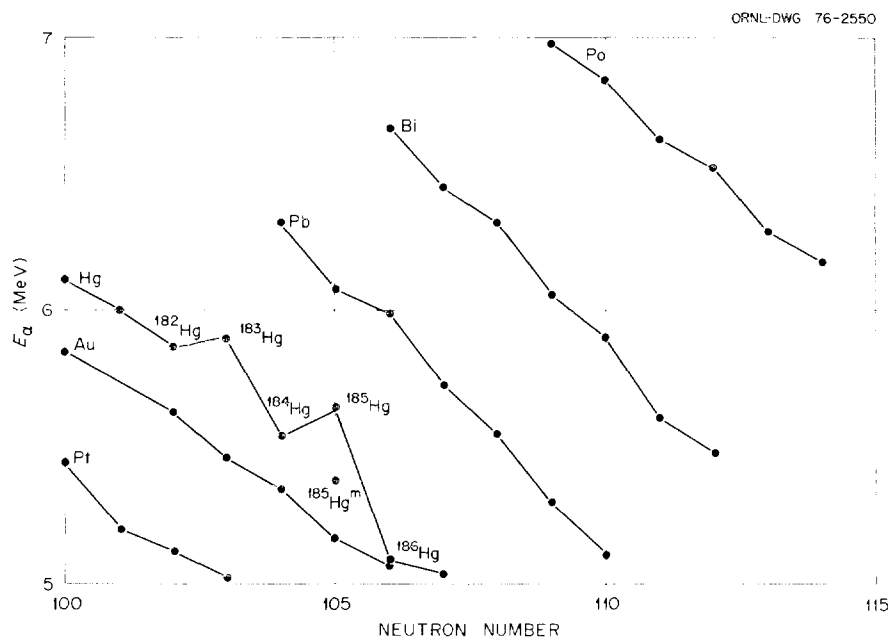


Fig. 1.15. Alpha-decay energy systematics in the mercury region. Note the abrupt discontinuities for the E_{α} of $^{182-186}\text{Hg}$. This may be related to the sharp increase in the nuclear charge radius observed (ref. 8) in going from ^{186}Hg to ^{185}Hg , contrasting with the smooth variance for the heavier mercury nuclei with $A = 187$ to 204 .

1. Virginia Polytechnic Institute and State University, Blacksburg.
2. Tennessee Technological University, Cookeville.
3. University of Alabama in Birmingham.
4. K. S. Toth et al., Oak Ridge National Laboratory, Oak Ridge, Tenn., unpublished results, 1974.
5. Y. LeBeyec and H. Gauvin, Institute for Nuclear Physics, Orsay, France, private communication, 1975.
6. J. H. Hamilton et al., *Phys. Rev. Lett.* **35**, 562 (1975).
7. P. G. Hansen et al., *Nucl. Phys.* **A148**, 249 (1970).
8. J. Bonn et al., *Phys. Lett.* **38B**, 308 (1972).

DECAY OF ^{194}Pb

E. L. Robinson¹ B. H. Ketelle²
B. O. Hannah¹

Both multiscaled gamma singles and gamma-gamma coincidence spectra were obtained in studying the decay of ^{194}Pb . Sixty-nine gamma transitions are identified by half-life as belonging to the decay of ^{194}Pb . All the strong lines and a number of the less intense lines are fitted into a proposed decay scheme.

Internal conversion coefficients were measured for the 204-, 225-, 368-, and 582-keV lines. The first three are largely $M1$ transitions, whereas the 582-keV line has a large $E2$ admixture. Both the low intensity of the annihilation peak and the failure to observe a positron spectrum with the proper half-life support the con-

clusion that ^{194}Pb decays predominantly by electron capture.

There is evidence from both systematics and from considerations of available shell-model levels that there exists a 1^+ level in ^{194}Tl , which should permit a strong Gamow-Teller transition in the decay of ^{194}Pb . A probable candidate for this is the 1519.48-keV level, which is highly populated and which decays to the 2^- ground state with an intensity of 102% relative to the 204-keV first excited state to ground state transition.

1. University of Alabama in Birmingham.
2. Chemistry Division.

FEASIBILITY STUDIES OF UNISOR EXPERIMENTS IN THE $A \approx 60-80$ REGION

A. C. Rester ¹	J. Galambos ¹
H. Kawakami ²	A. DeLima ²
R. M. Ronningen	J. L. Wood ⁴
H. K. Carter ³	E. F. Zganjar ⁵
M. D. Barker ¹	J. H. Hamilton ²

Presently, there is considerable research activity centered in the nuclear region $A \approx 60-80$. There is an interesting controversy^{6,7} over the nature of the anomalously low-lying 0^+ excited states in the even-

even nuclei, with N or Z approximately equal to 40. Also, in-beam gamma-ray spectroscopy experiments at ORNL and in Copenhagen⁸ have revealed unusual band structure in some of the nuclei in this region. In-beam studies and (p,t) reaction experiments are being conducted in this region at ORNL. Studies at UNISOR will provide a valuable complement to these measurements. Together with the extensive nuclear-model calculations being done at Vanderbilt and Emory Universities, the experiments form a unified program of intensive research.

To explore the feasibility of medium-mass UNISOR experiments, we used a helium gas-jet transport system to collect the activity from the reactions of ^{12}C and ^{16}O beams on ^{58}Ni and ^{64}Zn targets. Gamma-ray spectrum multiscaling measurements were taken at 60- to 95-MeV bombardment energies. The energies, intensities, and half-lives of the gamma rays were used to construct relative cross-section curves. The $^{64}\text{Zn}(^{12}\text{C},xx)$ results are shown in Fig. 1.16.

From this work, we conclude that neutron-deficient isotopes from copper to rubidium can be produced in sufficient quantity for experiments with the heavy-ion beams currently available at UNISOR. Those isotopes produced in large quantities which may be particularly

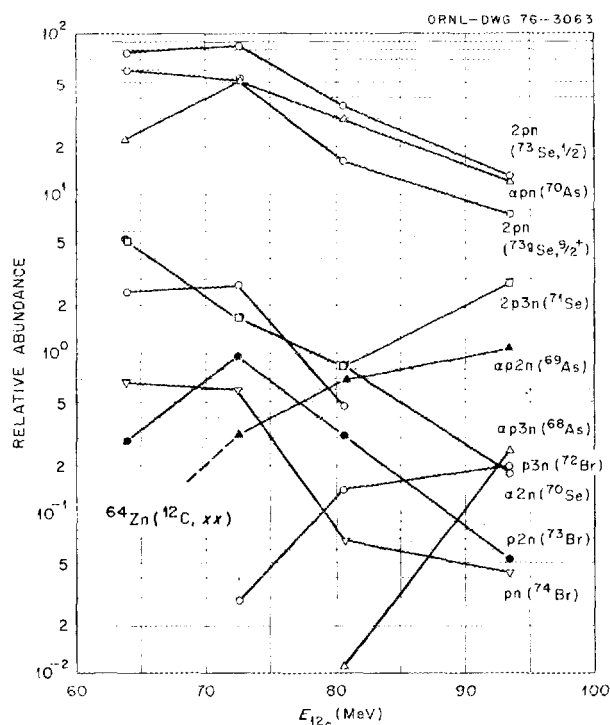


Fig. 1.16. Relative abundance of the most prominently observed isotopes in the radioactive decay spectra following the $^{64}\text{Zn}(^{12}\text{C},xx)$ reaction as a function of bombardment energy.

worthwhile for UNISOR experiments are ^{64}Ga , ^{68}As , ^{71}Se , ^{72}Br , ^{73}Br , ^{77}Rb , and ^{78}Rb , with half-lives ranging from 2.5 to 6 min.

1. Emory University, Atlanta, Ga.
2. Vanderbilt University, Nashville, Tenn.
3. UNISOR, Oak Ridge Associated Universities, Oak Ridge, Tenn.
4. Georgia Institute of Technology, Atlanta.
5. Louisiana State University, Baton Rouge.
6. A. C. Rester and J. Hadamann, *Proc. Int. Conf. Nucl. Phys., Munich* 2, 140 (1973).
7. J. H. Hamilton et al., *Phys. Rev. Lett.* 32, 239 (1974).
8. M. L. Halbert et al., *Bull. Am. Phys. Soc.* 20, 1172 (1975).

GYROMAGNETIC RATIO OF THE FIRST EXCITED 2^+ STATE IN ^{126}Xe

K.S.R. Sastry¹ A. V. Ramayya²
 R. S. Lee² J. H. Hamilton²
 R. L. Mlekodaj³ N. R. Johnson⁴

The gyromagnetic ratios of the first excited 2^+ states of a large number of even-even nuclei have been measured in recent years, using a variety of experimental techniques. The g factors for the lighter neodymium and samarium isotopes show a sharp drop as the closed $N = 82$ shell is approached from the region of higher neutron number; this behavior is contrary to theoretical expectation. The even-even isotopes $^{124-136}\text{Xe}$ and $^{130-138}\text{Ba}$ span the neutron region $70 \leq N \leq 82$. It would be of interest to see if the g factors for these nuclei with neutrons on the lower side of the closed $N = 82$ shell show similar behavior. Thus we have initiated measurements in this mass region, using the time-integrated perturbed angular correlation method. The present work is concerned with the 389-keV first excited 2^+ level in ^{126}Xe .

Radioactive ^{126}I was produced by the $^{126}\text{Te}(p,n)^{126}\text{I}$ reaction at the Oak Ridge 86-in. cyclotron. The high enrichment ($\approx 98\%$) of the target and the optimized bombarding energy greatly reduced contamination from other isotopes. The ^{126}I was converted to AgI , along with minimal amounts of stable iodine, a form well suited for implantation using the UNISOR facility in the off-line mode. The ^{126}I ions were accelerated to 65 keV and implanted into 2- μm -thick iron foils held at room temperature. A separation efficiency of about 5% was achieved, and three such implantations were performed. The foils were rolled into a thin cylinder and placed between the pole faces of a small electromagnet with a field of 1.5 kG. The precession of the angular correlation pattern was then measured, using a $\text{Ge}(\text{Li})\text{-NaI}$ coincidence system.

The angle of precession was found to be -54 ± 10 milliradians, the sign being inferred from the sense of the rotation. Using the value of 864 kOe for the internal field experienced by xenon atoms in the iron lattice, we obtained a value of $+0.22 \pm 0.05$ for the g factor of the 389-keV 2^+ level in ^{126}Xe . This is in reasonable agreement with the experimental value reported by Gordon et al.,⁵ using the Coulomb excitation recoil implantation method. Our result is also in good agreement with the theoretical value of 0.26 calculated by Kisslinger and Sorensen,⁶ using the pairing-plus-quadrupole model and quasi-particle random-phase approximation, including only particles in the outer shells. However, the hydrodynamical value of the g factor for ^{126}Xe is 0.43, whereas calculations by Greiner⁷ give 0.36.

1. University of Massachusetts, Amherst.
2. Vanderbilt University, Nashville, Tenn.
3. UNISOR, Oak Ridge Associated Universities, Oak Ridge, Tenn.
4. Chemistry Division.
5. D. M. Gordon et al., *Phys. Rev. C* 12, 628 (1975).
6. L. S. Kisslinger and R. A. Sorensen, *Rev. Mod. Phys.* 35, 853 (1963).
7. W. Greiner, *Nucl. Phys.* 80, 117 (1966).

UNISOR DEVELOPMENT

R. L. Mlekodaj ¹	E. H. Spejewski ¹
H. K. Carter ¹	A. G. Schmidt ¹
E. L. Robinson ^{1,2}	B. O. Hannah ^{1,2}
F. T. Avignone III ^{1,3}	L. L. Collins ⁴
G. M. Gowdy ^{1,5}	

Ion-Source Development

The Nielsen-type⁶ oscillating-electron ion source has been tested for the on-line separation of rare-earth product nuclei. Figure 1.17 shows the arrangement used, which consists of an $80\text{-}\mu\text{g}/\text{cm}^2$ carbon window to isolate the target from the corrosive CCl_4 ion-source vapors. The window, however, allows most reaction recoils to pass into the ion source, where they are stopped on the graphite-felt catcher. The previous low efficiency obtained for this system ($\sim 0.01\%$) was thought to perhaps be due to the slow diffusion out of the graphite catcher ($T \cong 1200^\circ\text{C}$). A new graphite-felt catcher ohmically heated to 1700°C has not, however, given a significant improvement in efficiency. Replacement of the graphite catcher with one of tungsten was tested to eliminate the possibility of formation of refractory compounds between the carbon and the

rare-earth products. The tungsten catcher was operated at about 2000°C , yet this arrangement also gave a similarly low efficiency. These experiments indicate that the limiting factor is not connected with the catcher but, rather, may be connected with a low chlorination probability or with the fact that the overall source temperature is too low. Future investigations of on-line separation of rare earths with plasma ion sources will be done with much higher-temperature ion sources, applying existing target, window, and catcher techniques.

The carbon window and external target techniques developed for CCl_4 use with rare-earth products can have other applications. It has been found, for example,

ORNL-DWG 72-10024RA

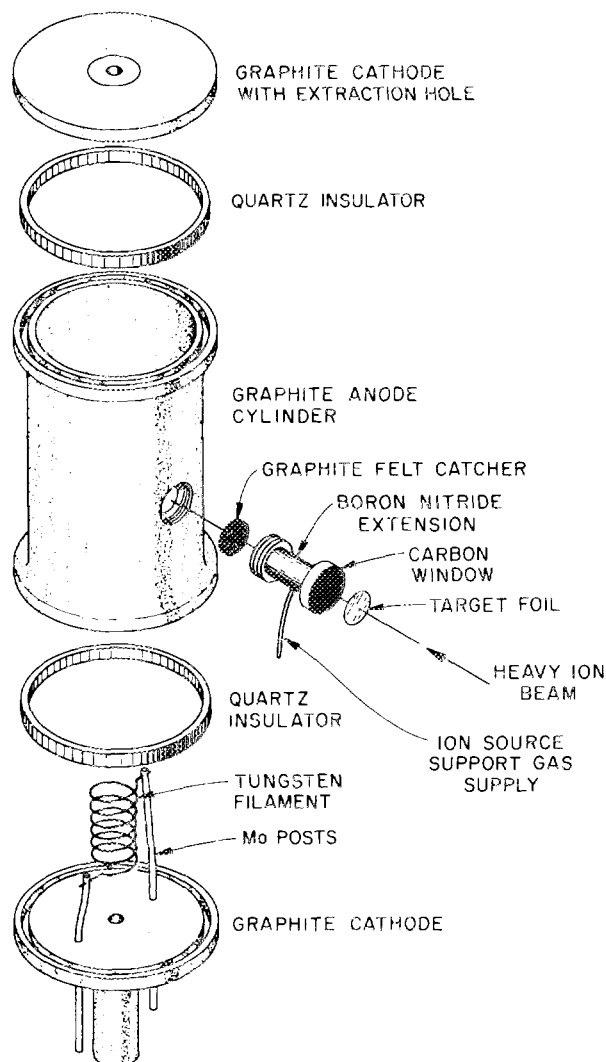


Fig. 1.17. UNISOR on-line ion source with carbon window.

that the use of CCl_4 as the ion-source support gas improved the efficiency for the on-line separation of lead and bismuth isotopes. The carbon window can also be applied in cases when a lower melting-point target must be isolated from the high temperature of the ion source.

A new ion-source variation has been tested where the target or carbon window is placed directly on the graphite felt. Thus the lower temperature region between the target or window and the graphite catcher (see Fig. 1.17) is eliminated. This lower temperature region could tend to retain low-vapor-pressure products. The limited experience to date indicates that this arrangement functions at least as well as the earlier ion sources for products of Hg, Tl, Pb, and Bi.

Several new forms of targets have been successfully applied. One new type was isotopically enriched tungsten evaporated on a substrate of tantalum. These targets were quite satisfactory even though the two metals would normally separate during operation and the target would be destroyed upon removal. The evaporation and sputtering of the ion-source filament material that caused problems in early ion-source designs has been used to fabricate targets directly in the ion source. Rhenium targets were made by using a rhenium wire for the ion-source filament and placing a substrate of thin tantalum in the anode wall. Rhenium deposits of 1 to 2 $\text{mg cm}^{-2} \text{ hr}^{-1}$ are collected during ion-source operation. The graphite-felt catcher has also been used as a substrate onto which target material has been directly evaporated.

A new surface-ionization ion-source system, designed mainly with on-line rare-earth separation in mind, has been constructed and will soon undergo testing. This type of source holds great promise because off-line efficiencies for this type of source for rare earths can exceed 80%. The main problem area anticipated is the ion-source window, which must be thin enough to transmit a large fraction of the reaction recoils yet be strong enough to withstand temperatures of 2000°C or more, in addition to bombardment by an intense heavy-ion beam. Tantalum and carbon windows will be used initially.

Tape-Transport Development

The capabilities of the tape-transport system have been substantially increased during the last year. Two new arrangements involving a three-detector array for simultaneous counting of one sample have been developed for on-line use. In one case, an x-ray detector and a thin-transmission-mount alpha detector are posi-

tioned in close geometry, one on either side of the collection tape. A Ge(Li) detector is then positioned behind the alpha detector for detection of the transmitted gamma rays. The second system is based on the collection tape traveling out to a small roller where the tape turns 180° and then returns. The tape is positioned so that the collected sample stops at the center of the roller. This system is typically used with a cooled Si(Li) electron detector looking directly at the source and two Ge(Li) gamma-ray detectors at $\pm 90^\circ$ relative to the electron detector. Two types of three-parameter coincidence data (gamma-gamma-time and gamma-electron-time) are then recorded simultaneously, as well as gamma and electron multispectrum scaling.

A new higher-resolution on-line electron detector has been installed on the tape-transport system and is now providing much improved on-line electron data. The on-line electron detector situation has also been improved by the addition of a turbomolecular pump to the tape-transport vacuum system. This pump will provide cleaner, more effective pumping at the electron detector position. The turbomolecular pumping system will also serve as the pumping system for an on-line Gerholm electron spectrometer system. The assembly of the Gerholm system has been completed and will be added to the tape-transport system.

Side-Mass Facilities

The UNISOR fast tape-pulling system⁷ has been expanded to two units so that sources from two different side masses can be rapidly extracted from the collection chamber. In addition, an alpha detector has been added to one of these units, allowing alpha-particle experiments to be carried out directly in the collection chamber.

The off-line electron detector system was modified to allow use of a Ge(Li) gamma-ray detector for close-geometry electron-gamma experiments. The vacuum of the off-line electron detector has also been upgraded.

Data Acquisition

The TP-5000 data acquisition system has been improved with Tennecomp's new faster software system — TPOS. The Tennecomp system has also been interfaced for direct data transfer to the on-line SEL computer. The data analysis capabilities of the TP-5000 have been greatly expanded during the past year by user-developed programs that include automated peak-fitting programs and skewed-Gaussian peak-fitting programs.

A new analyzer system, the Tracor Northern TN-1700, has been acquired and placed in service. The

multispectrum scaling capability of this programmable analyzer has made it a most valuable addition to the UNISOR facility.

1. UNISOR, Oak Ridge Associated Universities, Oak Ridge, Tenn.
2. University of Alabama in Birmingham.
3. University of South Carolina, Columbia.
4. University of Tennessee, Knoxville.
5. Georgia Institute of Technology, Atlanta.
6. O. Almén and K. O. Nielsen, *Nucl. Instrum. Methods* **1**, 302 (1957).
7. H. K. Carter and R. L. Mlekodaj, *Nucl. Instrum. Methods* **128**, 611 (1975).

HEAVY-ION MACROPHYSICS

STRONGLY DAMPED COLLISIONS INVOLVING MEDIUM-MASS TARGETS

A large amount of experimental data on strongly damped collisions exists for 5- to 10-MeV/nucleon beams of nitrogen through xenon on targets ranging from silver to uranium. The reaction mechanism termed "strongly damped," "deeply inelastic," or "quasi-fission" appears to be present to a varying extent in all systems studied. Fewer data are available for medium-mass targets ($A \sim 60$). To understand the nature of this reaction mechanism, it is important to have systematic data showing how its characteristics vary with projectile, target, and bombarding energy. To this end, several reactions involving medium-mass targets are currently being studied at ORIC; preliminary analyses are described below.

$^{20}\text{Ne} + \text{Ni}$

M. L. Halbert	F. Plasil
D. C. Hensley	R. L. Ferguson ²
R. G. Stokstad	F. E. Obenshain
A. H. Snell ¹	F. Pleasonton

These experiments included bombardment of nickel by 164- and 173-MeV ^{20}Ne . The reaction products were detected with an ionization-chamber-silicon position-sensitive detector (PSD) telescope (described elsewhere in this report³). The telescope covered a range of 9° at one setting and offered excellent separation of Z values from 2 to at least 30. Figure 1.30 (see ref. 3) is an example of the computer printout for a typical set of data.

Principal features of the spectra are illustrated in Fig. 1.18, which shows spectra of even- Z products from 173-MeV ^{20}Ne on nickel at 15° and 22° (lab). These

were obtained by masking arrays such as in Fig. 1.30 and projecting onto the energy axis. For products with Z well removed from that of the beam, a single broad peak is observed. When assuming a two-body final state and a mass corresponding to the most stable isotope of element Z , the Q value for the peak is about -75 MeV, becoming somewhat more negative with increasing angle of observation and slightly less negative with increasing Z . The width is between 20 and 40 MeV.

For products with Z near that of the beam, a sharper peak is seen at an energy corresponding to the same velocity as the beam. These particles may be due to decay of an excited projectile-like fragment; in support of this is the fact that the particles are much more intense for Z below 10.

The Z distributions for the deep-inelastic peak show an odd-even effect, the even- Z products being more intense. This is illustrated in Fig. 1.19. There is generally a decrease of cross section with increasing Z . The 164-MeV ^{20}Ne data, taken with a lower gas pressure in the ΔE counter to observe products with higher Z , suggest that the yield increases again above $Z = 21$, the maximum being at about $Z = 25$. (This latter result pertains to $\sim 30^\circ$ only and has not yet been verified for angle-integrated yields.)

Figure 1.19 also shows a strong decrease in yield for a given Z as a function of angle; this is seen more clearly in Fig. 1.20. The angular distributions for $Z \geq 14$ are approximately $1/\sin \theta_{\text{c.m.}}$. For $Z < 14$, the forward peaking is stronger.

Estimates of the total cross section for each Z were made by extrapolating in several ways over the unmeasured angles. These in turn were summed over Z to give an estimate of the total cross section for the strongly damped processes. The uncertainty in these estimates comes partly from the extrapolation ($\sim 10\%$), but mainly from the lack of adequate knowledge of the low- Z yields. For $^{20}\text{Ne} + \text{Ni}$ at 173 MeV, the deep-inelastic cross section summed for $6 \leq Z \leq 18$ is 500 ± 40 mb.

$^{16}\text{O} + \text{Ni}$

R. G. Stokstad D. C. Hensley

The $^{16}\text{O} + \text{Ni}$ reaction was studied at a bombarding energy of 113 MeV by using two solid-state counter telescopes having silicon ΔE counters with thicknesses of 13 and 25 μ respectively. (These studies were begun before the position-sensitive counter telescope became available.) Figure 1.21 shows a spectrum of oxygen ions scattered at 32° , which illustrates rather well the elastic

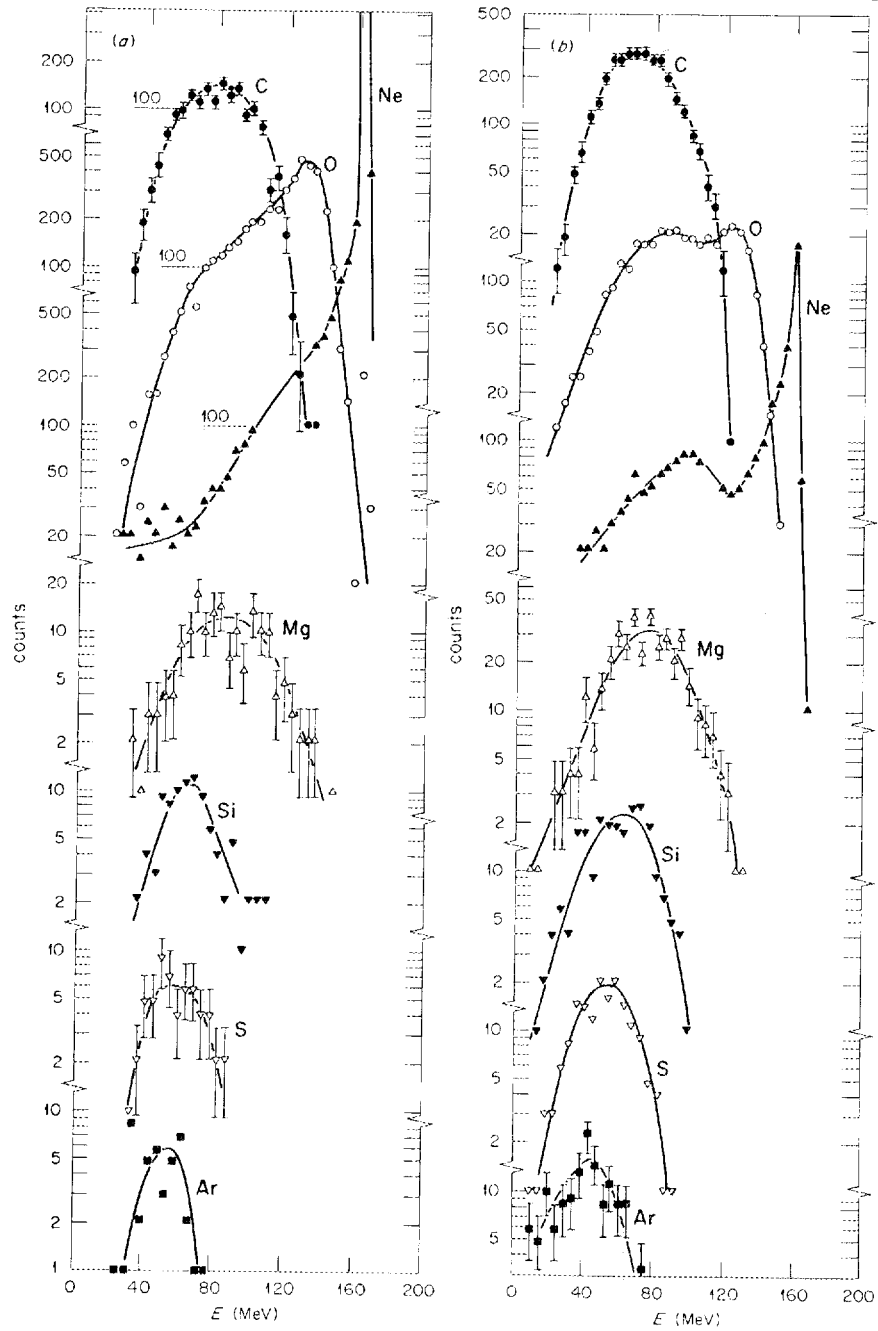


Fig. 1.18. Spectra of even- Z reaction products observed at (a) 15° and (b) 22° in the bombardment of nickel by $173\text{-MeV } ^{20}\text{Ne}$. The energy scale is based on the measured pulse height in the stopping detector; it does not include any correction for energy loss of the particles in the window and gas of the ionization chamber or in the target.

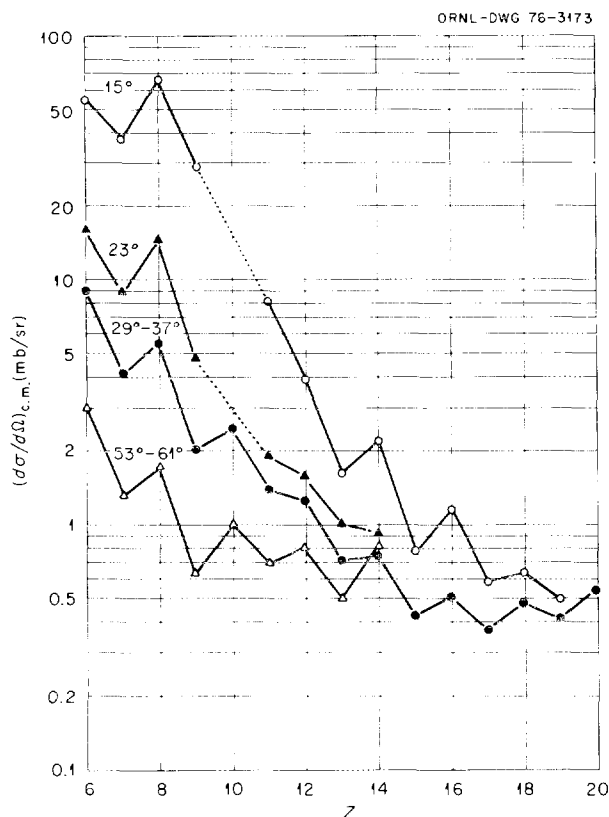


Fig. 1.19. The Z distribution of reaction products from 173-MeV ^{20}Ne on nickel for various laboratory angles. The two lower curves are sums of nine angles in 1° steps.

scattering, inelastic scattering to low-lying excited states, and the broad bump representing the strongly damped collisions. Also shown are spectra for carbon and nitrogen reaction products. Note that, although the deep-inelastic yields for nitrogen and oxygen are comparable, the carbon yield is about a factor of 2 higher. The major fraction of the carbon yield is ^{12}C . As the angle of observation is decreased to angles smaller than the grazing angle, the shape of the strongly damped peak for nitrogen and carbon changes. This is illustrated in Fig. 1.22 for the case of carbon. Here it is seen that, at forward angles, the position of maximum intensity moves up in energy until it attains an energy per nucleon equal to that of the scattered beam. In the case of nitrogen ions, one also observes transfer reactions to individual low-lying states with appreciable intensity at forward angles. In general, for $Z \leq 8$, it has not been possible to reliably separate the yields at forward angles into two components, one presumably arising from quasi-elastic scattering and the other from a strongly damped process. Thus the differential cross sections for

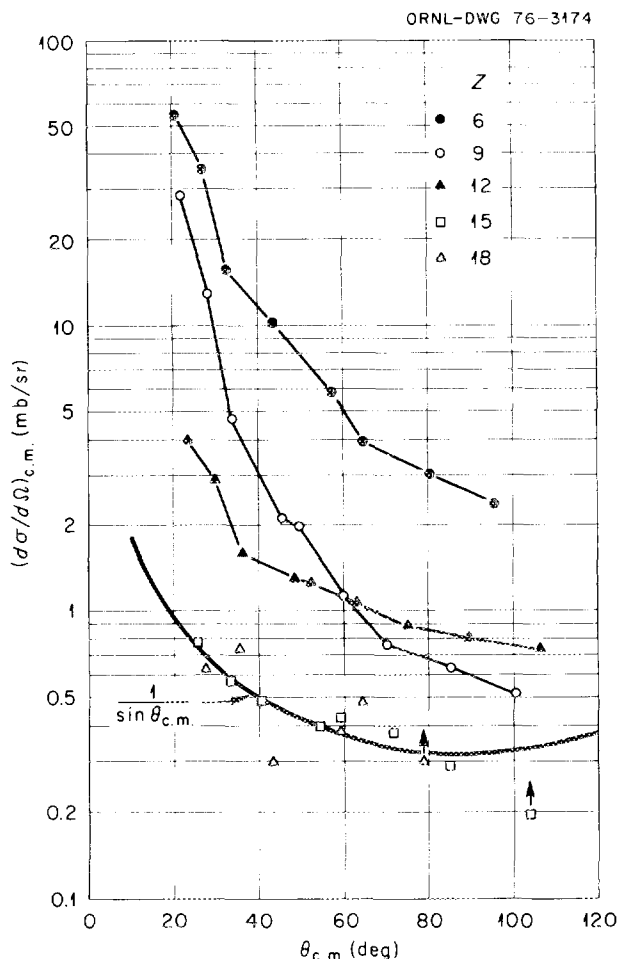
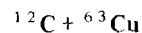


Fig. 1.20. Angular distributions for products of selected Z values from 173-MeV ^{20}Ne on nickel. The points beyond about 50° are from sums of spectra covering an interval of 9° (lab). The $1/\sin \theta$ curve is normalized to the $Z = 15$ distribution.

inelastic products with $Z = 5$ to 9 all rise more rapidly than $1/\sin \theta_{c.m.}$.



R. A. Dayras M. L. Halbert
C. B. Fulmer D. C. Hensley
R. G. Stokstad

The reaction $^{12}\text{C} + ^{63}\text{Cu}$ was studied at an energy of 130 MeV by using a 0.15-mg/cm^2 -thick target and the position-sensitive counter telescope. The energy distributions of reaction products with $3 \leq Z \leq 16$ were determined at angles between $\theta_{\text{lab}} = 10^\circ$ and 59° . For $Z > 6$, the energy distributions are peaked around $Q = -80$ MeV, with a width that varies between 20 and 40

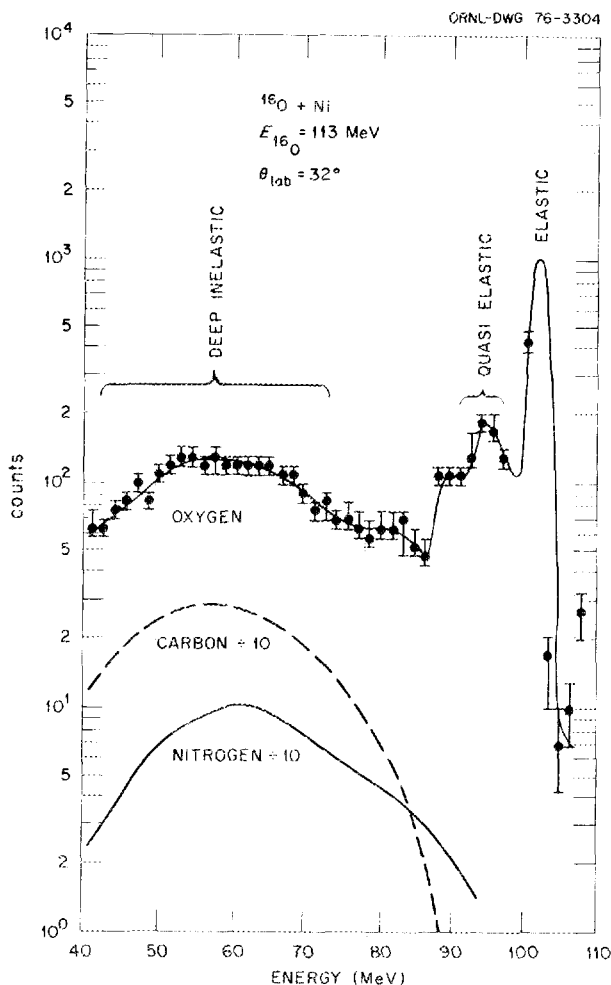


Fig. 1.21. Spectrum of oxygen, nitrogen, and carbon ions observed at $\theta_{\text{lab}} = 32^\circ$ and produced by 113-MeV ^{16}O ions on nickel.

MeV. This is a remarkably negative Q value when considering the fact that the energy available in the center of mass is only 109 MeV. For products with $Z \leq 6$, the spectra at forward angles contain sizable contributions from quasi-elastic events that cannot be separated from the strongly damped component. The angle-integrated yields show an odd-even effect, with even values of Z showing the higher yields.

A remarkable feature of this reaction is the appearance of two components in the energy spectra for yields with $Z \geq 8$. Neither of these components is quasi-elastic. This is illustrated for $Z = 10$ in Fig. 1.23, which shows spectra at three angles — 15° , 31° , and 55° . At the largest angle, only one peak, having a Q value of ~ -70 MeV, is present. The relative kinetic energy implied by this is about 15% greater than that expected

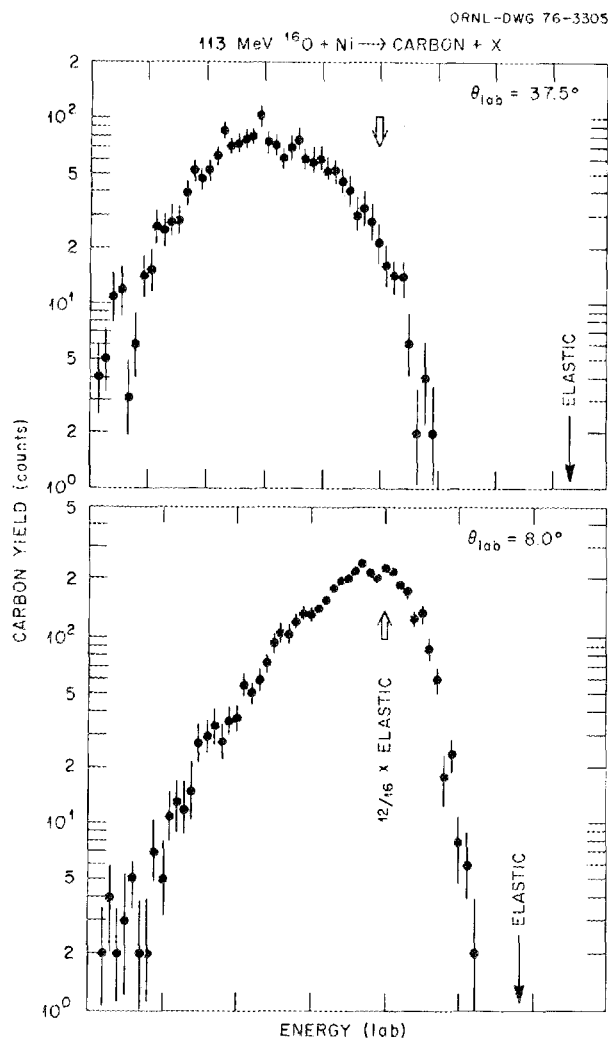


Fig. 1.22. Spectra of carbon reaction products at two laboratory angles. The single arrow denotes the laboratory energy, E_i , of the elastically scattered projectiles. The double arrow is $\frac{12}{16} \times E_i$.

for a Coulomb separation energy at a distance of $1.2(A_1^{1/3} + A_2^{1/3})$ fm. This peak, therefore, can be taken to represent the strongly damped process as seen also in $^{16}\text{O} + \text{Ni}$ and $^{20}\text{Ne} + \text{Ni}$.

At more forward angles an additional peak appears at an even lower energy. The angular distribution for this component is much more forward-peaked. The Q value corresponding to this second component is so negative (~ -95 MeV) that, if one assumes a two-body final state, the fragments must have been very elongated at the point of scission.

Figure 1.24 shows angular distributions ($do/d\theta$ in millibarns per radian in the center-of-mass system) for

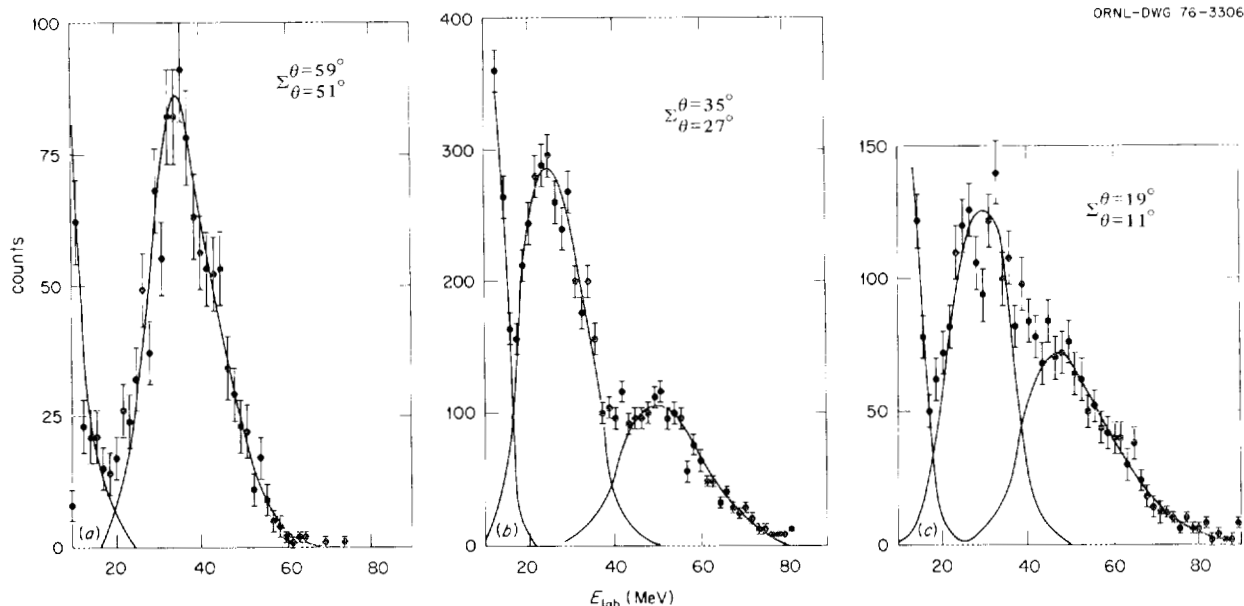


Fig. 1.23. Energy spectra at three angles for neon ions produced in the $^{12}\text{C} + ^{63}\text{Cu}$ reaction. Note the clear presence of two components at $\sim 31^\circ$ and the asymmetric nature of the peak at $\sim 15^\circ$, which also suggests two components. The decomposition of the yield into two components as shown in *b* and *c* is done only as a guide to the eye. The rapid rise in the yield at energies below ~ 15 MeV represents evaporation residues which have the same energy loss as the neon ions at low energies.

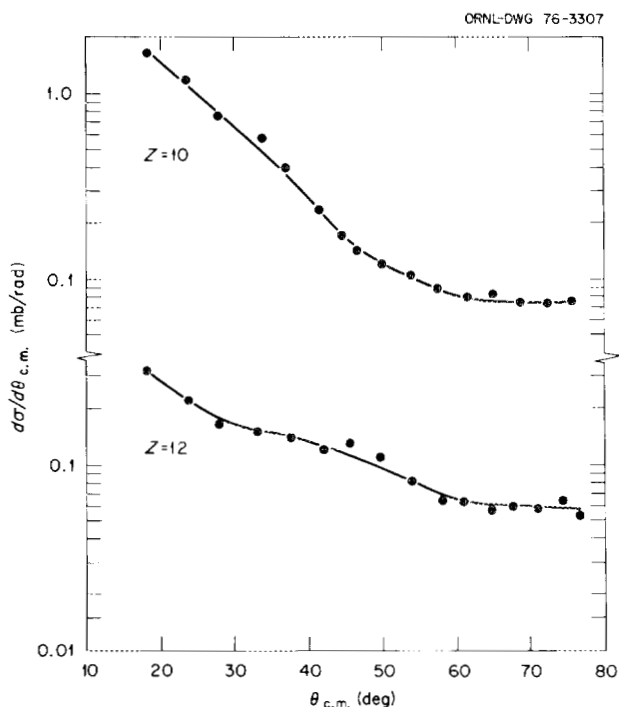


Fig. 1.24. Center-of-mass angular distributions, in millibarns per radian, for the total yield of neon and magnesium products from bombardment of ^{63}Cu with 130-MeV ^{12}C ions. The presence of two components in the yield is also apparent in the shape of the angular distribution for neon ions. The component having the lower energy is more forward-peaked.

the entire yields of neon and magnesium. In the case of neon, and somewhat less so for magnesium, the presence of two components is clearly indicated. At large angles the higher energy component is seen to have an angular distribution given by $d\sigma/d\Omega \sim 1/\sin\theta$. This indicates a lifetime of the complex system that is sufficiently long to produce a full rotation. If the forward-peaked component therefore corresponds to a shorter "sticking time," it is not clear why the scission process should produce in this case a smaller separation energy. It is also possible that the presence of two components may be connected with the phenomenon of scattering to negative angles or to some unspecified mechanism that produces a three-body final state. It will be interesting to explore this further.

Comparison of Results

All systems studied at ORIC thus far have certain spectral features in common: a broad deep-inelastic peak well below the elastic region and, at forward angles and for Z near that of the beam, a sharper peak at the same velocity as the projectile. The intensity of the products with Z less than that of the projectile is much greater than for high Z . An odd-even alternation in the intensity of the yield with Z is observed, with even values of Z having larger yields. This suggests that the light fragments emerge from the collision in an

excited state and subsequently decay to more tightly bound even-even nuclei.

The Q values of the deep-inelastic peak may be related to the Coulomb energy of two charged spherical fragments by

$$E_{\text{c.m.}} + Q = \frac{Z_1 Z_2 e^2}{r_0 (A_1^{1/3} + A_2^{1/3})}. \quad (1)$$

In general, it was found that the value of r_0 deduced from Eq. (1) varies with the scattering angle and the Z of the fragment. Table 1.2 lists measured Q values and deduced values of r_0 for fragments having the same Z as the beam and at large angles where quasi-elastic contributions should be small. This comparison of the three reactions emphasizes the difference between the carbon-induced reactions and the other two, the former experiencing a higher energy loss (and hence a larger deduced Coulomb separation distance).

The angular distributions are generally peaked forward more sharply than $1/\sin \theta$ except for the high- Z products of the ^{20}Ne reactions, which are well described by $1/\sin \theta$. The angle-integrated cross sections summed over the measured products may be compared with the total reaction cross section, as estimated from the quarter-point recipe. For 173-MeV ^{20}Ne on nickel, $\sigma_{\text{D.I.}}/\sigma_{\text{reac}} \approx 25\%$; this ratio is 16% for $^{12}\text{C} + ^{63}\text{Cu}$. For $^{16}\text{O} + \text{Ni}$ at 113 MeV, the ratio is about 22%, but it is only 3 to 4% at 96 MeV.⁴ This remarkably rapid change with energy will be investigated in future experiments.

A significant feature of the carbon-induced reactions is the presence of two components in the energy spectra for $Z > Z_{\text{beam}}$. This phenomenon appears to be absent in the oxygen- and neon-induced reactions, at least in the preliminary analyses we have performed to date.

Table 1.2. Approximate energies of deep-inelastic peaks at large angles

Reaction	Beam energy (MeV)	Laboratory angle (degrees)	$-Q$ (MeV)	r_0 (± 0.1) ^a (fm)
$^{12}\text{C} + ^{63}\text{Cu}$	130	51	81	1.45
$^{16}\text{O} + \text{Ni}$	96 ^b	40	31	1.16
$^{16}\text{O} + \text{Ni}$	113	25, 32.5, 45	45	1.16
$^{20}\text{Ne} + \text{Ni}$	164	26, 42	71	1.19
$^{20}\text{Ne} + \text{Ni}$	173	33	75	1.13

^aRadius parameters derived from Eq. (1) and the measured Q value.

^bFrom ref. 4.

Further investigation will be required to understand this phenomenon.

1. Consultant.
2. Chemistry Division.
3. See this report, R. G. Stokstad, D. C. Hensley, and A. Snell, "Position-Sensitive Counter Telescope."
4. R. Albrecht et al., *Phys. Rev. Lett.* **34**, 1400 (1975).

HEAVY-ION-INDUCED FUSION, FISSION, AND QUASI FISSION

The aim of this program is to provide an understanding of the macroscopic characteristics of interactions between complex nuclei that may be related to such fundamental properties of nuclei as viscosity, moments of inertia, and compressibility. For a given system, we measure the individual cross sections for the reaction products (evaporation residues, fission fragments, quasi-fission products, etc.) in an effort to account for the total reaction cross section. In addition, we measure mass, energy, and charge distributions of fission and quasi-fission fragments and evaporation residues. We obtain charge distributions and evaporation-residue cross sections with ΔE - E telescopes, in which ΔE is measured by a gas-filled ionization chamber or proportional counter and E is measured by a solid-state detector. Mass distributions are obtained by time-of-flight measurements at Berkeley and Orsay.

Competition Between Fission and Particle Emission in the ^{135}Tb Compound Nucleus

F. Plasil R. L. Hahn¹
R. L. Ferguson¹ F. E. Obenshain
F. Pleasonton

In this study at ORIC we investigated the reactions $^{20}\text{Ne} + ^{133}\text{Cs} \rightarrow ^{153}\text{Tb}^*$ and $^{12}\text{C} + ^{141}\text{Pr} \rightarrow ^{153}\text{Tb}^*$. Fission excitation functions for these two systems were presented earlier,² and it was pointed out that excitation functions for evaporation-residue products were required for an unambiguous analysis of the data.^{2,3} The analysis consists of calculations of fission and particle emission competition with angular-momentum-dependent fission barriers.^{4,5} Results obtained for ^{153}Tb should provide a test for this angular-momentum-dependent fission theory.⁵

We attempted to measure the evaporation-residue excitation functions for the two reactions but were able to obtain satisfactory results only for the highest energy points in each case (165 MeV for ^{20}Ne and 120 MeV for ^{12}C). At lower bombarding energies a map of E vs

ΔE shows that the low-energy tail of the slit-scattered projectiles merges with the low- ΔE portion of the evaporation-residue region; it is impossible to resolve the two types of events. This appears to be a fundamental limitation of our ΔE - E method, and we may be forced to use theoretical predictions for the energy dependence of fusion to generate the evaporation-residue excitation function.

1. Chemistry Division.
2. F. Plasil, p. 107 in *Proceedings of the International Conference on Reactions Between Complex Nuclei*, Nashville, June 1974, vol. 2, R. L. Robinson et al., Eds., North-Holland, Amsterdam, 1974.
3. F. Plasil et al., *Phys. Div. Annu. Prog. Rep. Dec. 31, 1974*, ORNL-5025 (1975), p. 32.
4. F. Plasil and M. Blann, *Phys. Rev. C* **11**, 508 (1975).
5. S. Cohen, F. Plasil, and W. J. Swiatecki, *Ann. Phys. (N. Y.)* **82**, 557 (1974).

Neon-Induced Fission of Nickel

F. Pleasonton	R. L. Hahn ¹
R. L. Ferguson ¹	F. Hubert ²
F. E. Obenshain	A. H. Snell ³
F. Plasil	

Fission is predicted to compete favorably with other modes of deexcitation for compound nuclei in all mass regions when the angular momentum of the system is sufficiently high.⁴ Thus, characteristics of the fission process can now be determined over a greatly increased range of mass, excitation energy, and angular momentum. Comparisons of fission properties with theoretical predictions over such broad ranges provide stringent tests of theory.

We have attempted to determine fission-fragment mass and kinetic-energy distributions and angular correlations for fission of the relatively very light compound nucleus formed in the reaction $\text{Ni} + {}^{20}\text{Ne}$. Surface-barrier detectors were used to measure the kinetic energies of two coincident fragments resulting from bombardments of a natural nickel target with 160-MeV ${}^{20}\text{Ne}^{6+}$ ions from ORIC.

A preliminary analysis of these data, based on a simple two-body breakup of the target-plus-projectile system, appears to support the theoretical predictions^{5,6} that this very light system fissions asymmetrically. However, this conclusion must be considered tentative, because the mass distributions obtained are very sensitive to the precise values of the measured energies and because, during the data analysis, we became aware of possibly serious uncertainties in the energy calibrations. It is likely that definitive measure-

ments and answers to theoretical questions will have to wait until we can repeat the experiment with the time-of-flight method.

1. Chemistry Division.
2. Centre d'Études Nucléaires, Bordeaux, France.
3. Consultant.
4. F. Plasil and M. Blann, *Phys. Rev. C* **11**, 508 (1975).
5. U. L. Businaro and S. Gallone, *Nuovo Cimento* **5**, 315 (1957).
6. R. Y. Cusson and K.T.R. Davies, private communication and contribution to this annual report.

Argon and Krypton Reactions with Copper and Silver at Energies of 4 to 8 MeV/amu

R. L. Ferguson ¹	B. H. Erkilli ²
F. Plasil	R. H. Stokes ²
H. C. Britt ²	H. H. Gurbrod ³
M. Blann ⁴	

Counter telescope measurements have been made of reactions ${}^{40}\text{Ar} + {}^{109}\text{Ag}$ at energies ranging from 169 to 337 MeV at the LBL Super-Heavy-Ion Linear Accelerator (Super-HILAC). Cross sections for evaporation-residue products have been extracted and compared with predictions of a particle-evaporation model that includes angular-momentum-dependent fission competition.⁵ As was reported earlier,⁶ above about 200 MeV, the excitation function for evaporation-residue products appears to be determined by fission competition. In the above experiment we have also measured elastic scattering and fission-like products and found that it was possible to decompose each fission-fragment charge distribution⁷ into a quasi-fission component and a fission component. These decompositions of integrated charge distributions are shown in Fig. 1.25. Also shown are distributions for the $\text{Kr} + \text{Cu}$ system. In this case decomposition is impossible because the masses of the target and projectile are similar to those obtained in a symmetric mass division of the compound system.

We have also measured the evaporation-residue cross sections for $\text{Kr} + \text{Cu}$ at 494, 604, and 708 MeV. The results involve large experimental errors due to the difficulty of measuring the very forward-peaked angular distribution of these products. In recent measurements we have taken data at $1\frac{1}{2}^\circ$ with respect to the beam in an effort to improve the accuracy of our results. The cross sections that we have obtained so far are consistent with the evaporation-fission competition model.⁸

Most recently we have measured the mass and charge distributions of evaporation-residue products simul-

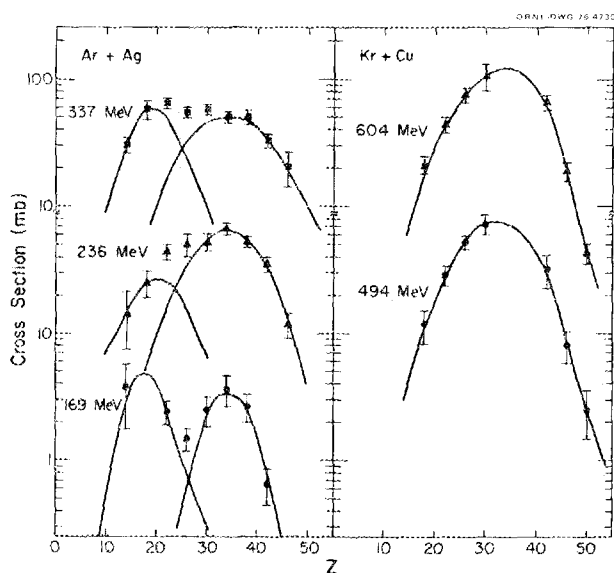


Fig. 1.25. Yield-charge distribution for the reactions $^{40}\text{Ar} + ^{109}\text{Ag}$ and $^{80}\text{Kr} + ^{65}\text{Cu}$. Laboratory energies are indicated. The solid lines in the $^{40}\text{Ar} + ^{109}\text{Ag}$ case indicate decomposition into a quasi-fission component (centered near $Z = 18$) and a fission component.

taneously from ^{86}Kr bombardments of ^{65}Cu . At 3° (lab) the average mass number was found to be ~ 128 , corresponding to 23 evaporated nucleons. The width of the distribution was 7.5 amu. The average charge was ~ 60 , and the width of the charge distribution was ~ 5 units. These numbers, however, are only tentative due to calibration uncertainties. In the future, by further analysis of the data, we plan to look for structure in these distributions and compare it with evaporation calculations.

1. Chemistry Division.
2. Los Alamos Scientific Laboratory, Los Alamos, N.M.
3. Gesellschaft für Schwerionenforschung, Darmstadt, Germany.
4. University of Rochester, Rochester, N.Y.
5. F. Plasil and M. Blann, *Phys. Rev. C* **11**, 508 (1975).
6. M. Blann et al. *Phys. Div. Annu. Prog. Rep. Dec. 31, 1974*, ORNL-5025 (1975), p. 33.
7. U. L. Businaro and S. Gallone, *Nuovo Cimento* **5**, 315 (1957).
8. S. Cohen, F. Plasil, and W. J. Swiatecki, *Ann. Phys. (N.Y.)* **82**, 557 (1974).

Quasi Fission in Argon and Copper Bombardments of Gold

C. Ngô¹ B. Tamain¹
 J. Péter¹ F. Hanappe²
 F. Plasil M. Berlinger²

The purpose of studying the $\text{Cu} + \text{Au}$ system at 443 MeV was to compare the results with those obtained at

365 MeV and thus to obtain information on the energy dependence of quasi fission.³ It was found that quasi fission continued to account for a large fraction of the total reaction cross section and that the events were well separated from other events (such as quasi-elastic events) except near the grazing angle. The angular distribution $d\sigma/d\theta$ was found to have a broad peak forward of the grazing angle and to have a finite value at 0° . This may imply the existence of nuclear orbiting at this higher energy. The mass distributions, as a function of angle, showed a similar behavior to those at the lower energy, but they were somewhat broader. The contribution of fission was larger at 443 MeV than at 365 MeV.

Previous experiments with argon on targets such as gold were all carried out at energies relatively high above the interaction barrier. The purpose of our study of $\text{Ar} + \text{Au}$ at 220 MeV was to see whether, at an energy close to the interaction barrier, quasi fission can be observed as a well-separated process. This was indeed found to be the case. Quasi-fission events formed a characteristic peak at all angles (except at the grazing angle, where they merged with partially damped events). The peak was well separated from the fission peak. The angular distribution of quasi fission was found to peak forward of the grazing angle, as was the case in studies with heavier ions such as copper and krypton. Thus, the quasi-fission process also occurs in systems other than those involving very heavy ions such as copper and krypton. It is likely that the extent of the quasi-fission contribution does not depend on the specific system involved, but rather on the relative magnitude of the Coulomb (and centrifugal) potentials and of the forces driving toward fusion, such as the nuclear potential and the incident momentum.

1. Institut de Physique Nucléaire, Orsay, France.
2. Université Libre de Bruxelles, Belgium.
3. Experiments conducted at Orsay, France.

FUSION OF $^{14}\text{N} + ^{12}\text{C}$ AT HIGH ENERGIES

R. G. Stokstad J. A. Biggerstaff
 J. Gomez del Campo¹ A. H. Snell²
 P. H. Stelson

The cross section for the fusion of heavy ions at high energies is of interest because it depends on the properties of the entrance channel and can give information on the highly excited compound nucleus. Experimental data for very light systems have not been available, however, possibly because the evaporation residues produced at higher bombarding energies have

masses comparable to or even less than the projectile. In this case, separation of the products of inelastic direct reactions and of fusion is no longer routine. Fusion measurements at high energies and for light systems, however, are of particular interest because systems having fewer nucleons might exhibit phenomena qualitatively different from those observed for heavy systems. Possible differences are (1) a dependence of σ_f on microscopic properties of the entrance channel or (2) a limitation of σ_f imposed by angular momentum restrictions in the compound nucleus rather than by the entrance channel.

Beams of ^{14}N at seven energies over the range of 43.8 to 178.1 MeV were used to bombard a carbon foil having an areal density of $272 \mu\text{g}/\text{cm}^2$. Reaction products with $Z = 3$ to 12 were identified with a ΔE - E counter telescope in which the ΔE detector was an ionization chamber 9.5 cm long and filled with methane at a typical pressure of 20 torr.³ Angular distributions were measured over the range of 4° to 40° (lab). In some measurements, an ionization chamber incorporating a solid-state PSD was used.⁴

The yields of neon, sodium, and magnesium nuclei are clearly the residues of compound-nucleus formation followed by evaporation of light particles. These residues have a velocity distribution centered about the velocity of the compound nucleus and broadened by the recoil imparted by light-particle emission. The yields of lighter elements, however, may contain contributions from two-body reactions in which one or more nucleons are transferred. These contributions appear with a velocity characteristic of that of the projectile and thus have an energy typically higher than that for an evaporation residue of the same mass.

We believe that it is possible to separate these two components with sufficient confidence to enable the extraction of fusion cross sections. The separation relies on the expectation that the energy distributions for the evaporation residues change consistently from element to element. As the Z of the residue decreases, the centroid of the energy distribution decreases and the width increases. These considerations have been quantified by developing a Monte Carlo computer code,⁵ which uses the Hauser-Feshbach prescription, including angular momentum, for the statistical decay of the compound system. In this way, the relative intensities, energy distributions, and angular distributions of the evaporation residues may be predicted in the laboratory system. We emphasize, however, that our analysis of the reaction products is not directly dependent on this model; the calculations serve only to give confidence that the peak shapes assumed in the analyses of the

energy spectra correspond to those expected for evaporation residues.

The foregoing remarks are illustrated in Fig. 1.26*a*, which shows measured and calculated energy spectra for sodium and nitrogen nuclei produced at bombarding energies of 86.3 and 167.1 MeV respectively. Similar agreement has also been obtained at other bombarding energies from 43 to 178 MeV for the energy spectra and for angular distributions of other elements. The change in the elemental distribution of the evaporation residues with bombarding energy is as would be expected from the decay of a compound nucleus formed with increasing excitation energy and angular momentum. A comparison of measured and predicted relative yields for evaporation residues at two energies is shown in Fig. 1.26*b*.

The experimental results are presented in Fig. 1.27. Figure 1.27 also includes measurements by Kuehner and Almqvist⁶ of the fusion cross section at lower energies. Above 40 MeV, the average fusion cross section, σ_f , is 812 ± 27 mb. Considering a systematic error of $\pm 7\%$ of σ_f , this corresponds to a critical radius parameter $r_{\text{cr}} = 1.08 \pm 0.04$ fm. A good fit to the low- and high-energy data is given by the model of Glas and Mosel⁷ with the parameters $r_{\text{cr}} = 1.06$, $V(R_{\text{cr}}) = 0.0$, $r_B = 1.47$, and $V(R_B) = 6.3$ (Fig. 1.27).

The values of σ_f at high energies therefore may be explained by an entrance-channel requirement that the colliding ions penetrate to a critical radius. In the present case this radius corresponds to a combined nuclear density ρ_c in the overlap region of $0.6\rho_0$ to $0.9\rho_0$, where ρ_0 is the central density. This value is comparable to the value $\rho_c \sim \rho_0$ obtained for heavier systems⁸ ($r_{\text{cr}} \sim 1.0 \pm 0.07$).

An alternative explanation of the limitation on σ_f involves the maximum angular momentum of the compound nucleus ^{26}Al for a given excitation energy (the yrast line). This is shown in Fig. 1.27*b*. Here, the values of J_c defined by $\sigma_f = \pi\lambda^2(J_c + 1)^2$ are plotted vs excitation energy in ^{26}Al . The data determine a straight line on a $J_c(J_c + 1)$ scale, which, in a rotational model, indicates a moment of inertia $2J/h^2 = 7.7 \pm 0.7 \text{ MeV}^{-1}$ and a band-head excitation energy of ~ 15 MeV. The above moment of inertia corresponds, for example, to a strongly deformed ^{26}Al nucleus ($\beta \sim 0.5$ for a prolate rigid rotor) or to a ^{12}C nucleus and ^{14}N nucleus orbiting at a separation of $(1.06 \pm 0.05)(A_1^{1/3} + A_2^{1/3})$ fm. The band head is located, perhaps not coincidentally, at the separation energy for $^{26}\text{Al} \rightarrow ^{12}\text{C} + ^{14}\text{N}$. Thus, the observed values of σ_f at energies greater than 40 MeV may be explained by postulating a compound nucleus that, for excitation energy E_X , has a maximum

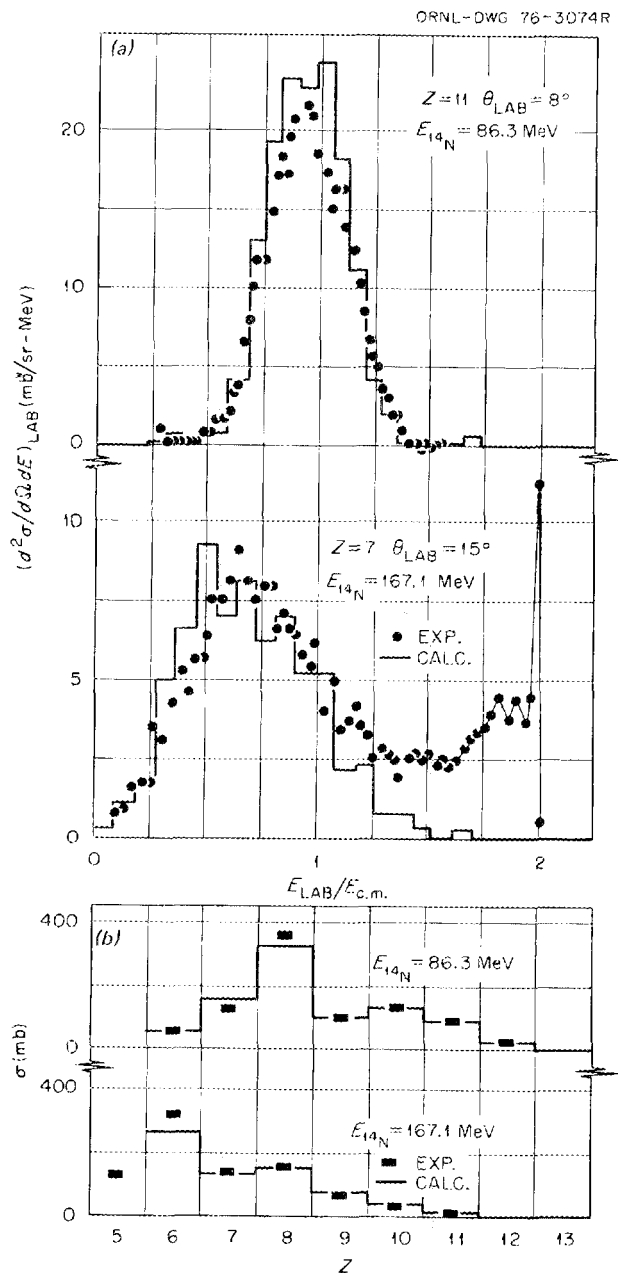


Fig. 1.26. Representative energy spectra and elemental yields for $^{12}\text{C} + ^{14}\text{N}$ reaction products. (a) Energy spectrum of sodium ions at $\theta_{\text{lab}} = 8^\circ$ ($E_{14\text{N}} = 86.3$ MeV). The histogram is the result of a Monte Carlo calculation, normalized to the total yield of all evaporation residues, $Z = 6$ to 12. Energy spectrum of nitrogen ions at $\theta_{\text{lab}} = 15^\circ$ ($E_{14\text{N}} = 167.1$ MeV). Again, the calculation of the evaporation-residue component (histogram) is normalized to the total angle-integrated yield of all residues, $Z = 5$ to 12. (b) Comparison of measured and predicted evaporation residues. The predicted values, having been normalized to the total yield, have only a relative significance.

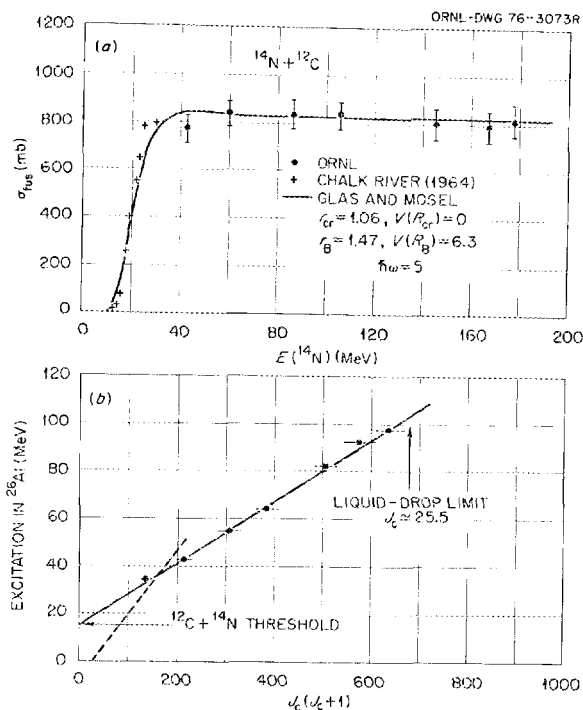


Fig. 1.27. Deduced fusion cross sections and critical angular momenta. (a) The measured fusion cross sections (solid points) as a function of bombarding energy (lab). The data shown as crosses are from ref. 6. The dashed line is a theoretical prediction (ref. 7) discussed in the text. (b) The measured critical angular momenta as a function of excitation energy in ^{26}Al . The dotted line corresponds to a moment of inertia $\mathcal{J} = 0.55\mathcal{J}_r$, where \mathcal{J}_r is the rigid-body value; it is an estimate for the ground-state moment of inertia.

angular momentum J_c given by

$$E_x = (7.7 \text{ MeV}^{-1})^{-1} J_c(J_c + 1) + 15 \text{ MeV}. \quad (1)$$

The present experimental results alone cannot distinguish between these alternative origins for the limitation on σ_f (entrance channel or compound nucleus). However, when assuming only that an equilibrated compound nucleus is formed in this reaction (regardless of the origin of the limitation on σ_f), the experimental data suggest that the ^{26}Al nucleus (1) is very deformed for excitation energies E_x and angular momenta J_c similar to those given by Eq. (1) and (2) has been formed with an angular momentum nearly equal to the limit for a rotating liquid drop,⁹ $\sim 25.5\hbar$.

1. On sabbatical leave from Instituto de Fisica, University of Mexico, Mexico City.

2. Consultant with the Physics Division.

3. See this report, A. H. Snell, "Modification of a Proportional Counter to an Ionization Chamber."
4. See this report, R. G. Stokstad, D. C. Hensley, and A. H. Snell, "Position-Sensitive Counter Telescope."
5. See this report, J. Gomez del Campo and R. G. Stokstad, "Monte Carlo Hauser-Feshbach Computer Code."
6. J. A. Kuehner and E. Almqvist, *Phys. Rev.* **134B**, 1229 (1964).
7. D. Glas and U. Mosel, *Nucl. Phys.* **A237**, 429 (1975).
8. J. Galin et al., *Phys. Rev. C* **9**, 1018 (1974).
9. S. Cohen, F. Plasil, and W. J. Swiatecki, *Ann. Phys.* **82**, 557 (1974).

**TRANSFER REACTIONS THAT LEAD TO
THE NUCLEI ^{245}Cf AND ^{244}Cf :
INTERACTION OF ^{16}O AND ^{20}Ne WITH ^{239}Pu**

R. L. Hahn¹ P. F. Dittner¹
F. Hubert² K. S. Toth

In a continuation of studies of transfer reactions, previously reported for the reactions of $^{12}\text{C} + ^{239}\text{Pu}$,^{3,4} we have measured excitation functions for reactions on ^{239}Pu induced by ^{16}O and ^{20}Ne beams, leading to the radioactive nuclides ^{245}Cf and ^{244}Cf . The experiments involved the use of helium gas-jet and radiochemical separation techniques.

Preliminary analysis of the data indicates that (1) the magnitudes of the cross sections for the reactions $X + ^{239}\text{Pu} \rightarrow ^{245,244}\text{Cf}$, when projectile X is either ^{12}C , ^{16}O , or ^{20}Ne , are about the same, with maximum values of 7 to 10 μb , and (2) the shapes (i.e., energy dependence) of the excitation functions obtained with the ^{12}C , ^{16}O , and ^{20}Ne beams are all very similar when plotted as a function of excitation energy.

These results strongly imply that a common transfer mechanism is operating in all of these reactions. Result (1) indicates that the californium products are not produced by compound-nucleus reactions or by radioactive decay of nuclides with Z greater than that of californium, because the cross sections for such reactions on plutonium decrease, due to increasing competition from fission, as the Z of the projectile increases. Result (2) indicates that some common excited intermediate californium nucleus (such as ^{247}Cf), formed by the transfer of a common aggregate (such as ^8Be) from the projectile to the ^{239}Pu target nucleus, is probably involved in all these reactions.

To test these ideas further, we plan to measure recoil ranges and angular distributions of the californium nuclei produced in these reactions and then compare the results with predictions of a model of the kinematics of transfer reactions.

1. Chemistry Division.

2. Guest Scientist in Chemistry Division from Centre d'Études Nucléaires, Bordeaux, France.

3. R. L. Hahn et al., *Phys. Div. Annu. Prog. Rep. Dec. 31, 1974*, ORNL-5025 (1975), p. 36.

4. R. L. Hahn et al., *Phys. Rev. C* **10**, 1889 (1974).

**MONTE CARLO HAUSER-FESHBACH
COMPUTER CODE**

J. Gomez del Campo¹ R. G. Stokstad

A computer code has been developed for predicting the relative intensities, energy spectra, and angular distributions of evaporation residues produced in heavy-ion reactions such as $^{12}\text{C} + ^{14}\text{N}$. The Hauser-Feshbach prescription for the decay of the compound nucleus is used in conjunction with the Monte Carlo method to calculate cross sections in the laboratory system. Angular momentum is included explicitly and found to be extremely important, particularly at high bombarding energies. Approximations that have been made are (1) a "constant-temperature" expression for the densities of levels in the residual nuclei, (2) a $1/\sin \theta_{\text{c.m.}}$ emission probability, and (3) a sharp-cutoff approximation for the transmission coefficients.

The code requires less than 16K of memory and presently executes on the CDC 3200 computer at the Van de Graaff. The rate at which the code can "evaporate" particles depends on the maximum angular momentum of the compound nucleus, J_{max} . For $J_{\text{max}} = 12$, the rate is ~ 37 particles per second, but for $J_{\text{max}} \sim 26$, the rate drops to about 23 particles per second. These two angular momenta correspond to ^{14}N bombarding energies of 43 and 167 MeV respectively. Because the average number of particles evaporated by the compound nucleus is 2 and 5 in these two cases, the corresponding running times for 10^5 fusion events are 1.5 and 6 hr respectively. (The IBM 360-91 would be about 40 times as fast.)

Comparison of the predictions of the code with experimental data for the $^{12}\text{C} + ^{14}\text{N}$ reaction has been made over a wide range of bombarding energies, from 43 to 167 MeV. The agreement has been quite satisfactory. Figure 1.28 shows some typical comparisons. The code has been of value in understanding the spectra observed in the $^{12}\text{C} + ^{14}\text{N}$ reaction and will be of general use in extrapolating angular distributions to very forward angles where measurements are not possible.

1. On sabbatical leave from Instituto de Física, University of Mexico, Mexico City.

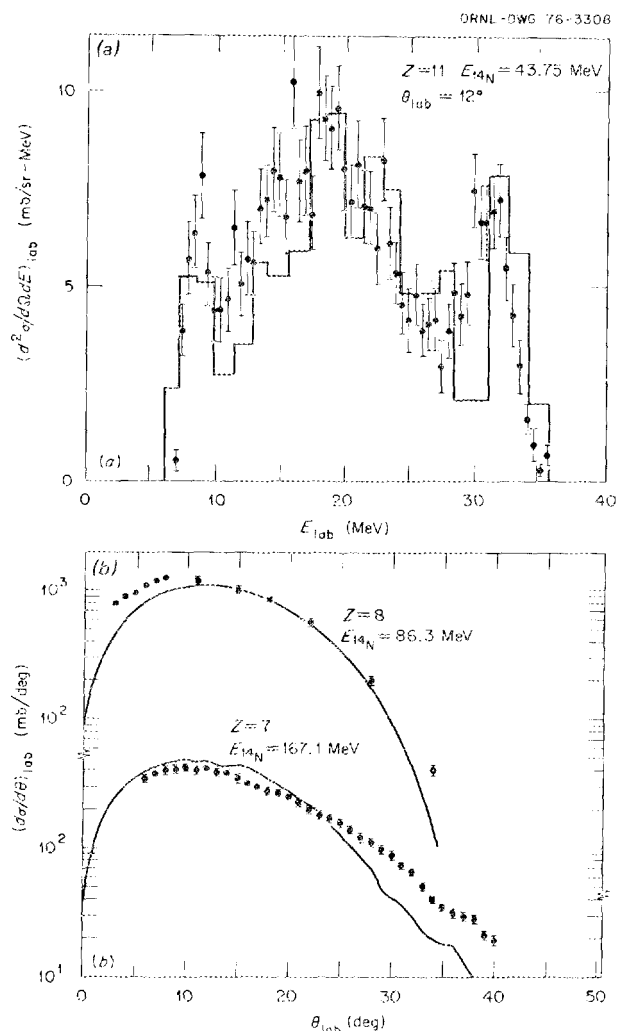


Fig. 1.28. Comparison of Monte Carlo predictions to the experimental data. (a) Energy spectrum for sodium residues at $\theta_{\text{lab}} = 12^\circ$, $E_{^{14}\text{N}} = 43.7$ MeV. The central peak corresponds to evaporation of two protons and a neutron; the highest and lowest energy peaks arise from alpha-particle emission at backward and forward angles, respectively, in the center-of-mass system. The experimental data are shown with error bars, the calculation as a histogram. (b) Predicted and measured angular distributions for oxygen residues produced at $E_{^{14}\text{N}} = 86.3$ MeV, and predicted and measured angular distributions for nitrogen residues produced at 167.1 MeV.

MODIFICATION OF A PROPORTIONAL COUNTER TO AN IONIZATION CHAMBER

A. H. Snell¹

Ionization chambers offer certain advantages over proportional counters, which may be exploited provided that the particles to be detected deposit sufficient

energy in the sensitive region that electronic noise is not a significant factor. This is usually the case for heavy ions. The type of proportional counter telescope that has been used in heavy-ion studies at ORNL in the last few years has been converted to an ionization chamber telescope by a simple modification. The thin wire (a few thousandths of an inch in diameter) was replaced with a 0.040-in.-diam nickel rod to prevent electron multiplication.

A cylindrical Frisch grid was constructed from 93%-transmission nickel mesh by wrapping the mesh around a $\frac{3}{8}$ in.-diam form. The grid was then placed around the 0.040-in.-diam anode. Other than minor changes in electrical connections, no other modifications were necessary. The counter performed quite satisfactorily and has been used extensively in the studies of the fusion of $^{12}\text{C} + ^{14}\text{N}$ and in other heavy-ion reactions.

1. Consultant with the Physics Division.

POSITION-SENSITIVE COUNTER TELESCOPE

R. G. Stokstad D. C. Hensley
A. H. Snell¹

Solid-state PSDs provide good energy resolution and a large solid angle without loss of angular resolution. Many heavy-ion experiments require these characteristics in addition to the identification of the detected particles. Because the Frisch-grid ionization chamber is widely used as the energy-loss detector in a counter telescope and because it can be made large, we have combined these two types of detectors into a single system. Figure 1.29 is a schematic diagram of this counter telescope.

Presently, the detector is used in the 30-in. scattering chamber, where it subtends an angle of 9° , the total solid angle being about 3 msr. We have used pure methane at pressures varying from 10 to 80 torr, typical electrode voltages of several hundred volts, and Formvar entrance windows of 40 to 80 $\mu\text{g}/\text{cm}^2$. The electronic noise of the ΔE portion is ~ 50 keV when using an ORTEC-124 preamplifier.

The data are stored in nine separate two-dimensional ΔE by $E + \Delta E$ arrays, each corresponding to $\Delta\theta \approx 1^\circ$ and having a maximum size of 55,000 channels. A new mode of on-line data processing using the Systems Engineering Laboratory (SEL) computer was developed for this detection system and is described elsewhere in this report.² Rates of up to 3 kHz have been accommodated, and results are available in the form of two-dimensional arrays during the experiment.

ORNL-DWG 76-331C

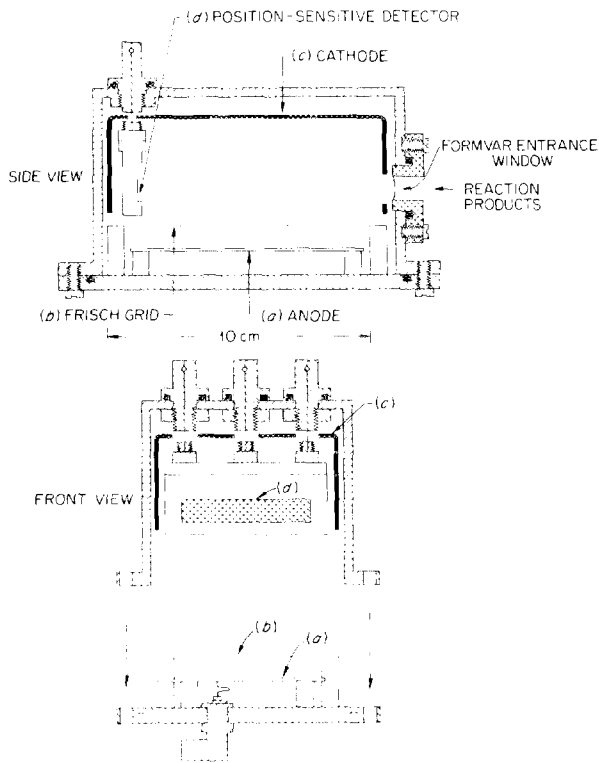


Fig. 1.29. Schematic diagram of the ΔE - E PSD. A mask having eight thin vertical bars covers the solid-state detector (ORTEC) and is used to provide a convenient position calibration. (a) Anode; (b) Frisch grid (97% transmission nickel mesh); (c) cathode; (d) solid-state detector.

The performance of the detector is illustrated in Fig. 1.30, which shows a $\Delta E \times E$ array for the products of the reaction $^{20}\text{Ne} + \text{Ni}$ at 173 MeV. A projection onto the ΔE axis of all events in a narrow region of $\Delta E + E$ centered about 15 MeV is shown in Fig. 1.31. Here one can see the resolution of adjacent elements up to $Z \sim 28$. Most of the observed spread in ΔE originates with energy-loss straggling. It appears that higher values of Z would also be resolved if they were produced in this reaction with sufficient energy and intensity. Because the thickness of the ΔE detector can be varied easily, it has been possible to use the detector for a variety of reactions and for observation of alpha particles as well as heavy ions.

1. Consultant with the Physics Division.

2. See this report, D. C. Hensley, "ORIC Data Acquisition System Development."

GAMMA-RAY MULTIPLICITIES IN $^{20}\text{Ne} + ^{150}\text{Nd}$ BOMBARDMENTS

D. G. Sarantites¹ J. H. Barker¹
S. A. Gronemeyer¹ M. L. Halbert
E. Eichler² D. C. Hensley
N. R. Johnson² R. A. Dayras

The measurement of the number of gamma rays accompanying nuclear reactions has been shown to be a promising tool for studying nuclear reaction mechanisms, especially for investigating the distribution of angular momentum in the parent nuclei. It is particularly interesting to study heavy-ion reactions near 7 MeV/nucleon, a point at which other types of experiments suggest that the compound-nucleus mechanism gives way to different processes.

A multidetector apparatus consisting of eight lead-shielded 5.08- by 7.62-cm NaI detectors, a reaction chamber with a 90° port for a Ge(Li) counter, and a support stand was constructed at Washington University. The NaI counters view the target at various angles between 45° and 140° to the beam. This apparatus and the associated electronic equipment were brought to ORIC in December and used in a four-shift trial run. We successfully acquired data on gamma-ray multiplicities, relative intensities, excitation functions, and related quantities from the bombardment of a ^{150}Nd target with ^{20}Ne at 128, 144, 165, and 173 MeV.

The NaI detectors furnished only yes- no signals as to whether or not a pulse in coincidence with the Ge(Li) detector had occurred above threshold (~100 keV). The events were tagged according to the number of NaI counters that had been triggered and were sorted into sixteen 8K spectra in the ORIC computer by a specially developed data-acquisition program. One of these spectra was used to store Ge(Li) singles (no NaI coincidences). Eight spectra were for the 1-fold NaI coincidence events for each of the eight NaI counters. The seven other spectra contained 2-fold, 3-fold, . . . , 8-fold events without regard to which of the NaI counters had been triggered. For the analyses done thus far, the eight 1-fold spectra were summed to one spectrum. Figure 1.32 shows an example of these spectra for the 128-MeV ^{20}Ne beam.

Preliminary analysis gives the following results.

1. Most of the discrete gamma rays correspond to known transitions in the ground-state band of xn and αxn products, with x from 5 to 10. As the bombarding energy is increased, progressively more neutrons are emitted, as expected. At the higher

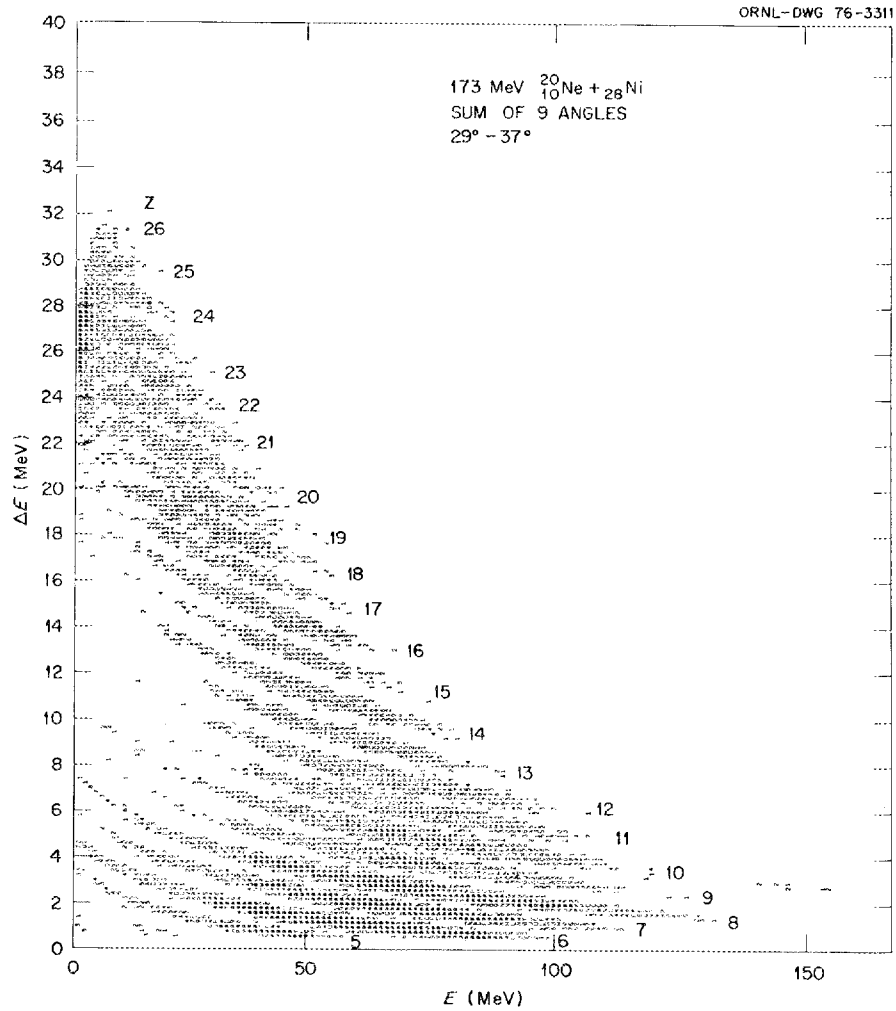


Fig. 1.30. A $\Delta E \times E$ array of products from the reaction 173-MeV $^{20}\text{Ne} + \text{Ni}$. Spectra at nine angles from 29° to 37° have been summed. Channels having fewer than four counts ($\Delta E < 20$ MeV) and six counts ($\Delta E \geq 20$ MeV) have been suppressed to better display the contours of constant Z . The energy scale for the ΔE axis is only approximate.

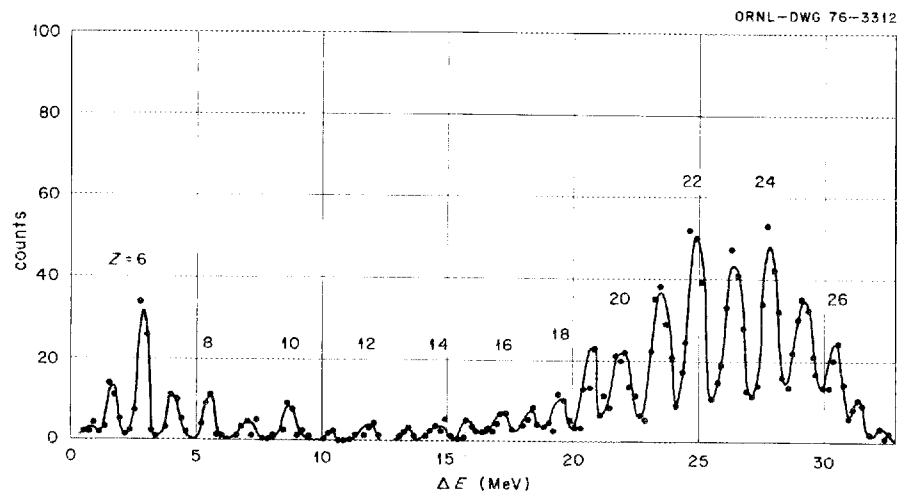


Fig. 1.31. A projection on the ΔE axis of events in a narrow energy region centered about 15 MeV (see Fig. 1.30). No counts were suppressed here.

bombarding energies, the αxn products carry more than half of the $xn + \alpha xn$ observed cross section.

- For a given exit channel, the average gamma-ray multiplicity $\langle M \rangle$ for the observed $(J+2) \rightarrow J$ transitions is independent of J .
- The average multiplicities vary from about 10 to 30 (see Fig. 1.33). They vary smoothly as a function of beam energy (increasing with energy for a given exit channel) and as a function of x (decreasing with x at a given beam energy). For a given x and beam energy, $\langle M \rangle$ is smaller for the αxn channels than for xn channels. The weighted average of $\langle M \rangle$ for all observed channels is about 20 and is substantially independent of beam energy.
- The standard deviation of the Multiplicity distribution is found to vary between 5 and 8, increasing with increasing bombarding energy or decreasing number of emitted neutrons.
- The skewness is negative.
- The relative intensities indicate that side feeding is important in populating the lowest members of the ground-state band at low but not high beam energies.

Future plans include extension of these experiments to other reactions forming the same compound system, measurement of neutrons and alpha energies, measure-

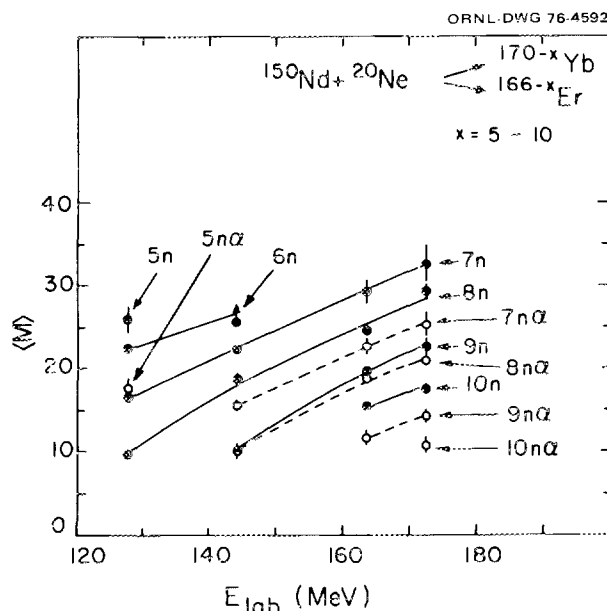


Fig. 1.33. Average multiplicities for various exit channels as a function of bombarding energy.

ments of NaI pulse heights, and angular correlation studies.

- Washington University, Saint Louis, Mo.
- Chemistry Division.
- Saint Louis University, Saint Louis, Mo.

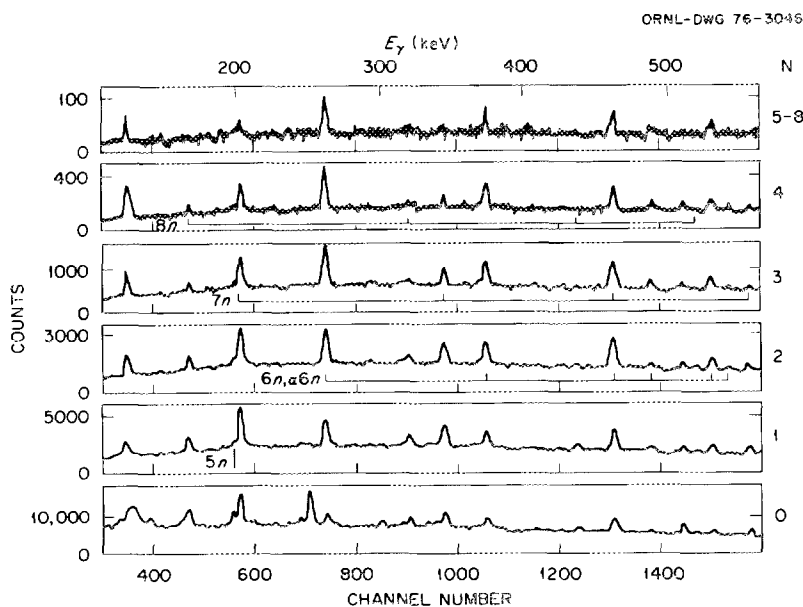


Fig. 1.32. Ge(Li) spectra in N -fold coincidence with the NaI detectors in the bombardment of ^{150}Nd by 128-MeV ^{20}Ne . Known gamma rays for the dominant channels are marked.

HEAVY-ION MICROPHYSICS

REACTION $^{14}\text{C}(^6\text{Li}, ^6\text{He})^{14}\text{N}$ AND DISTRIBUTION OF GAMOW-TELLER STRENGTHC. D. Goodman D. C. Hensley
W. R. Wharton¹

Many allowed beta decays proceed with rates that are orders of magnitude slower than the rates implied by the weak interaction and lepton dynamics. This puzzle has long been recognized in nuclear physics, but, although the effect seemed to be due to a general feature of nuclear structure, the beginnings of a real understanding of the effect did not come until analog states were discovered with the (p,n) reaction.² Analog states are connected by the same matrix element that appears in an allowed Fermi beta decay, and, insofar as the states are perfect analogs, no Fermi strength is left over for any other states.

The situation cannot be quite so simple for Gamow-Teller (G.T.) decays, but because they also are inhibited, the suggestion has been made that G.T. strength is also concentrated in an energy region that is not accessible to the beta decay.³ No systematic mapping of the G.T. strength has ever been done, but Wharton and Debevec have shown that the $(^6\text{Li}, ^6\text{He})$ reaction can be used as a probe of the G.T. strength.⁴

The decay of ^{14}C is an extreme example of an inhibited G.T. decay: the rate is about 10^6 times slower than it would be if there were no nuclear structure inhibition. We have exploited the smallness of the G.T. matrix element, $\langle ^{14}\text{N}_{g.s.} || \sigma \tau || ^{14}\text{C} \rangle$, to show first that the $L = 0$ part of the cross section does not contain large contributions from processes not proportional to the G.T. matrix element; that is, that it is in fact proportional to the G.T. matrix element. Second, we have mapped the G.T. strength between $^{14}\text{C}_{g.s.}$ and ^{14}N up to about 12 MeV of excitation in ^{14}N and have found that the 3.95-MeV state contains at least 90% of the G.T. strength, and possibly all of it. Thus we can rephrase the traditional description of the retarded beta decay of ^{14}C to say that it does not result from an accidental cancellation of the G.T. matrix to the ground state of ^{14}N but rather that it is a consequence of the concentration of the G.T. strength in the 3.95-MeV state. The measured differential cross sections are shown in Figs. 1.34 and 1.35.

Because we can map the G.T. strength over a large region of excitation, we are able to find sum strength that cannot be found through beta decay. The sum strength is sensitive to the wave function of the initial state alone, whereas the matrix element measures the

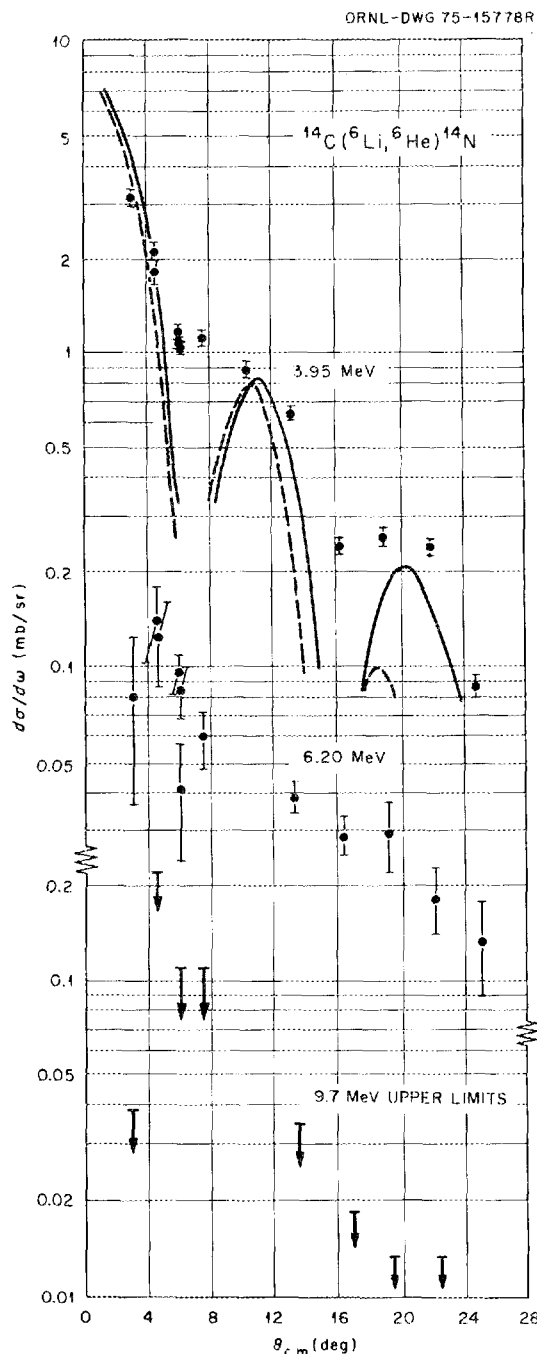


Fig. 1.34. Angular distributions for the $^{14}\text{C}(^6\text{Li}, ^6\text{He})$ reaction populating three 1^+ excited states in ^{14}N , at 3.95-, 6.2-, and 9.70-MeV excitation. The cross section for the 1^+ state at 9.7 MeV contains contributions from the 2^+ state at 9.51 MeV. Two distorted-wave Born approximation (DWBA) calculations for the $L = 0$ part of the reaction, each with the same normalization, are shown using an optical potential for $^6\text{Li} + ^{18}\text{O}$ (set 1) from ref. 3 and for $^6\text{Li} + ^{12}\text{C}$ (set 2) with $U = 159.5$ and $W = 8.0$ taken from ref. 4.

overlap of the initial and final states. We find that the theoretical wave function for ^{14}C of Visscher and Ferrel⁵ and that of Cohen and Kurath⁶ both overestimate the sum strength.

Our future plans are to extend the mapping of the G.T. strength to other mass regions and to map the

strength between ^{37}Cl and ^{37}Ar to provide data that might be useful in calculating the neutrino-detection efficiency of ^{37}Cl more precisely.

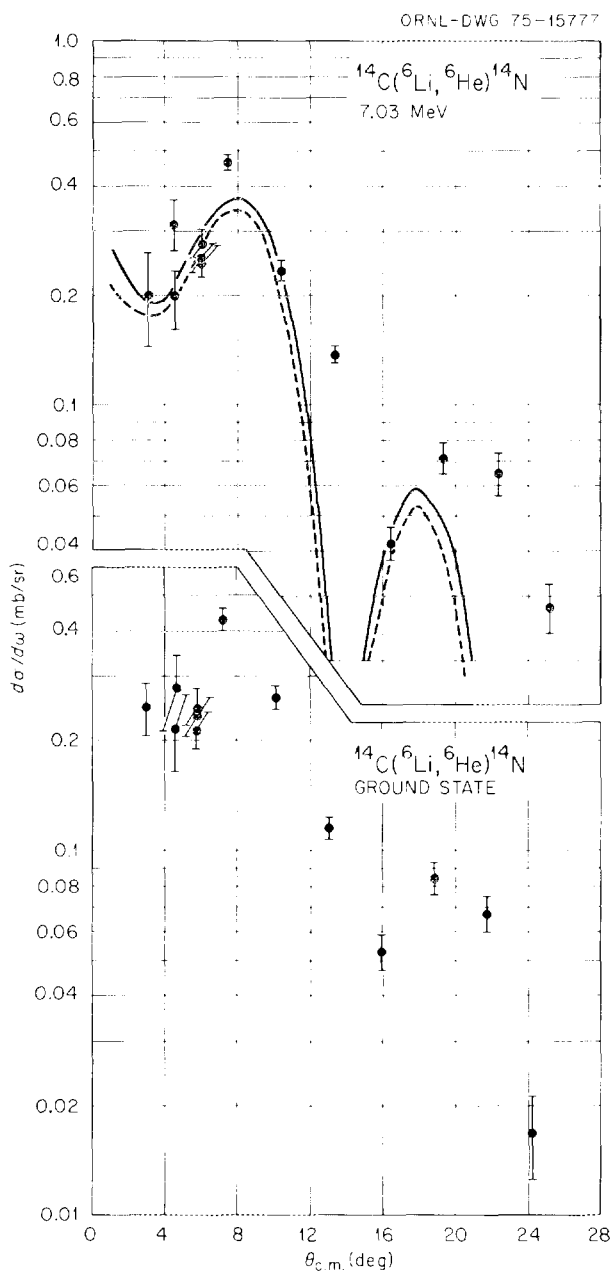


Fig. 1.35. Angular distributions for the $^{14}\text{C}(^6\text{Li},^6\text{He})$ reaction populating the 1^+ ground state and the 2^+ state at 7.03 MeV in ^{14}N . Two DWBA calculations for the $L = 2$ part of the reaction are shown, using the potentials described in the caption of Fig. 1.34.

1. Rutgers University, New Brunswick, N.J. Present address: Carnegie-Mellon University, Pittsburgh, Pa.

2. J. D. Anderson, C. Wong, and J. W. McClure, *Phys. Rev.* **126**, 2170 (1972).

3. M. Morita et al., *Prog. Theor. Phys. Suppl.* **48**, 41 (1971).

4. W. R. Wharton and P. T. Debevec, *Phys. Rev. C* **11**, 1963 (1975).

5. W. M. Visscher and R. A. Ferrell, *Phys. Rev.* **107**, 781 (1957).

6. S. Cohen and D. Kurath, *Nucl. Phys.* **73**, 1 (1965).

$^{12}\text{C} + ^{12}\text{C}$ REACTIONS

R. M. Wieland¹ A. H. Snell²
 C. B. Fulmer P. H. Stelson
 D. C. Hensley R. G. Stokstad
 S. Raman G. R. Satchler
 L. D. Rickertsen

Progress in understanding the mechanisms involved in $^{12}\text{C} + ^{12}\text{C}$ induced reactions has continued on both experimental and theoretical fronts. In the previous period, elastic and inelastic scattering had been measured at seven energies spanning the range from 74.2 to 117.1 MeV (lab).³ It was decided that additional measurements at intervening energies were necessary to establish the continuous and regular evolution of the structure in the angular distributions near 90° and to provide a more complete test of any reaction model. The new experimental data were taken at bombarding energies of 78.8, 93.8, 105, 112.0, 117.1, 121.6, and 126.7 MeV and with a different form of PSD having 25 individual sections spaced 0.6° apart. This detector offered a much improved efficiency over the previous detector. The experimental results for the elastic and inelastic scattering compare favorably with the previous results and do indeed show a regular change in the structure of the angular distributions with bombarding energy.

The inelastic scattering to the 2^+ (4.43-MeV) state and the mutual excitation of these states is known to be very intense as a result of the large $E2$ transition matrix element connecting the ground and the first excited state of ^{12}C . This raises the question as to whether single or multiple nucleon transfers might also be strong processes. Measurements of these processes would be important for a reaction model that included the effect of "double transfer" on the elastic scattering.

Because relatively few experimental data on these particular transfer reactions at high energies were

available, we chose to measure fairly complete angular distributions at 93.8 MeV, using two solid-state ΔE - E counter telescopes for this purpose. Figure 1.36 shows a representative energy spectrum for one of the reaction products, ^{10}B . There are only a few strong peaks in the spectrum even though a large number of excited states are available. Figure 1.37 compares elastic and inelastic angular distributions (at 93.8 MeV) with those for representative one-nucleon and two-nucleon (pn) transfer reactions. Data for nn , pp , and $p2n$ transfers are not shown in Fig. 1.37; these were observed in some of the ΔE - E spectra with cross sections much smaller than those of the one-nucleon and pn transfer reactions. The angular distributions for proton and neutron transfer reactions are similar (as would be expected from isospin symmetry) and are more forward-peaked than for pn transfer reactions.

Both the selectivity of the transfer reactions and the structure in the angular distributions are typical of direct reaction processes. We see in Fig. 1.37 that cross sections for the strongest transfer reactions are a factor $\gtrsim 10$ smaller than for elastic or inelastic scattering to low-lying states. The single transfer is of interest in addition to its usefulness in calibration for calculations of double-transfer processes; it will be valuable to know how well the optical potentials derived from elastic scattering will do in DWBA analysis of these transfer reactions.

Significant progress has been achieved in the analysis of the elastic and inelastic scattering. We found that the

shallow real potentials introduced by the Yale group produced quite adequate fits to the experimental data at angles less than $\theta_{c.m.} \sim 45^\circ$. However, at angles greater than 60° , the quality of the fits deteriorated, with the predicted cross sections tending to be too small. Various attempts were made using Woods-Saxon potentials to improve this situation, but none was particularly successful. The introduction of potentials derived from the folding model,⁴ however, has resulted in a marked improvement in the overall quality of the fits in the back-angle region while maintaining an equally good quality in the forward-angle region. Although both types of potential are similar in the external region, $6 \lesssim r \lesssim 7$ fm, the folded potentials are significantly more attractive in the region $r < 5$ fm. It also appears that good fits to the data require that the scattering be sensitive to the potential in the region 3 to 5 fm. This is because shallow imaginary Woods-Saxon potentials provide superior fits to the data and, it may be shown, are sufficiently transparent that a change in the real potential at $r \sim 3$ fm has a noticeable effect on the predicted cross sections. It thus appears that the real potential in this interior region of 3 to 5 fm is more attractive than has been indicated by optical-model analyses of data at lower energies.

Folded potentials derived by using several forms for the nucleon-nucleon interaction were investigated. The Gaussian interaction required a normalization factor of $N \sim 0.6$, whereas a Yukawa interaction gave $N \sim 1.0$. In all cases, the fits to the data were comparable, and the

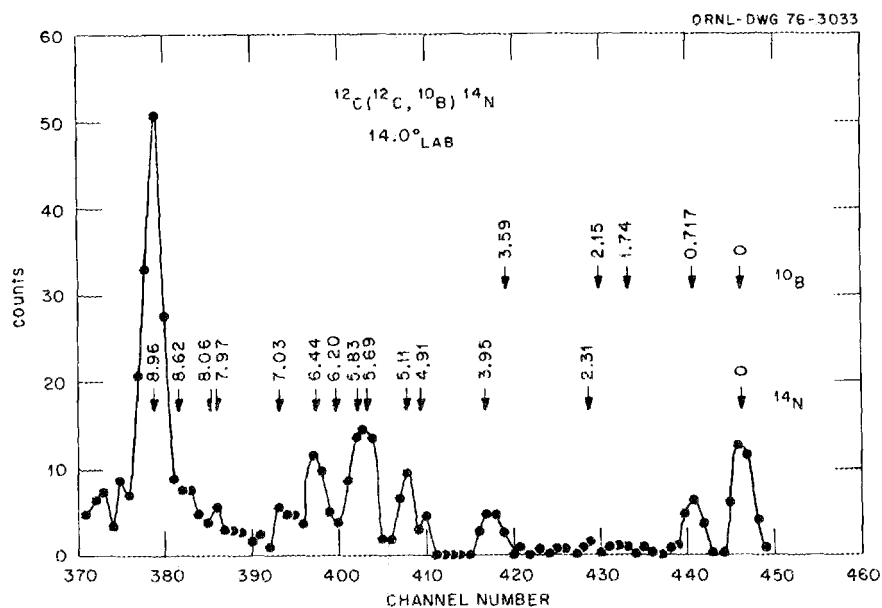


Fig. 1.36. Energy spectrum of ^{10}B ions observed in the $^{12}\text{C}(^{12}\text{C}, ^{10}\text{B})^{14}\text{N}$ reaction at $E_{\text{lab}} = 93.8$ MeV and $\theta_{\text{lab}} = 14^\circ$. Excited states in ^{14}N below 9 MeV and in ^{10}B below 3.6 MeV are indicated by the arrows to illustrate the selective nature of the reaction.

value of N was independent of the bombarding energy and similar to the values of N found for a variety of different heavy-ion systems including, for example, $^{16}\text{O} + ^{208}\text{Pb}$. Recently, a more "realistic" nucleon-nucleon interaction has been derived by Bertsch et al.⁵ from the Reid potential. Although we have not investigated this potential as extensively for the elastic scattering, it appears to give comparable results for $N = 1.05$. The important feature seems to be the greater strength of the folded potential in the interior region, and not so much the particular form of the interaction used in the folding procedure.

Figure 1.38 shows measured and predicted angular distributions for the elastic and inelastic scattering at

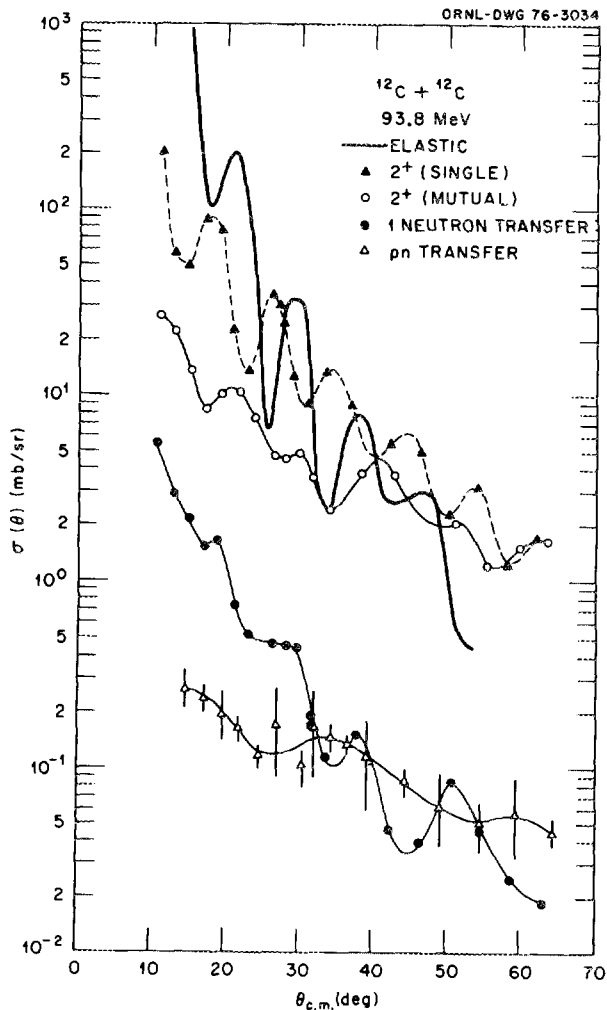


Fig. 1.37. A comparison of the angular distributions for elastic and inelastic scattering and for transfer reactions at 93.8 MeV. Data are shown for the transfer to the ground states; the data for the excited states are similar.

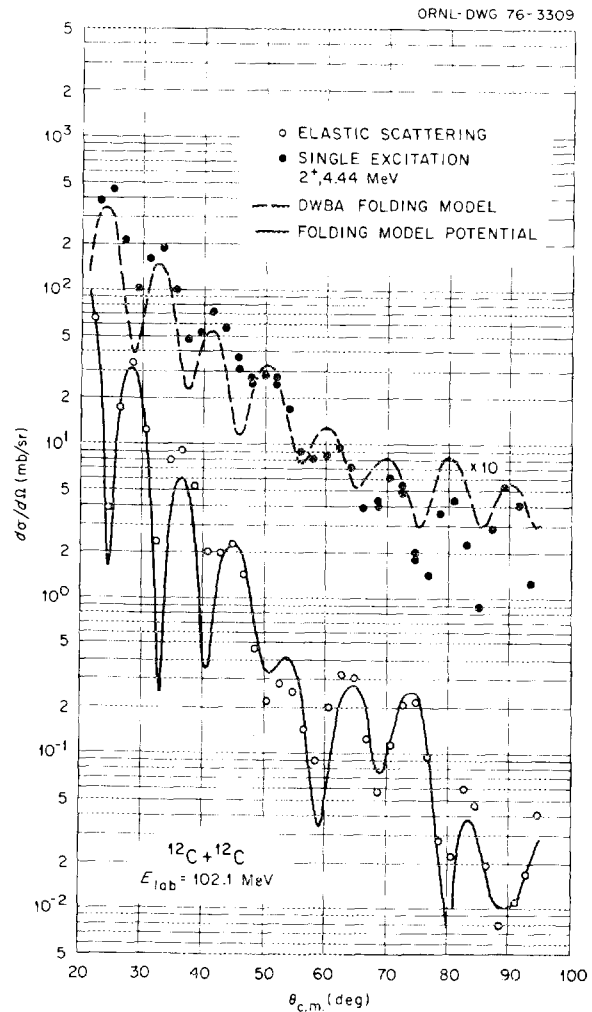


Fig. 1.38. Elastic and inelastic scattering at 102 MeV. The inelastic scattering is the sum of the two reactions $^{12}\text{C}[^{12}\text{C}, ^{12}\text{C}(2^+)]^{12}\text{C}$ and $^{12}\text{C}(^{12}\text{C}, ^{12}\text{C})^{12}\text{C}(2^+)$. The theoretical curves are obtained using real potentials from the folding model and transition densities as described in the text and with an imaginary potential given by $W = 13.9$ MeV, $r_0 = 1.22$, and $a = 0.54$.

102 MeV. The potentials were obtained from the "realistic" interaction described above. The excitation of the 2^+ state was calculated with the DWBA using a folding-model form factor. In this case, the transition density was taken from electron-scattering data with the assumption that the neutron and proton densities are the same. Complex coupling was included by deforming the Woods-Saxon imaginary potential. Because the normalization for the real potential and the parameters for the imaginary potential were determined by the elastic scattering, the calculation of the 2^+

excitation does not involve any adjustable parameters. The agreement is seen to be quite good in this case.

1. Oak Ridge Associated Universities faculty research participant, 1975, from Franklin and Marshall College, Lancaster, Pa.
2. Consultant with the Physics Division.
3. R. G. Stokstad et al., *Phys. Div. Annu. Prog. Rep. Dec. 31, 1974*, ORNL-5025 (1975), p. 46.
4. J. B. Ball et al., *Nucl. Phys. A252*, 208 (1975).
5. G. Bertsch et al., to be published.

NUCLEAR REORIENTATION EFFECT FOR INELASTIC HEAVY-ION SCATTERING

F. Todd Baker¹ Alan Scott¹
D. C. Hensley D. L. Hillis
E. E. Gross

We have begun a survey of the ($^{12}\text{C}, ^{12}\text{C}'$) reaction at 41 MeV from *s-d*-shell nuclei. The projectile energy is sufficiently high for the angular distributions for excitation of the first 2^+ states to have distinct diffraction structure. Coupled-channels (CC) calculations reveal that the predicted phase of this diffraction structure is quite sensitive to the assumed quadrupole moment of the excited state; this sensitivity is due mainly to interference between the direct ($0^+ \rightarrow 2^+$) and direct-plus-reorientation ($0^+ \rightarrow 2^+ \rightarrow 2^+$) nuclear (not Coulomb) amplitudes.

Preliminary calculations show ^{26}Mg to be prolate and ^{28}Si to be oblate. Data for excitation of the first 2^+ state of ^{30}Si are quite different from the ^{28}Si data, which suggests that ^{30}Si is probably prolate. We plan to continue this survey by acquiring data from ^{24}Mg and ^{32}S .

1. University of Georgia, Athens.

INELASTIC SCATTERING AND TRANSFER REACTIONS FROM ^{12}C IONS ON ^{90}Zr

S. T. Thornton^{1,2} J.L.C. Ford, Jr.
D. E. Gustafson^{1,2} K. S. Toth
D. C. Hensley

Studies of heavy-ion reactions to final states indicate that kinematically well-matched one-nucleon transfer reactions³⁻⁵ may be well described by DWBA calculations. However, in cases of poor kinematic matching the angular distributions predicted by the DWBA do not agree with the data, although reasonable spectroscopic factors may be obtained.³⁻⁷

Because of the simple shell-model picture in the ^{90}Zr mass region, we have studied the $^{90}\text{Zr}(^{12}\text{C}, ^{12}\text{C}')^{90}\text{Zr}^*$,

$^{90}\text{Zr}(^{12}\text{C}, ^{11}\text{C})^{91}\text{Zr}$, and $^{90}\text{Zr}(^{12}\text{C}, ^{11}\text{B})^{91}\text{Nb}$ reactions at 98-MeV incident energy. Angular distributions have been obtained for transitions to several states of the residual nuclei. Nuclear-Coulomb interference effects were observed in the inelastic scattering. By using DWBA calculations with collective form factors, deformation parameters β_N and β_C were obtained for the lowest 2^+ and 3^- states in ^{90}Zr . The transfer reactions were analyzed using a finite-range, recoil DWBA code, and spectroscopic factors were obtained for comparison with results from previous light-ion bombardments.

The 98-MeV ^{12}C ions obtained with ORIC were used to bombard a target of $50 \mu\text{g}/\text{cm}^2$ of enriched ^{90}Zr evaporated onto a thin carbon foil. The reaction products were detected in a 60-cm-long position-sensitive proportional counter located at the focal plane of the broad-range magnetic spectrograph.

The Q values for the $^{90}\text{Zr}(^{12}\text{C}, ^{11}\text{C})$ and $^{90}\text{Zr}(^{12}\text{C}, ^{11}\text{B})$ reactions are -11.519 and -10.798

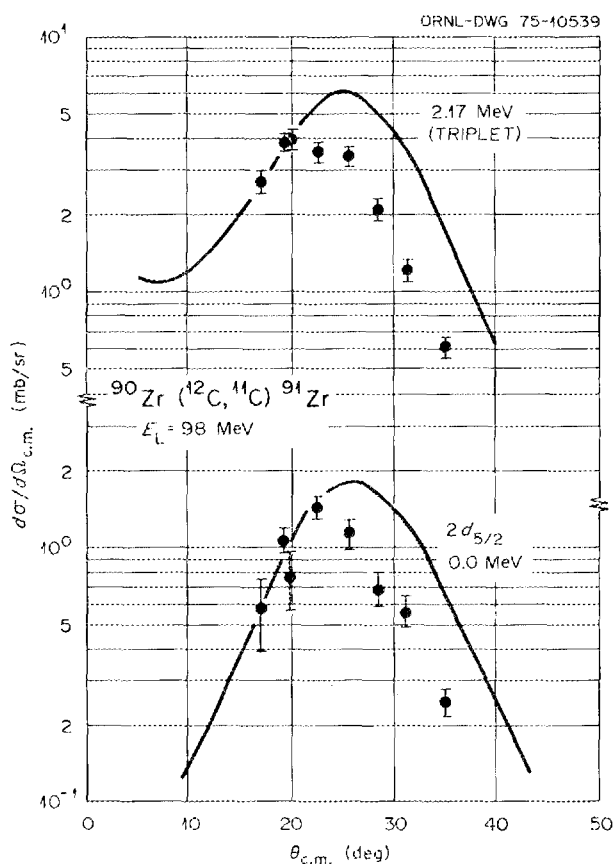


Fig. 1.39. Center-of-mass angular distributions for the $^{90}\text{Zr}(^{12}\text{C}, ^{11}\text{C})^{91}\text{Zr}$ reaction measured at an incident energy of 98 MeV in the present experiment. The data at 2.17 MeV probably represent contributions from two or more levels. The solid lines are DWBA predictions.

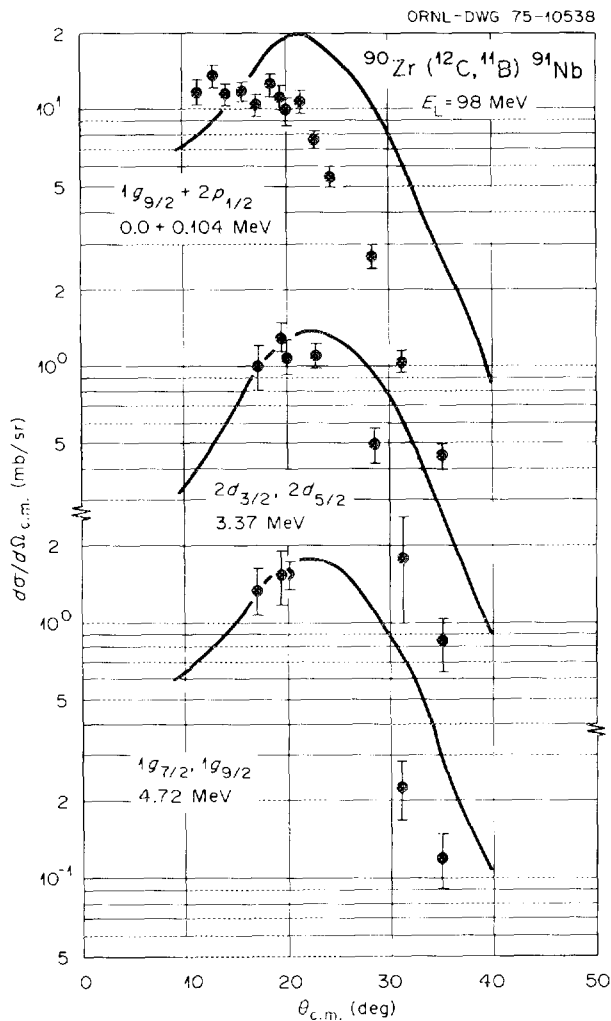


Fig. 1.40. Center-of-mass angular distributions for the $^{90}\text{Zr}(^{12}\text{C}, ^{11}\text{B})^{91}\text{Nb}$ reaction measured at an incident energy of 98 MeV in the present experiment. The ground state and the 0.104-MeV state were unresolved. The solid lines are DWBA predictions. For the 3.37- and 4.72-MeV levels, predictions were made with two choices of nj that resulted in similar angular distribution shapes.

MeV respectively. The difference in the entrance and exit channels orbital angular momentum is about $7\hbar$, and for this reason, effects due to poor angular momentum matching are possible.

The fits to the angular distributions for states observed in ^{91}Zr and ^{91}Nb are shown in Figs. 1.39 and 1.40. The results of the finite-range, recoil DWBA calculations are not in good agreement with the transfer reaction data. The magnitudes of the calculated cross sections are reasonable and yield spectroscopic factors consistent with light-ion-induced results. However, the theoretical curves disagree with the shape of the

measured angular distributions. The predicted peak angle of the angular distributions is about 5° larger than the observed peak angles. Reasonable changes in the optical-model parameters will not account for the discrepancy.

We believe that these transfer reaction data, therefore, indicate a clear failing of the DWBA. The present reactions should populate good single-particle states, and the incident energy is well above the Coulomb barrier. The disagreement seems to be associated with the large angular momentum mismatch between the entrance and exit channels.

1. Department of Physics, University of Virginia, Charlottesville (research supported in part by the National Science Foundation).
2. Travel to Oak Ridge supported in part by the Oak Ridge Associated Universities and the Southern Regional Education Board.
3. J.L.C. Ford, Jr., et al., *Phys. Rev. C* **10**, 1429 (1974).
4. K. S. Low and T. Tamura, *Phys. Rev. C* **10**, 789 (1975).
5. D. G. Kovar, p. 189 in *Proceedings of the International Conference on Reactions Between Complex Nuclei, Nashville, Tenn., June 1974*, vol. 2, R. L. Robinson et al., Eds., North-Holland, Amsterdam, 1974.
6. J. S. Larsen et al., *Phys. Lett.* **42B**, 205 (1972).
7. F. D. Becchetti et al., *Phys. Rev. C* **12**, 894 (1975).

ELASTIC AND INELASTIC SCATTERING OF 70-MeV ^{12}C IONS FROM THE EVEN NEODYMIUM NUCLEI

D. L. Hillis¹ L. D. Rickertsen
 E. E. Gross C. R. Bingham²
 D. C. Hensley A. Scott³
 F. T. Baker³

Measurements of differential cross sections for the scattering of 70-MeV ^{12}C ions from the 0^+ , 2^+ , 4^+ , and 3^- states of $^{142,144,146,148,150}\text{Nd}$ have been completed. In addition, we have obtained cross sections for exciting the 2^+ state of the beam projectile and the 6^+ state of ^{150}Nd . When analyzed with the coupled channels (CC) method, these data show an unexpected sensitivity to electric multipole moments.

Elastic scattering systematics are summarized in Fig. 1.41, where the ratio-to-Rutherford cross sections for all isotopes are displayed. The main feature here is the dampening of oscillations with increasing target mass and increasing target β_2 deformation. This effect is undoubtedly due to the removal of elastic flux by excitation of the low-lying 2^+ state and the rotational band built on this state. The strong-coupling effects apparent in the elastic scattering data of Fig. 1.41

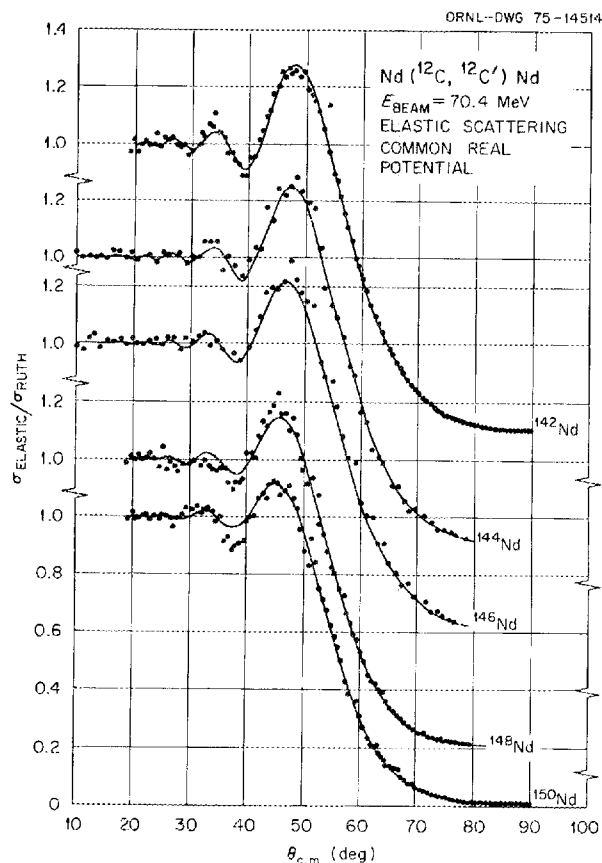


Fig. 1.41. Elastic scattering data for 70.4-MeV ^{12}C scattered from the even neodymium isotopes. The calculations (solid curves) are optical-model fits with the parameters of Table 1.3.

prompted us to search for an optical potential that had a real part common to all the neodymium nuclei and an imaginary part that accounted for the differences between them. It was then hoped that a CC analysis^{4,5} starting with such a potential would eventually lead to a more universal potential because the many absorptive effects would be explicitly handled. These hopes were essentially realized.

The fits of Fig. 1.41 are optical-model fits with the parameters of Table 1.3. The real part of the potential is common to all targets, but a drastic change in imaginary geometry is then required to fit the more deformed ^{148}Nd and ^{150}Nd . These potentials were used in DWBA calculations for inelastic excitation, and they were used as the starting potentials in a CC analysis of the data.

The main features of these calculations are illustrated in Fig. 1.42 for the ^{144}Nd data and in Fig. 1.43 for the ^{150}Nd data. In these calculations, we have taken the view that nuclear deformation lengths should be equal

to Coulomb deformation lengths and that, where available, we take Coulomb matrix elements from previous Coulomb excitation measurements.^{6,7} Before performing the CC calculations with the couplings shown in Fig. 1.42, we made a search on W and a' with couplings only between the 0^+ and 2^+ states. When this new potential was used in a full CC calculation

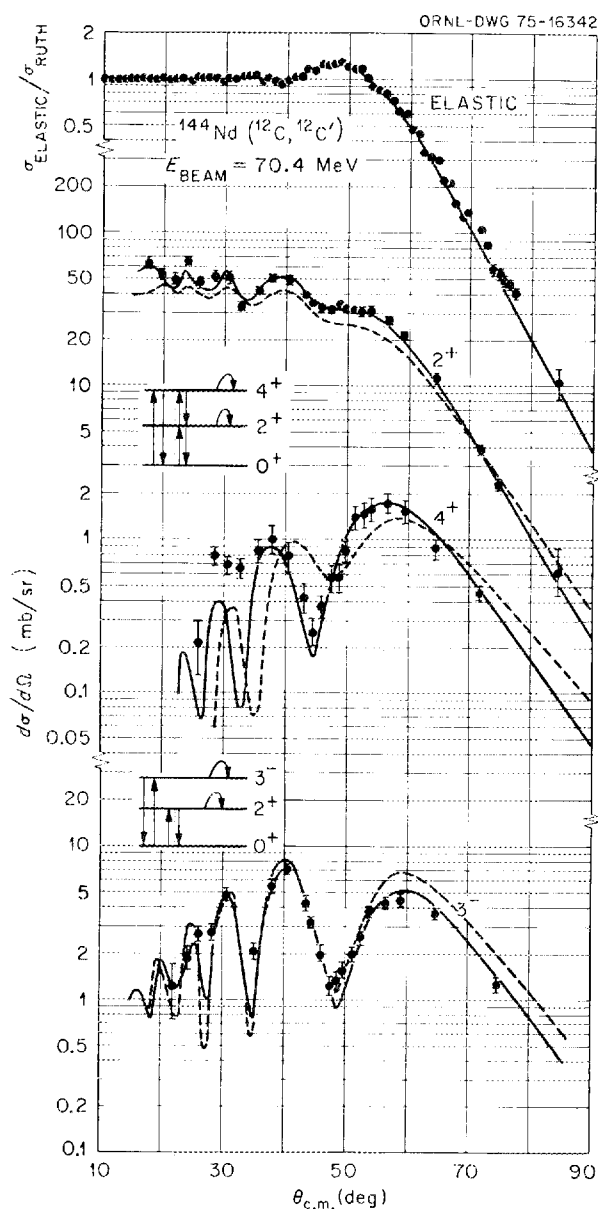


Fig. 1.42. 70.4-MeV ^{12}C elastic and inelastic scattering from ^{144}Nd . The dashed curves are DWBA calculations, and the solid curves are CC calculations including the couplings shown as insets. Known matrix elements (refs. 6 and 7) are used throughout with $\beta_4^C = 0.053$ deduced from the CC analysis.

including the 4^+ state or the 3^- state, we still had an excellent fit to elastic scattering.

The dotted curves of Fig. 1.42 are the DWBA calculations, which fail to account for various features

Table 1.3. Optical-model parameter set with a common real geometry obtained from fitting the elastic scattering

	^{142}Nd	^{144}Nd	^{146}Nd	^{148}Nd	^{150}Nd
V (MeV)	20	20	20	20	20
r_0 (fm)	1.315	1.315	1.315	1.315	1.315
a (fm)	0.562	0.562	0.562	0.562	0.562
W (MeV)	11.6	12.1	16.3	120.7	142.0
r'_0 (fm)	1.341	1.341	1.341	1.023	1.023
a' (fm)	0.414	0.414	0.414	0.769	0.769
r_c (fm)	1.25	1.25	1.25	1.25	1.25
σ_R (b)	1.249	1.271	1.322	1.547	1.609
χ^2/N	1.9	1.6	3.4	1.8	2.8
β	0.104	0.111	0.138	0.167	0.279

in the data. If the nuclear deformation lengths are reduced by about 30%, then the 3^- state can be fitted. To fit the 2^+ data, an additional upward normalization of the Coulomb deformation length by $\sim 10\%$ is required. The DWBA single-step calculation fails entirely for the 4^+ state. These findings are due to multistep effects, such as recoupling to the ground state in the case of the 2^+ state, quadrupole reorientation in the case of all states, and double $E2$ excitation in the case of the 4^+ state. All these effects can be properly handled in a CC calculation with the excellent results shown as the solid curves in Figs. 1.42 and 1.43. The quadrupole moments for the 3^- states were derived from those measured⁶ for the 2^+ states when assuming a rotational-model relationship. The hexadecapole deformation, β_4 , was the only parameter not derivable from previous Coulomb excitation measurements.

These results demonstrate that Coulomb excitation effects can be extended straightforwardly into the

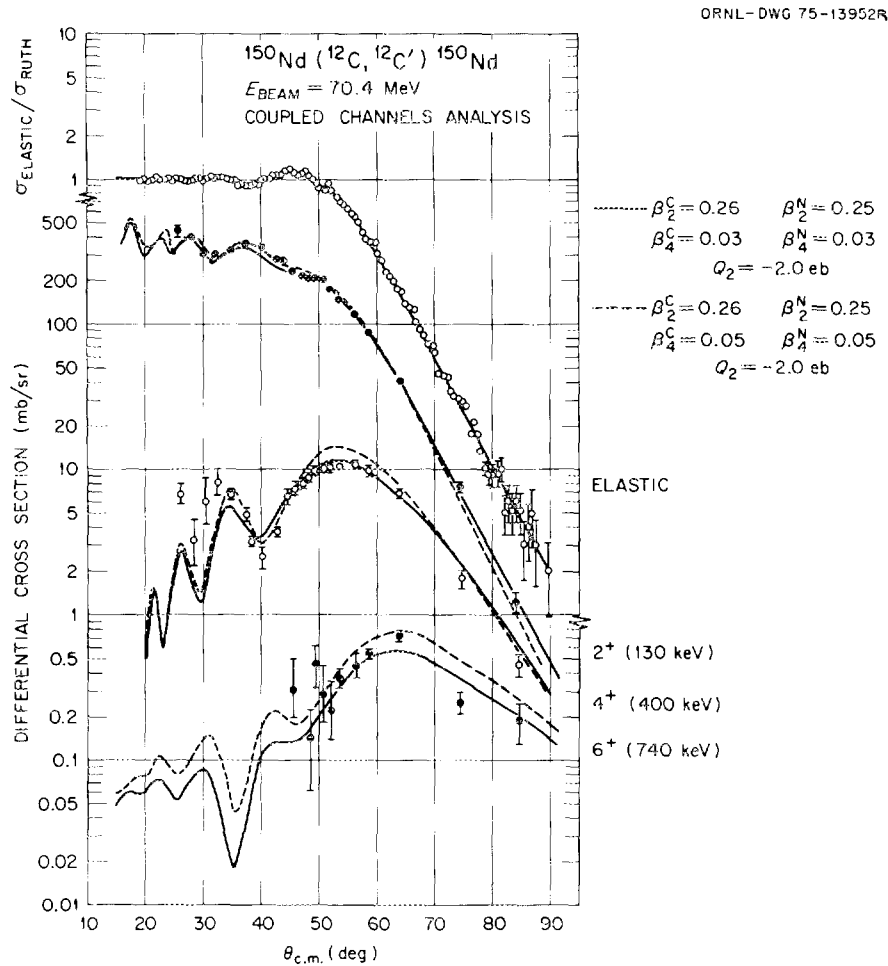


Fig. 1.43. 70.4-MeV ^{12}C elastic and inelastic scattering from ^{144}Nd . The curves are CC calculations using known matrix elements (refs. 6 and 7) and show the sensitivity to the unknown β_4 .

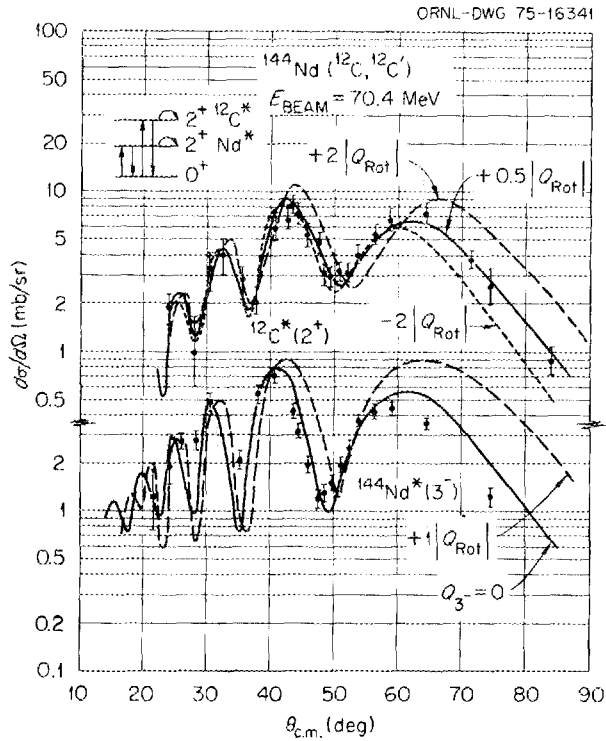


Fig. 1.44. Excitation of the 2^+ (4.43-MeV) state in the ^{12}C projectile and the 3^- (1.51-MeV) state in ^{144}Nd at 70.4-MeV (lab) energy. The curves are CC calculations that illustrate the sensitivity of the calculation and the data to the assumed sign and magnitude of quadrupole moments. Couplings included in the calculations for ^{12}C are shown as an inset in this figure, whereas the couplings used for the 3^- state calculation are shown in Fig. 1.42.

nuclear force domain. Heavy-ion inelastic scattering above the Coulomb barrier can then be used as a probe of nuclear multipole moments as illustrated in Figs. 1.43 and 1.44. Figure 1.43 shows the sensitivity to the value of β_4 . The value of β_2 and the quadrupole moment of the 2^+ state were taken from previous Coulomb excitation measurements.⁶ In Fig. 1.44 we show the 3^- ^{144}Nd data compared to CC calculations with various assumed values for the static quadrupole moment to show the sensitivity to this quantity. The large-angle data, dominated by nuclear excitation, are quite sensitive to the sign and magnitude of the assumed quadrupole moment. Also shown are similar calculations for the 2^+ state of the ^{12}C projectile with the same conclusion. The best fit is consistent with an oblate shape for ^{12}C with a 2^+ static quadrupole moment $\approx 0.5|Q_{\text{Rot}}|$.

1. Oak Ridge Graduate Fellow from the University of Tennessee, Knoxville, under appointment from Oak Ridge Associated Universities.

2. Consultant from University of Tennessee, Knoxville.
3. University of Georgia, Athens.
4. T. Tamura, *Rev. Mod. Phys.* **37**, 679 (1965).
5. J. Raynal, the computer program ECIS, private communication.
6. P. A. Crowley, J. R. Kerns, and J. X. Saladin, *Phys. Rev. C* **3**, 2049 (1971).
7. O. Hansen and O. Nathan, *Nucl. Phys.* **42**, 197 (1963).

MICROSCOPIC DESCRIPTION OF INELASTIC ^{12}C SCATTERING FROM ^{208}Pb

G. R. Satchler D. C. Hensley
 J. L. C. Ford, Jr. E. E. Gross
 K. S. Toth D. E. Gustafson^{1,2}
 S. T. Thornton²

It has been customary to analyze data on the inelastic scattering of heavy ions by using the collective (or deformed optical potential) model.³ However, a more microscopic approach has enjoyed considerable success with light-ion data.⁴ In this, the transition density for the target nucleus, $\rho_{tr}(\mathbf{r})$, is obtained from structure calculations and folded with an effective nucleon-nucleon interaction v . In the heavy-ion case this is further folded into the density distribution $\rho_p(r)$ (assumed spherical) of the projectile. The resulting transition potential,

$$U_{tr}(\mathbf{r}) = \int \rho_p(r_2) \rho_{tr}(\mathbf{r}_1) v(\mathbf{r}_1 - \mathbf{r}_2 - \mathbf{r}) d\mathbf{r}_1 d\mathbf{r}_2,$$

may then be used to calculate the inelastic scattering, for example, in DWBA. This approach is an extension of the double-folding model of the optical potential for elastic scattering,⁵ and we should demand consistency between the elastic and inelastic results.

A previous calculation of this type⁶ used the macroscopic collective model to generate the transition density ρ_{tr} . Instead, we use the results of microscopic random-phase approximation (RPA) hole-particle calculations,⁷ which have previously been shown⁴ to give a good account of the 2^+ and 3^- excitations in the $^{208}\text{Pb}(p,p')$ reaction using a similar model.

The 98-MeV incident ^{12}C ions were scattered from a target consisting of 100 $\mu\text{g}/\text{cm}^2$ of enriched ^{208}Pb evaporated onto a 40- $\mu\text{g}/\text{cm}^2$ carbon foil, and the reaction products were detected in a 60-cm-long position-sensitive proportional detector placed in the focal plane of a broad-range spectrograph. The experimental procedure has been described elsewhere.⁸ Angular distributions were measured between 24° and 58° in the center-of-mass system for the 3^- , 5^- , and 2^+ states at 2.61, 3.20, and 4.10 MeV in ^{208}Pb respectively. An additional state was observed at about 5.5

MeV in ^{208}Pb for which a definite spin assignment has not been made. Figures 1.45 and 1.46 display the measured inelastic angular distributions; only statistical errors are shown, and it is estimated that the total uncertainties are at least $\pm 10\%$. At a center-of-mass angle of about 42° , where nuclear absorption begins to reduce the elastic cross section below the Rutherford value, interference effects are seen in the inelastic data, particularly for the 3^- level.

Microscopic calculations were made for the three lowest states using the RPA transition densities⁵ [the 5^- density was increased by 15% to match the observed $B(E5)$ value^{9,10}]. A spin-independent Gaussian form was chosen for v . The present work also assumed a Gaussian form, $0.313 \exp(-0.2763r^2)$ (with r in femtometers), for the ^{12}C density; this gave the same results for elastic scattering as the shell-model form previously used.^{5,11,12} Each choice for v was nor-

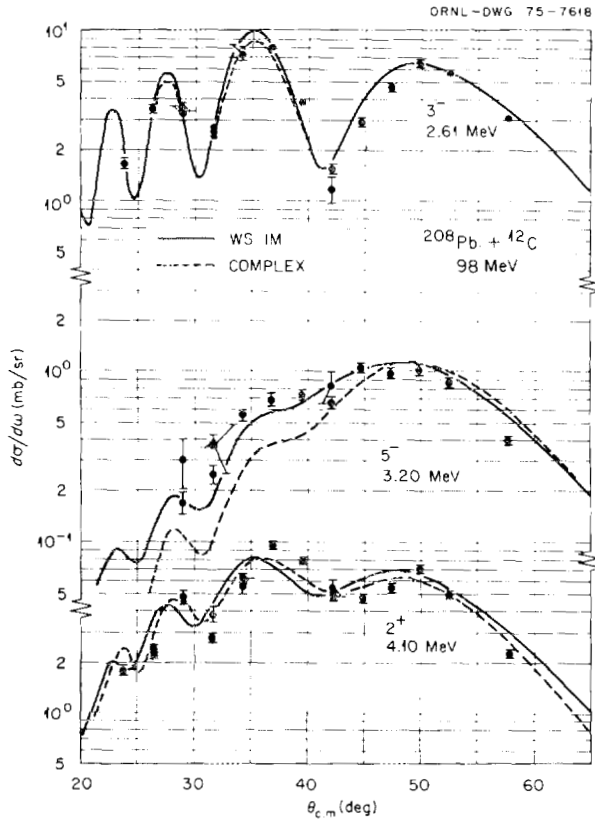


Fig. 1.45. Measured differential cross sections for inelastic scattering of ^{12}C ions from ^{208}Pb at an incident energy of 98 MeV. Only statistical errors are shown. The curves are microscopic calculations using RPA transition densities and a Gaussian interaction of 1-fm range. WSIM refers to a deformed Woods-Saxon imaginary coupling term; COMPLEX implies a complex strength for the Gaussian interaction.

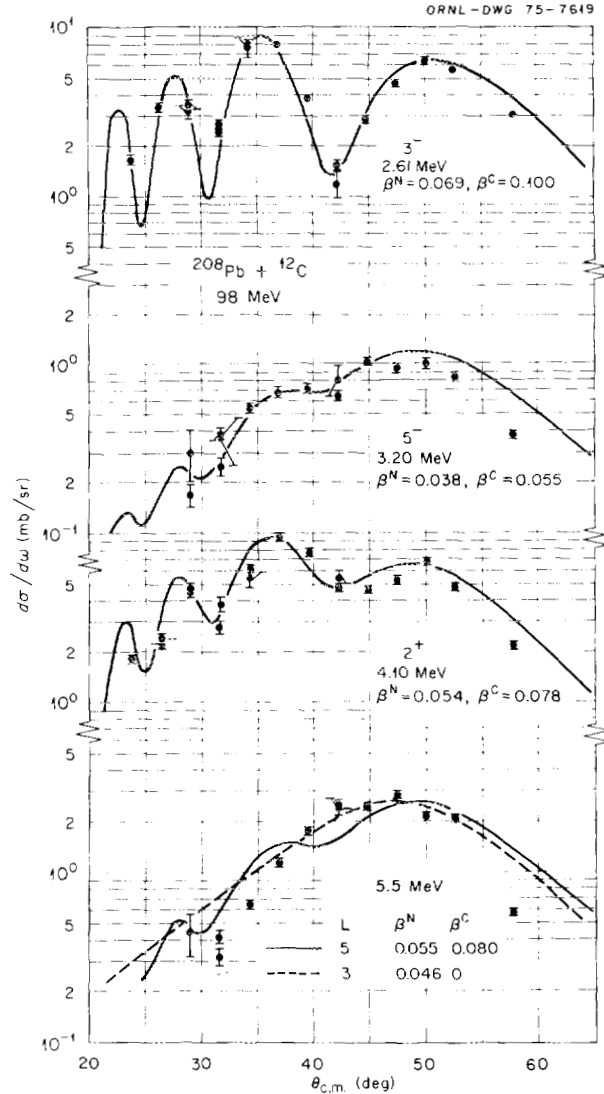


Fig. 1.46. Measured differential cross sections compared to collective-model predictions. β^N and β^C refer to the potential and charge deformation parameters used. A Woods-Saxon potential was used with $V = 40$ MeV, $W = 25$ MeV, $R = 10.32$ fm, and $a = 0.56$ fm.

malized by fitting the elastic data¹¹ at 96 MeV, and the corresponding folded optical potentials were used in the DWBA calculations of the inelastic scattering. Coulomb excitation was included, assuming $B(E2) = 2965e^2 \text{ fm}^4$, $B(E3) = (0.58 \times 10^6)e^2 \text{ fm}^6$, and $B(E5) = (4.5 \times 10^8)e^2 \text{ fm}^{10}$ (ref. 9) respectively. The imaginary interaction, which is essential in order to fit the data, was chosen in the two ways described above; the Woods-Saxon form that fits the elastic data^{11,12} has $W = 15$ MeV, $R = 10.76$ fm, and $a = 0.52$ fm, in a standard notation. This was used in the inelastic calculations

with deformation parameters $\beta_2^N = 0.036$, $\beta_3^N = 0.073$, and $\beta_5^N = 0.038$. These were obtained in the usual way from the $B(EL)$ values using a charge radius of 7.11 fm and scaling so that $\beta R = \text{constant}$.

As shown in Fig. 1.45, good fits were obtained with a Gaussian v with a range of 1 fm, except that the 2^+ cross section had to be increased by a factor of 2 (the same 2^+ enhancement is needed when the collective model is used -- see below -- and is not understood). The strengths, obtained from fitting the elastic data, are $(115.5 + 79.2i)$ MeV, or 126.2 MeV if the Woods-Saxon imaginary part is used. The latter version gives a slightly better fit to the elastic scattering and is significantly better for the 5^- inelastic excitation (see Fig. 1.45).

Consequently, we conclude that the present data require an interaction with a range shorter than that of the bare interaction between nucleons.

For comparison, results for the conventional collective model³ are shown in Fig. 1.46. Good fits are obtained, although again the data require that the 2^+ coupling strength be increased by about 40%. A group with an excitation energy near 5.5 MeV has been reported with either $L = 5$ (ref. 13) or $L = 3$ (refs. 14 and 15). As seen in Fig. 1.46, the present data agree best with $L = 5$ unless the scattering is due to an $L = 3$ transition without Coulomb excitation, which seems very unlikely for such a strong transition.

We used the codes ATHENA, DWUCK, and GENOA. In the DWBA calculations, 250 ($L = 2$) or 203 ($L = 3, 5$) partial waves were used, and the integrations were carried out to 45 fm ($L = 2$) or 35 fm ($L = 3, 5$).

1. Research participation at Oak Ridge National Laboratory sponsored in part by Oak Ridge Associated Universities.

2. University of Virginia, Charlottesville (research supported in part by the National Science Foundation).

3. See, for example, J.L.C. Ford, Jr., et al., *Phys. Rev. C* 8, 1912 (1973).

4. See, for example, G. R. Satchler, *Z. Phys.* 260, 209 (1973).

5. See review by G. R. Satchler, *Proceedings of the International Conference on Reactions Between Complex Nuclei, Nashville, Tenn., June 1974*, vol. 2, R. L. Robinson et al., Eds., North-Holland, Amsterdam, 1974.

6. C. B. Dover, P. J. Mofa, and J. P. Vary, *Phys. Lett.* 56B, 4 (1975).

7. P. Ring and J. Speth, *Nucl. Phys.* A235, 315 (1974).

8. J.L.C. Ford, Jr., et al., *Phys. Rev. C* 10, 1429 (1974).

9. A. R. Barnett and W. R. Phillips, *Phys. Rev.* 186, 1205 (1969).

10. M. Nagao and Y. Torizuka, *Phys. Lett.* 37B, 383 (1971).

11. G. R. Satchler, *Phys. Lett.* 55B, 167 (1975).

12. J. B. Ball et al., to be published in *Nuclear Physics*.

13. H. W. Kendall and J. Oeser, *Phys. Rev.* 130, 245 (1963).

14. J. Alster, *Phys. Rev.* 141, 1138 (1966).

15. M. B. Lewis, F. E. Bertrand, and C. B. Fulmer, *Phys. Rev. C* 7, 1966 (1973).

ANALYSIS OF THE ($^{12}\text{C}, ^{13}\text{C}$) AND ($^{12}\text{C}, ^{11}\text{B}$) REACTIONS INDUCED BY ^{12}C ON ^{208}Pb

K. S. Toth E. E. Gross
J.L.C. Ford, Jr. D. C. Hensley
G. R. Satchler S. T. Thornton¹
T. C. Schweizer¹

Earlier, we determined angular distributions for the ($^{12}\text{C}, ^{13}\text{C}$) and ($^{12}\text{C}, ^{11}\text{B}$) reactions induced on ^{208}Pb by 77-, and 98-, and 116-MeV ^{12}C ions.² Surprisingly, these data showed that for the proton-stripping reaction the peak angles remained constant with increasing excitation energy in ^{209}Bi . Last year, we presented new data that had been obtained for the same two reactions at a bombarding energy of 98 MeV.³ These new distributions were measured in smaller angular increments, and once again the same effect was noted for the ($^{12}\text{C}, ^{11}\text{B}$) reaction.

The full finite-range (recoil included) DWBA code LOLA is available at ORNL and has been used to analyze all four single-nucleon transfer reactions induced by ^{11}B incident on ^{208}Pb .⁴ Except for the ($^{11}\text{B}, ^{10}\text{B}$) case, which suffers from an unfavorable matching between incoming and outgoing orbits, the predictions were in good agreement with the data. It was of interest to see if DWBA calculations could account for the $^{12}\text{C} + ^{208}\text{Pb}$ results.

Elastic scattering measurements of 96-MeV ^{12}C ions from ^{208}Pb had already been made.⁵ For completeness we measured elastic scattering in the exit channels, that is, 86.1-MeV ^{13}C on ^{207}Pb and 74.6-MeV ^{11}B on ^{209}Bi . The three sets of data, together with the optical-model fits to the angular distributions, are shown in Fig. 1.47. The parameters derived from these fits were then used to analyze the transfer-reaction results.

The LOLA predictions and experimental data (at 98 MeV) for the ($^{12}\text{C}, ^{13}\text{C}$) and ($^{12}\text{C}, ^{11}\text{B}$) reactions are shown in Figs. 1.48 and 1.49 respectively. It is seen that the DWBA accounts reasonably well for the ($^{12}\text{C}, ^{13}\text{C}$) angular distributions except perhaps at forward angles where count-rate problems were encountered from the large elastic scattering cross section. In Fig. 1.49, however, one notes that whereas the experimental peak angles stay constant with excitation energy in ^{209}Bi , the predicted values shift to larger values. This is also evident in Fig. 1.50, where we show the 77- and 116-MeV data for the ($^{12}\text{C}, ^{11}\text{B}$) reaction; disagreement is most marked at the 77-MeV bombarding energy. The

dashed curve that fits the differential cross section for the 3.12-MeV ^{209}Bi state was calculated by arbitrarily increasing the ^{11}B r_0 parameter from the elastic scattering value of 1.308 to 1.4 fm. We should add that the 98-MeV data could also be fitted if the r_0 value was increased to 1.35 fm.

As in the ($^{11}\text{B}, ^{10}\text{B}$) case mentioned above, the ($^{12}\text{C}, ^{11}\text{B}$) reactions suffer from mismatching between the entrance and exit channels. This may account for the failure of the DWBA analysis. However, the

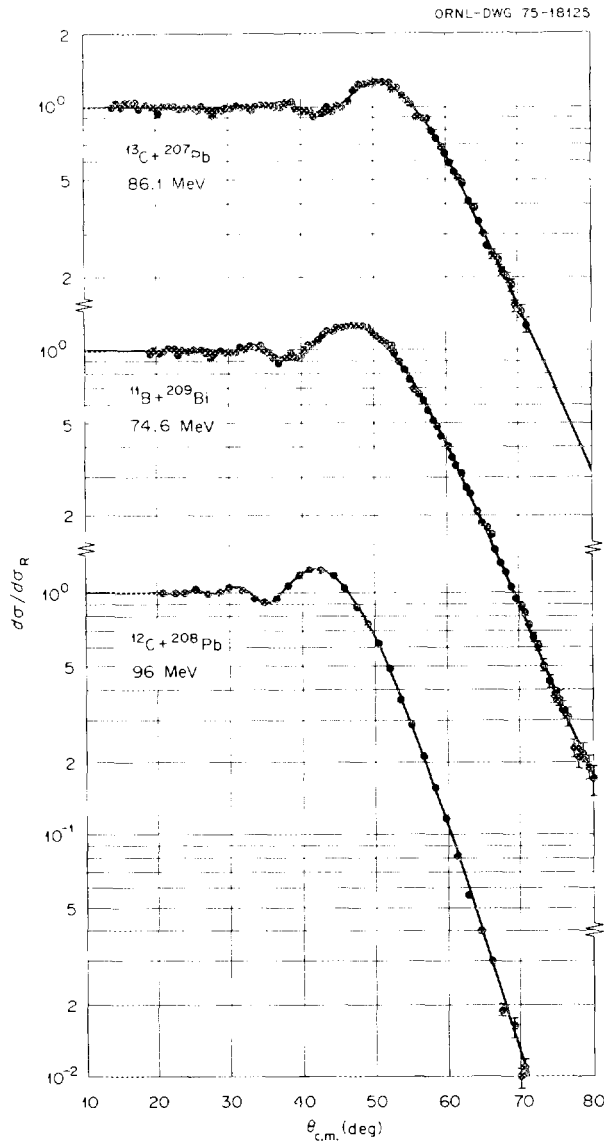


Fig. 1.47. Elastic scattering angular distributions for 96-MeV ^{12}C on ^{208}Pb , 74.6-MeV ^{11}B on ^{209}Bi , and 86.1-MeV ^{13}C on ^{207}Pb . Curves through the data points are optical-model fits. Parameters derived from these fits were used in DWBA analyses of the $^{208}\text{Pb}(^{12}\text{C}, ^{13}\text{C})^{207}\text{Pb}$ and $^{208}\text{Pb}(^{12}\text{C}, ^{11}\text{B})^{209}\text{Bi}$ transfer-reaction data.

indications are that at all three bombarding energies the disagreement with the data becomes progressively more pronounced as the excitation energy in ^{209}Bi increases.

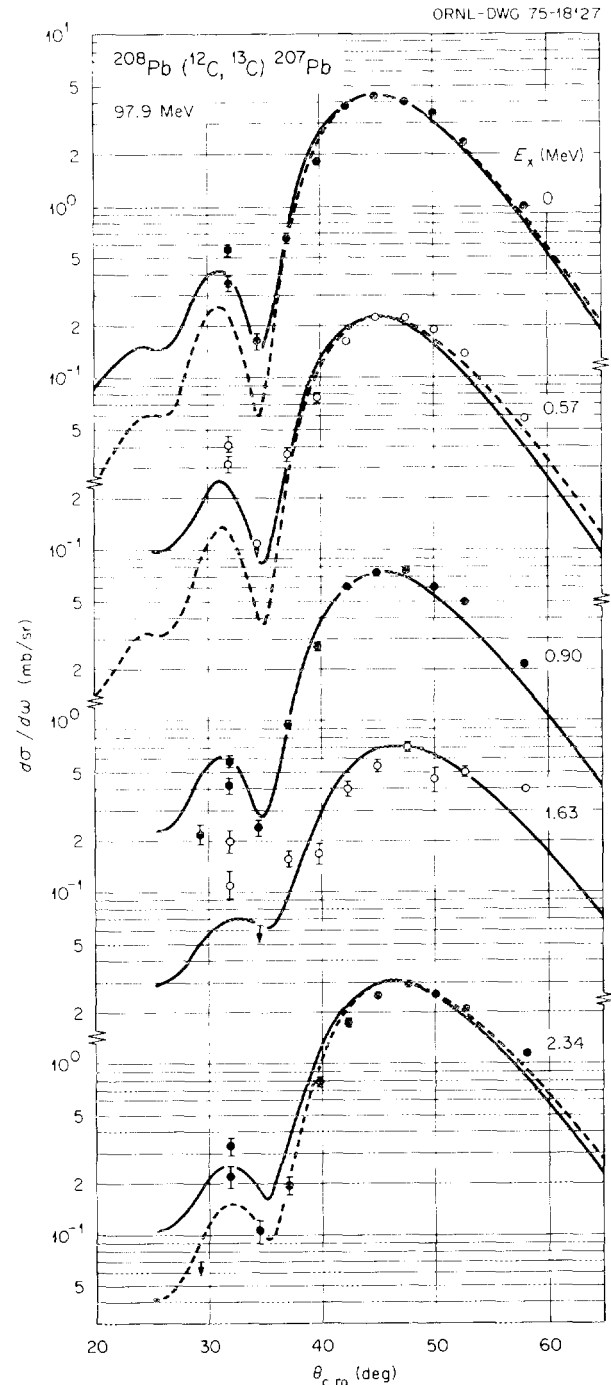


Fig. 1.48. Angular distributions obtained at an incident energy of 97.9 MeV for $^{208}\text{Pb}(^{12}\text{C}, ^{13}\text{C})^{207}\text{Pb}$ reactions leading to residual states in ^{207}Pb . Curves are DWBA calculations; solid and dashed curves represent calculations made with a Woods-Saxon and a folded potential respectively.

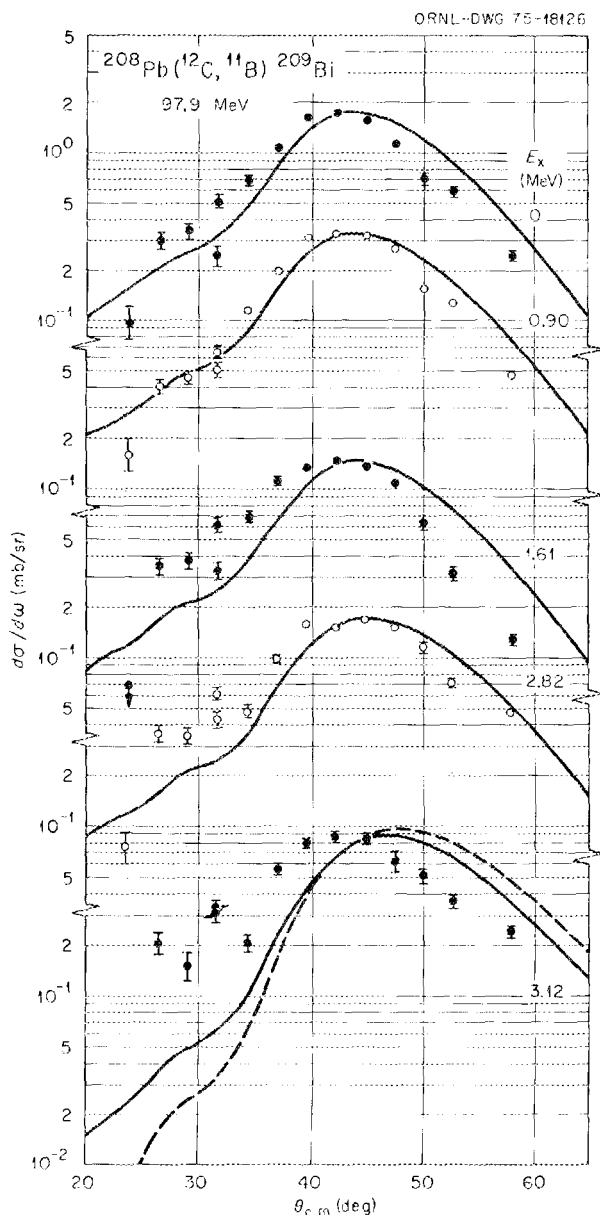


Fig. 1.49. Angular distributions obtained at an incident energy of 97.9 MeV for $^{208}\text{Pb}(^{12}\text{C}, ^{11}\text{B})$ reactions leading to residual states in ^{209}Bi . Curves are DWBA calculations; solid and dashed curves represent calculations made with a Woods-Saxon and a folded potential respectively. Note that the data, in contrast to the predictions, do not show a shift in the peak angle with increasing excitation energy in ^{209}Bi .

Unfortunately, the quality of the $^{208}\text{Pb}(^{11}\text{B}, ^{10}\text{B})$ data was such that it was not possible to say whether this same specific effect was also present in that instance.

The spectroscopic factors extracted for both the ($^{12}\text{C}, ^{13}\text{C}$) and ($^{12}\text{C}, ^{11}\text{B}$) reactions on ^{208}Pb were close to values obtained in other light- and heavy-ion

experiments. The same was true for the $^{208}\text{Pb}(^{11}\text{B}, ^{10}\text{B})$ reaction⁴ despite the fact that the calculations did not reproduce the angular distributions. This has also been found (see elsewhere in this report) for transfer reactions induced by ^{12}C on ^{90}Zr .

We conclude by saying that it is now apparent that the DWBA does not account for all of the features found experimentally for heavy-ion single-nucleon transfer reactions. Perhaps this is an indication that CC effects must be considered even in the case of closed-shell target nuclei.

1. University of Virginia, Charlottesville.
2. J. S. Larsen et al., *Phys. Lett.* **92B**, 205 (1972).
3. K. S. Toth et al., *Phys. Div. Annu. Prog. Rep. Dec. 31, 1974*, ORNL-5025 (1975), p. 42.
4. J.L.C. Ford, Jr., et al., *Phys. Rev. C* **10**, 1429 (1974).
5. J. B. Ball et al., *Nucl. Phys.* **A252**, 208 (1975).

HEAVY-ION-INDUCED TRANSFER REACTIONS ON ^{148}Nd

H. Oeschler¹ G. B. Hagemann³
M. L. Halbert² B. Herskind³

In an experiment done at the Niels Bohr Institute, transfer reactions induced by ^{16}O and ^{18}O beams on ^{148}Nd were measured with a time-of-flight setup at 72-MeV incident energy. The angular distributions are bell shapes having their maxima at angles somewhat below the grazing angle. The excitation in the final nuclei takes place, if possible, near the optimum Q value and is spread over 5 MeV for the one-particle transfer reactions and up to 10 MeV for the multi-particle transfers. The cross sections for the individual channels are explained mostly by Q -window considerations. In spite of the differences in the individual channels the total transfer cross section integrated over excitation energy, angle, and all channels turns out to be the same for both ^{16}O and ^{18}O beams. This cross section amounts to 20% of the total reaction cross section and nicely fills the gap between the measured fusion cross section and the total reaction cross section obtained from optical-model calculations based on elastic scattering data.

1. On leave from Max-Planck-Institut für Kernphysik, Heidelberg, Germany.
2. Exchange visitor at Niels Bohr Institute, University of Copenhagen, Denmark, 1974-1975.
3. Niels Bohr Institute, University of Copenhagen, Denmark.

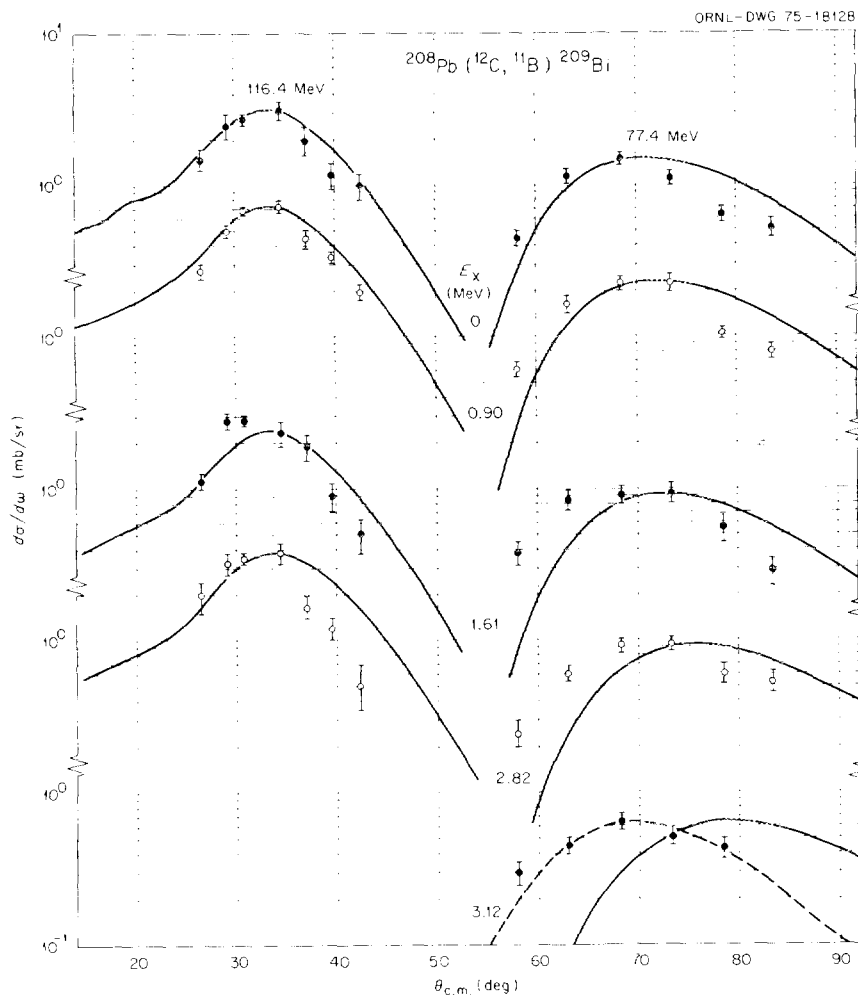


Fig. 1.50. Angular distributions measured at incident energies of 77.4 and 116.4 MeV for the $^{208}\text{Pb}(^{12}\text{C}, ^{11}\text{B})^{209}\text{Bi}$ reaction. Curves represent DWBA analyses. Note the marked shift in peak angle with increasing excitation energy for the predicted curves at 77.4 MeV, in contrast to the data. The dashed curve, which fits the data points for the 3.12-MeV ^{209}Bi excited state, was obtained by arbitrarily increasing the $^{11}\text{B} r_0$ parameter from the elastic scattering value of 1.308 to 1.4 fm.

DECAY RATES FOR EVEN-EVEN $N = 84$ ALPHA EMITTERS AND THE SUBSHELL CLOSURE AT $Z = 64$

W.-D. Schmidt-Ott¹ K. S. Toth

A proton subshell at 64 was first suggested when a discontinuity in the progression of alpha-decay energies for $N = 84$ nuclides was noted at $Z = 64$.² To obtain some theoretical understanding of this subshell closure, Macfarlane, Rasmussen, and Rho³ made calculations using a Gaussian residual force in a Bardeen-Cooper-Schrieffer (BCS) treatment for the proton system of 82-neutron nuclei. By assuming a sufficient spacing between the $d_{5/2}$ and $h_{11/2}$ proton orbitals, their calculations produced a discontinuity in theoretical

binding energies at $Z = 64$. In addition, they calculated relative reduced alpha-decay transition probabilities for the $N = 84$ even nuclei. Once again these theoretical reduced widths indicated a significant dip at $Z = 64$. Maxima were predicted at about $Z = 60$ and $Z = 74$ with the reduced widths decreasing in magnitude as the 50- and 82-proton closed shells were approached. Contrastingly, reduced widths determined from the then available experimental data for ^{144}Nd , ^{146}Sm , ^{148}Gd , ^{150}Dy , ^{152}Er , and ^{154}Yb indicated a general constancy in value except for a dramatic reduction (by about a factor of 2) for ^{150}Dy , that is, at $Z = 66$.³ The ^{150}Dy reduced width was based on an alpha-decay branching ratio of 0.18 ± 0.02 .⁴ A recent measurement, using a high-resolution Ge(Li) x-ray

detector, gave a value of 0.32 ± 0.05 .⁵ This higher value produced a ^{150}Dy reduced width very much in line with those for the other $N = 84$ even alpha emitters. The newer branching ratio has now been confirmed with values of 0.31 ± 0.03 , obtained once again from $K\alpha_1$ x-ray intensities, and 0.36 ± 0.03 , obtained from the ^{150}Dy electron-capture decay scheme.⁶

This large decrease in the ^{150}Dy partial alpha-decay half-life prompted us to examine the data currently available for these $N = 84$ nuclei. It was found that, with the exception of ^{150}Dy , no significantly different half-life measurements had been reported since the survey made in ref. 3. However, the alpha-decay energies of ^{144}Nd , ^{148}Gd , ^{150}Dy , and ^{152}Er were now much more accurately determined. Further, we were in a position to obtain a new determination of the ^{154}Yb alpha-decay energy. Bowman, Hyde, and Eppley⁷ have made available a list of accurate energies for about 40 alpha-emitting nuclides, many of them in the rare-earth region. Most of these, including ^{150}Dy and ^{152}Er , now have quoted errors of ± 3 keV. We reexamined our earlier spectral data⁸ where ^{154}Yb had been observed in the midst of a large number of nuclides appearing on this list.⁷ With the aid of these internal calibration standards we determined the E_α of ^{154}Yb to be 5.318 ± 0.005 MeV. The energy used in ref. 3 was 5.33 ± 0.02 MeV.

As had been done in ref. 3, the reduced widths (δ^2) were calculated using the alpha-decay formalism developed by Rasmussen.⁹ The δ^2 values were determined with the most up-to-date decay energies and half-lives available in the literature. In Fig. 1.51a we have plotted these reduced widths; in Fig. 1.51b we show the δ^2 values listed in Table I of ref. 3. The new determinations shown in Fig. 1.51a, in contrast to those in Fig. 1.51b, indicate that the dip occurs at $Z = 64$ as the BCS calculations predicted.³ Also, in agreement with the calculations, the new reduced widths show an increase in value as $Z = 60$ and $Z = 72$ are approached. Both indications would be more apparent if the error limits in the ^{146}Sm δ^2 value were reduced. The errors are due mainly to the 20-keV uncertainty in the nuclide's alpha-decay energy. Thus a new measurement that could decrease the ^{146}Sm E_α uncertainty to ~ 5 keV would be of great value. We should add that the error limits shown in Fig. 1.51a for the reduced widths are extreme; that is, the upper (lower) limit in each instance was calculated by using the shortest (longest) half-life and the smallest (largest) decay energy. It is not clear how the error limits were determined in ref. 3. However, if the same procedure had been followed, the errors should have been much greater than those shown in Fig. 1.51b because of the large uncertainties in the experimental decay energies available at that time.

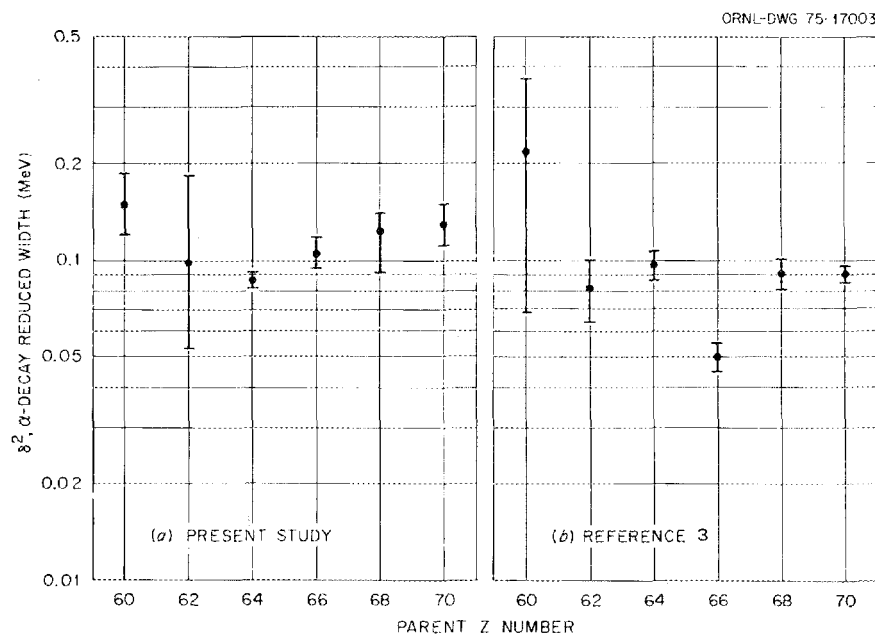


Fig. 1.51. Reduced widths (δ^2) for $N = 84$ even alpha emitters. (a) Calculated using up-to-date experimental information; (b) taken from Table I of ref. 3.

1. E. Physikalisches Institut der Universität, Göttingen, Germany.
2. J. O. Rasmussen, S. G. Thompson, and A. Ghiorso, *Phys. Rev.* **89**, 33 (1953).
3. R. D. Macfarlane, J. O. Rasmussen, and M. Rho, *Phys. Rev.* **134**, B1196 (1964).
4. R. D. Macfarlane and D. W. Seegmiller, *Nucl. Phys.* **53**, 449 (1963).
5. C. R. Bingham et al., *Phys. Rev. C* **7**, 2575 (1973).
6. K. S. Toth, C. R. Bingham, and W.-D. Schmidt-Ott, *Phys. Rev. C* **10**, 2550 (1974).
7. J. D. Bowman, E. K. Hyde, and R. E. Eppley, *Nuclear Chemistry Annual Report*, LBL-1666, Lawrence Berkeley Laboratory, Berkeley, Calif., 1972, p. 4.
8. K. S. Toth et al., *Phys. Rev. C* **7**, 2010 (1973).
9. J. O. Rasmussen, *Phys. Rev.* **113**, 1593 (1959).

PRODUCTION AND INVESTIGATION OF TUNGSTEN ALPHA EMITTERS, INCLUDING THE NEW ISOTOPES ^{165}W AND ^{166}W

K. S. Toth¹ C. R. Bingham²
W.-D. Schmidt-Ott¹ M. A. Ijaz³

The first alpha-radioactive tungsten isotopes, $^{162,163,164}\text{W}$, were discovered by Eastham and Grant⁴ in ^{24}Mg bombardments of ^{144}Sm and ^{147}Sm targets. The purpose of the present investigation was to identify unreported tungsten nuclides with mass numbers slightly greater than 164. The search for these

possible alpha emitters was made by bombarding ^{156}Dy with $^{16}\text{O}^{5+}$ ions accelerated in the ORIC. In addition, to confirm the data of Eastham and Grant,⁴ $^{162,163,164}\text{W}$ were produced by using the more energetic but much less intense $^{16}\text{O}^{6+}$ beam. The ORIC gas-jet-capillary system⁵ was used to transport product nuclei to a collection chamber where they were assayed for alpha radioactivity with (1) an annular Si(Au) detector to study the activity at the collection point and (2) a planar detector, offset by 145° with respect to the collection spot, to determine half-lives.

Figure 1.52 shows an alpha spectrum measured with the planar detector at an ^{16}O bombarding energy of 137.1 MeV. In addition to well-established rare-earth alpha emitters and ^{164}W , two new alpha groups can be seen with energies of 4.909 ± 0.005 and 4.739 ± 0.005 MeV. On the basis of yield curves, $^{14}\text{N} + ^{156}\text{Dy}$ cross bombardments, and alpha-decay energy systematics (Fig. 1.53), these groups were assigned to the new isotopes ^{165}W and ^{166}W respectively.

To confirm the results of Eastham and Grant⁴ we bombarded ^{156}Dy with $^{16}\text{O}^{6+}$ ions ranging in incident energies from 188.6 to 148.1 MeV. Due to low production yields, spectra were accumulated using only the annular detector; half-life information was not obtained. The half-life of ^{164}W ($E_\alpha = 5.146$ MeV), however, was determined in the 137.1-MeV multiscale

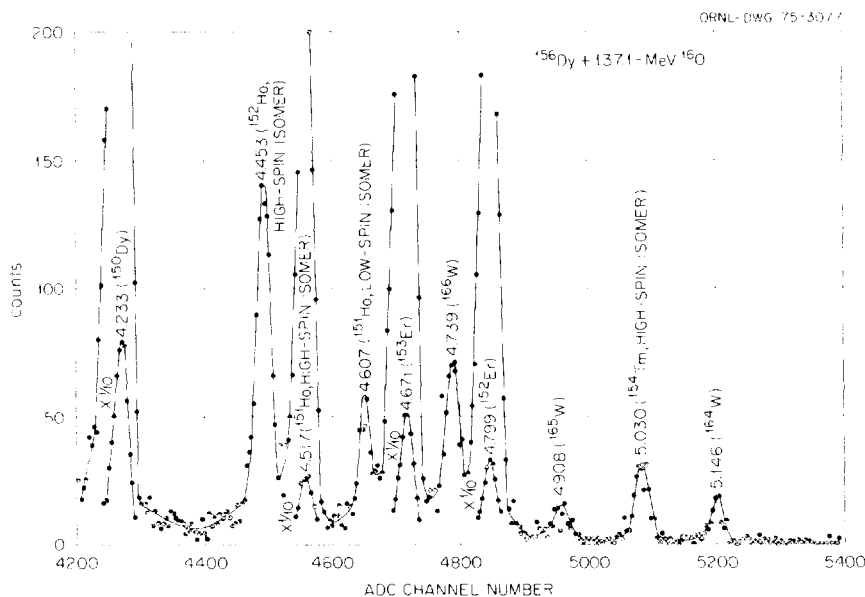


Fig. 1.52. Spectrum accumulated with a planar detector during a 10-hr half-life measurement made in a multiscale mode with ten separate spectra each 2 sec in duration. The incident energy of the ^{16}O ions was 137.1 MeV. In addition to well-established rare-earth nuclides and ^{164}W (reported in ref. 4), two new alpha groups are seen at 4.909 and 4.739 MeV. These are assigned (as labeled) to ^{165}W and ^{166}W respectively.

measurements (see Fig. 1.52). Figure 1.54 shows spectra measured at 188.6, 179.3, and 158.9 MeV. The 5.146-MeV group is seen to decrease in intensity with increasing bombarding energy, whereas the ^{163}W 5.384-MeV group is most intense at 179.3 MeV. A weak but distinct group is seen at the highest energy, 188.6 MeV; its energy was found to be 5.528 MeV, in agreement with the value of 5.53 MeV reported for ^{162}W .⁴ This variation with bombarding energy for the three alpha groups is consistent with the mass assignments proposed for them by Eastham and Grant.⁴

Table 1.4 summarizes available decay information for tungsten alpha emitters. A slight discrepancy was found between our results and those of ref. 4 for both the half-life and decay energy of ^{164}W .

In Fig. 1.53 we have plotted experimentally determined total alpha-decay energies (Q_α) for hafnium, tungsten, osmium, iridium, and platinum isotopes. Included in the figure are Q_α values predicted by Zeldes, Grill, and Simievic⁶ and by Meyers and Swiatecki^{7,8} for the same isotopes and for neighboring tantalum nuclides. These two mass formula predictions were selected because they have been found to be in good agreement with experimental values for osmium nuclides (see Fig. 1.53). Two points should be noted.

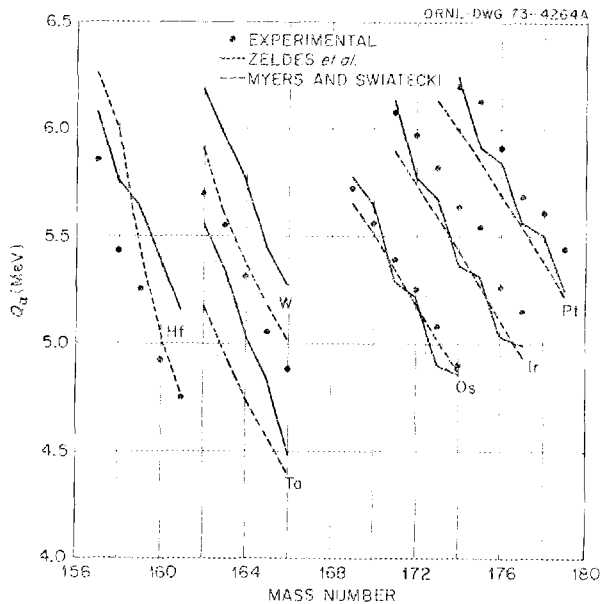


Fig. 1.53. Experimental and predicted Q_α values for hafnium, tungsten, osmium, iridium, and platinum alpha emitters. Predicted values for neighboring tantalum isotopes are also included. Note that the energies determined in this study for ^{165}W and ^{166}W fit in well with the general alpha-decay systematics in this mass region.

First, the energies determined in this work for ^{165}W and ^{166}W fit well not only as an extension of the data of Eastham and Grant⁴ but also into the general alpha-decay systematics in this mass region. Second, although the two sets of predicted Q_α values agree with experimental osmium decay energies, they tend to

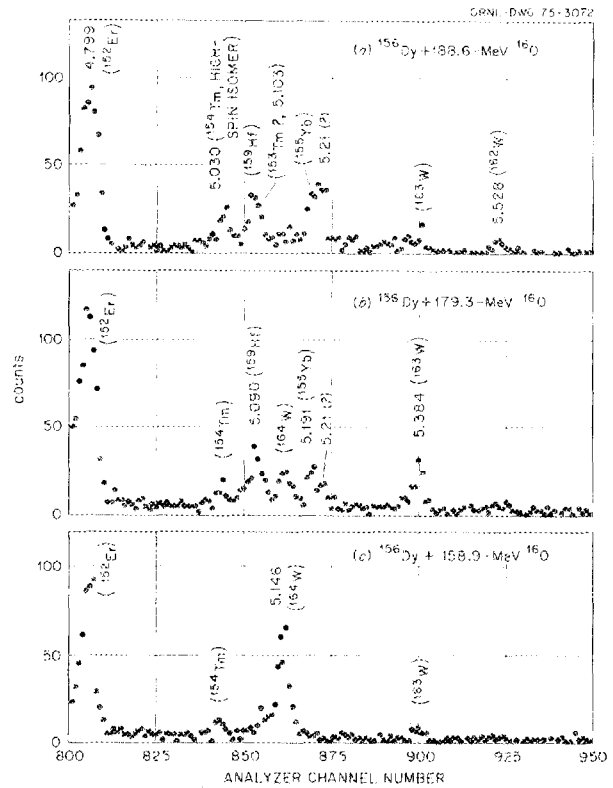


Fig. 1.54. Spectra measured when ^{156}Dy was bombarded with 188.6-, 179.3-, and 158.9-MeV ^{16}O ions. The alpha groups assigned in ref. 4 to ^{163}W and ^{164}W are clearly observed. In addition, a weak but distinct alpha group is seen at 5.528 MeV; this energy agrees with the value of 5.53 MeV reported in ref. 4 for ^{162}W ($T_{1/2} < 0.25$ sec).

Table 1.4. Decay information for $^{162-166}\text{W}$

Isotope	$T_{1/2}^a$ (sec)	E_α^a (MeV)	$T_{1/2}^b$ (sec)	E_α^b (MeV)
^{162}W		5.528 ± 0.010	< 0.25	5.53 ± 0.01
^{163}W		5.384 ± 0.010	2.5 ± 0.3	5.385 ± 0.005
^{164}W	5.5 ± 0.5	5.146 ± 0.005	6.3 ± 0.5	5.153 ± 0.005
^{165}W	5.1 ± 0.5	4.909 ± 0.005		
^{166}W	16 ± 3	4.739 ± 0.005		

^aFrom present work.

^bFrom ref. 4.

overestimate hafnium and tungsten energies and underestimate iridium and platinum energies.

1. UNISOR, Oak Ridge, Tenn.
2. University of Tennessee, Knoxville.
3. Virginia Polytechnic Institute and State University, Blacksburg, Va.
4. D. A. Eastham and I. S. Grant, *Nucl. Phys.* **A208**, 119 (1973).
5. W.-D. Schmidt-Ott and K. S. Toth, *Nucl. Instrum. Methods* **121**, 97 (1974).
6. N. Zeldes, A. Grill, and A. Simievic, *K. Dan. Vidensk. Selsk., Mat. Fys. Medd.* **3(5)** (1967).
7. W. D. Meyers and W. J. Swiatecki, *Nucl. Phys.* **81**, 1 (1966).
8. W. D. Meyers and W. J. Swiatecki, Lawrence Berkeley Laboratory report UCRL-11980, Berkeley, Calif.

NEW INFORMATION CONCERNING THE DECAY OF ^{147m}Tb

K. S. Toth C. R. Bingham¹
E. Newman A. E. Rainis²

In a study³ of terbium nuclides, we reported on the decay of the 1.9-min $^{147}\text{Tb}(h_{11/2})$ high-spin isomer to levels in ^{147}Gd . A tentative level at 1778.9 keV was proposed because (1) a 1778.9-keV gamma ray had a half-life of ~ 2 min and (2) an extremely weak 381.2-keV gamma ray appeared to have a similar half-life and its energy was such that it fit as a transition between the tentative 1778.9-keV level and one at 1397.7 keV. Recently, we have been investigating dysprosium isotopes with $A \leq 149$, produced in ^{12}C and ^{14}N bombardments of ^{142}Nd and ^{141}Pr respectively. As before, a capillary transport system is used to extract recoil products from a helium gas-jet reaction chamber to a shielded area where gamma-ray counting can be made. Data accumulated in these experiments show that the 1778.9-keV transition does not belong to the decay of 1.9-min ^{147}Tb and, therefore, the tentative level of the same energy does not exist in ^{147}Gd .

The conclusion is inescapable because the intensity of the 1778.9-keV gamma ray with respect to those of the most intense ^{147}Tb gamma rays, that is, 1397.7 and 1797.8 keV, was found to vary from experiment to experiment, depending on the bombarding energy, the projectile used, the amount of target material, etc. Coincidence data also show that the 1778.9-keV transition is not in coincidence with annihilation radiation and rare-earth K x rays. The gamma ray is thus associated with neither a highly neutron-deficient isotope nor a rare-earth nuclide.

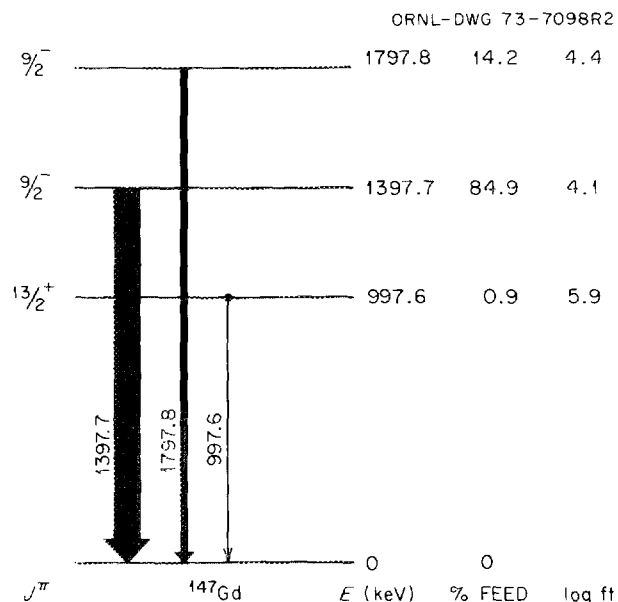


Fig. 1.55. Revised ^{147m}Tb decay scheme. New information has shown that a tentative level at 1778.9 keV does not exist in ^{147}Gd . In addition, a recent in-beam study (ref. 5) has shown that the $9/2^-$ assignment (from ref. 4) for the 997.6-keV level is incorrect. Instead, the assignment for the level is $13/2^+$; this agrees with the log ft value of 5.9 obtained in our decay measurements.

From a recent survey of known nuclides, it appears that a candidate which fits both the transition's energy and half-life is ^{28}Al . The source of the ^{28}Al could be its production from the aluminum gas-jet reaction chamber by neutron capture on ^{27}Al and/or heavy-ion-induced single-neutron transfer on ^{27}Al .

In the original investigation, three firm levels in ^{147}Gd were observed to be populated in the decay of the $^{147}\text{Tb}(h_{11/2})$ isomer. Two of these levels, 1397.7 and 1797.8 keV, were found to be fed strongly (log ft values $\lesssim 4.4$), prompting $9/2^-$ assignments for both states. The third level, at 997.6 keV, was populated weakly (log ft value ~ 5.9) even though an in-beam gamma-ray investigation⁴ had assigned a $9/2^-$ spin to that state as well. This particular dilemma has now been resolved. A recent in-beam study⁵ has shown that the spin of the 997.6-keV level is $13/2^+$. The revised ^{147m}Tb decay scheme is shown in Fig. 1.55.

1. University of Tennessee, Knoxville.
2. U.S. Army Ballistics Research Laboratory, Aberdeen Proving Ground, Md.
3. E. Newman et al., *Phys. Rev. C* **9**, 674 (1974).
4. J. Kownacki et al., *Nucl. Phys.* **A196**, 498 (1972).
5. P. Kleinheinz et al., *Phys. Lett.* **53B**, 442 (1975).

**ROTATIONAL BANDS IN THALLIUM NUCLEI
BY (H.L.,xn)**

L. L. Riedinger¹ N. R. Johnson³ A. C. Kahler⁴
P. Hubert² E. Eichler³ G. J. Smith⁵
R. L. Robinson P. H. Stelson

The even-even mercury nuclei are known to be quite regular in the spacings of the ground-state quasi-rotational band for $A = 190$ and higher. However, for $A = 188$ and lighter, the mercury nuclei exhibit low-lying prolate minima, evidenced partially by sudden changes in the spacings in the ground-state quasi bands. To investigate the behavior of the mercury cores in the presence of high- j protons, we have begun investigations of bands built on the $h_{9/2}$ and $i_{13/2}$ states in $^{189,191,193}\text{Tl}$. The reactions used to study the prompt in-beam gamma rays were $^{175}\text{Lu}(^{20}\text{Ne},4n)^{191}\text{Tl}$, $(^{20}\text{Ne},6n)^{189}\text{Tl}$, and $^{181}\text{Ta}(^{16}\text{O},4n)^{193}\text{Tl}$. The $^{191,193}\text{Tl}$ nuclei were previously studied by Newton, Stephens, and Diamond.⁶

Gamma-ray excitation function and coincidence measurements have been performed on each isotope, but angular distribution measurements to aid in spin assignments have not been completed. Consequently, the levels assigned are still tentative. The systematic behavior of the $h_{9/2}$ band is shown in Fig. 1.56. The levels for $A = 193-199$ were deduced by Newton, Stephens, and Diamond,⁶ whereas the states for 189 and the upper five levels in 191 come from our

measurements. The spacings in the band are amazingly constant for the light Tl nuclei, indicating that the mercury core is rather unchanging. The sequential spins of levels lead one to conclude that the band is a high- Ω strongly coupled structure built on an oblate shape, as discussed previously.⁶ The even-even mercury nuclei ($A \geq 190$) are known to have quasi-rotational bands that are quite regularly spaced up to $I = 10$. However, in ^{188}Hg the yrast band switches over to a prolate structure at $I = 6$.⁷ This strange behavior of the core should be reflected in irregular spacings further up in the $h_{9/2}$ band of ^{189}Tl , contrary to the quite regular ^{191}Tl case. We intend to extend our measurements on ^{189}Tl to test this possibility.

In each of the Tl nuclei studied here, a band built on the $i_{13/2}$ proton state is observed. This level is coming down in energy for the lighter Tl nuclei; the transition from the $^{13/2}^+$ state to the $^{1/2}^-$ of the $h_{9/2}$ band is 480, 613, and 736 keV in the $A = 189, 191,$ and 193 cases respectively. Work is continuing on the structure of these bands.

1. Consultant from the University of Tennessee, Knoxville.
2. Visitor from University of Bordeaux, France.
3. Chemistry Division.
4. Graduate Student, University of Tennessee, Knoxville.
5. Postdoctoral Fellow under appointment with Oak Ridge Associated Universities; presently at Brookhaven National Laboratory, Upton, N.Y.
6. J. O. Newton, F. S. Stephens, and R. M. Diamond, *Nucl. Phys. A236*, 225 (1974).
7. J. H. Hamilton et al., *Phys. Rev. Lett.* **35**, 562 (1975).

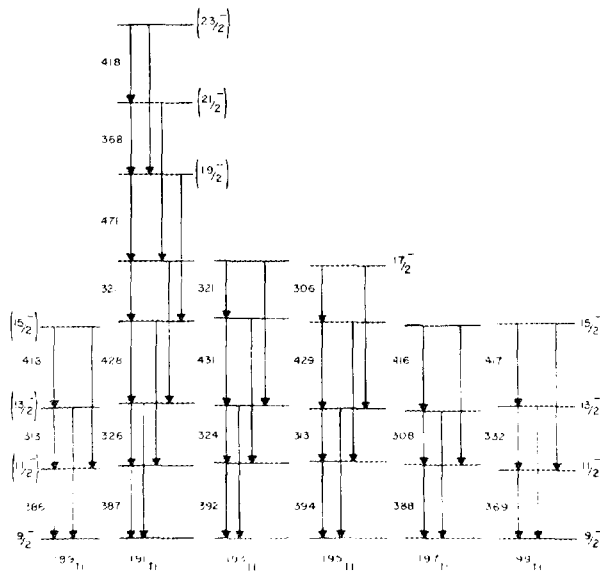


Fig. 1.56. Systematic behavior of $h_{9/2}$ band in the light Tl nuclei. Results on $A = 189$ and 191 are from the present work; other cases are from ref. 6.

**BANDS IN ^{164}Yb FROM
LUTETIUM DECAY**

C. R. Hunter¹ D. L. Hillis²
L. L. Riedinger² C. R. Bingham²
K. S. Toth

As do a number of different neutron-deficient rare-earth nuclei, the ground-state rotational band of ^{164}Yb backbends at $I = 14$. Of interest in these cases is the behavior of any observed excited (side) bands as they cross the ground band or higher-lying decoupled bands. Some (H.L.,xn γ) data were taken at ORIC on ^{164}Yb , resulting in the assignment of the yrast cascade up to $I = 20$ or 22 .³ A side band was partially observed but was difficult to assign and interpret because most of its intensity went to the ground band around $I = 10$. Because nothing was known about the vibrational band heads in ^{164}Yb , we performed measurements on the ^{164}Lu decay to learn about the low-spin members of

excited bands and thus to complement data on the high-spin members from (H.L., $xn\gamma$) experiments.

The ^{164}Lu activity was produced in the $^{155}\text{Gd}(^{14}\text{N},5n)$ reaction at 79 MeV. Recoils from the thin target were stopped in a helium atmosphere and transported to a low-level counting area with a gas-jet system. Sources of ^{164}Lu (3.17 min) were collected and counted in gamma-ray singles and coincidence experiments. The level scheme resulting from our work is shown in Fig. 1.57. All transitions have been placed with the aid of the coincidence measurements. Previously, only the low-energy 2^+ , 4^+ , and 6^+ levels were known. Most of the levels populated have low spins; therefore, the lutetium parent is thought to be low-spin. We did, however, observe some population of the 6^+ state, possibly indicating the existence of a high-spin isomer in lutetium. Because these gamma rays are quite weak, we were unable to measure half-lives different from the other peaks. Future work with the UNISOR facility is needed to produce cleaner sources so that this question can be answered.

The most strongly populated levels in ^{164}Yb are those at 864 and 1004 keV, which we call the 2^+ and 3^+ members of the gamma-vibrational band. The acquisi-

tion of conversion-electron data was not possible with the helium gas-jet system at the time of these measurements; so we have no conversion coefficients to aid in spin assignments. However, the heavier ytterbium nuclei are well studied and the trends are quite smooth. Based on the systematics and on the branching ratios from the states, we confidently assign the first two members of the gamma band. There are candidates for the 4^+ and 5^+ members also, but the arguments are not as strong. A 2^+ level at 1074 keV appears to be $K=0$ and may thus be part of a beta-vibrational band. There are also candidates for the 0^+ and 4^+ members of this band.

Figure 1.58 shows the systematics of the gamma bands in $^{164,166,168}\text{Yb}$. The $A=166$ results are from de Boer et al.,⁴ those for $A=168$ are from Charvet et al.⁵ The decrease in the band-head energy for the light nuclei, along with an increase in the spacings between the levels, indicate a nucleus with decreasing deformation and greater softness to shape vibrations. In addition, the deviation of the members from regular spacings ($J=2$ and 4 are pushed down relative to 3 and 5) increases for ^{164}Yb , indicating greater interactions between the gamma band and higher bands, especially

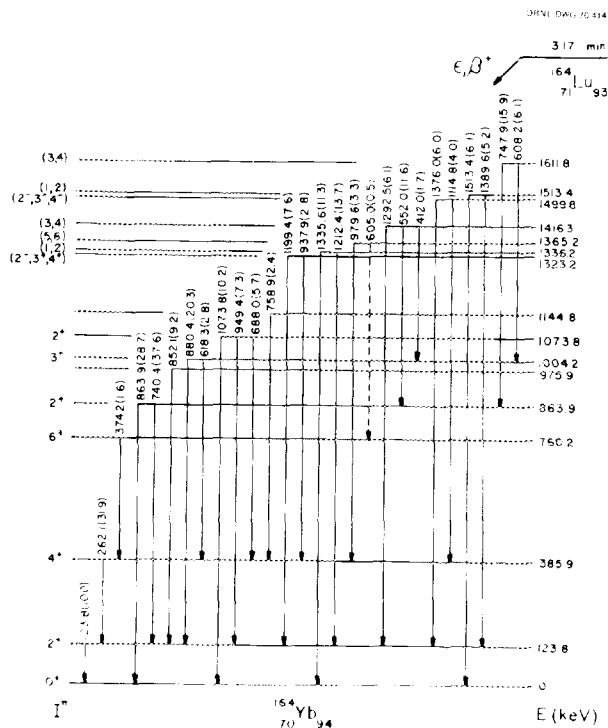


Fig. 1.57. Level scheme of ^{164}Yb populated by lutetium decay. Gamma-ray intensities are given in parentheses.

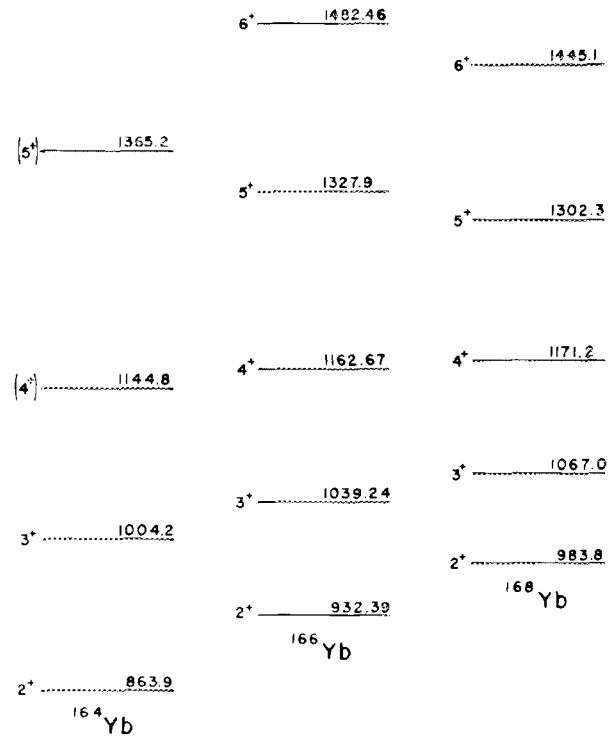


Fig. 1.58. Comparison of gamma-vibrational bands in the light ytterbium nuclei.

ones with $K = 0$ that have only even- I members. Mixing parameters extracted from the branching ratios show that the odd-spin members have wave functions that are more nearly pure gamma vibration than do the even-spin members. The trends established for these bands should enable us to better interpret side bands seen in the $(H.l., x\gamma)$ measurements.

1. Work performed toward M.S. degree at the University of Tennessee, Knoxville.
2. University of Tennessee, Knoxville.
3. L. L. Riedinger et al., *Phys. Div. Annu. Prog. Rep. Dec. 31, 1973*, ORNL-4937 (1974), p. 33.
4. F.W.N. de Boer et al. *Nucl. Phys. A225*, 317 (1974).
5. A. Charvet et al., *Nucl. Phys. A197*, 490 (1972).

LIFETIMES OF STATES IN A DECOUPLED BAND IN ^{165}Yb

E. Eichler N. R. Johnson
P. Hubert¹ L. L. Riedinger²

In recent years, there has been an intense interest in the so-called backbending phenomenon in which a rotational band shows a rather abrupt change in moment of inertia at high spin (about $I = 14$ for an even-even nucleus). The major emphasis has been in the development of detailed level schemes for these nuclei. Although the spectroscopic data amassed thus far favor the "rotation-alignment" explanation of this phenomenon, a more complete verification is needed.

To provide this more rigorous test of the models, we have measured the lifetimes of several members of the band³ in ^{165}Yb using the Doppler-shift recoil-distance method. With the reaction $^{130}\text{Te}(^{40}\text{Ar}, 5n)$, using a 162-MeV ^{40}Ar beam, we produced ^{165}Yb recoils with velocities of 1.8% c .

The lifetimes and $B(E2)$ values obtained from an analysis of the singles data are displayed in Table 1.5. In columns 4, 5, and 6 we show the calculated $B(E2)$ values for the weak-coupling, rotation-alignment, and strong-coupling schemes respectively. Note that there is

a rather definite ruling out of the weak-coupling approach. The strong-coupling scheme appears to be ruled out on the basis of the $^{3/2}^+ \rightarrow ^{2/2}^+$ transition $B(E2)$ value, as well as by the fact that we do not observe $\Delta I = 1$ transitions which are expected to compete with $\Delta I = 2$ gamma rays if strong coupling is present. Therefore, the rotation-alignment picture appears to be the correct description for this nucleus.

1. Centre d'Études Nucléaires de Bordeaux-Mérignac, Université de Bordeaux, France.
2. Physics Department, University of Tennessee, Knoxville.
3. L. L. Riedinger et al., *Phys. Rev. Lett.* 33, 1346 (1974).

MEASUREMENTS OF LIFETIME AND MULTIPLE COULOMB EXCITATION IN ^{162}Dy

P. P. Hubert¹ N. R. Johnson E. Eichler

Previous measurements² on the Coulomb excitation of ^{162}Dy with ^{20}Ne and ^{35}Cl ions have shown what appeared to be possible deviations from the rotational model for the 6^+ and 8^+ states. In an effort to clarify this point, we decided to make a direct measurement of the $E2$ matrix elements from these rotational states. For this, the half-lives of the 4^+ , 6^+ , and 8^+ members of the ground-state rotational band of ^{162}Dy have been determined by the Doppler-shift recoil-distance method. These levels were populated by multiple Coulomb excitation produced by a 146.6-MeV $^{40}\text{Ar}^{8+}$ beam at ORIC. The target was a 1.5-mg/cm² foil enriched to 96.26% in ^{162}Dy .

The basic principle of the measurement is to record gamma rays emitted from the recoil nucleus in coincidence with the backscattered heavy ions for different separations between the target and the plunger. Gamma rays emitted when the recoil nucleus is in flight give a shifted component, whereas those emitted when the recoil nucleus is stopped in the plunger give an unshifted component. The ratio $[R = u/(u + s)]$ of unshifted gamma-ray peak intensities to the sum of the unshifted and shifted gamma-ray peak intensities is a

Table 1.5. Lifetimes of states in ^{165}Yb

Transition	$T_{1/2}$ (psec)	$B(E2)$ values			
		Experimental	Weak coupling	Rotation alignment	Strong coupling
$1\frac{7}{2}^+ \rightarrow 1\frac{3}{2}^+$	87 ± 8	1.40 ± 0.13	0.83	1.38	1.45
$2\frac{1}{2}^+ \rightarrow 1\frac{7}{2}^+$	10.5 ± 1.1	1.46 ± 0.14	1.17	1.29	1.53
$2\frac{5}{2}^+ \rightarrow 2\frac{1}{2}^+$	4 ± 1	0.94 ± 0.23	1.20	1.06	1.57

function of the half-life of the level. The method, apparatus, and data analysis are described in detail elsewhere.³⁻⁶ Figure 1.59 shows the results for the 4^+ , 6^+ , and 8^+ states of ^{162}Dy ; Table 1.6 gives a summary of the half-lives and the computed experimental $B(E2)$

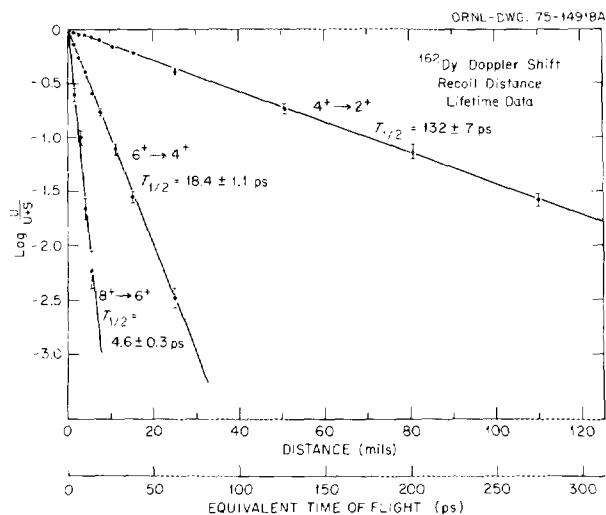


Fig. 1.59. Plot of ratios of unshifted gamma-ray peak intensities to sum of unshifted and shifted gamma-ray peak intensities as a function of target-stopper separation for ^{162}Dy .

values and compares these results with the pure rotational values.

During the same experiment, we were able to determine the relative Coulomb excitation probabilities for states up to the 12^+ member of the ground-state rotational band. The probability ratios $R[(I+2)/I]$, where I is the nuclear spin, compared to the theoretical values calculated with the Winther-de Boer code using rotational $E2$ and $E4$ matrix elements are given in Table 1.7, together with the results of Sayer et al.,² obtained with ^{20}Ne and ^{35}Cl beams. As is shown, the agreement between these two experiments is good, except for the ratio $R(12^+/10^+)$ where the present result, obtained with much better accuracy, is closer to the theoretical value.

We conclude from these measurements that within experimental uncertainties, both the results on the lifetimes and those on Coulomb excitation probabilities are consistent with the rigid-rotor predictions and show that the nucleus ^{162}Dy is a good rotor up to 12^+ .

1. NATO Fellow: on leave of absence from Centre d'Études Nucléaires de Bordeaux-Gradignan, Université de Bordeaux, France.
2. R. O. Sayer et al., *Phys. Rev. C* **9**, 1103 (1974).
3. M. W. Guidry, thesis, University of Tennessee, Knoxville.

Table 1.6. Summary of half-life and $B(E2)$ data for ^{162}Dy

Transition	$T_{1/2}$ (psec)	Experimental $B(E2)$ ($e^2 b^2$)	$B(E2)/B(E2)_{\text{rot}}$
$2^+ \rightarrow 0^+$	2150 ± 20^a	1.05 ± 0.01	1^b
$4^+ \rightarrow 2^+$	132 ± 7	1.50 ± 0.08	1.00 ± 0.06
$6^+ \rightarrow 4^+$	18.4 ± 1.1	1.57 ± 0.09	0.95 ± 0.06
$8^+ \rightarrow 6^+$	4.6 ± 0.3	1.64 ± 0.11	0.95 ± 0.07

^aAveraged mean of six measurements (from information on ^{162}Dy to be published in *Nuclear Data Sheets*).

^bNormalized to unity.

Table 1.7. Coulomb excitation probability ratios

Incident ion	Energy (MeV)	$R(I+2/I)$ experimental ^a			
		$R(I+2/I)$ theory			
		$R(6/4)$	$R(8/6)$	$R(10/8)$	$R(12/10)$
$^{20}\text{Ne}^b$	72.8	1.00 ± 0.07	0.80 ± 0.07		
$^{35}\text{Cl}^b$	127.6	0.81 ± 0.03	0.87 ± 0.03	1.07 ± 0.11	1.78 ± 0.67
^{40}Ar	146.6	0.98 ± 0.14	0.93 ± 0.17	1.22 ± 0.19	1.00 ± 0.20

^aTheoretical values were calculated with the Winther-de Boer code using rotational $E2$ and $E4$ matrix elements. $B(E2; 0^+ \rightarrow 2^+) = 5.128 e^2 b^2$ and $B(E4; 0^+ \rightarrow 4^+) = 0.073 e^2 b^4$ are the same as reported in ref. 2.

^bData taken from ref. 2.

4. N. R. Johnson et al., *Phys. Rev. C* **12**, 1927 (1975).
 5. E. Eichler et al., *Chem. Div. Annu. Prog. Rep. May 20, 1974*, ORNL-4976 (1975), p. 18.
 6. M. W. Guidry and R. J. Sturm, *Chem. Div. Annu. Prog. Rep. May 20, 1974*, ORNL-4976 (1975), p. 20.

HIGH-SPIN STATES IN ^{74}Se

M. L. Halbert¹ G. B. Hagemann³
 P. O. Tjømm² B. Herskind³
 I. Espe² M. Neiman³
 H. Oeschler⁴

Gamma-ray transitions from the bombardment of ^{64}Ni by ^{16}O , up to 81 MeV, were studied in a variety of experiments. Four transitions in coincidence with four previously known transitions in ^{74}Se were discovered. Information on energies, angular distributions, intensities, multiplicities, and lifetimes were obtained for these transitions. Excitation functions for this and several other channels were measured. Statistical calculations are in satisfactory agreement with experiment.⁵

1. Exchange visitor at Niels Bohr Institute, University of Copenhagen, Denmark, 1974-1975.
 2. University of Oslo, Norway.
 3. Niels Bohr Institute, University of Copenhagen, Denmark.
 4. On leave from the Max-Planck-Institut für Kernphysik, Heidelberg, Germany.
 5. Full report to appear in *Nuclear Physics*, 1976.

LIGHT-ION REACTIONS

INELASTIC PROTON EXCITATION OF GIANT RESONANCES IN *sd*-SHELL NUCLEI

F. E. Bertrand E. E. Gross
 D. C. Kocher E. Newman¹

The existence of a giant quadrupole resonance (GQR) is well established in nuclei with $A \gtrsim 40$. However, for *sd*-shell nuclei there have been conflicting reports of quadrupole strength in the giant-resonance region. Early proton inelastic scattering results^{2,3} on ^{27}Al were consistent with $\lesssim 50\%$ depletion of the isoscalar $E2$ EWSR strength in a broad structure (≈ 10 MeV wide) centered at an excitation energy of ≈ 20 MeV. However, (α, α') measurements^{4,5} on several *sd*-shell nuclei did not show a peaking of $E2$ strength, and alpha-capture results reported $\approx 30\%$ of the $E2$ EWSR strength spread uniformly over a large energy region.⁶ In an effort to resolve this apparent discrepancy, inelastic scattering measurements were made on ^{24}Mg , ^{26}Mg , ^{27}Al , and

^{28}Si , using 60.8-MeV protons from ORIC. The scattered particles were detected on nuclear emulsion plates placed in the focal plane of the broad-range magnetic spectrograph. The energy resolution was ≈ 100 keV (FWHM).

Figure 1.60 shows the inelastic spectra in the excitation energy range of 10 to 32 MeV for the four targets studied. Although narrow resonance structure is prominently seen near 19 to 20 MeV in all the spectra, only for the ^{27}Al and, to a lesser extent, ^{28}Si is a large, broad resonance peak observed. The present Al data⁷ are in good agreement with those previously published.²

A comparison is made in Figs. 1.61 and 1.62 between spectra from the (p, p') and (α, α') reactions on ^{27}Al and ^{28}Si . For both nuclei, no structure is observed in the 16- to 24-MeV region in the (α, α') reaction, although structure is present in the proton spectra. The alpha particle having zero isospin does not excite the isovector ($T = 1$) giant dipole resonance (GDR) to any observable extent. However, the (p, p') reaction has been shown to excite the GDR.⁸ Thus the absence of resonance structure in the alpha data suggests that the (p, p') structure may arise predominantly from excitation of the GDR.

The cross sections for the resonance structure observed in the (p, p') reaction on ^{24}Mg , ^{27}Al , and ^{28}Si near 20 MeV are shown in Fig. 1.63. The cross sections were obtained by subtracting an assumed smooth continuum from the resonance region. The calculated $E1$ cross sections are based on two different GDR models described by Satchler,³ the Goldhaber-Teller (GT) and Jensen-Steinwedel (JS) models. Normalization of the $E1$ calculation is based on the percent of the $E1$ sum-rule strength measured by total photonuclear reactions^{9,10} within the excitation energy limits shown in Fig. 1.63. For each of the nuclei studied, the $E1$ cross section predicted by the JS model is adequate to account for the measured cross section. Use of the GT model requires no more than 30% depletion of the $E2$ EWSR strength in the resonance region to provide good agreement with the measurements. This result is in good agreement with $E2$ EWSR limits set by the (α, α') and alpha-capture measurements.

Recently, several *sd*-shell nuclei have been studied using 150-MeV alpha inelastic scattering.¹¹ In *sd*-shell nuclei, the cross section for $E2$ excitation by 150-MeV alphas is 3 to 5 times greater than at 96 MeV. Thus, smaller GQR strength could be more readily observed at the higher energy. The 150-MeV alpha data show $\approx 30\%$ $E2$, $T = 0$, EWSR depletion in a resonance peak for ^{28}Si . This value is in excellent agreement with the

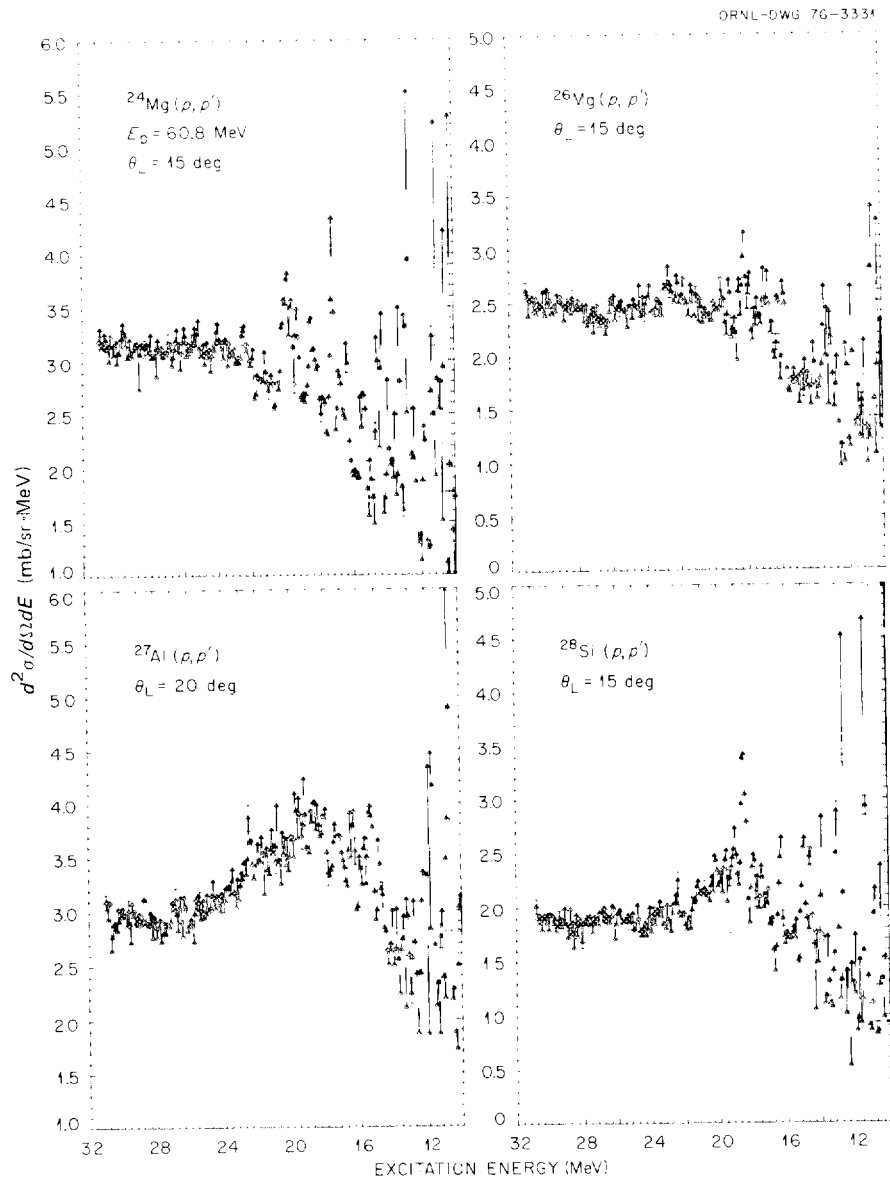


Fig. 1.60. Inelastic proton spectra from ^{24}Mg , ^{26}Mg , ^{27}Al , and ^{28}Si . The uncertainties shown in the spectra are statistical only.

(p,p') data if the GT model rather than the JS model is used for the $E1$ excitation.

In conclusion, we find good agreement between the several measurements of GQR strength in sd -shell nuclei. The amount of GQR strength observed in these nuclei, $\lesssim 30\%$ EWSR, is considerably less than the 80 to 90% observed in heavy nuclei. This difference may be partially explained by the larger depletion of $E2$ strength in the bound states for sd -shell nuclei⁵ than for heavier nuclei.^{1,2} In addition, the GQR strength in these

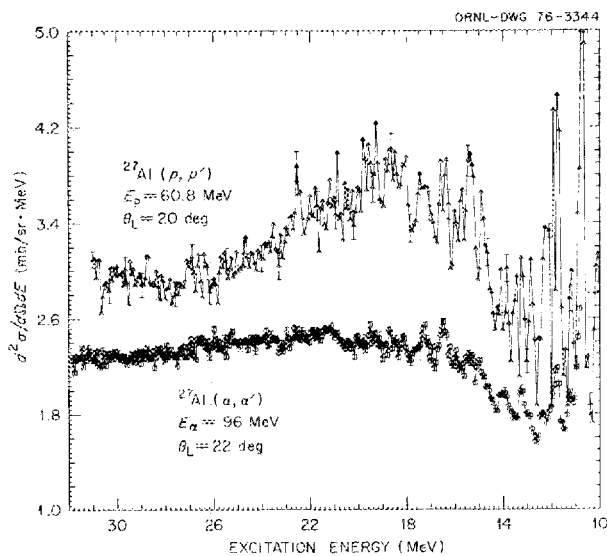


Fig. 1.61. Comparison of (p,p') and (α,α') spectra from ^{27}Al . The (α,α') data, taken from ref. 3, are arbitrarily normalized.

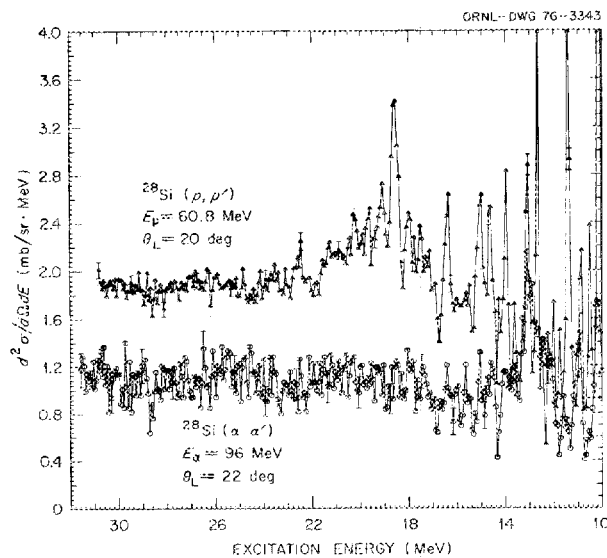


Fig. 1.62. Comparison of (p,p') and (α,α') spectra from ^{28}Si . The (α,α') data, taken from ref. 3, are arbitrarily normalized.

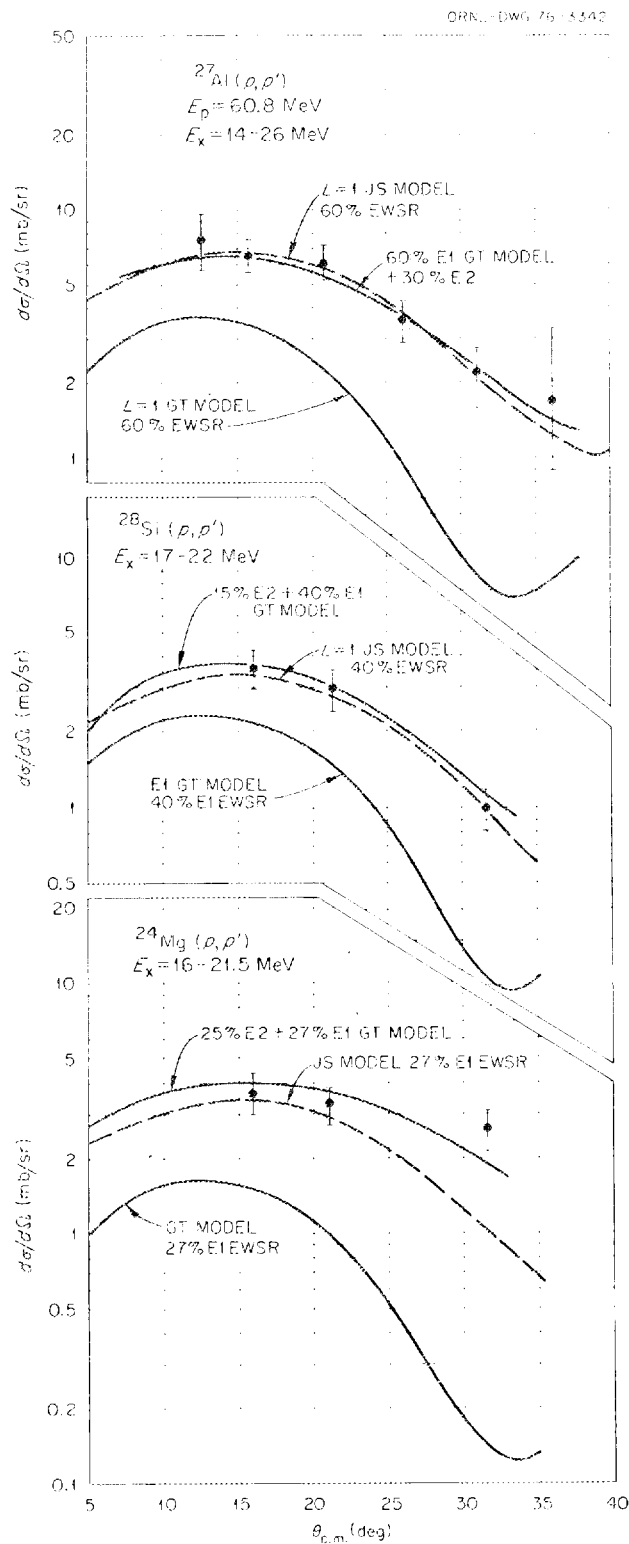


Fig. 1.63. Angular distribution for resonance structure measured in (p,p') reaction on ^{27}Al , ^{28}Si , and ^{24}Mg . The cross sections were obtained over the excitation energy regions indicated.

nuclei may be fragmented and spread over a very large energy region, as is the case for the GDR.¹⁰ Such fragmentation of the GQR strength would make observation of the resonance above the underlying continuum difficult.

1. Chemical Technology Division.
2. M. B. Lewis and F. E. Bertrand, *Nucl. Phys.* **A196**, 337 (1972).
3. G. R. Satchler, *Nucl. Phys.* **A195**, 1 (1972).
4. J. M. Moss et al., *Phys. Rev. Lett.* **34**, 12 (1975).
5. P. P. Singh and G. C. Yang, p. 162 in *Proceedings of the International Conference on Nuclear Structure and Spectroscopy*, Amsterdam, Sept. 9, 1974, vol. 1, H. P. Blok and A. I. L. Dieperink, Eds., Scholar's Press, Amsterdam, 1974.
6. E. Kuhlmann et al., *Phys. Rev. C* **11**, 1525 (1975).
7. Some of the $Al(p,p')$ data presented here were obtained with the assistance of M. B. Lewis.
8. C. C. Chang, F. E. Bertrand, and D. C. Kocher, *Phys. Rev. Lett.* **34**, 221 (1975).
9. J. M. Wyckoff et al., *Phys. Rev. B* **137**, 576 (1965).
10. J. Ahrens et al., *Nucl. Phys.* **A251**, 479 (1975).
11. K. T. Knöpfle, private communication.
12. M. B. Lewis, F. E. Bertrand, and C. B. Fulmer, *Phys. Rev. C* **7**, 1966 (1973).

EXCITATION OF GIANT RESONANCES IN ²⁰⁸Pb AND ¹⁹⁷Au VIA PROTON INELASTIC SCATTERING¹

F. E. Bertrand D. C. Kocher

The giant resonance regions in ²⁰⁸Pb and ¹⁹⁷Au have been investigated by inelastic scattering of 61-MeV protons with an energy resolution of about 100 keV. Cross sections for the GQR at $E_x \approx 63A^{-1/3}$ MeV exhaust about 90% of the EWSR strength for an isoscalar $E2$ excitation in both nuclei. The angular distribution for the GQR plus the GDR in ²⁰⁸Pb is compared with both macroscopic and microscopic DWBA calculations. A pronounced fine-structure resonance is observed in ²⁰⁸Pb at $E_x \approx 56A^{-1/3}$ MeV (9.4 MeV). The angular distribution for this resonance is well described by DWBA calculations for an $E2$ or $E3$ excitation, but not for an $E0$ excitation. The spectra for ²⁰⁸Pb and ¹⁹⁷Au show little evidence for a resonance at $E_x \approx 53A^{-1/3}$ MeV, interpreted as an $E0$ excitation in recent electron inelastic scattering studies. The spectra in the bound-state region for ¹⁹⁷Au show a pronounced structure centered at $E_x \approx 4$ MeV, for which the angular distribution is best described by DWBA calculations for $E3$ or $E4$ excitations.

¹. Abstract of paper to be submitted to the *Physical Review*.

STUDY OF THE STRUCTURE OF THE EVEN-EVEN ISOTOPES OF GERMANIUM WITH THE (p, t) REACTION

A. C. Rester¹ R. Auble J. B. Ball

In a study² of the systematics of two-phonon energy levels, it was found that the even-even nuclei with anomalously low-lying first 0^+ excited states could be fitted into a regular pattern showing a strong correlation between the lowering of the energies of these 0^+ energy levels and the closure of $p_{1/2}$ neutron and proton subshells. An explanation² of this phenomenon based on the coupling of phonon and pairing vibrational modes was proposed. Other groups (e.g., ref. 3) have suggested that the behavior of these unusual energy levels may be explained with a nuclear coexistence model in which such an anomalous 0^+ state would be the deformed head of a rotational band "coexisting" in the same nucleus with vibrational structure based on the supposedly spherical 0^+ ground state. As is discussed in ref. 2, (p, t) reactions on the even-even $N \approx 40$ nuclei can provide a good test of the two theories.

Measurements of the reactions ⁷⁶Ge(p, t)⁷⁴Ge and ⁷⁴Ge(p, t)⁷²Ge at 35-MeV proton energy with the broad-range spectrograph at ORIC have now been completed, and the exposed photographic plates are being scanned. Preliminary results from the 10⁹ plates indicate that the 0^+ state in ⁷²Ge is excited much more intensely than the 0^+ state in ⁷⁴Ge, relative to their ground states, as is expected from the pairing-phonon vibrational explanation. Detailed calculations of the structure of the even isotopes of germanium with an improved pairing-plus-quadrupole model of Kumar are almost completed. Wave functions for the reaction analysis have been generated as well.

1. Emory University, Atlanta, Ga.
2. J. Hadermann and A. C. Rester, *Nucl. Phys.* **A231**, 120 (1974).
3. J. H. Hamilton et al., *Phys. Rev. Lett.* **32**, 239 (1974).

INELASTIC SCATTERING OF 30-MeV POLARIZED PROTONS FROM ^{90,92}Zr AND ⁹²Mo

R. de Swiniarski¹ M. Bedjiam² J. Y. Grossiord²
G. Bagieu¹ C. B. Fulmer³ M. Gusakov²
M. Massaad¹ J. R. Pizzi²

Previous studies⁴ of inelastic scattering of polarized protons from the low-lying 2^+ states in ^{90,92}Zr and ⁹²Mo at 20 MeV have shown poor agreement between the coupled-channels (CC) or DWBA collective-model

calculations and the analyzing powers, whereas cross sections for these states were generally well reproduced by these calculations. Moreover, differences in the analyzing powers for the 2^+ states in these nuclei have been observed mainly at large angles; the ^{90}Zr and ^{92}Mo data were similar, but different from the analyzing power of ^{92}Zr . Good agreement was obtained, however, between the analyzing power (from the 20-MeV experiment) of the first 2^+ state in ^{90}Zr and the CC collective-model calculations⁵ where the ratio $\lambda = \beta_{\text{LS}}/\beta_{\text{central}}$ (β_{LS} is the spin-orbit deformation and β_{central} is the deformation of the central potential) was increased to 3.0. Raynal⁵ has suggested a possible relation of this parameter λ to the nuclear structure which, therefore, could vary from nucleus to nucleus. Recently, however, Verhaar⁶ has given an interesting and simple explanation for the observed tendency of λ to be somewhat greater than 1.0, based on the fact that the range of the central two-body force is longer than that of the two-body spin-orbit force. In the sd shell, for instance,^{7,8} there is strong evidence that this ratio is close to 1.5. It has also been suggested from an experimental point of view that this ratio may be energy dependent,⁹ such behavior may result from either a possible resonance-like phenomenon or a contribution from the giant resonance.

Inasmuch as compound nucleus effects may be important at 20 MeV and therefore partly responsible for the disagreement between the collective-model calculation and the analyzing power observed at this energy, a new measurement of these data at a higher energy is needed. We have obtained data at an energy of 30 MeV with a beam from the Grenoble cyclotron. An overall resolution of 80 to 100 keV (FWHM) was obtained for most of the data. Up to 3 nA of energy-analyzed polarized protons were delivered on the target, with a polarization of $\sim 70\%$, which was measured with a carbon polarimeter. Enriched targets of $\sim 1\text{-mg}/\text{cm}^2$ thickness were used.

The good resolution achieved permitted extraction of analyzing powers for several low-lying states, such as

the 2^+ , 3^- , and 5^- . The data were analyzed with the CC code ECIS 74 of Raynal¹⁰ in the framework of the collective model as well as with the distorted-wave approximation and the microscopic model with Schaeffer code DWBA 70.¹¹ Figure 1.64 compares the CC collective-model (vibrational) calculations with our measured values of the analyzing powers for the low-lying 2^+ and 3^- states in the three nuclei and also for the 5^- in ^{90}Zr and ^{92}Mo . The optical model parameters listed in Table 1.8 were obtained by using the code Magali¹⁰ searching on all parameters with the elastic cross section and polarization data simultaneously; the same parameters were used for both ^{90}Zr and ^{92}Zr .

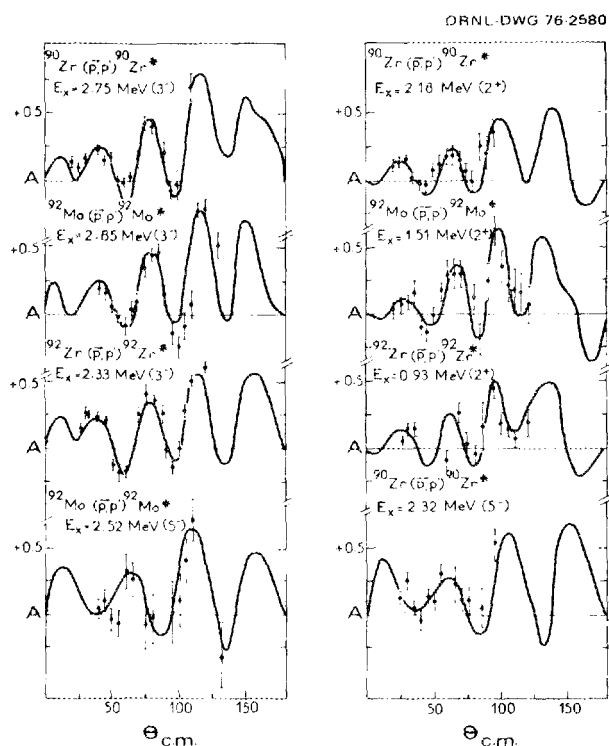


Fig. 1.64. Analyzing powers predicted by CC collective model compared with experimental results.

Table 1.8. Optical model parameters used to perform collective-model calculations

Deformation parameters were obtained by normalizing experimental cross sections with DWBA calculations.

Target	V_0 (MeV)	r_0 (MeV)	a_0 (f)	W_V (MeV)	W_D (MeV)	r_I (f)	a_I (f)	V_{LS}	r_{LS}	a_{LS}	β_{3^+}	β_{3^-}	β_{5^-}
^{90}Zr	56.7	1.11	0.77	4.0	4.88	1.37	0.65	6.17	0.89	0.54	0.07	0.13	0.08
^{92}Zr	56.7	1.11	0.77	4.0	4.88	1.37	0.65	6.17	0.89	0.54	0.12	0.17	
^{92}Mo	51.7	1.16	0.75	3.28	4.58	1.35	0.63	7.65	1.06	0.75	0.10	0.15	0.08

Figure 1.64 shows the excellent agreement obtained by the CC collective model for the analyzing powers of the low-lying 2^+ , 3^- , and 5^- states in the three nuclei. The calculations used the full Thomas term for the deformed spin-orbit optical potential and a ratio $\lambda = \beta_{LS}/\beta_{central}$ of 1.5 that has been found to give the best agreement for the 2^+ data. Good agreement for the 3^- and 5^- states could also be obtained by keeping the deformation parameters constant ($\beta_{LS} = \beta_{central}$). It is suggested that the ratio λ of the spin-orbit deformation over the central deformation is energy dependent because values of this factor as large as 3.0 are needed to reproduce the 20-MeV data. It is interesting to note the good agreement obtained by the calculations for the analyzing power of high-spin states like the 5^- in ^{90}Zr and ^{92}Mo , for which there are no previous data.

Macroscopic model calculations for the low-lying 2^+ states in the three nuclei were also performed and are described elsewhere.^{1,2} Good agreement was obtained with the cross-section data for all three targets. The analyzing powers predicted by the macroscopic model, however, are in poor agreement with the data (especially for ^{90}Zr and ^{92}Mo) in contrast to the good agreement obtained with the collective-model calculations.

1. Institut des Sciences Nucléaires, Grenoble, France.
2. Institut de Physique Nucléaire, Lyon, France.
3. On assignment at Institut des Sciences Nucléaires, Grenoble, France, 1974-1975.
4. C. Glashauser et al., *Phys. Rev.* **184**, 1217 (1969).
5. J. Raynal, in lectures presented at the "Nuclear Theory Course," Trieste, 1971, DPh/in°/71/1, Saclay, France.
6. B. J. Verhaar, *Phys. Rev. Lett.* **32**, 307 (1974).
7. R. de Swiniarski et al., to be published in *Nuclear Physics*.
8. R. de Swiniarski et al., *Can. J. Phys.* **51**, 1293 (1973).
9. P. J. Van Hall et al., private communication; to be published.
10. J. Raynal, "Magali," DPh/T/69-42, Saclay, France, unpublished.
11. R. Schaeffer, unpublished thesis, Paris, France.
12. R. de Swiniarski et al., submitted to *Physics Letters*.

EXCITATION OF NEUTRON-HOLE STATES IN THE $^{206}\text{Pb}(p,p')$ REACTION AT 61 MeV

Alan Scott¹ C. T. Chung²
F. T. Baker¹ M. Owais³
M. L. Whiten⁴

The purpose of our experiment on the excitation of neutron-hole states in the $^{206}\text{Pb}(p,p')$ reaction at 61 MeV was to compare the cross sections for excitation of

two-neutron-hole states in ^{206}Pb which are simply connected⁵ to the single-neutron-hole states excited in our recent experiment on ^{207}Pb with 61-MeV protons. Comparison of the ^{207}Pb results with those for lower-energy protons showed the core-coupling parameter A_L to be larger for 20-MeV protons than for those at 61 MeV by 58%, 153%, and 200% for transfers of $L = 2$, $L = 4$, and $L = 7$ respectively.⁶

Track counting of the nuclear plates is in progress.¹⁻³ Excitations of natural parity states involving transfers of $L = 2$, $L = 4$, and $L = 7$ are clearly measurable, in addition to many other states.

1. University of Georgia, Athens.
2. Graduate student, University of Georgia, Athens.
3. Paine College, Augusta, Ga.
4. Armstrong State College, Savannah, Ga.
5. W. A. Lanford and G. M. Crawley, *Phys. Rev. C* **9**, 646 (1974).
6. Alan Scott, M. Owais, and W. G. Love, submitted to *Nuclear Physics*.

^3He AND ALPHA-PARTICLE SCATTERING FROM ^{27}Al AND $^{28,29,30}\text{Si}$

G. Bagieu¹ R. de Swiniarski¹ D. H. Koang¹
A. J. Cole¹ C. B. Fulmer² G. Mariolopoulos¹

Previously measured angular distributions of elastic scattering of ^3He and alpha particles from neighboring even and odd nuclei show significant differences.^{3,4} For example, at angles beyond $\sim 50^\circ$, the distributions for ^{59}Co ($I = 7/2$) have minima that are appreciably less deep. These differences have been accounted for by a quadrupole contribution^{5,6} to the elastic scattering from the $I \neq 0$ nucleus. For an $I = 1/2$ nucleus, the quadrupole contribution is zero; hence data from neighboring targets that include an $I = 1/2$ nucleus are favorable cases for further study of target spin effects to determine whether there are effects that cannot be accounted for by a quadrupole contribution.

We explored ^3He and alpha-particle scattering for evidence of target spin effects in a different mass region with a group of targets that includes an $I = 1/2$ nucleus. With 45-MeV ^3He and 41-MeV alpha-particle beams from the Grenoble cyclotron, angular scattering distributions were measured for ^{27}Al ($I = 5/2$), ^{28}Si ($I = 0$), ^{29}Si ($I = 1/2$), and ^{30}Si ($I = 0$). The silicon targets were in oxide form ($>95\%$ enrichment in the principal isotope) evaporated onto plastic backing.⁷ The oxygen and carbon impurities limited inelastic scattering measurements to angles beyond $\sim 45^\circ$.

The measured ^3He elastic scattering data are presented in Fig. 1.65. At angles forward of $\sim 55^\circ$ the four

angular distributions are very similar. At larger angles, data from the three silicon targets are similar but different from that of ^{27}Al . The differences are qualitatively like those observed earlier³ for ^{59}Co and ^{60}Co but are larger in relative magnitude. The similarity

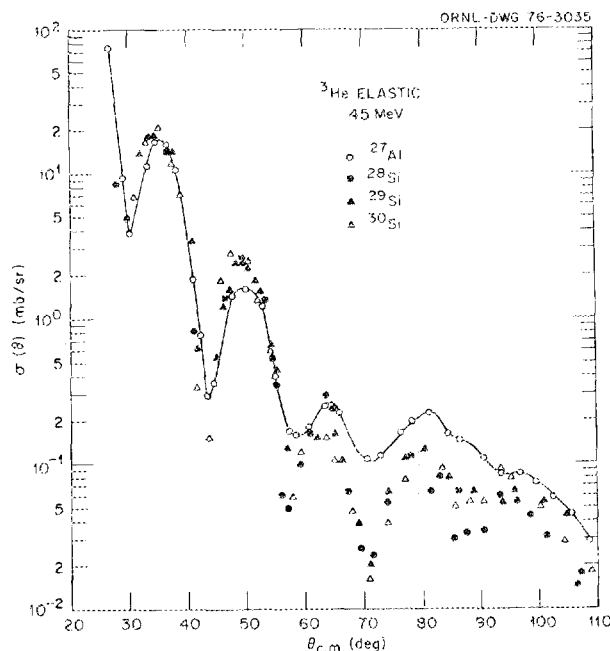


Fig. 1.65. 45-MeV ^3He elastic scattering from ^{27}Al , ^{28}Si , ^{29}Si , and ^{30}Si . The curve through the ^{27}Al data is to guide the eye.

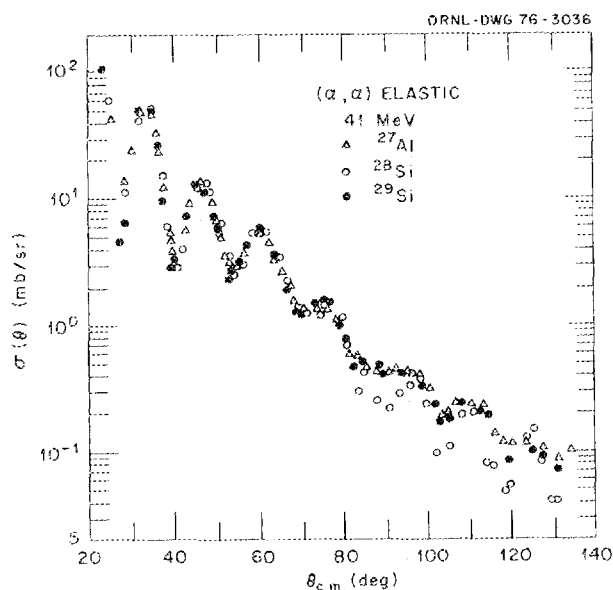


Fig. 1.66. 41-MeV alpha-particle elastic scattering from ^{27}Al , ^{28}Si , and ^{29}Si .

of the elastic angular distributions for the three silicon targets (which include the $I = 1/2$ isotope ^{29}Si) suggests that for ^3He scattering, target spin effects are due principally to quadrupole contributions.

Figure 1.66 presents the measured alpha-particle elastic scattering data for ^{27}Al , ^{28}Si , and ^{29}Si . At angles forward of $\sim 75^\circ$ the angular distributions are almost identical. At larger angles, in contrast to the ^3He results shown in Fig. 1.65, data from the two $I \neq 0$ targets, ^{27}Al and ^{29}Si , are similar but different from those of the $I = 0$ target, ^{28}Si . A further complication in the alpha-particle data is the puzzling differences between the data from ^{28}Si and the data from ^{30}Si (the latter are not shown in Fig. 1.66), which are both $I = 0$ targets. Analyses of the data, including inelastic scattering measurements, are under way.

1. Institut des Sciences Nucléaires, Grenoble, France.
2. On assignment at Institut des Sciences Nucléaires, Grenoble, France, 1974-1975.
3. C. B. Fulmer and J. C. Hafele, *Phys. Rev. C* **7**, 63 (1973).
4. C. B. Fulmer and J. C. Hafele, *Electronuclear Div. Annu. Prog. Rep. Dec. 31, 1970*, ORNL-4649 (1971), p. 47.
5. N. M. Clarke, *J. Phys. (London)* **A7**, 16 (1974).
6. G. R. Satchler and C. B. Fulmer, *Phys. Lett.* **50B**, 309 (1974).
7. We are indebted to D. C. Hensley for preparing the silicon targets.

SELECTIVE ENHANCEMENT OF A PROBABLE PARTICLE-HOLE STATE IN $^{16}\text{O}(^3\text{He},t)^{16}\text{F}$

C. D. Goodman D. C. Kocher
F. E. Bertrand R. L. Auble

We reported in last year's progress report¹ that the $(^3\text{He},t)$ reaction at 70 MeV on several $N = Z$ targets did not show any selective excitation of the GDR. However, in $^{16}\text{O}(^3\text{He},t)^{16}\text{F}$ the spectrum is dominated by a very large peak, as shown in Fig. 1.67, that corresponds to the analog in ^{16}F of about 19.2 MeV of excitation in ^{16}O . The angular distribution for the peak is shown in Fig. 1.68. Figure 1.69 shows where this peak fits on an isobar diagram.

We believe that the peak corresponds to a large peak observed in back-angle electron scattering,² $^{16}\text{O}(e,e')^{16}\text{O}$, at an excitation of 18.7 MeV in ^{16}O (the energy discrepancy is probably within experimental error).

The angular distribution is similar to that for a 2^- state observed in $^{12}\text{C}(^3\text{He},t)^{12}\text{N}$. Therefore, we suspect that we are seeing a concentration of $L = 1$ particle-hole

NUCLEAR CHEMISTRY

MEASUREMENT OF THE ELECTRON-CAPTURE
BRANCH OF THE DECAY OF $^{225}\text{No}^1$

R. J. Silva² C. E. Bemis, Jr.²
P. F. Dittner² D. C. Hensley

The granddaughter nuclide, 223-sec ^{255}No , produced by the decay of the daughter nuclide $^{259}\text{104}$, has been used in the identification of $^{263}\text{106}$ by its discoverers.³ However, quantitative analysis required the postulation in ^{255}No of a substantial decay branch ($\sim 50\%$) via electron capture (EC), a mode of decay not observed in the identification experiments. We have produced ^{255}No in the $^{249}\text{Cf}(^{12}\text{C}; \alpha, 2n)$ reaction using the $^{12}\text{C}^{4+}$ beam at an energy of 86 MeV, accelerated at ORIC. After traversing a 1-mil beryllium vacuum isolation window and a 0.5-mil beryllium target backing, the $^{12}\text{C}^{4+}$ energy (~ 73 MeV) matched the maximum in the excitation function for this reaction. The recoiling reaction products were collected on aluminum catcher disks in a helium gas-jet apparatus. The catcher disks were periodically (~ 10 min) transferred to the laboratory via a pneumatic tube.

To determine the EC branch of ^{255}No , the alpha decay of the parent, its EC daughter (27-min ^{255}Md), and the EC daughter of ^{255}Md (20.1-hr ^{255}Fm) were observed. Because these activities and others having similar alpha-particle energies can also be produced directly in the bombardment of ^{249}Cf by ^{12}C ions, it was necessary to do radiochemical separations. Initially, the nobelium was chemically separated from the trivalent actinides produced in the irradiation by solvent-extraction chromatography. The extraction column separations were carried out with bis(2-ethylhexyl)-phosphoric acid (HDEHP) adsorbed on Bio-Glass 500 (particle size, 200 to 325 mesh). The beads were loaded with 400 mg of HDEHP per gram of support. The column was heated to 70°C and run under pressure to attain an elution rate of ~ 5 sec per drop. The activity was loaded in ~ 5 drops of 0.1 N HCl and eluted with 0.1 N HCl . Under these conditions, monovalent and divalent ions are only weakly adsorbed and pass through the column in a few column volumes, whereas trivalent and tetravalent ions are adsorbed strongly.

In the case of nobelium, the activity was removed from the catcher disk with 0.1 N HCl and loaded on the column. The first ten elution drops were collected on a platinum disk, quickly dried, and placed in one of four counters. The total elapsed time for the separation was about 3 min. Four $\text{Si}(\text{Au})$ alpha detectors allowed us to

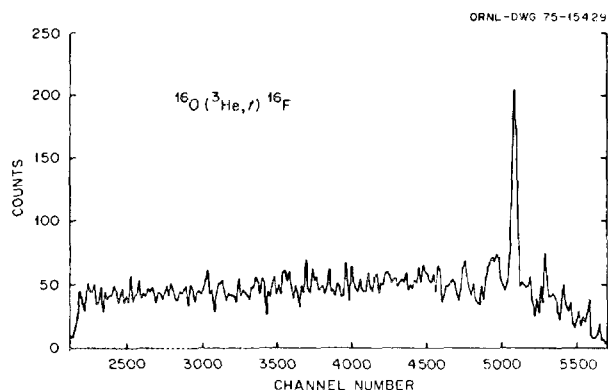


Fig. 1.67. Energy spectrum of tritons from $^{16}\text{O}(^3\text{He},t)^{16}\text{F}$ at 17.5° (lab) angle.

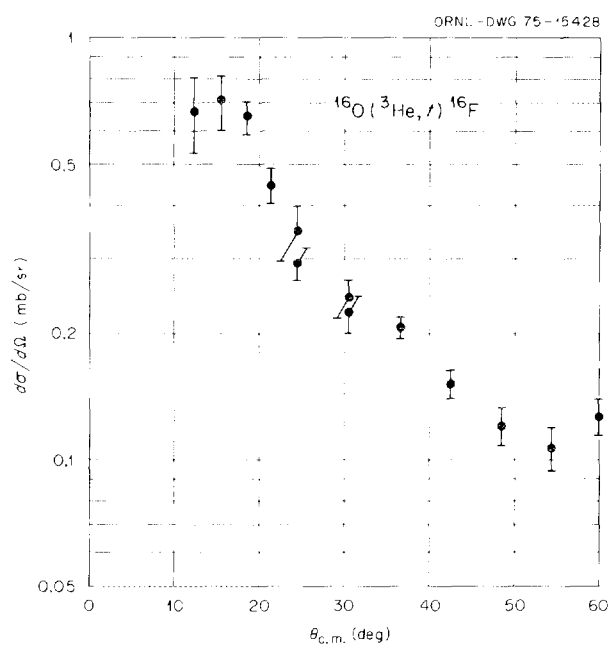


Fig. 1.68. Differential cross section for the large peak shown in Fig. 1.67.

strength. Because we do not expect a particle-hole state, as such, to be an eigenfunction of the nuclear Hamiltonian and because there are five 2^- states that belong to the $(p)^{-1}(sd)^1$ configuration, it seems surprising that the strength is concentrated. We plan to investigate this reaction with better resolution, at more forward angles, and at another energy to help us to make a more definite interpretation.

1. C. D. Goodman et al., *Phys. Div Annu. Prog. Rep. Dec. 31, 1974*, ORNL-5025 (1975), p. 65.

2. I. Sick et al., *Phys. Rev. Lett.* **23**, 1117 (1969).

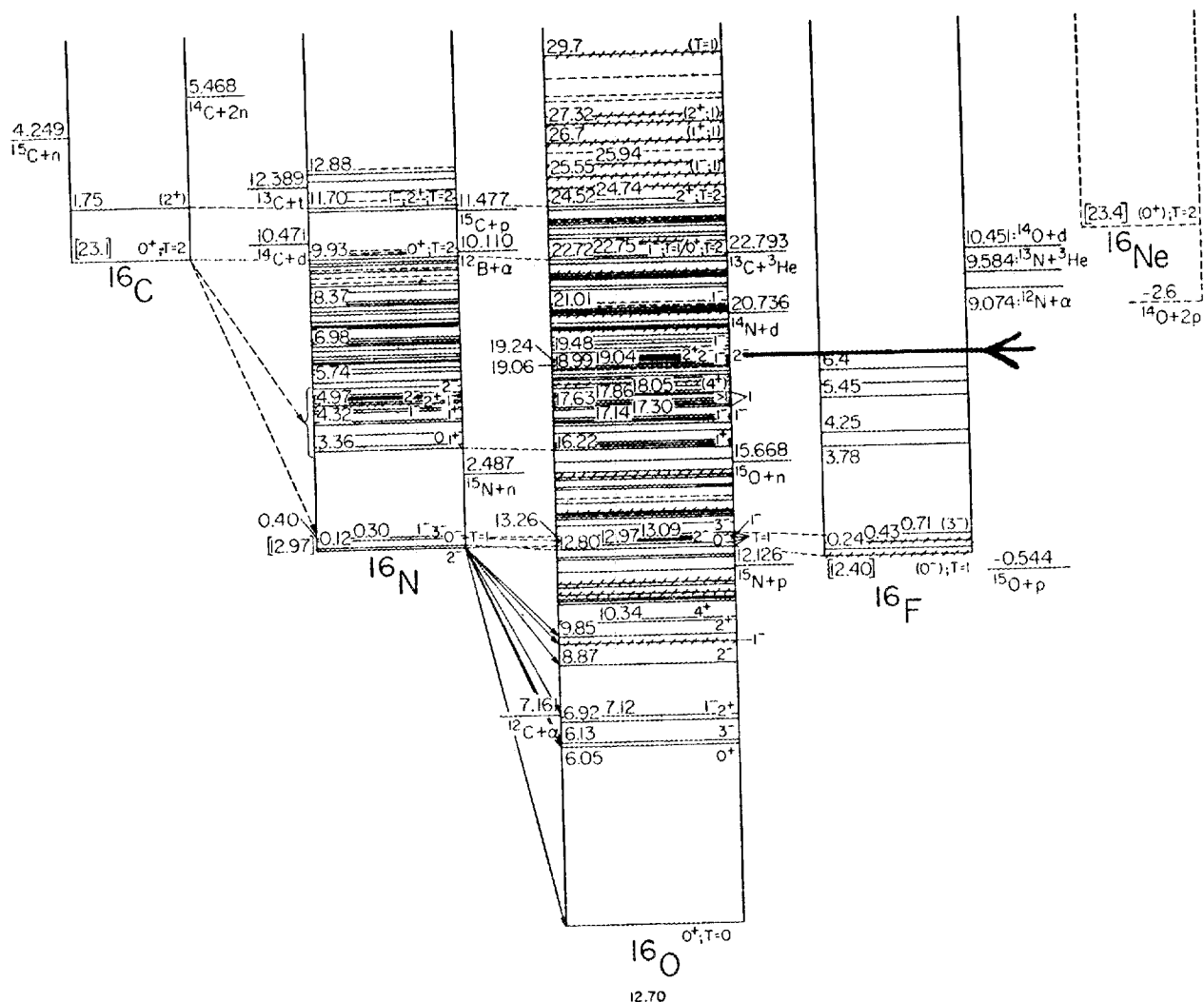


Fig. 1.69. Isobar diagram of levels for $A = 16$, showing the location of the large peak of Fig. 1.67.

measure the alpha energy spectra from each sample at a geometry of $\sim 28\%$.

Thirty-two 10-min bombardments were made. The first 28 samples were counted for 40 min each. During this period, all of the ^{255}No and about 64% of the ^{255}Md decay were detected. The last four samples were counted for about 48 hr. These longer counts enabled us to measure the amount of ^{255}Fm as well. From these data, using an average value⁴⁻⁶ of $8.8 \pm 0.8\%$ for the alpha branch of ^{255}Md , we determine the EC branch of ^{255}No to be $38.6 \pm 2.5\%$.

1. An account of this work has appeared in *Chem Div. Annu. Prog. Rep. Nov. 1, 1975*, ORNL-5111 (1976), p. 61.

2. Chemistry Division.
3. A. Ghiorso et al., *Phys. Rev. Lett.* **33**, 1490 (1974).
4. P. R. Fields et al., *Nucl. Phys.* **A154**, 407 (1970).
5. T. Sikkeland et al., *Phys. Rev.* **140**, B277 (1965).
6. R. W. Hoff et al., UCRL report 72898, 1971.

DECAY PROPERTIES AND L X-RAY IDENTIFICATION OF ELEMENT $^{260}105$

P. F. Dittner¹ R. J. Silva¹
 C. E. Bemis, Jr.¹ R. L. Hahn¹
 D. C. Hensley J. R. Tarrant¹
 L. D. Hunt¹

As part of our continuing study² of the identification and properties of transfermium elements, we carried

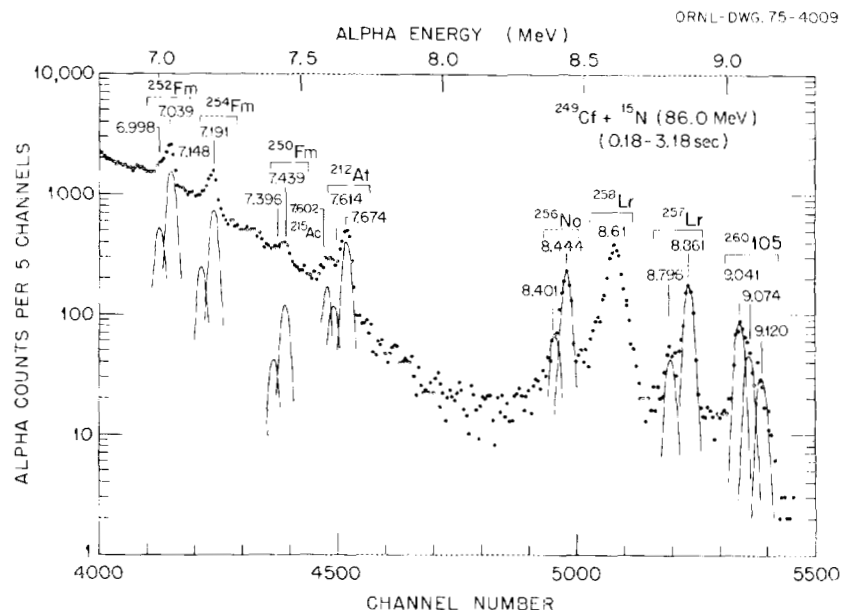


Fig. 1.70. Alpha spectrum of activities produced in the $^{249}\text{Cf} + ^{15}\text{N}$ reaction at 86.0 MeV.

out an experiment to identify, by observation of characteristic x rays, the atomic number of the previously reported³ isotope $^{260}105$. We produced $^{260}105$ in the $^{249}\text{Cf}(^{15}\text{N},4n)$ reaction using 99-MeV $^{15}\text{N}^{4+}$ ions accelerated at the ORIC facility. After an energy loss of about 14 MeV in the beryllium target chamber window and target backing, the ^{15}N ions had an energy optimized for this reaction. The reaction products recoiling out of the ^{249}Cf target were transferred to our counting station via a tape transfer system. The tape was advanced about every 3 sec so that the spot of collected activity faced an Si(Au) surface-barrier alpha and fission detector and was viewed through the tape by an intrinsic germanium photon detector.

We measured the energies of the emitted alpha particles, fission fragments, and photons and determined the time from the end of irradiation associated with any individual event and/or the time between two events (such as alpha and x ray). During about 200,000 irradiation and counting cycles, we observed 850 alpha events grouped into three peaks at 9.041, 9.074, and 9.120 MeV, with relative intensities of 0.53, 0.28, and 0.19, respectively (see Fig. 1.70), and a half-life of 1.52 ± 0.13 sec, which we ascribe to the decay of $^{260}105$. In coincidence with these alpha events, we saw ~ 150 L x-ray events whose energies and relative intensities are in excellent agreement with the calculated values⁴⁻⁶ (see Fig. 1.71) for the L x rays of lawrencium ($Z = 103$). To establish a genetic link between the $^{260}105$

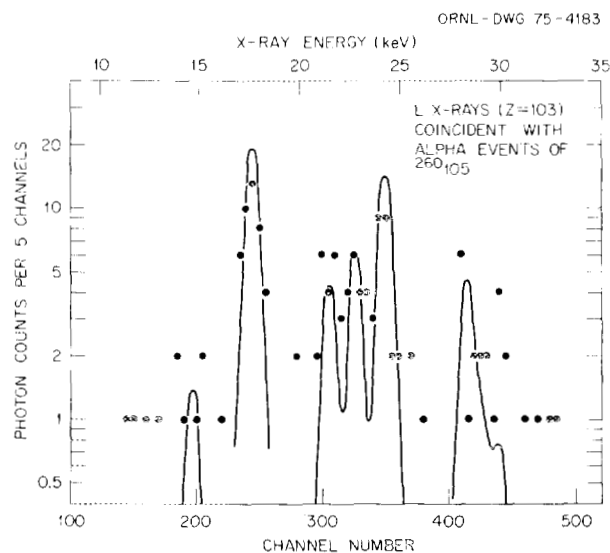


Fig. 1.71. L x-ray spectrum in coincidence with alpha events having $9.0 \leq E \leq 9.2$ MeV.

and its daughter ^{256}Lr , whenever an alpha event having an energy between 9.0 and 9.2 MeV occurred, the tape was stopped and the same spot was viewed by the Si(Au) detector for 35 sec to observe the alpha decay of the daughter. The spectrum for this "extended mode" corresponds, in the energies and the relative intensities of the alpha groups and in half-life, with the known

properties^{7,8} of ^{256}Lr . Thus, we have identified the atomic number of $^{260}105$ on the basis of the coincident L x-ray spectrum, and its mass number from the genetic link to the ^{256}Lr daughter.

-
1. Chemistry Division.
 2. An account of this work has appeared in *Chem. Div. Annu. Prog. Rep. Nov. 1, 1975*, ORNL-5111 (1976), p. 57.
 3. A. Ghiorso et al., *Phys. Rev. Lett.* **24**, 1498 (1970).
 4. C. C. Lu, F. B. Malik, and T. A. Carlson, *Nucl. Phys.* **A175**, 289 (1971).
 5. J. H. Scofield, Lawrence Livermore Laboratory, University of California, Livermore, report UCRL-51231, 1972.
 6. T. A. Carlson, private communication of calculated L x-ray intensities, 1974.
 7. K. Eskola et al., *Phys. Rev.* **C4**, 632 (1971).
 8. P. F. Dittner et al., to be published.

ATTEMPTED PRODUCTION OF $^{256}104$ ¹

P. F. Dittner² R. L. Hahn²
 R. J. Silva² J. R. Tarrant²
 C. E. Bemis, Jr.² L. D. Hunt²
 D. C. Hensley

The nuclide $^{256}104$ has been reported^{3,4} to be a ~ 5 -msec spontaneous fission (SF) activity as produced in the $^{208}\text{Pb}(^{50}\text{Ti},2n)$ reaction. However, no definitive elemental or isotopic identifications were possible in this prior work as only fission fragments were detected. The SF half-life for $^{256}104$, ~ 5 msec, was taken as evidence supporting a substantially different empirical trend for the even- A isotopes of $Z = 104$ than for the isotopes of fermium ($Z = 100$) and nobelium ($Z = 102$). Taking the result for $^{256}104$ together with the SF half-lives of $^{258}104$ (11 msec)⁵ and $^{260}104$ (0.1 sec),⁶ one would be tempted to predict substantially longer SF half-lives for other neutron-rich even-even nuclides in this region than had previously been predicted.

Because of the somewhat speculative nature of this prior work on $^{256}104$ and the importance of this nuclide in determining SF half-life trends, we have attempted to provide independent experimental evidence based on an x-ray identification using the coincident alpha-x-ray technique. Previous empirical trends suggested that the nuclide $^{256}104$ should have an SF half-life of ~ 10 sec and should undergo predominantly alpha decay ($8.5 \lesssim E_{\alpha_0} \lesssim 9.2$ MeV) with a total half-life in the range ~ 0.2 to 1.0 sec. Observing L -series x rays that follow the $\sim 20\%$ alpha-branching decay of $^{256}104$ to the 2^+ ground-band rotational state in ^{252}No would identify the nuclide. Additional identification information would be provided by observation

of the time-correlated direct genetic link with the known daughter nuclide, ^{252}No .

Initial experiments using the $^{244}\text{Cm}(^{16}\text{O},4n)$ reaction were unsuccessful because of poor recoil yields from the target, and our major efforts were made by using the $^{249}\text{Cf}(^{12}\text{C},5n)$ reaction, a less favorable reaction because the predicted cross section is about five times smaller than for $^{16}\text{O} + ^{244}\text{Cm}$. Approximately 200,000 bombardments using a tape transport assembly at bombardment-counting-time cycles of 1.5 sec were performed. The predicted yield for $^{256}104$ under our experimental conditions was expected to be ~ 1 alpha count/hr.

No obviously new alpha groups were readily apparent in our spectrum in the energy range of 8.5 to 9.2 MeV. The simultaneous production of 4.83-sec $^{257}104$ from the $(^{12}\text{C},4n)$ reaction interfered with the L x-ray identification, and no definitive information could be derived from the time-correlated genetic link aspect of our experiments. Obviously, better experiments can be performed by using the $^{244}\text{Cm}(^{16}\text{O},4n)$ reaction as we had planned originally. No interference from $^{257}104$ is expected when using this latter reaction.

-
1. An account of this work has appeared in *Chem. Div. Annu. Prog. Rep. Nov. 1, 1975*, ORNL-5111 (1975), p. 62.
 2. Chemistry Division.
 3. G. N. Flerov, p. 459 in *Proceedings of the International Conference on Reactions Between Complex Nuclei, Nashville, Tenn., June 1974*, vol. 2, R. L. Robinson et al., Eds., North-Holland, Amsterdam, 1974.
 4. Yu. Ts. Oganessian et al., *JETP Lett. (Engl. Transl.)* **20**, 265 (1974).
 5. A. Ghiorso et al., *Phys. Rev. Lett.* **22**, 1317 (1969).
 6. G. N. Flerov et al., *At. Energ.* **17**, 310 (1964) [*Sov. At. Energy (Engl. Transl.)* **17**, 1046 (1964)].

X-RAY IDENTIFICATION AND DECAY PROPERTIES OF ISOTOPES OF LAWRENCIUM¹

C. E. Bemis, Jr.² D. C. Hensley
 P. F. Dittner² R. L. Hahn²
 R. J. Silva² J. R. Tarrant²
 L. D. Hunt²

During the course of our experiment to identify element 105,³ and in a separate experiment where we bombarded a ^{249}Cf target with ^{11}B and then with ^{10}B , we produced several isotopes of lawrencium. The isotopes ^{258}Lr and ^{257}Lr were produced by the $^{249}\text{Cf}(^{15}\text{N}; \alpha, xn)$ reaction, where $x = 2$ and 3 respectively. The same equipment described in the $^{260}105$ article³ allowed us to determine the half-life,

Table 1.9. Experimental results of $^{255-258}\text{Lr}$ isotopes

Isotope	Half-life (sec)		Alpha-particle energy (MeV)		Intensity (%)	
	This work	Ref. 3 ^a	This work	Ref. 3 ^a	This work	Ref. 3 ^a
^{255}Lr	21.5 ± 5.0	22 ± 5	8.429 ± 0.018	8.37 ± 0.02	40 ± 10	~50
			8.370 ± 0.018	8.35 ± 0.02	60 ± 10	~50
^{256}Lr	25.9 ± 1.7	31 ± 3	8.624 ± 0.025	8.64 ± 0.02	4.2 ± 1.1	3 ± 2
			8.517 ± 0.015	8.52 ± 0.02	19.1 ± 1.5	19 ± 3
			8.472 ± 0.015	8.48 ± 0.02	13.3 ± 1.5	13 ± 3
			8.430 ± 0.015	8.43 ± 0.02	38.3 ± 2.9	34 ± 4
			8.390 ± 0.015	8.39 ± 0.02	18.8 ± 2.2	23 ± 5
^{257}Lr	0.646 ± 0.025	0.6 ± 1	8.319 ± 0.015	8.32 ± 0.02	6.3 ± 1.5	8 ± 2
			8.861 ± 0.012	8.87 ± 0.02	85 ± 4	81 ± 2
^{258}Lr	4.35 ± 0.59	4.2 ± 0.6	8.796 ± 0.013	8.81 ± 0.02	15 ± 4	19 ± 2
			8.648 ± 0.010	8.68 ± 0.02	10 ± 2	7 ± 2
			8.614 ± 0.010	8.65 ± 0.02	35 ± 5	16 ± 3
			8.589 ± 0.010	8.62 ± 0.02	45 ± 7	47 ± 3
			8.54 ± 0.020	8.59 ± 0.02	10 ± 5	30 ± 4

^aSee this report, P. F. Dittner et al., "Decay Properties and *L* X-Ray Identification of Element $^{260}_{105}$."

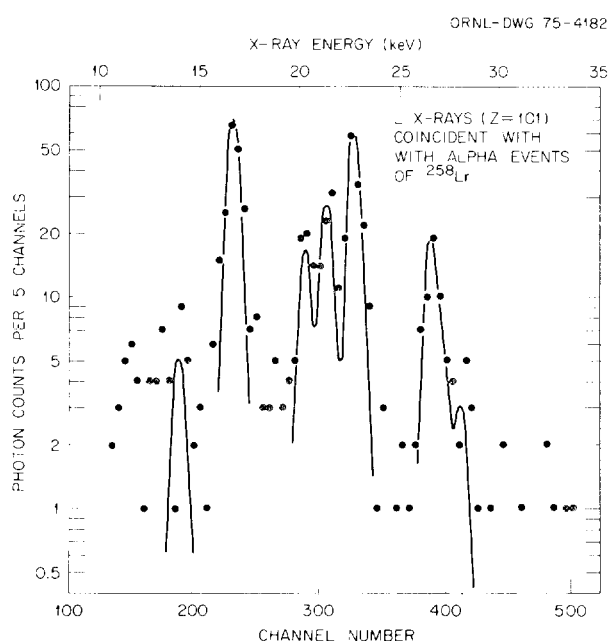


Fig. 1.72. Prompt photon spectrum coincident with alpha groups assigned to the decay of ^{258}Lr . The unique energy signature confirms the atomic number as $Z = 101$; thus the alpha-decay parent is confirmed to be $Z = 103$.

energies, and relative intensities of the alpha groups of ^{258}Lr and ^{257}Lr (see Table 1.9). In addition, ~600 *L*-series x rays of mendelevium ($Z = 101$) were seen in coincidence with the alpha events of ^{258}Lr (Fig. 1.72), thus identifying the atomic number of lawrencium as 103.

In another experiment, ^{256}Lr and ^{255}Lr were produced via the $^{249}\text{Cf}(^{11}\text{B},4n)$ and $^{249}\text{Cf}(^{10}\text{B},4n)$ reactions respectively. The experimental apparatus used was identical with our earlier work on the x-ray identification of nobelium.⁴ The half-lives and alpha-decay properties of ^{256}Lr and ^{255}Lr are shown in Table 1.9. Our results are in excellent agreement with previous measurements⁵ and, in some cases, of higher precision. Further, the x-ray identification of ^{258}Lr is the first unequivocal confirmation of the atomic number of lawrencium: earlier genetic linkage experiments are fraught with uncertainty because the mendelevium daughters either are not well characterized or do not undergo alpha decay.

1. An account of this work has appeared in *Chem. Div. Annu. Prog. Rep. Nov. 1, 1975*. ORNL-5111 (1976), p. 58.
2. Chemistry Division.
3. See this report, P. F. Dittner et al., "Decay Properties and *L* X-Ray Identification of Element $^{260}_{105}$."
4. P. F. Dittner et al., *Phys. Rev. Lett.* **26**, 1037 (1971).
5. K. Eskola et al., *Phys. Rev. C* **4**, 632 (1971).

DETERMINATION OF THE HALF-WAVE AMALGAMATION POTENTIAL OF NOBELIUM (ELEMENT 102)

R. E. Meyer¹ P. F. Dittner¹
W. J. McDowell² R. J. Silva¹
J. R. Tarrant¹

The half-wave amalgamation potential of nobelium, element 102, has been determined for the reaction No^{2f}

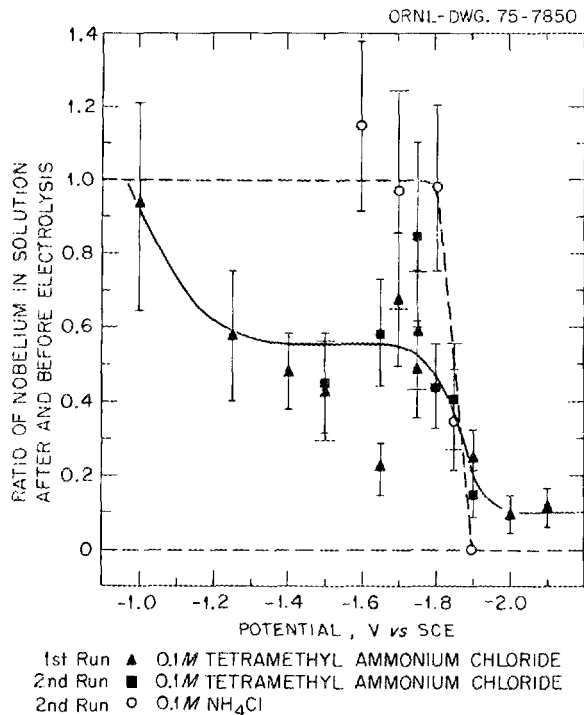


Fig. 1.73. Ratios of nobelium activities in solution plotted vs potential.

+ $2e^- \rightarrow \text{No}$ (amalgam).³ The nobelium isotope ^{255}No , with a half-life of 223 sec, was produced a few hundred atoms at a time by the reaction $^{249}\text{Cf}(^{12}\text{C}, \alpha 2n)^{255}\text{No}$ at ORIC. The nobelium activity was caught on an anodized aluminum disk and transferred pneumatically to the laboratory where it was washed into a small electrolysis cell with solvent (0.1 M tetramethyl ammonium chloride or 0.1 M NH_4Cl) and electrolyzed into a mercury cathode. Comparisons of the nobelium activity in the solution phase were made before and after electrolysis. By repeating the experiment at various electrode potentials (maintained constant by use of a potentiostat), the half-wave amalgamation potential was determined to be -1.85 ± 0.1 V vs the saturated calomel electrode, as shown in Fig. 1.73. The half-wave potential is estimated by taking the midpoint of the final drop in the ratio. The lower ratios at intermediate potentials for the runs with tetramethyl ammonium chloride can be explained by an adsorption phenomenon. By combining this measurement with the systematics of Nugent,⁴ we may estimate the standard potential for the $\text{No}-\text{No}^{2+}$ couple to be -2.6 V vs the standard hydrogen potential. Thus, by making use of only a few cyclotron-produced atoms, a fundamental and important thermodynamic property of nobelium was estimated.

1. Chemistry Division.
2. Chemical Technology Division.
3. An account of this work has appeared in *Chem. Div. Annu. Prog. Rep. Nov. 1, 1975*, ORNL-5111 (1976), p. 30.
4. L. J. Nugent, *J. Inorg. Nucl. Chem.* **37**, 1767 (1975).

EN Tandem Program

HIGH-SPIN STATES OF THE $K^\pi = 3/2^+$ AND $1/2^+$ BANDS OF ^{23}Na

D. E. Gustafson¹ J. L. C. Ford, Jr.
S. T. Thornton¹ P. D. Miller
T. C. Schweizer¹ R. L. Robinson
P. H. Stelson

The present experiment was undertaken to investigate high-spin states in ^{23}Na by examining the $^{12}\text{C}(^{15}\text{N}, \alpha)^{23}\text{Na}$ reaction in the framework of the statistical model employing Hauser-Feshbach (H-F) formalism. Previous heavy-ion-induced reactions in this mass region have indicated that the primary reaction mechanism should be of a compound-nuclear nature.^{2,3} In the present experiment, suggestions for spin-parities of the levels populated have been extracted from a comparison of energy-averaged angular distributions with H-F calculations. From the high-spin suggestions we have considered the possible rotational-band structure of the $K^\pi = 3/2^+$ ground-state and $K^\pi = 1/2^+$ bands. Energy-level predictions for high-spin states from shell-model calculations have been compared with the energy levels of high-spin states suggested from the H-F analysis for several of the higher spins ($J^\pi \geq 13/2^+$).

In the present work a ^{15}N beam was extracted from a duoplasmatron charge-exchange source and accelerated with the ORNL EN tandem accelerator. The reaction alpha particles were detected at the focal surface of an Enge split-pole spectrograph with a Borkowski-Kopp-type^{4,5} counter. At $\theta_{\text{lab}} = 7^\circ$ we measured excitation functions for states from 0 to 18 MeV of excitation energy in the bombarding energy range $E_{\text{lab}} = 36.0$ to 39.2 MeV in 400-keV steps. Cross sections were also measured at $\theta_{\text{lab}} = 15^\circ, 22^\circ,$ and 28° for four of these bombarding energies, and at 38.5° and 66.0° for 38.0 MeV. The excitation energies observed were limited at the more backward angles.

The $^{12}\text{C}(^{15}\text{N}, \alpha)^{23}\text{Na}$ reaction populates many levels, as may be seen in Fig. 1.74. Many of the more strongly populated levels are labeled by their excitation energies (taken from ref. 6) for the known low-lying levels, and determined from an alpha calibration of the magnetic spectrograph for the higher-lying energy lev-

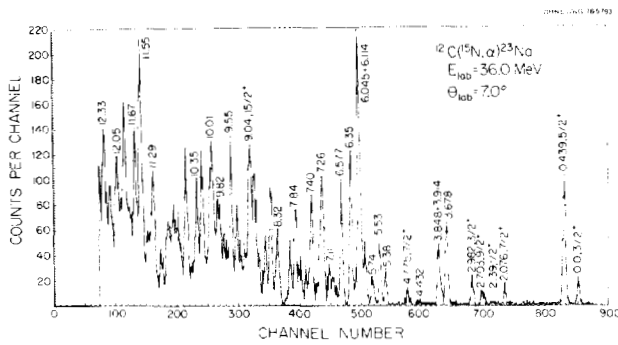


Fig. 1.74. A portion of the alpha spectrum from the $^{12}\text{C}(^{15}\text{N}, \alpha)^{23}\text{Na}$ reaction. Peaks are labeled by excitation energy from ref. 6 or from the present work ($\pm 30 \text{ keV}$).

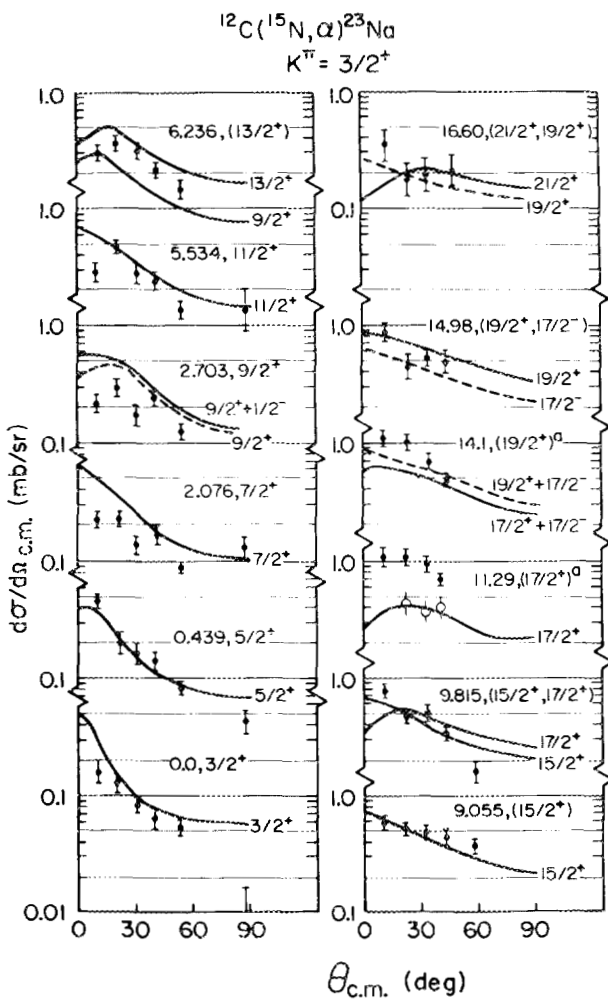


Fig. 1.75. Angular distributions for established and proposed $K^\pi = 3/2^+$ band members. Solid and dashed lines are the H-F calculations as discussed in the text for the spins indicated. States marked with a superscript *a* are unresolved multiple peaks with the suggested band member in parentheses. The open circles for the 11.29-MeV state represent peak-fitted contributions of the dominant state of the multiplet.

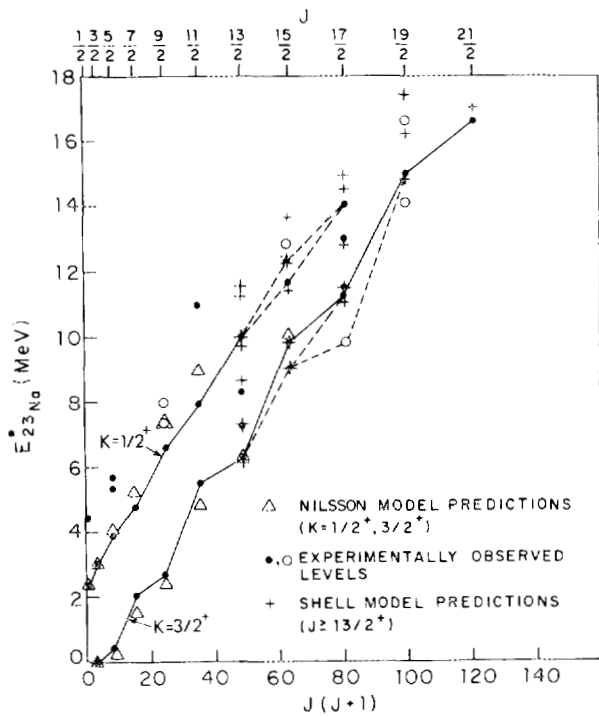


Fig. 1.76. Plot of the proposed $K^\pi = 3/2^+$ and $1/2^+$ rotational bands. The dots and open circles represent the H-F suggestions for spin values of experimentally observed levels; the dots represent the presently preferred spin values. Crosses indicate levels from shell-model calculations (ref. 7) for $J^\pi > 13/2^+$; the open triangles indicate Nilsson-model predictions (ref. 9) for the $K^\pi = 1/2^+$ and $3/2^+$ bands.

els. The excitation energies determined in the present experiment are quoted to $\pm 30 \text{ keV}$. Energy-averaged angular distributions for the proposed $K^\pi = 3/2^+$ ground-state band members and the corresponding H-F calculations for these states are shown in Fig. 1.75.

Remarkably good agreement is seen when comparing the high-spin states proposed in the present experiment to predictions for the energy levels of high-spin states obtained from large-basis shell-model calculations.⁷ Indications that the shell-model calculations give good agreement with the rotational structures and also account for states that are not in these bands implies that the extensive shell-model calculations consider the collective shapes of these bands implicitly, as is also the case in the ^{22}Na nucleus.⁸ Figure 1.76 displays our suggestions for the $K^\pi = 3/2^+$ (ground-state) and $K^\pi = 1/2^+$ bands in the form of a plot of excitation energy vs $J(J+1)$. Those experimentally observed high-spin states which have two spin possibilities are shown with the favored spin as a solid point and the other possible spin as an open circle. The band members according to

shell-model calculations⁷ and Nilsson model calculations⁹ are indicated by the crosses and open triangles respectively.

1. University of Virginia, Charlottesville.
2. J. Gomez del Campo et al., to be published in the *Physical Review*.
3. J.L.C. Ford, Jr., et al. *Z. Phys.* **269**, 147 (1974).
4. C. J. Borkowski and M. K. Kopp, *Rev. Sci. Instrum.* **39**, 1515 (1968).
5. C. J. Borkowski and M. K. Kopp, *IEEE Trans. Nucl. Sci. NS-17*, 390 (1970).
6. P. M. Endt and C. Van der Leun, *Nucl. Phys.* **A214**, 1 (1973).
7. B. H. Wildenthal, unpublished.
8. B. M. Freedom and B. H. Wildenthal, *Phys. Rev. C* **6**, 1633 (1972).
9. G. G. Frank et al., *Can. J. Phys.* **51**, 1155 (1973).

STUDY OF THE COHERENCE WIDTHS Γ IN ^{28}Si MEASURED BY THE $^{12}\text{C}(^{16}\text{O},\alpha)^{24}\text{Mg}$ REACTION

J. Gomez del Campo¹ J.L.C. Ford, Jr.
M. E. Ortiz¹ R. L. Robinson
A. Dacal¹ P. H. Stelson
S. T. Thornton²

The coherence width Γ of highly excited compound-nuclear states depends on the excitation energy and total angular momentum J of the compound system, and possibly the excitation energy of the state in the final nucleus populated by the compound-nucleus decay.³ Heavy-ion reactions may be a useful technique with which to investigate these effects because these reactions form compound systems at high excitation energy with high angular momentum.

Natural carbon foils with thicknesses of 7 to 10 $\mu\text{g}/\text{cm}^2$ were bombarded by ^{16}O ions from the Oak Ridge tandem accelerator at laboratory energies between 40 and 46 MeV. The reaction products were detected by a 60-cm-long position-sensitive proportional counter located at the focal plane of a split-pole magnetic spectrograph.

Figure 1.77 displays the alpha-particle spectrum recorded at a bombarding energy of 40.4 MeV and laboratory angle of 7° . The energy resolution of the order of 60 keV made it possible to sufficiently resolve states such as the 4^+ and 2^+ levels at 4.12 and 4.23 MeV respectively. The states in ^{24}Mg are labeled in Fig. 1.77 by the presently measured values for the excitation energies, whereas the spins and parities are generally those of ref. 4.

Excitation functions for the $^{12}\text{C}(^{16}\text{O},\alpha)^{24}\text{Mg}$ reaction leading to the levels or multiplets listed in Table 1.10

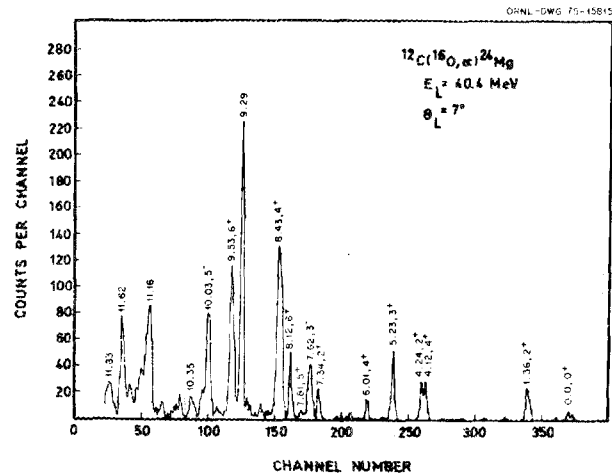


Fig. 1.77. A $^{12}\text{C}(^{16}\text{O},\alpha)^{24}\text{Mg}$ spectrum obtained at a bombarding energy of 40.4 MeV and a laboratory angle of 7° .

were measured in 200-keV intervals for incident energies (lab) between 40 and 46 MeV. The table also presents experimental and theoretical Γ values for levels in ^{24}Mg whose spin and excitation energy values are those of refs. 4, 5, and 6. Some of the levels in ^{24}Mg that were not resolved are indicated by brackets in the table.

The coherence widths Γ were obtained from the excitation functions by the usual techniques⁷⁻¹¹ of autocorrelation functions and counting maxima per unit energy. Table 1.10 shows as Γ_A the resulting Γ values using the autocorrelation functions, including corrections for finite energy resolution and sample size in the manner described by Halbert et al.⁷ The tabulated errors are the relative standard deviations as defined in ref. 4. The Γ_M of Table 1.10 correspond to the coherence widths obtained from counting the number of maxima in the excitation functions, and the tabulated errors are based on an estimation of the uncertainties in the number of maxima.

The coherence widths obtained from the autocorrelation functions show large deviations from one level to another (Table 1.10). However, the variation of the Γ_M values from level to level is less and indicates no significant dependence on the spin of the final nucleus. Because of the effects of finite sample length, the method of counting maxima should in the present case be the more reliable method of determining Γ . Similar conclusions have also been drawn from other analyses of the $^{12}\text{C}(^{16}\text{O},\alpha)^{24}\text{Mg}$ reaction,⁷ as well as from other heavy-ion reactions.¹²

The coherence width Γ can be evaluated in terms of the statistical model by calculating the partial widths

Table 1.10. Γ values (in keV) extracted from the fluctuation analyses of the $^{12}\text{C}(^{16}\text{O},\alpha)^{24}\text{Mg}$ reaction at bombarding energies between 40 and 46 MeV

E_x^a	J^d	Γ_A	Γ_M	Γ_{th}
1.369	2^+	120 ± 28	152 ± 30	139
4.123	4^+	145 ± 32	101 ± 30	120
4.239	2^+	81 ± 19	130 ± 22	156
5.236	3^+	130 ± 30	114 ± 16	163
6.010	4^+	135 ± 30	114 ± 38	132
7.348	2^+	91 ± 21	114 ± 38	184
7.553	1^-			222
7.616	3^-	166 ± 37	91 ± 10	159
7.812	5^{+b}	69 ± 15	101 ± 13	123
8.120	6^+	42 ± 9	91 ± 23	110
8.358	3^-			166
8.436	4^+	214 ± 46	114 ± 38	145
8.654	2^+	79 ± 19	114 ± 16	242
8.864	2^-	122 ± 27	130 ± 52	243
9.002	2^+	77 ± 18	114 ± 38	250
9.283	2^-			212
9.300	4^+	76 ± 16	91 ± 10	152
9.300	4^-			176
9.520	6^+	126 ± 27	130 ± 22	118
9.827	1^+	73 ± 20	114 ± 16	293
10.027	5^-	280 ± 62	114 ± 16	112
10.161	3^{-c}	64 ± 15	91 ± 10	154
10.355	2^+	118 ± 28	101 ± 13	231
10.578	5^{-c}	113 ± 25	152 ± 30	142
10.683	0^+	58 ± 16	114 ± 16	330
10.822				
10.922	2^+	69 ± 16	114 ± 38	242
11.017	2^+	168 ± 39	101 ± 13	244
11.163	(3^-)			202
11.220	4^+	88 ± 19	83 ± 9	168
11.313	(3^-)	85 ± 23	130 ± 52	202
11.457	2^+	72 ± 17	83 ± 9	254
11.594	5^-	86 ± 18	114 ± 16	148
11.693	4^+			173
11.860	8^{+d}	120 ± 25	130 ± 22	98
11.980	2^+	90 ± 21	101 ± 13	268
12.050	4^+			176
12.120	(5^-)	112 ± 23	130 ± 22	153

^aValues from ref. 4.

^bFrom ref. 5.

^cThis spin included in the H-F calculations.

^dFrom refs. 5 and 6.

$\Gamma_{J\pi}$ of compound-nucleus levels at a given excitation energy E_x and spin-parity J^π . The computation of Γ , given in the last column of Table 1.10, has been made using an H-F treatment and the parameters given in ref. 13.

Figures 1.78 and 1.79 show the dependence of the coherence width Γ on the excitation energy in ^{28}Si . The first three experimental points are those obtained by Halbert et al.,⁷ averaging the Γ values for the ground state and first four excited states. We obtained the

ORNL-DWG 76-2969

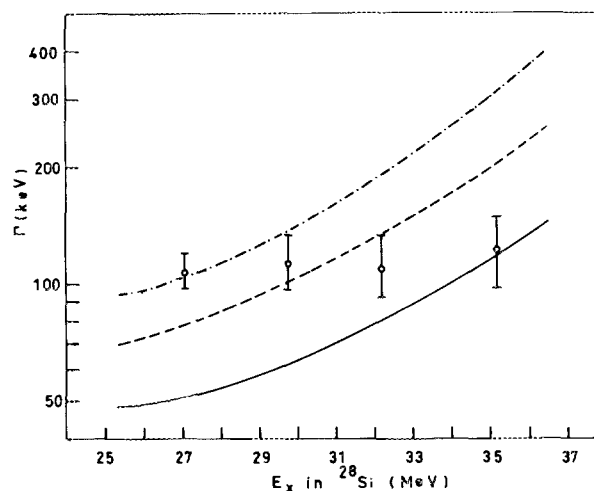


Fig. 1.78. The dependence of the coherence width Γ on the excitation energy in the compound nucleus ^{28}Si . The first three points are from ref. 7. The curves were calculated using the values $\Delta = 3.89$ MeV, $\mathcal{J}/\hbar^2 = 4.26$, and $a = 3.86, 3.54$, and 3.26 MeV^{-1} for the dot-dashed, solid, and dashed curves respectively.

ORNL-DWG 76-2970

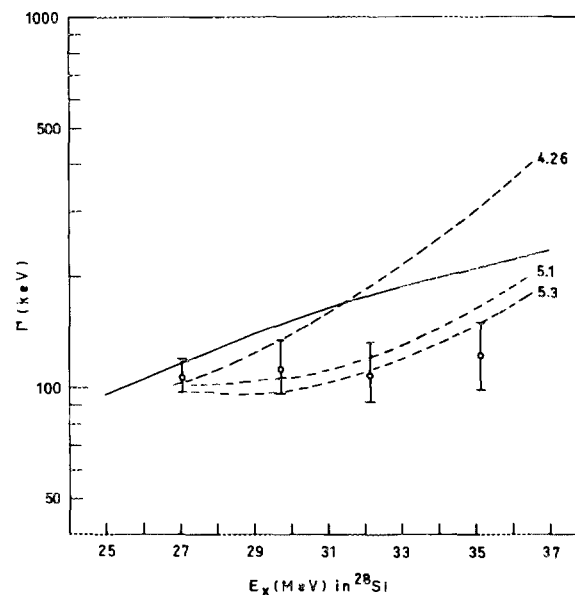


Fig. 1.79. The dependence of the coherence width Γ on the excitation energy in the compound nucleus ^{28}Si . The first three points are from ref. 7. The dashed curves were calculated using the values of 3.86 MeV^{-1} and 3.89 MeV for a and Δ respectively. However, the moment of inertia \mathcal{J}/\hbar^2 was varied as indicated. The solid line is the result obtained by using the expression $\Gamma = 14 \exp(-4.69 \sqrt{A/E_x})$ (see ref. 14).

from coincidence with the 90° detector. Coincidence spectra are essential to eliminate effects of side feeders.

The lifetimes in the central yrast cascade show a regular decrease. They yield an almost constant deformation, extracted from the $B(E2)$ values, except perhaps for the 4^+ level, where our results may be somewhat longer than reported from Coulomb excitation. A comparison of the two ^{74}Se positive-parity bands to the levels in ^{72}Se , where a coexistence model was invoked,² suggests that they may be built on spherical and deformed shapes. However, in contrast to ^{72}Se , every like-spin member of both bands in ^{74}Se is close and so there may be considerable mixing of many different levels. It is not clear yet what motion characterizes the yrast cascade above the 10^+ state, where there is a break in the moment of inertia plot

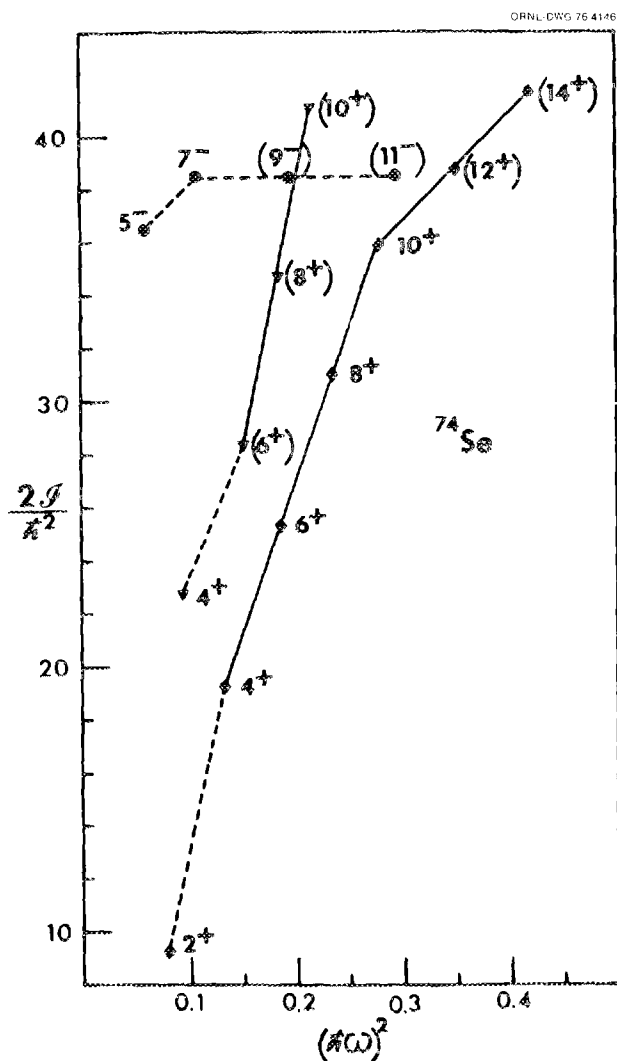


Fig. 1.81. Moment of inertia extracted for states of ^{74}Se .

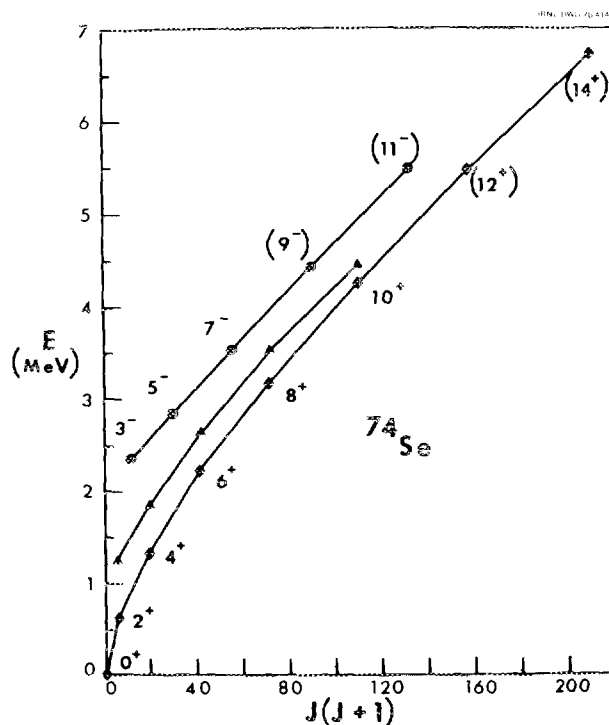


Fig. 1.82. Energies of levels in three ^{74}Se bands plotted vs $J(J+1)$.

(see Fig. 1.81). Further analysis of these positive-parity levels is in progress.

The most striking new feature of ^{74}Se is the discovery of the negative-parity band built on a collective (~ 9 spu) 3^- level reported at 2350 keV in Coulomb excitation studies.⁴ In Fig. 1.82 we have plotted the energy levels of these bands vs $J(J+1)$. One can see from these plots that the negative-parity band fits the one-parameter (linear) rotational formula extremely well, whereas such a fit for the two positive-parity bands is less successful.

For the negative-parity band, Fig. 1.82 shows that $\hbar^2/2I$ is remarkably constant compared to the positive-parity bands and is about 26.0 keV. This is much closer to the irrotational value of 34.4 keV than the rigid-body value of 2.5 keV calculated for $\beta = 0.3$. The deformation of the negative-parity level as extracted from lifetimes of the (9^-) and (11^-) levels is larger than for the positive-parity levels. This is the first time that a negative-parity band built upon a collective 3^- level has been studied to such high spins in medium-mass nuclei. In ^{66}Zn , negative-parity levels are reported but are attributed to excited neutron configuration states.⁵

1. Vanderbilt University, Nashville, Tenn.

2. J. H. Hamilton et al., *Phys. Rev. Lett.* **32**, 239 (1974).
3. J. Hadermann and A. C. Rester, *Nucl. Phys. A* **231**, 120 (1974).
4. J. Barette et al., *Nucl. Phys. A* **235**, 154 (1974).
5. J. F. Bruandet et al., *Phys. Rev. C* **12**, 1739 (1975).

TESTS OF THE COEXISTENCE OF SPHERICAL AND DEFORMED SHAPES IN ^{72}Se

J. H. Hamilton¹ V. Maruhn-Rezwani
 H. L. Crowell¹ J. A. Maruhn
 R. L. Robinson N. C. Singhal¹
 A. V. Ramayya¹ H. J. Kim
 W. E. Collins² R. O. Sayer³
 R. M. Ronningen¹ T. Magee⁴
 L. C. Whitlock⁴

Final results for the lifetimes of the 4^+ to (12^+) states in the yrast cascade in ^{72}Se were obtained from coincidence spectra where the gate transitions were higher yrast states to eliminate side feeders. This is the first time to our knowledge that lifetimes have been measured for the yrast states from spin 4^+ to (12^+) in a complex decay populated by a nuclear reaction where all feeder problems were eliminated by gamma-gamma coincidence work. The lifetimes are $4.5^{+1.5}_{-1.0}$, 2.6 ± 0.7 , $0.75^{+0.10}_{-0.08}$, 0.35 ± 0.07 , and 0.25 ± 0.04 psec respectively. These values reveal a pattern of increasing deformation to the 6^+ state and constant beyond that, as would be expected in a coexistence model.⁵ Our results do not agree with values of the 4^+ to (12^+) lifetimes extracted from singles data in refs. 6 and 7, where side feeders and extraneous gamma rays in the vicinity of the transition of interest create serious difficulty. Our results clearly show that coincidence data are essential in the extraction of lifetimes in some if not all such cases.

A recent theoretical work⁸ has suggested that no second minimum exists in ^{72}Se ; if correct, this would invalidate our earlier interpretation.⁶ To further test our interpretation we have used the Greuss-Greiner approach^{9,10} of varying the potential to see what type of potential energy surface can reproduce the experimental levels and our $B(E2)$ values. The data used and the resulting theoretical values are shown in Fig. 1.83 together with the potential energy surface. The fit used six parameters in the potential energy and one for an anharmonic kinetic term. The latter proved to be necessary to give both the correct moment of inertia for the rotational band and the level spacing of the vibrational levels.

The potential energy surface has three minima, with all of the experimental levels being located in the

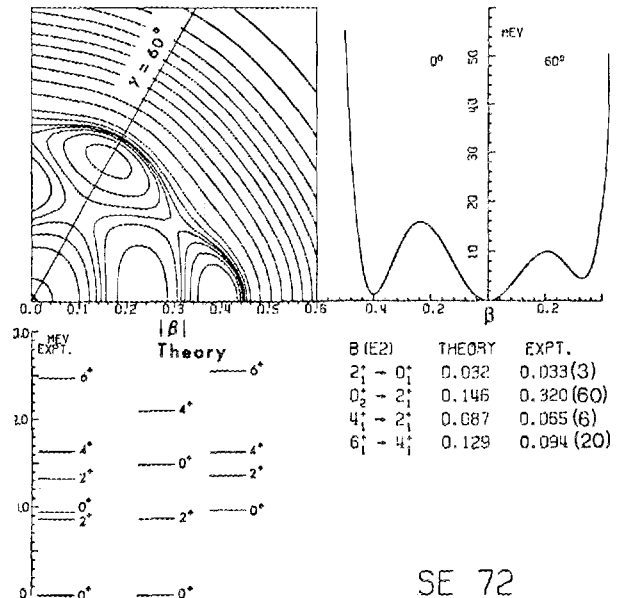


Fig. 1.83. Potential energy surface in a β and γ plot. In the right-hand part of the figure are shown cuts through the surface at $\gamma = 0^\circ$ and $\gamma = 60^\circ$ plotted as a function of β . The units of $B(E2)$ are $10^{-48} \text{ e}^2 \text{ cm}^4$.

spherical and prolate minima only. The third minimum on the oblate axis has little influence on these states, and its existence or nonexistence cannot be inferred from presently known experimental data. It should be borne in mind that these are least-square-fit results, so that those parts of the potential energy surface which have no bearing on the experimental quantities are just a by-product of the fit in the important areas and need not be meaningful physically. This is simply an expression of the fact that the experimental data are not sufficient to determine the surface in its entirety. The main intention of the present fit is to show that the coexistence of spherical and deformed minima is able to explain the data. The low-spin states of the rotational band built on the 0^+ state are distorted considerably by the interaction with the spherical 2^+ state. This makes the application of the $I(I+1)$ rule and of the spherical vibrator or simple rotator model for the explanation of the low-energy spectrum highly doubtful. Additional support for the potential energy surface comes from the prediction of 4_2^+ and 6_2^+ states in the near-spherical minimum at 2095 and 3254 keV respectively. These states could be mixed with more deformed ones. States are seen at 2406 and 3214 keV with the predicted branching ratios to the lower 4^+ and 2^+ states.

1. Vanderbilt University, Nashville, Tenn.
2. Fisk University, Nashville, Tenn.
3. Computer Sciences Division.
4. Mississippi College, Clinton, Miss.
5. J. H. Hamilton et al., *Phys. Rev. Lett.*, **32**, 239 (1974).
6. I. M. Lemberg et al., p. 376 in *Twenty-Fifth Nuclear Structure Conference of the Soviet Academy of Sciences, Leningrad, 1975*, U.S.S.R. Academy of Sciences, Abstracts, 1975.
7. K. E. G. Löbner et al., *Z. Phys.* **A274**, 251 (1975).
8. F. Dickmann and K. Dietrich, private communication.
9. G. Gneuss and W. Greiner, *Nucl. Phys.* **A171**, 449 (1971).
10. L. V. Bernus et al., *International Conference on Gamma-Ray Transition Probabilities, Delhi, India, November 1974*, in press.

^{46}Ti HIGH-SPIN STATES

H. J. Kim R. L. Robinson
R. Ronningen¹

The high-spin states in ^{46}Ti determined via the in-beam study of gamma rays from the $^{39}\text{K}(^{12}\text{C}, \alpha p \gamma)^{46}\text{Ti}$ reactions for incident energies of 32 to 39 MeV are shown in Fig. 1.84. Also shown are the high-spin states in ^{50}Cr for comparison. The level and transition energies are very similar and suggest that they may be the simple shell-model states. Since they are

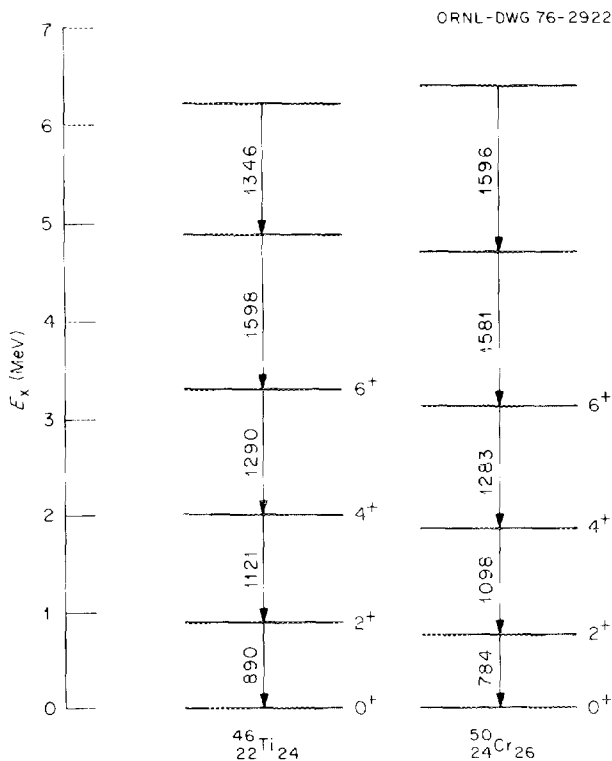


Fig. 1.84.

conjugate to each other, a common set of shell-model states can exist in both. It is hoped that the analysis of experimental angular distributions and direction correlations from oriented states (DCO) ratios, which is in progress, will lead to spin assignments for the higher-lying two new states.

1. Vanderbilt University, Nashville.

^{50}Cr HIGH-SPIN STATES

H. J. Kim W. K. Tuttle III¹ R. O. Sayer³
R. L. Robinson R. Ronningen² J. C. Wells, Jr.⁴

Based on their analysis of in-beam gamma-ray spectra resulting from the $^{40}\text{Ca}(^{16}\text{O}, 2p\alpha\gamma)^{50}\text{Cr}$ and $^{40}\text{Ca}(^{12}\text{C}, 2p\gamma)^{50}\text{Cr}$ reactions, Kutschera et al.⁵ made an 8^+ assignment to the 4.744-MeV level of ^{50}Cr , which decays exclusively to the 6^+ level via a 1581-keV gamma-ray transition. They then used this spin, in turn, to make still further assignments to higher-lying states. Figure 1.85 summarizes their results. Also shown for

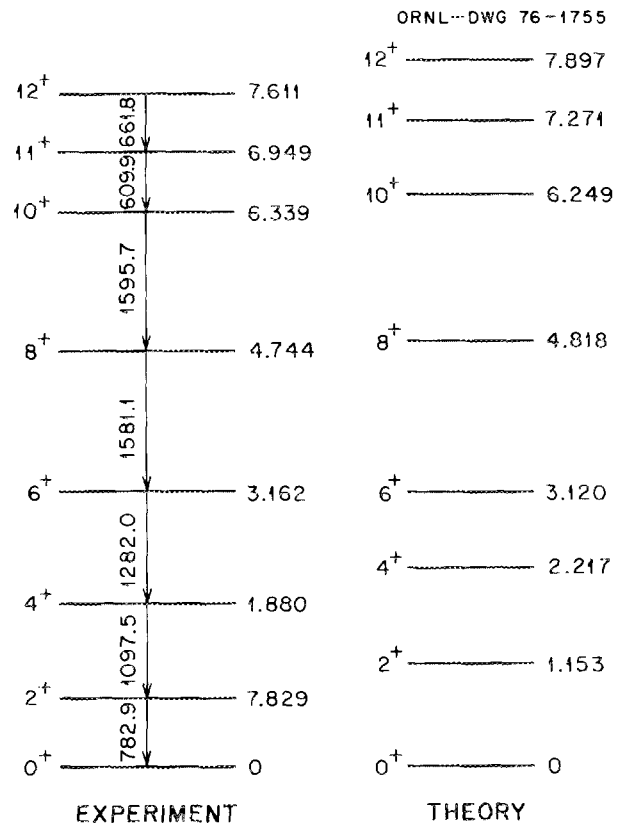


Fig. 1.85. Experimental and theoretical ^{50}Cr level scheme. Only the yrast levels are shown.

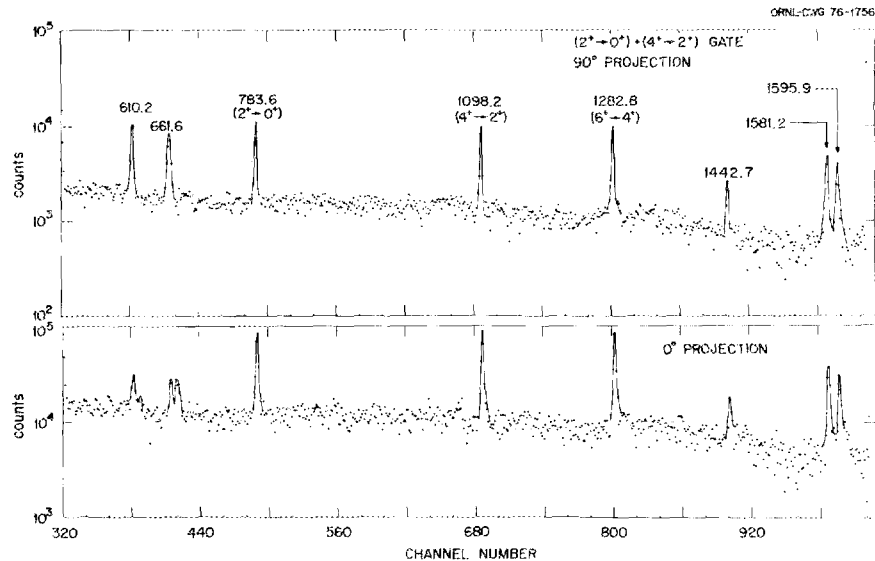


Fig. 1.86. 0° and 90° coincidence spectra projected from the two-parameter gamma-gamma coincidence matrix.

comparison are the calculated shell-model states as given in ref. 5. They measured gamma-ray angular distributions, linear polarizations (at 90° only), and gamma-gamma coincidence relations, but did not measure DCO ratios.^{6,7} As has been demonstrated, DCO ratio measurements for a cascade such as that of ^{50}Cr (see Fig. 1.85) would provide additional bases for the spin assignments.^{6,7}

We measured the DCO ratios between the 1581-keV and subsequent $6^+ \rightarrow 4^+$, $4^+ \rightarrow 2^+$, and $2^+ \rightarrow 0^+$ cascade gamma rays from ^{50}Cr levels populated via the $^{40}\text{Ca}(^{12}\text{C}, 2p\gamma)$ reaction at 38 MeV. A typical pair of coincidence spectra from which DCO ratios were deduced is shown in Fig. 1.86. (DCO ratios are essentially those of corresponding gamma-ray peak areas, 90° projection vs 0° projection, after correcting for detection efficiency differences.) The angular distributions of relevant gamma rays were also measured at 38 MeV. The present angular distribution of the 1581-keV gamma rays is consistent with the 8^+ assignment, but the DCO ratios are not. The DCO ratios from any pair of gamma rays for the $8^+ \rightarrow 6^+ \rightarrow 4^+ \rightarrow 2^+ \rightarrow 0^+$ cascade should be $R = 1$, whereas the observed average value of the ratio is $R_{\text{exp}} = 1.27 \pm 0.07$. This rather large discrepancy warrants an alternative spin assignment, and presently we are analyzing all available experimental results (i.e., angular distributions, polarizations, and DCO ratios) hoping to find an alternative assignment that resolves this discrepancy.

1. Present address: Department of Nuclear Medicine, Madigan Army Hospital, Fort Lewis, Wash.

2. Vanderbilt University, Nashville, Tenn.
3. Computer Sciences Division.
4. Tennessee Technological University, Cookeville, Tenn.
5. W. Kutschera et al., *Phys. Rev. Lett.* **33**, 1108 (1974).
6. J. A. Grau et al., *Phys. Rev. Lett.* **32**, 677 (1974).
7. H. J. Kim et al., *Nucl. Phys.* **A250**, 211 (1975).

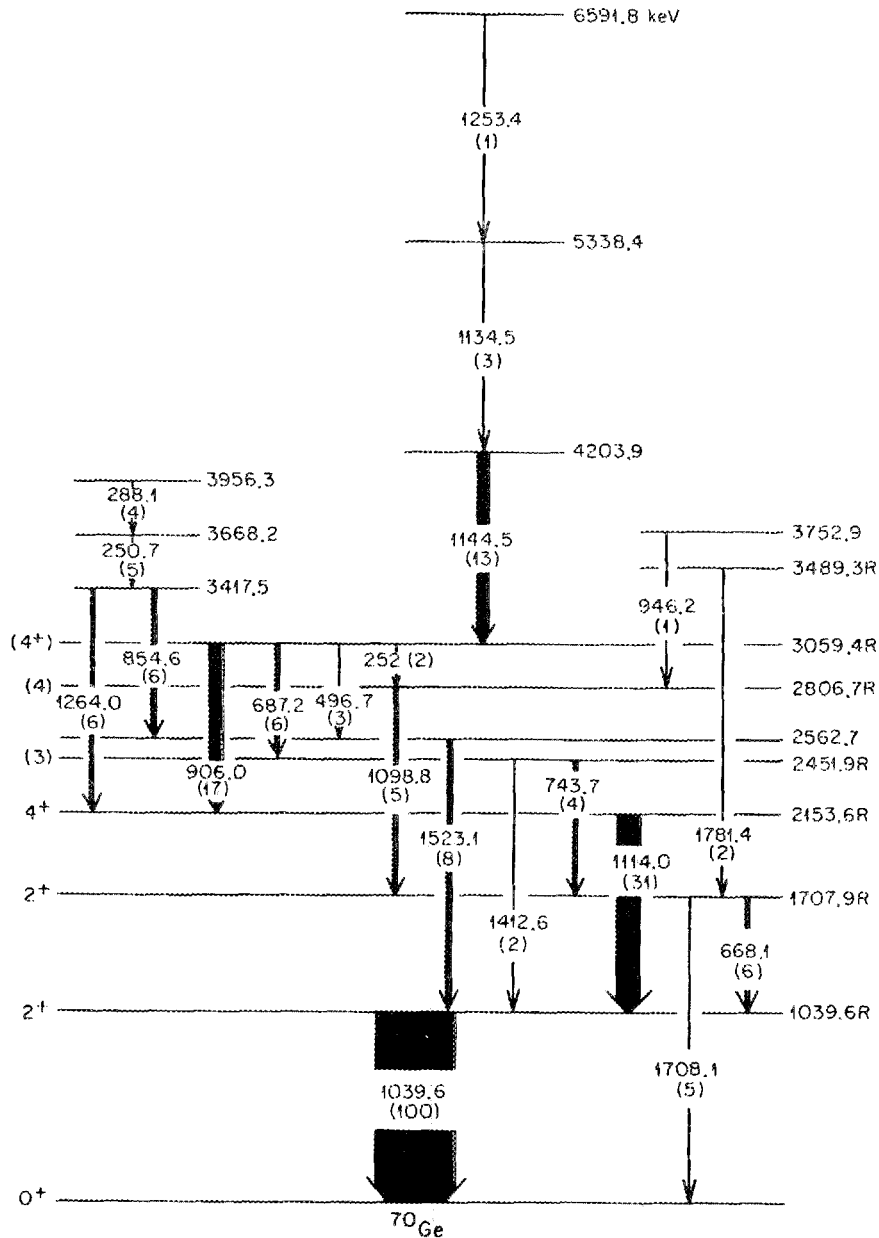
HIGH-SPIN STATES IN ^{68}Ge

A. P. de Lima¹ H. Kawakami¹ R. B. Piercey¹
 B. van Nooijen¹ A. V. Ramayya¹ R. L. Robinson
 R. M. Ronningen¹ J. H. Hamilton¹ H. J. Kim
 W. K. Tuttle III²

Recent studies of neutron-deficient nuclei in the region $Z > 28$, $N < 50$ have established band structures and unusual behavior in level energy spacings. Anomalous low-lying 0^+ excited states and rotational-like level spacings are two fascinating aspects of these studies. (For studies on ^{72}Se and ^{74}Se see J. H. Hamilton et al. and R. B. Piercey et al. in this same progress report.)

The germanium isotopes are interesting because in ^{70}Ge a 0^+ excited state lies just above the first excited state of $J^\pi = 2^+$, and in ^{72}Ge the 0^+ state is the first excited state. Thus we have done in-beam gamma-ray spectroscopy on the more neutron-deficient ^{68}Ge via the $^{12}\text{C}(^{58}\text{Ni}, 2p)^{68}\text{Ge}$ reaction with a beam energy of 39 MeV. Angular distributions and gamma-gamma coincidence measurements were made.

Preliminary analysis of our coincidence data agrees with the results of Nolte et al.³ for the yrast band up to (8^+). However, we tentatively assign a 1124-keV gamma

Fig. 1.88. Levels of ^{70}Ge .

Our preliminary $B(E\lambda)$ values are presented in Table 1.11. Interesting results are evident, some of which deviate from what we have found in our similar studies of gadolinium and hafnium nuclei.³ Although the β - and γ -type vibrational states decrease in energy and increase in strength with decreasing mass for the rare-earth region in general, the trend for the $2^+\beta$, $B(E2)$ strength for $^{156,158}\text{Dy}$ is reversed from this. Also for ^{164}Er , a possible⁴ fourth 2^+ state at 1483 keV is nearly five times as collective as the $I^\pi K = 2^+0$ state

at 1315 keV. Other collective states with $I^\pi = 2^+$ or 3^- are also weakly excited in ^{158}Dy , $^{162,164}\text{Er}$, and ^{168}Yb .

The $B(E3)$ strength for each nucleus is found mostly in one state, with an average value of $\sim 0.22 e^2 b^3$, except in ^{164}Er , where two $I^\pi = 3^-$ states share nearly that strength.

Our $B(E2)$ and $B(E3)$ measurements should provide good tests of collective models for this region because such models must not only predict the strengths and

Table 1.11. Experimental results for $B(E\lambda; 0^+_g \rightarrow I = \lambda)$

Nucleus	Level energy (keV)	Level	$B(E\lambda)$ ($e^2 \text{ b}^\lambda$)
^{156}Dy	138	2^+_g	3.67(5)
	891	$2^+_1\gamma$	0.187(11)
	829	$2^+_1\beta$	0.008(5)
	1367	3^-	0.22(7)
^{158}Dy	99	2^+_g	(4.91)
	946	$2^+_1\gamma$	0.149(10)
	1085	$2^+_1\beta$	0.051(9)
	1398	3^-	0.25(4)
	1610	(2^+)	<0.023
^{162}Er	101	2^+	4.95(3)
	897	$2^+_1\gamma$	0.167(8)
	1166	$2^+_1\beta$	0.041(6)
	1351	3^-	0.19(4)
	(1616)	(3^-)	<0.072
^{164}Er	91	2^+_g	5.37(3)
	860	$2^+_1\gamma$	0.146(7)
	1315	$2^+_1\beta$	0.0052(34)
	1434	3^-	0.106(19)
	1484	(2^+)	0.025(9)
	1568	3^-	0.065(24)
^{168}Yb	88	2^+_g	5.68(3)
	984	$2^+_1\gamma$	0.131(5)
	1234	$2^+_1\beta$	0.048(5)
	1475	3^-	0.22(3)
	1603	($2^+, 3^-$)	0.021(5) or 0.093(22) ($e^2 \text{ b}^2$) ($e^2 \text{ b}^3$)

trends of $2^+_1\gamma$, $2^+_1\beta$, and 3^- states but must describe the other observed collective modes.

The $B(E2)$ strengths of the 2^+_g states should be of interest for experiments and calculations involving properties of ground bands of these backbending nuclei. Also of interest is the measure of hexadecapole deformations for such neutron-deficient systems; $E4$ moments for these nuclei are now being extracted.

out in serious disagreement with calculations based on statistical evaporation of particles from a compound nucleus. Cross sections for this channel were based on in-beam intensities of the 429- and 674-keV gamma rays, which, according to Nolte et al.,³ were the $4 \rightarrow 2$ and $2 \rightarrow 0$ transitions of ^{74}Kr . However, Nolte et al.⁴ more recently have suggested energies of 455.7 and 557.8 keV for these two transitions. Also, several beta-decay studies⁵⁻⁷ of ^{74}Kr have become available since our original work was done. Reanalyzing our data with this new information, we obtained the limits (none of the ^{74}Kr in-beam or decay gamma rays were observed) on the cross sections given in Table 1.12. These are consistent with the calculated cross sections.

1. Vanderbilt University, Nashville, Tenn.
2. University of Tennessee, Knoxville.
3. R. M. Ronningen et al., to be published.
4. P. O. Tjøm and B. Elbek. *Nucl. Phys.* **A107**, 385 (1968).

ABSOLUTE CROSS SECTIONS FOR THE $^{61}\text{Ni}(^{16}\text{O},3n)^{74}\text{Kr}$ REACTION

J. C. Wells, Jr.¹ H. J. Kim
R. L. Robinson J.L.C. Ford, Jr.

In our earlier paper,² which reported the cross sections for a variety of channels from the $^{61}\text{Ni}(^{16}\text{O},X)$ reaction, one channel, the $^{61}\text{Ni}(^{16}\text{O},3n)^{74}\text{Kr}$, stood

1. Tennessee Technological University, Cookeville, Tenn.
2. J. C. Wells, Jr., et al., *Phys. Rev. C* **11**, 879 (1975).
3. E. Nolte et al., *Phys. Lett.* **33B**, 294 (1970).
4. E. Nolte et al., *Z. Phys.* **268**, 267 (1974).
5. H. Schmeing et al., *Nucl. Phys.* **A242**, 232 (1975).
6. Ali Coban, *J. Phys. (London)* **A7**, 1705 (1974).
7. E. Roeckl et al., *Z. Phys.* **266**, 65 (1974).

Table 1.12. Experimental and calculated cross sections for the $^{61}\text{Ni}(^{16}\text{O},3n)^{74}\text{Kr}$ reaction

$E_{^{16}\text{O}}$ (MeV)	σ (mb)	
	Experimental	Calculated
42	<0.15	0
44	<0.25	0
46	<0.40	0.010
48	<0.55	0.10
50	<0.65	0.27

HEAVY-ION NEUTRON YIELDS

J. K. Bair P. D. Miller
J. Gomez del Campo¹ P. H. Stelson

Determinations of the total neutron yields resulting from the $^{12,13}\text{C}$ bombardment of thin $^{12,13}\text{C}$ targets have been made. Figure 1.89 shows these data. Because, at sufficiently high energies, more than one neutron can be produced per neutron-producing event, the yield is plotted as $\sigma \cdot \nu$, where σ is the usual cross section and ν is the average number of neutrons produced per neutron-producing event. The data shown have not been corrected for the 1.1% of ^{13}C in the $^{\text{NA}}\text{C}$ target or for the 3% of ^{12}C in the enriched ^{13}C target. A preliminary error analysis indicates that the results are reliable to 5% (in addition to the errors shown in the figure).

Similar data are now available for ^{13}C on $^{16,18}\text{O}$. Data for $^{16,18}\text{O}$ on carbon have been previously reported.²

1. Universidad de Mexico, Mexico 20, D.F.

2. J. K. Bair et al., *Phys. Div. Annu. Prog. Rep. Dec. 31, 1972*. ORNL 4844 (1973), p. 45.

INTERACTION BARRIERS FOR THE $^{16,18}\text{O}$ PLUS NICKEL, COPPER, AND ZINC SYSTEMS

R. L. Robinson J. K. Bair

The cross sections for the $^{58,60,61,62,64}\text{Ni}$, $^{63,65}\text{Cu}$, and $^{64,66,67,68,70}\text{Zn}$ ($^{16,18}\text{O},xn$) reactions reported by Bair et al.¹ have been compared with the total reaction cross section calculated with the sharp-cutoff model and the parabolic barrier potential. To extract the total reaction cross sections from the experimental results, which only give cross sections for

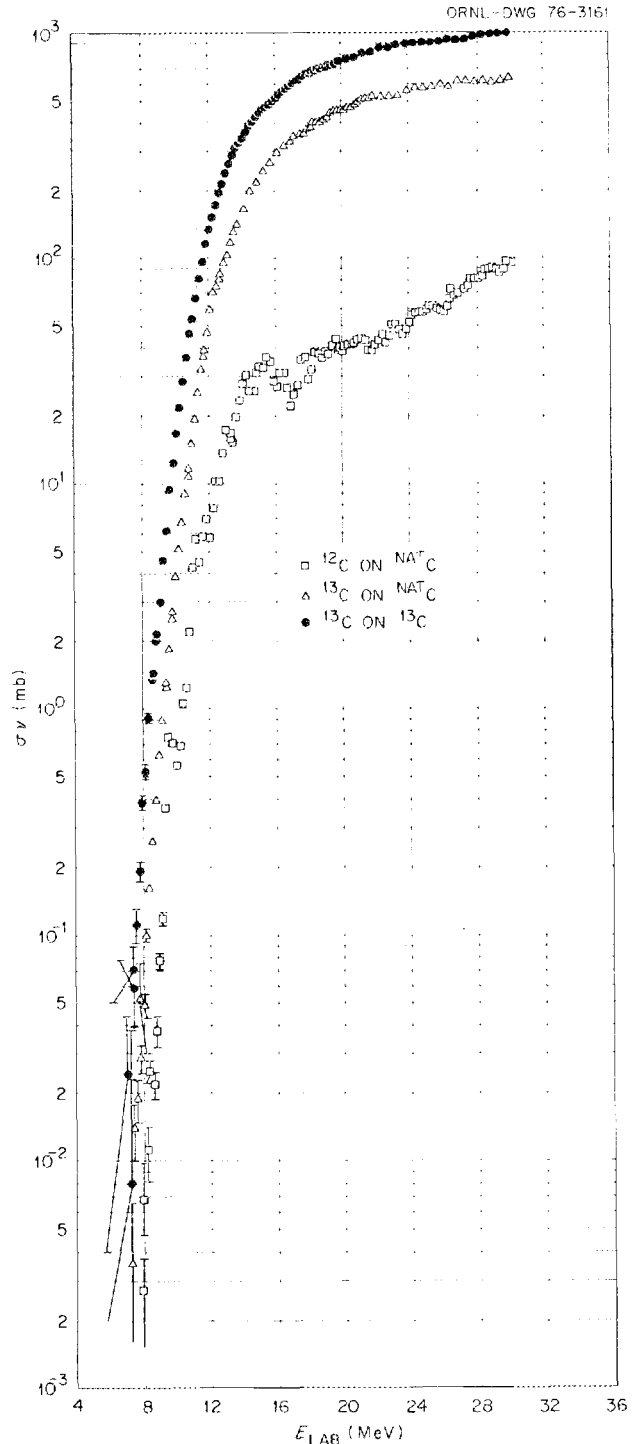


Fig. 1.89. Neutron yield for the indicated reactions. Target thicknesses were 20 to 50 $\mu\text{g}/\text{cm}^2$.

neutron-emitting channels, we used a computer program which assumes particles are statistically evaporated from a compound nucleus.²

The total reaction cross section for the sharp-cutoff model is calculated from the expression

$$\sigma_R = \pi R_f^2 \left[1 - \frac{V(R_f)}{E_{c.m.}} \right] \quad (1)$$

where R_f is the distance between the centers of the target and projectile at contact and $V(R_f)$ is the potential energy at that radius. A plot of σ_R vs $1/E_{c.m.}$, according to Eq. (1) will give a straight line with a zero intercept at $1/V(R_f)$. An example is shown in Fig. 1.90. The deviation of the experimental points near the energy axis from a straight line results from penetration, an effect not covered by this simple picture. The total reaction cross section for the parabolic-barrier model, which does account for penetration, is given by

$$\sigma_R = \frac{R_0^2 \hbar \omega_0}{2E_{c.m.}} \ln(1 + e^{2\pi(E_{c.m.} - V_0)/\hbar \omega_0}), \quad (2)$$

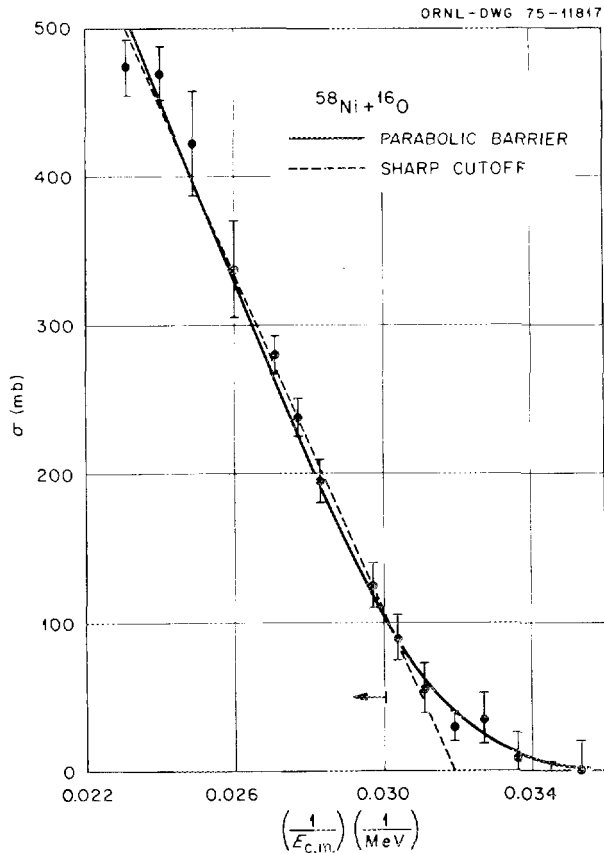


Fig. 1.90. Experimental and calculated total reaction cross section vs $1/E_{c.m.}$ for ^{16}O bombardment of ^{58}Ni .

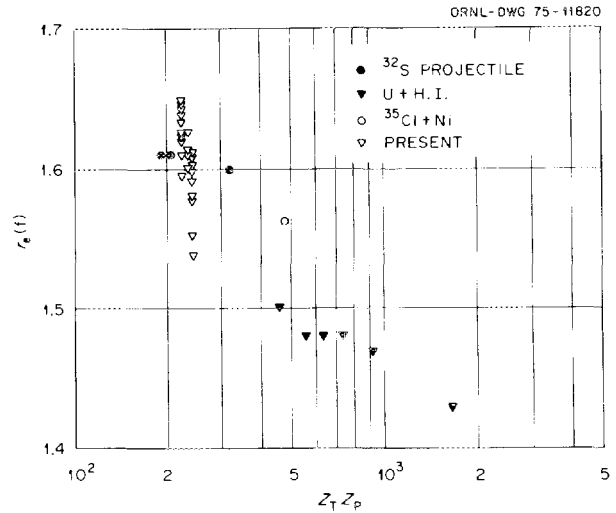


Fig. 1.91. Values extracted for the interaction radius r_e with the parabolic-barrier model for heavy-ion-induced reactions.

where R_0 , V_0 , and $\hbar\omega_0$ are the radius, height, and curvature, respectively, of the parabolic potential barrier for s waves.³ Nuclear deformation is included by assuming the interaction barrier has a uniform distribution of values between $V_0 - \Delta$ and $V_0 + \Delta$. For the comparison with the experimental data, Δ and $\hbar\omega$ were given values of 3.0 and 4.0 MeV respectively. An example of a fit is illustrated in Fig. 1.90.

Values extracted from the interaction barrier for the interaction radius

$$r_e = \frac{Z_P Z_T e^2}{V_0 (A_P^{1/3} + A_T^{1/3})}$$

for all projectile-target combinations fall in the range of 1.54 to 1.65 fm. As illustrated by Fig. 1.91, these compare favorably with interaction radii found from other heavy-ion-induced reactions.^{4,5}

1. J. K. Bair et al., private communication; *Bull. Am. Phys. Soc.* **17**, 530 (1972).
2. R. L. Robinson, H. J. Kim, and J.L.C. Ford, Jr., *Phys. Rev. C* **9**, 1402 (1974).
3. C. Y. Wong, *Phys. Rev. Lett.* **31**, 766 (1973).
4. L. C. Vaz and J. M. Alexander, *Phys. Rev.* **10**, 464 (1974).
5. W. Scobel et al., *Phys. Rev. C* **11**, 1701 (1975).

2. Nuclear Data Project

R. L. Auble¹ D. J. Horen² W. B. Ewbank
B. Harmatz Y. A. Ellis D. C. Kocher¹
F. E. Bertrand¹ H. J. Kim¹ M. J. Martin
F. K. McGowan¹ M. R. Schnorak

INTRODUCTION

This year has seen the culmination of Nuclear Data Project (NDP) efforts in several areas. The Evaluated Nuclear Structure Data File (ENSDF) has been developed to where it can serve as the focus for NDP evaluation activities. Standard ENSDF data sets are being used routinely to produce computer-printed nuclear data sheets as well as drawings. Additional output formats are being developed to meet the needs of other users. The project's file of keyword-indexed references to nuclear structure literature has also been used in new ways during the year: a volume of cumulated references to the experimental nuclear structure literature (1969 to 1974) was issued as a supplement to Vol. 16 of *Nuclear Data Sheets*;³ the contents of the cumulated volume were also placed on the RECON system for direct interactive search by any qualified user.

The standard formats⁴ developed by the NDP for the representation of nuclear structure data are gaining wider understanding and acceptance as the existence of ENSDF becomes known. Tape copies of data sets containing adopted levels and decay schemes have been sent on request to several laboratories in the United States, Europe, and the Soviet Union. The data center at the Leningrad Institute of Nuclear Physics (LIMP) has also used the standard formats to describe results of nuclear physics experiments.⁵

EVALUATED NUCLEAR STRUCTURE DATA FILE (ENSDF)

General Description

The ENSDF was designed to organize nuclear structure information in standard format⁴ into convenient blocks and to provide tools for storing and retrieving

the information as needed. The file is maintained in two parts on magnetic disks at ORNL. The permanent file (on private disk ENSDF1) is normally off line and is linked to the computer only when needed. A temporary buffer file (private disk NSDF00, which is always available to the IBM/360 system at ORNL) is used for more active data sets, such as those currently being revised. The contents of NSDF00 can be retrieved, edited, and revised remotely via the Time-Sharing Option (TSO) network.

Information in the ENSDF is organized into "data sets" of three general types:

1. adopted levels -- summarizing the properties (energy, spin, parity, half-life, decay modes) of each level known in a nucleus;
2. decay schemes -- providing the best available half-lives, decay energies, and intensities for the decay of each radioactive nucleus; and
3. reaction data -- giving, for each nuclear reaction, the nuclear structure information (including spectroscopic information, but excluding cross sections) derivable from that reaction.

Current Status

At the end of 1975, the permanent file had grown to include information on about 1200 nuclei across the periodic table. The information is contained in the following data sets: 1170 sets of adopted levels, 850 decay schemes, and 1250 sets of reaction data. These 3270 data sets organize the information on over 120,000 punched cards into easily retrievable blocks. Another 35,000 cards are held on the buffer disk during preparation of nuclear data sheets.

Nuclear Data Sheets from ENSDF

For several years, the drawings in *Nuclear Data Sheets* have been produced from standard ENSDF data sets. During 1975, the NDP took steps to begin the preparation of the printed data sheets from the data file. A standard page layout for presentation of tabular data was first used for $A = 75$.⁶ The addition of a text editor and use of the special 160-character print train now produce acceptable computer-composed pages for photoreproduction.⁷

The combined capability of selecting certain data from ENSDF and preparing it in readable tabular form has also been used to prepare lists in response to a number of special requests. Examples are:

1. a listing of all levels with known lifetimes, $A = 45$ to 90;
2. tabulation of half-lives for nuclei with $A = 80$ to 100 and $A = 140$ to 150;
3. tabulations of levels and gamma rays observed in (H.L., $x\gamma$) reactions, $A = 140$ to 190;
4. $K = 0$ bands in even nuclei, $A = 140$ to 190.

Decay Radiations from ENSDF

One additional output format for information from ENSDF has been tested. The MEDLIST program, which calculates absolute intensities for both atomic and nuclear radiations following radioactive decay, normally prepares a tabular format for photoreproduction (e.g., see publication ORNL-5114). The program was extended in 1975 to provide a list of these radiations in a card-image format, easily readable by FORTRAN programs. Many conventions of the ENDF/B-IV tapes were adopted to facilitate inclusion of ENSDF data in some future version of ENDF. Radiations from 191 radioactive nuclei were written onto a tape, which has been sent to several users for testing. A copy is also available on data cell for testing by ORNL users of radioactivity data.

NUCLEAR STRUCTURE REFERENCES

General Description

In support of its data evaluation program, the NDP conducts a search of the world's scientific literature for reports of nuclear structure results. All relevant work, whether published, preprint, laboratory report, or abstract, is tagged with keywords that describe the appropriate nuclei, reactions, measured data types, and deduced nuclear properties. The keywords are entered into a nuclear structure reference file, which is cumulated at intervals so that an up-to-date tabulation of

relevant articles on a subject is always available at the NDP. During 1975, 3000 published articles and 2000 preliminary reports were tagged and added to the master reference file, which now includes some 55,000 entries.

"Recent References" Cumulation

At four-month intervals, newly published experimental articles are selected from the reference file and published as a "Recent References" issue of *Nuclear Data Sheets*. The complete file is also used to fulfill requests for references on special topics. During 1975, the contents of 18 issues of "Recent References" were cumulated and reorganized into a volume titled *Nuclear Structure References, 1969-1974*, which was published as a supplement to *Nuclear Data Sheets*.³

Nuclear Structure References on RECON

In early 1975, the cumulated file of nuclear structure references for 1969 to 1974 was prepared for inclusion among the reference files available for searching from the RECON network. The file can be searched for keyword descriptions and references on nuclear structure topics from any of 27 directly connected RECON sites within the United States. Since the introduction in mid-1975 of a dial-up version of RECON, any ERDA-approved user can search the files from any telephone. The RECON version of the NDP reference file does not take full advantage of the keyword structure, but it does provide an interactive search capability that can include combinations of key terms (isotope, reaction, etc.). The RECON file can also be used to search on author or publication year, and can provide printed references if needed.

PUBLICATIONS

During 1975 the NDP prepared nine A -chain issues for publication in *Nuclear Data Sheets*, as well as two issues of "Recent References" and the cumulation of nuclear structure references for 1969 to 1974, described above. The A -chain issues contain complete revisions of nuclear data sheets for 46 mass values. Fifteen of these involved a Nuclear Information Research Associates (NIRA) author or coauthor. Twenty-three of the revised A chains were prepared entirely by computer from ENSDF. The numerical information contained in all revised A chains is included in ENSDF.

Photoready copy for an appendix to NBS Handbook 80, *A Manual of Radioactivity Procedures*, was prepared by the MEDLIST program from standard ENSDF

data sets. The tables of radiations (atomic and nuclear) from 191 radioactive isotopes have also been collected in slightly different format as a laboratory report.⁸

SPECIAL SERVICES

The NDP has responded to special requests for nuclear structure information on the average of once a week during 1975. The requests range from the small (precision of the ^{139}Ce half-life) to the average [bibliography to the (n,γ) reaction] to the extensive (magnetic tape containing adopted levels and level properties for all nuclei). Simple requests can often be answered from existing compilations or from indexed reference listings contained in the NDP library. Most special responses involve a mixture of data printouts from ENSDF and reference lists from the nuclear structure reference file. For users of large quantities of

data, a number of special subsets of ENSDF have been prepared on magnetic tape, and these tapes are copied for distribution.

-
1. Part-time assignment to Nuclear Data Project.
 2. Nuclear Data Project Director, January–November 1975.
 3. W. B. Ewbank et al., "Nuclear Structure References, 1969–1974," *Nucl. Data Sheets* **16**, suppl. (1975).
 4. W. B. Ewbank et al., *Nuclear Structure Data File -- a Manual for Preparation of Data Sets*, ORNL-5054 (June 1975).
 5. I. A. Kondurov and Yu. V. Sergeenkov, *Bulletin of the LINP Data Center*, No. 2, Leningrad Institute of Nuclear Physics, U.S.S.R., September 1975, p. 3.
 6. D. J. Horen and M. B. Lewis, *Nucl. Data Sheets* **16**, 25 (1975).
 7. *Nucl. Data Sheets* **16**(3) was prepared entirely by computer from ENSDF.
 8. M. J. Martin, Ed., *Nuclear Decay Data for Selected Radionuclides*, ORNL-5114 (March 1976).

3. Experimental Atomic Physics

ATOMIC STRUCTURE AND COLLISION EXPERIMENTS

I. A. Sellin¹ K. H. Liao¹ R. S. Thoe¹
 S. B. Elston¹ D. J. Pegg¹ H. C. Hayden²
 J. P. Forester¹ R. S. Peterson¹ P. M. Griffin

Our principal research activity concerns the atomic structure and collision phenomena of highly stripped ions in the range $Z = 10$ to 35. The primary objective of our research is the study of atomic structure of highly ionized heavy ions and their modes of formation and destruction in collisions. The decay of excited states of these ions, by radiative and also by electron emission processes, is the phenomenon we study in carrying out these experiments. Our major tools are the various heavy-ion accelerators at ORNL; x-ray, soft-x-ray, and extreme-ultraviolet spectrometers; electron spec-

trometers; and a variety of peripheral equipment associated with these devices.

Our main experimental activities of the past year are summarized in the succeeding paragraphs.

Characteristic and Noncharacteristic X-Ray Emission Produced by Heavy-Ion Impact

We have continued the study of the production of both characteristic (CR) and noncharacteristic (NCR) x rays in symmetric ion-atom collisions at medium projectile energies. The NCR angular distribution measurements planned a year ago on the C-C, O-C, Al-Al, and Si-Al collision systems have yielded corresponding NCR x-ray polarizations that are very large – typically in the range 0.5 to 1.0 – and are sensitively dependent both on x-ray photon energy and

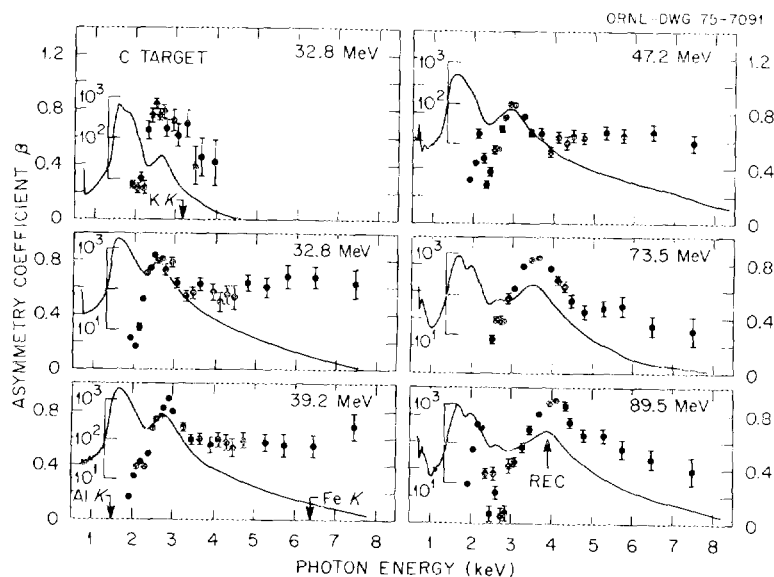


Fig. 3.1. Plots of the polarization β vs photon energy E for NCR x rays emitted in Al-Al collisions at various incident aluminum beam energies. Smoothed semilogarithmic plots of the x-ray intensity in counts observed at 90° to the beam are also shown, after absorption in a $12\text{-}\mu$ detector window and a $50\text{-}\mu$ Mylar absorber. Positions of the characteristic, united-atom, and REC x rays are noted.

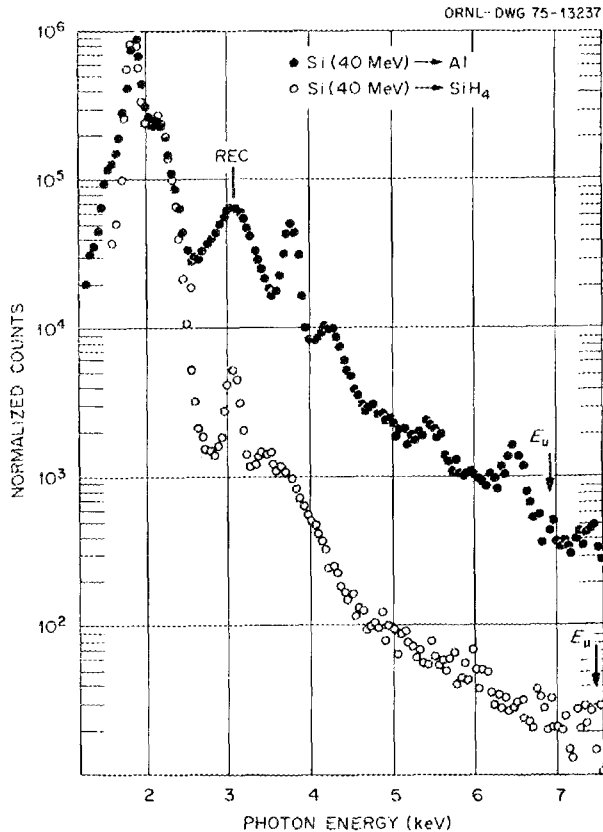


Fig. 3.2. X-ray spectra for Si^{6+} (40 MeV) on Al and SiH_4 . The x-ray spectra have been normalized to the silicon K x-ray lines. Impurity peaks at 3.7, 5.4, and 6.4 keV in the solid aluminum target are probably due to K x rays of calcium, chromium, and iron. The peak at 3.1 keV is due to REC in the solid target and argon K x rays in the gas target.

on projectile beam energy.³⁻⁶ Some of the results are shown in Figs. 3.1 and 3.2.

A principal motivation for these experiments is the possibility of access to the spectroscopy of superheavy atoms and molecules and, through them, to the quantum electrodynamics of strong, so-called supercritical fields. Recently, Muller, Smith, and Greiner⁷ predicted a unique signature for molecular K x rays in the form of a directional anisotropy in their emission, peaked at 90° to the beam direction and largest near the limiting combined-atom x-ray energy. Alignment corresponding to anisotropic σ - vs π -state production can also lead to asymmetry of this form, and the size of the asymmetry observed in the present experiments seems to imply considerable alignment. Hence, the uniqueness of the proposed induced-radiation signature now seems in doubt.

Beyond confirming the existence of directional anisotropies in NCR emission, the present work raises

important questions concerning the role of alignment in producing the anisotropies of the observed magnitude and in the validity of the induced-radiation theory.

Such angular distribution measurements have been extended for Al-Al collisions to higher beam energies at ORIC. Our motivation was to see at what level and at what beam energy the measured polarization near the united-atom limit would peak. We anticipated a decline at higher beam energies, as was apparent from the C-C and O-C data. As Fig. 3.1 shows, the new polarization data (closed circles) saturate as a function of beam energy near the united-atom limit, indicated by the symbol Fe K , and approaches unity at the variable position of a peak (labeled REC) in the intensity spectra (solid lines). This REC peak, which grows rapidly in intensity with beam energy, is due to radiative electron capture, in which, for example, a loosely bound target electron fills a vacancy in the onrushing projectiles, energy and momentum being balanced by an emitted x-ray photon. The interpretation of the saturating polarization and the analysis of cross sections for both REC and other continuum x-ray production are activities presently under way and will continue.

A more recent set of experiments concerns new experimental results of Bell et al.⁸ for 55-MeV $\text{S} \rightarrow \text{Al}$ and 48-MeV $\text{S} \rightarrow \text{Ne}$ collisions, which indicated that the production of NCR radiation was similar for gas and solid targets when normalized to the characteristic line of the projectile ion. Such a result would indicate that a one-collision mechanism for NCR production, in which a vacancy in the K shell is produced and filled during the collision, is as important as the two-collision model proposed by Saris and colleagues. Our new experiments concern more nearly symmetric collision partners, and we have found that the yield of x rays near the combined-atom K x-ray limit (E_u) for 40-MeV $\text{Si}^{6+} \rightarrow \text{SiH}_4$ is significantly smaller than the yield of NCR for 40-MeV $\text{Si}^{6+} \rightarrow \text{Al}$.⁹ Figure 3.2 provides comparative raw data from 40-MeV aluminum ions in silicon and SiH_4 . Since analyses of present results and more experimentation are contemplated for the coming year, further discussion will be deferred to a subsequent report.

Electron Spectroscopy on Core-Excited States of the Alkalis and on More Highly Ionized Lithium-Like, Beryllium-Like, and Boron-Like Ions

Atoms and ions may frequently be excited to states that, in turn, spontaneously decay by electron rather

than photon emission. Such a radiationless transition is called autoionization. For this process to be energetically possible, the excited state must be degenerate in energy with a state in some ionization continuum; that is, the excitation energy of the state must be greater than the energy required to liberate a single outer-shell electron. The simultaneous excitation of two loosely bound outer-shell electrons or the excitation of a more tightly bound inner-shell electron to a higher orbital will satisfy this energy requirement. It is the latter process, known as core excitation, that has been studied in our recent experiments on the alkalis.

The literature concerning photoelectron, electron-impact, and ion-impact spectroscopy of autoionizing states of the permanent gases is extensive. Similar results on the equally fundamental alkali metals had, until our recent work, been comparatively rare and usually of lesser accuracy, especially in the case of optically forbidden states. In the past year we have finished the analysis and published the first data on a number of optically forbidden core-excited states of Li, Na, Mg⁺, and K; we have also published pertinent details of a method (projectile electron spectroscopy) that allows ready access to large numbers of such levels in many alkali and alkali-like systems.¹⁰⁻¹⁴ We note that the data have attracted attention from investigators in Berlin (Stolterfoht and colleagues at the Hahn-Meitner Institute) and in Freiburg, West Germany (Mehlhorn and colleagues at the University of Freiburg), who have subsequently developed similar experiments on the alkalis and alkaline earths.

A comparison of our results with theory and with other available data has been published.¹¹ It can be seen that, where available, excellent agreement with other experiments is obtained, that experimental accuracy exceeds that provided by current theoretical techniques, and that a substantial number of previously unknown levels have been discovered and their energies established.

The spectrum of the autoionizing decay of core-excited states of potassium following the passage of a 70-keV K⁺ beam through a helium-gas target cell was also studied. The lines present in the spectrum represent the autoionizing decay of states formed from core-excited configurations of the type $3p^5 4snl$ ($n \geq 3$), $3p^5 3dnl$ ($n \geq 3$), $3p^5 4pnl$ ($n \geq 3$), etc. The energy scale chosen was based upon the likely supposition that two prominent peaks are associated with the $J = \frac{1}{2}$ and $\frac{3}{2}$ levels of the optically allowed term $(3p^5 4s^2)^2 P^o$, which had been observed in earlier photoabsorption work.¹⁵ The fine-structure splitting between these two levels in our spectrum is in good agreement with the photoabsorption data.

Higher resolution measurements of projectile electron spectra from metastable and intermediate-lived states of lithium-like, beryllium-like, and boron-like states of oxygen, fluorine, and silicon ions and sodium-like chlorine ions than had been carried out previously have also been made. An example is provided in Fig. 3.3, which depicts the lowest-lying features of electron spectra from three-, four-, and five-electron excited states of fluorine with one K vacancy (the inset shows the previous lower-resolution data). In the figure, electrons are observed at an average time delay of a few tenths of a nanosecond following excitation, a delay that is long on the time scale of allowed autoionization processes.

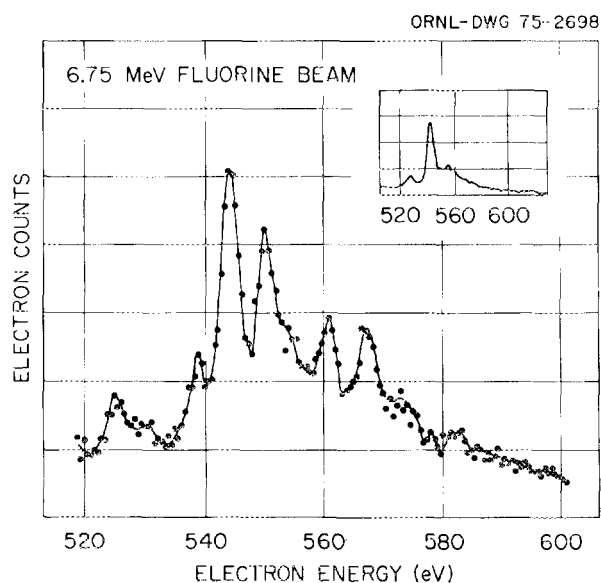


Fig. 3.3. Spectra of autoionizing electrons from highly ionized fluorine undergoing decay in flight, plotted in rest frame of emitting ion. The continuous curve is drawn to aid the eye. The inset shows previous lower resolution spectrum over the same energy range.

Extreme-Ultraviolet Spectra and Lifetimes of Multiply Ionized Metal Ions

The sputter ion source in use at the ORNL tandem accelerator is ideal for producing beams of metal ions such as silicon, iron, nickel, etc., at energies of ~ 1 MeV per nucleon. Stripping at these energies produces moderate to high degrees of ionization of ions in this Z range in the L and M shells. In collaboration with S. Bashkin (University of Arizona), T. Kruse (Rutgers University), and K. Jones and D. Pisano (Brookhaven National Laboratory), we have very recently begun investigating the spectra and lifetimes of $\Delta n = 0$ L -shell resonance transitions in beryllium-like, boron-like, and

carbon-like silicon transitions and $\Delta n = 0$ *M*-shell resonance transitions in magnesium-like iron. A typical spectrum is shown in Fig. 3.4.

Many lines of other stages of ionization of both silicon and iron (e.g., Si VI to Si XII) have also been observed in the range 100 to 400 Å (ref. 16), and, as usual, many previously unknown and yet to be identified transitions have been observed. The $\Delta n = 0$ resonance transitions, for example, $2s^2 - 2s2p$ transitions in beryllium-like silicon or $3s^2 - 3s3p$ transitions in magnesium-like iron, are particularly interesting to study for a number of reasons. First, such transitions often have lifetimes in the accessible 10- to 100-psec range, making reasonably accurate lifetime measurements feasible despite limited beam intensities and spatial resolution. Second, apart from our measurements, there seem to be no other *L*- or *M*-shell resonance transition probability measurements beyond $Z = 10$, and theoretical values for *A* (the Einstein *A*

coefficient) often have uncertainties approaching 50%. Third, such *A* values have high astrophysical significance. Fourth, such lines occur profusely in plasmas whose vacuum enclosure walls contain such metallic elements, so that line identification and *A*-value measurements have considerable plasma diagnostic value.

Atomic Collision Experiments Using the ORNL Multiply Charged Ion Source Facility

An investigation of electron-capture processes using B^{q+} ($q = 1$ to 4) incident on thin H_2 , He, and Ar targets in the projectile energy range ~ 5 to 60 keV has been made. The use of an atomic hydrogen target will be undertaken soon. Interesting enhancements of electron-capture cross sections by incident B^{3+} beams vs B^{4+} beams have been observed. This work has been done in collaboration with J. E. Bayfield, L. Gardner, and

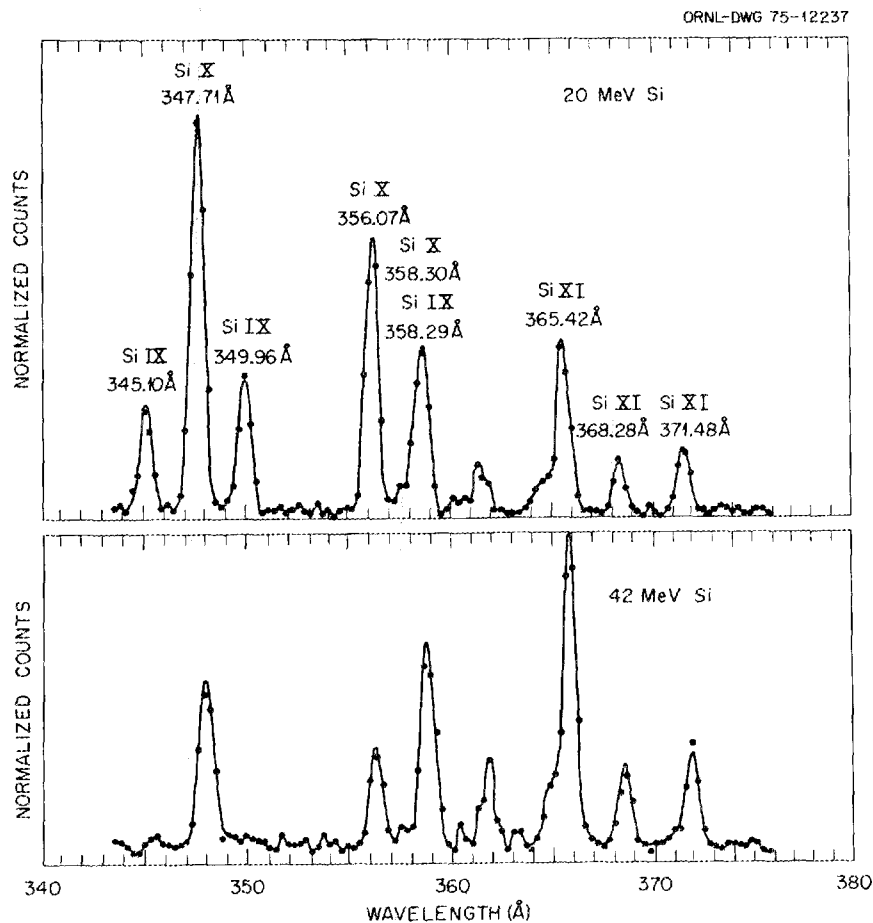


Fig. 3.4. Comparison of foil-excited spectra obtained using 20-MeV (upper) and 42-MeV (lower) silicon ion beams in the region 343 to 377 Å.

P. Koch of Yale University and D. H. Crandall and M. L. Mallory of ORNL.

Preliminary measurements have been made of the projectile charge-state dependence of neon K x-ray production in Ne^{q+} on neon collisions at keV energies, in which the Fano-Lichten molecular promotion model is generally thought to be approximately valid. Conversion of the data to absolute cross-section data awaits a calibration experiment with Ne^+ beams. Neon K x-ray production by incident $3+$, $4+$, and $5+$ ions at 60 keV has been found to scale approximately as 1:1.7:4.2.

1. University of Tennessee, Knoxville.
2. University of Connecticut, Storrs.
3. R. S. Thoe et al., to be published in *Beam-Foil Spectroscopy: Heavy Ion Atomic Physics*, I. A. Sellin and D. J. Pegg, Eds., Plenum Press, New York, 1976.
4. R. S. Thoe et al., p. 312 in *Electronic and Atomic Collisions*, J. S. Risley and R. Geballe, Eds., University of Washington Press, Seattle, Wash., 1975.
5. R. S. Thoe et al., p. 78 in *Proceedings of the Third Conference on Applications of Small Accelerators*, Denton, Tex., Oct. 21-23, 1974, ERDA CONF-74-1040 P1, ERDA Technical Information Center, Oak Ridge, Tenn., 1975.
6. R. S. Thoe et al., *Phys. Rev. Lett.* **34**, 64 (1975).
7. B. Muller, K. Smith, and W. Greiner, *Phys. Rev. Lett.* **33**, 469 (1974).
8. F. Bell et al., *Phys. Rev. Lett.* **35**, 841 (1975).
9. R. S. Peterson et al., to be published in *Beam-Foil Spectroscopy: Heavy Ion Atomic Physics*, I. A. Sellin and D. J. Pegg, Eds., Plenum Press, New York, 1976.
10. I. A. Sellin, to be published in *Beam-Foil Spectroscopy*, S. Bashkin, Ed., Springer-Verlag, Heidelberg, Germany, 1976.
11. D. J. Pegg et al., *Phys. Rev. A* **12**, 1330 (1975).
12. D. J. Pegg, to be published in *Beam-Foil Spectroscopy: Heavy Ion Atomic Physics*, I. A. Sellin and D. J. Pegg, Eds., Plenum Press, New York, 1976.
13. D. J. Pegg et al., p. 869 in *Electronic and Atomic Collisions*, J. S. Risley and R. Geballe, Eds., University of Washington Press, Seattle, Wash., 1975.
14. D. J. Pegg et al., *Phys. Lett.* **50A**, 447 (1975).
15. H. Beutler, *Z. Phys.* **91**, 131 (1934).
16. P. M. Griffin et al., to be published in *Beam-Foil Spectroscopy: Heavy Ion Atomic Physics*, I. A. Sellin and D. J. Pegg, Eds., Plenum Press, New York, 1976.

CHARGE-TRANSFER MEASUREMENTS

D. H. Crandall D. C. Kocher

A number of atomic physics experiments are in progress using the heavy-ion-source test stand as a source of slow multicharged ions.¹ Experiments to measure charge-transfer cross sections for ions of carbon, nitrogen, and oxygen in various gases were started in March 1975.² At velocities below 4×10^8 cm/sec, charge transfer is the dominant inelastic process in collisions of multicharged ions with atoms or

molecules, thus playing an important role in many physical phenomena, especially in high-temperature plasmas found in fusion research and astrophysics. Due to the difficulty in obtaining usable fluxes of multicharged ions at low velocities, only a small amount of experimental work has been done.^{3,4} Some of the relevant cross sections, including electron capture and electron ionization and excitation, have been computed, particularly by astrophysicists.

As a first step in the systematic study of these collisions the electron-capture cross section of multicharged ions of carbon, nitrogen, and oxygen have been measured in H_2 gas in the energy range 10 to 110 keV. The single-electron-capture cross sections for oxygen ions from charge state 3 to charge state 6 as a function of ion velocity or energy are shown in Fig. 3.5. Of considerable interest in collisions of multicharged ions is the question of how the cross section should scale as the charge state q . For high energies, where the Born approximation is applicable, computations suggest that the cross section should scale as q^2 . Referring to Fig. 3.5, one can see that this scaling is not verified in the low-energy region. The cross section σ_{43} (going from charge state 4 to charge state 3) is approximately three times σ_{32} . For initial charge state 5, the cross section is smaller than that for charge state 4, which is a consequence of potential curve crossing in the near-adiabatic energy region.⁵

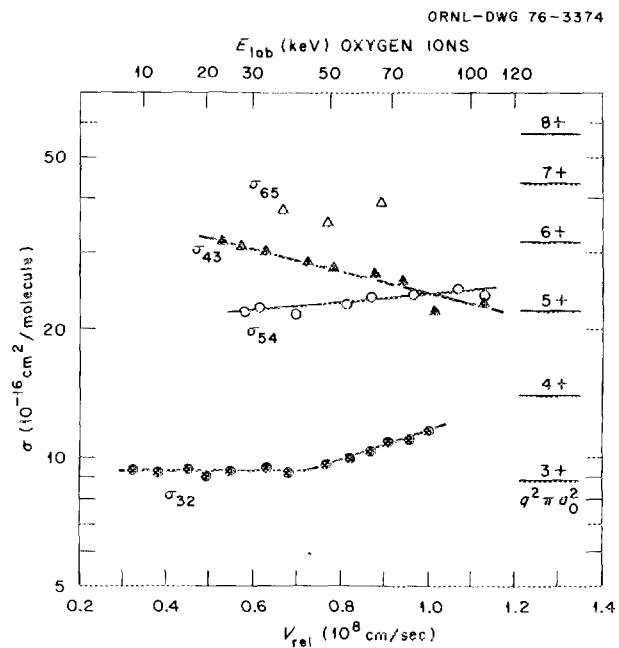


Fig. 3.5. Single electron capture for various ions of oxygen colliding with molecular hydrogen.

An interesting feature of these data is that the cross sections do not decrease at the lowest energies, indicating that potential interaction at fairly large internuclear separation is the primary source of electron transfer. This in turn implies that the electrons are transferred into excited states of the ion, since the potential curves of the excited states are the ones that cross at large nuclear separations.

Data similar to the O^{7+} cross sections have been obtained for C^{4+} and O^{7+} in H_2 . These measurements are being extended to hydrogen atom targets.

From both theoretical and experimental considerations, single- and double-electron-capture cross sections of the reaction $C^{4+} + He$ are particularly interesting. Double-electron-capture cross sections have usually been observed to be one to two orders of magnitude less than the single-electron-capture cross section. Results for both single and double electron capture of C^{4+} in He are shown in Fig. 3.6. For energies of 5 to 10 keV the measured cross sections are approximately equal, with double capture increasing at lower energies. Theoretical results are also shown for the two cases.

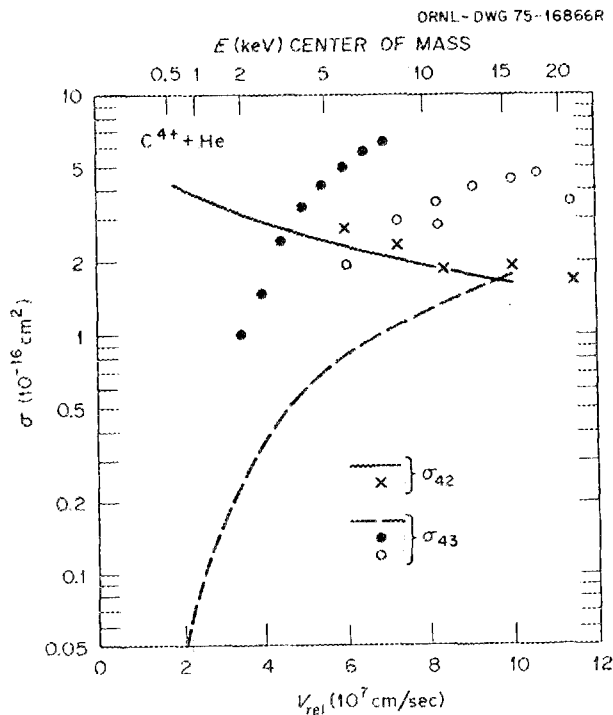


Fig. 3.6. Cross sections for single and double electron capture from C^{4+} incident on helium. Solid curve - present calculation of σ_{42} for $C^{4+} + He \rightarrow C^{2+} + He^{2+}$. Crosses - present experiment for σ_{42} . Dashed curve - present calculation of σ_{43} for $C^{4+} + He \rightarrow C^{3+} + He^+$. Open circles - present experiment for σ_{43} . Closed circles - σ_{43} from ref. 3.

Extremely good agreement between theory and experiment was found for the double electron capture, but agreement to within a factor of 2 was found for single capture.

1. M. L. Mallory and D. H. Crandall, *IEEE Trans. Nucl. Sci. NS-23(2)* (1976).
2. D. H. Crandall, p. 190 in *Ninth International Conference on Physics of Electronic and Atomic Collisions*, J. S. Risley and R. Geballe, Eds., University of Washington Press, Seattle, Wash., 1975.
3. H. J. Zwally and D. W. Koopman, *Phys. Rev. A* **2**, 1851 (1970).
4. H. Klinger, B. Müller, and E. Salzborn, *J. Phys. B* **8**, 230 (1975).
5. D. H. Crandall et al., submitted to *Physical Review Letters*.

ELECTRON-IMPACT EXCITATION AND IONIZATION CROSS SECTIONS

D. H. Crandall R. N. Phaneuf¹
P. O. Taylor¹

For modeling plasma behavior and interpreting line radiation from a plasma, the electron-impact excitation and ionization cross sections are crucial data. An experiment has been designed and an apparatus fabricated to measure the excitation of beryllium- and lithium-like ions and the ionization of charge states 3 to 6. A multicharged ion beam from the heavy-ion-source facility will be crossed at right angles with a modulated electron beam in a chamber whose base pressure is 10^{-9} to 10^{-10} torr. With this residual pressure, the signal-to-noise ratio is approximately 10^{-2} , necessitating the use of beam-modulation techniques. Measurements are under way.

1. Participants, Joint Institute Laboratory Astrophysics, Boulder, Colo.

MULTIPLE-ELECTRON-LOSS CROSS SECTIONS FOR 60-MeV I^{10+} IN SINGLE COLLISIONS WITH XENON

L. B. Bridwell¹ G. D. Alton P. D. Miller
J. A. Biggerstaff C. M. Jones Q. Kessel²
B. W. Wehring³

The production of highly ionized beams of heavy ions has been a subject of intensive investigation in several laboratories during the last decade. The resulting technology provides the basis on which many high-energy heavy-ion accelerators operate. Along the path of an ion as it traverses a stripping medium, the charge

state of a particular ion may fluctuate many times. The charge-state distribution of such a beam of particles reaches equilibrium after traversing a certain thickness of the stripping medium. A recent survey shows that extensive information has been accumulated concerning charge-state distributions of heavy ions as they emerge from both solid and gaseous targets.⁴ Most of these, however, have been obtained with experimental apparatus that confines the emerging beam within a very small solid angle in the forward direction. The work by Kessel shows that the emerging charge-state distributions produced in single-event scattering depend strongly on the distance of closest approach.⁵ We have previously reported a series of experiments in which absolute yields of highly charged ions were obtained from high-atomic-number stripping gases at target thicknesses somewhat above that of single-collision processes but somewhat less than equilibrium thickness.^{6,7} That work was performed specifically for determining design parameters for a terminal stripper in a large tandem accelerator. The present results were obtained using the same apparatus but with a smaller target thickness to examine single scattering events and to obtain cross sections for the loss of several electrons in a single collision.

The experimental apparatus is virtually identical to that reported earlier.^{6,7} A momentum-analyzed beam of 60-MeV I^{10+} ions was produced in the ORNL tandem accelerator. The exit apertures of the differentially pumped target-gas cell were slotted to permit measurements at scattering angles through 3° .

Charged particles scattered at a given angle were analyzed with an electrostatic charge-state analyzer that has been described previously.⁸ The charge-state resolution was determined by a 1.03-mm-high vertical collimator positioned at the entrance to the analyzer. The angular resolution was determined by a slot in a 4.1-mm-wide mask positioned directly in front of the detector, which was 429 cm from the center of the target. The resulting angular resolution was $\Delta\theta = 0.054^\circ$ and the solid angle was $\Delta\Omega = 2.9 \times 10^{-7}$ sr. Pressures in the flight tube before and after the target cell were approximately 2×10^{-6} torr throughout the measurements. Target-gas pressures were 5.1×10^{-3} and 11.9×10^{-3} torr, and the scattering angles were 0.05° , 0.10° , and 0.20° .

Figure 3.7 shows the charge-state distribution measured at xenon pressures of 5.1×10^{-3} and 11.9×10^{-3} torr at a scattering angle of 0.2° . The similarity in shape suggests that these target thicknesses are essentially in the single-collision region, although there is some evidence of electron pickup at the higher pressure.

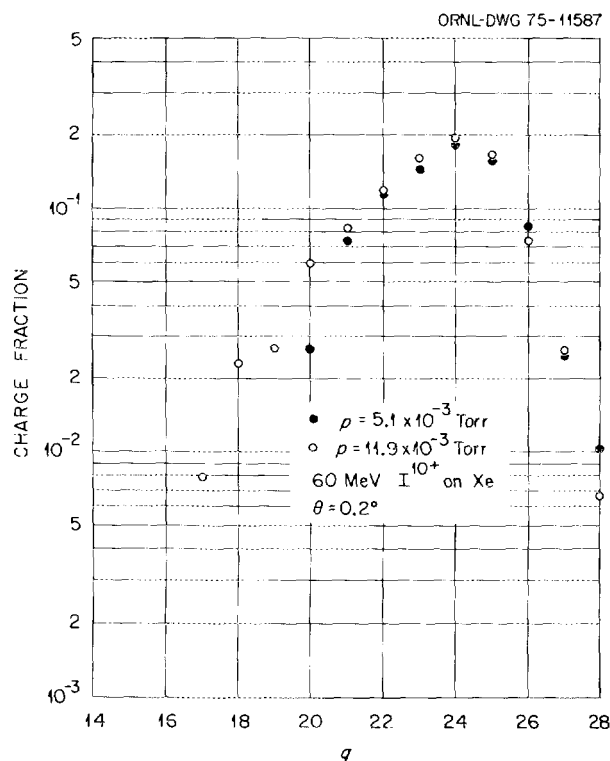


Fig. 3.7. Charge-state distributions for 60-MeV I^{10+} on xenon at a scattering angle of $\theta = 0.2^\circ$.

Figure 3.8 shows the differential scattering cross section plotted against the number of electrons removed for the three scattering angles observed. For a Δq of 15, the last N -shell electron must be removed in the collision. At a scattering angle of $\theta = 0.05^\circ$, the range of θ actually extends from 0.025° to 0.075° , so that the distance of closest approach, r_0 , varies from 0.17 to 0.26 Å. Self-consistent-field calculations^{9,10} show that the radii of maximum radial charge density are approximately 0.13 Å for the M shell and 0.42 Å for the N shell in iodine or xenon. At the minimum distance of closest approach within the allowed range for $\theta = 0.05^\circ$, the M -shell electrons of the iodine-xenon system are just beginning to merge during the collision. This may result in the excitation or removal of one or more of the M -shell electrons, which then leads to ionization cascades where all of the electrons in the N shell are removed. The much higher probability of removing 10 to 12 electrons probably results from similar processes but with the initial electron excitation or removal occurring in the N shell. At $\theta = 0.10^\circ$ the range of r_0 extends from 0.13 to 0.17 Å. In this case, the merging of the M shells within the iodine-xenon system is substantial; therefore, M -shell electron excitations are more probable. Finally, at $\theta = 0.2^\circ$ the interpenetration

of the M shells is complete, with r_0 extending from 0.09 to 0.11 Å. The probability of removing all N -shell electrons relative to other processes then becomes greater. At these selected scattering angles, L -shell interpenetration did not occur; thus very little M -shell ionization was observed. Numerical integration of the differential cross sections for the removal of 11, 12, 13, and 14 electrons over the angular range observed yields the results shown in Table 3.1.

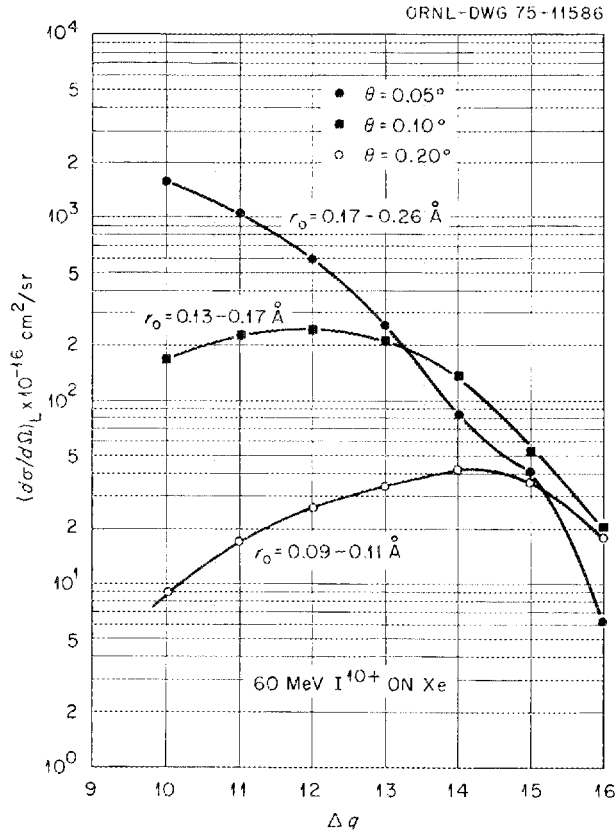


Fig. 3.8. Differential scattering cross sections for the removal of Δq electrons in a single collision between 60-MeV I^{10+} and xenon at angles of 0.05° , 0.10° , and 0.20° .

Table 3.1. Total removal cross sections for Δq electrons from 60-MeV I^{10+} when scattered by xenon gas in single collisions

Δq	Total σ (10^{-18} cm 2)
11	16 ± 4
12	8.7 ± 0.9
13	2.8 ± 0.5
14	1.9 ± 0.3

From these data and those reported earlier,^{5,6} it is clear that very high charge-state ions are produced in single collisions with the target atoms. With the large magnitude of the cross sections for these events, it is possible to make experimentally useful beams of such ions with a relatively simple gas cell, provided that a sufficiently large acceptance solid angle is employed.

1. Murray State University, Murray, Ky.
2. University of Connecticut, Storrs.
3. University of Illinois, Urbana.
4. H. D. Betz, *Rev. Mod. Phys.* **44**, 465 (1972).
5. Q. Kessel, *Phys. Rev. A* **2**, 1881 (1970).
6. G. D. Alton et al., *IEEE Trans. Nucl. Sci.* **NS-22**, 1685 (1975).
7. P. D. Miller et al., *Phys. Div. Annu. Prog. Rep. Dec. 31, 1974*, ORNL-5025 (1974), p. 178.
8. C. D. Moak et al., *Phys. Rev.* **176**, 426 (1968).
9. F. Herman and S. Skillman, *Atomic Structure Calculations*, Prentice-Hall, Inc., Englewood Cliffs, N.J., 1963.
10. J. T. Waber and D. T. Cromer, *J. Chem. Phys.* **42**, 4116 (1965).

SCREENING BY BOUND K ELECTRONS IN ELECTRONIC STOPPING

S. Datz J. Gomez del Campo²
P. F. Dittner¹ P. D. Miller
J. A. Biggerstaff

In previous studies on the motion of fast ions passing through crystal channels it was established that (1) well-channeled ions interact only with relatively slow conduction and valence electrons that simulate an electron gas; (2) a considerable fraction of oxygen ions ($q = 6+, 7+, 8+$) at ~ 2 MeV/amu pass through channels (up to 1 μm thick) with no charge-changing collisions;³ and (3) the stopping power for these ions is closely proportional to q^2 , implying that bound electrons screened the nuclear charge by one unit each.⁴ A quantitative test of this latter point has been made by measuring the stopping power for channeled B^{5+} , $C^{5+,6+}$, $N^{5+,6+,7+}$, $O^{6+,7+,8+}$, and $F^{7+,8+,9+}$ at 2 MeV/amu. For one-electron systems the screening ranged from 0.91 for carbon to 0.97 for fluorine, whereas for the two-electron systems the screening per electron was approximately 0.92. A comparison of channeled-ion stopping powers for bare nuclei ($Z = 5$ to 9) with proton stopping in the same medium also permits the extraction of higher-order Z effects⁵ (Z_1^3 and Z_1^4) on electronic stopping over a much larger range than has

been investigated heretofore ($Z = 1, 2$). The data have been accumulated and the treatment is proceeding.

-
1. Chemistry Division.
 2. University of Mexico, Mexico City.
 3. S. Datz et al., *Radiat. Eff.* **12**, 163 (1972).
 4. C. D. Moak et al., *Phys. Rev. B* **10**, 2681 (1974).
 5. J. Lindhard, *Nucl. Instrum. Methods*, in press.

PLANAR CHANNELING AND HYPERCHANNELING OF CHARGE-STATE- SELECTED 27.5-MeV OXYGEN IONS IN SILVER

S. Datz B. R. Appleton¹
C. D. Moak J. A. Biggerstaff
T. S. Noggle¹

The trajectories of ions penetrating crystal channels are controlled by the interaction between the charged particle and a continuum potential made up of an orderly sum of the atoms in crystal rows or planes. For most ions, charge capture and loss probabilities are so large that the formal charge on the projectile must be treated as a statistical average over a distribution. However, in some cases, charge-changing probabilities can be strongly suppressed, and one objective of the present work was to ascertain whether the change in restoring force due to different ion charge state could be measured. Previously we reported that 20- to 40-MeV $O^{6+,7+,8+}$ ions channeled in gold and silver have electron capture and loss cross sections such that (1) crystals up to $\sim 5000 \text{ \AA}$ thick are "thin targets" for charge exchange and, hence, capture and loss cross sections may be measured² and (2) the energy loss of transmitted particles that had not undergone charge exchange were accurately proportional to the square of the ion's charge, that is, the nuclear charge minus the number of bound electrons.^{3,4}

We therefore measured channeled-ion energy loss spectra for 27.5-MeV oxygen ions in silver (4150 \AA thick) as a function of input ($7+$ or $8+$) and exit ($7+$ or $8+$) charge state. For both planar channeling and hyperchanneling, the charge-state effect on stopping power is seen for the minimum energy-loss portion but decreases rapidly with increasing transverse energy, indicating a rapid rise in charge-changing probability with increasing amplitude. Although the effect of ion charge on restoring force could not be determined, two new aspects of channeling were disclosed. These are (1) equilibrium charge distributions as a function of amplitude and (2) the observation of a peak in the exit energy distribution at a greater than random energy loss

when the crystal was tilted into a planar blocking direction.

An additional observation was the appearance of two peaks in the energy loss spectrum measured for $8+$ in, $7+$ out, corresponding to electron capture at the exit and entrance surfaces of the crystal.

-
1. Solid State Division.
 2. S. Datz et al., *Radiat. Eff.* **12**, 163 (1972).
 3. S. Datz et al., p. 63 in *Atomic Collisions in Solids*, Plenum Press, New York, 1975.
 4. C. D. Moak et al., *Phys. Rev. B* **10**, 2681 (1974).

ELECTRON EMISSION FROM FAST OXYGEN AND COPPER IONS EMERGING FROM THIN GOLD CRYSTALS IN CHanneled AND RANDOM DIRECTIONS

S. Datz J. A. Biggerstaff
B. R. Appleton¹ T. S. Noggle¹
H. Verbeek²

The spectrum and yield of electrons accompanying the emergence of a fast ion from a solid contain information relating to the excitation state of the ion inside the solid and the nature of the response of the electron plasma to the moving projectile. We have measured yields, energy distributions, and angular distributions of electrons emitted by 27.5-MeV oxygen and 20- and 30-MeV copper ions emerging from a thin (3000-\AA) gold crystal in both channeled (110) and random directions. In the case of oxygen we concentrated attention on the electrons observed in a peak with velocities closely corresponding to the emergent-ion velocity³ ($\sim 900\text{-eV}$ electrons). Under channeling conditions the yield of these electrons was lower than for random orientation, and, moreover, the yield for channeled ions depended on the charge state of the entering ion ($6+$ or $8+$). For entering charge state $6+$, the ratio of the random yield to the channeled yield was 2.0, and for $8+$ entrance charge it was 3.0. Because the electrons are emitted from exiting ions, the dependence of yield on input charge simply reflects the dependence of exit charge on input charge and the lack of charge equilibrium for channeled ions.⁴ The exit charge distributions were measured and found to be 0.2 ($6+$), 0.5 ($7+$), and 0.27 ($8+$) for random emergence and also closely the same for channeled ions with initial charge state $6+$. (Note: This does not mean equilibrium is achieved.) For initial charge state $8+$, the exit charge fractions were 0.12 ($6+$), 0.35 ($7+$), and 0.53 ($8+$). The ratio of emergent ions that retain electrons (i.e., non- $8+$ ions) for $6+$ in to those for $8+$ in ($0.7/0.47 \cong 1.5$) is

thus identical to the ratio of the electron yields. This observation implies that the totally stripped 8+ ions do not contribute to this peak and that the electrons in this peak do not, in this case, arise from capture to continuum states. Instead, in agreement with Burch,⁵ who measured electrons lost in single collisions of oxygen ions at these energies, we propose that they are electrons removed from the moving ion in the last ionizing collision. The fact that the random yield is higher by a factor of 2 than for the 6+ channeled-ion yield is explained by the larger ionization probability in random collisions.

For the copper ions, where charge equilibrium should be rapid and charge-changing cross sections higher, no sensible difference in the yield of electrons traveling at the ion's velocity is observed for channeled and random 20-MeV copper, but for 30-MeV copper the channeled gave greater yields than the random. The absolute yields here are in the order of 2×10^{-2} electron per ion.

The yields of higher energy electrons, arising from violent collisions with electrons in the medium, are reduced for channeled ions because of the lower electron density penetrated. The total yield of electrons with energies from ~ 100 to 1200 eV integrated over $\sim 15^\circ$ of forward scattering angle was no greater than ~ 0.5 electron per ion. For copper ions at 30 MeV, for example, differences in charge-state distributions from gases ($\bar{q} = 9.3$) and solids ($\bar{q} = 13.6$) are anticipated.⁶ The theory of Betz and Grodzins⁷ concerning the excitation states of heavy ions in solids would predict the loss of about four Auger electrons per ion upon emergence from the solid. The $3p3d3d$ Auger electron energies, for example, should be ~ 50 eV, which, translated to the laboratory system, corresponds to energies of ~ 500 eV for forward scattering. The observed spectra show no departure from the smooth distribution anticipated from electron collision theory, and no evidence for the presence of Auger electrons could be adduced.

SPATIAL ION TEMPERATURE MEASUREMENTS

D. P. Hutchinson K. Vander Sluis
J. Waldman¹

Spatial electron and ion plasma temperatures can be measured using coherent Thomson scattering. Analysis of the spectrum of scattered photons from a plasma provides the electron temperature if the wavelength of the incident laser beam is less than $1 \mu\text{m}$ for a scattering angle of a few degrees. Increasing the incident wavelength to 200–500 μm results in the scattered spectrum containing ion temperature information.

Feasibility studies have shown that spatial temperatures in a plasma whose density is 10^{14} cm^{-3} can be determined from a 1-MW CH_3F laser operating at a wavelength of 496 μm . Present technology indicates that a 1-MW CH_3F laser can be obtained when optically pumped by a 150-J CO_2 laser operating at a wavelength of 9.55 μm rather than the normal 10.6- μm wavelength. Commercial CO_2 tunable lasers are not available at this power level. To force the CO_2 laser to oscillate at 9.55 μm , a 25-cm SF_6 gas cell has been placed in the CO_2 laser optical cavity. The SF_6 strongly absorbs and suppresses the 10- μm band lines but has high transmission for the 9- μm band lines. A few milliwatts of 9.55- μm radiation from an idler cw laser, which has a diffraction grating as one of the optical elements, is injected into the CO_2 laser cavity through a 0.5-mm hole in the gold-coated back reflector of the CO_2 laser. This cw signal overrides the spontaneous emission that normally starts the laser oscillating and locks the CO_2 oscillator to the injection frequency. Using this method a 10-J, normal 10.6- μm , CO_2 pulsed laser has produced 10 J of 9.55- μm energy. The next step in the development of 1 MW of 496- μm power will be to modify a commercial CO_2 laser to operate in the 9.55- μm mode, which will pump a CH_3F laser using either waveguide or unstable resonator techniques.

A 30-W cw CO_2 tunable laser has been used to optically pump a cw waveguide-resonator CH_3F laser. Sufficient power has been obtained to use the 496- μm radiation as an interferometer source to measure electron line density in present toroidal machines and as a local oscillator for a far-infrared heterodyne receiver needed in the Thomson scattering experiment. The system is now undergoing upgrading by replacing the optics and increasing the CO_2 pump power to provide 100 mW at 496 μm .

-
1. Solid State Division.
 2. Visiting scientist from Max-Planck-Institut für Plasma-physik, EURATOM Association, D-8046, Garching, Germany.
 3. K. Dettman, K. G. Harrison, and M. W. Lucas, *J. Phys. B* 7, 269 (1974).
 4. S. Datz et al., *Radiat. Eff.* 12, 163 (1972).
 5. D. Burch, University of Washington, Seattle, Wash., private communication.
 6. H. D. Betz, *Rev. Mod. Phys.* 44, 465 (1972).
 7. H. D. Betz and L. Grodzins, *Phys. Rev. Lett.* 25, 211 (1970).

-
1. Consultant, Lowell Institute, Lowell, Mass.

STARK MEASUREMENTS OF ELECTRIC FIELDS IN ORMAK

K. Vander Sluis P. M. Bakshi¹

Previous investigation of the intensity profile of the hydrogen Balmer lines radiated by the ORMAK plasma indicated satellite structure due to static and dynamic electric fields. Analysis of the spacing of the harmonics suggests electric fields of 5×10^4 V/cm existing in the plasma. Since electric fields of this magnitude are not expected in the apparently stable plasma, an intensive effort has been made to validate these measurements. By appropriate changes in the detector system, the signal-to-noise ratio has been increased by a factor of 10. Since a computer is used in the signal analysis, a systematic study has been made to eliminate the computer as a source of the harmonic signals. Correlation of the satellite lines with plasma impurity-line radiation revealed that lines of N III coincided with the shifted hydrogen δ line. At the present time, the statistics of the line shape for a single time interval during a pulse are so poor that reliable electric field strengths are not obtainable. On averaging many sets of data, the lines are broadened, presumably from the electric field fluctuating from pulse to pulse. Measurements are now being conducted to detect forbidden transitions of helium when small quantities of helium are added as plasma contaminants.

Theoretical studies have been pursued to determine the feasibility of using the Stark shift of impurity-line radiation in measuring electric fields. One disadvantage of hydrogen Balmer-series line radiation is that the radiation originates at the plasma periphery. By using impurity radiation, the plasma center is accessible for study. Of most interest is the manner in which the wavelength and the required resolution scales with Z . The hydrogen Lyman-alpha equivalent wavelength for C VI, N VII, and O VIII are 34, 25, and 19 Å respectively. For these ions the wavelength scales as Z^{-2} and the Stark displacement as Z^{-1} , which results in an effective scaling of Z^{-3} . Resolutions of the order of 10^{-5} are required, which for O VIII would result in a resolution of 3.4×10^{-4} Å. These resolutions are not obtainable by known techniques. Thus Lyman or Balmer series line studies are impossible.

Another possibility exists in going to higher principal quantum numbers n . As n increases, the wavelength increases and also Stark splitting increases as $n(n-1)$. This scaling implies that electric fields in the plasma center are amenable to measurement by using O VIII lines from states $n \geq 8$. Present plans are to investigate

the spectra of lines being emitted by the ORMAK plasma to determine if lines that originate from high terms are present.

1. Consultant, Boston College, Brighton, Mass.

ENERGY-MOMENTUM NEUTRAL-PARTICLE ANALYZER

J. A. Ray C. F. Barnett

A velocity-energy analyzer has been designed and fabricated for the ELMO Bumpy Torus (EBT) experiment to determine whether neutral impurities escaping the plasma are influencing ion temperatures as measured by the present energy analyzer. The components of the analyzer include an N_2 gas stripping cell to convert the neutrals to ions, a Wien velocity filter, a 45° parabolic single-channel energy analyzer, and a channel electron-multiplier detector. Since the EBT plasma is continuous in time, the spectrum will be scanned by programming both the Wien filter and energy analyzer to a step change in electrode voltage. A major requirement of the EBT analyzer is the ability to measure the flux of particles for energies less than 100 eV. Difficulties are encountered in this energy range due to both the extremely low efficiency ($\sim 10^{-6}$) of the stripping cell to convert neutrals to ions and the inability to determine neutral-particle fluxes. Recent measurements have shown that when neutral particles are incident on a surface, up to 70–90% of the particles are reflected as neutrals, which also results in an energy reflection coefficient from 0.1 to 0.5. Thus, large errors are introduced when thermal detectors, which are now relied on, are used to measure absolute neutral-particle fluxes. To overcome these difficulties, design studies are in progress to replace the N_2 gas cell with a cesium heat pipe and to design a thermal detector in which reflected particles are intercepted by the sensitive detector walls.

EXCITED ELECTRONIC STATES OF HYDROGEN MOLECULES

C. F. Barnett T. J. Morgan¹
J. A. Ray

Previous observations of Rydberg or highly excited electronic states of H_2 and D_2 have failed to confirm the quantum-mechanical calculations of level population, lifetimes, and observed quantum beats.² Recent theoretical results of A. Russek of the University of Connecticut suggest that upper electronic levels ($n \geq 10$) of the molecules are being populated from

lower levels ($n \sim 4$) by overlap of the vibrational states. To verify this hypothesis, an H_2^+ beam was accelerated to energies of 100 to 400 keV and passed through an H_2 gas cell, where electron capture collisions formed energetic H_2^* molecules in all states of excitation. The excited H_2^* molecules were passed through an intense longitudinal electric field, which ionized all states $n \geq 10$. Following the field ionizer was a 30-cm drift region in which the lower vibrational levels would have sufficient time to repopulate the $n \geq 10$ levels. By passing the H_2^* beam through an identical second electric field it was found that the $n \geq 10$ levels were repopulated as predicted by theory. However, on performing the same experiment with H^* atoms, we also found the $n \geq 10$ levels repopulated. This observation suggests that the levels $n \geq 10$ are not being completely ionized by the first ionizer because the transit time through the electric field is approximately the same as the mean lifetime for ionization. Another explanation for the H^* repopulation is the mixing of the $n = 9$ with the $n = 10$ level through overlap of angular-momentum states. Work is continuing to elucidate the H^* observations and to attempt to devise an experiment to overcome this difficulty.

1. Consultant, Wesleyan University, Middleton, Conn.

2. C. F. Barnett, J. A. Ray, and A. Russek, *Phys. Rev. A* **5**, 2110 (1972).

NEUTRAL-PARTICLE REFLECTION

E. Ricci

Measurements of the reflection coefficients for 0.3- to 5-keV H^0 incident on copper, stainless steel, and gold have been principally concerned with characterizing the surface condition. Measurements with helium-ion backscattering indicated that after any surface-cleaning procedure the surfaces become contaminated in a few minutes. Experiments with cleaning surfaces by ultraviolet radiation in the presence of approximately 1 mm of oxygen indicate that carbon and other contaminants can be readily removed from a surface but that an O_2 contaminant remains on the surface. Presumably, the cleaning action is the result of chemically active O_3 reacting with the surface impurities. To provide clean surfaces for a longer period of time, the base pressure in the system has been decreased to 10^{-9} torr. To increase the reliability of the data at low energies the apparatus has been moved to a low-energy ion source where the beam intensity is one or two orders of magnitude greater than previously available.

ABSOLUTE X-RAY-PRODUCTION CROSS SECTIONS FOR HEAVY IONS INCIDENT ON A WIDE VARIETY OF TARGETS

P. D. Miller	R. P. Chaturvedi ²
G. D. Alton	R. M. Wheeler ²
J. L. Duggan ¹	F. Elliott ³
F. D. McDaniel ¹	K. A. Kuenhold ³
R. Mehta ¹	J. McCoy ³
G. Monigold ¹	L. A. Rayburn ⁴
J. Tricomi ¹	S. J. Cipolla ⁵
G. Pepper ¹	A. Zander ⁶
J. Lin ⁷	

For the past three years a large group consisting of the above authors has been investigating the systematic behavior of x-ray production by heavy ions. A Si(Li) detector with approximately 170-eV resolution has been used, and absolute cross sections have been determined by detecting Rutherford scattered particles. The absolute efficiency and energy calibration of the x-ray detector are determined by a series of precisely calibrated sources. The bombarding particles used have been: boron, carbon, oxygen, fluorine, and chlorine. In each case the energy range covered has been from 0.5 to 3.0 MeV/amu. Some of the authors have participated in supplementary measurements using proton, helium, and lithium beams (these measurements have been made at North Texas State University and Florida State University).

In the K shell, most elements for which it is possible to prepare thin solid targets on carbon-foil backings have been investigated in the target atomic number range from $Z = 20$ through $Z = 47$. In each case absolute $K\alpha$ and $K\beta$ production cross sections have been determined, and the corresponding energy shifts, reflecting multiple ionization of the target atom, have been determined. Errors in the cross sections are typically of the order of 10%, and the energy-shift measurements are accurate to about 10 eV. Typical examples of the cross-section data are shown in Fig. 3.9, where total K x-ray-production cross sections are plotted for nitrogen ions incident on a series of the heavier targets. The significance of the various theoretical curves is as follows: BEA — binary encounter approximation;⁸ PWBA — plane-wave Born approximation;⁹ BE — corrected for the effect of increased binding of the electron in the target nucleus due to the close passage of the positive bombarding particle;¹⁰ CD — corrected for the effect of Coulomb deflection of the incident ion;¹⁰ POL — corrected for the effect of the polarization of the target electronic wave function due to the passage of the incident ion;¹¹ and

REL – corrected for relativistic corrections to the target wave function.¹² For each of the theoretical curves, the calculated ionization cross section has been multiplied by the single-vacancy fluorescence yields given by Bambynek et al.¹³ The principal uncertainty in the comparison of theory with experiment is these fluorescence yields, since the energy shifts of the K x rays indicate that there is multiple ionization of the L shell present, and there is no detailed theory of fluorescence yields of multiply ionized atoms. Figure 3.10 shows typical energy-shift data for carbon ions on four of the lighter K -shell targets. The abscissa is the square of the ratio of the velocity of the bombarding ion to the average velocity of the L -shell electrons. In general, the peak energy shifts occur for this ratio in the neighborhood of 1; however, for heavier targets there is a significant shift toward a lower value of the ratio at which the energy shifts peak.

The L -shell x rays were investigated for the same incident ions and energy range for an assortment of targets ranging from $Z = 50$ to $Z = 82$. Absolute cross sections were deduced for all of the resolvable satellites. These data are being analyzed. More detailed de-

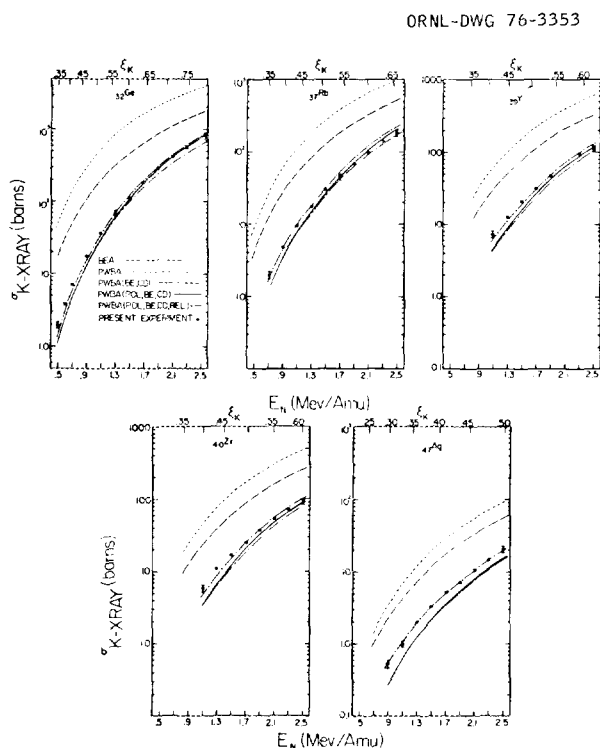


Fig. 3.9. Experimental ^{14}N ion-induced x-ray-production cross sections compared with various theoretical predictions (see text). The parameter ξ_k is the ratio of the collision time to the target electron orbit time.

ORNL-DWG 76-3354

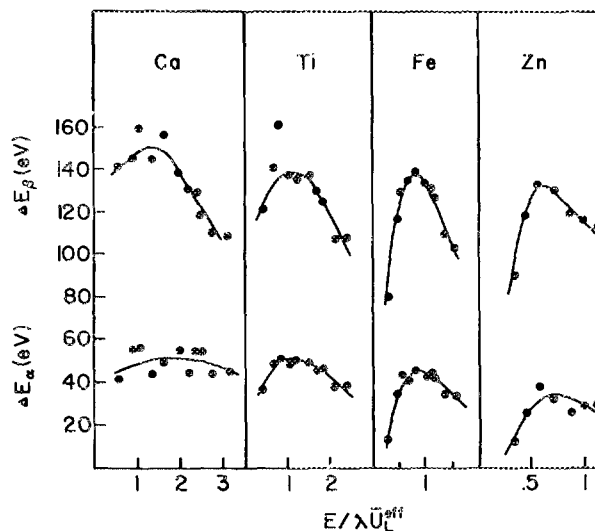


Fig. 3.10. The shifts in the characteristic energies of $K\alpha$ and $K\beta$ x rays of calcium, titanium, iron, and zinc in terms of $E_1/\lambda\bar{U}_L^{\text{eff}}$. The lines through the data points in this figure are not theoretical fits but are drawn to help visualize the results.

scriptions of the experiments and their analyses are given in refs. 14–21.

1. North Texas State University, Denton.
2. State University of New York College at Cortland.
3. University of Tulsa, Tulsa, Okla.
4. University of Texas, Arlington.
5. Creighton University, Omaha, Neb.
6. East Texas State University, Commerce.
7. Tennessee Technological University, Cookeville, Tenn.
8. J. H. McGuire and K. Ormidvar, *Phys. Rev. A* **10**, 182 (1974).
9. E. Merzbacher and H. Lewis, p. 166 in *Encyclopedia of Physics*, S. Flugge, Ed., vol. 34, Springer-Verlag, Berlin, 1958.
10. G. Basbas, W. Brandt, and R. Laubert, *Phys. Rev. A* **7**, 983 (1973).
11. K. W. Hill and E. Merzbacher, *Phys. Rev. A* **9**, 156 (1974).
12. An approximate correction is given by J. S. Hansen, *Phys. Rev. A* **8**, 822 (1973).
13. W. Bambynek et al., *Rev. Mod. Phys.* **44**, 716 (1972).
14. R. M. Wheeler et al., "K X-Ray Production Cross Sections for Fourteen Elements from Calcium to Palladium for Incident Carbon Ions," to be published in *Physical Review A*, March 1976.
15. J. Tricomi et al., "K Shell X-Ray Production in Ge, Rb, Y, Zr, and Ag by ^{14}N Ion Impact," submitted for publication in *Physical Review A*.
16. F. D. McDaniel and J. L. Duggan in *Proceedings of the Fourth International Conference on Beam Foil Spectroscopy and Heavy-Ion Atomic Physics, Gatlinburg, Tenn., Sept. 15–19, 1975*, Plenum Press, New York, 1976.

17. J. Tricomi et al., "K X-Ray Production Cross Sections for Elements of $Z = 20$ to 37 by Incident Cl Ions of 16--43 MeV Energy," paper presented at the Fall Meeting of the Texas Section of the American Association of Physics Teachers, Midwestern University, Wichita Falls, Tex., Nov. 1-2, 1974.

18. J. Tricomi et al., "Inner Shell Ionizations Produced by Fast Chlorine Ions," paper presented at the 78th Texas Academy of Science Meeting, Sam Houston State University, Huntsville, Tex., Mar. 20-22, 1975.

19. R. Mehta et al., *Bull. Am. Phys. Soc.* 21, 33 (1976).

20. F. D. McDaniel et al., "A Systematic Study of K-Shell X Rays from Ti and Rb for Incident Ions ^1H , ^4He , ^7Li , ^{12}C , ^{14}N , ^{19}F , ^{28}Si , and ^{35}Cl in the Range from 1-3 MeV/amu," abstract submitted to the Tucson Meeting of the American Physical Society, Dec. 3-6, 1975.

21. J. Tricomi et al., "K Shell X-Ray Production by ^{14}N Ions Incident on Thin Targets of Ge, Rb, Y, Zr, and Ag," abstract submitted to the Tucson Meeting of the American Physical Society, Dec. 3-6, 1975.

CONTROLLED FUSION ATOMIC DATA CENTER

C. F. Barnett M. I. Wilker

In view of delays caused by updating and insufficient manpower, the compilation *Cross Sections of Interest to Thermonuclear Research* has been rescheduled for publication in April 1976. The compilation has grown to approximately 800 pages with 2500 data sets. In cooperation with the Atomic Transition Probabilities Data Center of the National Bureau of Standards, a bimonthly publication entitled *Atomic Data for Fusion* was started in January 1975. One of the major

objectives of the newsletter has been to place in the hands of fusion researchers tabulated numerical data pertinent to high-temperature plasmas many months before the data appear in the published literature. Because the data have not gone through the refereeing process, the data center staff makes an attempt to evaluate data before placing them into the newsletter. Topics covered by the newsletter include atomic structure, atomic transition probabilities, particle interactions with surfaces, and atomic collision cross sections.

Searching and evaluation of the current published literature has continued with the bibliographical data entered into the computer storage file. A small effort was begun to transform tabulated cross-section data into reaction-rate data for both Maxwellian-Maxwellian and beam-Maxwellian distributions. Future plans include storing cross sections, reaction rates, and analytical expressions for reaction rates in the CTR Livermore computer for on-line retrieval.

During the past year, discussions have been held with the International Atomic Energy Agency (IAEA), Neutron Data Section, in regard to the participation of the IAEA in data compilation and analysis in the field of atomic data for controlled fusion. Approval has been granted for the IAEA to start a small two-year test program in January 1977. The exact role that the IAEA will perform is unclear, but it seems probable that they will have as a major task the coordination of the efforts in many countries.

4. Accelerators

HEAVY-ION LABORATORY

HEAVY-ION FACILITY PROJECT

J. B. Ball	J. W. Johnson
J. A. Martin	R. F. King ⁴
J. A. Biggerstaff	J. D. Larson ⁴
R. S. Lord	M. L. Mallory
C. M. Jones	J. E. Mann
R. L. Robinson	G. S. McNeilly ³
J. K. Bair	W. T. Milner
R. M. Beckers ¹	S. W. Mosko
E. Eichler ²	J. A. Murray ¹
K. N. Fischer ³	J. D. Rylander ¹
J.L.C. Ford, Jr.	R. O. Sayer ³
C. D. Goodman	J. A. Steed ¹
E. D. Hudson	N. F. Ziegler

Activity on the new Heavy-Ion Facility project which began last year has continued on schedule this year, the major concentration of effort being on design. The elevation view in Fig. 4.1 illustrates the major features of the project: the 25-MV folded tandem electrostatic accelerator, injection of beams from the tandem accelerator into ORIC for energy boosting, and a building to house the tandem, its injector, and auxiliary equipment. Also included in the building addition are two experimental areas for use of beams directly from the tandem accelerator.

Detailed design of the building addition was provided by the architect-engineering firm of Chas. T. Main, Inc. This work, begun in late December 1974, was finished in December 1975. The drawing and specification package will be issued to prospective building contractors early in 1976 with bids due in mid-February. An architectural rendition of the final design is shown in Fig. 4.2.

Site preparation for the building addition was started in late July and was 65% complete by the end of the year. A view of this activity is shown in Fig. 4.3. This work is expected to be completed by mid-February,

1976, about one month prior to the scheduled start of building construction.

On the basis of competitive bids, National Electrostatics Corporation (NEC) was selected to build the tandem electrostatic accelerator. Final approval by the Energy Research and Development Administration (ERDA) of the contract with NEC was received in May. The accelerator system to be supplied and installed under this contract is shown schematically in Fig. 4.4. The system comprises all of the components shown, including the high-voltage generator, the pressure vessel, the injector platform with ion source, and the interconnecting beam transport and vacuum components. Also included, but not shown in the figure, are a computer-based control system and a complete gas-handling system with liquid-storage vessels. The complete technical specifications on which the accelerator system is based are available as an ORNL technical memorandum (ORNL/TM-4942). For specific details about the system the reader is referred to these specifications and to the *Heavy-Ion Laboratory Newsletters* which are published quarterly.

The design of the ORIC modifications required to adapt the cyclotron for use as an energy booster is proceeding on schedule with 50 of 192 projected design drawings completed. Included in this portion of the project are all components of the injection-transfer beam line connecting the tandem accelerator to the ORIC. Fabrication of some of the components has now begun with the first package of modifications scheduled to be installed in ORIC late in 1976.

Formal ground-breaking ceremonies for the project took place on April 5, 1975. About 125 people were in attendance to hear a talk by ERDA Administrator Robert Seamans and remarks by ERDA Assistant Administrator John Teem, U.S. Congresswoman Marilyn Lloyd, University of Tennessee Chancellor Jack Reese, and ORNL Director Herman Postma.

Overall completion of the facility is still projected for late 1978 with initial testing scheduled for early 1979.

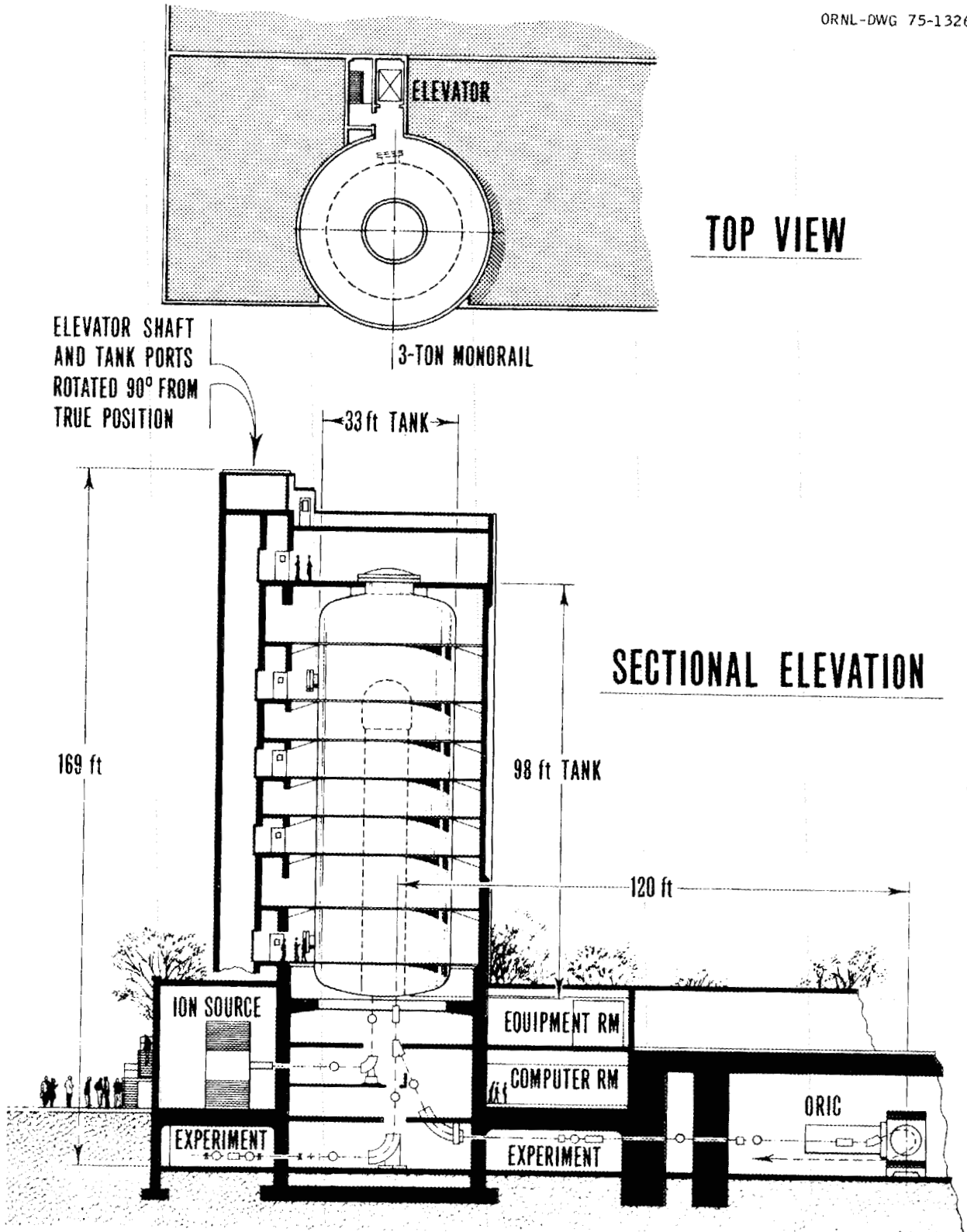


Fig. 4.1. Elevation view of the new Heavy-Ion Facility.

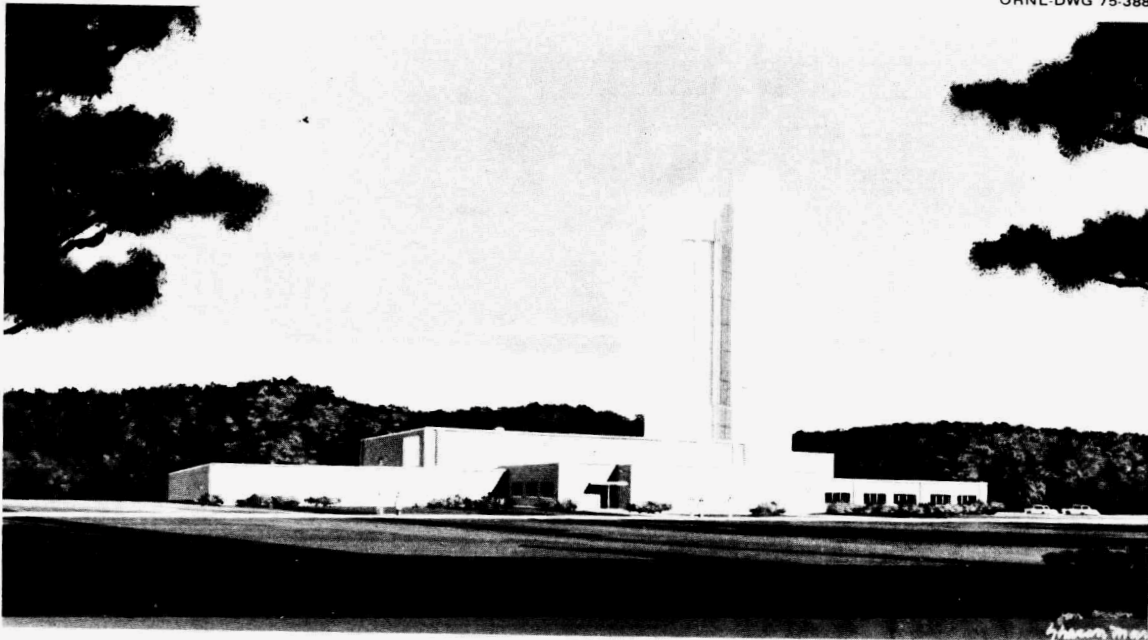


Fig. 4.2. Artist's conception of the ORIC building with the addition of the tower for the "folded" tandem.



Fig. 4.3. Site preparation activities behind the ORIC building. The area at the right of the photograph is for a small building to house the SF₆ compressors and storage vessels.

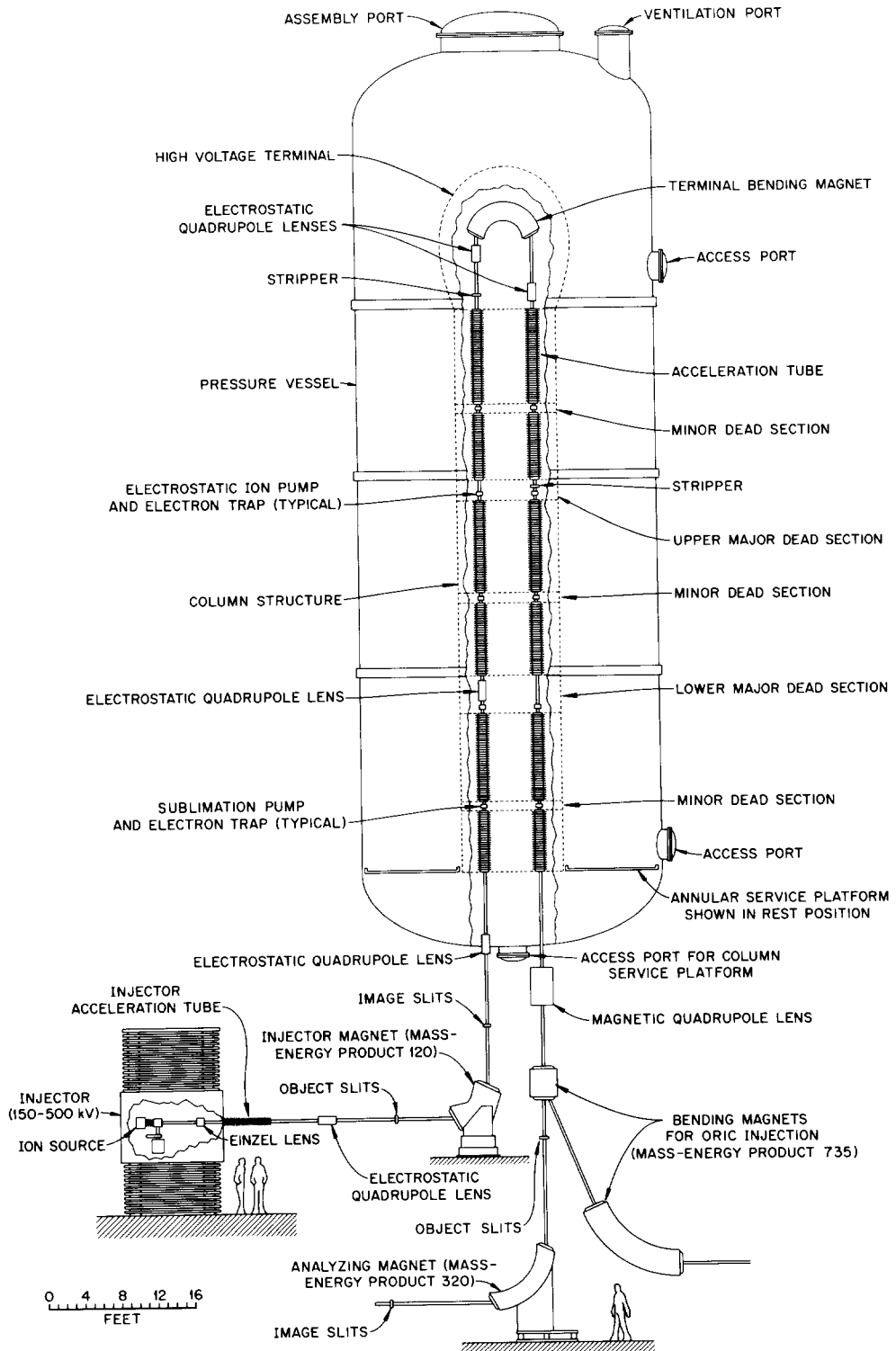


Fig. 4.4. Schematic of the 25-MV tandem accelerator system.

A users' organization for the facility became functional this year with the first annual meeting held in October. About 70 people from outside ORNL and 58 ORNL staff scientists met to ratify the charter proposed for the group by a six-member executive committee.

1. UCC-ND Engineering.
2. Chemistry Division.
3. UCC-ND Computer Sciences.
4. Consultant.

HEAVY ION FACILITY – PHASE II PROPOSAL

J. B. Ball	J. E. Mann
J. A. Martin	G. S. McNeilly ¹
J. A. Biggerstaff	S. W. Mosko
E. D. Hudson	J. A. Murray ²
R. S. Lord	R. L. Robinson

Phase II of the expansion of facilities for research with heavy ions is being planned to extend the range of beams useful for nuclear research to include the full range of atomic masses and to significantly increase the maximum energy available for the lighter heavy ions. A new $K = 300$ to 400 separated-orbit cyclotron will serve as an energy booster for beams from either the 25-MV tandem or the ORIC, and additional experimental areas which can be served by beams from either the 25-MV tandem or the new cyclotron are to be provided. The separated-sector cyclotron (SSC) will accelerate heavy ions to at least 10 MeV per nucleon for the full range of masses through uranium and will provide light ions in the range through $A = 40$ with energies up to about 75 MeV per nucleon. The range of performance in energy vs ion mass is seen in Fig. 4.5.

The arrangement of the facility (Fig. 4.6) was planned so that construction of the project would not interfere significantly with the continuing research programs of the phase I project; the plan will also allow changes at a later time to transport beams from either the SSC or 25-MV tandem to existing ORIC experimental areas, including the UNISOR facility. The new building will be a high-bay structure adjacent to the phase I facility and to the existing ORIC facilities. The addition will be approximately 190 ft long, 60 ft wide, and 47 ft high. A 35-ton bridge crane is provided to handle cyclotron components, experimental equipment, and movable shielding.

The new experimental areas will provide 6000 ft² of additional space, arranged in two large rooms. Each of these spaces will be served with three beam lines. The

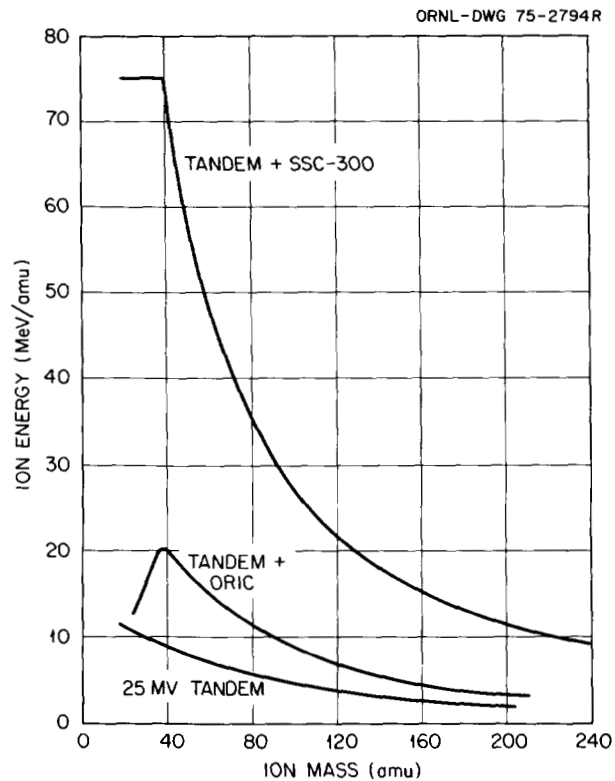


Fig. 4.5. Ion energy vs ion mass for the $K = 300$ SSC with ion injection from the 25-MV tandem. This is for the case of gas stripping in the tandem terminal with foil stripping before injection into the SSC. Also shown are curves for the tandem plus ORIC (phase I) and the tandem alone.

larger of the two rooms is envisioned as providing space for a large spectrometer to be added later.

A plan-section drawing of the SSC (Fig. 4.7) illustrates the main features of the design. The principal characteristics of the cyclotron are given in Table 4.1. Two of the opposing spaces between the sector magnets contain rf cavities. The others will contain beam-injection and -extraction equipment and diagnostic probes. The ion-injection system is adjustable in radius to meet the requirements of different beams from the tandem and the matching requirements for beams from ORIC.

The magnet sector angle is 52° , a choice that gives strong axial and radial ion focusing well away from resonances due either to magnet imperfections or to the fourfold magnet periodicity. Additional details of magnet design and its ion-focusing characteristics are given in another section of this report.³

The cyclotron rf system consists of quarter-wave coaxial resonators. The dees and respective ground planes are cone-shaped structures. Smaller resonators

operating at twice the main rf frequency are mounted within the main resonators. These harmonic resonators serve to effectively "flattop" the accelerating voltage waveform to increase the phase acceptance. The system is expected to increase the phase acceptance for the 0.1%-energy-spread output beam from $\pm 3^\circ$ to $\pm 10^\circ$. This feature eases bunching requirements for tandem beams and provides better phase matching for beams from ORIC.

The vacuum system for the cyclotron will be designed to provide a base operating pressure of 1×10^{-7} torr to avoid significant losses from charge-changing processes. The system volume of approximately 100,000 liters is to be pumped by a system of helium-cooled cryopumps

aided by small oil-diffusion pumps for noncondensable gases. The system will provide a pumping speed of 140,000 liters/sec for air and 10^6 liters/sec for water vapor. Pump-down time is estimated to be 15 hr.

During the past year a formal preconceptual design study was completed to define the scope and cost of the proposed addition. A conceptual design study to further refine the project design is authorized for 1976. Some changes in the design are being reviewed. Among the modifications being considered are an increase in the size of the cyclotron to $K = 400$, a change to a vertical half-wave resonator system possibly without second-harmonic resonators, and a change in rf range to increase the upper frequency limit to approximately 20

ORNL-DWG 75-9812

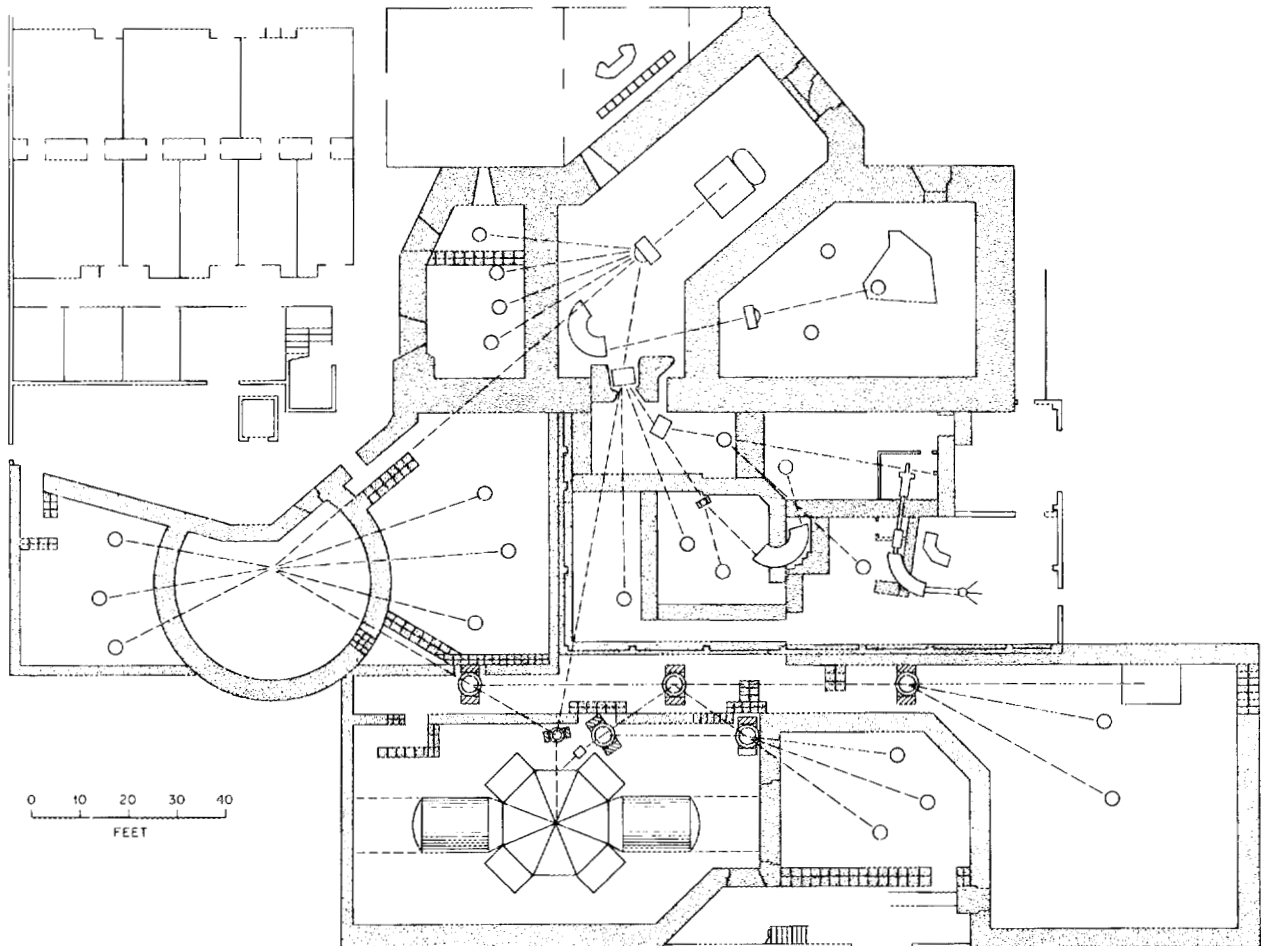


Fig. 4.6. First-floor plan view of the Heavy-Ion Laboratory; the phase II addition is shown at the bottom.

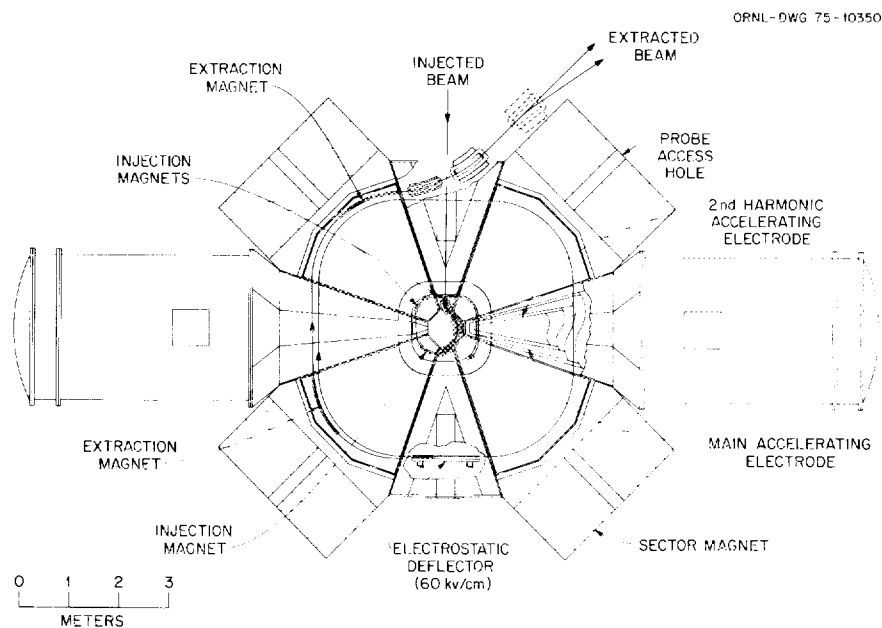


Fig. 4.7. Plan view of the separated-sector cyclotron.

Table 4.1. Characteristics of the separated-sector cyclotron

General	
Maximum energy ^a (MeV/A)	
Uranium, $^{238}\text{U}^{43+}$	10
Carbon, $^{12}\text{C}^{6+}$	75
Maximum $B\rho^a$ (kG-cm)	2540
Energy constant, ^a K ($E = Kq^2/A$)	310
Maximum magnetic field (kG)	15
Extraction mean radius (m)	2.83
Injection radius (m)	0.73–1.07
Magnet system	
Number of sectors	4
Sector angle (deg)	52
Gap (cm)	10
Steel weight (metric tons)	1450
Main coil power (kW)	300
Trimming coil power (kW)	300
Radio-frequency system	
	Main/harmonic cavities
Number of cavities	2/2
Frequency range (MHz)	6–14/12–28
Rf voltage, peak (kV)	250/100
Maximum rf excitation power (kW)	200/50
Amplitude stability	1:10 ⁴
Phase stability (deg)	±0.1

^aWith higher magnet power the design is capable of $B_{\text{max}} = 17.32$ kG, $B\rho = 2930$ kG-cm, and $K = 400$ and corresponding higher energies.

MHz to better match the requirements for high-energy ions.

1. UCC-ND Computer Sciences.
2. UCC-ND Engineering.
3. See this report, E. D. Hudson et al., "Magnet-Model Studies for Separated-Sector Heavy-Ion Cyclotrons."

BEAM-BUNCHER TEST PROGRAM

W. T. Milner N. F. Ziegler
S. W. Mosko R. F. King¹

The optimum injection of beams from the 25-MW tandem accelerator into ORIC requires that the incident beam be bunched into 6° or less of the cyclotron rf period. The double-drift harmonic beam-bunching system²⁻⁴ is especially attractive for this application because of its theoretical capability to bunch a large fraction of the electrostatic accelerator dc beam into the required pulses. A program to install and evaluate a prototype double-drift harmonic beam-bunching system on the EN tandem accelerator is under way. A portion of the EN tandem injection beam line has been redesigned to accommodate this equipment, and design of the bunching system is in progress. This program will include not only bunching-system evaluation but also the development of beam-pulse detection equipment and a CAMAC-based control system.

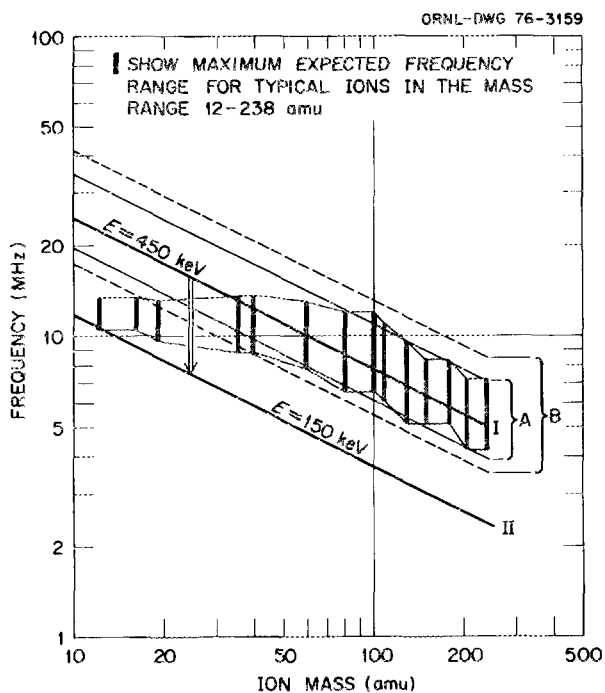


Fig. 4.8. *A* and *B* define the regions of 90 and 80% voltage efficiency about line I (i.e., at 450-keV ion energy) for a buncher whose first-harmonic element is 6 cm long. Corresponding regions about line II (for 150-keV ion energy) will have the same width, on this scale, as those about line I.

A study has been carried out in which the probable range of ORIC operating parameters was determined for a number of ions in the mass range of 12 to 238 amu. A consideration of the range of orbit frequencies that might be required for these ions shows that buncher elements of fixed length (6 and 3 cm for the first- and second-harmonic elements respectively) can be used to cover the entire range of operating frequencies. Figure 4.8 shows the frequency range that can be covered by a fixed-length buncher system operating on 450-keV ions. The region below mass 60 can be accommodated easily by reducing the ion-injection energy. For example, carbon ions will require injection energies of around 200 keV or less. Note that a frequency range of 1.8 to 1.0 can be attained, at fixed ion energy and buncher length, with only 10% loss in buncher voltage efficiency.

1. Consultant.

2. *Phys. Div. Annu. Prog. Rep. Dec. 31, 1974*, ORNL-5025 (1975), p. 155.

3. W. T. Miltner et al., *IEEE Trans. Nucl. Sci.* NS-22, 1697 (1975).

4. R. Emigh, p. 338 in *Proceedings of the 1966 Linear Accelerator Conference*, Los Alamos Laboratory Report LA-3609, 1966.

DEPENDENCE OF ^{12}C AND ^{16}O CHARGE-STATE YIELDS ON STRIPPER-GAS FLOW

R. O. Sayer¹ E. G. Richardson

In contrast to the more typical emphasis on high charge states, successful injection of ^{12}C and ^{16}O beams from the 25-MV folded tandem Van de Graaff into ORIC will require acceleration of charges 3 and 4, respectively, at relatively high terminal voltage, V_t . To investigate the intensities expected for these beams we have measured charge-state yields as a function of stripper-gas flow in the ORNL EN tandem. Typical results for analyzed beam current as a function of pressure in the high-energy tube are shown in Figs. 4.9 and 4.10. These data indicate that ample charge 3 and 4 intensities at $V_t = 6$ MV can be achieved at reduced gas pressures.

With regard to yields at higher V_t , the ^{12}C data at 6 MV show that, by a suitable reduction in gas flow, one can move 2 units away from equilibrium to charge 2 while suffering only about a 40% loss in intensity. At $V_t = 15$ MV the most probable charge is about 5, so that an adequate intensity for $^{12}\text{C}^{3+}$ with optimum gas flow can be expected. A similar argument can be made in the ^{16}O case. Therefore it seems likely that sufficiently intense low-charge beams of ^{12}C and ^{16}O at moderately high V_t will be available for injection into ORIC. Nonetheless, measurements in the 15 to 25 MV range are desirable.

We are indebted to Art McDonald and G. F. Wells for helpful discussions.

1. Computer Sciences Division.

MAGNET-MODEL STUDIES FOR SEPARATED-SECTOR HEAVY-ION CYCLOTRONS

E. D. Hudson	G. S. McNeilly
R. S. Lord	S. W. Mosko
L. L. Riedinger ¹	M. A. Barre ²
J. A. Martin	M. P. Bourgarel ²
F. Irwin	T. T. Luong ²
	M. Ohayon ²

A four-sector model of a 2200-metric-ton $K = 440$ separated-sector cyclotron (SSC) magnet has been built to 0.15 scale. Magnetic field measurements have been made using a single Hall-effect element that was positioned by a high-precision numerically controlled table. A list of full-scale characteristics is given in Table 4.2. The SSC is proposed as the second-stage accelerator to follow the 25-MV tandem electrostatic accelerator.

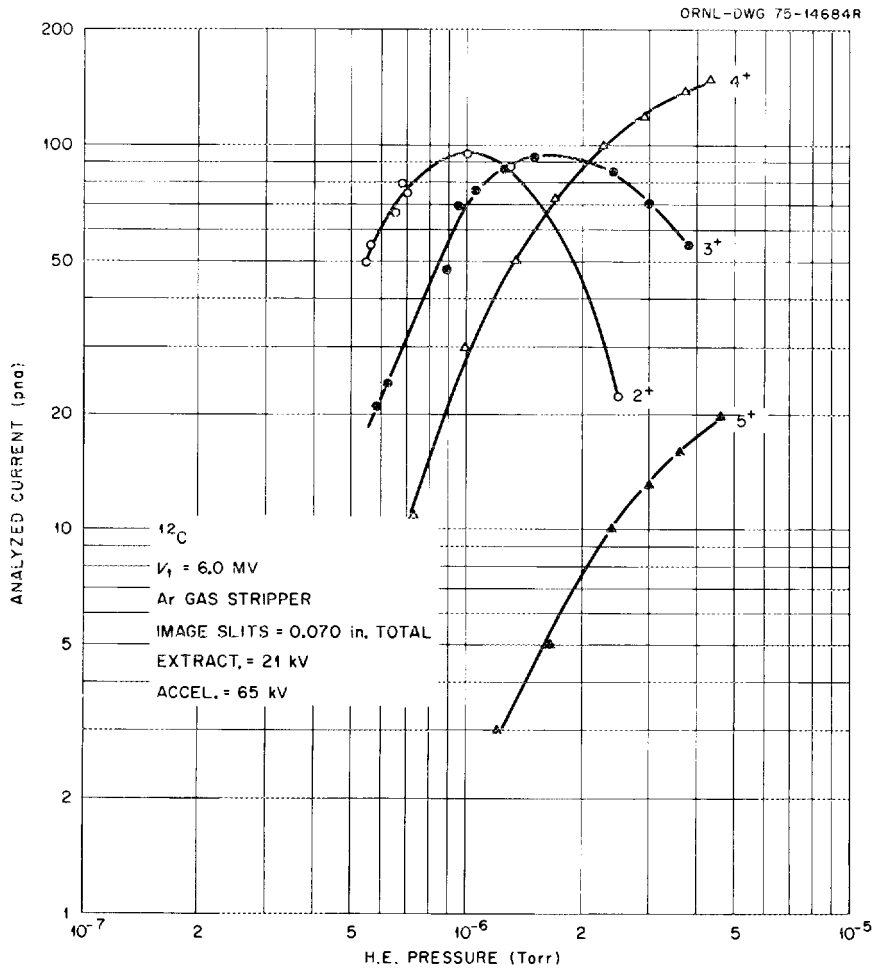


Fig. 4.9. Analyzed current in pna for charge 2, 3, 4, and 5 ¹²C beams vs high-energy tube pressure at $V_1 = 6.0$ MV.

These measurements were also made to provide magnetic field design information for the GANIL project. Four members of the GANIL project (Fig. 4.11) spent several weeks during May, June, and July at ORNL taking data on the model.

The magnetic field profile of the model was experimentally mapped at excitation levels of 5, 8, 12, 14, 16, and 18 kG. Figure 4.12 displays a normalized comparison of the average magnetic field as a function of radius for 8 and 16 kG. This average at each point has been calculated along a path of constant radius rather than along the particle path. The average is smooth to within 0.01% of the maximum field, that is, 1 or 2 G out of 16 kG. Between the limits of the injection and extraction radii, the 8- and 16-kG fields are similar in shape to within 0.5%. The near absence of saturation effects at 16 kG, the operating point of the full-scale magnet,

leads to very nearly the same dynamics of particle orbits at low and high field levels.

The effective magnetic angles at several radii are in very good agreement with the calculated values and the design value of 52°, demonstrating that the steps around the pole edge provide an excellent approximation of the desired Rogowski profile. The constancy of the magnetic angle as a function of radius also demonstrates the success of the pole-edge design. We find, in addition, that the magnetic angle at a given radius is constant to within 0.5° from 8 to 16 kG. This once again shows the near absence of saturation effects over this important range.

The results of General Orbit Code calculations with ¹²C⁶⁺ and ²³⁸U³⁶⁺ injected into the 16-kG field are graphed in Fig. 4.13. Here the orbits at successive radii were isochronized by adjusting the field level as a

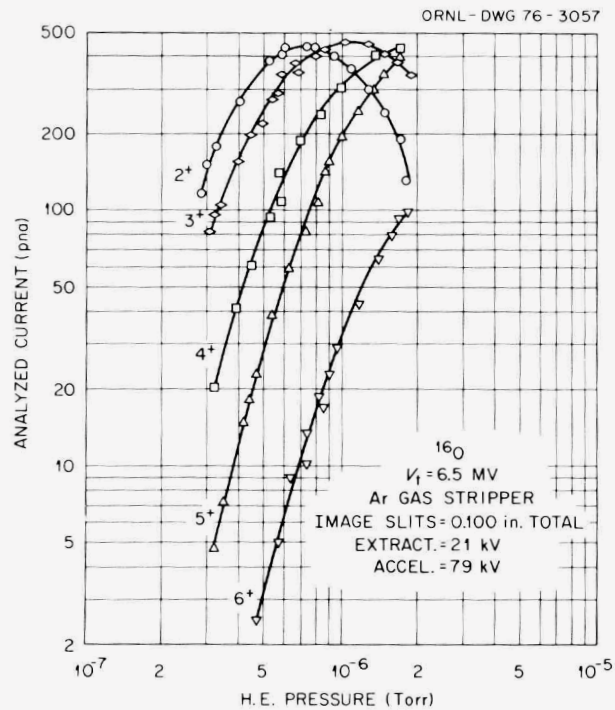


Fig. 4.10. Analyzed current in pna for charge 2, 3, 4, 5, and 6 ^{16}O beams vs high-energy tube pressure at $V_t = 6.5 \text{ MV}$.

function of radius, with this difference eventually to be furnished by trimming coils. This resonance diagram demonstrates the operating region of the proposed cyclotron and shows that with the 52° sector we will be free of instabilities caused by the essential resonances.

Table 4.2. Characteristics of the full-scale separated-sector cyclotron magnet

Energy constant, K (MeV)	440
Energy gain	9–19
Magnetic field (kG)	16
Number of sectors	4
Sector angle of magnet (deg)	52
Gap (cm)	10.2
Pole radius, min (cm)	40.6
Pole radius, max (cm)	358.0
Yoke radius, max (cm)	572.8
Yoke width (cm)	332.7
Yoke height (cm)	553.7
Sector weight (tons)	600
Sector weight (metric tons)	540
Beam extraction radius (cm)	328.9
ρ at injection, min (cm)	43.2
ρ at injection, max (cm)	63
ρ at extraction (cm)	188.7
Ampere turns per sector at 16 kG	148,000
Power per sector (kW)	100

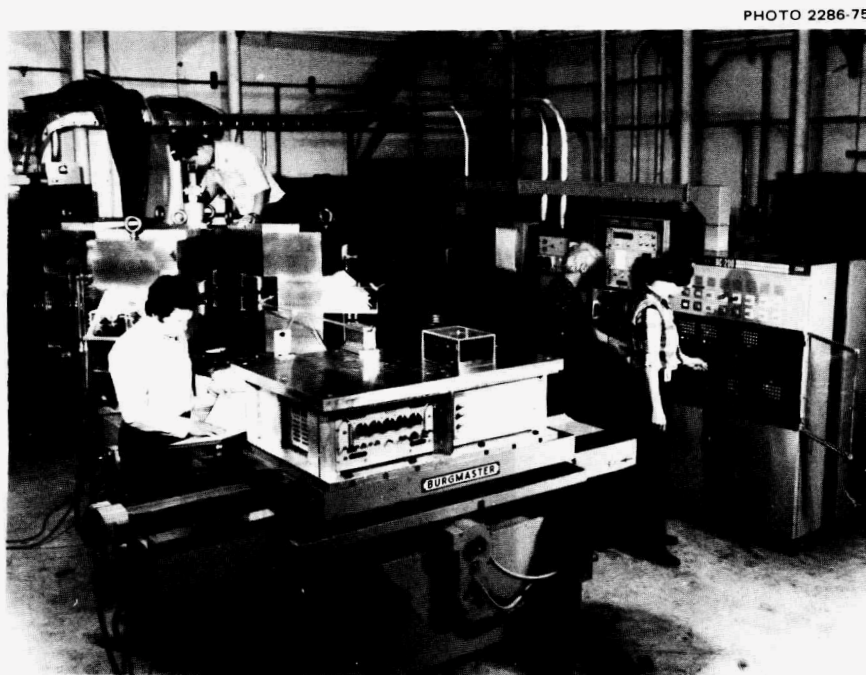


Fig. 4.11. Members of the GANIL project (France) working with the 0.15-scale model of a 2200-metric-ton cyclotron magnet are, from left, Maurice Ohayon, Thanh-Tam Luong, Michele Barre, and Marie-Paule Bourgarel.

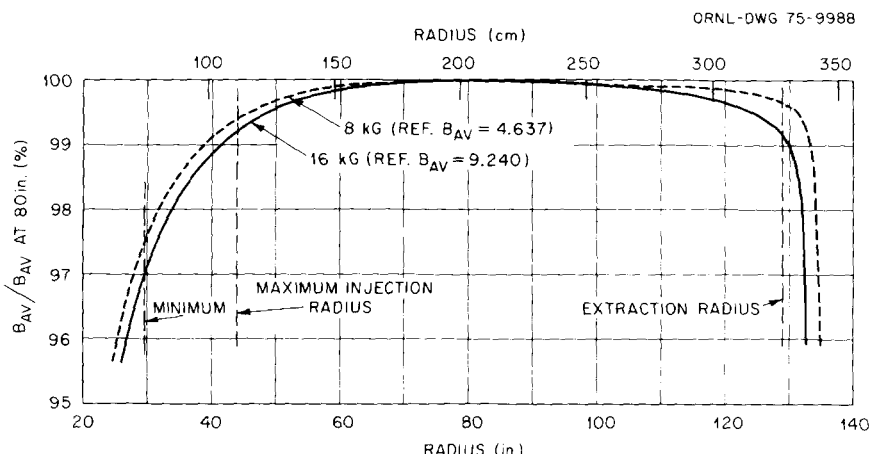


Fig. 4.12. Average magnetic field as a function of full-scale radius for the 8- and 16-kG fields. Note that there is, at most, 0.5% difference in field shape between the two in the range between the injection and extraction radii.

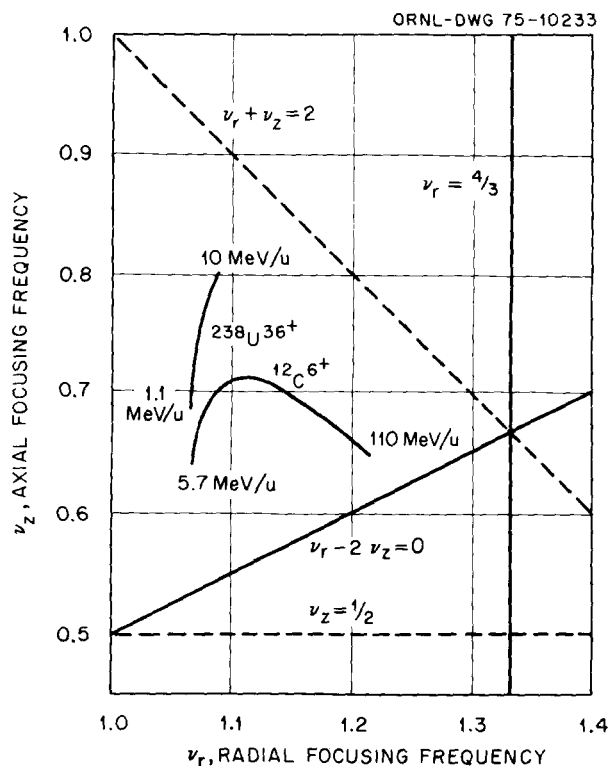


Fig. 4.13. Resonance diagram describing acceleration of ^{12}C and ^{238}U .

The range of ν_r and ν_z values is quite satisfactory for the successful operation of a four-sector cyclotron.

1. University of Tennessee, Knoxville.
2. Project GANIL, France.

INGRID PROPOSAL

M. J. Saltmarsh R. E. Worsham

Some of the major technological difficulties that will be encountered in the search for commercial fusion power are associated with the radiation damage to structural materials caused by the 14-MeV neutrons emitted from a *d-T* plasma. Investigation of this effect is severely hampered by the lack of suitably intense sources of energetic neutrons that are capable of simulating the spectrum expected at the first wall of a fusion reactor.

In response to this need a proposal has been prepared and submitted to the ERDA Division of Controlled Thermonuclear Research for the construction of an intense neutron generator for radiation-induced damage (INGRID).¹ The proposal represents a collaborative effort involving several ORNL divisions (Metals and Ceramics, Physics, Reactor, Solid State, and Thermonuclear) and staff from the Accelerator Division at the Fermi National Accelerator Laboratory.

The INGRID facility is based on the *d-Li* concept, which also forms the basis of similar proposals by Brookhaven National Laboratory (BNL)² and Hanford Engineering Development Laboratory (HEDL).³ A 100-mA 40-MeV beam of deuterons produced by a linac with a 100% duty factor would be used to bombard a 2.5-cm-thick jet of liquid lithium (Fig. 4.14). Neutrons are produced mainly in the forward direction, providing an experimental volume of several hundred cubic centimeters at fluxes $\geq 10^{14}$ neutrons $\text{cm}^{-2} \text{sec}^{-1}$, equivalent to the flux on the first wall of a fusion device operating at a wall loading of 1 MW/m².

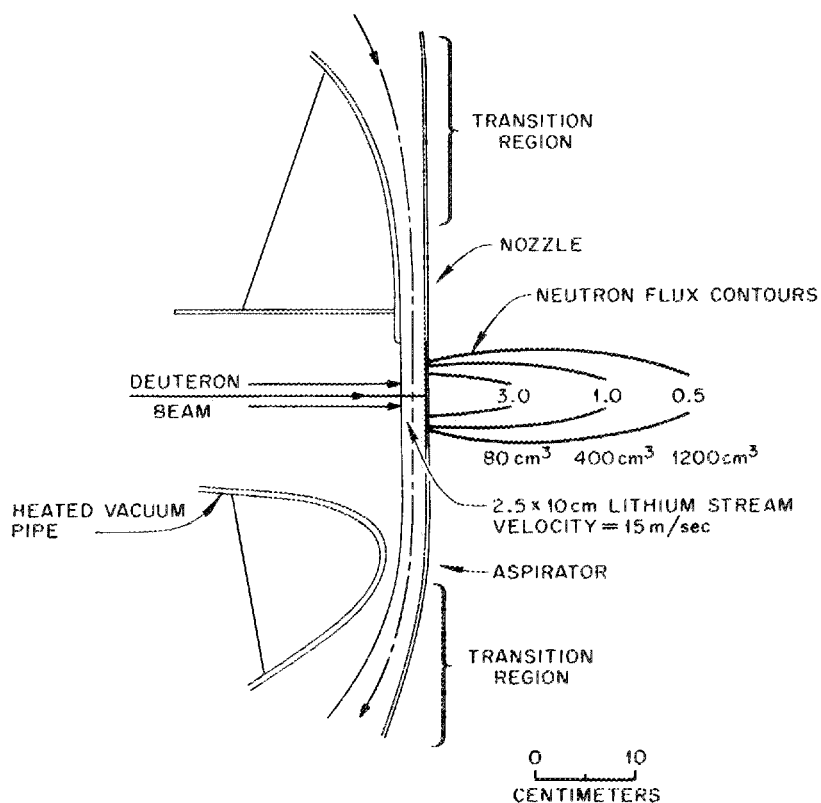


Fig. 4.14. The d -Li interaction region, showing the downward-flowing lithium jet. The neutron flux contours (given in units of 10^{14} neutrons $\text{cm}^{-2} \text{sec}^{-1}$) and their associated experimental volumes correspond to a 100-mA 40-MeV deuteron beam with a circular beam spot. The intensity profile was assumed to be Gaussian with a diameter of 2 cm (FWHM).

Analysis of the effects of the resultant neutron energy spectrum shows them to be very similar to the effects expected from a fusion spectrum, in terms of both atomic displacement and nuclear transmutation rates.

A plan view of the facility is shown in Fig. 4.15. The major components are the following.

1. The ion source and high-voltage column, capable of producing a 200-mA dc beam of 350-keV d^+ ions.
2. A 60-MHz cw linac, approximately 45 m long, to accelerate 100 to 150 mA of the injected beam to energies of 20 to 40 MeV.
3. A beam-transport system to send the beam through $\pm 45^\circ$ to one of the two irradiation cells.
4. A lithium circuit that pumps liquid lithium to one of the two lithium targets, each of which consists of a 10- by 2.5-cm jet of lithium moving at 15 m/sec across the end window of the beam-pipe vacuum

system. The one free surface of the jet is exposed to the vacuum to eliminate the need for a window. The 4 MW of beam power dissipated in the lithium circuit is transferred to a secondary heat-transfer fluid, tentatively chosen to be Dowtherm.

5. The irradiation facilities, consisting of the heavily shielded irradiation cells containing the lithium target, the probes that hold the samples to be irradiated and carry the experimental services through the shielding, and the hot-cell facilities used for dismantling or repairing experiments.

The facility must be conservatively engineered because irradiation times of a few days to years will be needed.

The overall cost, including some prototype development work, is estimated to be \sim \$70 million assuming INGRID to be an FY 1978 project. The time required

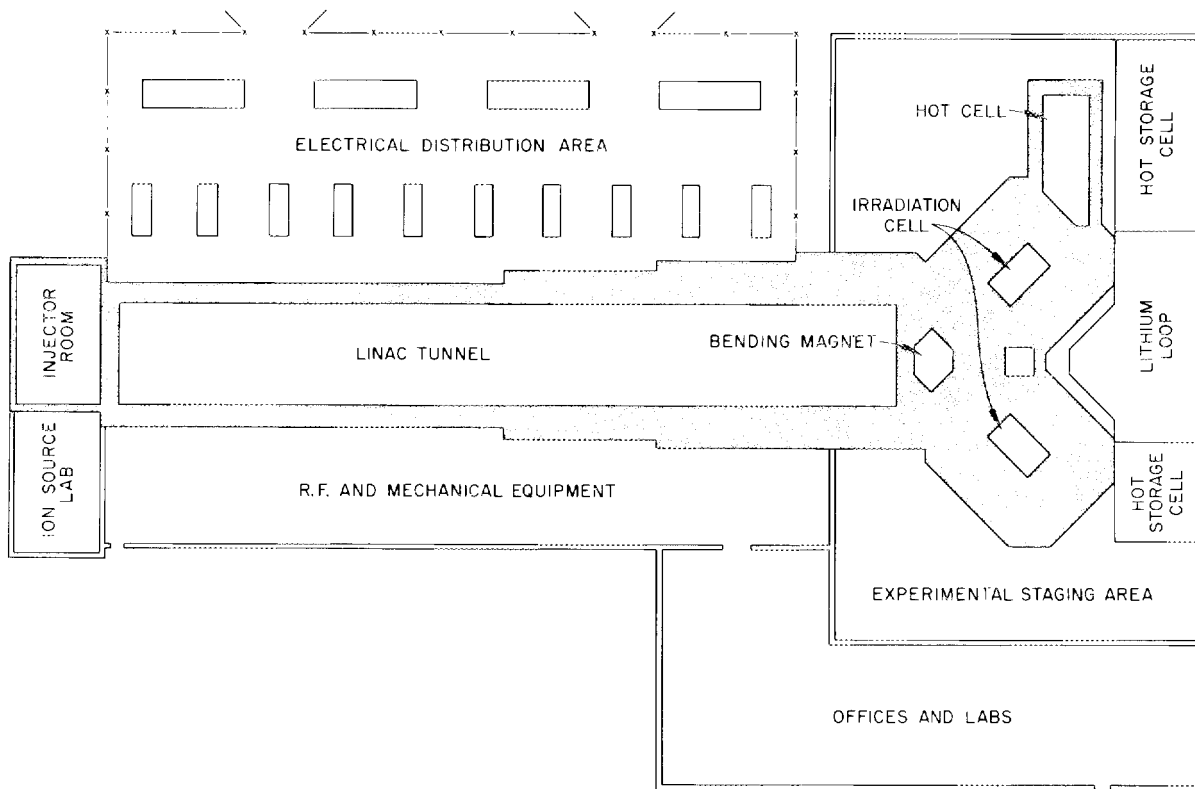


Fig. 4.15. Schematic plan view of the proposed INGRID facility. The overall length of the building is approximately 300 ft.

for construction is estimated at approximately four years.

1. M. J. Saltmarsh and R. E. Worsham, Eds., *INGRID, a Proposal for an Intense Neutron Generator for Radiation Induced Damage Studies in the CTR Materials Program*, ORNL/TM-5233 (January 1976).

2. P. Grand, Ed., *Proposal for an Accelerator-Based Neutron Generator*, BNL-20159, Brookhaven National Laboratory, Upton, N.Y., July 1975.

3. *CTR Materials Irradiation Testing Facility (CMIT) Proposal*, Hanford Engineering Development Laboratory, Richland, Wash., November 1975.

ORIC OPERATIONS

C. A. Ludemann	G. A. Palmer
M. B. Marshall	J. W. Hale
H. L. Dickerson	N. R. Johnson ¹
C. L. Viar	A. D. Higgins ²
H. D. Hackler	E. W. Sparks ³
C. L. Haley	R. C. Cooper ⁴

The ORIC operated on a 15-shift-per-week schedule essentially throughout CY 1975. Table 4.3 shows a time

analysis for the year. With ORNL's engineering staff concentrating on the new Heavy-Ion Facility project, scheduled downtime was devoted primarily to repairs and preventive maintenance. Our limited means are being used to improve the operation and reliability of existing systems rather than to expand the research capabilities of ORIC.

A comparison with statistics for the previous year shows that ORIC was operable 1017 hr more in 1975 than in 1974. A 26 to 35% improvement was experienced in unscheduled outage, depending on how one interprets the figures. The success of the program is the direct result of the hard work performed by the cyclotron operators.

Table 4.4 is a summary of the research bombardments for the year. It illustrates the broad nature of the research activity as well as the breadth of collaboration. It should be noted also that ~19% of the bombardments were for materials research and the production of plutonium isotopes for environmental research.

Table 4.5 summarizes beam use by type of particle. Approximately 80% of the research was conducted with projectiles heavier than helium. The state of radiation

Table 4.3. Time analysis of ORIC operations for CY 1975

	Hours	Percent
Beam on target	3038	48.3
Beam adjustment	349	5.5
Target setup	112	1.8
Startup and machine shutdown	579	9.2
Machine research	384	6.1
Total machine-operable time	4462	70.9
Source change	418	6.6
Vacuum outage	76	1.2
Rf outage	78	1.2
Power supply outage	162	2.6
Electrical-component outage	183	2.9
Mechanical-component outage	6	0.1
Water-leak outage	168	2.7
Radiation outage	0	0.0
Total unscheduled outage	1091	17.3
Scheduled maintenance	671	10.7
Scheduled engineering	72	1.1
Total scheduled downtime	743	11.8
Total time available	6296	100
Total research experiments	3925 ^a	~62

^aIncludes 640 hr for materials research and 88 hr for plutonium isotope production.

safety at ORIC during 1975 remained good. There were no personnel exposures beyond permissible limits, and there were no radioactivity releases resulting in a spread of contamination beyond zoned areas. The maximum integrated dose received by any individual associated with cyclotron operations was 0.58 rem, the average for the group being 151 millirems. The cyclotron operators, who receive the highest exposures, had doses that averaged 405 millirems, the highest single exposure being that indicated above. No responses significantly above background variance were observed by continuously operating air monitors in and around the facility, indicating effective containment of particulate radioactive materials.

Three major scheduled shutdowns will considerably reduce ORIC research time in 1976. The shutdowns are for (1) the removal of the "fringe-field concentrator" and installation of a new vertical positioning magnet, (2) the complete mapping of the cyclotron's magnetic field, and (3) the installation of a new dee. All three projects are being undertaken in preparation for ORIC's role as the energy booster for the 25-MV tandem.

1. Chemistry Division.
2. Plant and Equipment Division.
3. Instrumentation and Controls Division.
4. Health Physics Division.

ORIC DEVELOPMENT

C. A. Ludemann	E. D. Hudson
S. W. Mosko	R. S. Lord
E. E. Gross	J. E. Mann

As previously mentioned, our limited engineering resources were expended in improving the operation and reliability of existing systems at the cyclotron, not for expanding its research capabilities.

In the area of the rf system, a new screen-bypass capacitor for the power amplifier was installed and the germanium transistor servo-drivers were upgraded to use silicon transistors. In the area of vacuum improvements, a 60-W (at 15°K) helium refrigerator was installed to supply coolant for the machine's cryopanel. Vacuum monitoring equipment has been fabricated for all beam lines and will be installed in early 1976.

Beam current monitoring was improved by the replacement of the two tube-type integrators with two NIM-based units and the addition of two nanoammeters. Design of the new power-supply regulators for the trim and harmonic coils was completed and the first unit was being installed at the end of the year. The control computer was tested by using it to operate 19 power supplies during five weeks of routine cyclotron operation. These tests were successful and the computer control of all magnet systems is expected to be completed by mid-1976.

The 153° analyzing magnet was recalibrated. Since the original calibration, the slit mechanisms have been replaced and the nuclear fluxmeter location has been slightly changed. To recalibrate the system at low field (about 2 kG), a 1-mm-wide ²⁴⁴Cm alpha source¹ was placed at the entrance slit location, and the image of this source was viewed with a solid-state position-sensitive detector at the exit slit location. The magnetic field at the nuclear fluxmeter location required to bend the 5.805-MeV alpha particles along the beam orbit was found to be reproducible to 0.5 G in 2 kG provided the magnet was taken to saturation for about 30 min before making the measurements.

The absolute calibration was extended in the same way to ~4 kG by observing singly charged 5.805-MeV alpha particles from the source. The remaining calibration was accomplished by extracting a ~74-MeV ²⁰Ne⁴⁺ beam from the cyclotron and recording the magnetic fields (at the nuclear fluxmeter location) required to bend the 5+, 6+, 7+, and 8+ beams to the exit slit location. These beams result from stripping by residual gas in the ORIC beam piping (~1 × 10⁻⁵ torr). The magnetic rigidity of 74-MeV ²⁰Ne⁸⁺ is very close to that of 5.8-MeV ⁴He¹⁺, and we need only to assume

Table 4.4. Research bombardments at ORIC in 1975

Research activity	Investigators	Cyclotron time (8-hr shifts)
UNISOR ^a	Spejewski, Mlekodaj, Carter, Schmidt, Robinson, et al.	80
Heavy-ion fusion, fission, and transfers	Plasil, Ferguson, Pleasonton, Hahn, Obenshain, Snell, Hubert ^b	44
Materials research	Horak, Saltmarsh, Smith, Wiffen, Bloom, Washburn, Ullmaier, Jenkins, Noggle, Reiley, Auble, Ludemann	80
Accelerator development	Ludemann, Mallory, Hudson, Lord, Martin, Hale	34
Doppler-shift lifetime measurements	Johnson, Eichler, Hubert, ^b Yates, ^c Sarantites, Lindblad, ^d Urbon ^e	19
Coulomb-nuclear interference	Hillis, ^f Gross, Riedinger, ^f C. Bingham, ^f Halbert, Hensley, Scott, ^g Martin, ^h Baker ^g	28
Production of ²³⁷ Pu and ²³⁶ Pu	Mackey, Ottinger, Ratledge, Gross, Ludemann, Johnson	11
Identical-particle scattering	Halbert, Stelson, Snell, Fulmer, Raman, Stokstad, Hensley	11
Excitation of giant resonances	Bertrand, Kocher, Gross, Goodman, Auble	5
Atomic physics	Sellin, Mowatt, ^f Pegg, ^f Griffin, Haselton, ^f Peterson, ^f Laubert, ^f Datz, Thoe ^f	16
Backbending of rotational bands	Riedinger, ^f Stelson, Hensley, Robinson, Johnson, Sayer, Smith, Eichler	14
⁶ Li-induced reactions	H. Bingham, Halbert, Hensley, Goodman, Wharton, ⁱ Debevec ^j	21
Transplutonium chemistry	Silva, Peterson, ^f Tarrant, Dittner, Hunt, Case, Meyer, Niedhart ^k	
Heavy-ion transfer reactions	Ford, Toth, Hensley, Thornton, ^l Gross, Ball, Gustafson, ^l Riley, ^m Snell	6
Proportional-counter tests and miscellaneous experiments	Hensley, Gross, Hillis, ^f Stokstad, Snell	3
Spectroscopy of ⁹² Mo and ²⁰⁶ Pb	Scott, ^g Baker, ^g Wiggins ^g	2
Transfer-reaction studies with recoil nuclei	Hahn, Dittner, Toth, Hubert ^b	25
Properties of elements 104, 105, 106	Bemis, Silva, Hensley, Dittner, Keller, Hahn, Tarrant, Hunt	53
High-spin states in medium-mass nuclei	Robinson, Kim, Halbert, Wells, ⁿ Sayer, Rester, ^o Hamilton, ^h Ronningen	10
(p,t) Reactions of germanium isotopes	Rester, ^o Rao, ^o Rohrer, ^o Wood, ^o Auble	4
Deep inelastic scattering	Stokstad, Hensley, Halbert	18
Limits on fusion cross sections	Stokstad, Biggerstaff, Snell, Stelson	14
Search for short-lived isomers	Gross, Cleary, Hensley, Toth, Hungerford, ^p C. Bingham ^f	2
Multiplicity measurements	Sarantites, ^e Gronemeyer, ^e Barker, ^q Halbert, Eichler, Johnson, Hensley	4
Isospin nonconservation	Goodman, Hensley, Stokstad	4

^aUNISOR is a consortium of 12 universities, Oak Ridge National Laboratory, and Oak Ridge Associated Universities.

^bUniversity of Bordeaux, France.

^cUniversity of Kentucky, Lexington.

^dResearch Institute for Physics, Stockholm, Sweden.

^eWashington University, St. Louis, Mo.

^fUniversity of Tennessee, Knoxville.

^gUniversity of Georgia, Athens.

^hVanderbilt University, Nashville, Tenn.

ⁱRutgers University, New Brunswick, N.J.

^jArgonne National Laboratory, Argonne, Ill.

^kTechnische Hochschule, Darmstadt, Germany.

^lUniversity of Virginia, Charlottesville.

^mUniversity of Texas, Austin.

ⁿTennessee Technological University, Cookeville.

^oEmory University, Atlanta, Ga.

^pUniversity of Houston, Houston, Tex.

^qSt. Louis University, St. Louis, Mo.

Table 4.5. Analysis of ORIC beam use by type of particle

Particle	Energy (MeV)	Total hours assigned	Percent
Nuclear research			
Lithium	25--61	192	4.9
Boron	67--86	36	0.9
Carbon	41--180	527	13.4
Nitrogen	43--160	602	15.4
Oxygen	100--140	520	13.3
Neon	52--173	898	22.9
Aluminum	40--90	96	2.5
Argon	145--165	172	4.4
Nickel	76	32	0.8
Total, heavy-ion experiments		3075	78.5
Protons	30--61	96	2.4
Deuterons	23--40	96	2.4
³ He	70	40	1.0
Alphas	32--60	618	15.7
Total, light-ion experiments		850	21.5
Total, nuclear research experiments		3925	100.0
Machine research			
Heavy ions		248	96.9
Light ions		8	3.1
Total		256	100.0

that the radius of curvature does not change in a few gauss variation near 4×10^3 G. The main limitation of this method is the error associated with determining the peak intensity point of a broad energy spread. The better the resolution of the primary beam, the easier it is to determine the peak location. Within this limitation, the method appears to be a quick and easy way of obtaining an absolute calibration for heavy-ion beam-analysis systems.

1. Made by C. E. Bemis of the Chemistry Division using an isotope separator.

ORIC DATA-ACQUISITION SYSTEM DEVELOPMENT

D. C. Hensley

More than an order of magnitude improvement in throughput capability for data acquisition into large two-dimensional arrays has been achieved with the development of a quasi-listing program.

Many of the "two-dimensional" experiments at ORIC were increasingly restricted by the limited throughput

capability of the existing data-acquisition programs. These programs handled the necessary large two-dimensional arrays but had a maximum throughput capability of only ~ 400 events/sec. This capability decreased as the size of the array was increased or as the distribution of counts throughout the array became more random. More and more of our experiments required larger arrays with a more random distribution of counts and, at the same time, needed greater throughput capability.

A program has been developed which uses the excellent buffer I/O capability of disk storage units and which has achieved actual throughput rates of ~ 4 kHz (it has a theoretical capability for many cases of ~ 8 kHz). The conceptual form of the program is similar to that for the combined MEGASTRIP and PUSSE programs developed by W. T. Milner. Basically, the program does a presorting of all input data and lists them into an array on disk. When the list array fills, the program begins both to list into a second dedicated array and to update the experimenters' two-dimensional array from the first list array. Much effort has been expended to ensure that the use of all disk I/O activity and interrupts is optimized. The program is limited to 1 million channels by the size and capability of the present ORIC computer system, although the actual throughput capability of the program should be largely independent of the actual array size. As long as the input rate stays below the maximum throughput capability of the program, the front-end deadtime is scarcely affected by the overall computer activity.

Our charged-particle experiments now routinely handle event rates of 1 kHz into 500,000 channels, and gamma-ray multiplicity experiments use an event rate of 4 kHz into 128,000 channels. The program has been adapted to off-line processing of list-mode data stored on magnetic tape and may be extended to handle multiscaling of either charged particles or gamma rays.

DEVELOPMENT OF A GAS-JET-TO-TAPE TRANSPORT SYSTEM

H. K. Carter¹ E. H. Spejewski¹
 J. L. Wood² K. S. Toth
 R. L. Mlekodaj¹ R. J. Silva³

A helium gas-jet transport system⁴ has been used extensively for radioactive decay work at ORIC for several years. With expanded use it became apparent that the collection chamber needed to be redesigned to increase its flexibility and to make more efficient use of cyclotron time. Therefore, some means of automating sample collection and data acquisition needed to be

developed. To accomplish these objectives we have connected a copy of the original reaction chamber⁵ to the UNISOR tape transport system⁶ by a 1.3-mm-ID, 13-m Teflon capillary. The activity in the gas jet is deposited on the Mylar tape at the first port and can be moved to either of the other two detector stations. The configuration of the tape transport allows a much greater variety of experiments to be performed as well as allowing a second experiment to be set up while another is being run. The tape motion and data collection are controlled by the PDP-11-based data-acquisition system, thus providing full automation.

We have found the operating parameters of this system to compare favorably with the older (shorter capillary) system. It is quite easy to run at efficiencies (vis-à-vis a direct-catch measurement) of 20%. Standard cluster-generation techniques⁴ were used primarily. However, it appears that passing the helium over heated NH_4Cl increases the efficiency by about a factor of 2. The transport time has not been measured accurately; however, we detected a 3-sec activity but did not detect a 0.1-sec activity. To illustrate the usefulness of this system we have obtained excellent coincidence data in 2 to 4 hr on previously unstudied decay schemes far from the line of stability, for example, ^{189m}Au .

To be able to do alpha or electron spectroscopy it will be necessary to move the source from the high-pressure region into a vacuum region. We have tested an adaptation of a vacuum tape seal⁷ and found that less than 20% of the gas-jet-deposited activity is wiped off in passing through the seal. Work is continuing on this aspect of the problem.

1. UNISOR, Oak Ridge Associated Universities, Oak Ridge, Tenn.
2. Georgia Institute of Technology, Atlanta.
3. Chemistry Division.
4. W.-D. Schmidt-Ott and K. S. Toth, *Nucl. Instrum. Methods* **121**, 97 (1974).
5. K. S. Toth et al., *Phys. Rev. C* **2**, 1480 (1970).
6. H. K. Carter et al., *Phys. Div. Annu. Prog. Rep. Dec. 31, 1972*, ORNL-4844 (1973), p. 142.
7. H. K. Carter and R. L. Mlekodaj, *Nucl. Instrum. Methods* **128**, 611 (1975).

ORIC HARMONIC-BEAM SPACE-CHARGE EFFECT

M. L. Mallory K. N. Fischer E. D. Hudson

We have experimentally detected a heavy-ion beam loss when two harmonic beams are simultaneously accelerated from the ion source in ORIC. This loss is dependent upon the pressure in the cyclotron acceleration chamber. Two helium-cooled cryopanel were

installed in the ORIC magnet gap, resulting in lower pressure in the acceleration chamber. In beam-transmission experiments with helium-cooled cryopanel, an argon beam increased in intensity, as expected for the lower pressure. Therefore, use of the cryopanel was recommended for beams limited by accelerator intensity, such as O^{5+} .

The cryopanel were first used with an $^{18}\text{O}^{5+}$ beam during a two-week period in July 1974. A third week of running without the cryopanel followed, and the experimenter reported that operation with the cryopanel resulted in a decrease of the oxygen-beam intensity. In March 1975, a series of measurements was made of the oxygen-beam intensity with the cryopanel at room temperature and at 20°K which verified the difference. Results of these measurements are presented in Fig. 4.16. In Fig. 4.16, ORIC beam intensity is plotted as a function of the square of the radius from

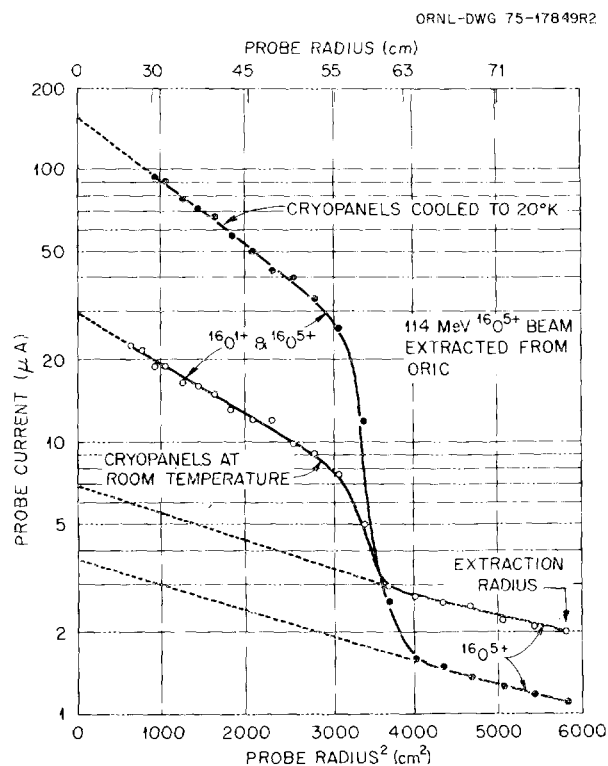


Fig. 4.16. The beam intensity vs probe position squared as measured from the center of ORIC for an extracted (first harmonic) $^{16}\text{O}^{5+}$ beam. The large step in the intensity at ~ 58 cm is identified as the maximum radius for the (fifth harmonic) $^{16}\text{O}^{1+}$ beam. The two curves were obtained for room-temperature and 20°K cryopanel (better vacuum) with the same operating conditions of the cyclotron and ion source. The intensity of the beam at 76 cm unexpectedly decreased for the better vacuum conditions. The dashed lines are projections of the $^{16}\text{O}^{5+}$ and $^{16}\text{O}^{1+}$ beams.

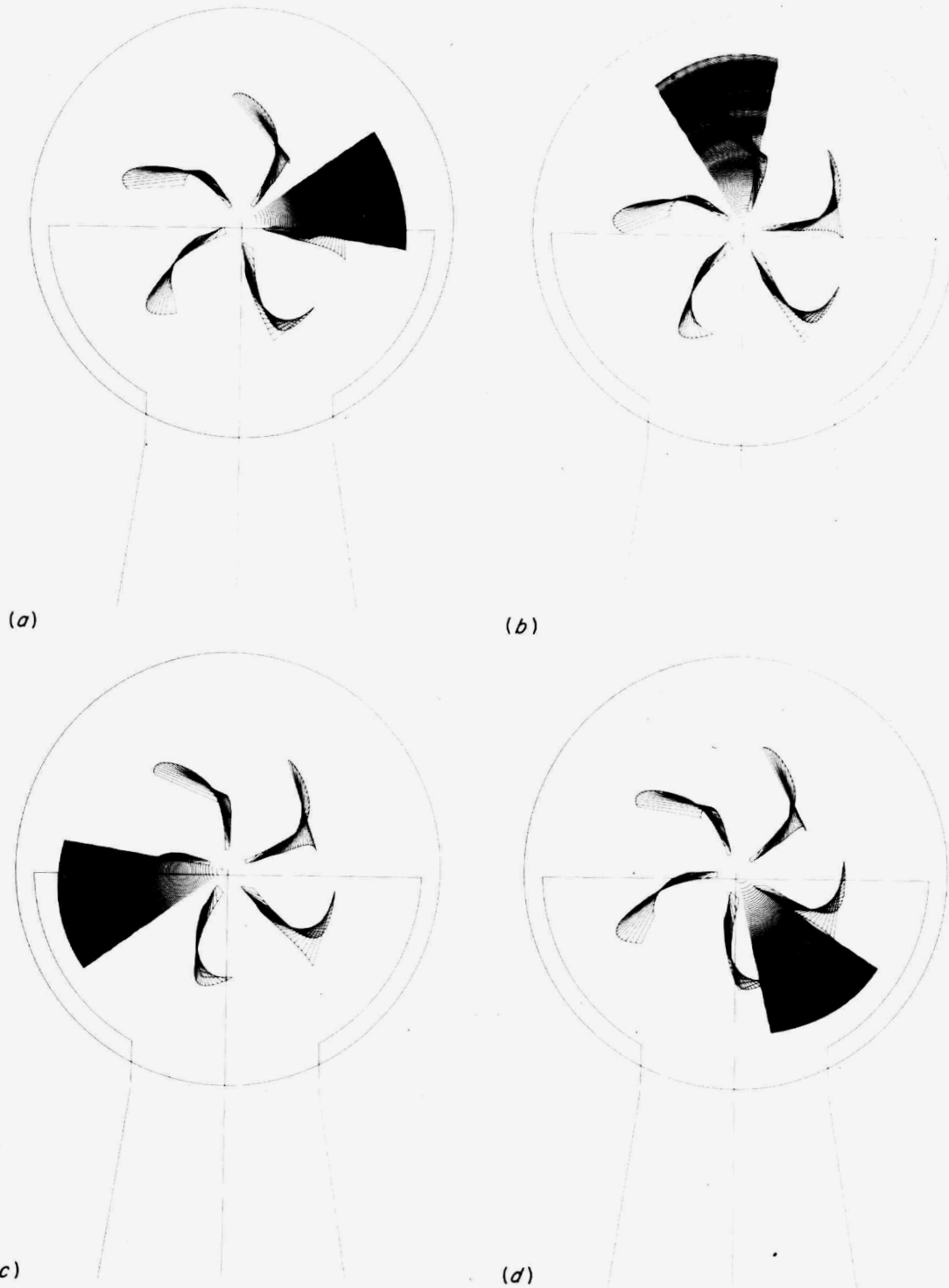


Fig. 4.17. The phase bursts for $^{16}\text{O}^{1+}$ and $^{16}\text{O}^{5+}$ for one complete rf oscillation are shown. Each figure is $\sim 1/4$ cycle from the preceding figure. The main significance is that the $^{16}\text{O}^{5+}$ phase bursts, which extend from 2.5- to 76-cm radius, pass through the five $^{16}\text{O}^{1+}$ phase bursts. This overlap between the $^{16}\text{O}^{1+}$ and $^{16}\text{O}^{5+}$ phase bursts results in a space-charge beam loss. The decelerating phase bursts of $^{16}\text{O}^{1+}$ have been deleted for clarity and are expected to contribute little to the space-charge loss because their intensity is reduced by self-space-charge and charge-transfer loss processes in the outgoing beam.

the cyclotron center both when the cryopanel are at 20°K and at room temperature. The beam intensity extracted from the cyclotron is directly proportional to the intensity measured at 76 cm and is less for the beam with the helium-cooled cryopanel. The other significant feature in Fig. 4.16 is the beam loss that occurs at ~58 cm; this is identified as the maximum radius for the harmonic beam $^{16}\text{O}^{1+}$. Figure 4.17a-d illustrates the computed phase-acceleration histories of $^{16}\text{O}^{1+}$ and $^{16}\text{O}^{5+}$ beam bursts for one rf cycle at intervals of $\sim 1/4$ rf cycle. The $^{16}\text{O}^{5+}$ beam (extending from 2.54 to 76 cm) was assumed to have an acceptance phase width of 48°. The five "buckets" of the accelerated beam of $^{16}\text{O}^{1+}$ are also shown. The significant feature of Fig. 4.17a-d is that the $^{16}\text{O}^{5+}$ beam bursts are passing through the high-intensity beam buckets of $^{16}\text{O}^{1+}$ as they are being accelerated to full radius. This is due to the difference in angular rotation frequency of $^{16}\text{O}^{5+}$ and $^{16}\text{O}^{1+}$.

For the harmonic-beam conditions described above, the axial force balance must be integrated over the time that the beams overlap in θ ; this is shown by

$$m_1 \frac{d^2 z_1}{dt_1^2} + m_1 \omega_1^2 \nu_{z_1}^2 z_1 - q_1 \int_{\theta_1=0}^{2\pi} E_{z_2} d\theta_1 = 0, \quad (1)$$

where the subscripts 1 and 2 refer to the different harmonic beams, m is the particle mass, ω is the angular rotation frequency, ν_z is the axial betatron frequency, z is the particle distance from the median plane, q is the particle charge, E_z is the beam-burst electric field, and θ is the particle azimuthal position in the cyclotron. The average beam current (I) limit for no focusing of the higher harmonic beam can be shown to be

$$I_2 = \frac{2\epsilon_0 \nu_{z_1}^2 z_1 V_2 \omega_1}{[h_2 - h_1]}, \quad (2)$$

where ϵ_0 is the dielectric constant of free space, V is the voltage gain per turn, and h is the harmonic number.

The results of Eq. (2) lead one to conclude that the space-charge force from high-intensity beams must be considered for beam losses of accompanying low-intensity harmonic beams.

Only a small number of ORIC beams are affected by space-charge forces. The principal beams thus affected are listed in Table 4.6.

The trajectories of $^{16}\text{O}^{1+}$ and $^{16}\text{O}^{5+}$ starting from the ion source are shown in Fig. 4.18. The $^{16}\text{O}^{5+}$ beam was started at an rf phase of 20°, dee voltage of 70 kV, and a magnetic field of 18.4 kG. The $^{16}\text{O}^{1+}$ starting phase was assumed to be 70°. The orbits do not continuously overlap, suggesting that a beam interceptor can be

Table 4.6. Simultaneously accelerated beams in ORIC

High-charge-state beam	h	Low-charge-state beam	h
$^6\text{Li}^{3+}$	1	$^6\text{Li}^{1+}$	3
$^{12}\text{C}^{5+}$	1	$^{12}\text{C}^{1+}$	5
$^{12}\text{C}^{6+}$	1	$^{12}\text{C}^{2+}$	3
$^{14}\text{N}^{5+}$	1	$^{14}\text{N}^{1+}$	5
$^{16}\text{O}^{5+}$	1	$^{16}\text{O}^{1+}$	5
$^{16}\text{O}^{6+}$	1	$^{16}\text{O}^{2+}$	3
$^{18}\text{O}^{5+}$	1	$^{18}\text{O}^{1+}$	5
$^{19}\text{F}^{6+}$	1	$^{19}\text{F}^{2+}$	3
$^{20}\text{Ne}^{6+}$	1	$^{20}\text{Ne}^{2+}$	3

ORNL-DWG 75-17847

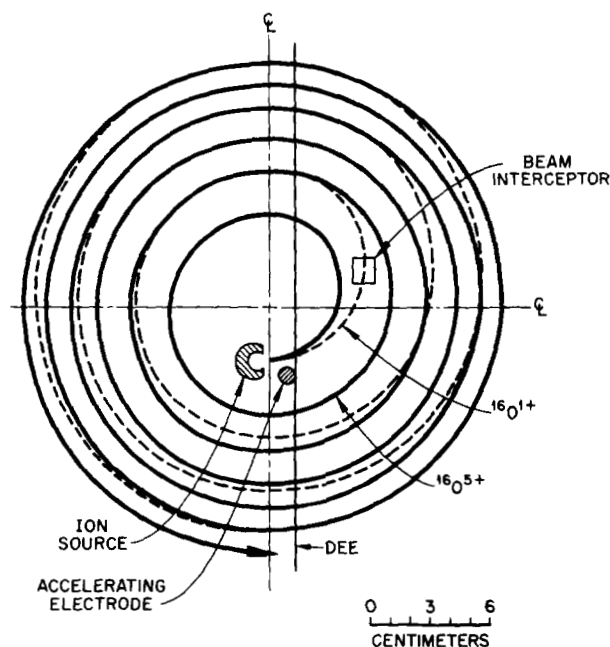


Fig. 4.18. The central-region orbit trajectories of $^{16}\text{O}^{1+}$ and $^{16}\text{O}^{5+}$ starting from the ion source. The starting phases are 70° and 20° for $^{16}\text{O}^{1+}$ and $^{16}\text{O}^{5+}$ respectively. An ideal location for a low-charge beam interceptor is shown in the dee. Its position should be variable for the different mass beams and cyclotron settings.

installed so that the undesirable harmonic beam can be dumped. An ideal location for the beam interceptor is indicated in Fig. 4.18.

ION-SOURCE-DEVELOPMENT PROGRAM

NEGATIVE-ION-SOURCE TEST FACILITY

G. D. Alton

The negative-ion-source test facility, previously described,¹ has operated almost flawlessly since startup

and is presently being used to test and evaluate a new negative-ion source based on the sputtering principle^{2,3} and to study the negative surface ionization of heavy molecular ions such as UF_6 by heated platinum metal. All aspects of the facility have met expectations — including the special compression lens employed to maximize the beam transmission through the limited direction of the magnet chamber (1.59 cm, acceptance $\sim 14\pi$ cm·milliradians). The effect of the lens on the ion beam improves the transmission through the system by a factor of ~ 2 . Preliminary measurements for low-atomic-weight ions such as carbon indicate a transmission efficiency of $\sim 90\%$. However, it is expected that the efficiency will be somewhat lower for heavier ions. During the next calendar year, the facility will be used principally for negative-ion-source development, and an effort will be made to incorporate additional ion-source diagnostic equipment such as emittance-measuring and energy-analyzing devices.

1. G. D. Alton et al., *Phys. Div. Annu. Prog. Rep. Dec. 31, 1974*, ORNL-5025 (1975), p. 194.

2. G. D. Alton, *IEEE Trans. Nucl. Sci. NS-23*, 223 (1976).

3. See this report, G. D. Alton, "Preliminary Evaluation of Mueller-Hortig Geometry Negative-Ion Source."

NEGATIVE-ION-SOURCE DEVELOPMENT

G. D. Alton

The Middleton-Adams Sputter Source¹

As indicated in last year's report,² several major difficulties were experienced with the vendor-supplied sputter source which seriously affected its performance. Almost without exception, the difficulties were associated with the surface ionization source; consequently, the source was totally redesigned (Fig. 4.19) in an effort to eliminate or reduce the problems. The previously reported modifications² were incorporated in the design and have since been thoroughly evaluated.

The ionizer and vacuum-seal designs have worked perfectly without failure or vacuum leaks during the past calendar year. During this period, a single ionizer has been employed, and it is still in use. Although the ionizer heater-assembly modifications (described earlier²) reduced the number of heater failures due to burnout and mechanical breakage, the burnout problem persisted even after redesign. Another heater-assembly design has been incorporated which has proved to be more reliable and less expensive. The new design has virtually eliminated the heater element problem.

The heating elements are now wound at our laboratory from molybdenum or tungsten wire in the form of

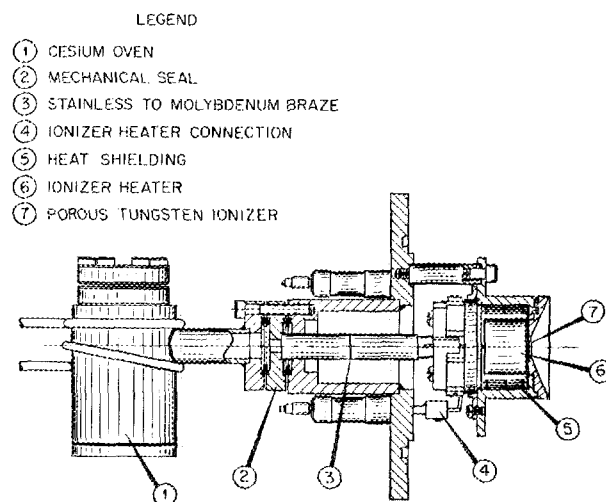


Fig. 4.19. The ORNL surface ionization source.

a spiral. Molybdenum is preferred because of crystallization problems that occur whenever tungsten is heated to high temperatures. After winding, the element is uniformly coated with aluminum oxide to provide electrical insulation. Since incorporation of this design, only one heater has been burned out and that because of overdriving with the power supply. The cost of a heating element has been reduced by a factor of ~ 5 over those commercially procured.

By incorporating the indicated modifications, the original problems associated with the Middleton-Adams source¹ have been eliminated, and the source now operates very stably over periods of time approaching 1000 hr between major cleaning operations.

Charge-Exchange Source

The problem of a continuous instability in the charge-exchange source was diagnosed. The instability was produced by the incorrect polarity of the einzel-lens coolant lines with respect to their surrounding electrostatic shield. A Penning ionization gage (PIG) configuration resulted which led to periodic loading and unloading of the lens and negative-ion-extraction power supplies. The problem was eliminated by feeding the coolant lines through the vacuum housing at another point.

Coolant was added to the magnet of the duoplasmatron, allowing the use of solid wire tantalum filaments instead of the conventional oxide-coated platinum gauze. The length of uninterrupted run time has been increased to more than one week and the anode lifetime has been increased by several times as a direct conse-

quence of the added coolant. The mass spectrum emitted by the source is also much cleaner with the solid wire filament than it is with the oxide-coated filament.

These improvements have led to significantly more stable operation and longer lifetime for the charge-exchange source.

1. R. Middleton and C. T. Adams, *Nucl. Instrum. Methods* **118**, 329 (1974).

2. G. D. Alton, *Phys. Div. Annu. Prog. Rep. Dec. 31, 1974*, ORNL-5025 (1975), p. 194.

PRELIMINARY EVALUATION OF MUELLER-HORTIG GEOMETRY NEGATIVE-ION SOURCE

G. D. Alton

Introduction

Since the discovery by Krohn,¹ in 1962, that yields of negative ions are greatly enhanced by sputtering in the presence of alkali metals, several negative-ion sources utilizing this principle have been developed.²⁻⁶ In recent months, a sputter source based on the Mueller-Hortig source has been designed and is presently being developed at ORNL at the negative-ion-source test facility.⁷

The original ion source of Mueller and Hortig clearly demonstrated the wide range of ions and high-intensity capabilities of a source that incorporates simultaneous sputtering and cesium surface activation. However, the design, although possessing the same potential, lacked the flexibility, versatility, and long lifetime demonstrated by the later Middleton-Adams source.³ The source geometry, however, has the following desirable aspects:

1. Negative ions are generated over a planar area, permitting the design of an ion-extraction system with good optical properties.
2. Quantitatively one can argue that the emittance may be lower than the conventional conical geometry because of the direction with which the particles leave the sample surface with respect to the extraction direction.

The important features of a modified Mueller-Hortig source recently designed and constructed at ORNL are described below.

Description of the Source

The ion source, shown schematically in Fig. 4.20, utilizes the surface ionization source⁸ to produce a 1- to 8-mA beam of Cs⁺ ions. The ions are accelerated to energies between 20 and 30 keV and focused onto the sample surface by an einzel lens which will be described later. The incorporation of the surface ionization source extends the source lifetime to >500 hr.

The einzel lens used to focus the ion beam onto the sample surface is designed to compress the beam more strongly in the horizontal than in the vertical direction to partially compensate for the oblique angle of incidence (10°) and to produce a more circular beam image as viewed along the negative-ion-extraction axis. Observation of the wear and deposits patterns on the negative-ion-extraction electrodes indicates that the shape is almost circular.

The sample wheel contains 18 samples in a circular arrangement around the wheel; a particular sample may be selected by indexing into the beam position. The sample wheel may also be moved in and out to compensate for misalignment or beam steering by the positive-ion lens. The results given here were obtained without coolant on the wheel, which may affect the negative-ion yields; the coolant will be added later to evaluate the effect.

A gridded electrode, biased 1.5 kV positive with respect to the generation surface, is used initially to accelerate the negative-ion beam. The ions are then further accelerated by the anode electrode at housing potential. The special einzel lens and negative-ion-extraction systems were designed by using the Herrmannsfeldt computer code.⁹

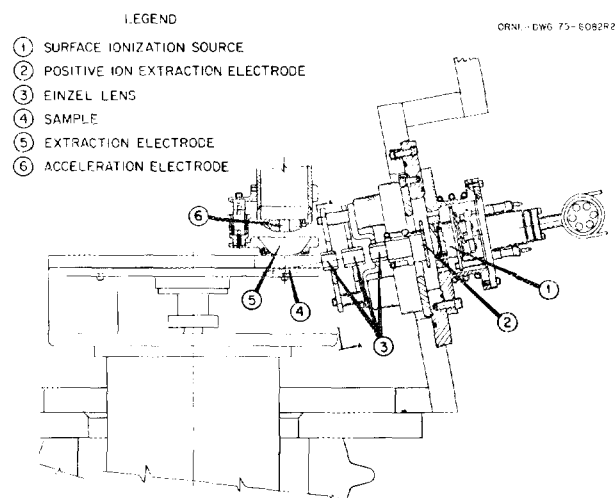


Fig. 4.20. The ORNL negative sputter source.

Source Operation

The source has thus far exhibited excellent operational characteristics. The surface ionizer is heated to $\sim 1100^{\circ}\text{C}$ by an annular cylindrical heater that surrounds the ionizer; the cesium oven is operated typically at $\sim 230^{\circ}\text{C}$. The dependence of the negative-ion yield on positive-ion lens voltage is shown in Fig. 4.21. As anticipated, the current is strongly dependent on how well the beam is focused on the sample surface.

Negative-Ion Yields

A partial list of the negative-ion species that have been produced to date is shown in Table 4.7. The source is seen to be a good producer of many elemental and molecular ions and is an excellent producer of ions from high-electron-affinity, high-vapor-pressure materials.

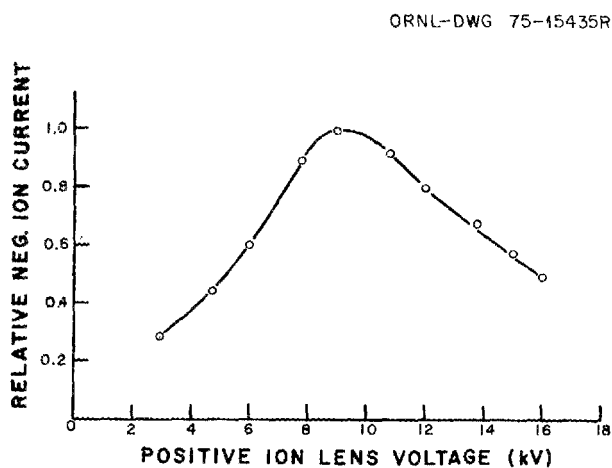


Fig. 4.21. Dependence of the negative-ion yield on positive-ion lens voltage.

The source is equipped with a gas feed system from which high-vapor-pressure materials can be fed. The sample surface, onto which the material is fed, may be selected by the indexing mechanism. The effect of the sample surface on the generation rates of several ions is shown in Table 4.8. The yield of a particular negative ion is seen to be dependent on the chemical properties of the sample surface.

Discussion

The results just described are preliminary, and during the next calendar year the source will be evaluated further. In particular, attempts will be made to maximize the negative-ion yields by incorporation of coolant on the sample wheel and investigation of the effects produced by using an oven for vaporizing additional surface cesium. With the incorporation of these features, along with the optimization of the negative-ion-

Table 4.7. Partial list of negative ions generated in the ORNL sputter source

Ion	Ion current (μA)	Ion	Ion current (μA)
Al^-	0.2	I^-	26
AlO^-	3	Ni^-	~ 0.2
Ag^-	0.250	NiO^-	~ 0.3
Ag^- ^a	1.2	Pb^-	0.03
Au^-	6	PbO_2^-	0.48
C^-	25	Pt^-	3.0
C_2^-	20	S^-	44
Cl^-	100	Ta^-	0.03
Cu^-	0.5	TaO_2^-	2.0
CuO^-	0.8	TaO_3^-	0.6
F^-	40	Ti^-	0.04
Fe^-	0.1	TiO^-	0.200
FeO^-	0.8	TiO_2^-	0.07

^aSintered silver powder saturated with cesium.

Table 4.8. Influence of the positive-ion impact surface on the rate of negative-ion generation

Ion species	Feed material	Ion current (μA) from ion generation surface of --										
		Al	Ag	Au	C	Cu	Fe	Ni	Pb	Ta	Ti	Pt
Cl^-	CCl_4	100	57	24	27	40	40	30	11	42	40	14
F^-	SF_6	25	6	5	8.5	15	17	12	9	35	40	3
I^-	CH_3I	26	7	4.8	16	13	13	15	10	4	23	9
O^-	O_2	30	1.5	3.5	7	7	20	15	3	10	20	1
S^-	CS_2	44	4.7	2.3	20	16	19	13	2.1	18	35	3.4

extraction system, the source is expected to reach maximum potential.

1. V. E. Krohn, *J. Appl. Phys.* **33**, 3523 (1962).
2. M. Mueller and G. Hortig, *IEEE Trans. Nucl. Sci.* **NS-16**, 38 (1969).
3. R. Middleton and C. T. Adams, *Nucl. Instrum. Methods* **118**, 329 (1974).
4. P. Tykesson, H. H. Andersen, and J. Heinemeier, *IEEE Trans. Nucl. Sci.* **NS-23(2)** (1976).
5. K. R. Chapman, *IEEE Trans. Nucl. Sci.* **NS-23(2)** (1976).
6. H. V. Smith, Jr., and H. T. Richards, *Nucl. Instrum. Methods* **125**, 497 (1975).
7. G. D. Alton, *IEEE Trans. Nucl. Sci.* **NS-23(2)** (1976).
8. See this report, G. D. Alton, "Negative-Ion-Source Development."
9. W. B. Herrmannsfeldt, SLAC report 166, Stanford University, Stanford, Calif., 1973.

VAN DE GRAAFF LABORATORY

TANDEM VAN DE GRAAFF OPERATIONS

G. D. Alton	J. W. Johnson
R. P. Cumby	E. G. Richardson
J.L.C. Ford, Jr.	N. F. Ziegler

The research activities on the tandem for the year 1975, together with the principal ions accelerated and approximate beam-time utilization for each activity, are listed in Table 4.9. The research time was equally divided between nuclear physics research and atomic physics or solid-state research. The experimental program on the accelerator is largely devoted to heavy-ion research.

Finances have made it necessary to limit the operations of the tandem. From January until May the accelerator ran half time (one week on, one week off). Since May, however, the scheduled operation of the machine has been increased to about two-thirds of the available time. Despite these restrictions, the accelerator was used for approximately 4000 hr of research time (including hours between 4:30 PM and 8:00 AM and on weekends, during which the research groups operated the machine).

Difficulties with the ion sources required an amount of time equal to about 10% of the total research hours. Most of this lost time was in the first part of the year and was due to sparking in the charge-exchange source. However, this problem was solved by relocating the high-voltage feedthrough for the first einzel lens of the source. Since that time both the charge-exchange duoplasmatron and Middleton-type sputter source have given routine and reliable operation.

The principal downtimes of the Van de Graaff accelerator itself were three days required to replace resistors and springs in the column and four days to replace the drive motor and terminal alternator. The actual failure in the second downtime was in the bearing of the terminal alternator, but both it and the drive motor were replaced because both had operated for a total of 11,810 hr. They had been installed in October 1972 and were replaced in December 1975.

The atomic physics and solid-state physics programs on the tandem are expected to increase in the future. These efforts will probably require new beam lines dedicated to new and specialized instruments for the anticipated research. Furthermore, these atomic physics and solid-state physics applications, as well as the heavy-ion nuclear research, will require an improved high vacuum from the high-energy end of the accelerator tank out to the experimental stations. The necessary improvements to the existing beam lines and additional beam lines are being planned.

CN VAN DE GRAAFF OPERATIONS

F. K. McGowan	G. F. Wells
M. B. Lewis ¹	F. A. DiCarlo
M. J. Saltmarsh	R. P. Cumby ²
C. H. Johnson	Martha Inman
N. H. Packan ¹	

The 5.5-MV accelerator is now used routinely for heavy-ion-induced radiation-damage studies³ by the Radiation Effects Group of the Metals and Ceramics Division. During CY 1975, the 4-MeV ⁵⁸Ni ion beam was used to irradiate 140 samples requiring 356 hr of ion beam on target. The heavy-ion-induced radiation damage ranged from 1 to 350 dpa per sample. The average irradiation per sample corresponded to a dose of 90 dpa, which, on the average, was produced at a rate of 35 dpa/hr (70 dpa is equivalent to a fluence $\sim 10^{23}$ neutrons/cm²). In the present arrangement of the radiation-damage facility, the effective sample area, produced by the 10- by 10-mm beam defining aperture upstream from the damage chamber, is 1.11 cm². Therefore, a dose of 1 dpa requires 300 μ C of ⁵⁸Ni²⁺ ions incident on target, and the average rate of 35 dpa/hr corresponds to 3.0 μ A of 2+ ions spread uniformly over the 10- by 10-mm aperture. Several samples have been irradiated at a dose rate of 50 dpa/hr (4.2 μ A of 2+ ions).

The Danfysik ion source was refurbished 18 times during 1975. With an initial charge of 200 mg of ⁵⁸Ni in the ion source, the average useful lifetime is about 80 hr when operating with a normal beam of 1.5 particle-

Table 4.9. Research activities on the tandem Van de Graaff accelerator

Type	Projectile	Investigators	Approximate percent of utilized beam time
Atomic physics	$p, {}^{12}\text{C}, {}^{16}\text{O}, {}^{19}\text{F}, {}^{27}\text{Al}, {}^{28}\text{Si}, {}^{35}\text{Cl}, {}^{48}\text{Ti}, {}^{56}\text{Fe}$	Sellin, ^a Elston, ^a Pegg, ^a Thoe, ^a Peterson, ^a Hayden, ^b Griffin, Forester, ^a Laubert ^c	12
Atomic collisions in solids	${}^{12}\text{C}, {}^{14}\text{N}, {}^{16}\text{O}, {}^{63}\text{Cu}, {}^{127}\text{I}$	Datz, Biggerstaff, Miller, Verbeck, ^d Appleton, ^e Noggle, ^e Dittner, ^f Gomez del Campo ^g	12
Enge-magnet heavy-ion reaction studies	${}^{10}\text{B}, {}^{15}\text{N}, {}^{16}\text{O}$	Ford, Gomez del Campo, ^g Miller, Stelson, Robinson, Thornton ^h	12
Coulomb excitation	$\alpha, {}^{16}\text{O}$	Milner, Robinson, Stelson, Raman, Dagenhart, ⁱ Tuttle ^a	10
X-ray studies	${}^{10}\text{B}, {}^{12}\text{C}, {}^{14}\text{N}$	Duggan, ^j Chaturvedi, ^k Gray, ^k Kauffman, ^l Pepper, ^j Light, ^j E. Robinson, ^m Miller, McCoy, ⁿ Carlton, ^o Alton	10
Beam-foil spectroscopy	${}^{28}\text{Si}, {}^{56}\text{Fe}, {}^{63}\text{Cu}$	Bashkin, ^p Jones, ^q Pisano, ^q Sellin, ^a Pegg, ^a Griffin	9
Coulomb excitation and lifetime measurements	$\alpha, {}^{16}\text{O}$	Hamilton, ^r Ronningen, ^r Garcia-Bernmudez, ^r Ramayya, ^r Riedinger, ^a Sayer	7
In-beam gamma-ray studies	${}^6, {}^7\text{Li}, {}^{12}\text{C}$	Robinson, Sayer, Smith, ^s Milner, Lin, ^t Wells, ^t Hamilton, ^r Ronningen, ^r Ramayya ^r	7
Heavy-ion-produced neutron cross sections	${}^{12}, {}^{13}\text{C}, {}^{16}\text{O}$	Bair, Stelson, Miller	7
(${}^{15}\text{N}, \alpha$) reaction	${}^{15}\text{N}$	Gomez del Campo, ^g Andrade, ^g Dacal, ^g Ortiz, ^g Ford	4
High-charge-state stripping studies	${}^{56}\text{Fe}, {}^{127}\text{I}$	Miller, Biggerstaff, Alton, Jones, Kessel, ^b Bridwell, ^u Wehring ^v	4
Fission	${}^{35}\text{Cl}, {}^{81}\text{Br}, {}^{127}\text{I}$	Pleasanton, Ferguson, ^f Obenshain, Snell, Hubert ^w	4
Oxygen diffusion in Zircaloy	p	Saltmarsh, Bertrand, Perkins ^x	4
Radiation damage studies	p	Chen, ^e Abraham ^e	1

^aUniversity of Tennessee, Knoxville.^bUniversity of Connecticut, Storrs.^cNew York University, New York City.^dMax-Planck-Institut für Plasmaphysik, Garching, Germany.^eSolid State Division.^fChemistry Division.^gUniversity of Mexico, Mexico City.^hUniversity of Virginia, Charlottesville.ⁱIsotopes Division.^jNorth Texas State University, Denton.^kState University of New York College at Cortland.^lKansas State University of Agriculture and Applied Science, Manhattan.^mUniversity of Alabama, Tuscaloosa.ⁿUniversity of Tulsa, Tulsa, Okla.^oMiddle Tennessee State University, Murfreesboro.^pUniversity of Arizona, Tucson.^qBrookhaven National Laboratory, Upton, N.Y.^rVanderbilt University, Nashville, Tenn.^sORAU Postdoctoral Fellow, Oak Ridge, Tenn.^tTennessee Technological University, Cookeville.^uMurray State University, Murray, Ky.^vUniversity of Illinois, Urbana.^wCentre d'Études Nucléaires de Bordeaux-Gradignan, France.^xMetals and Ceramics Division.

μA on target (during 1450 hr of operation the lifetimes have ranged between 60 and 113 hr). A summary of the use of the ^{58}Ni ion beam is given in Table 4.10. Approximately one-third of the beam time is not used effectively while loading and removing samples from the present radiation-damage chamber. With the implementation of the new radiation-damage chamber, 50% use of the beam time for irradiation of samples should be achieved easily.

In addition to irradiation of samples, a major part of the year has been devoted to (1) developing a monitoring system to measure both the on-line intensity and uniformity of the heavy-ion beam and (2) preparations for upgrading the performance of the terminal. The heavy-ion beam requirements for radiation-damage bombardments are rather severe; a large area of 1 cm^2 must be uniformly irradiated without rastering and with large intensity. This is accomplished with a ring lens⁴ which focuses the positive-ion beam onto the 10- by 10-mm entrance aperture to the radiation-damage target chamber. A beam profilometer (Physicon model MS-10), located between the aperture and target chamber, scans the beam at a rate of 10 Hz with two vanes sweeping nearly parallel to the X and Y axis respectively. A block diagram of the monitoring system is shown in Fig. 4.22. The current loop to the digitizer is calibrated and checked periodically by replacing the target assembly with a Faraday cup.

The profilometer output signals are also monitored by oscilloscope displays and a signal-averager analyzer to

Table 4.10. Use of the ^{58}Ni ion beam in 1975

Activity	Total hours	Percent
Irradiation of 140 samples (12,545 dpa or 35 dpa/hr)	356	25
Loading and removing samples from damage chamber (~3.5 hr per sample)	488	35
Calibration of beam profile monitor to provide the total ion flux incident on the target (~100 calibrations)	190	13
Microaperture scan of the beam profile at the target position	30	2
Accelerator startup time and preparation of the ion beam for an irradiation (1 hr per sample)	140	10
Startup time after refurbishing the ion source (12 hr)	216	15
Total	1420	100

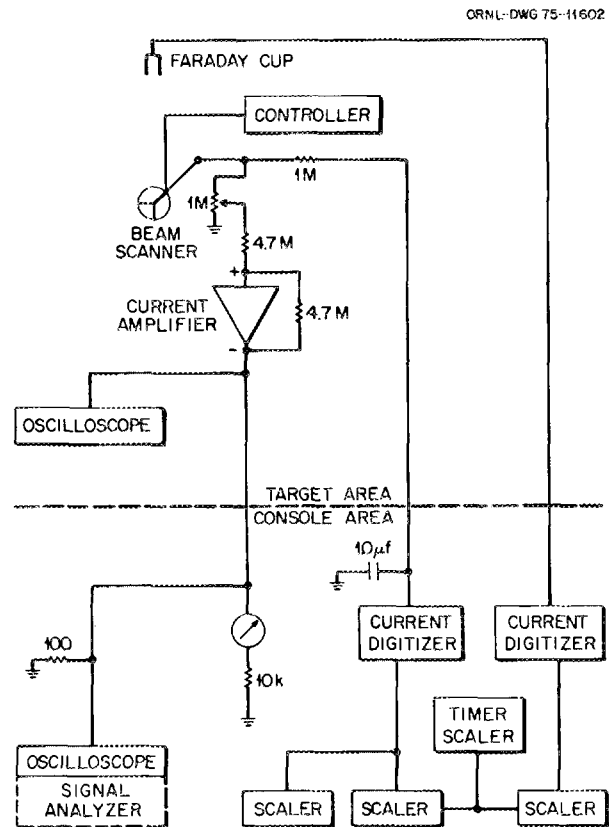


Fig. 4.22. Block diagram of heavy-ion beam monitoring system.

assist the Van de Graaff operator in preparing a uniform beam profile at the target, that is, adjustment of extractor, einzel lens, crossed-field analyzer, gap lens, beam steering, and ring lens. The usual oscilloscope display of the beam profile is not ideal because plasma oscillations in the ion source give rise to small oscillations on each observed profile. The oscilloscope display associated with the signal averager solves this problem by time averaging. Therefore, the signal averager provides more detail of the beam profile for the operator. The signal-averager analyzer also provides the experimenter with a digitized accumulation of the scans of the beam profile for an irradiation.

A second beam profilometer is located upstream of the ring lens. This profilometer display assists the operator in preparing an ion beam emanating from the crossover, formed near the focal point of the 90° analyzing magnet, with axial symmetry and with approximately Gaussian divergence.

1. Metals and Ceramics Division.
2. Instrumentation and Controls Division.

3. M. B. Lewis et al., p. 15 in *Proceedings of a Symposium on Experimental Methods for Charged-Particle Irradiations, Gatlinburg, Tenn., Sept. 30, 1975*, CONF 75-0947, ERDA Technical Information Center, Oak Ridge, Tenn., 1975.

4. C. H. Johnson, *Nucl. Instrum. Methods* **127**, 163 (1975).

OAK RIDGE ELECTRON LINEAR ACCELERATOR

J. A. Harvey¹ T. A. Lewis²
H. A. Todd² J. G. Craven³

The Oak Ridge Electron Linear Accelerator (ORELA) was operated for neutron experiments for 5138 hr during 1975. Operation was reduced from six days per

week to five days per week in May and to a conservative manner to reduce operating expenses. At high powers (>40 kW) the electron beam is swept vertically to decrease local heating and the possibility of burning out the tantalum targets. A larger heat exchanger was added to the target cooling-water system to allow the target to dissipate 75 kW average power while keeping the cooling-water temperature below 100°C.

The research activities at ORELA in 1975 are listed in Table 4.11. Because experiments can be operated on several flight paths simultaneously the total number of experimenter hours shown for the various activities is much larger than the 5138 hr of accelerator operation.

Table 4.11. Neutron experiments performed at ORELA in 1975

Type of experiment	Elements, isotopes, etc.	Neutron energies (min, max)	Experimenters	Beam time (hr)
Total cross sections	C, F, Na, Mg, Fe, Cu, V, ^{6,7} Li, ⁵⁸ Fe, ^{58,59,60,61,62,64} Ni, ^{63,65} Cu, ^{64,66,67,68,70} Zn, ¹⁰⁰ Mo, ²⁰⁸ Pb, ^{233,238} U, ²⁴⁰ Pu, ²⁴⁹ Bk	0.005 eV, 40 MeV	Auchampaugh, ^a Benjamin, ^b Fowler, Garg, ^c Gwin, Harvey, Hill, Ingle, Johnson, Larson, le Rigoleur, ^d Olsen, Perey, Perez, Raman, Todd, Weigmann ^e	4,200
Capture cross sections	Mg, Cr, Fe, Zr, Mo, ^{54,56,57} Fe, ²⁸ Si, ^{58,59,60} Ni, ¹⁴⁰ Ce, ²³² Th, ²³⁵ U, ^{240,242} Pu, ²⁴¹ Am	0.01 eV, 2 MeV	Allen, ^f deSaussure, Earle, ^g Garg, ^c Hill, Halperin, le Rigoleur, ^d Macklin, Pandey, ^c Perey, Perez, Todd, Weigmann, ^e Weston, Winters ^h	2,300
Fission cross sections	²³² Th, ^{235,238} U, ^{239,240} Pu, ^{243,245} Cm	0.01 eV, 14 MeV	Dabbs, deSaussure, Difilippo, ⁱ Felvinci, ^j Gwin, Hill, Ingle, Luers, ^j Melkonian, ^j Perez, Raman, Todd, Weston	3,400
(n,γ) spectra	V, Ta, Au, ¹⁰⁰ Mo, ^{118,122,124} Sn, ¹⁴⁴ Nd, ¹⁷³ Yb, ^{206,207} Pb	0.4 eV, 20 MeV	Carlton, ^k Chapman, Gwin, Hill, Ingle, McClure, ^l Morgan, Newman, Raman, Slaughter, Weigmann, ^e Wells ^m	5,200
Other experiments	(n,xγ), V, Cr, Nb, Mo, Au; ⁵⁹ Ni(n,α), (p), ²³⁵ U, ²³⁹ Pu, ²⁵² Cf; integral neutron scattering, Al, SiO ₂ ; fission chamber efficiencies, ^{235,238} U, ²⁵² Cf; neutron flux measurements; response, NE-213; calibrations, Fe, Ta	0.01 eV, 20 MeV	Chapman, Gwin, Halperin, Harvey, Hill, Ingle, Morgan, Newman, Raman, Spencer, Todd, Weston	4,200
				19,300

^aLos Alamos Scientific Laboratory, Los Alamos, N.M.

^bSavannah River Laboratory, Aiken, S.C.

^cState University of New York College at Cortland.

^dCentre d'Études Nucléaires, Bruyere-le-Chatel, France.

^eBureau Central de Mesures d'Nucléaires, Geel, Belgium.

^fAustralian Atomic Energy Commission, Lucas Heights, Australia.

^gChalk River Nuclear Laboratories, Chalk River, Ontario, Canada.

^hDenison University, Granville, Ohio.

ⁱComision Nacional de Energia Atomica, Argentina.

^jColumbia University, New York City.

^kMiddle Tennessee State University, Murfreesboro.

^lGeorgia Institute of Technology, Atlanta.

^mTennessee Technological University, Cookeville.

During the year another flight path was instrumented with collimators, a shadow bar, a vacuum valve, and a beam stop to accommodate experimenters from the Solid State Division and various outside users.

The program for greatly improving the performance of ORELA for short-pulse (3 to 5 nsec) operation (by velocity modulation with time-dependent voltage gaps and drift/spacers) is progressing favorably within the constraints imposed by the limited manpower and funds available. Calculations have been made by R. G. Alsmiller, Jr., F. S. Alsmiller, and J. Barrish of the Neutron Physics Division and are favorable for a one-dimensional approximation model. These calculations are being expanded to more dimensions to better determine the magnetic field and gap-field effects. The tests of certain critical items of hardware being conducted by D. W. Bible, T. A. Lewis, and J. H. Todd are progressing favorably and are sufficiently far along to anticipate the completion of all necessary prototype systems within the next year.

More memory has been approved for the three SEL data-acquisition computers to enable each system to handle four simultaneous experiments. Increased functions of the system during data taking had resulted in insufficient core to perform tasks at the required time

when four experiments were running. A 1.5-million-word removable disk has been added to the peripheral-equipment controller (PEC) to be used by the PEC and connecting computers. On the PEC the disk will be used for storage of programs, local spooling of data to the line printer or Calcomp, and storage of local collected data for display and manipulations.

A PDP-15 display has been connected to the PEC, and an operating system has been written using the PEC disk. Programs and data files can easily be transferred between the PEC and PDP-10 disk. In addition to providing many features of the PDP-10/PDP-15 display system, the PEC/PDP-15 display system has a fast scan capability of data stored on the PEC disk. The PDP-15 displays are being modified to allow the central PDP-10 computer to control the display teletype as a normal time-sharing teletype. This modification increases teletype transmission from 800 to 1200 baud and eliminates all known problems that result in terminal hangups.

-
1. Co-Director of ORELA (with R. W. Peelle, Neutron Physics Division).
 2. Instrumentation and Controls Division.
 3. Computer Sciences Division.

5. Theoretical Physics

INTRODUCTION

G. R. Satchler

The year 1975 saw the nuclear theory efforts dominated by heavy-ion physics. Some exciting advances have been made in developing theoretical and computational tools for handling the complex problems posed by the collision of two nuclei. From studying these we hope to learn about the more general problem of large-amplitude collective motions of a quantal fluid. At one level (the "macroscopic" one), we regard the collision as a problem in fluid dynamics, the collision of two fluid drops. At another level (the "microscopic" one), we attempt to understand the process in terms of the motions of the individual nucleons and their forces; time-dependent Hartree-Fock theory is the tool here. At the same time, theoretical links are being forged between the microscopic and macroscopic levels. In the high-energy limit, where the individual nucleon motions are all-important, a classical approximation is also being studied, rather like the collision of two clusters of billiard balls. In addition to these new ventures, work continues on more conventional nuclear reaction and structure models, in close collaboration with the experimental effort at ORNL. One common theme runs through all these projects: the need for sophisticated and expensive computational machinery. Only through its use can the phenomena of interest be studied.

As the lists of authors of the various contributions testify, we continue to enjoy valuable collaboration and interaction with other nuclear theorists from many institutions outside ORNL. (In addition to numerous informal visits, a very productive four-day workshop on time-dependent Hartree-Fock theory was held in December.) Locally, we have seven staff members (of whom J. B. McGrory has been on loan to the Long-Range Planning Group since September 1, 1975) and two temporary appointees. In addition, we have benefited from two guest assignees, V. Maruhn-Rezwani and, since August, H. Feldmeier.

MACROSCOPIC NUCLEAR DYNAMICS AND HEAVY-ION COLLISIONS

J. J. Griffin ¹	J. A. Maruhn
J. A. McDonald ²	C. G. Trahern ³
T. A. Welton	C. Y. Wong

In the discussion of nuclear phenomena, it is convenient to introduce the concept of a nuclear fluid and to treat finite nuclei as small quantities of it. The dynamics of this fluid are then described by the time variations of the density field $n(\mathbf{r}, t)$, the velocity field

$\mathbf{u}(\mathbf{r}, t)$, and the entropy field $\sigma(\mathbf{r}, t)$. Our knowledge of the static and dynamic properties of the fluid is as yet incomplete. (For example, although its equilibrium density is known, its compressibility is uncertain. The novel capabilities of the new heavy-ion accelerators may lead to the systematic elucidation of these fluid properties.) In focusing our attention on a macroscopic description we hope to learn about the bulk properties of the nuclear fluid so as to enhance our understanding of complex nuclear phenomena. Furthermore, a macroscopic description is appropriate for the collisions of

heavy nuclei, where the complexity of the problem as yet precludes a fully microscopic description. Even though three-dimensional time-dependent Hartree-Fock (TDHF) calculations are possible, the assumptions required to make such a treatment feasible may preclude any dependable description of real nuclei. It is then quite possible that a theory of classical form, with constants adjusted for best fit to experiment, may survive as the method of choice for the description of a wide range of heavy-ion phenomena.

1. University of Maryland; presently on leave at Justus Liebig Universität, Giessen, West Germany.

2. Student from Princeton University, summer 1975, under the Exceptional Student Program.

3. Student from Rice University, summer 1975, under the Exceptional Student Program.

BASIS FOR A MACROSCOPIC DESCRIPTION

C. Y. Wong T. A. Welton
J. A. Maruhn J. A. McDonald¹

The theoretical foundation for a macroscopic description is sought by starting with the more fundamental microscopic theories. We can show, as previously with the time-dependent Hartree-Fock approximation,² or more recently with the exact many-body Schrödinger equation,³ that one can define unambiguously the macroscopic variables of density field, velocity field, and the total kinetic energy field (or equivalently, the entropy field). Furthermore, the equations of motion for these variables turn out to be analogous to the equations of motion in classical fluid dynamics. A completely macroscopic fluid-dynamical description requires, however, that the stress tensor and the heat flux be expressed as simple functions of the basic macroscopic variables n , u , and σ . The conditions under which such a completely macroscopic description can be a good one are examined by comparing the length and time scales for microscopic and macroscopic relaxations.⁴ We find that in the collision, for example, of two similar nuclei of mass $A/2$, a macroscopic description should be reasonably valid for $A \geq 40$ at nonrelativistic energies, except for those collisions in a nearly grazing impact, and we can therefore be confident of a useful range of application for such a description. What is not known well are the detailed expressions for quantities like the stress tensor and the heat flux in terms of the basic macroscopic variables such as density and the fluid velocity components. These can only be parameterized at present in reason-

ably standard form (the Navier-Stokes form of the stress tensor and a heat flux proportional to temperature gradient being simple illustrations). We hope that the important parameters in such expressions can be determined when we confront theoretical predictions with experiment and that, in fact, the functional forms of these expressions can be refined as new phenomena appear.

1. Student from Princeton University, summer 1975, under the Exceptional Student Program.

2. C. Y. Wong, J. A. Maruhn, and T. A. Welton, *Nucl. Phys.* **A253**, 469 (1975).

3. C. Y. Wong and J. A. McDonald, to be published.

4. C. Y. Wong, T. A. Welton, and J. A. Maruhn, to be published.

NUMERICAL SOLUTION OF THE FLUID-DYNAMICAL EQUATIONS

J. A. Maruhn T. A. Welton C. Y. Wong

At the time of writing, we do not have results to report for a fully three-dimensional calculation although such calculations are well under way and results are expected in the near future. Meanwhile, collisions in one dimension have been studied, partly to gain experience with the computational aspects of the problem and partly because we believe we can learn about some features of more realistic collisions in this way.

The equations used were:

mass conservation,

$$\frac{\partial n}{\partial t} + \frac{\partial}{\partial x} (nv) = 0; \quad (1)$$

momentum conservation,

$$\begin{aligned} \frac{\partial}{\partial t} (nv) + \frac{\partial}{\partial x} (nv^2) \\ = -\frac{\partial p}{\partial x} - n \frac{\partial V_I}{\partial x} + \frac{\partial}{\partial x} \left(\eta \frac{n}{n_0} \frac{\partial v}{\partial x} \right); \quad (2) \end{aligned}$$

and energy conservation,

$$\frac{\partial}{\partial t} (nW^{(t)}) + \frac{\partial}{\partial x} (nW^{(t)}v) = \eta(n) \left(\frac{\partial v}{\partial x} \right)^2. \quad (3)$$

The internal energy per particle is given by the equation of state,

$$W(n) = b_0 n^{2/3} + b_1 n + b_2 n^{4/3} + b_3 n^{5/3} + \frac{1}{4} \left(\frac{4\pi}{G} \right)^{2/3} \frac{2m^* (kT)^2}{\hbar^2 n^{2/3}}, \quad (4)$$

where the coefficients have been chosen to yield an equilibrium density of 0.17 nucleon/fm³, a corresponding binding energy of 16 MeV, and a compressibility of 134 MeV. The pressure is $P = n^2 \partial W / \partial n$, evaluated at a constant entropy. The thermal part of the internal energy, $W^{(t)}$, is defined as the last term on the right-hand side of Eq. (4). It is convenient to write the equation of energy conservation in terms of $W^{(t)}$, instead of the total energy density, because it is a small quantity compared to kinetic and total internal energy and would not be obtained accurately from the total energy density.

The long-range potential V_l was assumed to be given by

$$\frac{d^2 V_l(x)}{dx^2} - \alpha^2 V_l(x) = -4\pi\beta n(x), \quad (5)$$

so that it is of Yukawa type. We used $\beta = -280$ MeV and $\alpha = 2.1$ fm⁻¹. The Yukawa potential produces an additional binding energy linear in n in the nuclear matter limit, which has to be subtracted from the linear term in Eq. (4) to preserve the limiting properties of $W(n)$. A Coulomb potential was not included because of its singular behavior in the one-dimensional case.

We used an explicit Eulerian flux-corrected transport algorithm,¹ which ensures stability in the presence of extreme density or velocity gradients or even discontinuities, such as occur in the neighborhood of shocks. Although thus able to describe shock fronts only a few mesh-points wide, Eq. (3) does not then give the correct heating in the front because the derivation of Eq. (3) from the conservation equation for the total energy density assumes continuity of n and v . The resulting loss of total energy can be made rather small, however, by choosing the mesh sufficiently small, so that shocks extend over a larger number of mesh points. For the 256 mesh points actually used, the energy loss was less than 10 MeV during a collision.

Figure 5.1 shows a few sample results for the collision of two slabs with widths about equal to the diameter of ²⁰⁸Pb.

In Fig. 5.1a the initial lab energy is 18.8 MeV per nucleon. This corresponds to a relative speed of about

1.7 times the velocity of sound in nuclear matter for the equation of state assumed, so that the collision is supersonic and compression is expected to be important. The viscosity was set zero in this case. A zone of strong compression forms in the center with near-zero velocity; the remainder of the two slabs still stream in from the side. The maximum density reached is large because of the low incompressibility assumed. At time 125 fm/c a compressed composite system has been formed with almost no internal motion. The high pressure in the compressed state then causes gradual expansion, and the density slowly goes down to the equilibrium value at time ~ 210 fm/c, but internal motion has been built up to such an extent that it cannot be stable and starts fissioning at 286 fm/c.

Figure 5.1b shows a nonviscous collision with an initial energy of 75.2 MeV per nucleon. The main difference is the much stronger compression ratio of more than 2.5. Such strong compressions are not expected in a three-dimensional situation since then matter can flow out to the sides. The density becomes more stretched out before it starts to fission. Equation (4) favors fission as soon as the density goes below 0.11 fm⁻³ since then the lowering of the density becomes even more favorable energetically.

At very low energies there is the possibility of fusion; this has also been observed in the calculations. Figures 5.1c and d show the effects of viscosity on a collision with an initial energy of 18.8 MeV per nucleon.

Viscosity tends to smooth the density throughout the entire collision. The short-range oscillations in the density have vanished and the corresponding energy has been dissipated into heating. Viscosity also lowers the overall compression, because at the collision zone, kinetic energy is converted into heat as well as into compression. The third effect is a direct consequence of this heating: Because of the equation of state, a heated zone also has a higher pressure than the surroundings. Because we do not yet include thermal conductivity, the generated heat stays at the center of the collision (there is little convective motion in this region). Thus the heated region must have a lower density to be in pressure equilibrium with the surroundings. This is the physical explanation for the pronounced central dip seen in Fig. 5.1c and d. This dip later develops directly into the fission breakup in Fig. 5.1c, which thus proceeds more rapidly than in the inviscid case.

The collision in Fig. 5.1d, on the other hand, is so strongly damped that the central compression zone does not engulf the whole system, but the outer peaks survive and are pushed outward again, forming small fragments in the final breakup.

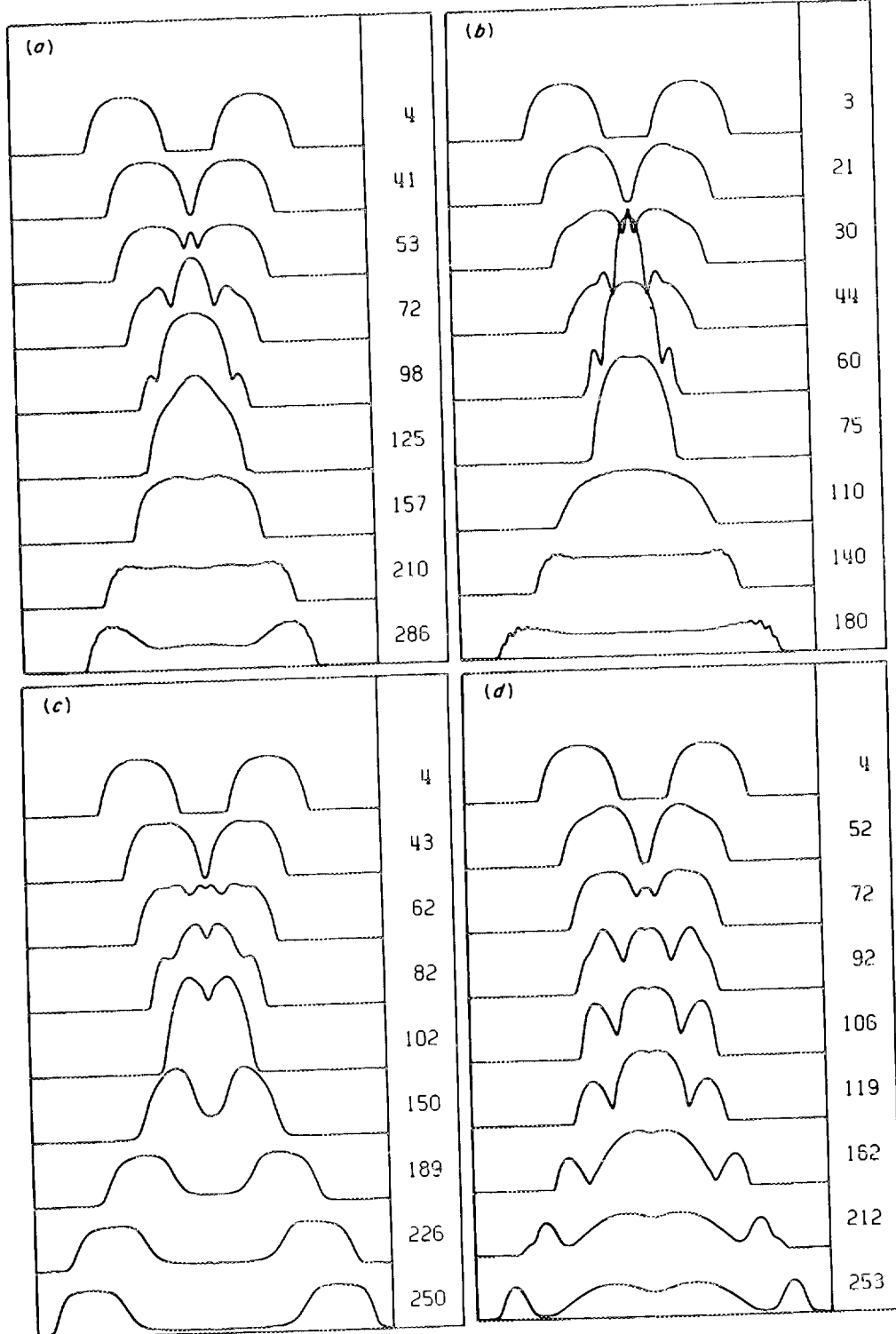


Fig. 5.1. Density as a function of time for a collision of two slabs. The numbers give the time (in fm/c) elapsed since starting time. The vertical distance between graphs corresponds to a density of 0.2 fm^{-3} . (a) Initial energy of 18.8 MeV per nucleon and zero viscosity; (b) initial energy of 75.2 MeV per nucleon and zero viscosity; (c) initial energy of 18.8 MeV per nucleon and $\eta_0 = 20 \text{ MeV}/c \cdot \text{fm}^2$; (d) initial energy of 18.8 MeV per nucleon and $\eta_0 = 50 \text{ MeV}/c \cdot \text{fm}^2$.

It is clear that merely by varying the one parameter of nuclear viscosity, a wide range of collision phenomena can be obtained. This could provide a means of learning about a realistic nuclear viscosity coefficient by comparing results of a full three-dimensional calculation with experiment.

1. J. P. Boris and D. L. Book, *J. Comput. Phys.* **11**, 38 (1973).

SPIN AND ISOSPIN DYNAMICS OF NUCLEAR FLUID

C. Y. Wong T. A. Welton J. A. Maruhn

We have considered the effects of the spin and isospin degrees of freedom on the dynamics of the nuclear fluid; we expect them to allow new kinds of sound wave to occur. To investigate these we start with the time-dependent Hartree-Fock (TDHF) equation with spin- and isospin-dependent central interactions. We then cast the TDHF equation into a set of conservation equations of the classical type, coupling the spin and isospin densities. With simple zero-range density-dependent interactions, we obtain the normal modes for the propagation of density variations and the corresponding sound speeds. In addition to the normal sound waves, in which the total density varies with space and time, there are the spin sound waves, in which the difference of the spin-up and spin-down densities varies with space and time; the isospin sound waves, in which the difference of neutron and proton densities varies with space and time; and finally, the spin-isospin sound waves, in which the difference of the "parallel" spin and isospin densities and the "antiparallel" spin and isospin densities varies with space and time.

A HAMILTONIAN FORMULATION FOR EULERIAN HYDRODYNAMICS

T. A. Welton C. G. Trahern¹

Current efforts to formalize a classical hydrodynamical description of heavy-ion collisions usually depend heavily on the use of the Eulerian description of the flow. The fixed coordinate mesh in this method is particularly convenient in view of the large deformations to be expected. The Eulerian equations, in spite of their apparent convenience, suffer from some serious disadvantages, among these being the problem of fluid surfaces. In order to achieve numerical stability, some artificial dissipation, explicit or implicit, must be

introduced. In this way, a conservative theory is converted into a theory with uncontrolled dissipation, with considerable attendant difficulty of interpretation. From another viewpoint, we may regard nuclear hydrodynamics as a considerable generalization of the familiar concept of collective motions. The Eulerian equations at best allow a purely classical description of these collective motions, but we may expect that a quantum treatment of the collective motions will, in fact, be required. Thus, a Hamiltonian theory that is equivalent to the Eulerian equations will permit such quantization by generally familiar methods.

To proceed, we first restrict our attention to one-dimensional flows. Note that the Lagrangian (mesh moving with fluid) description allows directly a Lagrangian ($\delta \int L dt = 0$) formulation. We write

$$L = \int dQ \left\{ \frac{1}{2} \rho_0(Q) \left(\frac{\partial x}{\partial t} \right)_Q^2 - \rho_0(Q) U \left[\left(\frac{\partial x}{\partial Q} \right)_t \right] \right\}, \quad (1)$$

where

$x(Q, t)$ = coordinate at the time t of the fluid element which was at position Q at the starting time,

$\rho_0(Q)$ = mass of fluid per unit range of starting position,

$\left(\frac{\partial x}{\partial t} \right)_Q = U$ = velocity of the fluid element currently at x ,

$\left(\frac{\partial x}{\partial Q} \right)_t$ = fractional compression of the fluid element at x , compared with its starting density,

$U \left(\frac{\partial x}{\partial Q} \right)$ = specific enthalpy of compression.

Isentropic flow has been assumed; otherwise the system is certainly not conservative.

A Hamiltonian and appropriate canonical momenta can be derived from Eq. (1) by familiar manipulations, but the resulting formalism has current fluid position as a coordinate, whereas the independent integration variable Q is a label that identifies a particular fluid element. We now make a transformation (which appears to be novel) in which label and coordinate are simply interchanged. That is, we write

$$L = \int dx \rho_0 [Q(x)] \left(\frac{\partial Q}{\partial x} \right)_t \left\{ \frac{1}{2} \left(\frac{\partial x}{\partial t} \right)_Q^2 - U \left[\left(\frac{\partial x}{\partial Q} \right)_t \right] \right\}, \quad (2)$$

where we hold in abeyance the question of the meaning of the new coordinate $Q(x, t)$. We complete the transformation by use of two familiar identities:

$$\left(\frac{\partial x}{\partial Q}\right)_t = 1/\left(\frac{\partial Q}{\partial x}\right)_t \equiv 1/\frac{\partial Q}{\partial x},$$

$$\left(\frac{\partial x}{\partial t}\right)_Q = -\frac{(\partial Q/\partial t)_x}{(\partial Q/\partial x)_t} \equiv -\frac{\partial Q/\partial t}{\partial Q/\partial x}. \quad (3)$$

Finally,

$$L = \int dx \rho_0(Q) \left(\frac{\dot{Q}^2}{2Q} - Q' U(Q') \right), \quad (4)$$

where $\dot{Q} \equiv \partial Q/\partial t$ and $Q' \equiv \partial Q/\partial x$.

This Lagrangian has precisely the form of a nonlinear field theory for a single field variable Q , which is a function of x and t . The resulting field equations are precisely equivalent to the desired Eulerian equations, but we now have a significant advantage. The above integral can be directly replaced by a sum over discrete cells. The Lagrangian form is fully retained, as is the positive definite character of the resulting Hamiltonian. Instability is then possible only if the method for numerical integration of the coupled equations of motion is a poor approximation.

The extension to two dimensions is not completely trivial, because we now have Q_1 and Q_2 , which may each be differentiated with respect to x or y . The correct formalism is

$$L = \int dx \int dy \rho_0(Q_1, Q_2) \left(\frac{1}{2J} \left\{ \left(\frac{\partial Q_2}{\partial x} \right)^2 + \left(\frac{\partial Q_2}{\partial y} \right)^2 \right. \right. \\ \left. \left. + \left(\frac{\partial Q_1}{\partial x} \right)^2 \dot{Q}_1^2 + \left[\left(\frac{\partial Q_1}{\partial x} \right)^2 + \left(\frac{\partial Q_1}{\partial y} \right)^2 \right] \dot{Q}_2^2 \right. \right. \\ \left. \left. - 2 \left(\frac{\partial Q_1}{\partial x} \frac{\partial Q_2}{\partial x} + \frac{\partial Q_1}{\partial y} \frac{\partial Q_2}{\partial y} \right) \dot{Q}_1 \dot{Q}_2 \right\} - J \cdot U(\rho_0 J) \right),$$

where $J = (\partial Q_1/\partial x)(\partial Q_2/\partial y) - (\partial Q_1/\partial y)(\partial Q_2/\partial x) =$ Jacobian of transformation $Q_1 Q_2 \rightarrow x, y$.

The Hamiltonian and the equations of motion are easily obtained, and the extension to three dimensions is now obvious. Extensive numerical testing of this

promising formulation has been started, and some ideas for approximate quantization have been devised.

1. Student from Rice University, summer 1975, under the Exceptional Student Program.

SIMPLE HYDRODYNAMICS IN DROPLET COLLISIONS

C. Y. Wong J. J. Griffin¹

The motions of the nuclear fluid in a heavy-ion reaction occur on a large spatial scale. The associated time scales can be made small or large, depending on the initial conditions. If the flow is mostly subsonic, a description based on the dynamics of an incompressible, sometimes viscous, fluid (hydrodynamics) can be used. We have initiated a program²⁻⁴ to study colli-

ORNL-DWG 75-16843

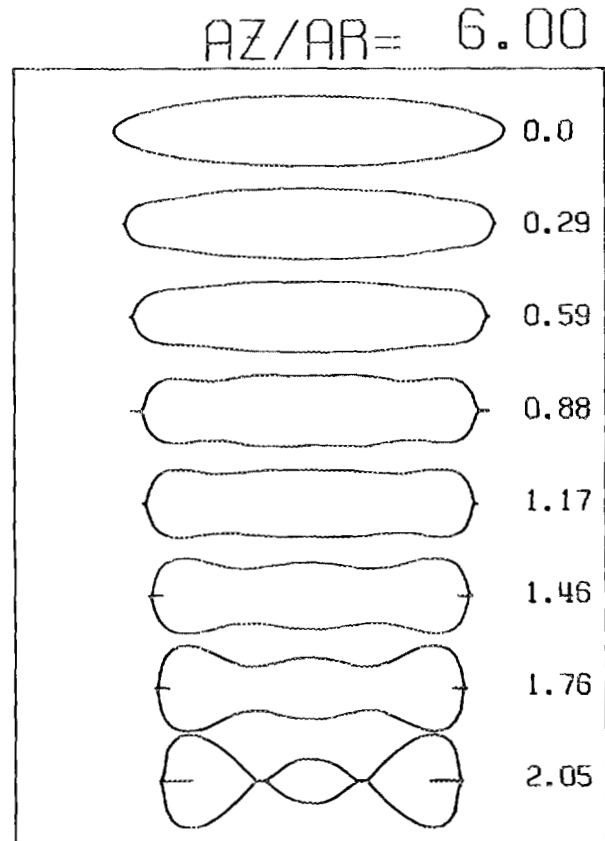


Fig. 5.2. Motion of a chargeless droplet stretched to the shape of a spheroid with an aspect ratio of 6. The numbers are the times, in units of $\sqrt{E_s^{(0)}/nR_0^2}$, where $E_s^{(0)}$ is the surface energy of a spherical drop of radius R_0 with the same volume.

sions between droplets of nuclear fluid in these terms. In our simple treatment, we represent the surface in terms of spherical harmonics and assume a linearized hydrodynamics for which solutions are already known. Simple hydrodynamics reproduces many experimental features such as (1) the rapid formation of a neck, (2) focusing of surface waves, (3) the formation of a toroidal-shaped droplet at the end point of maximal compression, and (4) shape of the neck for a non-head-on collision. However, hydrodynamics linearized for expansion with respect to a sphere cannot adequately describe the disintegration of a droplet. Accordingly, we investigated hydrodynamics linearized for a shape expanded with respect to spheroids of large aspect ratio and obtained the corresponding normal modes. This is particularly appropriate for the shape of the composite droplet at the end point of its maximal stretching in a head-on collision. We show in Fig. 5.2 the motion of such a droplet, which initially is a spheroid with an aspect ratio of 6. The droplet breaks into three pieces as it disintegrates. Instability of this kind is conveniently called "necklace" instability because disintegration results in a line of drops of similar sizes. We find that the greater the aspect ratio, the larger the number of drops created. For the collision of two equal drops of radius R and in the absence of viscosity, the number of drops should increase with $u\sqrt{R}$, where u is the relative velocity. Because the presence of charge enhances necklace instability, experimental search for the occurrence of such phenomena with heavy nuclear projectiles will be of interest.

1. University of Maryland, presently on leave at Justus Liebig Universität, Giessen, West Germany.

2. J. J. Griffin and K. K. Kan, *Colliding Heavy Ions: Nuclei as Dynamical Fluids*, ORO-4856-3, University of Maryland, College Park, 1975.

3. C. Y. Wong, *Selected Topics in Heavy-Ion Reactions*, ORNL/TM-5000, 1975.

4. J. J. Griffin and C. Y. Wong, *Bull. Am. Phys. Soc. II* **20**, 1158 (1975).

MICROSCOPIC MODELS OF NUCLEI AND HEAVY-ION COLLISIONS

J. P. Bondorf ¹	S. E. Koonin ⁵
R. Y. Cusson ²	S. J. Krieger ⁶
K. T. R. Davies	J. A. Maruhn
H. T. Feldmeier ³	V. Maruhn-Rezwani ⁷
S. Garpman ⁴	J. W. Negele ⁸
E. C. Halbert	P. J. Siemens ¹

Recently there has been renewed interest in the derivation and application of microscopic theories of

nuclear collective motion, especially because of heavy-ion reaction experiments that probe previously unexplored areas of nuclear dynamics. New approaches are currently being examined; the aim is to obtain a unified microscopic description of the statics and dynamics of a wide range of physical phenomena, including large-amplitude collective oscillations, fission, fusion, compound-nucleus formation, deep-inelastic scattering, and fragmentation. A microscopic approach may describe just the statics of the system, or it may aim to describe the full dynamics of collective motion. Both aspects are being studied with independent-particle theories, based on some form of the Hartree-Fock approximation. Static calculations use self-consistent constrained Hartree-Fock models, from which one obtains quantities appropriate to slow adiabatic motion. The dynamical calculations rely on time-dependent Hartree-Fock methods to provide detailed information on the time evolution of nuclear processes such as fission or heavy-ion reactions. In addition, a simplified approach is being used which treats the individual nucleon-nucleon collisions classically.

1. Niels Bohr Institute, Copenhagen, Denmark.

2. Consultant to ORNL from Duke University, Durham, N.C.

3. Guest assignee from Technische Hochschule Darmstadt, Germany, under NATO Fellowship.

4. Nordisk Institut for Teoretisk Atomfysik, Copenhagen, Denmark.

5. California Institute of Technology, Pasadena.

6. University of Illinois at Chicago Circle.

7. Guest assignee, presently consultant with Chemistry Division.

8. Massachusetts Institute of Technology, Cambridge.

ADIABATIC MODEL

R. Y. Cusson¹

The density-dependent self-consistent single-particle potential developed recently² has been used to give a microscopic description of several kinds of fission and heavy-ion properties. We have obtained heavy-ion interaction potentials for a number of systems.³ For example, the case of $^{12}\text{C} + ^{12}\text{C}$ is shown in Fig. 5.3. The calculated adiabatic cluster potential energy V_{cl} is plotted vs $R = \sqrt{Q_2^0/2\mu}$, which is a measure of the separation between the ions. The experimental potential was obtained from the analyses of ORNL data on $^{12}\text{C} + ^{12}\text{C}$ scattering described elsewhere in this report.⁴ (The scattering is only sensitive to the potential beyond 3 or 4 fm.) The calculated potential has too large a radius; this arises because the radius of the density of ^{12}C is calculated to be 0.4 fm larger than the

one obtained from electron scattering. This discrepancy could easily be remedied by readjusting the parameters of the calculation. In the internal region the potential has its minimum at a value of Q_2^0 , the total mass quadrupole moment, that is consistent with the ground state properties of the compound system, ^{24}Mg . The minimum is also in reasonable agreement with the experimental binding energy of ^{24}Mg . Thus we see that there does seem to exist a single microscopic, albeit semiphenomenological, energy operator, V_{cl} , which can simultaneously give the correct potential in the asymptotic limit of large separation as well as in the fused compound-nuclear region.

Further calculations were made for the heavy-ion-induced fission reaction $^{58}\text{Ni} + ^{20}\text{Ne} \rightarrow ^{78}\text{Sr} \rightarrow A_1 + A_2$, which is being studied experimentally at ORNL. Because the compound system, ^{78}Sr , has a fissility below the Businaro-Gallone critical value of 0.396 for zero angular momentum, the pure liquid-drop model predicts asymmetric fission. A cluster potential energy curve for $^{78}\text{Sr} \rightarrow ^{39}\text{K} + ^{39}\text{K}$, similar to Fig. 5.3, was first obtained. From this curve it was possible to confirm that for such a light fissioning system, the top of the fission barrier still occurs in the strong absorption region, as it does for other light systems. This simplifies the calculation of the absolute energy of the fission barrier because the shell structure of the compound system does not contribute to the barrier energy. For such a light system, sections of the potential-energy surfaces along the fission and fusion

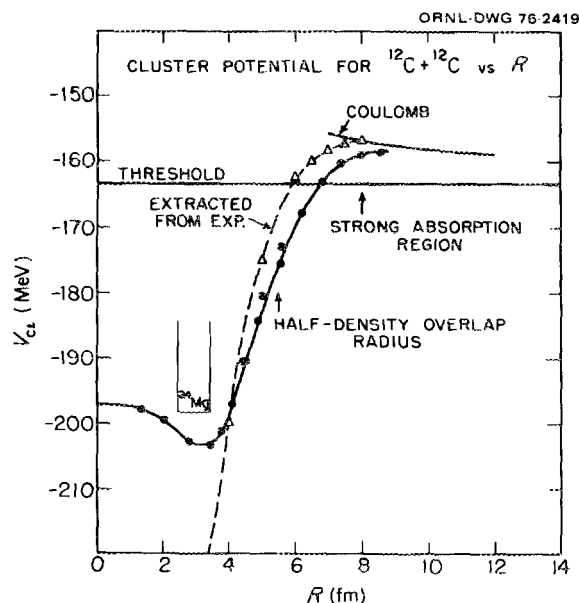


Fig. 5.3. Cluster potential energy for $^{12}\text{C} + ^{12}\text{C}$ ions.

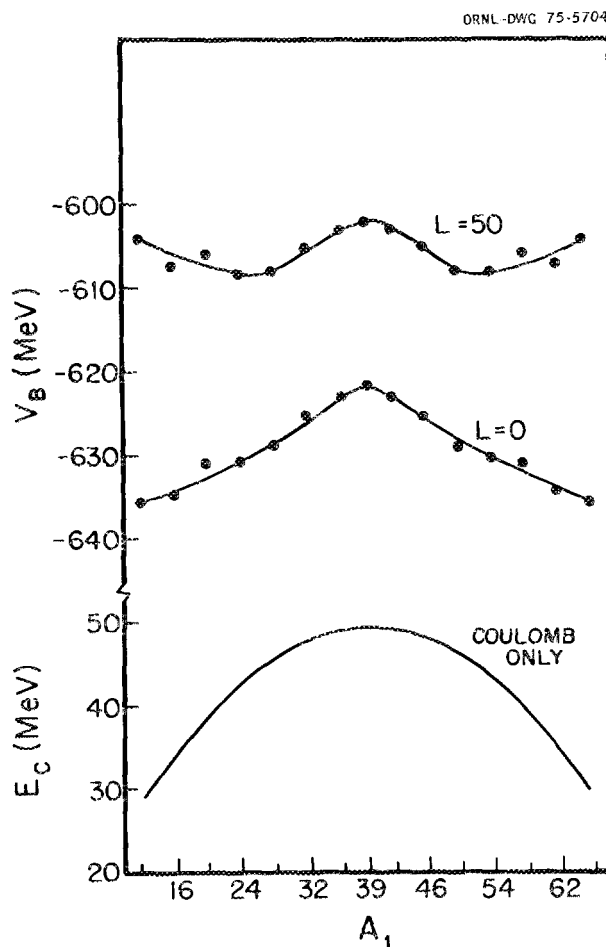


Fig. 5.4. Absolute energy of fission barrier of ^{78}Sr vs A_1 , the atomic number of one of the fragments.

valleys are similar and are shown in Fig. 5.4; the Coulomb energy is also shown. The potential energy corresponding to a nonzero value of the total angular momentum L was obtained by using the rigid-body values of the moments of inertia. Experimentally, it seems likely that much of the fission takes place from a compound nucleus with angular momenta in the neighborhood of 50. Figure 5.4 shows that the lowest barrier appears near $A_1 \approx 26$ (or 52), in agreement with preliminary experimental results showing a peak in the mass distribution near $A_1 = 29$. Thus the shell structure of the compound system does not appear to influence the fission systematics in this region of the periodic table as it does for heavy nuclei.

1. Consultant to ORNL from Duke University, Durham, N.C.
2. R. Y. Cusson et al., submitted to *Physical Review*.
3. R. Y. Cusson, R. Hilko, and D. Kolb, submitted to *Nuclear Physics*.

4. See this report, R. M. Wieland et al., " $^{12}\text{C} + ^{12}\text{C}$ Reactions."

DYNAMICS AND THE TDHF THEORY

R. Y. Cusson ¹	S. J. Krieger ⁴
K. T. R. Davies	J. A. Maruhn
H. T. Feldmeier ²	V. Maruhn-Rezwani ⁵
S. E. Koonin ³	J. W. Negele ⁶

New experimental results with heavy ions have prompted many questions concerning colliding droplets of nuclear fluid. For example, the simple process of converting the collective kinetic energy of a cluster into disordered heat energy might proceed, if it is analogous to its well-known classical counterpart, by particle-particle scattering due to the residual interaction. However, there are other possibilities. It is known that if a set of particles move in a highly time-dependent single-particle potential, the collective coherence of the motion may be converted into random motion. This is but one example where nuclear fluid dynamics may exhibit degrees of freedom not encountered in other types of fluid flow.

The ultimate explanation of nuclear collective dynamics must come from a microscopic description based on a realistic nucleon-nucleon force. An obvious approach is the time-dependent Hartree-Fock (TDHF) approximation, which was first proposed by Dirac nearly 50 years ago and is now becoming feasible with large computers. There are many motivations for applying TDHF to nuclei. TDHF is a truly microscopic theory, which requires as input only the nucleon-nucleon force: it is unnecessary to make an assumption as to the relevant collective coordinates. Moreover, although it is a fully quantal theory, its independent-particle nature permits a semiclassical interpretation, which often provides insights not obtainable in calculations that make use of much more complicated wave functions. We are encouraged by the significant successes that the static Hartree-Fock theory has had in providing descriptions of the energies and charge densities of nuclei. Finally, TDHF studies are expected to lead to a better understanding of existing approximation methods that are based on it, such as the random-phase approximation and adiabatic TDHF.

The numerical feasibility of TDHF calculations has been demonstrated recently for a one-dimensional system.⁷ These calculations, which describe collisions between slabs of nuclear matter in which the transverse degrees of freedom are frozen, resulted in a somewhat

unexpected richness of solutions corresponding to compound-nucleus formation, resonances, deep-inelastic processes, and fragmentation. Encouraged by this, we are applying the theory to more realistic two- and three-dimensional systems, including collisions of ions with unequal masses. More realistic nuclear forces are being included together with the effects of pairing. Some early results are reported in the following articles.

-
1. Consultant to ORNL from Duke University, Durham, N.C.
 2. Guest assignee from Technische Hochschule Darmstadt, Germany, under NATO Fellowship.
 3. California Institute of Technology, Pasadena.
 4. University of Illinois at Chicago Circle.
 5. Guest assignee, presently consultant with Chemistry Division.
 6. Massachusetts Institute of Technology, Cambridge.
 7. P. Bonche, S. E. Koonin, and J. W. Negele, *Phys. Rev. C*, January 1976, in press.

$^{12}\text{C} + ^{12}\text{C}$ AND THE TDHF MODEL

R. Y. Cusson¹ J. A. Maruhn

The same realistic single-particle potential that was used with the adiabatic model described in the preceding article was used to do a TDHF calculation² of the head-on collision of ^{12}C on ^{12}C . A harmonic oscillator basis was used. Figure 5.5 shows the resulting mass current distributions for several values of the time. Direct and exchange Coulomb forces as well as spin-orbit forces were included, and neutrons and protons were treated separately. The first time frame, at $t = 35$ fm/c, shows an early step in the collision where the system develops a stationary compression region in the center. The next stage, at $t = 44$ fm/c, shows that, as a reaction to the compression, the matter begins to flow radially outwards and back toward the initial position. This radial motion is short-lived, however, and quickly reverses itself. At $t = 85$ fm/c the two ^{12}C clusters are moving away from each other and would permanently separate if a substantial amount of collective kinetic energy had not already been lost to random motion. Thus at $t = 110$ fm/c the current distribution is in the process of reversing itself again. For this particular bombarding energy, the energy loss has not been high enough to allow the system to fall back towards the ^{24}Mg compound state. Thus in the fifth frame at $t = 165$ fm/c we can observe a metastable molecular state with a complicated internal oscillatory mode of the clusters. These oscillations continue while the system

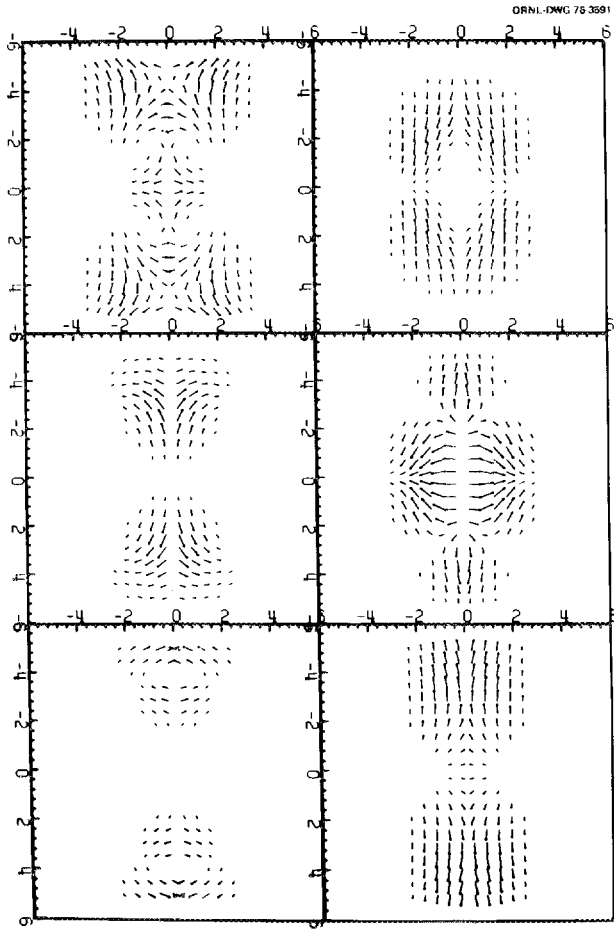


Fig. 5.5. Current distributions for head-on collisions of $^{12}\text{C} + ^{12}\text{C}$ at 6.4 MeV/A (c.m.) for the following times, from left to right, starting at the top and going down: $t = 110, 35, 165, 44, 321,$ and $85 \text{ fm}/c$.

slowly drifts apart, as shown in the last frame, at $t = 321 \text{ fm}/c$.

1. Consultant to ORNL from Duke University, Durham, N.C.
2. R. Y. Cusson and J. A. Maruhn, to be published in *Physics Letters*.

TWO-DIMENSIONAL TDHF CALCULATIONS

K.T.R. Davies S. E. Koonin²
H. T. Feldmeier¹ S. J. Krieger³
V. Maruhn-Rezwani⁴

Time-dependent Hartree-Fock (TDHF) calculations have also been performed in a two-dimensional coordinate space where it is assumed that the nuclear system is axially symmetric. The effective interaction used

consists of zero-range two- and three-body forces of the Skyrme type and a finite-range Yukawa force. Coulomb terms (except for exchange contributions) were included. This potential reproduces reasonably well the binding energies, radii, and densities of ^{16}O and ^{40}Ca . An effective charge was used in the calculations to avoid treating neutrons and protons separately, an approximation which should be valid for light systems. The head-on collision of $^{16}\text{O} + ^{16}\text{O}$ at a laboratory energy of 8.0 MeV per nucleon was studied previously.⁵

However, in order to compare TDHF results with experimental data, nonzero angular momenta (or impact parameters) must be studied. In a rigorous treatment, such systems would entail fully three-dimensional numerical calculations. While this is not impossible for the $^{16}\text{O} + ^{16}\text{O}$ system, such an approach becomes increasingly prohibitive for larger systems in terms of computing costs. Therefore we must consider how the effects of finite impact parameters may be treated without sacrificing the numerical simplicity of two-dimensional coordinate-space calculations. Therefore we consider an approximation in which the effect of the relative orbital angular momentum is accounted for by imagining the collision to occur in a frame rotating about an axis perpendicular to the scattering plane, while the system is assumed to remain axially symmetric about an axis in the scattering plane. The orientation of the z axis in real three-dimensional space is specified by the angle θ , whose time rate of change ω is given by

$$\omega = L/I(\rho), \quad (1)$$

where L is the relative orbital angular momentum and I is the instantaneous moment of inertia about the rotation axis. The total energy of the system is then modified as follows:

$$H \rightarrow H + L^2/2I(\rho). \quad (2)$$

The moment of inertia $I(\rho)$ is a functional of the density and depends on whether or not clumping of the ions due to tangential friction has occurred.

In Fig. 5.6 we show a polar plot of the trajectories for $^{16}\text{O} + ^{16}\text{O}$ at 8.0 MeV per nucleon. On the graph, r is the center-of-mass separation of the ions. Whereas the grazing partial waves ($l \geq 35$) suffer some small inward deflection due to the attractive tail of the nuclear potential, the influence of the strong interaction is most evident for $l \leq 30$. Head-on collisions ($l = 0$) penetrate deepest toward the compound system and bounce strongly with large energy loss. With increasing angular momentum ($l = 10$ to 25) the trajectory takes on a

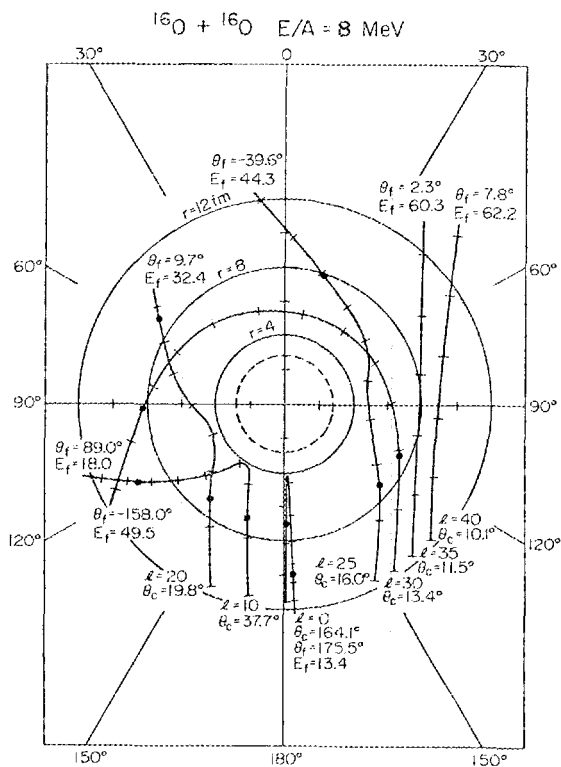


Fig. 5.6. r - θ trajectories for $^{16}\text{O} + ^{16}\text{O}$ at a c.m. energy of 8.0 MeV per nucleon. For each partial wave, we list θ_c , the scattering angle for a noninteracting-point Coulomb trajectory; θ_f , the scattering angle from the TDHF calculation; and E_f , the final center-of-mass relative fragment kinetic energy, in MeV. Tick marks indicate time intervals of 10^{-22} sec; the dots delineate times during which the ions "clutch." The dashed circle at $r = 2.8$ fm is the sharp-surface liquid-drop value for the compound system ^{32}S .

skimming characteristic under the influence of Coulomb, centrifugal, and nuclear forces. Because penetration is not as strong, the energy loss is less severe. In addition, the scission configuration becomes less elongated with increasing l . The $l = 30$ trajectory is of an orbiting type, just at the top of the "fusion" barrier. This interpretation is supported by the change in the initial curvature of the trajectory at $l = 30$.

In Fig. 5.7 we show the density at various times t for a TDHF calculation of $^{40}\text{Ca} + ^{40}\text{Ca}$ at 12.0 MeV per nucleon and $l = 20$. (The apparent deformation perpendicular to the direction of motion is simply due to a choice of unequal length scales for the plots.) The ions begin to clutch at $t = 0.16$, and at $t \approx 0.32$ they form a compound system. After various internal shape changes the system eventually begins to break apart, and scission occurs at $t = 0.9$. These qualitative pictures give

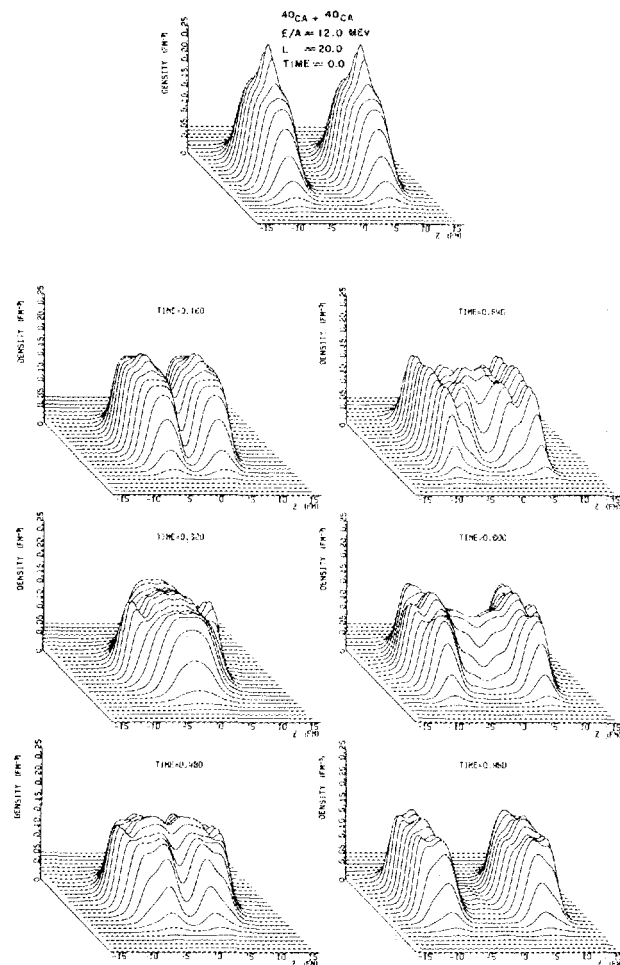


Fig. 5.7. Density distribution pictures for the reaction $^{40}\text{Ca} + ^{40}\text{Ca}$ at 12.0 MeV per nucleon and $l = 20$. The time is in units of 10^{-21} sec.

some idea of the richness of the structure involved in the shape changes obtained from a TDHF calculation.

1. Guest assignee from Technische Hochschule Darmstadt, Germany, under NATO Fellowship.
2. California Institute of Technology, Pasadena.
3. University of Illinois at Chicago Circle.
4. Guest assignee, presently consultant with Chemistry Division.
5. S. E. Koonin, to be published in *Physics Letters*.

THREE-DIMENSIONAL TDHF CALCULATIONS

J. A. Maruhn R. Y. Cusson¹

The assumptions made in the two-dimensional model discussed in the preceding article must be tested by exact calculations. With this in mind, we have devel-

oped a fully three-dimensional TDHF code. In the interest of computing speed, we have incorporated further simplifications of the Skyrme interaction and a combined coordinate-momentum space basis. With the present budgetary limitations, we expect to be restricted to studying systems no heavier than, say, Ni + Ni. Preliminary calculations for $\alpha + \alpha$ at 16 MeV per nucleon and impact parameters $b = 1, 2, 3, 4, 4.5,$ and 5 fm have been made. We find: (1) in the region $b = 2$ to 4 fm, the collective kinetic energy loss is considerably larger than for a head-on collision; this occurs via the formation of a molecular state that may perform several rotations while losing collective kinetic energy by radial oscillations before coming apart; (2) the two clusters tend to interpenetrate each other as in a two-fluid model with the result that the moment of inertia shows large deviations from the rigid-body value; and (3) for certain values of the impact parameter, the outgoing determinantal wave function factors, as it did before the collision, into two separate determinants representing the two clusters. Calculations for $^{16}\text{O} + ^{16}\text{O}$ and $^{40}\text{Ca} + ^{40}\text{Ca}$ are under way.

1. Consultant, Duke University, Durham, N.C.

CLASSICAL MICROSCOPIC DESCRIPTION OF HEAVY-ION COLLISIONS

J. P. Bondorf¹ H. T. Feldmeier² S. Garpman³
E. C. Halbert P. J. Siemens¹

In heavy-ion collisions, bombarding energies of a few hundred MeV per nucleon seem most favorable for producing shock zones of compressed nuclear matter. As an alternative to hydrodynamic ways of treating such collisions, we are investigating a microscopic description in which the classical paths of individual nucleons are followed. One aim is to make qualitative, rapid (and therefore economical) calculations of how the shock-zone characteristics and emergent-particle angular distributions depend upon the initial nuclear masses, the bombarding energy, and the nucleus-nucleus impact parameter.

Our present computer program, called SIMON, is a simple simulation code. Each run simulates one nucleus-nucleus collision, involving many nucleon-nucleon scatterings. Monte Carlo methods are used to determine the initial nucleon positions and velocities within the two separated nuclei. Nucleon-nucleon interactions are taken into account via cross sections rather than via explicit forces. Each nucleon's motion is approximated

as uniform in velocity, except for abrupt changes when nucleon-nucleon scatterings occur. The occurrence of each scattering and its exact time are determined by simple geometric considerations such as cross section, nucleon-nucleon impact parameter, and, sometimes, nucleonic hard-core radius. (There are alternative options available in SIMON.) The two new nucleon velocities, after each scattering, are determined by the impact parameter and/or by Monte Carlo methods. Within a run, all nucleon positions and velocities are known as functions of time. This allows calculation of such gross features as the space- and time-dependent particle density during collision, the space- and time-dependent mean-square nucleon velocity, and the angular distribution of particles emerging after collision.

There are two approximations basic to the present SIMON code: (1) classical-particle kinematics and (2) abrupt cross-section-induced changes in velocity (rather than continuous accelerations induced by smoothly varying nucleon-nucleon forces). These two simplifications are not justified in detail, for at the kinetic energies we consider, the de Broglie wavelength of a nucleon is of the same order of magnitude as the internucleon spacing, which in turn is of the same order as the mean free path for nucleon-nucleon scattering. However, we hope for some cancellation of detailed errors when we use these approximations in calculating gross features of the collision. We also make some other simplifications, reasonable enough at this stage but not basic to the SIMON method. At present we use nonrelativistic kinematics; also, we start with zero-temperature nuclei of spherical shape, and we neglect nuclear binding, Coulomb energy, nucleon spin, neutron-proton differences, and pion production. Furthermore, we allow only elastic and isotropic nucleon-nucleon scattering, with energy-independent density-independent cross section. These nonbasic simplifications may be modified in the future.

Local particle densities $\rho(\mathbf{r})$ are obtained by averaging over small volume elements, and emergent-particle angular distributions $W(\cos \theta)$ and $X(\phi)$ are obtained by averaging over appropriate solid-angle elements. Because of the Monte Carlo conditions defining each calculated nucleus-nucleus collision, there may be severe fluctuations of the local density (in time and space) and of the angular distributions. To reduce these fluctuations, we average over an ensemble of SIMON runs, all identical except for their Monte Carlo numbers. Figures 5.8–5.10 show some results obtained by averaging over nine head-on collisions between two mass 235 nuclei. For the nucleon-nucleon cross section we used $\sigma = 25$ mb, as suggested by experimental data in the energy region

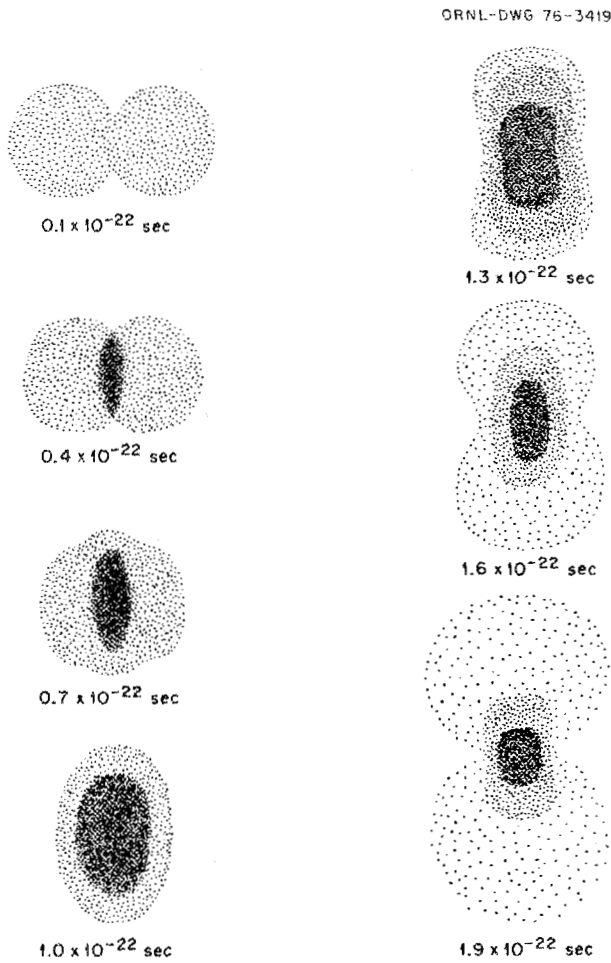


Fig. 5.8. Sketch of the cylindrically symmetric density calculated for a sequence of times during the head-on collision of two mass 235 nuclei.

of interest. The results shown were obtained with nucleon-nucleon scattering modeled as hard-sphere scattering, so that the distance of closest approach was $(\sigma/\pi)^{1/2} = 0.9$ fm. As Fig. 5.10 shows, this hard-sphere model yields a maximum particle density about twice that of normal nuclear matter. When we use the same σ , but with scattering models that allow nucleons to approach each other more closely than 0.9 fm, we find maximum densities $\gtrsim 3$ times normal. This sensitivity to the scattering mechanism is being studied in more detail.

1. Niels Bohr Institute, Copenhagen, Denmark.
2. Guest assignee from Technische Hochschule Darmstadt, Germany, under NATO Fellowship.
3. Nordisk Institut for Teoretisk Atomfysik, Copenhagen, Denmark.

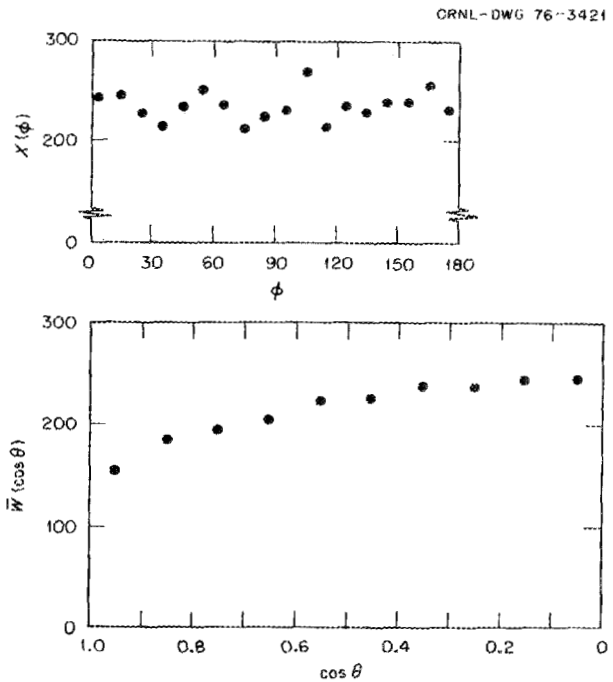


Fig. 5.9. Angular distributions of scattered emergent nucleons for head-on collisions between two mass 235 nuclei. $\bar{W}(\cos \theta)$ is $\frac{1}{2} W(\cos \theta) + \frac{1}{2} W(-\cos \theta)$, where $W(\cos \theta)$ is the number of nucleons with velocity vectors within the solid-angle interval defined by $\cos \theta \pm 0.05$. $X(\phi)$ is the number with velocities in the solid-angle interval defined by $\phi \pm 5^\circ$.

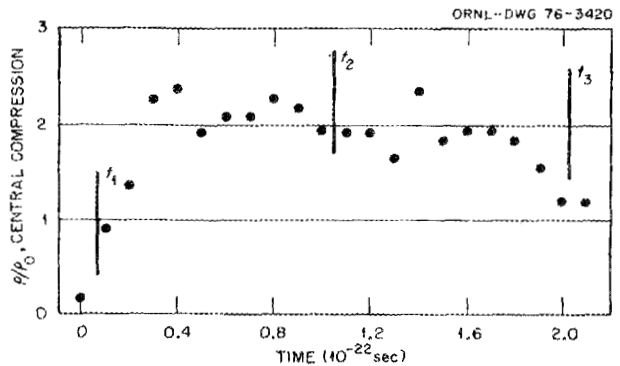


Fig. 5.10. The central density as a function of time for the collision of two mass 235 nuclei, where ρ_0 is the central density of each before the collision. At time t_1 the two first touch, at t_2 they would completely overlap if they did not interact, and at t_3 they would have completed passing through each other.

NUCLEAR REACTION THEORY

E. C. Halbert G. R. Satchler L. D. Rickertsen
L. W. Owen¹ J. B. McGrory

This section is concerned with more conventional nuclear reaction models: optical model, coupled chan-

nels, distorted-wave Born approximation (DWBA), etc. Most of the applications have been to heavy-ion reactions, although light ions have not been neglected entirely: work has continued on the excitation of giant multipole resonances by protons, alphas, and neutrons^{2,3} and on the role of two-step processes in charge-exchange reactions.^{4,5} This theoretical effort is usually pursued in close collaboration with the experimentalists at ORNL, and some of the results appear in the experimental sections of this report; these we only touch upon briefly.

Our activities have three broad motivations: (1) to provide the most sophisticated tools for the analysis of experimental data obtained at ORNL, (2) to see what we can learn from various types of data and hence to guide future experiments, and (3) to achieve a better understanding of the basic nuclear reaction mechanisms. Primarily our attention has been focused on direct or peripheral collisions; reactions of the fusion and deep-inelastic variety are better studied by the approaches described in the preceding articles.

1. Computer Sciences Division.
2. E. C. Halbert et al., *Nucl. Phys.* **A245**, 189 (1975).
3. F. P. Brady et al., *Phys. Rev. Lett.* **36**, 15 (1976).
4. L. D. Rickertsen et al., *Phys. Lett.* **59B**, 129 (1975).
5. L. D. Rickertsen et al., *Phys. Lett.*, in press.

SECOND-ORDER DWBA FOR HEAVY-ION INELASTIC SCATTERING

L. D. Rickertsen

The distorted-wave Born approximation (DWBA) requires much less computational effort than a coupled-channels (CC) calculation, and, in addition, the interpretation of the amplitudes leading to a given cross section is much simpler. Hence, it is of importance to understand the degree to which a DWBA analysis is adequate for a given reaction. The accurate data recently obtained at ORNL on the inelastic scattering of ^{12}C by neodymium isotopes at 70.4 MeV offered a

good opportunity to investigate this question, since the excitation of collective levels in both target and projectile, as well as the elastic scattering, was observed over a large range of angles. This energy is about 10 MeV above the Coulomb barrier, where the sensitivity to Coulomb-nuclear interference is optimal. The quadrupole coupling strength to the lowest 2^+ state of neodymium increases with mass number to values that are customarily thought to be so large that a CC treatment is necessary.

In our analyses of these data, we find that, although a first-order DWBA treatment is not adequate, a second-order DWBA treatment is sufficient and that it is not necessary to solve the coupled equations to all orders. In particular, we conclude that as long as the elastic scattering is reproduced well by a one-channel optical potential, the direct matrix element between any two channels is accurately given by the first-order DWBA term. To this must be added amplitudes corresponding to higher-order processes: self-coupling or reorientation and indirect transitions via other intermediate channels. Although these contributions are too complicated to be accounted for by simply modifying the optical potentials in the one-step DWBA calculation, we find it is sufficient to calculate them in a second-order DWBA, rather than solving the full coupled equations.

Figure 5.11 shows results for ^{144}Nd . Two calculations for the 3^- excitation are shown in Fig. 5.11a: a CC calculation taking into account the coupling to the 3^- and the 2^+ and 4^+ members of the ground-state rotational band to all orders and a DWBA calculation for the 3^- state where the 2^+ and 4^+ states have been ignored. In each case the optical parameters that were used reproduce the elastic scattering, and the inelastic results are indistinguishable; both are represented by the solid curve. The coupling strengths and optical parameters are given in Table 5.1. The quadrupole moment of the 3^- state was not included in either of these calculations. The dashed curve in Fig. 5.11a shows the result of including the quadrupole self-coupling in a second-order DWBA calculation. The intrinsic quadrupole moment of the 3^- state was taken arbitrarily to

Table 5.1. Optical parameters and coupling strengths for $^{12}\text{C} + ^{144}\text{Nd}$

Calculation	V	r_V	a_V	W	r_W	a_W	$\beta_2 R$	$\beta_3 R$	$\beta_4 R$
CC ^a	20.0	1.32	0.562	10.9	1.34	0.414	0.72	0.83	0.37
DWBA ^b	20.0	1.32	0.562	12.1	1.34	0.433	0.72	0.83	0.37

^aCC — parameters for the fully coupled-channels calculation.

^bDWBA — one-channel optical parameters and coupling strengths for the first- and second-order DWBA calculations.

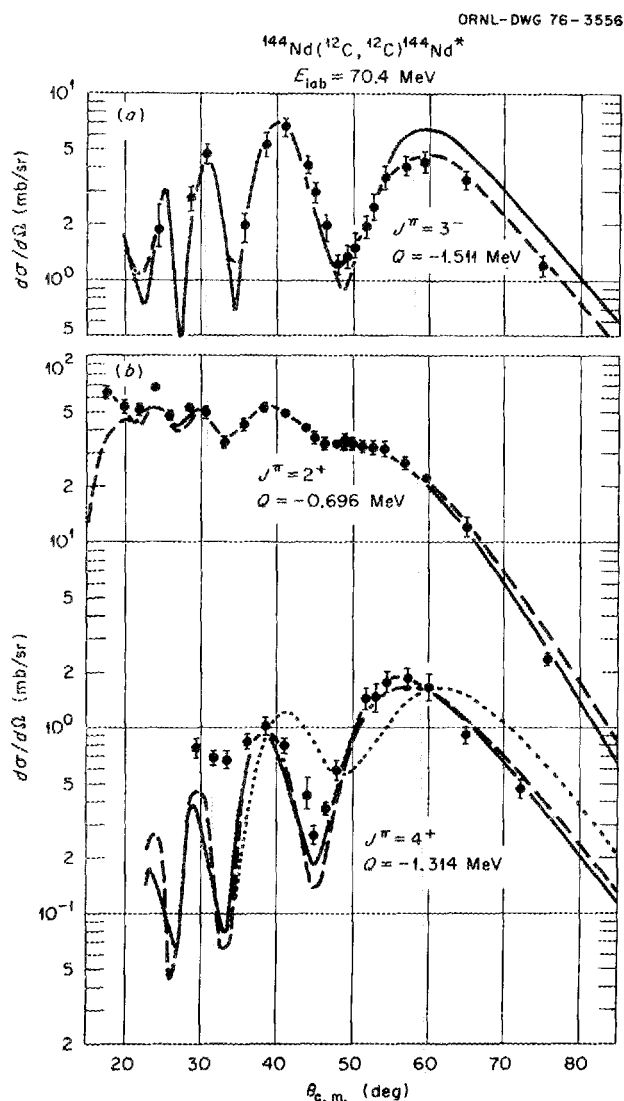


Fig. 5.11. Comparison of coupled-channel and second-order DWBA calculations for the inelastic scattering of 70.4-MeV ^{12}C on ^{144}Nd (see text for details). (a) Excitation of the lowest 3^- state of ^{144}Nd ; (b) excitation of the 2^+ and 4^+ rotational states of ^{144}Nd .

be the same as for the ^{144}Nd 2^+ state. Figure 5.11b shows analogous calculations for the excitation of the 2^+ and 4^+ rotational states. The solid curve corresponds to the full CC calculation (including reorientation couplings), and the dashed curve is the result of second-order DWBA calculations where the quadrupole coupling is taken only to second order. In each case the observed elastic scattering is reproduced. A major component of the 4^+ angular distribution is due to the two-step process by way of the 2^+ state, and the dotted curve corresponds to the DWBA calculation neglecting this contribution.

The character of these results persists for even stronger coupling. The quadrupole deformation for ^{150}Nd is nearly a factor of 3 larger than for ^{144}Nd , but calculations for the angular distributions taking this strength to all orders and to only second order differ by less than 30%. It appears that when the experimental data can be described by a CC analysis, a second-order DWBA will also be adequate for even the largest coupling strengths experimentally observed in this mass region. Finally, because there is nothing to distinguish the projectile from the target in these reactions except for the details of the coupling, these conclusions are expected to be valid for projectile excitation as well.

MICROSCOPIC DESCRIPTION OF HEAVY-ION SCATTERING

L. D. Rickertsen G. R. Satchler

By "microscopic" we mean a description in terms of nucleon-nucleon forces and individual nucleon motions rather than the usual one-body phenomenological optical-potential and collective models. In practice, we have only considered simple folding models in which an effective nucleon-nucleon interaction is folded into the density (or the transition density for inelastic scattering) of each of the two ions. Our treatment of higher-order processes is limited so far to the use of such potentials in coupled-channel calculations.

Previous studies of this folding model for elastic scattering, using what were then regarded as "realistic" interactions, showed that the model overpredicted the potential near the strong-absorption radius as deduced from measurements by as much as a factor of 2.¹ However, a new interaction derived by Bertsch et al.^{2,3} from G -matrix elements based upon the Reid potential has an appreciably shorter range and does give results in agreement with experiment (to within the uncertainties implicit in the density parameters) for a variety of heavy-ion scatterings ranging from $^{12}\text{C} + ^{12}\text{C}$ to $^{16}\text{O} + ^{208}\text{Pb}$. This interaction has also been applied to heavy-ion inelastic scattering ($^{12}\text{C} + ^{12}\text{C}$, $^{16}\text{O} + ^{28}\text{Si}$, and $^{16}\text{O} + ^{60}\text{Ni}$), using transition densities derived from electron scattering, thus leaving no adjustable parameters. We obtain agreement with measured cross sections. The validity of this interaction is being tested more widely, particularly on heavier systems, together with the role of higher-order corrections such as arise from the Pauli principle. Another form of the interaction, due to Eisen et al.^{4,5} and also derived from the Reid potential, is being tested; preliminary results indicate that it is also successful.

A previous study was made of the inelastic scattering of ^{12}C by ^{208}Pb using detailed one-particle, one-hole

wave functions of the random-phase-approximation type and Gaussian nucleon-nucleon interactions normalized to fit the observed elastic scattering.⁶ Again there were no free parameters, and agreement with the data was obtained. Some indication was found that the range required is shorter than that previously used. This appears to be a useful tool for exploring the range of the effective force and will be studied further, particularly with lighter systems where the Coulomb excitation contribution is not so dominant.

It has often been asserted that some data on heavy-ion elastic scattering demand shallow ion-ion potentials. We believe this question is far from settled. The folded potentials just discussed are very deep in the nuclear interior, and, for example, fits are obtained to $^{12}\text{C} + ^{12}\text{C}$ and $^{16}\text{O} + ^{28}\text{Si}$ scattering over a wide range of energies which are as good as those using a shallow potential. The elastic data are sensitive only to the surface region (although, for these light systems, they appear to probe the potential several fermis inside the strong-absorption radius); we hope that combining them with fusion measurements may provide more definitive information.

1. G. R. Satchler, *Phys. Lett.* **59B**, 121 (1975).
2. G. Bertsch et al., to be published.
3. W. G. Love, private communication.
4. Y. Eisen, B. Day, and E. Friedman, *Phys. Lett.* **56B**, 313 (1975).
5. B. Day, private communication.
6. G. R. Satchler et al., *Phys. Lett.*, in press.

SINGLE-NUCLEON TRANSFER REACTIONS

G. R. Satchler L. W. Owen¹

The work on single-nucleon transfer reactions was primarily directed toward the analysis of ORNL data on the one-neutron pickup and one-proton stripping reactions of $^{12}\text{C} + ^{208}\text{Pb}$, described elsewhere in this report. Two new theoretical features were involved: (1) the use of folding-model optical potentials to describe the elastic scattering and (2) inclusion of all the interaction terms that should properly appear in a first-order DWBA treatment.² The code LOLA³ was modified to accommodate these features.

Although the folded potentials are several hundred MeV deep, their use has little effect on the predicted transfer cross sections in shape or magnitude. The cross sections forward of the main peak tend to be slightly smaller, and those at larger angles somewhat larger, than those predicted using a 40-MeV-deep Woods-Saxon well. Including the other interaction terms³ (in the post

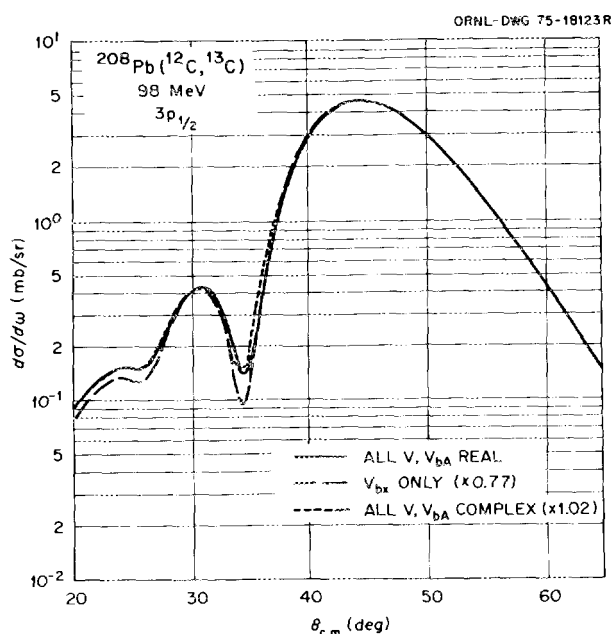


Fig. 5.12. Effects of the different interaction terms on a DWBA calculation of the $^{208}\text{Pb}(^{12}\text{C}, ^{13}\text{C})$ reaction.

representation) has very little effect on the angular distributions (none at all for the proton transfer; the effects on the neutron transfer are shown in Fig. 5.12). The cross-section magnitudes are changed by amounts $\lesssim 20\%$. However, the extra terms are necessary to give the post-prior equivalence that is required of the DWBA.

1. Computer Sciences Division.
2. R. M. DeVries, G. R. Satchler, and J. G. Cramer, *Phys. Rev. Lett.* **32**, 1377 (1974).
3. R. M. DeVries, *Phys. Rev. C* **8**, 951 (1973).

COUPLED-CHANNEL ANALYSIS OF $^{26}\text{Mg}(^{16}\text{O}, ^{14}\text{C})^{28}\text{Si}$ USING SHELL-MODEL SPECTROSCOPIC AMPLITUDES

E. C. Halbert¹

Calculations were made for the reaction $^{26}\text{Mg}(^{16}\text{O}, ^{14}\text{C})^{28}\text{Si}$ at 45 MeV using the coupled-channels Born approximation (CCBA). The new feature of the present work was the use of two-proton spectroscopic amplitudes from many-particle (*s,d*) shell-model calculations for ^{26}Mg and ^{28}Si . Our computed CC cross sections involve contributions from six separate form factors, characterized in obvious notation as: $0_{26}^+ \rightarrow 0_{28}^+$, $0_{26}^+ \rightarrow 2_{28}^+$, $2_{26}^+ \rightarrow 0_{26}^+$, $2_{26}^+ \rightarrow 2_{28}^+$ (transferred $L = 0, 2,$ and 4). Care was taken to ensure that the six transfer

form factors had phases consistent with the collective-model couplings used for the inelastic scattering. At 5 fm, the $2_{26}^+ \rightarrow 0_{28}^+$ form factor is three times the $0_{26}^+ \rightarrow 2_{28}^+$ form factor. The ratios as well as the magnitudes of the six form factors depend upon the detailed shell-model structure of the four states 0_{26}^+ , 0_{28}^+ , 2_{26}^+ , and 2_{28}^+ . In contrast, the form factors used by Nilsson et al.^{2,3} depended upon the L transfer but not upon the initial ^{26}Mg state or final ^{28}Si state, whereas the form factors of Sørensen⁴ depended upon L , but with state dependence entering only through the spins J_{26} and J_{28} in the multiplying Clebsch-Gordan coefficient ($J_{26} \ 0 \ L \ 0 | J_{28} \ 0$). In calculating cross sections for the reactions to the ground and first 2^+ states, we tried two different $^{26}\text{Mg} + ^{16}\text{O}$ optical-model potentials.²⁻⁴ Also, we investigated the effects of other changes, for example, varying the $0^+ - 2^+$ coupling strength for ^{28}Si , neglecting some of the six transfer form factors, and neglecting some state dependence of these form factors. The form factors and the magnitudes and angular dependences of the cross sections were found to be rather sensitive to these variations in the calculational details. However, none of the variations we tried provided a clear remedy for the principal difficulty of the earlier calculations — their failure to produce cross sections as large as those experimentally observed.²⁻⁴ This work is part of a more general investigation to see whether improvements in simultaneous-transfer calculations might increase the predicted cross sections by the one or two orders of magnitude needed to fit experiment or whether sequential transfer has to be included.

1. Work performed while on leave at the Niels Bohr Institute, Copenhagen, Denmark, 1974–1975, in collaboration with S. Landowne, B. S. Nilsson, and R. A. Broglia.

2. B. Nilsson et al., *Phys. Lett.* **47B**, 189 (1973).

3. S. Landowne, R. A. Broglia, and B. Nilsson, p. 49 in *Proceedings of the International Conference on Reactions between Complex Nuclei, Nashville, Tenn., June 1974*, R. L. Robinson et al., Eds., North-Holland, Amsterdam, 1974.

4. B. Sørensen, *Phys. Lett.* **53B**, 285 (1974).

SEMICLASSICAL SCATTERING WITH COMPLEX TRAJECTORIES

L. D. Rickertsen

For energies not too far above the Coulomb barrier, heavy-ion scattering into a particular angle can often be understood in terms of a small range of values of the relative angular momentum L between the target and the projectile. For example, the “quarter-point” angle (where $d\sigma/d\sigma_R = 1/4$) corresponds closely to the orbit whose transmission coefficient $T_L = 1/2$. Although

quantum mechanically one can never associate a given scattering angle with a single value of the angular momentum, this observed behavior strongly suggests the usefulness of semiclassical (or classical) approaches to heavy-ion scattering. A code has been written to calculate the elastic scattering cross sections for heavy ions in a WKB approximation. Although earlier attempts to use the WKB method have been unsuccessful, the method has recently been generalized by Knoll and Schaeffer¹ (and others) to allow the possibility of complex angular momenta. Using this procedure, the code BUMPPPO is able to reproduce angular distributions computed by the usual optical-model routines to better than 1% for all angles. For a single angle, the WKB method requires about 1/100 of the computing time required by the standard codes which integrate the Schrödinger equation directly, so that for a large number of angles the computing times for the two methods are comparable. Applications of this procedure to heavy-ion scattering by Knoll and Schaeffer and with BUMPPPO reveal that in regions where the calculated angular distribution falls smoothly, that is, is not diffractive, the cross section at a single angle is due to a single complex angular momentum. The real part of this angular momentum corresponds closely to the average of the L values which contribute in the quantum mechanical calculation; the imaginary part roughly corresponds to the width of the distribution of these partial-wave amplitudes. For angles where diffraction is evident in the calculated angular distributions, the WKB cross section is the result of the interference of a small number (~ 2 or 3) of amplitudes corresponding to different complex angular momenta. This conclusion was reached earlier with regard to the diffraction structure observed in heavy-ion and alpha-particle scattering.² Thus the WKB method is potentially able to reveal considerable physical insight as well as to provide a fast method of computation of the elastic scattering. Application of the method to inelastic scattering is in progress.

1. T. Knoll and R. Schaeffer, *Ann. Phys.*, to be published.

2. W. Frahn and R. Venter, *Nucl. Phys.* **A59**, 651 (1964).

NUCLEAR STRUCTURE THEORY

R. L. Becker E. C. Halbert
T.T.S. Kuo¹ A. D. MacKellar³
N. M. Larson² J. A. Smith⁴
J. B. McGrory J. P. Svenne⁵
B. H. Wildenthal⁶

At a fundamental level, understanding the saturation properties of nuclei in terms of the nucleon-nucleon

force remains one of the outstanding problems of nuclear theory. Work has continued on this difficult problem, using the Brueckner theory and its developments to evaluate higher-order corrections.

The shell model attempts to describe nuclear properties in terms of the motions of a few "valence" nucleons restricted to a relatively few independent-particle orbits. Thus one of its important functions continues to be to correlate experimental findings and to predict others of interest. Our efforts in this area have often been made in close collaboration with experimental groups.

In many cases it is difficult to separate structure and reaction theory; for example, the structure calculations of transfer form factors were an essential part of the two-nucleon transfer problem discussed in a preceding article. Similar intermingling occurs in the interpretation of giant multipole resonances excited by inelastic scattering.

1. State University of New York, Stony Brook.
2. Computer Sciences Division.
3. University of Kentucky, Lexington.
4. Visitor from New College, Sarasota, Fla., partially supported by a program administered by Oak Ridge Associated Universities. Present address: Department of Astronomy, Yale University, New Haven, Conn.
5. University of Manitoba, Winnipeg, Manitoba, Canada.
6. Michigan State University, East Lansing.

PROPAGATOR-RENORMALIZED BRUECKNER THEORY

R. L. Becker¹ N. M. Larson¹ A. D. MacKellar²
J. A. Smith³ J. P. Svenne⁴

For the past two years, motivated by a deficiency of the renormalized Brueckner-Hartree-Fock (RBHF) approximation with respect to the saturation properties of nuclei, we have been attempting to include nonlinear terms in the self-consistent field. The second-order terms are shown in column 3 of Fig. 5.13. Some preliminary results for ^{16}O were reported in last year's annual report.⁵ Another aspect of the Brueckner calculations is the desire for self-consistency of the effective interaction with respect to the single-particle wave functions and energies. Ensuring this self-consistency involves making Pauli and spectral corrections to the reaction matrix. Preliminary reaction-matrix corrections also were reported last year for ^{16}O .⁵ The code was so slow, however, as to provide a major obstacle to extending the applications to heavier nuclei. The bulk of the computational effort this year has been involved in making the Pauli-spectral and SORB

(second-order renormalized Brueckner theory) codes very much faster. Some sample results for ^{40}Ca , calculated with the Hamada-Johnston interaction, are shown in Table 5.2. In contrast to the case of ^{16}O , the residual Pauli and spectral corrections did not increase the radius, and the saturation properties are only slightly improved relative to RBHF calculations with the uncorrected matrix elements. Both the Pauli-spectral corrections and the second-order particle-hole terms are expected to increase in importance as one considers heavier nuclei. The codes now appear fast enough to handle an $N = Z$ nucleus with ~ 200 nucleons at reasonable expense. Some additional programming will be needed to ensure complete self-consistency in the presence of a neutron excess, spin-unsaturated shells, and a large Coulomb field; however, calculations in the lead and actinide regions now seem quite feasible at moderate cost.

A continuing interest in trying to include three-body contributions into the finite nuclear Brueckner calculations led to an investigation of the validity of Day's approximation for the Bethe-Goldstone defect function. This approximation neglects the dependence of the defect function on the energy of an interacting pair.

ORNL-DWG 76-3001

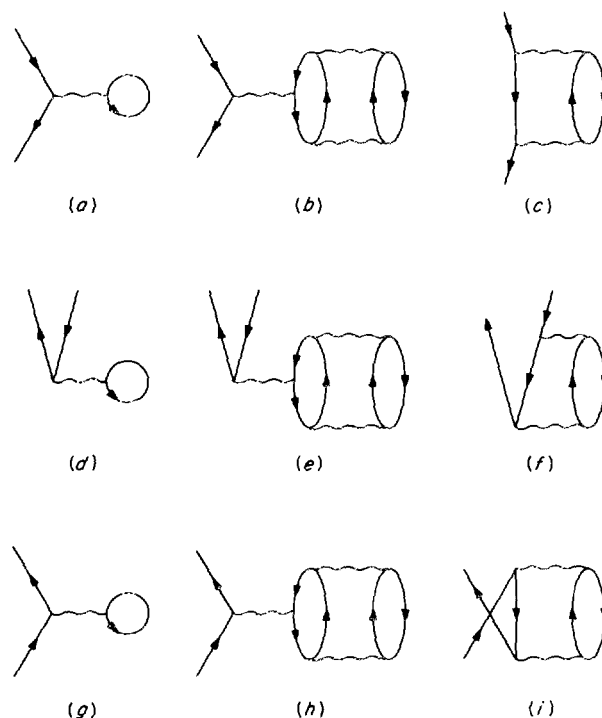


Fig. 5.13. Diagrams included in the SORB approximation for the self-consistent field.

Table 5.2. Effects of Pauli-spectral corrections of the reaction matrix and second-order terms in the self-consistent field to propagator-renormalized Brueckner calculations of $^{40}\text{Ca}^a$

Propagator ^b	SCF ^c	$(BE)^{\text{calc}}/(BE)^{\text{exp}}$ (%)	$r_{\text{chg}}^{\text{calc}}/r_{\text{chg}}^{\text{exp}}$ (%)	nlj	$\epsilon(2)^d$ (MeV)
SOC (^{16}O)	RBHF	81	86	$0f_{7/2}$	0.37
SOC (^{40}Ca)	RBHF	61	87.5	$1p_{3/3}$	1.06
RBHF ^c (^{40}Ca)	RBHF	66	87.4	$1p_{1/2}$	1.31
RBHF (^{40}Ca)	SORB	66	89	$0f_{7/2}$	0.88

^aAn oscillator basis with $\hbar\omega = 16.8$ MeV and a well depth of 44 MeV was used.

^bFor the propagator, SOC = single oscillator configuration and oscillator spectrum, and RBHF = renormalized Brueckner-Hartree-Fock configuration and spectrum.

^cSCF means self-consistent field.

^d $\epsilon(2)$ = second-order rearrangement energy of "particle" states.

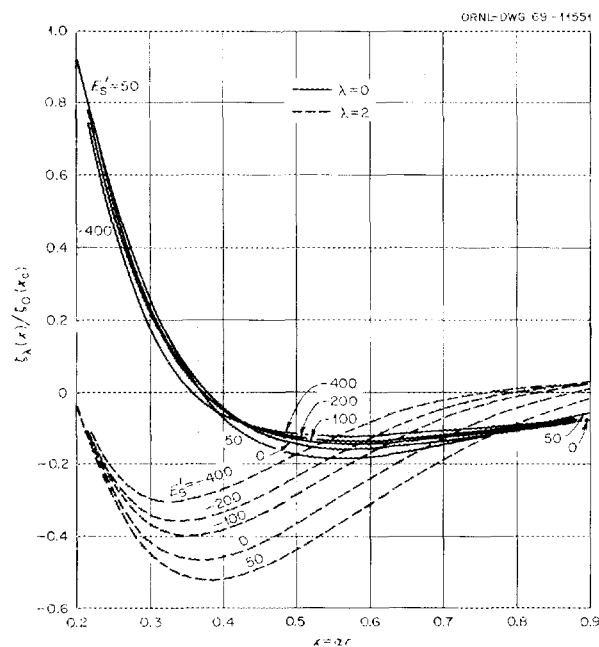
Figure 5.14 shows the energy dependence of relative s-state defect functions in an oscillator potential.^{6,7}

A level inversion usually occurs in self-consistent field calculations when only one of a pair of symmetry-related levels is occupied. An interpretation is offered: the single-particle energy of the level unoccupied in the A -particle system is its energy of removal from the $(A+1)$ -particle system.^{8,9} The correction of this energy to convert it to the corresponding energy in system A is simply given. When both symmetry-related levels are calculated in the same system, there is no level inversion. The usual prescription to occupy the lowest levels should be amended to state that the energies should all correspond to removal energies from system A . Our interpretation also explains abnormal spin-orbit splittings.

In seeking to ascertain how good the body densities calculated from self-consistent field theories are, it is important to know how reliable are the "experimental" densities inferred from elastic electron scattering. The usual analysis of the data is by finding a charge density that yields a charge form factor that fits the data. We have discovered, however, that the best empirical charge densities of light nuclei correspond to body probability densities with negative regions containing a total negative probability of about 1%.¹⁰ Moreover, the negative portions cannot be removed by adding a small positive exponential tail and subsequently renormalizing without seriously disrupting the fit to the data. We propose the alternative procedure of dividing the experimental charge form factor by the nucleon form factor to yield an experimental body form factor and then fitting this with a form factor obtained from a nonnegative body density. We have found that the analytic body form factor

$$f_b(q) = q^{-1} [A \sin(aq) e^{-\alpha q^2} + b^{-1} (1 - Aa) \sin(bq) e^{-\beta q^2}] ,$$

which corresponds to a nonnegative body density, together with the Hofstadter-Wilson double-pole form factor of the proton, yields excellent fits to the data on



Radial dependence of the Triplet Relative Defect Functions $\xi_\lambda(\bar{N}nljE_S'; x)$, $\lambda = j \pm 1$, for $\bar{N} = l = 0$, $j = 1$, $n = 5$, Divided by $\xi_0(0, 50, 1E_S'; x_c)$, for the Hamada-Johnston Interaction, $E_S' = 50, 0, -100, -200$, and -400 MeV, $\alpha = 0.4 F^{-1}$, and $\rho_{\text{max}} = 5$.

Fig. 5.14. Bethe-Goldstone defect functions.

^3He , ^4He , and ^{16}O . Further applications of our relatively simple method of mapping out regions of uncertainty in the density also have been made.^{11,12}

1. Computer Sciences Division.
2. University of Kentucky, Lexington.
3. Yale University, New Haven, Conn.
4. University of Manitoba, Winnipeg, Manitoba, Canada.
5. R. L. Becker and N. M. Larson, *Phys. Div. Annu. Prog. Rep. Dec. 31, 1974*, ORNL-5025 (1975), p. 12.
6. R. L. Becker, p. 96 in *Effective Interactions and Operators in Nuclei*, Springer, New York, 1975.
7. R. L. Becker and A. D. MacKellar, to be published.
8. R. L. Becker and J. P. Svenne, *Phys. Rev. C* **12**, 2067 (1975).
9. R. L. Becker and J. P. Svenne, *Inversion of Single-Particle Levels in Nuclear Hartree-Fock and Brueckner-HF Calculations with Broken Symmetry*, ORNL/TM-5174 (1975).
10. J. A. Smith and R. L. Becker, to be published.
11. R. L. Becker and J. A. Smith, *Phys. Div. Annu. Prog. Rep. Dec. 31, 1973*, ORNL-4937 (1974), p. 210.
12. R. L. Becker and J. A. Smith, paper submitted to *Physical Review C*.

NUCLEAR SHELL MODEL

J. B. McGrory E. C. Halbert T.T.S. Kuo¹
B. H. Wildenthal²

In the past year, we have continued to use the shell-model codes as an adjunct to the experimental program. As reported elsewhere,^{3,4} there continues to be interest in locating states of high spin in light nuclei, in both the (s , d) shell and (f , p) shell. In particular, lifetimes have been measured and tentative spin assignments proposed in ^{42}Ca . The spins are higher than allowed by the simple (f , p)² model for ^{42}Ca , so it is necessary to include other orbitals. A model space was chosen in which a ^{32}S core is assumed, and the ten extra nucleons are distributed over the $d_{3/2}$ and $f_{7/2}$ orbits, with up to five $f_{7/2}$ particles allowed. An effective residual interaction was chosen which leads to reasonable agreement for the known spectrum of states in ^{40}Ca . Within this model space for ^{42}Ca , both negative- and positive-parity levels can be calculated, and there is the potential for describing low-lying deformed $4p-2h$ states. The qualitative result of the calculation is that there are a number of high-spin states calculated to be at about the same energy as the high-spin states suggested by the measured spectrum; in fact, there are more states calculated than there are observed. The calculated $B(E2)$ values for transitions between these states indicate the existence of some sort of "rotational" band structure for these high-spin

states, but there are not enough experimental data with which to compare this prediction.

Work was completed on an extensive study of nuclei near the ^{208}Pb shell closure. The lead isotopes $^{204,205,206,210,211,212}\text{Pb}$ and ^{210}Po , ^{211}At , and ^{212}Rn were treated as systems of identical particles (or holes) built on a ^{208}Pb core. The Kuo-Herling interaction was used, with some empirical renormalization. The results were generally in good agreement with experiment. It was found that a simple seniority truncation scheme was very effective in reproducing the calculated shell-model results in untruncated spaces. Such a scheme should be useful in examining the structure of much lighter lead isotopes, for which data are now being accumulated.

There have been some investigations of more purely theoretical questions in the shell-model field this year. One concerned the infamous spurious state question. It was suggested by Gloeckner and Lawson⁵ that a useful prescription for "eliminating" such states would be to add to the shell-model effective residual interaction the Hamiltonian for the motion of the center of mass of the nucleus multiplied by a large coefficient. This large coefficient would mean that if a state had a significant admixture of states with the center of mass excited, that state would be pushed to a high energy. In a very simple shell-model space, the prescription appeared to be very useful. The approach was then applied to the Zuker-Buck-McGrory (ZBM) calculation of ^{16}O . Their prescription for eliminating the spurious states also eliminated the agreement between theory and experiment. We first tried to find an interaction that gave good agreement with experiment when the spurious states were projected out in this way, but we had no success. We next studied in some detail what was happening in the ZBM model when the spurious states were eliminated. We found that the ZBM model space actually contained very small admixtures of spurious states. To eliminate these small admixtures, a large and significant part of the model space had to be eliminated along with them. We concluded that it was more useful to accept the small spurious-state contamination than to throw away an important part of the model space. This analysis suggested that the Gloeckner-Lawson prescription was not generally useful.

1. State University of New York, Stony Brook.
2. Michigan State University, East Lansing.
3. J. Gomez del Campo et al., *Phys. Rev.* **12**, 1247 (1975).
4. See this report, D. E. Gustafson et al., "High-Spin States of the $K^\pi = \frac{3}{2}^+$ and $\frac{1}{2}^+$ Bands of ^{23}Na ."
5. D. H. Gloeckner and R. D. Lawson, *Phys. Lett.* **60B**, 5 (1975).

6. High-Energy and Medium-Energy Activities

H. O. Cohn
G. T. Condo¹
W. M. Bugg¹

E. L. Hart¹
H. R. Brashear²
T. H. Handler³

INTRODUCTION

Activities of the High-Energy Program at ORNL included participation in a π^-p experiment with 150-GeV/c pions at the Fermi National Accelerator Laboratory (FNAL). The experiment was done with a hybrid system employing the 76.2-cm bubble chamber and wire proportional counters. New data were obtained with the same setup for positive-pion interactions at the same momentum. Further effort was put into the study of low-energy physics with high-energy techniques by further analyzing data obtained at BNL of interaction of \bar{p} and K^- in plates inserted in a 76.2-cm bubble chamber. Measurement of interaction of pions in the 208.3-cm SLAC bubble chamber has continued, leading to completion of the measurement phase of a π^+ -deuterium interaction experiment and accumulation of data for a π^- -proton experiment.

VERY HIGH ENERGY PHYSICS

The principal experimental effort of the Oak Ridge high-energy physics group continues to be the hybrid bubble-chamber--proportional-wire-counter experiment at FNAL. During 1975, an additional experimental run yielded $\sim 200,000$ pictures exposed to a beam of 150-GeV/c positive pions. The data contained in this exposure are still in the measuring and preanalysis phase. Work is also continuing at ORNL in the design and construction of large drift chambers that will be inserted behind the bubble chamber to enhance the downstream capabilities, both in regard to the accuracy of momenta determinations and to the physical size of the angular acceptance of the region surveyed by the proportional-wire systems.

Work has also continued on the analysis of the initial experiment performed with the hybrid system at FNAL, namely, an exposure of the hydrogen bubble chamber to 147-GeV/c π^- mesons. This has resulted in the submission of several papers for publication. The first of these was concerned with measurement of the elastic, total, and topological cross sections for both π^-p and K^-p interactions. The latter particles were present in about 2% of the beam and were tagged by an upstream Cerenkov counter. Our measurements are, in the main, in agreement with others that have been made at these higher momenta. The most interesting feature of the data is that the scaling behavior of the partial topological cross sections, as predicted by Koba, Neilson, and Oleson,⁴ is verified by the π^-p data over a broad range of pion momenta. In another paper, the inclusive and semi-inclusive cross sections for ρ^0 production from 147-GeV/c π^-p interactions was discussed. The total observed ρ^0 cross section was 7.3 ± 1.3 mb, most of which occurred in the lower topology events (less than ten outgoing prongs). This value is substantially smaller than the 13.5 ± 1.3 mb value reported in π^-p interactions at 205 GeV/c.⁵ The principal difference in the two experiments is in the large value for the ρ^0 cross section reported at 205 GeV/c in the events of higher topology (≥ 10 prongs). The determination of partial resonance production cross sections in high-topology events is quite subjective, and the above differences are probably due to different assumed backgrounds and different parameters employed for the Breit-Wigner resonance-fitting procedure. A third paper presented evidence for the so-called clustering emission model of particle production at high energies. The data support the hypothesis that charge and transverse momenta are locally conserved on the rapidity axis.

LOW-ENERGY PHYSICS WITH HIGH-ENERGY TECHNIQUES

During the past year, an invited talk was given at the Fourth International Symposium of $\bar{N}N$ Interactions at Syracuse University. This talk summarized the world sample of stopping \bar{p} interactions with complex nuclei. Very few data exist concerning stopping \bar{p} interactions in nuclei heavier than deuterium, except for nuclear-emulsion data where the identification of the target nucleus is a well-known difficulty. Our previous experiment, which suggested the existence of a neutron halo in heavier nuclei, is virtually the only systematic study of stopping \bar{p} interactions. This result was criticized by Gerace, Sternheim, and Walker⁶ on the grounds that pion charge-exchange scattering in the parent nucleus could invalidate our evidence about the existence of a neutron halo. These authors assumed \bar{p} capture in the nuclear periphery and used free-particle pion-nucleon charge-exchange cross sections to arrive at their conclusion. In a short note⁷ we challenged the use of free-particle cross sections to infer secondary charge-exchange interactions following \bar{p} capture. K^- meson capture is an entirely analogous physical situation with the added virtue that one can identify specific charge-exchange reactions from the charge states of the emitted pions and hyperons. The use of free-particle π charge-exchange cross sections implies that charge exchange would be about an order of magnitude larger than is observed experimentally following K^- capture.

Work was also begun on an investigation of the various \bar{p} elastic and inelastic (annihilation and non-annihilation) scattering from the nuclei of carbon, titanium, tantalum, and lead. This work was initiated to check the reliability of calculations made by Pilkuhn⁸ based on a black-sphere model for the absorption of slow negative hadrons. It will also be the first measurement of low-momentum (~ 300 - to ~ 400 -MeV/c) \bar{p} interactions with complex nuclei.

π^+ -DEUTERON INTERACTIONS AT 15 GeV/c

We have completed the measurement phase of a 15-GeV/c π^+ -deuteron experiment being conducted in collaboration with Florida State University. The 500,000 frames of film obtained at SLAC with the 208.3-cm bubble chamber filled with deuterium were scanned for events with an identified stopping-proton track. A total of 55,000 events were measured at ORNL with the spiral reader. About 90% of the events passed the filtering program and yielded data suitable for processing through the three-view geometric-reconstruction program. After kinematic fitting of each event

to hypotheses of interest, data summary tapes were prepared. Analysis of the data has just begun, and the preliminary results are consistent with previous measurements at similar energies. We will search for production of higher-mass bosons and compare the data to predictions of theoretical models.

π^- -PROTON INTERACTIONS AT 8 GeV/c

We are continuing to scan and measure film obtained at SLAC with the hydrogen-filled 208.3-cm bubble chamber exposed to a beam of 8-GeV/c π^- . So far, 75,000 events have been measured on the spiral reader. Considerable effort has been spent on improving the efficiency and reliability of the filtering program. Our share of the film is one-third of a larger exposure done in collaboration with MIT and Tohoku University, Japan. We are planning to pool our data to obtain high statistical results. Preliminary data based on early measurements show the expected general features in the two- and three-pion mass distribution. We expect to study in detail A_2 meson production in association with $\Delta(1236)$ production, which will enable us to effect a meaningful check of the hypothesis of charge independence.

1. Consultant to ORNL from the University of Tennessee, Knoxville.
2. Instrumentation and Controls Division.
3. Guest assignee to ORNL from the University of Tennessee, Knoxville.
4. Z. Koba, H. B. Neilson, and P. Oleson, *Nucl. Phys.* **B40**, 317 (1972).
5. F. C. Winkelmann et al., *Phys. Lett.* **56B**, 101 (1975).
6. W. J. Gerace, M. M. Sternheim, and J. F. Walker, *Phys. Rev. Lett.* **33**, 508 (1974).
7. W. M. Bugg, G. T. Condo, and H. O. Cohn, *Phys. Rev. Lett.* **35**, 611 (1975).
8. H. Pilkuhn, *Z. Phys.* **A273**, 259 (1975).

THE $\pi^+ + d \rightarrow p + p$ REACTION AND THE DEUTERON D STATE

E. E. Gross	R. L. Burman ³
C. A. Ludemann	R. P. Redwine ³
M. J. Saltmarsh	W. R. Gibbs ³
B. M. Freedom ¹	E. L. Lomon ³
C. W. Darden ¹	K. Gabathuler ⁴
R. D. Edge ¹	P. Y. Bertin ⁵
T. Marks ¹	J. Alster ⁶
M. Blecher ²	J. P. Perroud ⁷
K. Gotow ²	B. Goplen ⁸

The D -state probability, P_D , of the deuteron has been the object of much study. The understanding of the

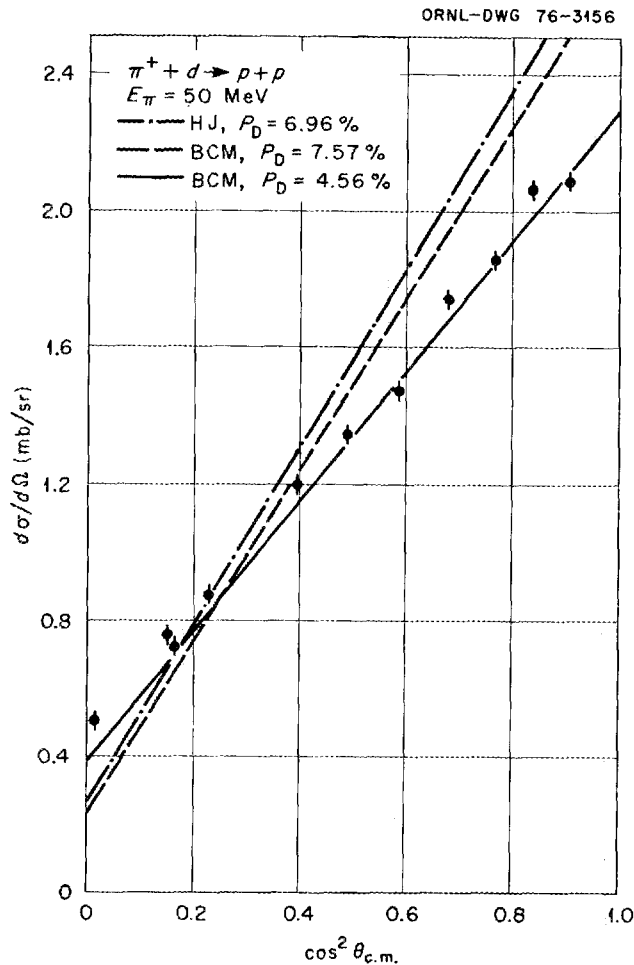


Fig. 6.1. Angular distribution for an incident pion energy of 50 MeV. The curves are calculated using either Hamada-Johnston (HJ) or boundary-condition-model (BCM) wave functions with the D -state percentages (P_D) indicated.

binding energy, the magnetic dipole moment, and the quadrupole moment of the deuteron requires a variation in P_D from 4 to 7%. Deuteron wave functions determined from a description of nucleon-nucleon scattering, deuteron electromagnetic form factors, and elastic π - d scattering contain a D -state admixture of 5 to 7%.

We have measured angular distributions for the $\pi^+ + d \rightarrow p + p$ reaction at incident energies of 40, 50, and 60 MeV. These data were taken using the low-energy pion channel at the Clinton P. Anderson Meson Physics Facility at the Los Alamos Scientific Laboratory. Because of the large momentum mismatch between the entrance and exit channels (i.e., $p_\pi \sim 100 \text{ MeV}/c$, $p_p \sim 400 \text{ MeV}/c$ each), this reaction should be sensitive to the high-momentum components of the deuteron wave function. Goplen, Gibbs, and Lomon⁹ and Goplen¹⁰ have shown that this reaction is sensitive to the D state of the deuteron.

Figure 6.1 shows the angular-distribution data measured at 50 MeV and the results of calculations for the differential cross section. The form of the reaction mechanism allows the pion to scatter from one nucleon to another before it is absorbed. The contributions from on- and off-momentum-shell terms are the same for each calculation. Only the form of the deuteron wave function and the D -state percentage were changed. The calculation using the Hamada-Johnston (HJ) wave function ($P_D = 6.96\%$) and that using the boundary-condition-model (BCM) wave function ($P_D = 7.57\%$) are essentially parallel, but both have a different slope from the calculation using the BCM ($P_D = 4.56\%$) wave function. This is interpreted to mean that the $\pi^+ + d \rightarrow p + p$ angular distribution is very sensitive to the magnitude of the D -state wave function but that it is not sensitive to the exact form of the radial wave function.

1. University of South Carolina, Columbia.
2. Virginia Polytechnic Institute and State University, Blacksburg.
3. Los Alamos Scientific Laboratory, Los Alamos, N.M.
4. Swiss Institute for Nuclear Physics, Villigen, Switzerland.
5. University of Clermont F^d, Clermont-Ferrand, France.
6. University of Tel-Aviv, Tel-Aviv, Israel.
7. University of Lausanne, Lausanne, Switzerland.
8. Science Applications, Inc., Albuquerque, N.M.
9. B. Goplen, W. R. Gibbs, and E. L. Lomon, *Phys. Rev. Lett.* **32**, 1012 (1974).
10. B. Goplen, Ph.D. thesis, University of New Mexico, 1975.

7. Molecular and Materials Research

Electron Spectroscopy

INTRODUCTION

T. A. Carlson W. B. Dress

During 1975, the principal effort of the electron spectroscopy program has been the construction of a chamber where photoelectron spectroscopy can be carried out under ultrahigh-vacuum conditions. The main thrust of our future program will be directed toward the study of the electronic structure of molecules adsorbed onto surfaces. In addition to clarifying the basic relationships between the photoelectron process and the electronic structure of molecules, these studies will provide new tools for research in heterogeneous catalysis. In particular, we have a strong interest in the nature of the angular distribution of ejected photoelectrons from a partially orientated molecule. To this end, two photon sources have been constructed: an x-ray source with changeable anodes and an He I discharge lamp (21.22 eV) with a device for polarization. Different ports allow a change in angle between the direction of the incoming photons and ejected photoelectrons, and the sample can rotate 360° about its axis.

As a test of the new chamber, both photoelectron- and photon-induced Auger spectra have been taken on an Mg-MgO system. In addition, experiments were made on aluminum, silicon, and sulfur compounds before the new chamber was put into place. The primary interest in these studies was the difference in chemical shifts of the core binding energies between measurements made using Auger data and x-ray photoelectron data. This difference has been called the "Auger parameter" and is related to the relaxation energy or polarizability of molecules.¹ It will be particularly interesting to measure this important quantity for molecules adsorbed on the surface, and studies of this nature are planned for the near future.

While the ultrahigh-vacuum chamber was under construction, a number of photoelectron spectra were taken on gaseous hydrocarbons. The greater sensitivity afforded by our new position-sensitive detector made these studies feasible. The main goal was the characterization of satellite structure arising from electron shakeup and, in particular, the influence of π orbitals associated with double-bonded carbon. A more detailed report is given in this section.

Finally, plans were made with the help of F. A. Grimm,² G. S. Painter,³ D. Dill,⁴ and J. Dehmer⁵ to set up a program for calculating photoelectron cross sections as a function of the angle of the ejected photoelectrons, using molecular orbital methods employing χ_α scattering. These results will be used to compare our earlier results on

randomly oriented gas molecules and to evaluate the anticipated results on molecules preferentially orientated on the surface.

1. C. D. Wagner, *Faraday Discuss. Chem. Soc.*, in press.
2. Consultant to ORNL from the University of Tennessee, Knoxville.
3. Metals and Ceramics Division.
4. Boston University, Boston, Mass.
5. Argonne National Laboratory, Argonne, Ill.

ULTRAHIGH-VACUUM CHAMBER AND DATA SYSTEM FOR ELECTRON SPECTROSCOPY

T. A. Carlson W. B. Dress
F. H. Ward¹

Major modifications were made last year to the electrostatic analyzer. These consisted of construction of an ultrahigh-vacuum (uhv) chamber and photon sources and the development of a new data-taking system. (See Fig. 7.1 for an overall schematic of the spectrometer.) The new chamber is a stainless steel bakeable bell jar with 11 ports. The system is pumped with an NRC-4 diffusion pump which is carefully trapped with a Granville-Phillips double-wall nitrogen trap. The system is designed to operate in the low 10^{-10} torr region. An ion gun is employed for in-situ cleaning of the sample. The sample holder is manipulated in x , y , and z directions and may be rotated about its axis by 360° .

Two types of photon sources have been designed and built. They can be placed in different ports to direct

their beams at angles of 45° , 55° , 90° , and 135° to the direction of the ejected photoelectrons. Both photon sources can be used in the source chamber simultaneously. One photon source produces characteristic soft x rays. Its anode and thus the nature of the characteristic x rays can be varied. At present, a mixed silver-aluminum anode is being used. The aluminum K_α x rays are used in obtaining core-level photoelectron spectra, whereas the silver L x rays are useful for producing *KLL* Auger spectra of the third-row elements. The second photon source produces 21.22-eV radiation by means of a helium gas-discharge lamp. Triple differential pumping is used to reduce the amount of helium in the chamber. A special feature is a rotatable reflection-type polarizer using three gold mirrors, which should yield 90% polarization; the design is taken from Horton et al.²

Ejected photoelectrons are transferred to the entrance slit of the analyzer by means of a three-element lens. This arrangement has several advantages. First, having the sample at a large distance from the spectrometer slit

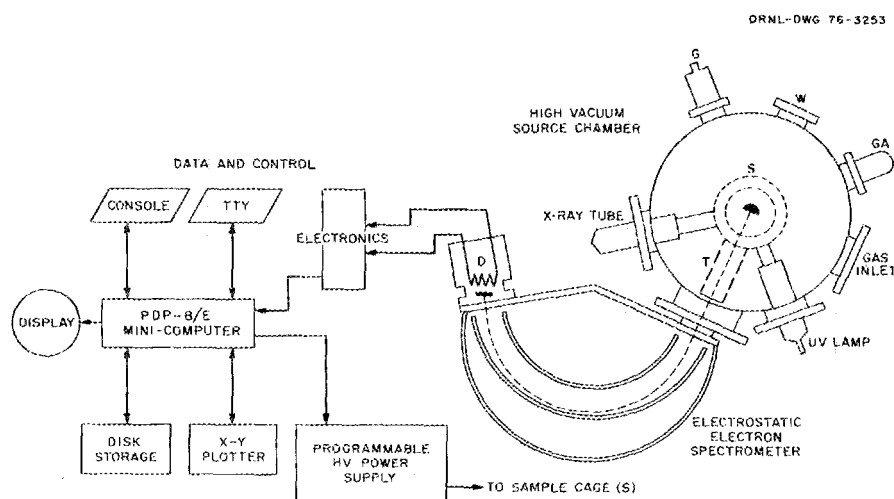


Fig. 7.1. Experimental arrangement. The schematic sketch of the source chamber shows the photon sources (x ray and uv), ion gun (G), window (W), ion gage (GA), transfer lens (T), and sample manipulator and source cage (S). The electrostatic analyzer indicates the relative position of the entrance slits and detector, with a typical electron orbit shown as a dotted line. A block diagram of the data-handling system depicts the major components of computer, detector electronics, disk storage, plotter, display scope, programmable power supply, and both Teletype terminals.

minimizes contamination from the spectrometer, which is not bakeable and is maintained at a pressure from 10^{-6} to 10^{-7} torr. Because of the small slit, the pressure in the uhv chamber can be maintained by differential pumping at 10^{-10} torr so long as direct line-of-sight contamination can be avoided. Second, the transfer lens also serves to accelerate or decelerate electrons to a constant voltage, which is of advantage in operating a position-sensitive detector. Third, the triple lens allows for efficient transfer of electrons even though the sample is set some distance back from the entrance, thus offering more room to manipulate the sample and the different photon sources.

Substantial improvement in data handling has also been achieved. A position-sensitive detector consisting of a channel-plate multiplier array³ and located at the focal plane of the electron spectrometer has been interfaced to a PDP-8/E minicomputer as shown in Fig. 7.1. A programmable power supply controlled by the computer determines the preacceleration of the electrons leaving the sample before they enter the spectrometer. Because the spherical-sector analyzing plates of the spectrometer are set to a predetermined voltage so that only electrons of a set energy are allowed to fall on the detector array, any portion of the spectrum may be selected, acquired, and stored for later analysis. The range in energy of each spectrum is about 5% of the kinetic energy of an analyzed electron and is distributed over 1024 data channels with a linearity of better than 2%.

A software system for on-line data acquisition and real-time control of the spectrometer has been developed, incorporating both direct experimenter control of the system as well as a "batch" capability that allows a set of instructions to be executed automatically without operator intervention. Various portions of the spectrum under study may be selected, counted for a predetermined live time, plotted on graph paper, displayed on the scope screen, and saved on the disk-storage device. A second Teletype terminal is devoted to any "background" tasks that will execute when the data system is momentarily idle. Such tasks could be the running of a Fortran program, development of other programs, and computing on previously acquired data.

In addition to the real-time system, a number of data-analysis programs in Fortran IV, Basic, and machine language are available. These programs allow correction of the energy scale, correction for detector response, peak integration, and data display and plotting. The system of programs is versatile and written with the outside user in mind. Changes to the system

are quick and easy to make, and a visiting worker could easily write his own special program using existing modules.

The complete spectrometer system, including high-vacuum source and data acquisition, has been tested, and a number of Auger spectra of the Mg-MgO system have been acquired and examined. The next phase is to explore surface orientation of adsorbed species using the polarized He I radiation. It is here that we expect the biggest benefit of our new data system to make itself felt in its ease and rapidity of handling the high counting rates and the many spectra we hope to obtain.

-
1. Plant and Equipment Division.
 2. V. G. Horton et al., *Appl. Opt.* **8**, 667 (1969).
 3. C. D. Moak et al., *J. Electron Spectrosc. Relat. Phenom.* **6**, 151 (1975).

STUDY OF SATELLITE STRUCTURE FOUND IN THE PHOTOELECTRON SPECTRA OF GASEOUS HYDROCARBONS

T. A. Carlson F. A. Grimm¹
W. B. Dress J. S. Haggerty²

Electron shakeup can occur in a molecule when an electron is suddenly ejected from a core level. This is manifested in the photoelectron spectrum by the appearance of satellite structure which occurs at a photoelectron energy lower than the main photoelectron peak by exactly the amount of excitation present in the electron-shakeup process. Electron shakeup is defined as the transferring of an electron (most probably an electron from the valence shell) into an excited bound state as the result of a sudden change in core potential.

It has been noted with unsaturated hydrocarbons in the solid phase that a rather sharp satellite peak is found at small energy separations from the main peak.³ It has been postulated that these peaks are due to the $\pi \rightarrow \pi^*$ transition involving the π orbital that results from the carbon-carbon double bond. In addition, the behavior of the low-excitation-energy peak with regard to relative excitation energy and intensity was correlated with properties of the carbon-carbon double bond. Because of the interest and importance of the solid-phase work, it is essential that the basic understanding of electron shakeup due to excitation of the π orbitals be examined with free molecules in the gas phase. Experimentally, photoelectron studies in the gas phase have a much better peak-to-background ratio, and contributions from characteristic energy losses can be determined and corrected. Theoretically, electron

shakeup calculations can be made using molecular orbital theory and can be compared directly with experiment.

We have carried out photoelectron studies using a magnesium K_{α} x-ray source on a group of unsaturated aliphatic hydrocarbons: ethylene, propylene, 1-butene, *trans*-2-butene, *cis*-2-butene, and butadiene, and for comparison, some saturated hydrocarbons: methane, propane, and cyclopropane. In each case, spectra were taken in the vicinity of the carbon 1s photoelectron peak. Studies were also made on CF_4 and furan. In each case, characteristic energy losses were determined by pressure studies and separate electron-impact measurements. During this work a similar investigation has been reported on gaseous benzene and some of its derivatives.⁴

Figure 7.2 shows two typical spectra of ethylene and propane. The dotted line gives the small contribution from inelastic collisions of photoelectrons passing through the gas. The satellite structure can be divided into two groups. One group is characterized by a relatively sharp peak at low excitation energy (about 6

to 8 eV) which is believed to result from the $\pi \rightarrow \pi^*$ transition and is usually from the highest-occupied to the lowest-unoccupied molecular orbital. In addition, there is a broad complex band that peaks at an excitation energy of about 20 eV and has a long tail. This satellite structure probably contains contributions from the excitation of σ orbitals and may also include contributions from electron shakeoff (transition to the continuum). The absence of a low-energy peak in propane as compared to ethylene is striking and gives confidence to the assignment of that peak to the carbon-carbon double bond.

In Table 7.1 are listed results on the intensities of the satellite structure. The broad excitation band is similar in each case, amounting to about 30% of the main peak. The sharp, low-energy excitation peak is found in each of the unsaturated hydrocarbons, and its intensity is roughly proportional to the ratio of the number of double bonds to the total number of carbon atoms in the molecule.

Theoretical calculations on the intensity of the $\pi \rightarrow \pi^*$ transition were made using the sudden approxi-

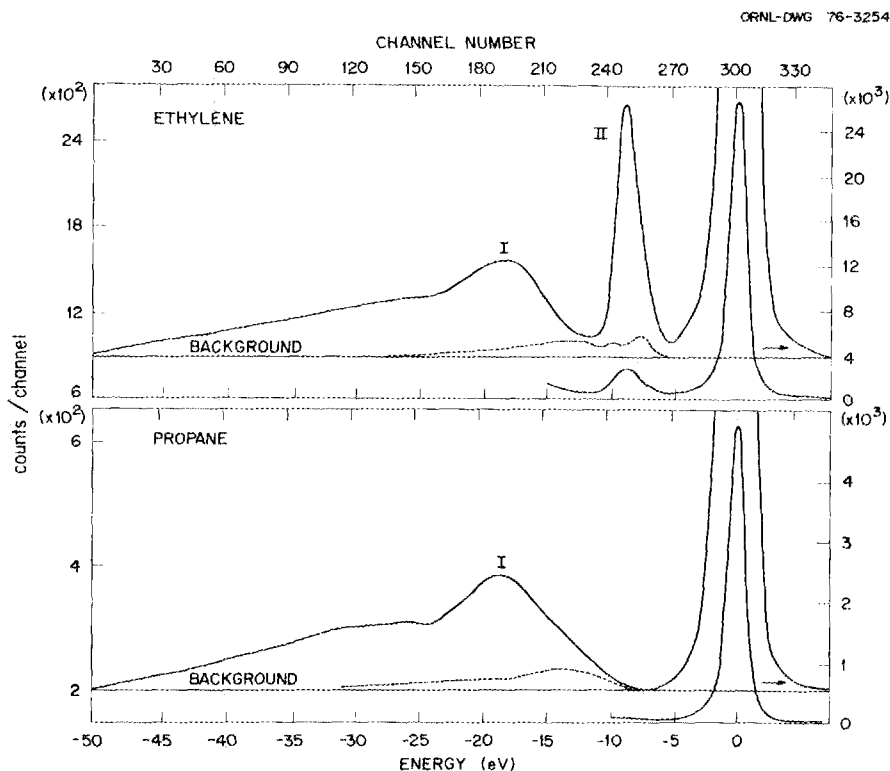
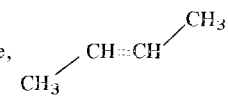
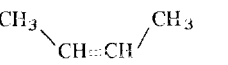


Fig. 7.2. Photoelectron spectra of ethylene and propane showing the satellite structure plotted as a function of kinetic energy relative to the main peak. Magnesium K_{α} x rays (1254 eV) were used as a photon source. The dotted curves are a measurement of the small contribution from inelastic collisions of the ejected photoelectrons passing through the gas samples as determined from electron-gun measurements. Regions I and II are as defined in Table 7.1.

Table 7.1. Intensity of satellite structure observed in the photoelectron spectra of gaseous hydrocarbons relative to main peak = 100

Molecule	Experimental		Theory ^c $\pi \rightarrow \pi^*$
	Region I ^a	Region II ^b	
Ethylene, H ₂ C=CH ₂	9.6	27.3	6.4
Propylene, H ₂ C=CH-CH ₃	6.7	31.4	4.1
1-Butene, H ₂ C=CH-CH ₂ -CH ₃	4.2	35.5	2.9
<i>trans</i> -2-Butene, 	4.8		2.8
<i>cis</i> -2-Butene, 	5.6		3.3
Butadiene, CH ₂ =CH-CH=CH ₂	15.6 (4.4) ^d	31.7	14.9 (8.1) ^d
Propane, CH ₃ -CH ₂ -CH ₃		33.7	

^aIntensity of low-excitation-energy satellite peak.

^bIntensity of higher-excitation-energy satellite band.

^cCalculation of low-energy $\pi \rightarrow \pi^*$ transitions, using Eq. (1) with CNDO/2 wave functions.

^dShows two distinct peaks; intensity of lower-excitation-energy peak given in parentheses.

mation, from which the transition probability to a given final state, $p_{i \rightarrow f}$, is taken as

$$p_{i \rightarrow f} = \left| \int \psi_f^* \psi_i d\tau \right|^2, \quad (1)$$

where ψ_i is the wave function for the initial neutral molecule, or, specifically, the frozen orbitals represented by that molecule with the provision that one electron from the 1s carbon shell has been removed, and ψ_f is the relaxed state of the ion with one electron missing from the 1s carbon shell. Equation (1) was solved by using CNDO/2 molecular orbitals and assuming that the final states can be approximated by using a nuclear charge of $Z+1$. No provision was made for coupling the unpaired spins. The comparison between theory and experiment in Table 7.1 is surprisingly good, considering the crudeness of the wave functions used. Furthermore, the calculations have not been normalized, which, when done, should bring the calculated values up slightly to even better agreement with theory. Specifically, the calculations showed that the shakeup due to $\pi \rightarrow \pi^*$ was substantial only when vacancies were created in the carbon attached to the double bond and that the transition rates were fairly independent of the molecule, thus confirming the observations that the intensities of the first satellite peaks were proportional to the relative number of

carbons associated with the double bonds. Butadiene has two double bonds and, curiously, also has two distinct peaks at low excitation energy in its photoelectron spectra. However, calculations show a much more complicated situation. Because, in butadiene there are two occupied π orbitals and two unoccupied π orbitals, a total of four different transitions are possible. In addition, a fairly intense transition was found involving σ orbitals which also appears in roughly the same energy range.

In conclusion, the sharp distinct satellite peak found in x-ray photoelectron spectra of unsaturated hydrocarbons can usually be attributed to the π orbital associated with the double-bonded carbons. With proper precaution, it would seem both legitimate and valuable to try to correlate the behavior of their satellite peaks with the double-bond behavior of molecules.

1. Consultant to ORNL from the University of Tennessee, Knoxville.

2. Oak Ridge Associated Universities Trainee, summer 1975, from Manhattan College, Bronx, N.Y.

3. D. T. Clark and D. B. Adams, *J. Electron Spectrosc. Relat. Phenom.* **7**, 401 (1975).

4. T. Ohta, T. Fujikawa, and H. Kuroda, *Chem. Phys. Lett.* **32**, 369 (1975).

HYPERFINE INTERACTIONS IN SOLIDS

F. E. Obenshain J. O. Thomson¹
 P. G. Huray¹ G. Pettit²
 C. M. Tung³

These investigations of hyperfine interactions in solids use experimental techniques of nuclear physics applied to solid-state physics and provide information about the environment of the atomic nucleus in metals, alloys, and compounds. Among these techniques are the Mössbauer effect, perturbed angular correlation (PAC), and time-differential perturbed angular correlation (TDPAC). These methods are complementary and give information about nuclear physics as well as solid-state physics. Together, these measurement techniques reflect in three distinct ways the changes in local behavior of the material under investigation. The electric monopole interaction (isomer shift) shows changes in the electronic charge density at the nucleus. The magnetic dipole interaction is a measure of the magnetic properties of the material, and the electric quadrupole interaction reflects the charge symmetry of the crystalline structure. When this information is combined with that from electron spectroscopy for chemical analysis (ESCA), neutron diffraction and inelastic scattering, magnetic susceptibility, and nuclear magnetic resonance data, a complete description of solids emerges.

Electron-Charge-Density Distributions Surrounding Impurity Atoms in Gold

Mössbauer isomer-shift measurements of ¹⁹⁷Au for 1-, 2-, and 4-at. % solid solutions of calcium, scandium, titanium, vanadium, chromium, manganese, iron, cobalt, nickel, copper, zinc, gallium, germanium, silver, cadmium, indium, tin, and antimony with high-purity gold have been extrapolated to 0 at. % to determine the influence of single impurities upon the electronic conduction band of gold. The screening "cloud" of electrons distributed about the impurities has been interpreted through a phase-shift analysis of electron scattering by a perturbation potential

$$V(\mathbf{r} - \mathbf{r}_j) = V_{\text{impurity}}(\mathbf{r} - \mathbf{r}_j) - V_{\text{Au}}(\mathbf{r} - \mathbf{r}_j)$$

located at the impurity site \mathbf{r}_j . Following the classical nuclear physics technique we have chosen to parameterize the impurity potential by assuming it to have the form of a square well of radius a (0.5 of the gold near-neighbor distance) and of variable depth depending on the angular momentum and spin of the incident

scattered electron of the gold conduction band. This technique has been used by Friedel and others to show that the residual electrical resistivity $1/\sigma$ brought about by 1 at. % of the impurities may be expressed in terms of the phase shift $\delta_l(k_F)$ of the incident wave function when evaluated at the gold Fermi level through

$$\frac{1}{\sigma} = \frac{2h}{e^2 k_F} \sum_{l=0}^{\infty} (l+1) \sin^2 [\delta_l(k_F) - \delta_{l+1}(k_F)] .$$

The expression is modified slightly for spin-dependent δ_l . It has also been demonstrated that preservation of electrical charge neutrality in a large sphere about the impurity requires that the various $\delta_l(k_F)$ satisfy the sum rule

$$N = \frac{2}{\pi} \sum_{l=0}^{\infty} (2l+1) \delta_l(k_F) ,$$

where N is the nominal charge difference Δz between the impurity and gold atoms. (We also correct for local lattice strains.)

We have extended these calculations to account for the incremental change in electron charge density at the 12 near-neighbor gold nuclei, at the 6 second-near-neighbor gold nuclei, etc. We then interpret changes in the Mössbauer isomer shift of the ¹⁹⁷Au nuclei (after volume corrections) as the average influence brought about by the presence of the impurity scattering "cloud."⁴ Residual electrical resistivity measurements, the excess nuclear charge Ne to be screened (the local magnetic moment), and the Mössbauer scattering measurements all extrapolated to $T = 0^\circ\text{K}$ thus provide an interpretation of three (four) unknown phase shifts that must satisfy three (four) simultaneous transcendental equations. We have done this for all impurities studied here and present the results in terms of the total scattered charge surrounding each impurity in terms of the various angular momenta and spin. Figure 7.3 shows the resulting variation of this fractional charge for the case of no local magnetic moment at $T = 0^\circ\text{K}$, that is, only s , p , and d types of scattered charge. The results are given relative to the electronic angular-momentum character of the conduction band of pure gold. (If this band is assumed to have pure s character, one s electron should be added to the values shown.) For comparison we have included in Fig. 7.3 the electronic states expected for a free atom of the impurity.

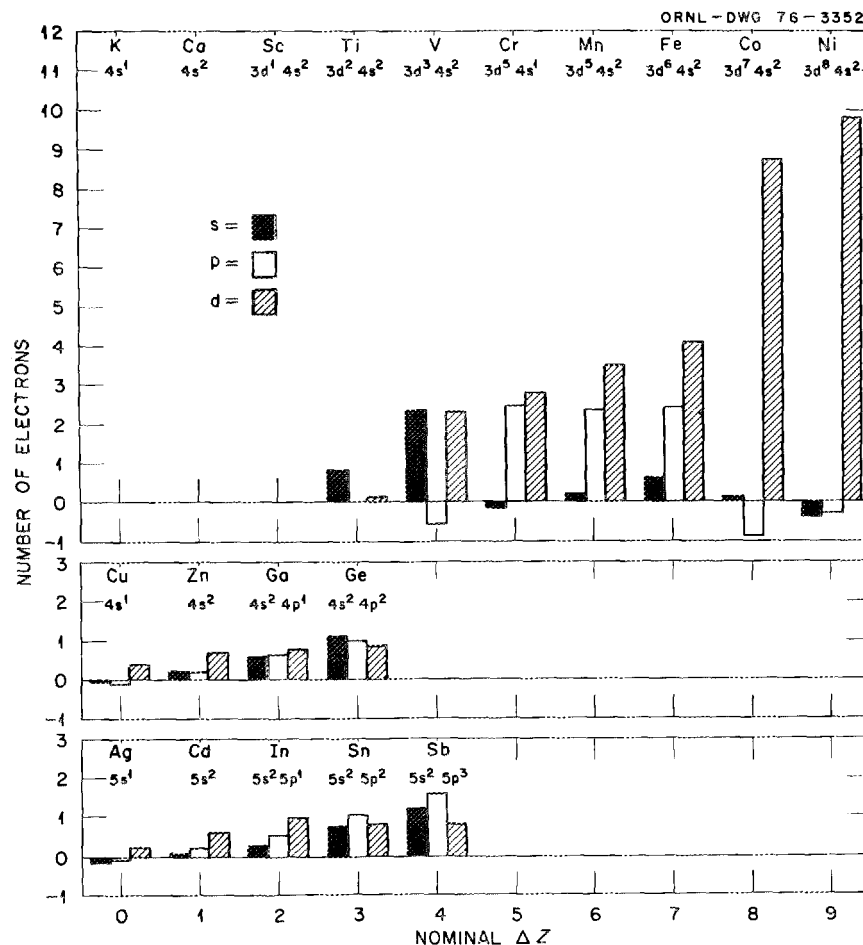


Fig. 7.3. Measured fractional s , p , and d charge of the electronic screening "cloud" about various impurities in pure gold metal at $T = 0^\circ\text{K}$. The results are given relative to the electronic angular momentum character of the pure-gold conduction band. The free-atom states expected for each impurity are given for comparison only.

Valence States of BaFeO_x

Barium ferrate^{5,6} and strontium ferrate⁷ are the only two known compounds of iron that exhibit ionic properties corresponding to Fe^{4+} and Fe^{6+} as well as Fe^{3+} . Samples of these compounds were prepared by a new technique⁸ here at ORNL, and the hyperfine interactions were studied by the Mössbauer effect. The electronic charge densities for these three ionic states have been calculated, and they indicate increasing charge density with increasing valence. With respect to pure iron, the isomer shift should become more negative the higher the valence state. This is observed experimentally; however, the relative magnitudes of the isomer shifts show that there is considerable covalent mixing for the three valence states.

The method of sample preparation used here was to react barium hydroxide and iron oxide in a high-

pressure-steam environment and to observe the hydrogen released. From this information an estimate of Fe^{4+} could be obtained. The use of the Mössbauer technique serves to identify the oxidation states present in the reacted sample.

The Mössbauer spectra showed that the three expected valence states were present in freshly prepared samples of BaFeO_x . The most negative isomer shift is taken to be BaFeO_4 for Fe^{6+} and, for the most positive, $2\text{BaO} \cdot \text{Fe}_2\text{O}_3$ for Fe^{3+} and BaFeO_3 for the Fe^{4+} that appears in between. The relative amounts of three charge states assuming similar recoilless fractions are 20% Fe^{5+} , 40% Fe^{4+} , and 40% Fe^{6+} . This is rather surprising, considering the difficulty in preparing Fe^{6+} .

When exposed to the atmosphere, the samples used showed a slow transition to an almost pure BaFeO_3 Fe^{4+} state, which then appears to be stable. The transformation of the Fe^{6+} to Fe^{4+} is to be expected

from energetics. However, the transformation of the Fe^{3+} to Fe^{4+} is not to be expected. Any other interpretation of our results would require unrealistic assumptions, for example, about the electric quadrupole interaction.

Electric Quadrupole Interaction at ^{161}Dy in Gd_2O_3

We have applied the time-differential perturbed angular correlation (TDPAC) and Mössbauer techniques to measure the electric quadrupole interaction at ^{161}Dy in Gd_2O_3 . Two previous Mössbauer effect studies of ^{161}Dy in Gd_2O_3 have been reported. In the first experiment a complex emission spectrum was observed, and this was interpreted in terms of two electric-field-gradient tensors, the larger having an interaction energy of ~ 1000 MHz.⁹ In the second experiment a unique electric field gradient was obtained with an electric quadrupole frequency of 485 MHz.¹⁰

For the present measurements with the TDPAC method a distribution of electric-field-gradient tensors was used to fit our data at both 20° and 650°C . With this model an average value for the field and an associated width is obtained from the experimental data. At room temperature (20°C) the average electric quadrupole frequency was ~ 557 MHz with a width of ~ 180 MHz. When the temperature was raised to 650°C the frequency decreased to ~ 235 MHz, whereas the width of the distribution increased to ~ 582 MHz.

The Mössbauer measurement at room temperature yielded a result that is consistent with this distribution-of-fields model. The source for the Mössbauer measurement is Gd_2O_3 that has been irradiated in the reactor to produce $^{161}\text{Dy}^*$ as in the TDPAC measurement. For the absorber we have used an ordered 50-at. % DyCu intermetallic compound. The alloy has cubic symmetry, and no electric field gradients are expected. The Mössbauer spectra tend to substantiate but do not prove this conclusion.

The Gd ions in Gd_2O_3 occupy two different types of lattice sites, and a unique electric field gradient would not be expected.

5. P. Gallagher, J. MacChesney, and D. Buchanan, *J. Chem. Phys.* **43**, 516 (1965).
6. V. Panyushkin, G. DePasquali, and H. Drickamer, *J. Chem. Phys.* **51**, 3305 (1969).
7. P. Gallagher, J. MacChesney, and D. Buchanan, *J. Chem. Phys.* **41**, 2429 (1964).
8. C. Bamberger, Chemistry Division.
9. V. Sklyarevsky et al., *Phys. Lett.* **6**, 157 (1963).
10. S. Mørup and G. Trumpp, *Phys. Status Solidi* **40**, 759 (1970).

RADIO-FREQUENCY SURFACE RESISTANCE OF LEAD NEAR THE CRITICAL TEMPERATURE

J. R. Thompson¹ C. M. Jones

Introduction

We are investigating the rf surface resistance, R_s , of lead up to and beyond the superconducting critical temperature, $T_c = 7.20^\circ\text{K}$. The work has been done using a lead-plated, helically loaded cavity constructed largely of OFHC copper.² The fundamental frequency of the cavity is $f_1 = 137$ MHz; most of the measurements reported here were performed at the second harmonic, $f_2 = 229$ MHz. To the best of our knowledge, this is the first detailed examination of surface resistance near T_c for a high-quality lead surface, particularly at comparatively low measurement frequencies. The objectives of this work are (1) to examine the critical-point behavior of R_s for superconducting lead, (2) to compare the results of theoretical calculations within the BCS framework with experiment for the temperature region where $T/T_c \gtrsim 0.5$ and to obtain the resulting material parameters for lead, and (3) to examine R_s in the anomalous resistance regime, $T > T_c$.

Previous experimental studies of R_s have concentrated on the low-temperature region, typically $T/T_c \lesssim 0.5$, where the experimental values, R_{expt} , can be described by

$$R_{\text{expt}} = R_{\text{BCS}} + R_{\text{res}}.$$

Here R_{BCS} is the temperature-dependent theoretical surface resistance, calculable^{3,4} as a function of the electronic mean free path l , the London penetration depth λ_L , the superconducting gap Δ , and the coherence length ξ_F ; R_{res} is an additional, temperature-independent residual resistance whose magnitude depends on the quality of the surface being studied. To within an additive constant, the agreement with theory is satisfactory for the low-temperature region.

At higher temperatures, however, it is important to establish the range of validity for the theory. For

1. Consultant to ORNL from the University of Tennessee, Knoxville.

2. Consultant to ORNL from Georgia State University, Atlanta.

3. Graduate student from the University of Tennessee, Knoxville.

4. Details of the model have been reported in *Phys. Div. Annu. Prog. Rep. Dec. 31, 1974*, ORNL-5025 (1975), p. 214.

example, as $T \rightarrow T_c$, the superconducting energy gap Δ is no longer constant but decreases from its low-temperature value and eventually vanishes at $T = T_c$. Experimentally, this behavior makes it desirable to measure R_s at a comparatively low frequency f as in this work, because direct absorption is caused by the breaking of Cooper pairs when $hf > 2\Delta$.

Experimental Measurements

The rf cavity and transmission lines were situated in a well-insulated dewar constructed of fiberglass and aluminum. To avoid the presence of significant external magnetic fields, the region near the cavity was shielded from the earth's magnetic field.

The temperature of the cavity was determined using a calibrated germanium resistance thermometer mounted on the exterior surface of the cavity. The resistance was measured using a constant current supply and a four-wire potentiometric technique. To verify that the resistor was calibrated accurately, it was checked where possible against the vapor pressure of ^4He , that is, $T < 5.2^\circ\text{K}$. Measurements of R_s below 5.2°K were performed by pressurizing the dewar up to pressures of ~ 1720 torr. Measurements above 5.2°K were performed by allowing the cavity to drift up in tempera-

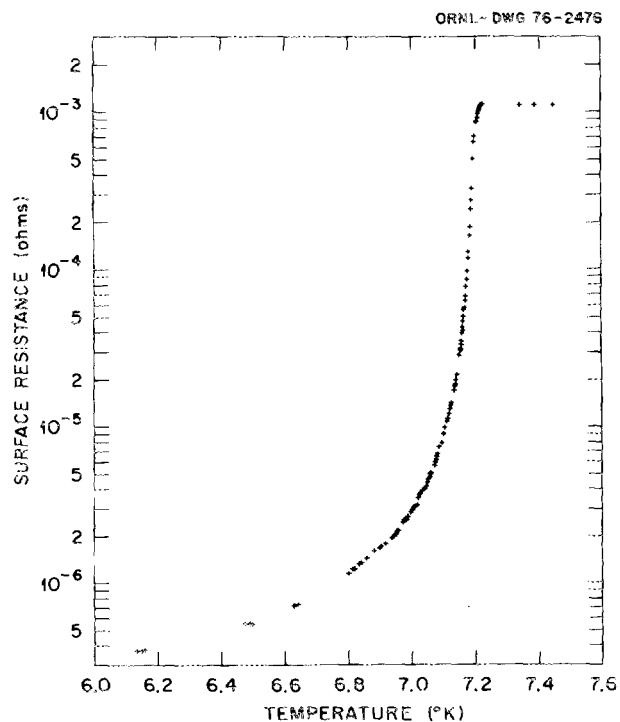


Fig. 7.4. The rf surface resistance of lead vs temperature T . The frequency is 229 MHz.

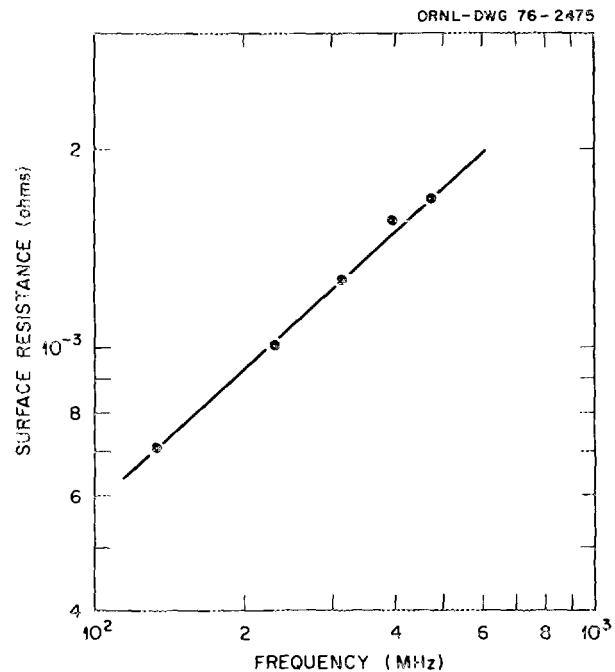


Fig. 7.5. The low-temperature normal-state surface resistance of lead vs frequency f . The line is a least-squares fit to the data, with $R_n = Af^\alpha$, $\alpha = 0.685 \pm 0.012$.

ture with only gaseous helium in the dewar. Details of the measurement technique have been described elsewhere.²

Discussion

In Fig. 7.4, the surface resistance R_s at $f_2 = 229$ MHz is plotted logarithmically vs temperature T . Just below $T_c = 7.20^\circ\text{K}$, the variation is very rapid. There, R_s increases by three orders of magnitude in an interval of $\sim 0.3^\circ\text{K}$ and by one decade in an interval of 0.03°K . This region of extremely rapid change is being analyzed in terms of the scaling laws and critical exponents as widely applied in critical phenomena.⁵ For the entire temperature range, the BCS expressions are being numerically evaluated.

At T_c the surface resistance abruptly changes slope and becomes nearly temperature-independent. Just above T_c , normal-state lead is in the anomalous resistance regime where the electronic mean free path l is comparable with the rf skin depth δ . When $l/\delta \rightarrow \infty$ the surface resistance approaches the extreme anomalous limit R_∞ . The normal-state surface resistance R_n , which is within a factor of 2 to 3 of R_∞ , has been measured as a function of frequency f . This is plotted as a function of frequency in Fig. 7.5. The line is a least-squares fit to the data of the equation $R_n = Af^\alpha$,

where $\alpha = 0.685$ with a standard deviation of 0.012. This value of α is surprising because, although the material is in the anomalous resistance regime, it is near the classical limit where α should equal $1/2$.^{6,7} We therefore infer an apparent weak frequency dependence in the electrical conductivity. Using R_n with reported values⁶⁻⁸ of R_∞ and σ/l , the mean free path at T_c^+ may be determined. We obtain $l \approx 0.53 \mu\text{m}$, thereby determining experimentally one of the material parameters needed for evaluation of the BCS expressions for surface resistance.

In conclusion, the surface resistance varies extremely rapidly with temperature near, but below, the critical temperature. Above T_c , the behavior is temperature-independent and yields values for the low-temperature mean free path.

1. Consultant from the University of Tennessee, Knoxville.
2. J. P. Judish, unpublished thesis, University of Tennessee, Knoxville, 1974.
3. D. C. Mattis and J. Bardeen, *Phys. Rev.* **111**, 412 (1958).
4. A. A. Abrikosov, L. P. Gor'kov, and I. M. Khalatnikov, *Sov. Phys. JETP (Engl. Transl.)* **35**, 182 (1959).
5. H. E. Stanley, *Introduction to Phase Transitions and Critical Phenomena*, Oxford Press, England, 1971.
6. G.E.H. Reuter and E. H. Sondheimer, *Proc. R. Soc. A* **195**, 336 (1948).
7. R. G. Chambers, *Proc. R. Soc. A* **215**, 481 (1952).
8. T. E. Faber and A. B. Pippard, *Proc. R. Soc. A* **231**, 336 (1955).

HIGH-RESOLUTION MICROSCOPY PROGRAM

R. E. Worsham W. W. Harris

In the hope of eliminating the high-voltage discharges that led to destruction of the field-emitter (FE) tips in the high-coherence microscope, the gun was rebuilt. The bushing was replaced with a ten-step accelerating tube and each of the 5.08-cm-long anode I--anode II insulators was replaced with two 2.54-cm units. Conditioning of the entire gun to 200 kV was possible.

To further protect the very delicate FE emitters and increase the reliability of the gun, a vacuum lock was added which permits exchange of emitters without loss of the ultrahigh vacuum. In addition, the emitter may be withdrawn from the gun into the lock for protection during high-voltage conditioning. A lock chamber pressure of 10^{-7} to 10^{-8} torr is adequate with the 1.59-cm opening into the gun chamber.

Following these modifications to the gun, the column was put back in operation with specimen used, first of all, to determine the capability of the microscope. With

thin ($<50\text{-\AA}$) carbon films, micrographs were obtained which showed, using an optical transform, that information corresponding to a resolution $<2 \text{ \AA}$ was present. Lattice images of K_2PtCl_4 crystallites were directly visible on the screen. A nearly continuous array of lattice images with about 30- to 40- \AA major dimension was observed in a thin carbon film. The half spacing of the lines measured 1.55 to 1.60 \AA . Apparently, neither fringes such as these nor comparable optical transforms have been obtained with other microscopes.

Further comparison of the high-coherence microscope with two commercial microscopes was made for the appearance of the image on the screen using identical (and/or same batches of) specimens. The contrast and resolution of the high-coherence column were markedly superior. Before further application of the microscope could be made, however, the funds were exhausted. All work was stopped temporarily. Near the end of this report period, work began anew to get the microscope back into operation.

INFRARED SPECTRA OF SO_3F^- AND $\text{SO}_3(\text{OH})^-$ IN SOLID SOLUTION

H. W. Morgan P. A. Staats

A study of the monovalent ions SO_3F^- and $\text{SO}_3(\text{OH})^-$ followed attempts to resolve isotopic structure in the spectrum of divalent SO_4^{2-} . The vibrational absorption bands of divalent ions in alkali-halide solid solutions are relatively broad, even at low temperatures. This is believed to arise from the random position of the vacancy necessary for charge compensation in a lattice of monovalent ions. Use of a divalent cation does produce narrow SO_4^{2-} absorption lines, but normally a complex is formed which lowers the symmetry and removes the degeneracy of the SO_4^{2-} normal modes of vibration.

The ions SO_3F^- and $\text{SO}_3(\text{OH})^-$ are similar, F^- and OH^- both being strongly electronegative and compa-

Table 7.2. Vibrational absorption frequencies of SO_3F^- and $\text{SO}_3(\text{OH})^-$ in solid solution (in cm^{-1})

Vibration	SO_3F^-		$\text{SO}_3(\text{OH})^-$	
	KBr	KI	KBr	KI
$\nu_1(A_1)$	1081	1074	1065	1058
$\nu_2(A_1)$	739	735	884	
$\nu_3(A_1)$	576	562	586	579
$\nu_4(E)$	1307	1297	1275	1262
$\nu_5(E)$	585	582	597	592
$\nu_6(E)$		414	413	

Table 7.3. Isotopic shift observed in spectrum of SO_3F^- in KBr matrix at 77°K

Isotope	$\nu_2(A_1)$	$\nu_4(E)$
^{32}S	737.0	1297.0
^{33}S	731.0	1288.0
^{34}S	726.5	1279.5

rable in mass. We have considered the $(\text{O}-\text{H})^-$ stretch and $-(\text{OH})^-$ bend distinct from the vibrations of the SO_3X group. The observed frequencies, shown in Table 7.2, indicate that this is a good approximation. The solid-solution bands show the expected narrow half widths, which could only be estimated at room temperature because of the presence of bands from excited vibrational states. At 77°K , the half widths are 2 cm^{-1} or less. At the lower temperature the vibrational bands involving isotopic sulfur atoms can be easily distinguished with the intensity ratio of approximately 100:5:1. The frequencies observed for SO_3F^- are given in Table 7.3.

The ions SO_3F^- and $\text{SO}_3(\text{OH})^-$ readily form solid solutions in KBr and KI. Solution in KCl, NaBr, and NaCl is more difficult due to the size of the ion. Solid solutions were normally prepared by heating the appropriate salt, in intimate contact with the alkali halide, at temperatures up to 150°C . At about 190°C , $\text{SO}_3(\text{OH})^-$ decomposes in the matrix to give SO_2 , SO_3 , and H_2O . The ion SO_3F^- is stable but above 250°C reacts with traces of moisture.

Earlier spectroscopic work had been performed on alkali salts of these two ions; Raman studies were made of aqueous solutions and infrared studies were made of the pure salt. Our work included laser Raman spectra of the pure salt for comparison. We confirm the assignments of Siebert¹ and disagree with the data of Walrafen, Irish, and Young,² while obtaining more precise frequencies and the first data on isotopic shifts.

1. H. Siebert, *Z. Anorg. Allg. Chem.* **289**, 15 (1957).

2. G. E. Walrafen, D. E. Irish, and T. F. Young, *J. Chem. Phys.* **37**, 662 (1962).

HELIUM IMPLANTATION IN POTENTIAL FIRST-WALL CTR MATERIALS

J. A. Horak¹ R. L. Auble
M. J. Saltmarsh J. W. Woods¹
C. K. Thomas¹

Fusion-reactor first-wall materials will be subjected to intense fluxes of energetic neutrons ($E_n \approx 14\text{ MeV}$)

which will induce much higher nuclear transmutation rates than can normally be attained in fission-reactor irradiations. The one exception occurs for nickel-containing alloys irradiated in a mixed fast-thermal-flux reactor [e.g., the High-Flux Isotope Reactor (HFIR) or the Oak Ridge Research Reactor (ORR)]. In this case the two-step reaction $^{58}\text{Ni}(n,\gamma)^{59}\text{Ni}(n,\alpha)^{56}\text{Fe}$ results in helium production rates similar to those expected for a fusion reactor. Fortunately, not only is helium regarded as the most important transmutation product from the radiation-damage standpoint, but early fusion reactors will almost certainly use stainless steel as a first-wall material. Fission irradiations will therefore provide the CTR program with information applicable to these early devices. Eventually, however, stainless steels may be superseded by one of the refractory metals, for which the helium generation rates in fission reactors are far too low. The effect of helium must be examined by preinjection of the samples before irradiation. For such a simulation procedure to be validated, correlation experiments are required to compare the postirradiation properties of samples that have been preinjected with helium and then irradiated with those of samples in which the helium and displacement damage have been produced simultaneously.

We are currently engaged in a program that includes both correlation experiments with stainless steels and the investigation of some refractory-metal alloys. For the preinjection of helium we have used the 60-MeV alpha beam from ORIC, employing a rotating wedge and scanning the specimen holder across the beam to ensure uniform helium deposition throughout the specimens. Figure 7.6 shows one of the specimen holders. An array of tensile specimens, a few of which are shown in the foreground, is backed by a thin sheet of some other metal of interest behind which cooling water is flowing. Helium is deposited both in the tensile specimens and in the backing sheet, from which an equal number of tensile specimens can be obtained.

Helium levels of 60 to 200 appm, which are relevant to those anticipated for early CTRs such as EPR-1, have been implanted in 300 tensile samples of type 316 stainless steel, Nimonic PE-16, V-20 wt % Ti, and V-15 wt % Cr-5 wt % Ti. Forty-seven of these samples combined with 27 samples containing no helium are currently under irradiation in EBR-II to produce the dpa (displacement per atom) levels relevant to early CTRs. An additional 115 tensile samples containing helium and 125 with no helium will be placed under irradiation in EBR-II in 1976. Included in these 125 are samples of the two vanadium alloys containing different amounts of cold work, which is a parameter that has

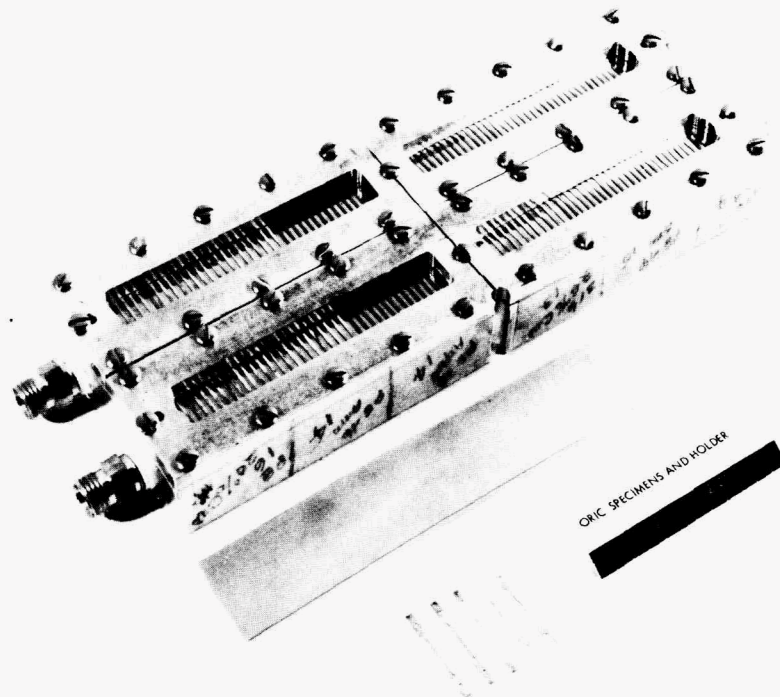


Fig. 7.6. Water-cooled specimen holder used to inject helium into tensile and sheet specimens of various alloys.

not been studied in previous irradiations of these alloys. The postirradiation mechanical properties of the 316 SS and the PE-16 samples will be compared with those of companion samples that have been irradiated at the same temperature and to the same helium and dpa levels in ORR. The correlation obtained by this comparison will provide valuable information on the use of helium preinjection followed by fast-neutron irradiation for studying the swelling and postirradiation mechanical properties of refractory-metal alloys that contain helium and dpa levels relevant to CTR applications.

Twenty-six tube samples of these alloys have also been implanted with helium (up to 60 appm). The tubes will be pressurized to produce stresses of the magnitude anticipated in the first wall of early CTRs and then irradiated in EBR-II. One-half of the tube length does not contain helium. Comparing the creep and fracture behavior of the two sections of the tubes will provide information on the effect of helium on the deformation processes in these alloys during and after irradiation.

1. Metals and Ceramics Division.

8. Publications

Prepared by Wilma L. Stair

The following listing of publications includes primarily those articles by Physics Division staff members and associates which have appeared in print during 1975. It is not possible to include open-literature publications for the entire calendar year, however, as some journals for 1975 will be received only after this report has gone to press; thus, five open-literature publications not previously reported in an annual report are included, and a few 1975 articles yet to be published will be listed in the annual report for the period ending December 31, 1976.

BOOK, JOURNAL, AND PROCEEDINGS ARTICLES

- Alexeff, I., H. Tamagawa, C. M. Jones, and P. D. Miller "Use of the Hot-Electron Minor Machine INTEREM as a High-Z Ion Source," *IEEE Trans. Plasma Sci.* (Proceedings Second IEEE International Conference on Plasma Science, Ann Arbor, Mich., May 1975) **PS-4B1**, 88 (1975).
- Allen, B. J., J. W. Boldeman, M. J. Kenny, A. R. Musgrove, H. Pe, and R. L. Macklin, "Neutron Capture Mechanism in Light and Closed Shell Nuclides," pp. 360–62 in vol. 1 of *Nuclear Cross Sections and Technology* (Proceedings of Conference, Washington, D.C., March 1975), R. A. Schrack and C. D. Bowman, Eds., National Bureau of Standards, 1975.
- Allen, B. J., A. R. de L. Musgrove, D. M. Chan, and R. L. Macklin, "Neutron Capture Cross Sections of the Calcium and Barium Isotopes," p. 275 in *Proceedings Kiev Conference on Neutron Physics, Kiev, U.S.S.R., May–June 1973*, Obninsk, U.S.S.R., 1974.
- Alton, G. D. (invited paper), "Ion Sources for Accelerators," pp. 11–30 in vol. 1 of *Proceedings Third Conference on Application of Small Accelerators, Denton, Tex., October 1974*, ERDA CONF-741040-P1, ERDA Technical Information Center, Oak Ridge, Tenn., 1975.
- Alton, G. D., "Review of the Heavy Ion Source Research and Development Program at the Oak Ridge National Laboratory," *IEEE Trans. Plasma Sci.* (Proceedings Second IEEE International Conference on Plasma Science, Ann Arbor, Mich., May 1975) **PS-4B1**, 88 (1975).
- Alton, G. D., J. A. Biggerstaff, L. Bridwell, C. M. Jones, Q. Kessel, P. D. Miller, C. D. Moak, and B. Wehring, "Absolute Charge State Yields of 20-MeV I Ions Scattered from Argon and Xenon," *IEEE Trans. Nucl. Sci.* (Proceedings 1975 Particle Accelerator Conference, Washington, D.C., March 1975) **NS-22**, 1685–89 (1975).
- Anastasio, M. R., T.T.S. Kuo, and J. B. McGrory, "Vertex-Function Approximations in the AHK Algorithm for the Effective Interaction," *Phys. Lett.* **57B**, 1–6 (1975).
- Appleton, B. R., J. A. Biggerstaff, T. S. Noggle, S. Datz, C. D. Moak, M. D. Brown, H. F. Krause, R. H. Ritchie, and V. N. Neelavathi, "Radiative Electron Capture by Channeled Oxygen Ions," pp. 499–507 in vol. 2 of *Proceedings Fifth International Conference on Atomic Collisions in Solids, Gatlinburg, Tenn., September 1973*, S. Datz, B. R. Appleton, and C. D. Moak, Eds., Plenum Press, New York, 1975.
- Artna-Cohen, Agda, "Nuclear Data Sheets for $A = 183$," *Nucl. Data Sheets* **16**, 267–316 (October 1975).
- Arvieux, J., M. Buenerd, A. J. Cole, P. de Saintignon, G. Perrin, and D. J. Horen, "Giant Resonances in f - p Shell Nuclei Studied by Inelastic Scattering of 80-MeV ^3He Ions," *Nucl. Phys.* **A247**, 238–50 (1975).

- Auble, R. L., "Nuclear Data Sheets for $A = 63$," *Nucl. Data Sheets* **14**, 119–53 (February 1975).
- Auble, R. L., "Nuclear Data Sheets for $A = 61$," *Nucl. Data Sheets* **16**, 1–24 (September 1975).
- Auble, R. L., "Nuclear Data Sheets for $A = 65$," *Nucl. Data Sheets* **16**, 351–82 (November 1975).
- Auble, R. L., "Nuclear Data Sheets for $A = 66$," *Nucl. Data Sheets* **16**, 383–416 (November 1975).
- Auble, R. L., "Nuclear Data Sheets for $A = 67$," *Nucl. Data Sheets* **16**, 417–44 (November 1975).
- Auchampaugh, G. F., J. Halperin, R. L. Macklin, and W. M. Howard, "Kilovolt $^{33}\text{S}(n,\alpha)$ and $^{33}\text{S}(n,\gamma)$ Cross Sections: Importance in the Nucleosynthesis of the Rare Nucleus ^{36}S ," *Phys. Rev. C* **12**, 1126–33 (1975); also, LA-UR-75-494.
- Avignone, F. T., III and S. Raman, "Internal Conversion Studies in ^{144}Nd ," *Phys. Rev. C* **12**, 963–66 (1975).
- Bair, J. K., J. A. Biggerstaff, C. M. Jones, J. D. Larson, J. W. McConnell, W. T. Milner, and N. F. Ziegler, "Design Considerations for the ORNL 25-MV Tandem Accelerator," *IEEE Trans. Nucl. Sci.* (Proceedings 1975 Particle Accelerator Conference, Washington, D.C., March 1975) **NS-22**, 1655–58 (1975).
- Baker, K. R., J. H. Hamilton, J. Lange, A. V. Ramayya, L. Varnell, V. Maruhn-Rezwani, J. J. Pinajian, and J. A. Maruhn, "Magnetic Properties of ^{166}Er and the Collective Mode," *Phys. Lett.* **57B**, 441–44 (1975).
- Ball, J. B., C. B. Fulmer, E. E. Gross, M. L. Halbert, D. C. Hensley, C. A. Ludemann, M. J. Saltmarsh, and G. R. Satchler, "Heavy Ion Elastic Scattering Survey, I: ^{208}Pb Target," *Nucl. Phys.* **A252**, 208–36 (1975).
- Ball, J. B., O. Hansen, J. S. Larsen, D. Sinclair, and F. Videbaek, " ^{16}O Induced One-Nucleon Transfer Reactions on Targets of ^{26}Mg , ^{27}Al , ^{30}Si , and ^{48}Ca ," *Nucl. Phys.* **A244**, 341–64 (1975).
- Barnett, C. F., "Atomic and Nuclear Cross Section Needs for the Controlled Thermonuclear Research Program," pp. 253–58 in vol. 1 of *Proceedings of Third Conference on Application of Small Accelerators, Denton, Tex., October 1974*, ERDA CONF-741040-P1, ERDA Technical Information Center, Oak Ridge, Tenn., 1975.
- Barrett, J. H., B. R. Appleton, T. S. Noggle, C. D. Moak, J. A. Biggerstaff, S. Datz, and R. Behrisch, "Hyperchanneling," pp. 645–68 in vol. 2 of *Proceedings of the Fifth International Conference on Atomic Collisions in Solids, Gatlinburg, Tenn., September 1973*, S. Datz, B. R. Appleton, and C. D. Moak, Eds., Plenum Press, New York, 1975.
- Barrett, B. R., E. C. Halbert, and J. B. McGrory, "Hidden Configurations and Effective Interactions: A Comparison of Three Different Ways to Construct Renormalized Hamiltonians for Truncated Shell-Model Calculations," *Ann. Phys.* **90**, 321–90 (1975).
- Becker, R. L. (invited paper), "Computation of the Reaction Matrix, G," pp. 96–118 in *Effective Interactions and Operators in Nuclei* (Proceedings of Tucson International Topical Conference on Nuclear Physics, Tucson, Arizona, June 1975), B. R. Barrett, Ed., Springer-Verlag, New York, 1975.
- Becker, R. L. and J. P. Svenne, "Interpretation of Inversions of Single-Particle Levels in Self-Consistent Field Theories," *Phys. Rev. C* **12**, 2067–71 (1975).
- Bendjaballah, N., J. Delaunay, and H. J. Kim, "High-Spin Yrast Cascade in ^{56}Co ," *Nucl. Phys.* **A244**, 322–28 (1975).
- Benjamin, R. W., C. E. Ahlfeld, J. A. Harvey, and N. W. Hill, "Neutron Total Cross Section of ^{248}Cm ," *Nucl. Sci. Eng.* **55**, 440–49 (1974).
- Bingham, H. G., M. L. Halbert, D. C. Hensley, E. Newman, K. W. Kemper, and L. A. Charlton, "Mirror States in $A = 15$ from 60-MeV ^6Li Induced Reactions on ^{12}C ," *Phys. Rev. C* **11**, 1913–23 (1975).
- Boldeman, J. W., B. J. Allen, A. R. de L. Musgrove, and R. L. Macklin, "Valence Component in the Neutron Capture Cross Section of ^{90}Zr ," *Nucl. Phys.* **A246**, 1–20 (1975).
- Boldeman, J. W., B. J. Allen, A. R. de L. Musgrove, and R. L. Macklin, "The Neutron Capture Cross Section of Natural Silicon," *Nucl. Phys.* **A252**, 62–76 (1975).
- Bugg, W. M., G. T. Condo, E. L. Hart, and H. O. Cohn, "Charge Exchange of Secondary Pions Produced by Slow Hadron Absorption in Complex Nuclei," *Phys. Rev. Lett.* **35**, 611–12 (1975).

- Burrows, T. W. and R. L. Auble, "Nuclear Data Sheets for $A = 144$," *Nucl. Data Sheets* **16**, 231–65 (October 1975).
- Carlson, G. H., W. L. Talbert, Jr., and S. Raman, "Nuclear Data Sheets for $A = 116$," *Nucl. Data Sheets* **14**, 247–96 (1975).
- Carlson, T. A., "The Nature of Secondary Electrons Created as the Result of Electron Shake Off and Vacancy Cascades," *Radiat. Res.* **64**, 53–69 (1975).
- Carlson, T. A., "Photoelectron Spectroscopy" (book chapter), *Ann. Rev. Phys. Chem.* **26**, 211–33 (1975).
- Carlson, T. A., *Photoelectron and Auger Spectroscopy*, Plenum Press, New York and London, 1975.
- Carlson, T. A., J. C. Carver, and G. A. Vernon, "Satellite Structure in the X-ray Photoelectron Spectra of the K Shell of Transition Metal Compounds," *J. Chem. Phys.* **62**, 932–35 (1975).
- Carter, H. K. and R. L. Mlekodaj, "A Simple Tape Vacuum Seal for Quick Sample Removal from High Vacuum," *Nucl. Instrum. Methods* **128**, 611–13 (1975).
- Chang, C. C., F. E. Bertrand, and D. C. Kocher, "Isolation of the Giant Quadrupole Resonance in ^{58}Ni Via Deuteron Inelastic Scattering," *Phys. Rev. Lett.* **34**, 221–24 (1975).
- Chrien, R. E., G. W. Cole, G. G. Slaughter, and J. A. Harvey, "Failure of Bohr's Compound Nucleus Hypothesis for the $^{98}\text{Mo}(n,\gamma)^{99}\text{Mo}$ Reaction," *Phys. Rev. C* **13**, 578–94 (1976).
- Cookson, J. A., M. Hussian, C. A. Uttley, J. L. Fowler, and R. B. Schwartz, "Absolute Calibration of Neutron Detectors in the 10–30 MeV Range," pp. 66–68 in vol. 1 of *Nuclear Cross Sections and Technology* (Proceedings of Conference, Washington, D.C., March 1975), R. A. Schrack and C. D. Bowman, Eds., National Bureau of Standards, 1975.
- Dabbs, J.W.T., N. W. Hill, C. E. Bemis, and S. Raman, "Fission Cross Section Measurements on Short-Lived Alpha Emitters," pp. 81–82 in vol. 1 of *Nuclear Cross Sections and Technology* (Proceedings of Conference, Washington, D.C., March 1975), R. A. Schrack and C. D. Bowman, Eds., National Bureau of Standards, 1975.
- Datz, S., B. R. Appleton, J. A. Biggerstaff, M. D. Brown, H. F. Krause, C. D. Moak, and T. S. Noggle, "Charge State Dependence of Stopping Power for Oxygen Ions Channeled in Silver," pp. 63–73 in vol. 1 of *Proceedings of the Fifth International Conference on Atomic Collisions in Solids, Gatlinburg, Tenn., September 1973*, S. Datz, B. R. Appleton, and C. D. Moak, Eds., Plenum Press, New York, 1975.
- Datz, S., B. R. Appleton, and C. D. Moak, Eds., vols. 1 and 2 of *Proceedings of the Fifth International Conference on Atomic Collisions in Solids, Gatlinburg, Tenn., September 1973*, Plenum Press, New York, 1975.
- Davies, R. W. and K.T.R. Davies, "On the Wigner Distribution Function for an Oscillator," *Ann. Phys.* **89**, 261–73 (1975).
- Davies, K.T.R. and A. J. Sierk, "Calculation of Coulomb Energies for Uniform Charge Distributions of Arbitrary Shape," *J. Comput. Phys.* **18**, 311–25 (1975); also LA-UR-74-790 (1974).
- Doukellis, G., C. McKenna, R. Finlay, J. Rapaport, and H. J. Kim, "Low Lying States of ^{96}Tc ," *Nucl. Phys.* **A229**, 47–60 (1974).
- Dress, W. B., C. Guet, P. Perrin, and P. D. Miller, "Observation of Two Photon Decay in n - p Capture," *Phys. Rev. Lett.* **34**, 752–55 (1975).
- Eagle, R., N. M. Clarke, R. J. Griffiths, C. B. Fulmer, and D. C. Hensley, "Inelastic Scattering of ^3He from Samarium Isotopes at 53 MeV," p. 35 in *Proceedings of Europhysics Conference on Nuclear Interactions at Medium and Low Energies, Harwell, England, March 1975*, Institute of Physics, AERE, 1975.
- Eagle, R., N. M. Clarke, R. J. Griffiths, C. B. Fulmer, and D. C. Hensley, "53 MeV ^3He Scattering from Samarium Isotopes," *J. Phys. G* **1**, 358–61 (1975).
- Ellis, Y. A., "Nuclear Data Sheets for $A = 187$," *Nucl. Data Sheets* **14**, 347–411 (March 1975).
- Ellis, Y. A. and B. Harmatz, "Nuclear Data Sheets for $A = 177$," *Nucl. Data Sheets* **16**, 135–94 (September 1975).
- Ewbank, W. B., "Computer-Readable Nuclear Data Sheets," pp. 309–12 in vol. 1 of *Nuclear Cross Sections and Technology* (Proceedings of Conference, Washington, D.C., March 1975), R. A. Schrack and C. D. Bowman, Eds., National Bureau of Standards, 1975.

- Ewbank, W. B., R. L. Haese, F. W. Hurley, and M. R. McGinnis, "Recent References (May 1974 through August 1974)," *Nucl. Data Sheets* **14**, 1–118 (January 1975).
- Ewbank, W. B., R. L. Haese, F. W. Hurley, and M. R. McGinnis, "Recent References (September 1, 1974 through December 15, 1974)," *Nucl. Data Sheets* **15**, 1–106 (May 1975).
- Ewbank, W. B., R. L. Haese, F. W. Hurley, and M. R. McGinnis, "Nuclear Structure References, 1969–1974," *Nucl. Data Sheets, Suppl.* **16**, 1–493 (1975).
- Ewbank, W. B., R. L. Haese, F. W. Hurley, and M. R. McGinnis, "Recent References (December 16, 1974 through August 15, 1975)," *Nucl. Data Sheets* **16**, 507–660 (December 1975).
- Fulmer, C. B. and D. A. Goldberg, "Excitation Functions for ${}^7\text{Be}$ Production by Light Ion Bombardment of ${}^{12}\text{C}$," *Phys. Rev. C* **11**, 50–53 (1975).
- Fulmer, C. B., J. C. Hafele, and N. M. Clarke, " ${}^3\text{He}$ Elastic Scattering from ${}^{208}\text{Pb}$ and ${}^{209}\text{Bi}$ at 71 MeV," *Phys. Rev. C* **12**, 87–89 (1975).
- Garcia Santibanez, F. and T. A. Carlson, "Multiplet Splitting of Mixed Spinels $\text{NiFe}_x\text{Cr}_{2-x}\text{O}_4$ and Its Relation to Magnetic Hyperfine Fields," *Phys. Rev. B* **12**, 965–69 (1975).
- Gari, M., J. B. McGrory, and R. Offermann, "Circular Polarization in ${}^{18}\text{F}$ as a Probe for Neutral Currents," *Phys. Rev. Lett.* **55B**, 277–80 (1975).
- Gari, M., A. H. Huffman, J. B. McGrory, and R. Offermann, "Calculation of Parity Mixing in ${}^{19}\text{F}$," *Phys. Rev. C* **11** (Communications), 1485–87 (1975).
- Gauvin, H., D. Guerreau, Y. Le Beyec, M. Lefort, F. Plasil, and X. Tarrago, "Cross Sections for Evaporation Residue Products in Argon-Induced Reactions," *Phys. Lett.* **58B**, 163–65 (1975).
- Gizon, J., A. Gizon, and D. J. Horen, "Band Structure in ${}^{131,132,133}\text{Ba}$ Observed by (${}^{12}\text{C},xn$) Reactions," *Nucl. Phys.* **A252**, 509–23 (1975).
- Gomez del Campo, J., D. E. Gustafson, R. L. Robinson, P. H. Stelson, P. D. Miller, J. K. Bair, and J. B. McGrory, "Population of High-Spin States in ${}^{23}\text{Na}$ through the ${}^{11}\text{B}({}^6\text{O},\alpha)$ Reaction," *Phys. Rev. C* **12**, 1247–59 (1975).
- Halbert, E. C., J. B. McGrory, G. R. Satchler, and J. Speth, "Hadronic Excitation of the Giant Resonance Region of ${}^{208}\text{Pb}$," *Nucl. Phys.* **A245**, 189–204 (1975).
- Hamilton, J. H., A. V. Ramayya, E. L. Bosworth, W. Lourens, J. D. Cole, G. Garcia-Bermudez, B. Martin, B. N. Subba Rao, L. L. Riedinger, C. R. Bingham, F. Turner, E. F. Zganjar, E. H. Spejewski, H. K. Carter, R. L. Mlekodaj, W. D. Schmidt-Ott, K. R. Baker, R. W. Fink, G. W. Gowdy, J. L. Wood, A. Zenoulis, B. D. Kern, K. J. Hofstetter, J. L. Weil, K. S. Toth, and M. A. Ijaz, "Crossing of Near-Spherical and Deformed Bands in ${}^{186,188}\text{Hg}$ and New Isotopes ${}^{186,188}\text{Tl}$," *Phys. Rev. Lett.* **35**, 562–65 (1975).
- Harmatz, B. and D. J. Horen, "Nuclear Data Sheets for $A = 173$," *Nucl. Data Sheets* **14**, 297–345 (March 1975).
- Harmatz, B., D. J. Horen, and Y. A. Ellis, "Ground States in the Neutron-Deficient $165 \leq A \leq 185$ Region," *Phys. Rev. C* **12**, 1083–86 (1975).
- Harvey, J. A. and N. W. Hill, "Neutron Total Cross Section of ${}^6\text{Li}$ from 10 eV to 10 MeV," pp. 244–45 in vol. 1 of *Nuclear Cross Sections and Technology* (Proceedings of Conference, Washington, D.C., March 1975), R. A. Schrack and C. D. Bowman, Eds., National Bureau of Standards, 1975.
- Haselton, H. H., R. S. Thoe, J. R. Mowat, P. M. Griffin, D. J. Pegg, and I. A. Sellin, "Lifetimes of the Metastable Autoionizing ($1s2s2p$) ${}^4P_{5/2}$ States of Lithiumlike Al^{10+} and Si^{11+} Ions; Comparisons with Theory Over the Isoelectronic Sequence $Z = 8-18$," *Phys. Rev. A* **11**, 468–72 (1975).
- Hillis, D. L., C. R. Bingham, D. A. McClure, N. S. Kendrick, Jr., J. C. Hill, S. Raman, J. B. Ball, and J. A. Harvey, "Nuclear Spectroscopy of ${}^{145}\text{Nd}$," *Phys. Rev. C* **12**, 260–78 (1975).
- Horen, D. J., J. Arvieux, M. Buenerd, J. Cole, G. Perrin, and P. de Saintignon, "Giant Resonance Region Observed in ${}^3\text{He}$ Scattering by ${}^{144,154}\text{Sm}$, ${}^{159}\text{Tb}$, ${}^{165}\text{Ho}$, ${}^{169}\text{Tm}$, and ${}^{208}\text{Pb}$," *Phys. Rev. C* **11**, 1247–50 (1975).
- Horen, D. J. and M. B. Lewis, "Nuclear Data Sheets for $A = 75$," *Nucl. Data Sheets* **16**, 25–54 (September 1975).

- Hudson, E. D., R. S. Lord, M. L. Mallory, J. E. Mann, J. A. Martin, and W. R. Smith, "Increased Intensity Heavy Ion Beams at ORIC with Cryopumping," *IEEE Trans. Nucl. Sci.* (Proceedings 1975 Particle Accelerator Conference, Washington, D.C., March 1975) **NS-22**, 1544–47 (1975).
- Jenkins, L. H., T. S. Noggle, R. E. Reed, M. J. Saltmarsh, and G. J. Smith, "High Energy Neutron Sputtering Yields from Gold and Niobium," *Appl. Phys. Lett.* **26**, 426–28 (1975).
- Johnson, C. H., "A Ring Lens for Focusing Ion Beams to Uniform Densities," *Nucl. Instrum. Methods* **127**, 163–71 (1975).
- Johnson, N. R., R. J. Sturm, E. Eichler, M. W. Guidry, G. D. O'Kelley, R. O. Sayer, D. C. Hensley, N. C. Singhal, and J. H. Hamilton, "Lifetimes of Rotational States in ^{232}Th ," *Phys. Rev. C* **12**, 1927–36 (1975).
- Kenny, M. J., P. W. Martin, L. E. Carlson, and J. A. Biggerstaff, "Gamma Ray Transitions Following keV Neutron Capture in $2s-1d$ Shell Nuclei," *Aust. J. Phys.* **27**, 771 (1974).
- Keyworth, G. A., C. E. Olsen, J. D. Moses, J.W.T. Dabbs, and N. W. Hill, "Spin Determination of Resonances in ^{235}U ," pp. 576–78 in vol. 1 of *Nuclear Cross Sections and Technology* (Proceedings of Conference, Washington, D.C., March 1975), R. A. Schrack and C. D. Bowman, Eds., National Bureau of Standards, 1975.
- Kim, H. J., "Nuclear Data Sheets for $A = 114$," *Nucl. Data Sheets* **16**, 107–33 (September 1975).
- Kim, H. J., "Nuclear Data Sheets for $A = 60$," *Nucl. Data Sheets* **16**, 317–49 (November 1975).
- Kim, H. J., R. Ballini, B. Delaunay, J. Delaunay, J. P. Fouan, and M. Pichevar, "Yrast Cascade in ^{60}Ni ," *Nucl. Phys.* **A250**, 211–20 (1975).
- Kim, H. J., R. L. Robinson, and W. T. Milner, "Lifetime of the 3.830-MeV State of ^{41}Ca ," *Phys. Rev. C* **11**, 1468–69 (1975).
- Kim, H. J., R. L. Robinson, and W. T. Milner, " ^{44}Ca Yrast Levels," *Phys. Rev. C* **11**, 2108–10 (1975).
- Kocher, D. C., "Nuclear Data Sheets for $A = 83$," *Nucl. Data Sheets* **15**, 169–201 (June 1975).
- Kocher, D. C., "Nuclear Data Sheets for $A = 90$," *Nucl. Data Sheets* **16**, 55–105 (September 1975).
- Kocher, D. C., "Nuclear Data Sheets for $A = 89$," *Nucl. Data Sheets* **16**, 445–505 (November 1975).
- Kolb, D. and C. Y. Wong, "Shape Isomerism in Mercury Isotopes," *Nucl. Phys.* **A245**, 205–20 (1975).
- Kopp, O. C. and P. A. Staats, "Measurement of Q for RbOH-Grown Quartz," *J. Phys. Chem. Solids* **36**, 356 (1975).
- Laubert, R., H. Haselton, J. R. Mowat, R. S. Peterson, and I. A. Sellin, "Symmetric Ion Atom Collisions at Medium Energies I: Characteristic X-rays," *Phys. Rev. A* **11**, 135–39 (1975).
- Laubert, R., H. H. Haselton, J. R. Mowat, R. S. Peterson, and I. A. Sellin, "Symmetric Ion-Atom Collisions at Medium Energies: Noncharacteristic Radiation," *Phys. Rev. A* **11** (Comments and Addenda), 1468–71 (1975).
- Lee, I. Y., J. X. Saladin, J. Holden, J. O'Brien, C. Baktash, C. Bemis, Jr., P. H. Stelson, F. K. McGowan, W. T. Milner, J.L.C. Ford, Jr., R. L. Robinson, and W. Tuttle, "Deformation Parameters of the Charge Distribution and the Optical Potential for Some Nuclei In and Near the Rare Earth Region," *Phys. Rev. C* **12**, 1483–94 (1975).
- Lemming, J. F. and R. L. Auble, "Nuclear Data Sheets for $A = 82$," *Nucl. Data Sheets* **15**, 315–34 (July 1975).
- Lewis, M. B., "Nuclear Data Sheets for $A = 68$," *Nucl. Data Sheets* **14**, 155–90 (February 1975).
- Lewis, M. B., "Effects of Spreading Widths Upon the Direct Nuclear Reaction Continuum," *Phys. Rev. C* **11**, 145–53 (1975).
- Lewis, M. B., F. K. McGowan, C. H. Johnson, and M. J. Saltmarsh, "The Oak Ridge CN Van de Graaff Facility for Heavy Ion Radiation Damage Studies," pp. 15–37 in *Proceedings of Experimental Methods for Charged-Particle Irradiations Symposium, Gatlinburg, Tenn., September 1975*, CONF-75-0947, David Kramer, Ed., ERDA Technical Information Center, Oak Ridge, Tenn., 1975.
- Lord, R. S., J. B. Ball, E. D. Hudson, M. L. Mallory, J. A. Martin, S. W. Mosko, R. M. Beckers, K. N. Fischer, G. S. McNeilly, and J. D. Rylander, "Energy Boosting of a Tandem Beam with the Oak Ridge Isochronous Cyclotron," *IEEE Trans. Nucl. Sci.* (Proceedings 1975 Particle Accelerator Conference, Washington, D.C., March 1975) **NS-22**, 1679–81 (1975).

- Macklin, R. L., J. Halperin, and R. R. Winters, "Gold Neutron Capture Cross Section from 3 to 500 keV," *Phys. Rev. C* **11**, 1270--79 (1975).
- Mallory, M. L. and E. D. Hudson "A Rotatable Cold Cathode Penning Ion Source," *IEEE Trans. Nucl. Sci.* (Proceedings 1975 Particle Accelerator Conference, Washington, D.C., March 1975) **NS-22**, 1669--71 (1975).
- Mallory, M. L., E. D. Hudson, and R. S. Lord, "Isochronous Cyclotron Harmonic Beam Experiments," *IEEE Trans. Nucl. Sci.* (Proceedings 1975 Particle Accelerator Conference, Washington, D.C., March 1975) **NS-22**, 1694--96 (1975).
- Maruhn-Rezwani, V., J. A. Maruhn, and W. Greiner, "Collective Description of Magnetic Properties of Even-Even Nuclei," *Phys. Lett.* **57B**, 109--12 (1975).
- McGowan, F. K. and W. T. Milner, "Reaction List for Charged-Particle-Induced Nuclear Reactions --- July 1973 to September 1974," *At. Data Nucl. Data Tables* **15**, 189--303 (1975).
- McGrory, J. B. and T.T.S. Kuo, "Shell Model Calculations of Two to Four Identical 'Particle' Systems Near ^{208}Pb ," *Nucl. Phys.* **A247**, 283--316 (1975).
- McGrory, J. B. and B. H. Wildenthal, "Further Comment on Spurious Center-of-Mass Motion," *Phys. Lett.* **60B**, 5--8 (1975).
- Milner, W. T., G. D. Alton, D. C. Hensley, C. M. Jones, R. F. King, J. D. Larson, C. D. Moak, and R. O. Sayer, "Transport of DC and Bunched Beams through a 25-MV Folded Tandem Accelerator," *IEEE Trans. Nucl. Sci.* (Proceedings 1975 Particle Accelerator Conference, Washington, D.C., March 1975) **NS-22**, 1697--1701 (1975).
- Moak, C. D., B. R. Appleton, J. A. Biggerstaff, S. Datz, and T. S. Noggle, "Velocity Dependence of the Stopping Power of Channeled Iodine Ions," pp. 57--62 in vol. 1 of *Proceedings of the Fifth International Conference on Atomic Collisions in Solids, Gatlinburg, Tenn., September 1973*, S. Datz, B. R. Appleton, and C. D. Moak, Eds., Plenum Press, New York, 1975.
- Moak, C. D., S. Datz, F. Garcia Santibanez, and T. A. Carlson, "A Position Sensitive Detector for Electrons," *J. Electron Spectrosc. Relat. Phenom.* **6**, 151--56 (1975).
- Mowat, J. R., B. R. Appleton, J. A. Biggerstaff, S. Datz, C. D. Moak, and I. A. Sellin, "Charge State Dependence of Si K X-ray Production in Solid and Gaseous Targets by MeV Oxygen Ion Impact," pp. 461--68 in vol. 1 of *Proceedings of the Fifth International Conference on Atomic Collisions in Solids, Gatlinburg, Tenn., September 1973*, S. Datz, B. R. Appleton, and C. D. Moak, Eds., Plenum Press, New York, 1975.
- Mowat, J. R., P. M. Griffin, H. H. Haselton, R. Laubert, D. J. Pegg, R. S. Peterson, I. A. Sellin, and R. S. Thoe, "Heliumlike ^{19}F : 2^3P_2 and 2^3P_0 Lifetimes," *Phys. Rev. A* **11**, 2198--2200 (1975).
- Multhauf, L. G., K. G. Tirsell, S. Raman, and J. B. McGrory, "Potassium-48," *Phys. Lett.* **57B**, 44--46 (1975).
- Musgrove, A. R. de L., B. J. Allen, and R. L. Macklin, "keV Neutron Resonance Capture in Barium-135," pp. 1--28 in Report AAEC/E327, December 1974.
- Musgrove, A. R. de L., B. J. Allen, J. W. Boldeman, and R. L. Macklin, "keV Neutron Resonance Capture in ^{138}Ba ," *Nucl. Phys.* **A252**, 301--14 (1975).
- Pandey, M. S., J. B. Garg, J. A. Harvey, and W. M. Good, "High Resolution Total Neutron Cross-Section in the ^{54}Fe and ^{56}Fe ," pp. 748--53 in vol. 1 of *Nuclear Cross Sections and Technology* (Proceedings of Conference, Washington, D.C., March 1975), R. A. Schrack and C. D. Bowman, Eds., National Bureau of Standards, 1975.
- Pegg, D. J., H. H. Haselton, R. S. Thoe, P. M. Griffin, M. D. Brown, and I. A. Sellin, "Core-Excited Autoionizing States in the Alkali Metals," *Phys. Rev. A* **12**, 1330--39 (1975).
- Plasil, F., "Experimental Summary," pp. 255--61 in *Proceedings of the International Workshop III on Gross Properties of Nuclei and Nuclear Excitations, Hirschegg, Austria, January 1975*, Technische Hochschule, Darmstadt, Germany, 1975.
- Plasil, F., "On Reaction Times for 'Quasi-Fission' and on the Critical Distance Concept in Heavy-Ion Fusion Reactions," pp. 95--104 in *Proceedings of the International Workshop III on Gross Properties of Nuclei and Nuclear Excitations, Hirschegg, Austria, January 1975*, Technische Hochschule, Darmstadt, Germany, 1975.

- Plasil, F. and M. Blann, "Consequences of Fission Deexcitation of Compound Nuclei Formed in Heavy Ion Reactions," *Phys. Rev. C* **11**, 508–19 (1975).
- Raman, S., N. B. Gove, and T. A. Walkiewicz, "Isospin Impurity of ^{64}Ga Ground State," *Nucl. Phys.* **A254**, 131–40 (1975).
- Raman, S. and H. J. Kim, "Nuclear Data Sheets for $A = 115$," *Nucl. Data Sheets* **16**, 195–229 (October 1975).
- Raman, S., C. W. Nestor, Jr., and J.W.T. Dabbs, "A Study of the ^{233}U - ^{232}Th Reactor as a Burner for Actinide Wastes," pp. 222–23 in vol. 1 of *Nuclear Cross Sections and Technology* (Proceedings of Conference, Washington, D.C., March 1975), R. A. Schrack and C. D. Bowman, Eds., National Bureau of Standards, 1975.
- Raman, S., T. A. Walkiewicz, and H. Behrens, "Superallowed $0^+ \rightarrow 0^+$ and Isospin-Forbidden $J^\pi \rightarrow J^\pi$ Transitions," *At. Nucl. Data Tables* **16**, 451–94 (1975).
- Ramayya, A. V., R. M. Ronningen, J. H. Hamilton, W. T. Pinkston, G. Garcia Bermudez, R. L. Robinson, H. J. Kim, H. K. Carter, and W. E. Collins, "Mean Life and Collective Effects of the 937 keV, 0^+ State in ^{72}Se : Evidence for Nuclear Coexistence," *Phys. Rev. C* **12**, 1360–63 (1975).
- Rickertsen, L. D., M. J. Schneider, J. J. Kraushaar, W. R. Zimmerman, and H. Rudolph, "Two-Step Processes in the ($^3\text{He},t$) Reaction to Analog and Anti-Analog States in ^{56}Co ," *Phys. Lett.* **60B**, 19–24 (1975).
- Robinson, E. L., J. K. Bair, and J. L. Duggan, "Absolute Neutron Yield of a Fluorescent Thyroid Scanner Source," *Health Phys.* **28**, 205–7 (1975).
- Rudolph, H., C. D. Zafiratos, R. F. Bently, and L. D. Rickertsen, "Two-Step Contributions to the $^{40}\text{Ar}(p,n)^{40}\text{K}$ Anti-Analog State Transition," *Phys. Lett.* **59B**, 129–31 (1975).
- Rutkowski, R. W. and E. E. Gross, "Reaction $^3\text{He}(d,t)2p$ at 23.5 MeV c.m.," *Phys. Rev. C* **12**, 362–69 (1975).
- Saethre, L. J., T. A. Carlson, Joyce J. Kaufman, and W. S. Koski, "Nitrogen Electron Densities in Narcotics and Narcotic Antagonists by X-ray Photoelectron Spectroscopy and Comparison with Quantum Chemical Calculations," *Mol. Pharmacol.* **11**, 492–500 (1975).
- Saltmarsh, M. J. (invited paper), "Radiation Damage Studies with Accelerators," pp. 259–69 in vol. 1 of *Proceedings of the Third Conference on Application of Small Accelerators, Denton, Tex., October 1974*, ERDA CONF-741040-P1, ERDA Technical Information Center, Oak Ridge, Tenn., 1975.
- Saltmarsh, M. J. (invited paper), "Uses of Accelerators in Energy R & D," *IEEE Trans. Nucl. Sci.* (Proceedings 1975 Particle Accelerator Conference, Washington, D.C., March 1975) **NS-22**, 940–45 (1975).
- Satchler, G. R., "Potentials for Heavy Ions Scattering from ^{208}Pb ," *Phys. Lett.* **B55**, 167–70 (1975).
- Satchler, G. R., "Energy Dependence of the Surface Absorption and $\text{Ni} + ^{16}\text{O}$ Scattering," *Phys. Lett.* **58B**, 408–10 (1975).
- Satchler, G. R., "A Critique of Folded Potentials for Heavy-Ion Scattering," *Phys. Lett.* **59B**, 121–24 (1975).
- Satchler, G. R., J.L.C. Ford, Jr., K. S. Toth, D. C. Hensley, E. E. Gross, D. E. Gustafson, and S. T. Thornton, "A Microscopic Description of Inelastic ^{12}C Scattering from ^{208}Pb ," *Phys. Lett.* **60B**, 43–46 (1975).
- Sayer, R. O., J. S. Smith, and W. T. Milner, "Rotational and Quasi-Rotational Bands in Even-Even Nuclei," *At. Nucl. Data Tables* **15**, 85–110 (1975).
- Schmidt-Ott, W. D., R. L. Mlekodaj, E. H. Spejewski, and H. K. Carter, "He-Jet On-Line Ion Source of the UNISOR Mass Separator," *Nucl. Instrum. Methods* **124**, 83–91 (1975).
- Schmidt-Ott, W. D., K. S. Toth, and E. F. Zganjar, "Absolute Cross Sections for ($^{14}\text{N},4n$) and ($^{14}\text{N},5n$) Reactions Induced on ^{141}Pr and ^{142}Nd ," *Phys. Rev. C* **11**, 154–57 (1975).
- Schmorak, M. R., "Nuclear Data Sheets for $A = 182$," *Nucl. Data Sheets* **14**, 413–600 (April 1975).
- Schmorak, M. R. and R. L. Auble, "Nuclear Data Sheets for $A = 170$," *Nucl. Data Sheets* **15**, 371–407 (July 1975).
- Spears, D. P., H. J. Fischbeck, and T. A. Carlson, "Satellite Structure in the Photoelectron Spectra of the Core Electrons of NO , N_2O , and H_2O ," *J. Electron Spectrosc. Relat. Phenom.* **6**, 411–20 (1975).

- Stelson, P. H. (invited paper), "The New Heavy-Ion Accelerator Facility at Oak Ridge," pp. 1–10 in vol. 1 of *Proceedings of the Third Conference on Application of Small Accelerators, Denton, Tex., October 1974*, ERDA CONF-741040-P1, ERDA Technical Information Center, Oak Ridge, Tenn., 1975.
- Thoe, R. S., I. A. Sellin, M. D. Brown, J. P. Forester, P. M. Griffin, D. J. Pegg, and R. S. Peterson, "Observation of Large and Strongly Energy Dependent Directional Anisotropies in Non-Characteristic K X-rays Emitted in Heavy Ion Collisions," *Phys. Rev. Lett.* **34**, 64–67 (1975).
- Thoe, R. S., I. A. Sellin, M. D. Brown, J. P. Forester, P. M. Griffin, D. J. Pegg, and R. S. Peterson (invited paper), "Energy Dependence of the Anisotropy of Non-Characteristic X-rays Emitted in Fast Ion-Atom Collisions," pp. 78–85 in vol. 1 of *Proceedings of the Third Conference on Application of Small Accelerators, Denton, Tex., October 1974*, ERDA CONF-741040-P1, ERDA Technical Information Center, Oak Ridge, Tenn., 1975.
- Thoe, R. S., I. A. Sellin, R. S. Peterson, D. J. Pegg, P. M. Griffin, and J. P. Forester, "Photon Energy Dependence of the Asymmetry of Non-Characteristic X-radiation in Si-Al, and Al-Al Collisions," p. 312 in *Abstracts of Papers of IXth International Conference on Physics of Electron and Atomic Collisions, Seattle, Wash., July 1975*, J. S. Risley and R. Geballe, Eds., University of Washington Press, Seattle/London, 1975.
- Thompson, J. R. and J. O. Thomson, "Mössbauer Studies of Dilute Ag:Fe and Ag:Co Alloys," pp. 477–78 in *AIP Conference Proceedings No. 24 -- Twentieth Conference on Magnetism and Magnetic Materials, San Francisco, Calif., December 1974*, Hugh C. Wolfe, Ed., American Institute of Physics, New York, 1975.
- Thomson, J. O., F. E. Obenshain, P. G. Huray, J. C. Love, and J. Burton, "Mössbauer Measurements with ^{197}Au in AuAl_2 , AuIn_2 and AuSb_2 ," *Phys. Rev. B* **5**, 1835–39 (1975).
- Thomson, J. O. and J. R. Thompson, "Investigation of Dilute Magnetic Impurities Via the Mössbauer Effect: Ag^{57}Fe and Ag^{57}Co ," *Phys. Rev. B* **12**, 2572–78 (1975).
- Thornton, S. T., J.L.C. Ford, Jr., E. Friedland, C. A. Wiedner, and M. Goldschmidt, " $^{13}\text{C} + ^{144}\text{Sm}$ Neutron Transfer Reaction," *Phys. Rev. C* **12**, 877–86 (1975).
- Toth, K. S., E. Newman, C. R. Bingham, A. E. Rainis, and W. D. Schmidt-Ott, "Observation of a 1^+ ($\pi h_{11/2}, \nu h_{9/2}$) State in ^{148}Tb Populated in the Decay of a New Isotope, ^{148}Dy ," *Phys. Rev. C* **11**, 1370–77 (1975).
- Toth, K. S., A. E. Rainis, C. R. Bingham, E. Newman, H. K. Carter, and W. D. Schmidt-Ott, "Excitation Energies of the $h_{11/2}$ and $d_{3/2}$ Neutron States in ^{145}Gd and ^{147}Dy ," *Phys. Lett.* **56B**, 29–32 (1975).
- Toth, K. S., W. D. Schmidt-Ott, C. R. Bingham, and M. A. Ijaz, "Production and Investigation of Tungsten Alpha-Emitters Including the New Isotopes, ^{165}W and ^{166}W ," *Phys. Rev. C* **12**, 533–40 (1975).
- Urone, P. P. and F. E. Bertrand, "Nuclear Data Sheets for $A = 78$," *Nucl. Data Sheets* **15**, 107–36 (June 1975).
- Urone, P. P. and D. C. Kocher, "Nuclear Data Sheets for $A = 79$," *Nucl. Data Sheets* **15**, 257–87 (July 1975).
- Wells, J. C., R. L. Robinson, H. J. Kim, and J.L.C. Ford, Jr., "Absolute Cross Sections for the $^{61}\text{Ni}(^{16}\text{O},X)$ Reactions," *Phys. Rev.* **11**, 879–85 (1975).
- Wells, J. C., Jr., R. L. Robinson, H. J. Kim, and J.L.C. Ford, Jr., "Absolute Cross Sections for the $^{63,65}\text{Cu}(^{16}\text{O},X)$ Reactions," *Phys. Rev. C* **12**, 1529–39 (1975).
- Welton, T. A., "Practical Resolution Enhancement in Bright Field Electron Microscopy by Computer Processing," pp. 196–97 in *Proceedings of the Thirty-Third Annual Meeting of the Electron Microscopy Society of America, Las Vegas, Nev., August 1975*, G. W. Bailey, Ed., Claitor's Publishing Division, Baton Rouge, La., 1975.
- Wigner, E. P. and J. L. Fowler, "Roundtable Discussion of the Significance and Accomplishments of the Conference," p. 964 in vol. 1 of *Nuclear Cross Sections and Technology* (Proceedings of Conference, Washington, D.C., March 1975), R. A. Schrack and C. D. Bowman, Eds., National Bureau of Standards, 1975.
- Wong, C. Y., J. A. Maruhn, and T. A. Welton, "Dynamics of Nuclear Fluid. I. Foundation," *Nucl. Phys.* **A253**, 469–89 (1975).
- Young, J. P., K. L. Vander Sluis, and G. K. Werner, "High Temperature Spectroscopic and X-ray Diffraction Studies of Californium Tribromide: Proof of Thermal Reduction to Californium (II)," *J. Inorg. Nucl. Chem.* **37**, 2497–2501 (1975).

- Zganjar, E. F., J. L. Wood, R. W. Fink, L. L. Riedinger, C. R. Bingham, B. D. Kern, J. L. Weil, J. H. Hamilton, A. V. Ramayya, E. H. Spejewski, R. L. Mlekodaj, H. K. Carter, and W. D. Schmidt-Ott, "Rotation Aligned Coupling and Axial Asymmetry in $^{189-195}\text{Au}$," *Phys. Lett.* **58B**, 159-62 (1975).
- Ziegler, N. F., "An Improved Van de Graaff Belt Charge Regulator," *IEEE Trans. Nucl. Sci.* (Proceedings Particle Accelerator Conference, Washington, D.C., March 1975) **NS-22**, 1730-31 (1975).
- Ziegler, N. F., "A 100 KV Regulator with 1/4 PPM Stability," CPEM 74 Digest (Proceedings Conference on Precision Electromagnetic Measurements, London, England, July 1974), *IEEE Cat. No. 74*, CH0770-81M, 297 (1975).

THESES

- Maruhn, Vida, "Collective Description of Magnetic Properties of Even-Even Nuclei," Ph.D. dissertation, University of Frankfurt, Germany, June 1975.
- Tuttle, W. K., III, "Levels in $^{113,115}\text{In}$ As Seen by the Coulomb Excitation and (HI,xn) Reactions," Ph.D. dissertation, University of Tennessee, December 1975.

ANNUAL REPORT

- Stelson, P. H., *Physics Division Annual Progress Report for the Period Ending December 31, 1974*, ORNL-5025 (May 1975).

TOPICAL REPORTS

- Becker, R. L. and J. P. Svenne, *Inversion of Single-Particle Levels in Nuclear Hartree-Fock and Brueckner-HF Calculations with Broken Symmetry*, ORNL/TM-5174 (December 1975).
- Dickens, J. K. and G. G. Slaughter, *Gamma-Ray Transitions in ^{181}Ta Observed in $^{181}\text{Ta}(n,n'\gamma)$ Reactions*, ORNL/TM-4881 (June 1975).
- Ewbank, W. B., M. R. Schmorak, F. E. Bertrand, M. Feliciano, and D. J. Horen, *Nuclear Structure Data File -- A Manual for Preparation of Data Sets*, ORNL-5054 (June 1975).
- Howard, F. T., *Tandem Accelerators, 1973-1974*, ORNL/TM-4934 (July 1975).
- Hutchinson, D. P. and K. L. Vander Sluis, *Proposed Spatial Ion Temperature Measurements with a Fir Laser*, ORNL/TM-5071 (October 1975).
- Jones, C. M., J. A. Biggerstaff, J. K. Bair, J. B. Ball, J. D. Larson, J. A. Martin, J. W. McConnell, W. T. Milner, J. A. Murray, and N. F. Ziegler, *Technical Specifications for a 25-MV Tandem Electrostatic Accelerator*, ORNL/TM-4942 (August 1975).
- Macklin, R. L., *LSFIT -- A Least Squares Computer Program to Fit Neutron Capture Cross Section Resonance Data from ORELA*, ORNL/TM-4810 (February 1975).
- Wong, C. Y., *Selected Topics in Heavy-Ion Reactions -- Lectures Given at Saclay, May 1975*, ORNL/TM-5000 (November 1975).

PUBLICATIONS PENDING AS OF FEBRUARY 24, 1976
(References Included If Known)

- Alton, G. D., "Preliminary Evaluation of a Modified Hortig-Geometry Negative-Ion Source Using a Negative-Ion Source Test Facility," *IEEE Trans. Nucl. Sci.* (International Conference on Heavy Ion Sources, Gatlinburg, Tenn., October 1975).
- Alvarez, I., Carmen Cisneros, C. F. Barnett, and J. A. Ray, "Negative-Ion Formation from Dissociative Collisions of H_2^+ , H_3^+ , and HD_2^+ in H_2 , He, and Xe," *Physical Review*.
- Alvarez, I., Carmen Cisneros, C. F. Barnett, and J. A. Ray, "Electron Capture and Stripping Cross Sections for Tl and K Ions and Atoms," *Physical Review*.
- Andersen, J. U., E. Laegsgaard, M. Lund, and C. D. Moak, " Z_1 Scaling for Impact-Parameter Dependence of Inner-Shell Ionization by Heavy Ions," *Proceedings Sixth International Conference on Atomic Collisions in Solids* (Amsterdam, Netherlands, September 1975).
- Appleton, B. R., R. H. Ritchie, J. A. Biggerstaff, T. S. Noggle, S. Datz, C. D. Moak, and H. Verbeek, "Energetic Heavy Ion Channeling as an Experimental Technique for Simulating Radiative Electron Capture by Plasma and Impurity Ions in a CTR Type Plasma," *Proceedings International Conference on Surface Effects in Controlled Fusion Devices* (San Francisco, Calif., February 1976).
- Auble, R. L., H. R. Hiddleston, and C. P. Browne, "Nuclear Data Sheets for $A = 131$," *Nucl. Data Sheets* **17**, 573-615 (April 1976).
- Auble, R. L., "Nuclear Data Sheets for $A = 69$," *Nucl. Data Sheets* **17**, 193-224 (February 1976).
- Barnett, C. F. (invited paper), "Atomic Physics in the Controlled Thermonuclear Research Program," *Proceedings International Collision Conference* (Seattle, Wash., July 1975).
- Becker, R. L. and J. P. Svenne, "Inversion of Single-Particle Levels in Nuclear Hartree-Fock and Brueckner-HF Calculations," *Canadian Journal of Physics*.
- Bendjaballah, N., J. Delaunay, A. Jaffrin, and H. J. Kim, "Evidence for a Cut-Off Effect in the Ground-State Rotational Band of ^{56}Fe ," *Nuclear Physics*.
- Bertrand, F. E., "Excitation of Giant Resonances Via Inelastic Hadron Scattering," *Proceedings Symposium on Highly Excited States in Nuclei* (Jülich, West Germany, September 1975).
- Bingham, C. R., L. L. Riedinger, F. E. Turner, B. D. Kern, J. L. Weil, K. J. Hofstetter, J. Lin, E. F. Zganjar, A. V. Ramayya, J. H. Hamilton, J. L. Wood, G. M. Gowdy, R. W. Fink, E. H. Spejewski, W. D. Schmidt-Ott, R. L. Mlekodaj, H. K. Carter, and K. S. R. Sastry, "Decay of Mass-Separated ^{190}Tl and ^{190}Hg ," *Physical Review C*.
- Boldeman, J. W., B. J. Allen, M. J. Kenny, A. R. de L. Musgrove, and R. L. Macklin, "Valence and Doorway State Effects in Neutron Capture Near Closed Shells," *Proceedings Third National Soviet Conference on Neutron Physics* (Kiev, U.S.S.R., June 1975).
- Brady, F. P., N.S.P. King, M. W. McNaughton, and G. R. Satchler, "Excitation of Analogs of Giant Dipole States Via the $^{27}Al(n,p)^{27}Mg$," *Phys. Rev. Lett.* **36**, 15-17 (1976).
- Bridwell, L. B., J. A. Biggerstaff, G. D. Alton, C. M. Jones, P. D. Miller, Q. Kessel, and B. W. Wehring, "Multiple Electron Loss Cross Sections for 60 MeV I^{+10} in Single Collisions with Xenon," *Proceedings Fourth International Conference on Beam-Foil Spectroscopy and Heavy Ion Atomic Physics* (Gatlinburg, Tenn., September 1975).
- Butler, H. M., C. B. Fulmer, and K. M. Wallace, "Neutron Shielding of Cyclotron Targets," *Health Physics*.
- Carlson, G. H., W. L. Talbert, Jr., and S. Raman, "Nuclear Data Sheets for $A = 118$," *Nucl. Data Sheets* **17**, 1-37 (January 1976).
- Carlson, T. A., "Primary Processes in Hot Atom Chemistry," *Nuclear Transformations in Solids*, North-Holland, Amsterdam, Netherlands.
- Carlson, T. A., "Photoelectron Spectroscopy" (book review), *American Scientist*.

- Carlson, T. A. "Satellite Structure in the Photoelectron Spectra of Transition Metal Compounds Ionized in the K Shell of the Metal Ion," *Proceedings Faraday Society Discussion on Electron Spectroscopy of Solids and Surfaces* (Vancouver, B.C., Canada, July 1975).
- Carlson, T. A. (invited paper), "Multiple Excitation in Free Molecules," *Proceedings NATO Advanced Study Institute* (Corry-Le-Rouet, France, August–September 1975).
- Cisneros, Carmen, I. Alvarez, C. F. Barnett, and J. A. Ray, "Differential Scattering and Total Cross Sections of Hydrogen and Deuterium Atoms in Nitrogen," *Physical Review*.
- Cisneros, Carmen, I. Alvarez, C. F. Barnett, and J. A. Ray, "Angular Distributions and Total Cross Sections for D^- Formation from Interaction of D^+ and D^0 with Cesium," *Physical Review*.
- Condo, G. T., W. M. Bugg, E. L. Hart, H. O. Cohn, and R. D. McCulloch, "Nuclear Absorption of Slow Antiprotons," *Proceedings IVth International Symposium on Nuclear-Antinuclear Interactions* (Syracuse, N.Y., May 1975).
- Crandall, D. H., R. E. Olson, E. J. Shipsey, and J. C. Browne, "Single and Double Charge Transfer in C^{4+} -He Collision," *Physical Review Letters*.
- Cusson, R. Y. and J. Maruhn, "Dynamics of $^{12}C + ^{12}C$ in a Realistic T.D.H.F. Model," *Physical Review Letters*.
- Dalton, B., "Non-Linear Realizations of the Direct Product of Two Lorentz Groups on an Antisymmetric Tensor Field," *Physical Review*.
- Datz, S., C. D. Moak, B. R. Appleton, J. A. Biggerstaff, and T. S. Noggle, "Hyper- and Planar-Channeling of Charge-State-Selected 27.5-MeV Oxygen Ions in Ag," *Proceedings Sixth International Conference on Atomic Collisions in Solids* (Amsterdam, Netherlands, September 1975).
- Davies, K.T.R., S. E. Koonin, J. R. Nix, and A. J. Sierk, "Macroscopic and Microscopic Approaches to Nuclear Dissipation," *Proceedings International Workshop III on Gross Properties of Nuclei and Nuclear Excitations* (Hirschegg, Austria, January 1975); also, LA-UR-75-5.
- Dayras, R. A., R. G. Stokstad, Z. E. Switkowski, and R. M. Wieland, "Gamma-ray Yields from $^{12}C + ^{13}C$ Reactions Near and Below the Coulomb Barrier," *Nuclear Physics*.
- de Swiniarski, R., G. Bagieu, M. Bedjidi, C. B. Fulmer, J. Y. Grossiord, M. Massaad, J. R. Pizzi, and M. Gusakow, "Inelastic Scattering of 30 MeV Polarized Protons from $^{90,92}Zr$ and ^{92}Mo ," *Proceedings Fourth International Symposium on Polarization Phenomena in Nuclear Reactions* (Zurich, Switzerland, August 1975).
- de Swiniarski, R., G. Bagieu, M. Massaad, Dinh-Lien Pham, M. Bedjidi, J. Y. Grossiord, M. Gusakow, J. R. Pizzi, and C. B. Fulmer, "Macroscopic and Microscopic Model Analysis of Inelastic Scattering of 30 MeV Polarized Protons from $^{90,92}Zr$ and ^{92}Mo ," *Physics Letters*.
- Dress, W. B., Jr., "Observation of Two Photons in n - p Capture," *Proceedings VI International Conference on High Energy Physics and Nuclear Structure* (Santa Fe, N.M., June 9–13, 1975).
- Ellis, Y. A., "Nuclear Data Sheets for $A = 216$," *Nucl. Data Sheets* 17, 329–39 (March 1976).
- Ellis, Y. A., "Nuclear Data Sheets for $A = 220$," *Nucl. Data Sheets* 17, 341–50 (March 1976).
- Ellis, Y. A., "Nuclear Data Sheets for $A = 224$," *Nucl. Data Sheets* 17, 351–66 (March 1976).
- Ewbank, W. B., R. L. Haese, F. W. Hurley, and M. R. McGinnis, "Recent References (August 16 through December 15, 1975)," *Nucl. Data Sheets* 18, 1–85 (May 1976).
- Fong, D., M. Heller, A. Shapiro, M. Widgoff, F. Bruyant, D. Bogert, M. Johnson, R. Burnstein, C. Fu, D. Petersen, M. Robertson, H. Rubin, R. Sard, A. Snyder, J. Tortora, D. Alyea, C-Y Chien, P. Lucas, A. Pevsner, R. Zdanis, J. Brau, J. Grunhaus, E. Hafen, R. Hulsizer, U. Karshon, V. Kistiakowsky, A. Levy, A. Napier, I. Pless, P. Trapagnier, R. Yamamoto, H. Cohn, T. C. Ou, R. Plano, T. Watts, E. Brucker, E. Koller, P. Stamer, S. Taylor, W. Bugg, G. Condo, T. Handler, E. Hart, H. Kraybill, D. Ljung, T. Ludlam, and H. Taff, "Inelastic Two-Prong Events in $147 \text{ GeV}/c \pi^- p$," *Physical Review*.
- Forester, J. P., R. S. Peterson, P. M. Griffin, D. J. Pegg, H. H. Haselton, K. H. Liao, I. A. Sellin, J. R. Mowat, and R. S. Thoe, "Autoionizing States in Highly Ionized Oxygen, Fluorine, and Silicon," *Proceedings Fourth International Conference on Beam-Foil Spectroscopy* (Gatlinburg, Tenn., September 1975).

- Fowler, J. L. (invited paper), "Summary for Panel on Significance and Accomplishments of the Conference," *Proceedings Conference on Nuclear Cross Sections and Technology* (Washington, D.C., March 1975).
- Friedland, E., M. Goldschmidt, C. A. Widener, J.L.C. Ford, Jr., and S. T. Thornton, "Spectroscopic Investigation of the $^{144}\text{Sm}(^3\text{He},\alpha)^{143}\text{Sm}$ Reaction," *Nuclear Physics*.
- Fulmer, C. B., D. C. Hensley, J. C. Hafele, C. C. Foster, N. M. O'Fallon, W. W. Eidson, and S. A. Gronemeyer, "Back-Angle ^3He and Alpha-Particle Elastic Scattering from ^{27}Al ," *Physical Review*.
- Gari, M., A. H. Huffman, J. B. McGrory, and R. Offermann, "Weak Interaction Theories and Parity Mixing in ^{18}F and ^{19}F ," *Proceedings Symposium on Interaction Studies in Nuclei* (Mainz, Germany, February 1975).
- Gomez del Campo, J., M. E. Ortiz, A. Dacal, J.L.C. Ford, Jr., R. L. Robinson, P. H. Stelson, and S. T. Thornton, "Study of the Coherence Widths in ^{28}Si Measured by the $^{12}\text{C}(^{16}\text{O},\alpha)$ Reaction," *Nuclear Physics*.
- Goodman, C. D., W. R. Wharton, and D. C. Hensley, "The Reaction $^{14}\text{C}(^6\text{Li},^6\text{He})^{14}\text{N}$ and the Distribution of Gamow-Teller Strength," *Physical Review Letters*.
- Gowdy, G. M., A. C. Xenoulis, J. L. Wood, K. R. Baker, R. W. Fink, J. L. Weil, B. D. Kern, K. J. Hofstetter, E. H. Spejewski, R. L. Mlekodaj, H. K. Carter, W. D. Schmidt-Ott, J. Lin, C. R. Bingham, L. L. Riedinger, E. F. Zganjar, K.S.R. Sastry, A. V. Ramayya, and J. H. Hamilton, "On-Line Mass Separator Investigation of New Isotope 2.9-Sec ^{116}I ," *Physical Review*.
- Griffin, P. M., D. J. Pegg, I. A. Sellin, K. W. Jones, D. Pisano, T. H. Kruse, and S. Bashkin, "Extreme Ultraviolet Spectra of Highly Stripped Si Ions," *Proceedings Fourth International Conference on Beam-Foil Spectroscopy and Heavy Ion Atomic Physics Symposium* (Gallinburg, Tenn., September 1975).
- Gustafson, D. E., J. Gomez del Campo, R. L. Robinson, P. H. Stelson, P. D. Miller, and J. K. Bair, "High Spin States of ^{26}Mg Populated in the $^{12}\text{C}(^{18}\text{O},\alpha)$ Reaction," *Nuclear Physics*.
- Gustafson, D. E., S. T. Thornton, T. C. Schweizer, J.L.C. Ford, Jr., P. D. Miller, R. L. Robinson, and P. H. Stelson, "High-Spin States of the $K^\pi = 3/2^+$ Bands of ^{23}Na ," *Physical Review*.
- Gustafson, D. E., S. T. Thornton, J.L.C. Ford, Jr., P. D. Miller, R. L. Robinson, and P. H. Stelson, "Preferential Population of the $K^\pi = 1/2^-$ Band of ^{23}Na Observed in the $^{12}\text{C}(^{15}\text{N},\alpha)$ Reaction," *Physical Review Letters*.
- Halbert, E. C., J. B. McGrory, G. R. Satchler, and J. Speth, "Hadronic Excitation of the Giant Resonance Region of ^{208}Pb ," *Proceedings Symposium on Highly Excited States in Nuclei* (Jülich, Germany, September 1975).
- Hamilton, J. H., K. R. Baker, C. R. Bingham, E. L. Bosworth, H. K. Carter, J. D. Cole, R. W. Fink, G. Garcia Bermudez, G. M. Gowdy, K. J. Hofstetter, M. A. Ijaz, A. C. Kahler, B. D. Kern, W. Lourens, B. Martin, R. L. Mlekodaj, A. V. Ramayya, L. L. Riedinger, W. D. Schmidt-Ott, E. H. Spejewski, B. N. Subba Rao, E. L. Robinson, K. S. Toth, F. Turner, J. L. Weil, J. L. Wood, A. Xenoulis, and E. F. Zganjar, "New Isotope ^{193}Pb and the Structure of ^{193}Tl ; Shape Coexistence in ^{188}Hg and in ^{189}Au ; and a New Ion Source: Recent UNISOR Research," *Izvestiya Akademii Nauk Uzbekskoi SSR*.
- Hamilton, J. H., H. L. Crowell, R. L. Robinson, A. V. Ramayya, W. E. Collins, R. M. Ronningen, V. Maruhn-Rezwani, J. Maruhn, N. C. Singhal, H. J. Kim, R. O. Sayer, T. Magee, and L. C. Whitlock, "Lifetime Measurements to Test the Coexistence of Spherical and Deformed Shapes in ^{72}Se ," *Phys. Rev. Lett.* **36**, 340-42 (1976).
- Harmatz, B., "Nuclear Data Sheets for $A = 167$," *Nucl. Data Sheets* **17**, 143-92 (January 1976).
- Hillis, D. L., E. E. Gross, D. C. Hensley, M. L. Halbert, L. L. Riedinger, C. R. Bingham, A. Scott, and D. Martin, "Elastic and Inelastic Scattering of 70-MeV ^{12}C Ions from ^{144}Nd ," *Physics Letters*.
- Hillis, D. L., E. E. Gross, D. C. Hensley, L. D. Rickertsen, C. R. Bingham, A. Scott, and F. T. Baker, "Multi-Step Processes in the Inelastic Scattering of 70.4-MeV ^{12}C from ^{144}Nd ," *Phys. Rev. Lett.* **36**, 304-6 (1976).
- Horen, D. J., "Nuclear Spectra," *Encyclopedia of Science and Technology*, McGraw-Hill, New York.
- Horen, D. J., "Nuclear Data Sheets for $A = 228$," *Nucl. Data Sheets* **17**, 367-90 (March 1976).
- Hudson, E. D., R. S. Lord, L. L. Riedinger, J. A. Martin, J. K. Bair, L. N. Howell, F. Irwin, J. W. Johnson, G. S. McNeilly, and S. W. Mosko, "Magnet Model Studies for Separated-Sector Heavy Ion Cyclotrons," *Proceedings VIIIth International Conference on Cyclotrons and their Applications* (Zurich, Switzerland, August 1975).

- Hudson, E. D., M. L. Mallory, and R. S. Lord, "Production of Positive Ion Beams from Solids," *IEEE Trans. Nucl. Sci.* (International Conference on Heavy Ion Sources, Gatlinburg, Tenn., October 1975).
- Hudson, E. D., J. A. Martin, M. L. Mallory, F. E. McDaniel, and F. Irwin, "Magnetic Field Trimming Studies for a Separated-Sector Cyclotron," *Proceedings VIIIth International Conference on Cyclotrons and their Applications* (Zurich, Switzerland, August 1975).
- James, G. D., J.W.T. Dabbs, J. A. Harvey, N. W. Hill, and R. H. Schindler, "Intermediate Structure Studies of ^{234}U Cross Sections," *Physical Review*.
- Johnson, C. H., "A Ring Lens for Producing Uniform Density Ion Beams," *Proceedings Symposium on Experimental Methods for Charged-Particle Irradiations* (Gatlinburg, Tenn., September 1975).
- Johnson, J. W., "Evaluation of Vacuum Components for Beam Lines for the ORNL 25-MV Heavy Ion Accelerator," *Proceedings Symposium on Applied Vacuum Science and Technology* (Tampa, Fla., February 1976).
- Jones, C. M. (invited paper), "Large Tandem Accelerators," *IEEE Trans. Nucl. Sci.* (International Conference on Heavy Ion Sources, Gatlinburg, Tenn., October 1975).
- Kern, B. D., J. L. Weil, J. H. Hamilton, A. V. Ramayya, C. R. Bingham, L. L. Riedinger, E. F. Zganjar, J. L. Wood, G. M. Gowdy, R. W. Bink, E. H. Spejewski, H. K. Carter, R. L. Mlekodaj, and J. Lin, "Mass Differences of Proton-Rich Atoms Near $A = 116$ and $A = 190$," *Proceedings of Conference on Atomic Masses and Fundamental Constants* (Paris, France, June 1975).
- Kim, H. J., "Nuclear Data Sheets for $A = 59$," *Nucl. Data Sheets* **17**, 485--517 (April 1976).
- Kim, H. J., J. Delaunay, and N. Bendjaballah, "Unambiguous Spin Assignments from In-Beam Gamma-Ray Data," *Physics Letters*.
- Kocher, D. C., "Nuclear Data Sheets for $A = 120$," *Nucl. Data Sheets* **17**, 39--95 (January 1976).
- Kocher, D. C., "Nuclear Data Sheets for $A = 74$," *Nucl. Data Sheets* **17**, 519--72 (April 1976).
- Laubert, R., R. S. Peterson, J. P. Forester, K. H. Liao, P. M. Griffin, H. Hayden, S. B. Elston, D. J. Pegg, R. S. Thoe, and I. A. Sellin, "Differences in the Production of Noncharacteristic Radiation in Gaseous and Solid Targets," *Physical Review Letters*.
- Lewis, M. B., F. K. McGowan, C. H. Johnson, and M. J. Saltmarsh, "The Oak Ridge CN Van de Graaff Facility for Heavy Ion Radiation Damage Studies," *Proceedings Symposium on Experimental Methods for Charged-Particle Irradiations* (Gatlinburg, Tenn., September 1975).
- Lord, R. S., E. D. Hudson, G. S. McNeilly, R. O. Sayer, J. B. Ball, M. L. Mallory, S. W. Mosko, R. M. Beckers, K. N. Fischer, J. A. Martin, and J. D. Rylander, "The Oak Ridge Isochronous Cyclotron as an Energy Booster for a 25-MV Tandem," *Proceedings VIIIth International Conference on Cyclotrons and their Applications* (Zurich, Switzerland, August 1975).
- Lowry, M., J. S. Schweitzer, R. Dayras, and R. G. Stokstad, "Cross Sections for ^6Li Production in the Reactions $^{10}\text{B} + ^{16}\text{O}$ and $^{12}\text{C} + ^{14}\text{N}$," *Nuclear Physics*.
- Ludemann, C. A., "Raise Your Hand if you Know What CAMAC Is!," *Proceedings 1976 National Computer Conference* (New York, June 1976).
- Macklin, R. L., "Neutron Capture Cross Section of Niobium from 2.6 to 700 keV," *Nuclear Science and Engineering*.
- Macklin, R. L., "The $^{165}\text{Ho}(n,\gamma)$ Standard Cross Section from 3 to 450 keV," *Nuclear Science and Engineering*.
- Mallory, M. L. and D. H. Crandall, "A Penning Multiply Charged Heavy Ion Source Test Facility," *IEEE Trans. Nucl. Sci.* (International Conference on Heavy Ion Sources, Gatlinburg, Tenn., October 1975).
- Mallory, M. L., K. N. Fischer, and E. D. Hudson, "Isochronous Cyclotron Harmonic Beam Space Charge Effect," *Nuclear Instruments and Methods*.
- Martin, J. A., "Accelerators for Heavy Ions," *Proceedings Seventh International Conference on Cyclotrons and their Applications* (Zurich, Switzerland, August 1975).

- Martin, J. A., "Oak Ridge Heavy Ion Research Laboratory," *Particle Accelerators (News & Views)*.
- Martin, J. A., "VIIth International Conference on Cyclotrons and their Applications," *Particle Accelerators (News & Views)*.
- Martin, M. J., Ed., "Nuclear Decay Data for Selected Radionuclides," *Appendix - A Manual of Radioactivity Procedures, NBS Handbook 80*, National Council on Radiation Protection and Measurements.
- Maruhn, J. A. and W. Greiner, "Collective Effects on Mass Asymmetry in Fission," *Physical Review*.
- Maruhn, J. A., T. A. Welton, and C. Y. Wong, "Remarks on the Numerical Solution of Poisson's Equation for Isolated Charge Distribution," *Journal of Computational Physics*.
- McGrory, J. B. (invited paper), "Shell Model Calculations of Electromagnetic Observables of Nuclei in the *sd*-Shell Region," *Proceedings International Conference on Gamma-ray Transition Probabilities* (Delhi, India, November 1974).
- McNeilly, G. S., E. D. Hudson, R. S. Lord, M. L. Mallory, J. E. Mann, J. B. Ball, and J. A. Martin, "Design Study for the Conversion of the Oak Ridge Isochronous Cyclotron from an Energy Constant of $K = 90$ to $K = 300$," *Proceedings VIIth International Conference on Cyclotrons and their Applications* (Zurich, Switzerland, August 1975).
- Moak, C. D., "Sources of Protons," *Fourth Edition McGraw-Hill Encyclopedia of Science and Technology*, Daniel N. Lapedes, Ed., McGraw-Hill, New York.
- Moak, C. D., "Channeling in Solids," *Fourth Edition McGraw-Hill Encyclopedia of Science and Technology*, Daniel N. Lapedes, Ed., McGraw-Hill, New York.
- Moak, C. D. (invited paper), "Stripping in Foils and Gases," *IEEE Trans. Nucl. Sci.* (International Conference on Heavy Ion Sources, Gatlinburg, Tenn., October 1975).
- Moak, C. D., B. R. Appleton, J. A. Biggerstaff, M. D. Brown, S. Datz, T. S. Noggle, and H. Verbeek, "The Velocity Dependence of the Stopping Power of Channeled Iodine Ions from 0.6 to 60 MeV," *Proceedings Sixth International Conference on Atomic Collisions in Solids* (Amsterdam, The Netherlands, September 1975).
- Mosko, S. W., D. B. Bates, R. R. Bigelow, E. K. Connongim, E. W. Pipes, and K. Sueker, "A 120-kA Pulsed dc Power System with Computerized Thyristor Triggering," *IEEE Trans. Nucl. Sci.* (Proceedings Sixth Symposium on Engineering Problems of Fusion Research, San Diego, Calif., November 1975).
- Mosko, S. W., E. D. Hudson, R. S. Lord, M. L. Mallory, J. E. Mann, J. A. Martin, G. S. McNeilly, J. B. Ball, K. N. Fischer, L. L. Riedinger, and R. L. Robinson, "A Separated-Sector Cyclotron Post-Accelerator for the Oak Ridge Heavy Ion Laboratory," *Proceedings VIIth International Conference on Cyclotrons and Their Applications* (Zurich, Switzerland, August 1975).
- Musgrove, A. R. de L., B. J. Allen, J. W. Boldeman, D.M.H. Chan, and R. L. Macklin, "keV Neutron Resonance Capture in ^{40}Ca ," *Nuclear Physics*.
- Musgrove, A. R. de L., B. J. Allen, J. W. Boldeman, and R. L. Macklin, "keV Neutron Capture Cross Sections of ^{134}Ba and ^{136}Ba ," *Nucl. Phys.* **A256**, 173-88 (1976).
- Obenshain, F. E., J. C. Williams, and L. W. Houk, "Hyperfine Interactions at ^{61}Ni in Ionic Nickel Compounds," *Journal of Inorganic and Nuclear Chemistry*.
- Peebles, P. Z., M. Parvarandeh, and C. M. Jones, "Shunt Impedance of Spiral Loaded Resonant RF Cavities," *Particle Accelerators*.
- Pegg, D. J. (invited paper), "Autoionizing States in the Alkalis," *Proceedings Fourth International Conference on Beam-Foil Spectroscopy* (Gatlinburg, Tenn., September 1975).
- Pegg, D. J., H. H. Haselton, R. S. Thoe, P. M. Griffin, M. D. Brown, and I. A. Sellin, "Autoionizing States Formed in $\text{Na}^+ + \text{He}$ and $\text{Mg}^+ + \text{He}$ Collisions at 70 keV $^+$," *Proceedings Ninth International Conference on Physics of Electronics and Atomic Collisions* (Seattle, Wash., July 1975).
- Pegg, D. J., H. H. Haselton, R. S. Thoe, P. M. Griffin, M. D. Brown, and I. A. Sellin, "Optically Inaccessible Core Excited States of Li and Na," *Physics Letters*.

- Pegg, D. J., H. H. Haselton, R. S. Thoe, P. M. Griffin, M. D. Brown, and I. A. Sellin, "Core-Excited Autoionizing States in the Alkalis," *Physics Review*.
- Peterson, R. S., R. S. Thoe, H. Hayden, S. B. Elston, J. P. Forester, K.-H. Liao, P. M. Griffin, D. J. Pegg, I. A. Sellin, and R. Laubert, "Differences in the Production of Noncharacteristic Radiation in Solid and Gas Targets," *Proceedings Fourth International Conference on Beam Foil Spectroscopy and Heavy Ion Atomic Physics* (Gatlinburg, Tenn., September 1975).
- Pichevar, M., J. Delaunay, B. Delaunay, H. J. Kim, Y. El Masri, and J. Vervier, "High Spin States in ^{59}Ni ," *Nuclear Physics*.
- Rainis, A. E., K. S. Toth, and C. R. Bingham, "Isomerism in the New $N = 81$ Isotope, ^{147}Dy ," *Physical Review*.
- Raman, S. (invited paper), "General Survey of Applications which Require Nuclear Data," *Proceedings IAEA Meeting on Transactinium Isotope Nuclear Data* (Karlsruhe, Germany, November 1975).
- Raman, S. (invited paper), "Some Activities in the United States Concerning the Physics Aspects of Actinide Waste Recycling," *Proceedings IAEA Meeting on Transactinium Isotope Nuclear Data* (Karlsruhe, Germany, November 1975).
- Raman, S., R. L. Auble, J. B. Ball, E. Newman, J. C. Wells, Jr., and J. Lin, "Levels in ^{144}Nd from the $^{143}\text{Nd}(d,p)$ and the $^{146}\text{Nd}(p,t)$ Reactions," *Zeitschrift fuer Physik*.
- Robinson, R. L., H. J. Kim, J. B. McGrory, G. J. Smith, W. T. Milner, R. O. Sayer, J. C. Wells, Jr., and J. Lin, "High-Spin States in ^{42}Ca ," *Physical Review*.
- Ronningen, R. M., J. H. Hamilton, A. V. Ramayya, L. L. Riedinger, G. Garcia Bermudez, J. Lange, W. Lourens, L. Varnell, R. L. Robinson, P. H. Stelson, and J.L.C. Ford, Jr., "Reduced Transition Probabilities of Vibrational States in Deformed Rare Earth Nuclei," *Proceedings International Conference on Gamma-ray Transition Probabilities* (Delhi, India, November 1974).
- Saltmarsh, M. J. and J. A. Horak (invited paper), "A Large-Volume Intense Neutron Source for CTR Materials Studies," *Proceedings International Conference on Radiation Test Facilities for the CTR Surface and Materials Program* (Argonne, Ill., July 1975).
- Sastry, K.S.R., A. V. Ramayya, R. S. Lee, J. H. Hamilton, R. L. Mlekodaj, and N. R. Johnson, "Gyromagnetic Ratio of the First 2^+ Excited State in ^{126}Se ," *Nuclear Physics*.
- Schmidt-Ott, W. D. and K. S. Toth, "Decay Rates for Doubly-Even $N = 84$ Alpha-Emitters and the Subshell Closure at $Z = 64$," *Physical Review*.
- Schmorak, M. R., "Nuclear Data Sheets for $A = 244-262$ (even- A)," *Nucl. Data Sheets* 17, 391-484 (March 1976).
- Sellin, I. A., "The Measurement of Autoionizing Ion Levels and Lifetimes by Projectile Electron Spectroscopy," chapter in *Topics in Modern Physics: Beam-Foil Spectroscopy*, Springer-Verlag, Heidelberg-New York-London, 1975.
- Sellin, I. A., "Applications of Beam-Foil Spectroscopy to Atomic Collisions in Solids," *Surface Science*.
- Sellin, I. A., "Highly Ionized Ions," *Advances in Atomic and Molecular Physics*, Academic Press, New York, 1976.
- Shamu, R. E., Ch. Lagrange, E. M. Bernstein, J. J. Ramirez, T. Tamura, and C. Y. Wong, "Quadrupole Deformation Parameters of $^{148,152,154}\text{Sm}$ Determined from Neutron Total Cross Sections," *Physical Review Letters*.
- Smith, J. S., III and R. O. Sayer, "A Program to Calculate and Plot the Nuclear Moment of Inertia Versus the Square of the Rotational Frequency," *Computer Physics Communications*.
- Stelson, P. H. (invited paper), "The Atomic Physics Potential of New Accelerators," *Proceedings Fourth International Conference on Beam Foil Spectroscopy and Heavy Ion Atomic Physics* (Gatlinburg, Tenn., September 1975).
- Stelson, P. H., "Coulomb Excitation," *Fourth Edition McGraw-Hill Encyclopedia of Science and Technology*, McGraw-Hill, New York.
- Stelson, P. H., "Future of Physics with Heavy Ions," *IEEE Trans. Nucl. Sci.* (International Conference on Heavy Ion Sources, Gatlinburg, Tenn., October 1975).

- Tamagawa, H., I. Alexeff, C. M. Jones, N. H. Lazar, and P. D. Miller, "Use of the Hot-Electron Mirror Machine INTEREM as a High-Z Ion Source," *IEEE Trans. Nucl. Sci.* (International Conference on Heavy Ion Sources, Gatlinburg, Tenn., October 1975).
- Tamain, B., F. Plasil, C. Ngo, J. Peter, M. Berlinger, and F. Hanappe, "On the Energy Dependence of Quasi-Fission," *Phys. Rev. Lett.* **36**, 18-20 (1976).
- Thoe, R. S., R. S. Peterson, I. A. Sellin, K. H. Liao, D. J. Pegg, J. P. Forester, and P. M. Griffin, "Polarization Measurements of the Non-Characteristic Radiation Emitted from Collision between High-Energy Al Ions," *Physics Letters*.
- Thoe, R. S., I. A. Sellin, J. Forester, P. M. Griffin, K. H. Liao, D. J. Pegg, and R. S. Peterson, "Observation of Saturation of Polarization of Noncharacteristic K X-rays Emitted in Heavy Ion Collisions," *Physical Review Letters*.
- Thoe, R. S., I. A. Sellin, K. H. Liao, R. S. Peterson, D. J. Pegg, J. P. Forester, and P. M. Griffin, "Angular Distribution Studies of Noncharacteristic X-radiation," *Proceedings Fourth International Conference on Beam-Foil Spectroscopy* (Gatlinburg, Tenn., September 1975).
- Thornton, S. T., D. E. Gustafson, J.L.C. Ford, Jr., K. S. Toth, and D. C. Hensley, "Inelastic Scattering and Transfer Reactions from ^{12}C Ions on ^{90}Zr ," *Physical Review*.
- Thornton, S. T., T. C. Schweizer, D. E. Gustafson, J.L.C. Ford, Jr., and M. J. LeVine, "Nuclear Structure Study of ^{141}Nd , ^{143}Nd , and ^{143}Pm by ^{13}C Induced Reactions on ^{142}Nd ," *Physical Review*.
- Toth, K. S., E. Newman, C. R. Bingham, and A. E. Rainis, "Comment Concerning the Tentatively Proposed 1778.9-keV level in ^{147}Gd ," *Physical Review (Comments)*.
- Tricomi, J., J. L. Duggan, F. D. McDaniel, P. D. Miller, R. P. Chaturvedi, R. M. Wheeler, J. Lin, K. A. Kuenhold, L. A. Rayburn, and S. J. Cipolla, "K Shell X-ray Production in Ge, Rb, Y, Zr, and Ag by ^{14}N Ion Impact," *Physical Review*.
- Tuttle, W. K., III, P. H. Stelson, R. L. Robinson, W. T. Milner, F. K. McGowan, S. Raman, and W. K. Dagenhart, "Coulomb Excitation of $^{113,115}\text{In}$," *Physical Review*.
- Vernon, G. A., G. Stucky, and T. A. Carlson, "Comprehensive Study of Satellite Structure in the Photoelectron Spectra of Transition Metal Compounds," *Inorganic Chemistry*.
- Wells, J. C., Jr., R. L. Robinson, H. J. Kim, and J.L.C. Ford, Jr., "Absolute Cross Sections for the $^{61}\text{Ni}(^{16}\text{O},3n)^{74}\text{Kr}$ Reaction," *Physical Review*.
- Wheeler, R. M., R. P. Chaturvedi, J. L. Duggan, J. Tricomi, and P. D. Miller, "K X-ray Production Cross Sections for Fourteen Elements from Calcium to Palladium for Incident Carbon Ions," *Physical Review*.
- Wong, C. Y., "Limits of the Nuclear Viscosity Coefficient in the Liquid Drop Model," *Physics Letters*.
- Wong, C. Y., "Time Scales in the Dynamics of Nuclear Systems," *Nuclear Physics*.
- Wong, C. Y., "On the Schrödinger Equation in Fluid Dynamical Form," *Journal of Mathematics and Physics*.
- Wong, C. Y. and K. S. Low, "Time-Dependent Hartree-Fock Formalism with Phenomenological Dissipation," *Proceedings International Workshop IV on Gross Properties of Nuclei and Nuclear Excitations* (Hirschegg, Austria, January 1976).
- Wong, C. Y. and H.H.K. Tang (invited paper), "Vibrational Frequency of a Non-Conducting Charged Liquid Drop," *Proceedings International Colloquium on Drops and Bubbles* (Pasadena, Calif., August 1974).
- Wong, C. Y., T. A. Welton, and J. A. Maruhn, "Dynamics of Nuclear Fluid II. Conditions for a Macroscopic Description," *Nuclear Physics*.
- Worsham, R. E., "Studies with Highly-Coherent Illumination and Liquid-Helium-Cooled Specimens," *Proceedings Sixth European Congress on Electron Microscopy* (Jerusalem, Israel, September 1976).
- Zucker, A. and J. B. Ball (invited paper), "The Heavy-Ion Accelerator Project at Oak Ridge," *Proceedings IV All-Union National Conference on Particle Accelerators* (Moscow, U.S.S.R., November 1974).

9. Papers Presented at Scientific and Technical Meetings

Prepared by Wilma L. Stair

American Chemical Society Meeting (St. Joseph Valley Section), South Bend, Indiana, January 13, 1975

H. W. Morgan (invited talk), "Coherent Light and Holography."

International Workshop III on Gross Properties of Nuclei and Nuclear Excitation, Hirschegg, Austria, January 13--18, 1975

K. T. R. Davies, S. E. Koonin, J. R. Nix, and A. J. Sierk, "Macroscopic Approaches to Nuclear Dissipation."

F. Plasil, "Experimental Summary."

F. Plasil, "On Reaction Times for Quasi-Fission and on the Critical Distance Concept in Heavy-Ion Fusion Reactions."

American Chemical Society Meeting (Kalamazoo Section), Kalamazoo, Michigan, January 14, 1975

H. W. Morgan (invited talk), "Coherent Light and Holography."

American Chemical Society (University of Michigan Section), Grand Rapids, Michigan, January 15, 1975

H. W. Morgan (invited talk), "Coherent Light and Holography."

American Chemical Society (University of Michigan Section), Ann Arbor, Michigan, January 16, 1975

H. W. Morgan (invited talk), "Coherent Light and Holography."

Twenty-fifth Annual National Conference of the Academy of Sciences of the U.S.S.R. on Nuclear Spectroscopy and Structure of the Atomic Nucleus, Leningrad, U.S.S.R., January 29--February 1, 1975

J. H. Hamilton, K. R. Baker, C. R. Bingham, E. L. Bosworth, H. K. Carter, J. D. Cole, R. W. Fink, G. Garcia Bermudez, G. W. Gowdy, K. J. Hofstetter, M. A. Ijaz, A. C. Kahler, B. D. Kern, W. Lourens, B. Martin, R. L. Mlekodaj, A. V. Ramayya, L. L. Riedinger, W. D. Schmidt-Ott, E. H. Spejewski, B. N. Subba Rao, E. L. Robinson, K. S. Toth, F. Turner, J. L. Weil, J. L. Wood, A. Xenoulis, and E. F. Zganjar, "New Isotopes ^{192}Pb and the Structure of ^{192}Tl ; Shape Coexistence in ^{188}Hg and in ^{189}Au ; and a New Ion Source: Recent UNISOR Research."

American Physical Society Meeting, Anaheim, California, January 29--February 1, 1975

J. A. Biggerstaff (invited talk), "New Measurements with Channeling," *Bull. Am. Phys. Soc.* **20**, 11 (1975).

D. Bogert, W. Barletta, D. Dauwe, M. Kenton, A. E. Snyder, R. D. Sard, D. G. Fong, M. Heller, A. Pevsner, R. A. Zdanis, O. Fu, D. V. Petersen, E. D. Alyea, Jr., J. Grunhaus, E. Hafen, P. Trepagnier, J. Wolfson, R. K. Yamamoto, W. M. Bugg, E. L. Hart, T. C. Ou, R. J. Plano, E. L. Koller, and P. Stamer, "Two-Body Correlations Among Mesons Produced by 147 GeV/c π^-p Interactions," *Bull. Am. Phys. Soc.* **20**, 14 (1975).

R. Y. Cusson and R. Hilko, "Realistic Heavy Ion Potentials from Constrained Self-Consistent B.H.F. Calculations," *Bull. Am. Phys. Soc.* **20**, 67 (1975).

D. G. Fong, M. Widgoff, P. Lucas, R. A. Zdanis, R. A. Burnstein, C. Fu, H. A. Rubin, A. E. Snyder, J. Tortora, E. D. Alyea, Jr., A. Levy, A. Napier, I. A. Pless, P. Trepagnier, G. T. Condo, R. J. Plano, T. L. Watts, P. Stamer, S. Taylor, M. Johnson, H. Kraybill, D. Ljung, T. Ludlam, and H. Taft, "Feynman-x and Rapidity Distributions of π^- and π^+ Mesons Produced by 147 GeV/c π^-p Interactions," *Bull. Am. Phys. Soc.* **20**, 14 (1975).

B. Hamatz, D. J. Horen, and Y. A. Ellis, "Anomalous Ground States in the Neutron-Deficient $171 \leq A \leq 181$ Region," *Bull. Am. Phys. Soc.* **20**, 96 (1975).

P. Lucas, C. Y. Chien, A. M. Shapiro, M. Widgoff, R. M. Robertson, H. A. Rubin, J. Tortora, E. D. Alyea, R. I. Hulsizer, U. Karshon, V. Kistiakowsky, A. Levy, A. Napier, I. A. Pless, G. T. Condo, E. L. Hart, T. L. Watts, E. B. Brucker, S. Taylor, M. Johnson, H. Kraybill, D. Ljung, T. Ludlam, and H. Taft, "Dependence of the Leading Particles in the 2, 4, and 6-Prong Final States Produced by 147 GeV/c π^-p Interactions," *Bull. Am. Phys. Soc.* **20**, 14 (1975).

L. G. Multhauf, K. G. Tirsell, and S. Raman, "Decay of ^{111}Sn ," *Bull. Am. Phys. Soc.* **20**, 74 (1975).

D. V. Petersen, R. A. Burnstein, R. M. Robertson, M. Heller, A. M. Shapiro, C. Y. Chien, A. Pevsner, R. D. Sard, E. D. Alyea, Jr., F. Bruyant, J. Grunhaus, E. Hafen, R. I. Hulsizer, U. Karshon, V. Kistiakowsky, W. M. Bugg, H. O. Cohn, T. C. Ou, E. B. Brucker, E. L. Koller, D. Bogert, W. Barletta, D. Dauwe, and M. Kenton, "Charged Prong Multiplicities Produced by 147 GeV/c K Incident on Protons," *Bull. Am. Phys. Soc.* **20**, 14 (1975).

A. E. Rainis, K. S. Toth, E. Newman, C. R. Bingham, H. K. Carter, and W. D. Schmidt-Ott, "Isomerism in the New $N = 81$ Isotope, ^{147}Dy ," *Bull. Am. Phys. Soc.* **20**, 74 (1975).

R. S. Thoe, I. A. Sellin, M. D. Brown, J. P. Forester, P. M. Griffin, D. J. Pegg, and R. S. Peterson, "Energy Dependence of the Directional Anisotropy Exhibited by Quasimolecular K X Radiation," *Bull. Am. Phys. Soc.* **20**, 75 (1975).

K. G. Tirsell, L. G. Multhauf, and S. Raman, "Decay of 20-min ^{46}K ," *Bull. Am. Phys. Soc.* **20**, 34 (1975).

Symposium on Interaction Studies in Nuclei, Mainz, Germany, February 1975

M. Gari, A. H. Huffman, J. B. McGrory, and R. Offermann, "Weak Interaction Theories and Parity Mixing in ^{18}F and ^{19}F ."

Western Regional Nuclear Conference, Manitoba, Canada, February 20--22, 1975

G. R. Satchler (invited talk), "Microscopic Description of Inelastic Scattering and the Excitation of Giant Resonances."

Conference on Nuclear Cross Sections and Technology (Topical Conference of the American Physical Society), Washington, D.C., March 3--7, 1975

B. J. Allen, J. W. Boldeman, M. J. Kenny, A. R. Musgrove, H. Pe, and R. L. Macklin, "Neutron Capture Mechanism in Light and Closed Shell Nuclides," *Bull. Am. Phys. Soc.* **20**, 150 (1975).

J. A. Cookson, M. Hussain, C. A. Uttley, J. L. Fowler, and R. B. Schwartz, "Absolute Calibration of Neutron Detectors in the 10--30 MeV Energy Range," *Bull. Am. Phys. Soc.* **20**, 137 (1975).

J. W. T. Dabbs, C. E. Bemis, N. W. Hill, and S. Raman, "Fission Cross Section Measurements on Short-Lived Alpha Emitters," *Bull. Am. Phys. Soc.* **20**, 137 (1975).

W. B. Ewbank, "Computer-Readable Nuclear Data Sheets," *Bull. Am. Phys. Soc.* **20**, 148 (1975).

J. L. Fowler (invited talk), "Panel and Roundtable Discussion of the Conference," *Bull. Am. Phys. Soc.* **20**, 175 (1975).

J. A. Harvey and N. W. Hill, "Neutron Total Cross Section of ${}^6\text{Li}$ from 100 eV to 3 MeV," *Bull. Am. Phys. Soc.* **20**, 145 (1975).

G. A. Keyworth, C. E. Olsen, J. D. Moses, J. W. T. Dabbs, and N. W. Hill, "Spin Determination of Resonances in ${}^{235}\text{U}$," *Bull. Am. Phys. Soc.* **20**, 159 (1975).

M. S. Pandey, J. B. Garg, J. A. Harvey, and W. M. Good, "High Resolution Total Cross Section in ${}^{54}\text{Fe}$ and ${}^{56}\text{Fe}$," *Bull. Am. Phys. Soc.* **20**, 166 (1975).

S. Raman, C. W. Nestor, Jr., and J. W. T. Dabbs, "The ${}^{233}\text{U}$ - ${}^{232}\text{Th}$ Reactor as a Burner for Actinide Wastes," *Bull. Am. Phys. Soc.* **20**, 144 (1975).

1975 Particle Accelerator Conference (Topical Conference of the American Physical Society), Washington, D.C., March 12–14, 1975

G. D. Alton, C. M. Jones, P. D. Miller, B. Wehring, J. A. Biggerstaff, C. D. Moak, Q. C. Kessel, and L. Bridwell, "Absolute Charge State Yields of 20 MeV Fe and I Ions Scattered from Xenon," *Bull. Am. Phys. Soc.* **20**, 195 (1975).

J. K. Bair, J. A. Biggerstaff, C. M. Jones, J. D. Larson, and W. T. Milner, "Design Considerations for the ORNL 25 MV Tandem Accelerator," *Bull. Am. Phys. Soc.* **20**, 202 (1975).

J. A. Biggerstaff, N. F. Ziegler, and J. W. McConnell, "Digital Control System for the ORNL 25 MV Tandem Accelerator," *Bull. Am. Phys. Soc.* **20**, 185 (1975).

E. D. Hudson, R. S. Lord, M. L. Mallory, and J. E. Mann, "Increased Intensity Heavy Ion Beams at ORIC with Cryopumping," *Bull. Am. Phys. Soc.* **20**, 216 (1975).

R. S. Lord, J. B. Ball, E. D. Hudson, M. L. Mallory, J. A. Martin, G. S. McNeilly, S. W. Mosko, R. M. Beckers, and J. D. Rylander, "Energy Boosting of a Tandem Beam with the Oak Ridge Isochronous Cyclotron," *Bull. Am. Phys. Soc.* **20**, 195 (1975).

M. L. Mallory and E. D. Hudson, "A Rotatable Cold Cathode Penning Ion Source," *Bull. Am. Phys. Soc.* **20**, 195 (1975).

M. L. Mallory, E. D. Hudson, and R. S. Lord, "Isochronous Cyclotron Harmonic Beam Experiment," *Bull. Am. Phys. Soc.* **20**, 196 (1975).

W. T. Milner, G. D. Alton, D. C. Hensley, C. M. Jones, R. F. King, J. D. Larson, and C. D. Moak, "Transport of DC and Bunched Beams through a 25 MV Folded Tandem Accelerator," *Bull. Am. Phys. Soc.* **20**, 196 (1975).

M. J. Saltmarsh (invited talk), "Uses of Accelerators in Energy Research and Development," *Bull. Am. Phys. Soc.* **20**, 180 (1975).

N. F. Ziegler, "An Improved Van de Graaff Belt Charge Regulator," *Bull. Am. Phys. Soc.* **20**, 204 (1975).

Europhysics Conference on Nuclear Interactions at Medium and Low Energies, Harwell, England, March 24–26, 1975

R. Eagle, N. M. Clarke, R. J. Griffiths, C. B. Fulmer, and D. C. Hensley, "Inelastic Scattering of ${}^3\text{He}$ from Samarium Isotopes at 53 MeV."

Conference on Deep Inelastic Processes and Compound Nucleus Formation, Stony Brook, New York, April 3–5, 1975

R. G. Stokstad (invited talk), "Limits on Fusion Cross Sections for Light Nuclei."

American Chemical Society Meeting, Philadelphia, Pennsylvania, April 6–11, 1975

R. G. Stokstad (invited talk), "Limits on Fusion Cross Sections for Light Nuclei."

G. A. Vernon, G. D. Stucky, and T. A. Carlson, "The Characterization of the $2p$ X-Ray Photoelectron Spectra of Transition Metal Compounds."

NNV-DPG Spring Meeting on Nuclear Physics, The Hague, Netherlands, April 7--11, 1975

W. D. Schmidt-Ott and K. S. Toth, "Decay Rates for Even-Even $N = 84$ Alpha-Emitters: Search for ^{148}Gd Electron Capture Decay."

American Physical Society Meeting, Washington, D.C., April 28--May 1, 1975

R. L. Becker (invited talk), "The Saturation Problem and Developments in the Many-Body Theory of the Self-Consistent Field," *Bull. Am. Phys. Soc.* **20**, 554 (1975).

R. F. Carlton, G. G. Slaughter, and S. Raman, "The $^{120}\text{Sn}(n,\gamma)^{121}\text{Sn}$ Reaction," *Bull. Am. Phys. Soc.* **20**, 687 (1975).

S. Datz, M. D. Brown, P. M. Griffin, R. S. Peterson, R. S. Thoe, and I. A. Sellin, "Charge State Dependence of X-Ray Production for Collisions of Ni (~ 1 MeV/nuc.) with SiH_4 ," *Bull. Am. Phys. Soc.* **20**, 639 (1975).

Y. A. Ellis, B. Harmatz, and D. J. Horen, "Some Aspects of Nilsson Orbital Properties," *Bull. Am. Phys. Soc.* **20**, 736 (1975).

J. L. C. Ford, Jr., K. S. Toth, E. E. Gross, D. C. Hensley, D. E. Gustafson, and S. T. Thornton, "Inelastic Scattering and Single-Nucleon Transfer Reactions Induced by 98-MeV ^{12}C Ions on ^{208}Pb ," *Bull. Am. Phys. Soc.* **20**, 576 (1975).

J. P. Forester, P. M. Griffin, H. H. Haselton, K. H. Liao, J. R. Mowat, D. J. Pegg, R. S. Peterson, I. A. Sellin, and R. S. Thoe, "Autoionizing States in Lithium-Like Silicon and Sodium-Like Chlorine," *Bull. Am. Phys. Soc.* **20**, 679 (1975).

D. L. Hillis, E. E. Gross, D. C. Hensley, C. R. Bingham, A. Scott, F. T. Baker, and D. Martin, "Coulomb-Nuclear Interference Effects in the Elastic and Inelastic Scattering of 70 MeV ^{12}C Ions from ^{144}Nd , ^{146}Nd , and ^{148}Nd ," *Bull. Am. Phys. Soc.* **20**, 575 (1975).

D. J. Horen, W. B. Ewbank, and S. Raman, "Neutron Separation Energy for ^{75}Se ," *Bull. Am. Phys. Soc.* **20**, 566 (1975).

P. G. Huray, F. E. Obenshain, and J. O. Thomson, "Temperature Dependence of the Mössbauer Isomer Shift and Recoilless Fraction for ^{197}Au ," *Bull. Am. Phys. Soc.* **20**, 609 (1975).

M. A. Ijaz, K. S. Toth, W. D. Schmidt-Ott, and C. R. Bingham, "Investigation of Tungsten Alpha-Emitters; New Isotopes $^{165},^{166}\text{W}$," *Bull. Am. Phys. Soc.* **20**, 715 (1975).

C. H. Johnson, "Ring Lens to Focus Ion Beams to Uniform Density," *Bull. Am. Phys. Soc.* **20**, 562 (1975).

E. T. Journey, J. A. Harvey, S. Raman, and N. W. Hill, "Thermal Neutron Capture and Absorption Cross Sections for ^{59}Ni ," *Bull. Am. Phys. Soc.* **20**, 560 (1975).

H. J. Kim, R. Ballini, B. Delaunay, J. P. Fouan, and M. Pichevar, "High-Spin States of ^{60}Ni ," *Bull. Am. Phys. Soc.* **20**, 565 (1975).

P. D. Kunz and L. D. Rickertsen, "Effects of Deuteron Continuum States in the Multi-Step (p - d , d - n) Reactions to Analogue States," *Bull. Am. Phys. Soc.* **20**, 666 (1975).

V. Maruhn-Rezwani and J. A. Maruhn, "Collective g -Factors and $E2/M1$ -Mixing Ratios in Even-Even Nuclei," *Bull. Am. Phys. Soc.* **20**, 735 (1975).

A. I. Namenson, A. Stolovy, and J. A. Harvey, "Neutron Resonances in Re Isotopes," *Bull. Am. Phys. Soc.* **20**, 561 (1975).

M. S. Pandey, J. B. Garg, J. A. Harvey, and W. M. Good, "High Resolution Total Cross Section in ^{63}Cu and ^{65}Cu ," *Bull. Am. Phys. Soc.* **20**, 561 (1975).

D. J. Pegg, H. H. Haselton, M. D. Brown, R. S. Thoe, P. M. Griffin, and I. A. Sellin, "Electron Spectra from the Autoionizing Decay of Collisionally Excited Mg^+ and K^+ Beams," *Bull. Am. Phys. Soc.* **20**, 674 (1975).

R. S. Peterson, J. P. Forester, P. M. Griffin, H. H. Haselton, K. H. Liao, J. R. Mowat, D. J. Pegg, I. A. Sellin, and R. S. Thoe, "Electron Spectra from Autoionizing States of Highly Stripped Oxygen and Fluorine," *Bull. Am. Phys. Soc.* **20**, 679 (1975).

G. A. Petitt and F. E. Obenshain, "TDPAC Study of ^{161}Dy in Gd_2O_3 and Gd Metal," *Bull. Am. Phys. Soc.* **20**, 615 (1975).

A. E. Rainis, K. S. Toth, C. R. Bingham, and W. D. Schmidt-Ott, "Observation of 1^+ ($\pi h_{11/2}, h_{9/2}$) States in $^{148,150,152}\text{Tb}$ Populated in the Decay of Their Dysprosium Parents," *Bull. Am. Phys. Soc.* **20**, 624 (1975).

L. D. Rickertsen, "Analysis of $^{12}\text{C} + ^{12}\text{C}$ Elastic and Inelastic Scattering," *Bull. Am. Phys. Soc.* **20**, 664 (1975).

R. L. Robinson, H. J. Kim, J. L. C. Ford, Jr., and J. C. Wells, Jr., "Absolute Cross Sections for $^{63}\text{Cu}(^{16}\text{O},X)$ Reactions," *Bull. Am. Phys. Soc.* **20**, 665 (1975).

M. Schmorak, "Nuclear Structure Properties of $A = 182$," *Bull. Am. Phys. Soc.* **20**, 669 (1975).

G. G. Slaughter and S. Raman, "Neutron Separation Energies of Tin Isotopes," *Bull. Am. Phys. Soc.* **20**, 560 (1975).

R. G. Stokstad, C. B. Fulmer, M. L. Halbert, D. C. Hensley, S. Raman, A. H. Snell, and P. H. Stelson, "Angular Distributions for $^{12}\text{C} + ^{12}\text{C}$ Elastic and Inelastic Scattering ($E_{\text{lab}} = 70\text{--}117$ MeV)," *Bull. Am. Phys. Soc.* **20**, 664 (1975).

R. Thoe (invited talk), "Directional Anisotropies in Non-Characteristic X-Ray Emission," *Bull. Am. Phys. Soc.* **20**, 607 (1975).

R. S. Thoe, I. A. Sellin, D. J. Pegg, J. P. Forester, K. H. Liao, R. S. Peterson, and P. M. Griffin, "Non-Characteristic Spectra from Symmetric and Asymmetric Collision Systems," *Bull. Am. Phys. Soc.* **20**, 675 (1975).

W. K. Tuttle III, P. H. Stelson, F. K. McGowan, W. T. Milner, S. Raman, and R. L. Robinson, "Coulomb Excitation of ^{113}In ," *Bull. Am. Phys. Soc.* **20**, 686 (1975).

J. L. Weil, B. D. Kern, E. F. Zganjar, J. L. Wood, R. W. Fink, C. R. Bingham, L. L. Riedinger, J. H. Hamilton, A. V. Ramayya, E. H. Spejewski, W. D. Schmidt-Ott, H. K. Carter, R. L. Mlekodaj, and J. Lin, "The Positron Decay of ^{189}Tl , ^{189}Hg , and ^{189}Au ," *Bull. Am. Phys. Soc.* **20**, 715 (1975).

J. C. Wells, Jr., S. Raman, G. G. Slaughter, and E. T. Jurney, "Energy Levels and Level Density in ^{144}Nd ," *Bull. Am. Phys. Soc.* **20**, 624 (1975).

C. Y. Wong, J. A. Maruhn, and T. A. Welton, "Hydrodynamics in Heavy-Ion Collisions," *Bull. Am. Phys. Soc.* **20**, 666 (1975).

Fourth International Symposium on Nuclear-Antinuclear Interactions, Syracuse, New York, May 2–4, 1975

G. T. Condo, W. M. Bugg, E. L. Hart, H. O. Cohn, and R. D. McCulloch, "Neutron Absorption of Slow Antiprotons."

American Chemical Society Meeting, Erie, Pennsylvania, May 7, 1975

H. W. Morgan (invited talk), "Coherent Light and Holography."

American Chemical Society Meeting, Painesville, Ohio, May 8, 1975

H. W. Morgan (invited talk), "Coherent Light and Holography."

American Chemical Society Meeting, Sharon, Pennsylvania, May 9, 1975

H. W. Morgan (invited talk), "Coherent Light and Holography."

American Chemical Society Meeting, Youngstown, Ohio, May 9, 1975

H. W. Morgan (invited talk), "Coherent Light and Holography."

Workshop on Deep Inelastic Collisions and Fusion in Heavy Ion Reactions, Saclay, France, May 12–30, 1975

C. Y. Wong (invited talk – series of six lectures), "Hydrodynamical Theory of Heavy-Ion Collisions."

1975 IEEE International Conference on Plasma Science, Ann Arbor, Michigan, May 14–16, 1975

I. Alexeff, H. Tamagawa, C. M. Jones, and P. D. Miller, "Use of the Hot-Electron Minor Machine INTEREM as a High-Z Ion Source."

G. D. Alton, "Review of the Heavy Ion Source Research and Development Program at the Oak Ridge National Laboratory."

Workshop on Heavy-Ion Reactions, Orsay, France, May 19–23, 1975

C. Y. Wong (invited talk), "Hydrodynamical Calculations."

Meeting on Macrophysical Aspects of Heavy-Ion Reactions, Orsay, France, May 20–22, 1975

C. Y. Wong (invited talk), "Hydrodynamical Calculations."

Third National Soviet Conference on Neutron Physics, Kiev, U.S.S.R., June 1975

J. W. Boldeman, B. J. Allen, M. J. Kenny, A. R. de L. Musgrove, and R. L. Macklin, "Valence and Doorway State Effects in Neutron Capture near Closed Shells."

International Conference on Effective Interactions and Operators in Nuclei, Tucson, Arizona, June 2–6, 1975

R. L. Becker (invited talk), "Computation of the Reaction Matrix G ."

Meeting on Atomic Masses and Fundamental Constants, Paris, France, June 2–6, 1975

B. D. Kern, J. L. Weil, J. H. Hamilton, A. V. Ramayya, C. R. Bingham, L. L. Riedinger, E. F. Zganjar, J. L. Wood, G. M. Gowdy, R. W. Fink, E. H. Spejewski, H. K. Carter, R. L. Mlekodaj, and J. Lin, "Mass Differences of Proton-Rich Atoms near $A = 116$ and $A = 190$."

Sixth International Conference on High Energy Physics and Nuclear Structure, Santa Fe, New Mexico, June 9–13, 1975

W. B. Dress, Jr. (invited talk), "Observation of Two Photons in n - p Capture."

American Physical Society Meeting, Knoxville, Tennessee, June 16–18, 1975

J. B. Ball (invited talk), "Status Report on the Heavy Ion Accelerator Project," *Bull. Am. Phys. Soc.* **20**, 826 (1975).

L. L. Collins, L. L. Riedinger, C. R. Bingham, G. D. O'Kelley, J. W. Wood, R. W. Fink, E. F. Zganjar, A. G. Schmidt, E. H. Spejewski, H. K. Carter, R. L. Mlekodaj, and J. H. Hamilton, "Decay of ^{195}Pb ," *Bull. Am. Phys. Soc.* **20**, 830 (1975).

H. L. Crowell, J. H. Hamilton, R. L. Robinson, A. V. Ramayya, W. E. Collins, W. T. Pinkston, R. M. Ronningen, N. C. Singhal, H. J. Kim, and R. O. Sayer, "Lifetime Measurements of High Spin States in ^{72}Se ," *Bull. Am. Phys. Soc.* **20**, 830 (1975).

E. E. Gross, "Calibration of an Analyzing Magnet Using an Alpha-Source and Heavy Ion Beams," *Bull. Am. Phys. Soc.* **20**, 829 (1975).

D. E. Gustafson, T. C. Schweizer, S. T. Thornton, J. L. C. Ford, Jr., P. D. Miller, R. L. Robinson, P. H. Stelson, and J. B. McGrory, "Selective Population of High Spin States in ^{23}Na ," *Bull. Am. Phys. Soc.* **20**, 829 (1975).

J. H. Hamilton, J. D. Cole, A. V. Ramayya, W. Lourens, B. N. Subba Rao, E. L. Bosworth, B. Martin, L. L. Riedinger, C. R. Bingham, E. F. Zganjar, E. H. Spejewski, H. K. Carter, R. L. Mlekodaj, R. W. Fink, J. L. Wood, G. W. Gowdy, B. D. Kern, and J. Weil, "On-Line Conversion Electron Measurements in the Decay of ^{183}Tl ," *Bull. Am. Phys. Soc.* **20**, 830 (1975).

R. C. Hunter, L. L. Riedinger, D. L. Hillis, C. R. Bingham, and K. S. Toth, "Decay of ^{164}Lu ," *Bull. Am. Phys. Soc.* **20**, 829 (1975).

J. A. Maruhn (invited talk), "Some Aspects of Collective Dynamics in Fission," *Bull. Am. Phys. Soc.* **20**, 815 (1975).

D. J. Pegg (invited talk), "Projectile Electron Spectroscopy of Autoionizing States in the Alkalis," *Bull. Am. Phys. Soc.* **20**, 826 (1975).

Thirtieth Annual Symposium on Molecular Structure and Spectroscopy, Columbus, Ohio, June 16--20, 1975

H. W. Morgan, P. A. Staats, and E. Silberman, "Vibrational Spectra of No^+ and No_2^+ ."

Faraday Society Discussions on Electron Spectroscopy of Solids and Surfaces, Vancouver, B.C., July 15--17, 1975

T. A. Carlson, "Satellite Structure in the Photoelectron Spectra of Transition Metal Compounds Ionized in the K Shell of the Metal Ion."

International Conference on Radiation Test Facilities for the CTR Surface and Materials Programs, Argonne, Illinois, July 15--18, 1975

M. J. Saltmarsh, A. P. Fraas, and J. A. Horak (invited talk), "A Large-Volume Intense Neutron Source for CTR Materials Studies."

Symposium on Intermediate Energy Heavy Ion Physics, Berkeley, California, July 17--19, 1975

J. B. Ball (invited talk), "Oak Ridge Plans for a Booster Cyclotron."

C. Y. Wong (invited talk), "Foundation of Nuclear Fluid Dynamics."

Ninth International Conference on Physics of Electronic and Atomic Collisions, Seattle, Washington, July 24--30, 1975

C. F. Barnett (invited talk), "Atomic Physics in the CTR Program."

D. J. Pegg, H. H. Haselton, R. S. Thoe, P. M. Griffin, M. D. Brown, and I. A. Sellin, "Autoionizing States Formed in $\text{Na}^+ + \text{He}$ and $\text{Mg}^+ + \text{He}$ Collisions at 70 keV."

R. S. Thoe, I. A. Sellin, R. S. Peterson, D. J. Pegg, P. M. Griffin, and J. P. Forester, "Photon Energy Dependence of the Asymmetry of Non-Characteristic X-Radiation in Si-Al and Al-Al Collisions."

Sixth Topical Conference on Particle Physics, Manoa, Hawaii, August 6--19, 1975

H. O. Cohn, "Nuclear Structure with High Energy Physics --- The Neutron Halo."

Thirty-third Annual Meeting, Electron Microscopy Society of America, Las Vegas, Nevada, August 11--15, 1975

T. A. Welton, "Practical Resolution Enhancement in Bright Field Electron Microscopy by Computer Processing."

1975 Nijenrode Summer School on Nuclear Spectroscopy, Nijenrode, Netherlands, August 11--23, 1975

G. R. Satchler (invited lecture series), "Direct Nuclear Reactions."

Seventh International Conference on Cyclotrons and Their Applications, Zurich, Switzerland, August 19--22, 1975

E. D. Hudson, J. A. Martin, F. E. McDaniel, and F. Irwin, "Magnetic Field Trimming Studies for a Separated-Sector Cyclotron."

E. D. Hudson, R. S. Lord, L. L. Riedinger, J. A. Martin, J. K. Bair, L. N. Howell, J. W. Johnson, G. S. McNeilly, F. E. McDaniel, and S. W. Mosko, "Magnet Model Studies for Separated-Sector Heavy Ion Cyclotrons."

R. S. Lord, E. D. Hudson, G. S. McNeilly, R. O. Sayer, J. B. Ball, M. L. Mallory, S. W. Mosko, R. M. Beckers, K. N. Fischer, J. A. Martin, and J. D. Rylander, "The Oak Ridge Isochronous Cyclotron as an Energy Booster for a 25 MV Tandem."

J. A. Martin (invited talk), "Accelerators for Heavy Ions."

G. S. McNeilly, E. D. Hudson, R. S. Lord, M. L. Mallory, J. E. Mann, J. B. Ball, and J. A. Martin, "Design Study for the Conversion of the Oak Ridge Isochronous Cyclotron from an Energy Constant of $K = 90$ to $K = 300$ MeV."

S. W. Mosko, E. D. Hudson, R. S. Lord, M. L. Mallory, J. E. Mann, J. A. Martin, G. S. McNeilly, J. B. Ball, K. N. Fischer, and R. L. Robinson, "A Separated-Sector Cyclotron Post-Accelerator for the Oak Ridge National Laboratory."

Fourth International Symposium on Polarization Phenomena in Nuclear Reactions, Zurich, Switzerland, August 25--29, 1975

R. de Swiniarski, G. Bagieu, M. Bedjiam, C. B. Fulmer, J. Y. Grossiord, M. Massaad, J. R. Pissi, and M. Gusakov, "Inelastic Scattering of 30 MeV Polarized Protons from $^{90,92}\text{Zr}$ and ^{92}Mo ."

NATO Advanced Study Institute on Photoionization and Other Probes of Many Electron Interactions, Carry-le-Rouet, France, August 31--September 13, 1975

T. A. Carlson (invited talk), "Multiple Excitation in Free Molecules."

Symposium on Target Techniques for On-Line Isotope Separators, Aarhus, Denmark, September 4--5, 1975

R. L. Mlekodaj, E. H. Spejewski, H. K. Carter, and A. G. Schmidt, "Target-Ion Source Techniques for Heavy-Ion Beams at UNISOR."

Fourth International Conference on Beam Foil Spectroscopy and Heavy Ion Atomic Physics, Gatlinburg, Tennessee, September 15--19, 1975

L. B. Bridwell, J. A. Biggerstaff, G. D. Alton, C. M. Jones, P. D. Miller, Q. Kessel, and B. W. Wehring, "Multiple Electron Loss Cross Sections for 60 MeV I^{+10} in Single Collisions with Xenon."

J. P. Forester, R. S. Peterson, P. M. Griffin, H. Haselton, K. H. Liao, J. R. Mowat, D. J. Pegg, I. A. Sellin, and R. S. Thoe, "Autoionizing States in Highly Ionized O, F, and Si."

P. M. Griffin, D. J. Pegg, I. A. Sellin, K. W. Jones, D. Pisano, T. H. Kruse, and S. Bashkin, "Extreme Ultraviolet Spectra of Highly Stripped Si Ions."

D. J. Pegg (invited talk), "Autoionizing States in the Alkalis."

R. S. Peterson, R. Laubert, R. S. Thoe, H. Hayden, S. Elston, J. Forester, K. H. Liao, P. M. Griffin, D. J. Pegg, and I. A. Sellin, "Differences in the Production of Non-Characteristic Radiation in Solid and Gas Targets."

P. H. Stelson (invited talk), "The Atomic Physics Potential of New Accelerators."

R. S. Thoe, I. A. Sellin, K. H. Liao, R. S. Peterson, D. J. Pegg, J. P. Forester, and P. M. Griffin, "Angular Distribution Studies of Non-Characteristic X-Radiation."

British Physical Society Meeting, Daresbury, England, September 17, 1975

G. R. Satchler (invited talk), "Scattering of Heavy Ions."

Sixth International Conference on Atomic Collisions in Solids, Amsterdam, Netherlands, September 22--26, 1975

J. U. Andersen, E. Laegsgaard, M. Lund, and C. D. Moak, " Z_1 Scaling for Impact-Parameter Dependence of Inner-Shell Ionization by Heavy Ions."

S. Datz, C. D. Moak, B. R. Appleton, J. A. Biggerstaff, and T. S. Noggle, "Hyper- and Planar-Channeling of Charge State Selected 27.5 MeV Oxygen Ions in Ag."

C. D. Moak, B. R. Appleton, J. A. Biggerstaff, M. D. Brown, S. Datz, T. S. Noggle, and H. Verbeek, "The Velocity Dependence of the Stopping Power of Channeled Ions from 0.6 to 60 MeV."

Symposium on Highly Excited States in Nuclei, Jülich, West Germany, September 23--26, 1975

F. E. Bertrand, "Excitation of Giant Resonances via Inelastic Hadron Scattering."

E. C. Halbert, J. B. McGrory, G. R. Satchler, and J. Speth, "Hadronic Excitation of the Giant Resonance Region of ^{208}Pb ."

G. R. Satchler (invited talk), "Hadronic Excitation of the Giant Resonance Region of ^{208}Pb ."

Symposium on Experimental Methods for Charged-Particle Irradiations, Gatlinburg, Tennessee, September 30, 1975

C. H. Johnson, "A Ring Lens for Producing Uniform Density Ion Beams."

M. B. Lewis, F. K. McGowan, C. H. Johnson, and M. J. Saltmarsh, "The Oak Ridge CN Van de Graaff Facility for Heavy Ion Radiation Damage Studies."

Conference on Radiation Effects and Tritium Technology for Fusion Reactors, Gatlinburg, Tennessee, October 1--3, 1975

J. B. Roberto, J. Narayan, and M. J. Saltmarsh, "15 MeV Neutron Damage in Cu and Nb."

American Chemical Society (Boulder Dam Section), Las Vegas, Nevada, October 9, 1975

H. W. Morgan (invited talk), "Coherent Light and Holography."

American Chemical Society (Sierra Nevada Section), Reno, Nevada, October 10, 1975

H. W. Morgan (invited talk), "Coherent Light and Holography."

American Chemical Society (Sacramento Section), Davis, California, October 13, 1975

H. W. Morgan (invited talk), "Coherent Light and Holography."

American Chemical Society (Fresno Section), Fresno, California, October 14, 1975

H. W. Morgan (invited talk), "Coherent Light and Holography."

American Chemical Society (Mojave Desert Section), China Lake, California, October 15, 1975

H. W. Morgan (invited talk), "Coherent Light and Holography."

American Chemical Society (Bakersfield Section), October 16, 1975

H. W. Morgan (invited talk), "Coherent Light and Holography."

American Chemical Society Meeting (Hawaiian Section), Honolulu, Hawaii, October 17, 1975

H. W. Morgan (invited talk), "Coherent Light and Holography."

Optical Society of America, Boston, Massachusetts, October 21--24, 1975

K. L. Vander Sluis, "Stark Structure on Hydrogen Spectra in ORMAK Plasma."

International Conference on Heavy Ion Sources, Gatlinburg, Tennessee, October 27--30, 1975

G. D. Alton, "Preliminary Evaluation of a Modified Hortig-Geometry Negative-Ion Source Using a Negative-Ion-Source Test Facility."

E. D. Hudson, M. L. Mallory, and R. S. Lord, "Production of Positive Ion Beams from Solids."

C. M. Jones (invited talk), "Large Tandem Accelerators."

M. L. Mallory and D. H. Crandall, "A Penning Heavy Ion Source Test Facility."

C. D. Moak (invited talk), "Stripping in Foils and Gases."

P. H. Stelson (invited paper), "Future of Physics with Heavy Ions."

H. Tamagawa, I. Alexeff, C. M. Jones, N. H. Lazar, and P. D. Miller, "Use of the Hot-Electron Mirror Machine INTEREM as a High-Z Ion Source."

American Physical Society Meeting, Austin, Texas, October 30--November 1, 1975

G. Bagieu, A. J. Cole, R. de Swiniarski, C. B. Fulmer, D. H. Kong, and G. Mariolopoulos, "41 MeV Alpha-Particle Scattering from ^{27}Al , $^{28,29,30}\text{Si}$," *Bull. Am. Phys. Soc.* **20**, 1156 (1975).

F. T. Baker, A. Scott, E. E. Gross, D. C. Hensley, and D. L. Hillis, "The Nuclear Reorientation Effect for ^{12}C Scattering from ^{28}Si and ^{26}Mg ," *Bull. Am. Phys. Soc.* **20**, 1190 (1975).

W. K. Dagenhart, P. H. Stelson, F. K. McGowan, W. T. Milner, S. Raman, and R. L. Robinson, "Coulomb Excitation of ^{115}Sn ," *Bull. Am. Phys. Soc.* **20**, 1187 (1975).

B. J. Dalton, "Fixed J , Fixed T Shell Model Level Densities for Arbitrary Orbitals," *Bull. Am. Phys. Soc.* **20**, 1185 (1975).

C. D. Goodman, F. E. Bertrand, D. C. Kocher, and R. L. Auble, " $(^3\text{He},t)$ on Several $N = Z$ Targets," *Bull. Am. Phys. Soc.* **20**, 1156 (1975).

R. S. Grantham, R. M. Ronningen, J. H. Hamilton, A. V. Ramayya, B. van Nooijen, H. Kawakami, R. B. Piercey, R. S. Lee, L. L. Riedinger, and W. K. Dagenhart, " $B(E2)$ Values of 2^+_{γ} , 2^+_{β} , and 2^+_{α} States in $^{162,164}\text{Er}$ and ^{168}Yb ," *Bull. Am. Phys. Soc.* **20**, 1190 (1975).

J. J. Griffin and C. Y. Wong, "Vibrational Instability in Droplets (and Nuclei?)," *Bull. Am. Phys. Soc.* **20**, 1158 (1975).

E. E. Gross, M. L. Halbert, D. C. Hensley, D. L. Hillis, C. Bingham, A. Scott, F. T. Baker, and T. A. Slaman, "Elastic Scattering of 70.4 MeV ^{12}C from Even Nd Isotopes," *Bull. Am. Phys. Soc.* **20**, 1192 (1975).

M. L. Halbert, P. O. Tjøm, G. B. Hagemann, B. Herskind, M. Neiman, and H. Oeschler, "High Spin States in ^{74}Se ," *Bull. Am. Phys. Soc.* **20**, 1172 (1975).

J. A. Harvey, J. Halperin, N. W. Hill, R. L. Macklin, S. Raman, and E. T. Jurney, "Total and Capture Cross Sections of ^{59}Ni for eV and keV Neutrons," *Bull. Am. Phys. Soc.* **20**, 1195 (1975).

D. L. Hillis, E. E. Gross, D. C. Hensley, C. R. Bingham, A. Scott, F. T. Baker, and T. A. Slaman, "Shape Effects in the Inelastic Scattering of 70 MeV ^{12}C Ions from $^{142,144,146,148,150}\text{Nd}$," *Bull. Am. Phys. Soc.* **20**, 1192 (1975).

D. J. Horen (invited talk), "Information Systems of the Nuclear Data Project," *Bull. Am. Phys. Soc.* **20**, 1153 (1975).

R. C. Hunter, L. L. Riedinger, D. L. Hillis, C. R. Bingham, and K. S. Toth, "Vibrational Bands in ^{164}Yb ," *Bull. Am. Phys. Soc.* **20**, 1154 (1975).

M. A. Ijaz, E. L. Robinson, K. S. Toth, C. R. Bingham, and J. Lin, "Search for Alpha Decay of Thallium 185, 186 Isotopes," *Bull. Am. Phys. Soc.* **20**, 1154 (1975).

C. H. Johnson, J. Halperin, R. L. Macklin, and R. R. Winters, "Neutron Total and Capture Cross Sections for ^{32}S ," *Bull. Am. Phys. Soc.* **20**, 1195 (1975).

R. L. Macklin, "The $^{165}\text{Ho}(n,\gamma)$ Standard Cross Section from 3 to 450 keV," *Bull. Am. Phys. Soc.* **20**, 1196 (1975).

J. A. Maruhn, C. Y. Wong, and T. A. Welton, "Fluid Dynamic Description of Heavy-Ion Collisions," *Bull. Am. Phys. Soc.* **20**, 1158 (1975).

J. B. McGrory and B. H. Wildenthal, "A Comment on the Projection of Spurious Center-of-Mass States in Truncated Shell-Model Calculations," *Bull. Am. Phys. Soc.* **20**, 1184 (1975).

R. B. Piercey, A. V. Ramayya, R. M. Ronningen, and J. H. Hamilton, "In-Beam Gamma-Ray Spectroscopy Following $^{60}\text{Ni}(^{16}\text{O},2p)^{74}\text{Se}$," *Bull. Am. Phys. Soc.* **20**, 1172 (1975).

A. V. Ramayya, J. H. Hamilton, J. D. Cole, B. van Nooijen, H. Kawakami, L. L. Riedinger, C. R. Bingham, K. S. R. Sastry, H. K. Carter, and F. T. Avignone, "Near Spherical and Deformed Bands in ^{186}Hg ," *Bull. Am. Phys. Soc.* **20**, 1154 (1975).

L. D. Rickertsen and D. L. Hillis, "Second-Order Coupling Effects in Heavy-Ion Inelastic Scattering," *Bull. Am. Phys. Soc.* **20**, 1167 (1975).

R. M. Ronningen, J. H. Hamilton, R. S. Grantham, A. V. Ramayya, B. van Nooijen, R. B. Piercey, R. S. Lee, H. Kawakami, L. L. Riedinger, and W. K. Dagenhart, "Coulomb Excitation of 2^+ Ground and 3^- Octupole Levels in $^{156,158}\text{Dy}$, $^{162,164}\text{Er}$, and ^{168}Yb ," *Bull. Am. Phys. Soc.* **20**, 1189 (1975).

M. J. Saltmarsh (invited talk), "Accelerators and Energy," *Bull. Am. Phys. Soc.* **20**, 1153 (1975).

W. K. Tuttle III, R. L. Robinson, H. J. Kim, R. O. Sayer, W. T. Milner, G. J. Smith, and R. M. Ronningen, "Levels in ^{113}In Populated by the $^{110}\text{Pd}(^6\text{Li},3n)$ Reaction," *Bull. Am. Phys. Soc.* **20**, 1173 (1975).

C. Y. Wong, J. A. Maruhn, and T. A. Welton, "Normal Sound, Spin Sound, Isospin Sound, and Spin-Isospin Sound in Nuclear Fluid," *Bull. Am. Phys. Soc.* **20**, 1158 (1975).

International Atomic Energy Agency Advisory Group Meeting on Transactinium Isotope Nuclear Data, Karlsruhe, West Germany, November 3–7, 1975

S. Raman (invited talk), "Some Activities in the United States Concerning the Physics Aspects of Actinide Waste Recycling."

S. Raman (invited talk), "General Survey of Applications Which Require Nuclear Data."

American Physical Society Meeting (Division of Plasma Physics), St. Petersburg, Florida, November 10–14, 1975

K. L. Vander Sluis, "Stark Structure on Hydrogen Spectra in ORMAK Plasma," *Bull. Am. Phys. Soc.* **20**, 1227 (1975).

Materials Science Symposium (American Society for Metals), Cincinnati, Ohio, November 11–13, 1975

T. A. Carlson (invited talk), "Use of Photoelectron Spectroscopy for Surface Analysis."

American Physical Society Meeting (Southeastern Section), Auburn, Alabama, November 13–15, 1975

W. E. Collins, A. Ashley, J. H. Hamilton, H. L. Crowell, and R. L. Robinson, "The Level Structure of ^{69}As ."

H. L. Crowell, J. H. Hamilton, A. V. Ramayya, R. M. Ronningen, N. C. Singhal, R. L. Robinson, and R. O. Sayer, "Angular Distribution Measurements in ^{72}Se ."

T. Magee, L. C. Whitlock, H. L. Crowell, J. H. Singhal, R. L. Robinson, and R. O. Sayer, "Mean Life of the 4^+ State in ^{72}Se ."

F. E. Obenshain (invited talk), "Heavy Ion Induced Fission near $A = 100$."

E. L. Robinson, B. O. Hannah, B. H. Ketelle, G. Schuster, and J. L. Weil, "Decay of ^{194}Pb ."

I. A. Sellin (invited talk), "Highly Ionized Ions."

F. E. Turner, L. L. Riedinger, C. R. Bingham, E. H. Spejewski, R. L. Mlekodaj, H. K. Carter, B. D. Kern, J. L. Weil, E. L. Robinson, and J. H. Hamilton, " $^{192}\text{Pb} \rightarrow ^{192}\text{Tl} \rightarrow ^{192}\text{Hg}$."

American Nuclear Society Meeting, San Francisco, California, November 16–21, 1975

C. F. Barnett and E. Ricci (invited talk), "Plasma-Wall Interface Studies for TOKAMAK Type Plasmas."

Sixth Symposium on Engineering Problems of Fusion Research, San Diego, California, November 18–21, 1975

S. W. Mosko, D. D. Bates, R. R. Bigelow, E. K. Cottongim, E. W. Pipes, and K. Sueker, "A 120 kA Pulsed dc Power System with Computerized Thyristor Triggering."

American Physical Society Meeting (Division of Electron and Atomic Physics), Tucson, Arizona, December 3–6, 1975

D. H. Crandall, D. C. Kocher, and T. J. Morgan, "Single and Double Charge Transfer of C^{4+} in Helium," *Bull. Am. Phys. Soc.* **20**, 1456 (1975).

R. S. Peterson, I. A. Sellin, H. Hayden, S. B. Elston, J. P. Forester, K. H. Liao, P. M. Griffin, D. J. Pegg, and R. Laubert, "Non-Characteristic X-Radiation Production in Solid and Gas Targets," *Bull. Am. Phys. Soc.* **20**, 1450 (1975).

American Physical Society Meeting, Pasadena, California, December 29–31, 1975

A. Gizon, J. Gizon, and D. J. Horen, "Band Structure in ^{132}Ba ," *Bull. Am. Phys. Soc.* **20**, 1496 (1975).

10. Omniana

Prepared by M. L. Halbert, Christine R. Wallace, and Wilma L. Stair

ANNOUNCEMENTS

The Controlled Fusion Atomic Data Center was transferred from the Thermonuclear Division to the Physics Division in July 1975. At the same time, several other people were transferred from Thermonuclear, which increased the technical staff of the Physics Division by four permanent and two temporary members.

During November, W. B. Ewbank was appointed Director of the Nuclear Data Project, and F. E. Bertrand was appointed Deputy Director.

PERSONNEL ASSIGNMENTS

During 1975 the Physics Division was host to at least 37 guests from the United States and abroad. Some of these were short-term assignments, variously sponsored by different organizations and institutions. Seven Physics Division staff members have been the guests of laboratories located outside the United States. A list of guests, staff assignments, and personnel changes follows:

Guest Assignees from Abroad

B. J. Allen, Australian Atomic Energy Commission, Lucas Heights, New South Wales, Australia -- Oak Ridge Electron Linear Accelerator Program (completed one-month assignment in March 1975)

E. I. Andrade, Universidad Nacional Autonoma de Mexico, Mexico -- Van de Graaff Program (completed one-month assignment in July 1975)

Michel Barre, Commissariat a l'Energie Atomique, Group GANIL, Institut de Physique Nucleaire, Orsay, France -- Heavy-Ion Project (completed two-month assignment in June 1975)

Marie-Paule Bourgairel, Commissariat a l'Energie Atomique, Group GANIL, Institut de Physique Nucleaire, Orsay, France -- Heavy-Ion Project (completed two-month assignment in June 1975)

A. A. Dacal, Universidad Nacional Autonoma de Mexico, Mexico -- Van de Graaff Program (completed one-month assignment in July 1975)

E. D. Earle, Atomic Energy of Canada Limited, Chalk River, Canada -- Oak Ridge Electron Linear Accelerator Program (completed two-week assignment in January 1975).

H. W. Feldmeier, NATO Fellowship from Technische Hochschule, Darmstadt, West Germany -- Theoretical Physics Program (began one-year assignment in September 1975)

Thanh-Tam Luong, Commissariat a l'Energie Atomique, Group GANIL, Institut de Physique Nucleaire, Orsay, France -- Heavy-Ion Project (completed two-month assignment in June 1975)

Vida Maruhn-Rezwani, University of Frankfurt, Frankfurt, West Germany -- Theoretical Physics Program (continued assignment begun November 1974)

P. S. Murty, Bhabha Atomic Research Centre, Trombay, India -- Electron Spectroscopy Program (began one-year assignment in May 1975)

Maria E. S. Ortiz, Universidad Nacional Autonoma de Mexico, Mexico -- Van de Graaff Program (completed one-month assignment in July 1975)

Hermann Weigmann, Central Bureau for Nuclear Measurements (CBNM), EURATOM, Geel, Belgium — Oak Ridge Electron Linear Accelerator Program (began eight-month assignment in July 1975)

Guest Assignees from the United States

B. J. Dalton, summer research participant (ORAU) from Fort Valley State College, Fort Valley, Georgia — Theoretical Physics Program (completed three-month assignment in September 1975)

Stuart Elston, University of Tennessee — Accelerator Atomic Physics Program (began one-year assignment in January 1975)

J. P. Felvinci, Columbia University — Oak Ridge Electron Linear Accelerator Program (completed six-week assignment in July 1975)

J. P. Forester, University of Tennessee — Accelerator Atomic Physics Program (continued assignment begun in September 1974)

L. D. Gardner, Yale University — Charge Exchange Cross Section Measurements Program (completed one-month assignment in December 1975)

J. B. Garg, State University of New York at Albany — Oak Ridge Electron Linear Accelerator Program (completed six-week assignment in August 1975)

Thomas Handler, University of Tennessee — High Energy Physics Program (continued assignment begun in November 1974)

E. L. Hart, University of Tennessee — High Energy Physics Program (completed six-year assignment in August 1975 — now consultant with ORNL Physics Division)

Howard Hayden, University of Tennessee — Accelerator Atomic Physics Program (began one-year assignment in June 1975)

D. L. Hillis, University of Tennessee — Oak Ridge Isochronous Cyclotron Program (began one-year assignment in January 1975)

A. C. Kahler III, University of Tennessee — Oak Ridge Isochronous Cyclotron Program (began one-year assignment in October 1975)

P. M. Koch, Yale University — Oak Ridge Isochronous Cyclotron Program (completed two-week assignment in December 1975)

Kuo-Hsien Liao, Columbia University — Accelerator Atomic Physics Program (completed ten-month assignment in October 1975)

B. R. Luers, Columbia University — Oak Ridge Electron Linear Accelerator Program (completed six-week assignment in July 1975)

Edward Melkonian, Columbia University — Oak Ridge Electron Linear Accelerator Program (completed six-week assignment in July 1975)

T. J. Morgan, summer research participant (ORNL) from Wesleyan University — Atomic Physics Program (completed two-month assignment in August 1975)

T. L. Nichols, University of Tennessee — Hyperfine Interactions Program (completed ten-month assignment in February 1975)

M. S. Pandey, State University of New York at Albany — Oak Ridge Electron Linear Accelerator Program (completed six-week assignment in August 1975)

R. S. Peterson, University of Tennessee — Accelerator Atomic Physics Program (continued assignment begun in July 1972)

P. O. Taylor, Joint Institute for Laboratory Astrophysics, University of Colorado — Controlled Fusion Atomic Data Center (began one-year assignment in October 1975)

R. Thoe, University of Tennessee — Accelerator Atomic Physics Program (completed two-year assignment in June 1975 — now consultant with ORNL Physics Division)

Cheng-May Tung, University of Tennessee — Electron Spectroscopy Program (began one-year assignment in August 1975)

R. R. Turtle, University of Tennessee — Accelerator Atomic Physics Program (completed seven-month assignment in May 1975)

W. K. Tuttle III, University of Tennessee — Van de Graaff Program (completed eleven-month assignment in November 1975)

J. Waldman, University of Lowell — Plasma Diagnostics Program (completed three-month assignment in September 1975)

R. M. Wieland, summer research participant (ORAU) from Franklin and Marshall College, Lancaster, Pennsylvania — Oak Ridge Isochronous Cyclotron Program (completed three-month assignment in August 1975)

University Isotope Separator at Oak Ridge (UNISOR)

G. M. Gowdy, Laboratory Graduate Participant Fellow — Oak Ridge Associated Universities (began one-year assignment in January 1975)

- H. K. Carter, Oak Ridge Associated Universities (indefinite assignment)
- R. L. Mlekodaj, Oak Ridge Associated Universities (indefinite assignment)
- A. V. Ramayya, Vanderbilt University (completed one-month assignment July 1975)
- E. L. Robinson, University of Alabama (completed one-year assignment in September 1975)
- A. G. Schmidt, Oak Ridge Associated Universities (continued postdoctoral appointment begun in September 1974)
- E. H. Spejewski, Oak Ridge Associated Universities (indefinite assignment)

Staff Assignments

- C. B. Fulmer -- Oak Ridge Isochronous Cyclotron Program. Completed in September 1975 a one-year assignment with the Institut des Sciences Nucléaires, University of Grenoble, Grenoble, France
- E. E. Gross -- Oak Ridge Isochronous Cyclotron Program. Completed in May 1975 a four-week assignment at the Grenoble Cyclotron Laboratory, Grenoble, France
- Edith C. Halbert -- Theoretical Physics Program. Completed in August 1975 a one-year assignment with the Niels Bohr Institute, Copenhagen, Denmark
- M. L. Halbert -- Oak Ridge Isochronous Cyclotron Program. Completed in August 1975 a one-year assignment with the Niels Bohr Institute, Copenhagen, Denmark
- J. B. McGrory -- Theoretical Physics Program. Began in October 1975 a one-year assignment with the ORNL Program Planning and Analysis Office
- C. D. Moak -- Van de Graaff Program. Began in February 1975 a six-month assignment with the University of Aarhus, Aarhus, Denmark; began in October 1975 a six-month assignment with the Daresbury Laboratory, Daresbury, England
- F. Plasil -- Physics of Fission Program. Completed in September 1975 a one-year assignment with the Laboratoire de Physique Nucléaire, University of Paris, Orsay, France
- K. S. Toth -- Oak Ridge Isochronous Cyclotron Program. Completed in October 1975 a five-month assignment at the Laboratory for Nuclear Reactions, Joint Institute for Nuclear Research, Dubna, U.S.S.R.

Personnel Changes

- C. F. Barnett -- Controlled Fusion Atomic Data Center. Transferred from Thermonuclear Division to Physics Division in July 1975
- D. H. Crandall -- Atomic Physics Program. Transferred from Thermonuclear Division to Physics Division in July 1975
- R. A. Dayras -- Oak Ridge Isochronous Cyclotron Program. Began two-year postdoctoral appointment in December 1975
- J. Gomez del Campo -- Van de Graaff Program. Began four-month appointment in October 1975
- D. P. Hutchinson -- Plasma Diagnostics Program. Transferred from Thermonuclear Division to Physics Division in July 1975
- J. W. Johnson -- Van de Graaff Program. Transferred from Instrumentation and Controls Division to Physics Division in September 1975
- M. B. Lewis -- Van de Graaff Program. Transferred from Physics Division to Metals and Ceramics Division in July 1975
- E. Newman -- Oak Ridge Isochronous Cyclotron Program. Transferred from Physics Division to Chemical Technology Division in July 1975
- R. A. Phaneuf -- Atomic Physics Program. Began one-year appointment with the Thermonuclear Division in October 1975 (on loan to the Physics Division)
- J. A. Ray -- Atomic Physics Program. Transferred from Thermonuclear Division to Physics Division in July 1975
- E. Ricci -- Surface Studies Program. Began loan assignment with the Physics Division from Analytical Chemistry in July 1975
- L. L. Riedinger -- Heavy Ion Project. Completed eight-month assignment in August 1975
- K. L. Vander Sluis -- Plasma Diagnostics Program. Transferred from Thermonuclear Division to Physics Division in July 1975
- G. K. Werner -- Infrared Spectroscopy Program. Transferred from Physics Division to Oak Ridge Gaseous Diffusion Plant in March 1975

**ADJUNCT RESEARCH PARTICIPANTS UNDER SUBCONTRACT WITH
UNION CARBIDE CORPORATION NUCLEAR DIVISION – ORNL**

Faculty members of colleges and universities who were under subcontract with ORNL and who participated in the activities of the Physics Division during 1975 are listed as follows:

- | | |
|--|--|
| P. M. Bakshi, Boston College – Controlled Fusion Atomic Data Center | D. J. Pegg, University of Tennessee – Accelerator Atomic Physics Program |
| C. R. Bingham, University of Tennessee – Oak Ridge Isochronous Cyclotron Program | G. A. Petitt, Georgia State University – Hyperfine Interactions Program (contract closed August 1975) |
| H. G. Blosser, Michigan State University – Heavy Ion Project | L. L. Riedinger, University of Tennessee – Heavy Ion Project |
| D. A. Bromley, Yale University – Nuclear Physics Program | A. B. Ritchie, University of Alabama – Electron Spectroscopy Program |
| W. M. Bugg, University of Tennessee – High Energy Physics Program | Reginald Ronningen, Vanderbilt University -- Van de Graaff Program |
| J. W. Burton, Carson-Newman College -- Hyperfine Interactions Program | Arnold Russek, University of Connecticut – Controlled Fusion Atomic Data Center |
| R. F. Carlton, Middle Tennessee State University – Oak Ridge Electron Linear Accelerator Program | I. A. Sellin, University of Tennessee – Accelerator Atomic Physics Program |
| T. P. Cleary, University of Tennessee – Oak Ridge Isochronous Cyclotron Program | A. J. Sierk, California Institute of Technology – Theoretical Physics Program (contract closed December 1975) |
| G. T. Condo, University of Tennessee -- High Energy Physics Program | R. M. Tate, University of Tennessee -- Van de Graaff Program |
| R. Y. Cusson, Duke University – Theoretical Physics Program | Robert Thoe, University of Tennessee – Accelerator Atomic Physics Program |
| Brian Gilbody, Queen's University, Belfast, Ireland – Controlled Fusion Atomic Data Center | E. W. Thomas, Georgia Institute of Technology – Controlled Fusion Atomic Data Center |
| J. Gomez del Campo, National University of Mexico -- Van de Graaff Program (contract closed September 1975) | J. R. Thompson, University of Tennessee -- Van de Graaff Program |
| F. A. Grimm, University of Tennessee – Electron Spectroscopy Program | J. O. Thomson, University of Tennessee – Hyperfine Interactions Program |
| E. L. Hart, University of Tennessee -- High Energy Physics Program | S. T. Thornton, University of Virginia – Van de Graaff Program |
| Philippe Hubert, Centre d'Etudes Nucléaires, Bordeaux, France – Oak Ridge Isochronous Cyclotron Program (contract closed September 1975) | H. Verheul, Free University, Amsterdam, Netherlands – Nuclear Data Project (contract closed April 1975) |
| P. G. Huray, University of Tennessee – Hyperfine Interactions Program | Lawrence Wilets, University of Washington – Theoretical Physics Program |
| Constance Kalbach, University of Tennessee – Oak Ridge Isochronous Cyclotron and Theoretical Physics Programs | R. R. Winters, Denison University – Oak Ridge Electron Linear Accelerator Program (contract closed August 1975) |
| Donald Malbrough, University of South Carolina -- Oak Ridge Isochronous Cyclotron Program at LAMPF | Additionally in 1975, the Physics Division had the participation of the following nonfaculty ORNL subcontract holders: |
| Earl McDaniels, Georgia Institute of Technology – Controlled Fusion Atomic Data Center | F. T. Howard, ORNL retiree -- Accelerator Information Project (contract closed November 1975) |

- D. D. Klema, undergraduate student from Princeton University -- Van de Graaff and Oak Ridge Isochronous Cyclotron Programs
- R. F. King, ORNL retiree -- Van de Graaff Program
- J. D. Larson, representing self -- Heavy Ion Project
- L. A. Slover, ORNL retiree -- Oak Ridge Isochronous Cyclotron Program
- A. H. Snell, ORNL retiree -- Oak Ridge Isochronous Cyclotron Program
- G. J. Smith, ORAU postdoctoral appointee -- Oak Ridge Isochronous Cyclotron Program (contract closed September 1975)

**ADJUNCT RESEARCH PARTICIPANTS UNDER CONTRACT
ARRANGEMENT WITH OAK RIDGE ASSOCIATED UNIVERSITIES**

Under arrangements with Oak Ridge Associated Universities ("S" contracts and "U" contracts), 81 university or college faculty members and students visited the Physics Division for consultation and collaboration during 1975. These individuals and their affiliation are listed below:

- | | |
|---|---|
| F. T. Avignone III, University of South Carolina | D. E. Johnson, North Texas State University |
| F. T. Baker, University of Georgia | H. Kawakami, Vanderbilt University |
| J. H. Barker, Saint Louis University | G. Kegel, Lowell Technological Institute |
| S. Bashkin, University of Arizona | K. W. Kemper, Florida State University |
| J. E. Bayfield, Yale University | B. D. Kern, University of Kentucky |
| R. A. Bragda, Georgia Institute of Technology | Q. C. Kessel, University of Connecticut |
| W. H. Brantley, Furman University | S. E. Koonin, California Institute of Technology |
| L. B. Bridwell, Murray State University | S. J. Krieger, University of Illinois at Chicago Circle |
| R. P. Chaturvedi, State University of New York at Cortland | T. H. Kruse, Rutgers -- the State University |
| S. J. Cipolla, Creighton University | K. A. Kuenhold, University of Tulsa |
| P. W. Coulter, University of Alabama, Tuscaloosa | K. Kumar, Vanderbilt University |
| R. H. Davis, Florida State University | W. S. Lewis, Georgia Institute of Technology |
| J. P. Draayer, Louisiana State U. and A. & M. C. | T. K. Lim, Drexel University |
| J. L. Duggan, North Texas State University | J. Lin, Tennessee Technological University |
| R. W. Fink, Georgia Institute of Technology | W. G. Love, University of Georgia |
| R. M. Gaedke, Trinity University | A. D. MacKellar, University of Kentucky |
| R. S. Grantham, Vanderbilt University | M. S. McCay, University of Tennessee at Chattanooga |
| T. J. Gray, Kansas State University | D. A. McClure, Georgia Institute of Technology |
| M. B. Greenfield, Florida A. & M. University | F. D. McDaniel, North Texas State University |
| M. A. Grimm, Jr., Georgia Institute of Technology | G. C. Monigold, North Texas State University |
| S. A. Gronemeyer, Washington University | J. R. Mowat, City University of New York |
| D. E. Gustafson, University of Virginia | J. W. Negele, Massachusetts Institute of Technology |
| J. H. Hamilton, Vanderbilt University | R. B. Piercey, Vanderbilt University |
| B. O. Hannah, University of Alabama in Birmingham | B. M. Preedom, University of South Carolina |
| E. V. Hungerford, University of Houston | A. R. Quinton, University of Massachusetts |
| M. A. Ijaz, Virginia Polytechnic Institute and State University | A. E. Rainis, West Virginia University |
| | A. V. Ramayya, Vanderbilt University |

- P. V. Rao, Emory University
 M. S. Rapaport, Georgia Institute of Technology
 R. B. Raphael, Oglethorpe University
 A. D. Ray, North Texas State University
 L. A. Rayburn, University of Texas at Arlington
 A. C. Rester, Emory University
 R. K. Rice, North Texas State University
 E. L. Robinson, University of Alabama in Birmingham
 J. R. Rowe, North Texas State University
 K.S.R. Sastry, University of Massachusetts
 T. C. Schweizer, University of Virginia
 A. Scott, University of Georgia
 J. Tricomi, North Texas State University
 B. Van Nooijen, Vanderbilt University
 G. Vourvopoulos, Florida A. & M. University
 T. A. Walkiewicz, Edinboro State College
 J. L. Weil, University of Kentucky
 J. C. Wells, Jr., Tennessee Technological University
 W. R. Wharton, Carnegie-Mellon University
 R. M. Wheeler, State University of New York at Cortland
 R. M. Wieland, Franklin and Marshall College
 B. H. Wildenthal, Michigan State University
 S. R. Wilson, North Texas State University
 R. R. Winters, Denison University
 J. L. Wood, Georgia Institute of Technology
 S. W. Yates, University of Kentucky
 A. R. Zander, East Texas State University
 E. F. Zganjar, Louisiana State U. and A. & M. C.

PHYSICS DIVISION SEMINARS

Physics Division seminars were held once a week on the average. The seminar cochairmen during most of the year were J. B. McGrory and W. B. Dress. On October 1, E. Eichler (Chemistry Division) replaced McGrory. The seminars listed below are announced to the entire Laboratory by being listed in the ORNL Technical Calendar. In addition, groups within the Division hold meetings of more specialized interest, such as the Nuclear Research Coffee meetings on alternate Wednesday afternoons and the Theoretical Circus on Fridays.

- January 15 – David Nagel, U.S. Naval Research Laboratory, “X-Rays from Plasmas and Projectiles”
 January 20 – G. Goldring, Weizmann Institute of Science, Rehovot, Israel, “Hyperfine Interactions and Gyromagnetic Ratios of Excited States of Light Nuclei”
 January 24 – J. R. Comfort, University of Groningen, Netherlands, “Particle-Hole Multiplets and Reaction Mechanisms in the Mass-90 Region”
 January 30 – J. L. Fowler, Physics Division, ORNL, “Neutrons and Energy; the Mystery of the Missing Ninth”
 February 12 – Charles Flaum, University of Rochester, “Experimental and Theoretical Investigations of Anomalous Behavior of Rotational States at High Spin”
 February 24 – J. N. Ginocchio, Yale University, “Statistical Mechanical Approach to Nuclear Structure”
 March 4 – Igor Alexeff, University of Tennessee, “Plasma Containment Devices as Sources of Multiply-Charged Ions”
 March 6 – K. Thomas R. Davies, Physics Division, ORNL, “Effect of Nuclear Viscosity on the Dynamics of Fission”
 March 20 – B. L. Cohen, The Institute for Energy Analysis, Oak Ridge, “Environmental Impacts of Plutonium Dispersal and Radioactive Waste Storage”
 March 24 – H. C. Pauli, Max-Planck-Institut für Kernphysik, Heidelberg, Germany, “Dynamic Excitation in Fission”
 April 1 – M. R. Mottleson, Niels Bohr Institutet, Copenhagen, Denmark, “What Can Angular Momentum Do to the Nucleus?”
 April 24 – Ole Hansen, Los Alamos Scientific Laboratory, “Resonances in the $^{12}\text{C}(^{12}\text{C},p)$ Reaction: A New Rotational Band in ^{24}Mg ”

- May 2 -- Klaus Eberhard, University of Washington, "Correlated Structure in $^{12}\text{C} + ^{12}\text{C}$ Induced Reactions"
- May 5 -- Charles Lewis, CERN, "Some Experiments in Nuclear π^- Absorption"
- May 8 -- H. Schrader, Institut Laue-Langevin, Grenoble, France, "Fission Yields with Mass Separator Lohengrin"
- May 12 -- Mikkel B. Johnson, Los Alamos Scientific Laboratory, "Nuclear Matter Theory for Pion Scattering from Nuclei"
- May 15 -- D. H. Youngblood, Texas A. & M. University, "Particle Decay from the Giant Resonance Region of ^{40}Ca "
- May 22 -- Marlan Scully, Optical Sciences Center, University of Arizona, "An Ion Beam X-Ray Laser: Superradiance in Action"
- May 28 -- E. Salzborn, Kansas State University, "Electron Capture Processes of Multiply Charged Argon Ions in Gas Targets at Energies from 10--90 keV"
- May 29 -- M. Kimura, Tohoku University, Sendai, Japan, "Pulsed Neutron Sources for Utilization for Condensed Matter Research"
- May 29 -- I. Bergström, Research Institute for Physics, Stockholm, Sweden, "On Effective Two- and Three-Body Interactions: A Lesson from High-Spin States in the Lead Region"
- June 5 -- W. B. Dress, Physics Division, ORNL, " $2\frac{1}{2}$ Years of Measurements with and on French Neutrons"
- June 17 -- A. K. Edwards, University of Georgia, "Collisional Excitation of Negative Ions and Neutral Atoms"
- June 19 -- Terrance Cleary, University of Wisconsin, "Nuclear Structure in the $A \approx 90$ Region from Reactions Induced by Vector Polarized Deuterons"
- June 24 -- L. C. Feldman, Bell Laboratories, Murray Hill, N.J., "X-Ray Yields from Ar-Al Collisions: Lifetime Effects"
- June 26 -- G. S. Hurst, "Resonance Ionization Spectroscopy on He (2^1S)"
- July 9 -- R. de Swiniarski, University of Grenoble, France, "Some Recent Experiments Done at the Grenoble Cyclotron"
- July 14 -- S. G. Nilsson, University of Lund, Sweden, "Nuclei at High Angular Momentum States"
- July 14 -- Gunter Kegel, Lowell Technological Institute, "Fast Neutron Scattering from U-238"
- July 22 -- Johann Rafelski, Argonne National Laboratory, "Spontaneous Neutralization of Charged Nuclear Matter"
- August 4 -- Paul Bonche, Saclay, "Nuclear Dynamics in One-Dimension in the Time-Dependent Hartree-Fock Approximation"
- August 5 -- V. S. Nikolayev, Moscow State University, U.S.S.R., "Atomic Cross Sections for Multi-Charged Ions"
- August 7 -- C. K. Gelbke, Max-Planck-Institut, Heidelberg, Germany, "Exchange Symmetries in Heavy-Ion Reactions"
- August 14 -- J. A. Maruhn, Physics Division, ORNL, "Collective Effects on Mass Distributions in Fission"
- August 21 -- Vida Maruhn-Rezwani, University of Frankfurt, West Germany, "Generalized Collective Model"
- September 2 -- Jiri Kopecky, Reactor Centrum, Petten, Netherlands, " (n, γ) Experiments at the High Flux Reactor at Petten"
- September 4 -- Bill Dalton, ORAU, "Statistical Methods for Finding Shell Model Level Densities"
- September 11 -- M. L. Halbert, Physics Division, ORNL, "Danish Photons Soft and Hard"
- October 9 -- Franz Plasil, Physics Division, ORNL, "Physics with the Very Heavy Ions -- French Connection"
- October 20 -- W. F. van Gunsteren, Free University, Amsterdam, "Relationship between Odd and Even Single Closed Shell Nuclei in a Low Seniority Approximation"
- October 27 -- S. M. Lee, Institute for Nuclear Physics, University of Cologne, West Germany, "Role of Resonances and Critical Angular Momenta in Heavy Ion Reactions"
- October 28 -- M. A. Nagarajan, Daresbury Nuclear Physics Laboratory, Daresbury, England, "Generator Co-ordinate Method for Nuclear Collisions"
- October 31 -- H. H. Andersen, Aarhus, Denmark, "Sputtering as a Tool for the Investigation of Atomic Collision Cascades in Solids"
- November 6 -- Hermann Weigmann, CBNM, Geel, Belgium, "Neutron Data Measurements at the Geel Linac"

November 13 – Peter Wurm, Max Planck Institute for Nuclear Physics, Heidelberg, and SUNY, Stony Brook, “Friction in Deep Inelastic Scattering”

November 17 – R. F. Casten, Brookhaven National Laboratory, “Nuclear Structure Research Using the (n, γ) Reaction”

December 10 – R. K. Adair, Yale University, “Prompt Leptons: Leptons Produced by the Direct Interaction of Hadrons”

COLLOQUIA AND SEMINARS PRESENTED AT OTHER INSTALLATIONS

Staff members of the Physics Division and other scientists associated with the Division frequently receive invitations to present seminars and colloquia at institutions both in the United States and abroad. Partial support for some of the requests was provided through the Traveling Lecture Program (TLP) administered by Oak Ridge Associated Universities. A number of lecture-demonstrations were supported by the local-section lecture program of the American Chemical Society.

Following is a list of seminars and colloquia presented in 1975:

J. B. Ball – University of Melbourne, Australia, February 29, 1975, “Plans for a New Heavy Ion Accelerator at Oak Ridge”; Florida State University, April 10, and Texas A. & M. University, May 29, “The New Heavy Ion Laboratory at Oak Ridge” (TLP); University of Tennessee, December 2, “Status Report on the Heavy Ion Accelerator Facility at Oak Ridge”

C. F. Barnett – National Bureau of Standards Workshop, March 3–4, “Atomic Data for CTR, Particularly on Heavy Ion Impurities”; National Bureau of Standards, Gaithersburg, Maryland, March 3, “Atomic Physics Research at ORNL” and “Controlled Fusion Atomic Data Center”

F. E. Bertrand – University of Georgia, April 17, “Excitation of Giant Resonances via Direct Reactions”; Texas A. & M. University, November 4, “Giant Resonances and the Nuclear Continuum”

C. R. Bingham – KVI, Groningen, Netherlands, November 11, “Initial Research with the On-Line Isotope Separator, UNISOR”; Free University, Amsterdam, Netherlands, December 4, “Structure of Light Mercury Isotopes with an Isotope Separator”

T. A. Carlson – University of Missouri, April 25, “Electron Spectroscopy for Surface Studies”; University of Illinois, November 12, “Use of Electron Spectroscopy for Surface Studies” (APS Visiting Scientist Program)

W. B. Ewbank – Instituut voor Kernfysisch Onderzoek, Amsterdam, January 24, “ENSDF (Evaluated Nuclear Structure Data File)”

J. L. Fowler – University of Tennessee, February 11, “The Neutron as a Probe for Nuclear Structure around Closed Shell Nuclei”

C. B. Fulmer – Institut des Sciences Nucléaires, Grenoble, France, January 24, “Heavy-Ion Scattering Studies at Oak Ridge”; Centre de Recherches Nucléaires de Strasbourg, Strasbourg, France, April 24, “Heavy-Ion Scattering Studies at Oak Ridge”; Kernfysisch Versneller Instituut, Groningen, Netherlands, September 2, “Some Experiences in the French Alps”; Natuurkundig Laboratorium der Vrije Universiteit, Amsterdam, Netherlands, September 4, “Some α -Particle and Heavy-Ion Scattering Experiments”; Wheatstone Physics Laboratory, King’s College, London, U.K., September 26, “Some Experiences in the French Alps”

C. D. Goodman – Kent State University, Kent, Ohio, September 17, “The Nuclear Reaction (${}^6\text{Li}, {}^6\text{He}$) as a Tool for Studying Nuclear Transitions Related to Gamow-Teller Beta Decays”

E. E. Gross – University of Texas at Arlington, February 5, and North Texas State University, February 6, “Heavy-Ion Research at Oak Ridge” (TLP); Clemson University, February 27, “Testing Time Reversal Invariance in Nuclear Physics” (TLP); Niels Bohr Institute, Copenhagen, Denmark, May 2, “70 MeV ${}^{12}\text{C}$ Scattering from ${}^{144}\text{Nd}$ ”; University of Groningen, Netherlands, May 6, “Heavy-Ion Research at ORIC”; Institut des Sciences Nucléaires, Grenoble, France, May 9, “Coulomb-Nuclear Interference Effects in 70 MeV ${}^{12}\text{C} + {}^{144}\text{Nd}$ Scattering”

R. L. Hahn – Randolph-Macon Women’s College, January 23; Davidson College, March 21; Union College, April 19; Huntingdon College, April 21; and Tuskegee Institute, April 21, “The Quest for New Elements” (TLP); Lawrence Berkeley Laboratory, December 16, “Reactions of ${}^{40}\text{Ar}$ with ${}^{160}\text{Dy}$, and ${}^{164}\text{Dy}$ and ${}^{174}\text{Yb}$ ”

- E. C. Halbert – Niels Bohr Institute, February 5, “Renormalization to Cell Effective Interactions for Truncated Many-Body Shell Models”
- M. L. Halbert – Hahn-Meitner Institut, West Berlin, January 31, “Heavy-Ion Elastic Scattering from ORIC; The Heavy-Ion Accelerator Project at Oak Ridge”
- J. B. McGroory – North Carolina State University, January 24; Vanderbilt University, March 14, “Successes and Failures of the Nuclear Shell Model” (TLP); Georgia State University, April 16, “Microscopic Description of Collective Nuclear Motion in Terms of the Nuclear Shell Model”
- M. L. Mallory – Michigan State University, November 17, “Metal Ion Source and Harmonic Beam Space Charge Effect”
- J. A. Martin – Gesellschaft für Schwerionenforschung, Darmstadt, September 2, “Heavy Ion Accelerators at Oak Ridge”
- J. A. Maruhn – Vanderbilt University, February 6, “Dynamic Theory of Mass Distributions in Fission”; Argonne National Laboratory, April 2, “Dynamic Theory of Mass Distributions in Fission”; Lawrence Berkeley Laboratory, July 15, “Some Practical Aspects of Implementing a Fluid-Dynamical Code for Heavy-Ion Reactions”; Los Alamos Scientific Laboratory, October 14, “Fluid-Dynamical Description of Heavy-Ion Reactions”; California Institute of Technology, October 24, “Fluid-Dynamical Description of Heavy-Ion Reactions”; Duke University, November 20, “Fluid-Dynamical Description of Heavy-Ion Reactions”; North Carolina State University, November 21, “Collective Theory of Mass Distributions in Fission”
- P. D. Miller – State University of New York at Cortland, February 4; University of Alabama, February 27; Auburn University, February 28; University of Kentucky, October 3, “Search for the Electric Dipole Moment of the Neutron” (TLP)
- R. L. Mleкодaj – Gesellschaft für Schwerionenforschung, Darmstadt, September 15, “The Status of the UNISOR Project”
- C. D. Moak – Rutgers – the State University, November 7, “Large Tandem Accelerators”; University of Oxford, England, November 17, “Physics with Heavy Ions”
- H. W. Morgan – (lectures sponsored by the American Chemical Society local-section lecture program are marked with an asterisk) Indiana University at South Bend, January 13; St. Joseph Valley Section, ACS,* January 13; Kalamazoo College,* January 14; Grand Valley State College, January 15; Hope College,* January 15; University of Michigan, Ann Arbor,* January 16; Wayne State University, January 17; Gannon College, May 7; Villa Maria College,* May 7; Northeastern Ohio Section, ACS,* May 8; Pennsylvania State University, May 9; Penn–Ohio Border Section, ACS,* May 9; Ball State University, June 23; University of Nevada at Las Vegas,* October 9; University of Nevada at Reno,* October 10; University of California at Davis, October 13; Sacramento State University,* October 13; California State University at Fresno,* October 14; Naval Weapons Center at China Lake,* October 15; California State College at Bakersfield,* October 16; University of Hawaii at Manoa,* October 17, “Coherent Light and Holography”
- F. E. Obenshain – University of Georgia, February 4, “Some Applications of the Mossbauer Effect”
- F. Pasil – Hahn-Meitner Institut, Berlin, February 21, “Heavy-Ion Induced Fission and Fusion”; University of Vienna, June 13; University of Marburg, June 16; Max-Planck-Institut, Heidelberg, June 18; University of Munich, June 20; University of Liverpool, July 9; University of Manchester, July 10; University of Lyon, July 18, “Fission et Fusion Induite par Ions Lourds”
- S. Raman – University of Tennessee, Nuclear Engineering Department, May 27, “The Actinide Waste Problem”
- L. L. Riedinger – Notre Dame University, December 10, “New Accelerator at Oak Ridge; Recent (HI,xn) Measurements”
- M. J. Saltmarsh – University of Virginia, March 19, “Some Practical Applications of Accelerators, Past, Present and Future”
- G. R. Satchler – Texas A. & M. University, April 8, “Microscopic Description of the Inelastic Scattering and the New Giant Resonances”; Oxford University, England, October 2, “Giant Resonances”
- A. G. Schmidt – University of Tennessee, April 16, “Multiple Multipole Mixtures in the Decay of ^{182}Ta ”
- E. H. Spejewski – Tennessee Technological University, January 27, “The UNISOR Project”
- P. H. Stelson – Instituto de Fisica, Mexico City, March 18, “Heavy Ion Facility at Oak Ridge”; March 19, “Backbending Phenomena in Nuclei”

- R. G. Stokstad – State University at New York, April 4, “Limits on Fusion Cross Sections for Light Nuclei”
- K. S. Toth – University of Tennessee, March 5, “ α -Decay in the Cis-Polonium Region”; Institute for Nuclear Research, Kiev, U.S.S.R., July 3, “Heavy-Ion Research at the Oak Ridge Isochronous Cyclotron”; Institute for Nuclear Physics, Gatchina, U.S.S.R., August 6, “Heavy-Ion Research at the Oak Ridge Isochronous Cyclotron”
- T. A. Welton – Virginia Polytechnic Institute and State University, June 2, “Coherence Effects in Optics”; University of Alabama, September 26; Clark College, October 15; University of Kentucky, November 21, “What is Life?” (TLP)
- C. Y. Wong – University of Puerto Rico, Mayaguez, February 4; University of Puerto Rico, Rio Piedras, February 8; Clemson University, South Carolina, March 13, “Toroidal Galaxies” (TLP); Texas A. & M. University, March 25, “Nuclear Hydrodynamics”; University of Maryland, April 17, “Foundation of Nuclear Hydrodynamics”; Centre d’Etudes Nucléaires, Saclay, France, May 12–30, series of five lectures on “Selected Topics in Heavy-Ion Reactions”

MISCELLANEOUS PROFESSIONAL ACTIVITIES OF DIVISIONAL PERSONNEL

Staff members are frequently involved in professional activities which are incidental to their primary responsibilities. During 1975 60% of the members of the Division acted as referees for 25 journals, principally *The Physical Review*, *Physical Review Letters*, and *Nuclear Physics*. Other activities during 1975 included those listed below. A listing as a member of a Users Group implies active participation in experiments at other laboratories.

- G. D. Alton – local arrangement committee for International Conference on Heavy Ion Sources; guest co-editor for Proceedings of International Conference on Heavy Ion Sources
- C. F. Barnett – Research Advisory Committee for ERDA–DCTR; panel member, National Academy of Science for Atomic Physics in the Energy Program; panel member, ERDA–DCTR fusion research plasma facility; proposal reviewer, ERDA–DCTR, ERDA, DPR, NSF, National Research Corporation; consultant to IAEA on atomic data; organized symposium for APS annual meeting, Anaheim, California, January 29, 1975; organized workshop – “Theoretical Atomic Physics in the CTR Program,” Oak Ridge, September 8, 1975
- R. L. Becker – reviewer for Division of Physical Research (ERDA) and National Science Foundation; lecturer, University of Tennessee
- F. E. Bertrand – chairman-elect, Indiana University Cyclotron Users Group; member, LAMPF Users Group
- T. A. Carlson – joint editor-in-chief of the *Journal of Electron Spectroscopy*; chairman of 1976 Gordon Conference on Electron Spectroscopy; lecturer at the NATO Advanced Study Institute on Photoionization and Other Problems of Many Electron Interactions, September 1975
- E. Eichler (Chemistry Division) – Physics Division Seminar Chairman since October 1; Heavy-Ion Laboratory Users Group Liaison Officer; member of Organizing Committee, Heavy-Ion Workshop
- J.L.C. Ford – member, National Heavy-Ion Laboratory Users Group Executive Committee; member, Superhilac and Brookhaven National Laboratory Users Groups
- J. L. Fowler – part-time professor, University of Tennessee; secretary for Nuclear Physics Commission of IUPAP; member of Fellowship Committee of Council of APS
- C. B. Fulmer – safety officer and radiation control officer for Physics Division; instructor for ORNL Personnel Development Programs
- C. D. Goodman – chairman of the ORNL Science and Technology Colloquium; Physics Division Quality Assurance Coordinator; representative from Nuclear Physics Division of APS to advise on Physics and Astronomy Classification Scheme (PACS); member of Indiana University Cyclotron Users Group
- E. E. Gross – UNISOR Executive Committee; ORIC Program Committee; reviewer for NSF and Research Corporation Proposals
- J. A. Harvey – labor coordinator for the Physics Division; Physics Division coordinator for ORNL Awards Committee; secretary–treasurer of the Division of Nuclear Physics of the American Physical Society (1967–1976); member, organizing committee of the 1976 International Conference on the Interactions of Neutrons with Nuclei; member of the editorial board of the *Atomic and Nuclear Data Tables*
- D. P. Hutchinson – Physics Division coordinator for Computer Microfiche Printout Committee

- C. H. Johnson -- member of Accelerators and Radiation Sources Review Committee
- N. R. Johnson (Chemistry Division) -- member of the ORIC Program Committee; member of Heavy-Ion Facility Users Organization; ORIC Scheduling Coordinator
- C. M. Jones -- member, Program Committee, 1975 Particle Accelerator Conference; member, local arrangements committee, International Conference on Heavy Ion Sources
- C. A. Ludemann -- reviewer of Physics Division ADP facilities; Physics Division representative, Union Carbide Nuclear Division Affirmative Action Program; member, LAMPF Users Group
- F. K. McGowan -- member, editorial board of *Atomic Data and Nuclear Data Tables*, journal published by Academic Press
- J. B. McGrory -- ORNL Ad Hoc Committee on Long Range ADP Acquisition; Physics Division ORIC Scheduling Committee; on leave to Program Planning and Analysis Group
- R. L. Macklin -- Physics Division Industrial Cooperation Officer; Criticality Safety Approvals Committee ORGDP
- M. L. Mallory -- co-editor, International Conference on Heavy Ion Sources
- J. A. Martin -- chairman, Meetings Committee of Technical Activities Board of IEEE; member, Administrative Committee of the IEEE Nuclear and Plasma Sciences Society; member, Editorial Advisory Board of *Particle Accelerators*; consultant, National Science Foundation Physics Section as member of Visiting Committees for Indiana University Cyclotron Project and Columbia University Synchrotron Improvement Project; member, Organizing Committee for the 1975 Particle Accelerator Conference, Washington, D.C.; member, International Organizing Committee for VIIth International Conference on Cyclotrons and Their Applications, Zurich, Switzerland, August 1975
- J. A. Maruhn -- lecturer, University of Tennessee
- S. W. Mosko -- member, ERDA Electrical Safety Criteria Committee; member, Program Committee of 1975 Particle Accelerator Conference
- F. Plasil -- chairman, ORNL Graduate Fellow Selection Panel; member, ORNL Ph.D. Recruiting Team; member, Lawrence Berkeley Laboratory Superhilar Users Executive Committee
- F. Pleasonton -- member, Review Committee for Phase II (separated-sector cyclotron) of Heavy-Ion Facility
- E. Ricci -- technical chairman, International Atomic and Nuclear Activation Analysis Conference, Gatlinburg, October 14--16, 1975; member, Executive Committee of American Nuclear Society Isotopes and Radiation Division; chairman, Committee Analytical Applications of American Nuclear Society Isotopes and Radiation Division
- M. J. Saltmarsh -- member, Technical Advisory Panel, LAMPF; member, American Society for Testing Materials Subcommittee E10.08 (Procedures for Radiation Damage Simulation); member, ORNL Proposal Review Committee (Seed Money Committee)
- G. R. Satchler -- member, Executive Committee, Division of Nuclear Physics, American Physical Society; member, Program Committee, Division of Nuclear Physics, American Physical Society; member, editorial board of *Atomic Data and Nuclear Data Tables*; member, Organizing Committee for Conference on Highly Excited States in Nuclei, Jülich, Germany, September 22--26, 1975
- P. A. Staats -- staff member, Fisk University Infrared Spectroscopy Institute; participated in organization of and directed laboratory portion of Twenty-Sixth Annual Fisk Infrared Institute, Fisk University, Nashville, Tennessee, August 11--15, 1975
- P. H. Stelson -- part-time faculty member, Department of Physics, University of Tennessee; associate editor of *Nuclear Physics*; member, executive committee of Southeastern Section of the American Physical Society; member, American Physical Society Division of Nuclear Physics Committee on Nuclear Data Compilations; member, advisory committee for the ORNL Instrumentation and Controls Division; member, nominating committee for Nuclear Division of the American Physical Society
- R. G. Stokstad -- member, Ad Hoc Panel on The Future of Nuclear Science (CNS--NAS); member, National Heavy-Ion Facility Users Group Charter Committee; reviewer of research proposals for the National Science Foundation and Brooklyn College
- K. S. Toth -- chairman, UNISOR Scheduling Committee; member, Major Nuclear Chemistry Facilities Committee of the American Chemical Society; helped arrange two sessions of invited speakers for the American Physical Society meeting held in Knoxville, Tennessee

T. A. Welton – completed three-year term on Council of Electron Microscopy Society of America; program chairman for 1975 annual meeting of above society; reviewed research proposals for ERDA and NSF;

part-time consultant to the ORGDP Gas Centrifuge Program; part-time professor and colloquium chairman, University of Tennessee Physics Department

GRADUATE THESIS RESEARCH

During 1975, Physics Division staff and associates served as advisors or supervisors for 16 students engaged in thesis research. All projects listed below were carried out with facilities operated at least in part by the Division. In 1975, four doctoral theses and one bachelor's thesis were completed.

Ph.D. Thesis Research

Candidate	Advisor(s)	Thesis Title or Field of Research
W. K. Dagenhart, University of Tennessee	P. H. Stelson	Coulomb Excitation of ^{115}Sn
J. P. Forester, University of Tennessee	I. Sellin, University of Tennessee	Heavy-Ion Atomic Collisions
L. D. Gardner, Yale University	M. L. Mallory	Charge Exchange Cross Sections
G. M. Gowdy, Georgia Institute of Technology	E. H. Spejewski, E. Eichler	Systematics of the Levels of Neutron-Deficient Odd-Mass Hg Isotopes
D. E. Gustafson, University of Virginia	S. T. Thornton, University of Virginia; J.L.C. Ford, Jr., R. L. Robinson, K. S. Toth	“High Spin States in ^{26}Mg and ^{23}Na Populated by Heavy Ion Reactions” (degree to be conferred in 1976)
D. L. Hillis, University of Tennessee	E. E. Gross; C. R. Bingham, L. L. Riedinger, University of Tennessee; M. L. Halbert, P. H. Stelson	“Shape Effects in the Elastic and Inelastic Scattering of 70.4 MeV ^{12}C Ions from the Even Neodymium Isotopes” (degree to be conferred in 1976)
A. C. Kahler III, University of Tennessee	L. L. Riedinger, University of Tennessee; UNISOR Staff	Rotational Bands in Tl and Au Nuclei
M. S. Pandey, State University of New York at Albany	J. A. Harvey, R. L. Macklin	“Study of High Resolution Neutron Total and Capture Cross Sections in Separated Isotopes of Copper” (degree conferred in 1975)
R. S. Peterson, University of Tennessee	I. Sellin, University of Tennessee	Heavy-Ion Atomic Collisions
R. Piercey, Vanderbilt University	J. H. Hamilton, Vanderbilt University; R. L. Robinson	High Spin States in ^{74}Se
Cheng-May Tung, University of Tennessee	F. Obenshain	Isomer Shift Studies in Dilute Au Alloys
W. K. Tuttle III, University of Tennessee	P. H. Stelson, R. L. Robinson	“Levels in $^{113,115}\text{In}$ as Seen by Coulomb Excitation and (H.I., xn) Reactions” (degree conferred December 1975)

Master's Thesis Research

Candidate	Advisor(s)	Thesis Title or Field of Research
B. O. Hannah, University of Alabama, Birmingham	E. L. Robinson, University of Alabama; E. H. Spejewski	Decay of ^{194}Pb and ^{194}Tl
R. C. Hunter, University of Tennessee	L. L. Riedinger, University of Tennessee; K. S. Toth	Decay of ^{164}Lu to ^{164}Yb
F. E. Turner, University of Tennessee	L. L. Riedinger, University of Tennessee; UNISOR Staff	Study of the $A = 192$ Chain: Pb-Tl-Hg

Bachelor's Thesis Research

Candidate	Advisor(s)	Thesis Title or Field of Research
J. A. Smith, New College, Sarasota	R. L. Becker	"On the Radial Proton Distributions of Light Nuclej" (degree conferred June 1975)

UNDERGRADUATE STUDENT GUESTS AND EMPLOYEES DURING 1975

- A. R. Bogdan,¹ student at Haverford College -- Heavy-Ion Project (completed ten-week assignment in August)
- H. E. Doughty II, employee of the University of Tennessee -- High Energy Physics Program
- Sally Fairman,² student at Carrolton College -- Plasma Diagnostics Program (completed three-month assignment in September)
- J. L. Gray,¹ student at University of Wisconsin -- Oak Ridge Electron Linear Accelerator Program (completed ten-week assignment in August)
- J. S. Haggerty,¹ student at Manhattan College -- Electron Spectroscopy Program (completed ten-week assignment in August)
- J. A. McDonald,² student at Princeton University -- Theoretical Physics Program (completed three-month assignment in September)
- T. L. Nichols, employee of University of Tennessee -- Hyperfine Interactions Program (completed ten-month assignment in February)
- Terry B. Sexauer,³ student at Center College -- Ion Source Development Program (completed five-month assignment in May)
- T. A. Slamon,¹ student at Pennsylvania State University -- Oak Ridge Isochronous Cyclotron Program (completed ten-week assignment in August)
- D. M. Tanner,¹ student at University of Southwest Louisiana -- Ion Source Development Program (completed ten-week assignment in August)
- C. G. Trahern,² student at Rice University -- Theoretical Physics Program (completed three-month assignment in August)
- Vickie D. Vandergriff, employee of University of Tennessee -- University of Tennessee High Energy Physics Program

1. Oak Ridge Associated Universities Trainee.

2. Oak Ridge National Laboratory Exceptional Student Program.

3. Southern Colleges and Universities Union.

ANNUAL INFORMATION MEETING

The 1975 Physics Division Information Meeting was held on May 19 and 20. Members of the Advisory Committee were:

R. M. Diamond, Lawrence Berkeley Laboratory

R. K. Middleton, University of Pennsylvania

J. R. Nix, Los Alamos Scientific Laboratory

H. E. Wegner, Brookhaven National Laboratory

W. Whaling, California Institute of Technology

INTERNAL DISTRIBUTION

- | | |
|-------------------------------------|---------------------------------------|
| 1. G. D. Alton | 49. C. D. Goodman |
| 2. R. L. Auble | 50. P. M. Griffin |
| 3. S. I. Auerbach | 51. E. E. Gross |
| 4. J. A. Auxier | 52. R. L. Hahn |
| 5. J. K. Bair | 53. E. C. Halbert |
| 6. J. B. Ball | 54. M. L. Halbert |
| 7. C. F. Barnett | 55. B. Harmatz |
| 8. S. E. Beall | 56. J. A. Harvey |
| 9. R. L. Becker | 57. D. C. Hensley |
| 10. P. R. Bell | 58. R. F. Hibbs |
| 11. C. E. Bemis | 59. D. J. Horen |
| 12. F. E. Bertrand | 60. E. D. Hudson |
| 13. J. A. Biggerstaff | 61. D. P. Hutchinson |
| 14. Biology Library | 62. C. H. Johnson |
| 15. A. L. Boch | 63. J. W. Johnson |
| 16. C. K. Bockelman (Consultant) | 64. N. R. Johnson |
| 17. C. J. Borkowski | 65. C. M. Jones |
| 18. D. N. Braski | 66. O. L. Keller |
| 19. T. A. Carlson | 67. G. G. Kelley |
| 20. H. P. Carter | 68. H. J. Kim |
| 21--23. Central Research Library | 69. D. C. Kocher |
| 24. R. E. Chrien (Consultant) | 70. M. O. Krause |
| 25. J. F. Clarke | 71--80. Laboratory Records Department |
| 26. H. O. Cohn | 81. Laboratory Records, ORNL R.C. |
| 27. W. C. Colwell | 82. J. D. Larson |
| 28. D. H. Crandall | 83. R. S. Livingston |
| 29. F. L. Culler | 84. R. S. Lord |
| 30. J.W.T. Dabbs | 85. C. A. Ludemann |
| 31. Alexander Dalgarno (Consultant) | 86. R. L. Macklin |
| 32. S. Datz | 87. F. C. Maienschein |
| 33. K.T.R. Davies | 88. M. L. Mallory |
| 34. R. A. Dayras | 89. J. E. Mann |
| 35. G. Desaussure | 90. M. B. Marshall |
| 36. H. L. Dickerson | 91. J. A. Martin |
| 37. W. B. Dress | 92. M. J. Martin |
| 38. E. Eichler | 93. J. A. Maruhn |
| 39. Y. A. Ellis | 94. F. K. McGowan |
| 40. H. A. Enge (Consultant) | 95. J. B. McGrory |
| 41. W. B. Ewbank | 96. C. J. McHargue |
| 42. D. E. Ferguson | 97. P. D. Miller |
| 43. R. L. Ferguson | 98. W. T. Milner |
| 44. J.L.C. Ford, Jr. | 99. R. E. Minturn |
| 45. J. L. Fowler | 100. C. D. Moak |
| 46. C. B. Fulmer | 101. H. W. Morgan |
| 47. J. H. Gillette | 102. S. W. Mosko |
| 48. J. Gomez del Campo | 103. J. Ray Nix (Consultant) |

- | | |
|--|---------------------------------|
| 104. F. E. Obenshain | 127. P. A. Staats |
| 105. ORNL – Y-12 Technical Library
Document Reference Section | 128–302. P. H. Stelson |
| 106. R. W. Peelle | 303. R. G. Stokstad |
| 107. F. G. Percy | 304. J. B. Storer |
| 108. J. J. Pinajian | 305. R. W. Stoughton |
| 109. F. Plasil | 306. E. G. Struxness |
| 110. F. Pleasonton | 307. D. A. Sundberg |
| 111. H. Postma | 308. E. H. Taylor |
| 112. S. Raman | 309. K. S. Toth |
| 113. J. A. Ray | 310. K. L. Vander Sluis |
| 114. E. Ricci | 311. C. L. Viar |
| 115. E. G. Richardson, Jr. | 312. Harvey Wegner (Consultant) |
| 116. L. D. Rickertsen | 313. J. R. Weir, Jr. |
| 117. R. L. Robinson | 314. G. F. Wells |
| 118. M. J. Saltmarsh | 315. T. A. Welton |
| 119. G. R. Satchler | 316. J. C. White |
| 120. R. O. Sayer | 317. M. K. Wilkinson |
| 121. M. R. Schmorak | 318. C. S. Williams |
| 122. H. E. Seagren | 319. E. O. Wollan |
| 123. M. J. Skinner | 320. Cheuk-Yin Wong |
| 124. G. G. Slaughter | 321. R. E. Worsham |
| 125. A. H. Snell | 322. N. F. Ziegler |
| 126. E. H. Spejewski | 323. A. Zucker |

EXTERNAL DISTRIBUTION

324. B. J. Allen, Physics Division, Australian Atomic Energy Commission, Sutherland, N.S.W., Australia
325. M. Baranger, 6-308-A, Massachusetts Institute of Technology, Cambridge, MA 02139
326. C. A. Barnes, Physics Division, California Institute of Technology, Pasadena, CA 91109
327. John Barnhart, Department of Physics, Southwestern at Memphis, Memphis, TN 38107
328. Ingmar Bergstrom, Nobel Institute of Physics, Stockholm 50, Sweden
329. V. B. Bhanot, Physics Department, Panjab University, Chandigari-3, India
330. Bibliotheque – Madame Belle, Universite de Grenoble, Institut des Sciences Nucleaires,
53, Rue des Martyrs, B. P. 21, 38 Grenoble, France
331. C. R. Bingham, Physics Department, University of Tennessee, Knoxville, TN 37916
332. M. Blann, Nuclear Structure Research Laboratory, University of Rochester, River Campus Station,
Rochester, NY 14627
333. E. Bleuler, Pennsylvania State University, University Park, PA 16802
334. S. D. Bloom, University of California, Lawrence Radiation Laboratory, P.O. Box 808, Livermore, CA
94550
335. H. G. Blosser, Cyclotron Laboratory, Michigan State University, East Lansing, MI 48823
336. A. Bohr, Copenhagen University, Niels Bohr Institute, Blegdamsvej 17, Copenhagen, Denmark
337. R. O. Bondelid, Cyclotron Branch, U.S. Naval Research Laboratory, Washington, D.C. 20390
338. J. A. Brink, Library Division, The Merensky Institute of Physics, University of Stellenbosch,
Stellenbosch, Republic of South Africa
339. H. Brinkman, Physics Department, University of Groningen, Westersingel 34, Groningen, Netherlands
340. D. A. Bromley, Nuclear Structure Laboratory, Yale University, New Haven, CT 06520
341. H. Bruckmann, Institut für Experimentelle Kernphysik, Kernforschungszentrum Karlsruhe, Postfach 947,
75 Karlsruhe, West Germany
342. W. M. Bugg, Physics Department, University of Tennessee, Knoxville, TN 37916

343. W. E. Burcham, Physics Department, University of Birmingham, P.O. Box 363, Birmingham, England
344. J. L. Burnett, Energy Research and Development Administration Headquarters, Washington, D.C. 20545
345. J. W. Burton, Carson-Newman College, Jefferson City, TN 37760
346. R. F. Carlton, Department of Physics, Middle Tennessee State University, Murfreesboro, TN 37130
347. David Clark, Lawrence Radiation Laboratory, University of California, Berkeley, CA 94720
348. B. L. Cohen, Department of Physics, University of Pittsburgh, Pittsburgh, PA 15213
349. G. T. Condo, Physics Department, University of Tennessee, Knoxville, TN 37916
350. H. E. Conzett, Lawrence Radiation Laboratory, University of California, Berkeley, CA 94720
351. R. Y. Cusson, Physics Department, Duke University, Durham, NC 27706
352. Gordon Czjzek, Institute für Angewandte Kernphysik, Kernforschungszentrum Karlsruhe, Postfach 3640, 7500 Karlsruhe, West Germany
353. Martin Deutsch, Laboratory for Nuclear Science, Massachusetts Institute of Technology, Cambridge, MA 02139
354. R. M. Diamond, Chemistry Division, Lawrence Berkeley Laboratory, Berkeley, CA 94720
355. R. M. Drisko, Physics Department, University of Pittsburgh, Pittsburgh, PA 15213
356. D. J. Eccleschall, U.S. Army Nuclear Defense Laboratory, Edgewood Arsenal, MD 21010
357. U. Facchini, Physics Department, University of Milan, Via Salidini 50, Milan, Italy
358. W. Falk, Cyclotron Laboratory, Department of Physics, University of Manitoba, Winnipeg 19, Manitoba, Canada
359. H. Faraggi-Mathieu, Centre d'Etudes Nucleaires de Saclay, B.P. No. 2, Gif-Sur-Yvette (S. and O.), France
360. G. N. Flerov, Laboratory for Nuclear Reactions, Dubna Joint Institute for Nuclear Research, Dubna, Moscow Oblast, U.S.S.R.
361. David Fossan, SUNY, Stony Brook, Dept. of Physics, Stony Brook, NY 11790
362. W. A. Fowler, California Institute of Technology, Pasadena, CA 91109
363. J. D. Fox, Dept. of Physics, Florida State University, Tallahassee, FL 32306
364. A. I. Galonsky, Cyclotron Laboratory, Michigan State University, East Lansing, MI 48823
365. W. Gentner, Max-Planck-Institut für Kernphysik, Saupfercheckweg, 69 Heidelberg, West Germany
366. J. H. Gibbons, Office of Energy Conservation, Department of the Interior, 18th & "C" Streets, Washington, D.C. 20240
367. W. A. Glaeser, Institut für Angewandte Kernphysik, Kernforschungszentrum Karlsruhe, Postfach 3640, 7500 Karlsruhe, West Germany
368. B. Goel, Cyclotron Laboratory, Kernforschungszentrum Karlsruhe, Postfach 97, 75 Karlsruhe, West Germany
369. G. S. Goldhaber, Physics Department, Brookhaven National Laboratory, Upton, Long Island, NY 11973
370. J. H. Goldstein, Physics Department, Emory University, Atlanta, GA 30322
371. M. Gouettefangeas, L'Energie Atomique, Direction de la Physique, Projet GANIL, Boite Postale No. 2, 91 Gif-Sur-Yvette, France
372. H. E. Gove, Nuclear Structure Research Laboratory, University of Rochester, River Campus Station, Rochester, NY 14627
373. A.E.S. Green, University of Florida, Gainesville, FL 32601
374. G. W. Greenlees, Physics Department, University of Minnesota, Minneapolis, MN 55455
375. J. J. Griffin, Physics Department, University of Maryland, College Park, MD 20740
376. R. J. Griffiths, Physics Department, Kings College, Strand, London, W.C. 2, England
377. H. A. Grunder, Lawrence Berkeley Laboratory, Berkeley, CA 94702
378. M. Micheline Guichard, Institut de Physique Nucleaire, B.P. No. 1, 91 Orsay, France
379. E. Guth, 116 Oklahoma Avenue, Oak Ridge, TN 37830
380. J. H. Hamilton, Department of Physics, Vanderbilt University, Nashville, TN 37203
381. S. S. Hanna, Physics Department, Stanford University, Stanford, CA 94305
382. E. L. Hart, Physics Department, University of Tennessee, Knoxville, TN 37916
383. B. G. Harvey, Lawrence Radiation Laboratory, University of California, Berkeley, CA 94720
384. D. W. Heikkinen, University of California, Lawrence Livermore Laboratory, P.O. Box 808, Livermore, CA 94550

385. D. L. Hendrie, Director 88-Inch Cyclotron, Lawrence Berkeley Laboratory, Berkeley, CA 94720
386. Hugh Henry, Department of Physics, DePauw University, Greencastle, IN 46135
387. N. P. Heydenburg, Physics Department, Florida State University, Tallahassee, FL 32306
388. Brigitte Hinkelmann, Institut für Angewandte Kernphysik, Kernforschungszentrum Karlsruhe, Postfach 947, 75 Karlsruhe, West Germany
389. R. L. Hirsch, Energy Research and Development Administration Headquarters, Washington, D.C. 20545
390. W. G. Holladay, Physics Department, Vanderbilt University, Nashville, TN 37203
391. H. D. Holmgren, Physics Department, University of Maryland, College Park, MD 20742
392. P. G. Huray, Physics Department, University of Tennessee, Knoxville, TN 37916
393. Institute for Energy Analysis, P.O. Box 117, Oak Ridge, TN 37830
394. C. Johnson, Triumf, University of British Columbia, Vancouver 8, B.C., Canada
395. D. L. Judd, Physics Division, Lawrence Radiation Laboratory, University of California, Berkeley, CA 94720
396. H. H. Jung, 2057 Geesthacht, Reaktorstation, Institut für Reine und Angewandte Kernphysik der Christian-Albrechts-Universität, Kiel, West Germany
397. J. A. Jungeman, Physics Department, University of California, Davis, CA 95616
398. H. Kamitsubo, Head, Cyclotron Laboratory, Institute of Physical and Chemical Research, Wako-Shi, Saitama, 351, Japan
399. D. G. Kamke, Institut für Experimentalphysik (I), Ruhr-Universität Bochum, 463 Bochum, West Germany
400. J. S. Kane, Energy Research and Development Administration Headquarters, Washington, D.C. 20545
401. K. W. Kemper, Physics Dept., Florida State Univ., Tallahassee, FL 32306
402. Dennis Kovar, Argonne National Laboratory, Argonne, IL 60439
403. S. J. Krieger, Physics Department, University of Illinois at Chicago Circle, Chicago, IL 60680
404. L. L. Lee, Physics Department, State University of New York, Stony Brook, NY 11790
405. T. D. Lee, Department of Physics, Columbia University, New York, NY 10027
406. I. Kh. Lemberg, Politechnicheskaja 26, Physical Technical Institute, Leningrad, K-21, U.S.S.R.
407. J. A. Lenhard, ERDA - ORO, Federal Office Building, Oak Ridge, TN 37830
408. Librarian, Atomic Energy Centre, P.O. Box 164, Ramna, Dacca, Bangladesh
409. Librarian, Cyclotron Laboratory, Michigan State University, East Lansing, MI 48823
410. Librarian, Information Service, University of Oxford, Department of Nuclear Physics, Keble Road, Oxford, England
411. Librarian, Institut des Sciences Nucleaires, B.P. 257 - Centre de Tri, 38044 Grenoble Cedex, France
412. J. C. Love, Department of Physics, Florida Institute of Technology, Melbourne, FL 32901
413. F. B. Malik, Physics Department, Swain Hall, Indiana University, Bloomington, IN 47401
414. Sven Malmkog, AB Atomenergi, Studsvik, Nykoping, Sweden
415. J. V. Martinez, Energy Research and Development Administration Headquarters, Washington, D.C. 20545
416. C. Mayer-Borick, KFA Jülich, 517 Jülich, Nordrhein-Westfalen, West Germany
417. T. Mayer-Kuckuk, Institut für Strahlen-und-Kernphysik der Universität, 53 Bonn, West Germany
418. R. J. McCarthy, Carnegie-Mellon University, Pittsburgh, PA 15213
419. A. Michaudon, Chef du Service de Physique Nucleaire, Commissariat à l'Energie Atomique, Centre d'Etudes de Bruyeres, le Chatel, P.P. No. 61, Montrouge 92120, France
420. D. R. Miller, Energy Research and Development Administration Headquarters, Washington, D.C. 20545
421. J.C.D. Milton, Physics Division, Atomic Energy of Canada Ltd., Chalk River, Canada
422. Ulrich Mosel, Institut für Theoretische Physik, Universität Giessen, 63 Giessen, West Germany
423. S. A. Moszkowski, Physics Department, University of California, Los Angeles, CA 90024
424. S. C. Mukherjee, Librarian, SAHA Institute of Nuclear Physics, 92, Acharya Prafulla Chandra Road, Calcutta-9, India
425. O. Nathan, Copenhagen University, Niels Bohr Institute, Blegdamsvej 17, Copenhagen, Denmark
426. Samuel Neff, Department of Physics, Earlham College, Richmond, IN 47374

427. H. W. Newson, Duke University, Durham, NC 27706
428. A. H. Nielsen, Dean, University of Tennessee, Knoxville, TN 37916
429. W. C. Parkinson, Cyclotron Laboratory, University of Michigan, Ann Arbor, MI 48105
430. P. Z. Peebles, Dept. of Electrical Engineering, University of Tennessee, Knoxville, TN 37916
431. D. J. Pegg, Physics Department, University of Tennessee, Knoxville, TN 37916
432. Max Peisach, Southern Universities Nuclear Institute, P.O. Box 17, Faure, 7131, South Africa
433. Elliott Pierce, Energy Research and Development Administration Headquarters, Washington, D.C. 20545
434. Tom Pinkston, Arts and Sciences, Vanderbilt University, Nashville, TN 37312
435. W. D. Ploughe, Van de Graaff Accelerator Laboratory, Dept. of Physics, 1302 Kinnear Road, Columbus, OH 43212
436. B. Povh, Max-Planck-Institut für Kernphysik, 69 Heidelberg, Saupfercheckweg, Postfach 124B, West Germany
437. L. W. Put, Kernfysisch Versneller Instituut, Universiteitscomplex Paddepoel, Groningen, Netherlands
438. L. J. Rainwater, Department of Physics, Columbia University, New York, NY 10027
439. Jacobo Rapaport, Department of Physics, Ohio University, Athens, OH 45701
440. John Rasmussen, Lawrence Berkeley Laboratory, Bldg. 70A, Berkeley, CA 94720
441. Patrick Richard, Physics Dept., Kansas State Univ., Manhattan, KS 66506
442. M. E. Rickey, Physics Department, Indiana University, Bloomington, IN 47401
443. Charles Ricker, Department of Physics, Albion College, Albion, MI 49224
444. L. L. Riedinger, Department of Physics, University of Tennessee, Knoxville, TN 37916
445. E. T. Ritter, Energy Research and Development Administration Headquarters, Washington, D.C. 20545
446. Louis D. Roberts, Physics Department, University of North Carolina, Chapel Hill, NC 27514
447. G. L. Rogosa, Energy Research and Development Administration Headquarters, Division of Physical Research, Washington, D.C. 20545
448. R. Ronningen, Department of Physics, Vanderbilt University, Nashville, TN 37203
449. L. Rosen, Los Alamos Scientific Laboratory, P.O. Box 1663, Los Alamos, NM 87544
450. Arthur E. Ruark, 7952 Orchid Street, N.W., Washington, D.C. 20012
451. Rainer Santo, Sektion Physik der Universität München, 8046 Garching, Beschleunigerlaboratorium (Forschungsgelände), West Germany
452. Christoph Schmelzer, Gesellschaft für Schwerionenforschung MBH, 6100 Darmstadt I, West Germany
453. F. H. Schmidt, Physics Department, University of Washington, Seattle, WA 98105
454. H. W. Schmitt, Environmental Systems Corporation, P.O. Box 2525, Knoxville, TN 37901
455. Roland J. Schuttler, Service SEPP, Cen/Far (Fort de Chatillon), Fontenay-Aux-Roses (Seine), France
456. A. Schwarzschild, Brookhaven National Laboratory, Upton, NY 11973
457. Alan Scott, Dept. of Physics and Astronomy, University of Georgia, Athens, GA 30601
458. I. A. Sellin, Department of Physics, University of Tennessee, Knoxville, TN 37916
459. R. Seltz, Centre de Recherches Nucleaires, B.P. 20 CR 67, Strasbourg-3, France
460. Rubby Sherr, Department of Physics, Princeton University, Princeton, NJ 08540
461. Lloyd Smith, Lawrence Radiation Laboratory, University of California, Berkeley, CA 94720
462. Hsu Loke Soo, Ag. Head, Department of Physics, Nanyang University, Singapore 22, Republic of Singapore
463. T. Springer, Kernforschungsanlage Jülich, Postfach 365, Jülich 517, West Germany
464. T. T. Sugihara, Director, Cyclotron Institute, Texas A & M University, College Station, TX 77843
465. Kazusuke Sugiyama, Department of Nuclear Engineering, Faculty of Engineering, Tohoku University, Sendai, Japan
466. Shigeya Tanaka, Japan Atomic Energy Research Institute, Tokai-Mura, Ibaraki-Ken, Japan
467. R. F. Taschek, Los Alamos Scientific Laboratory, P.O. Box 1663, Los Alamos, NM 87544
468. J. Teillac, Laboratoire de Physique Nucleaire d'Orsay, Facultes des Sciences, B.P. No. 1, Orsay (S. and O.), France
469. G. M. Temmer, Physics Department, Rutgers State University, New Brunswick, NJ 08903

470. Jacques Thirion, C.E.N. Saclay S.P.N.M.E., B.P. No. 2, Gif-Sur-Yvette 91, France
471. J. O. Thomson, Department of Physics, University of Tennessee, Knoxville, TN 37916
472. J. R. Thompson, Department of Physics, University of Tennessee, Knoxville, TN 37916
473. S. T. Thornton, Physics Department, University of Virginia, Charlottesville, VA 22901
474. A. G. Tibell, Gustaf Werner Institute, University of Uppsala, Uppsala, Sweden
475. J. P. Unik, Bldg. 200, Argonne National Laboratory, Argonne, IL 60439
476. Robert Vandenbosch, Department of Chemistry, University of Washington, Seattle, WA 98105
477. A. Van Der Woude, Kernfysisch Versneller Instituut der Rijksuniversiteit, Universiteitscomplex Paddepoel, Groningen, Netherlands
478. J. Vervier, Laboratoire du Cyclotron Louvain-la-Neuve, Rue de Namur, 1340 Ottignies, Belgium
479. R.G.P. Voss, Daresbury Nuclear Physics Laboratory, Daresbury, Nr. Warrington, Lancashire, England
480. Captain Arnold S. Warshawsky, U.S. Army Nuclear Agency, Attn: ATCN-W, Fort Bliss, TX 79916
481. Horst H. F. Wegener, Tandemlabor des Physikalischen Instituts der Universitat Erlangen-Nurnberg, 8520 Erlangen, Erwin-Rommel-Str.1, West Germany
482. F. Weller, Institute for Neutron Physics and Reactor Technology, Kernforschungszentrum Karlsruhe, Postfach 3640, Karlsruhe, West Germany
483. Joseph Weneser, Department of Physics, Brookhaven National Laboratory, Upton, Long Island, NY 11973
484. Ward Whaling, Division of Physics and Astronomy, California Institute of Technology, Pasadena, CA 91109
485. J. A. Wheeler, Department of Physics, Princeton University, Princeton, NJ 08540
486. S. L. Whetsone, Energy Research and Development Administration Headquarters, Washington, D.C. 20545
487. E. P. Wigner, Department of Physics, Princeton University, Princeton, NJ 08540
488. L. Wilts, Department of Physics, University of Washington, Seattle, WA 98105
489. D. H. Wilkinson, Nuclear Physics Laboratory, 21 Banbury Road, Oxford, England
490. H. B. Willard, Department of Physics, Case Western Reserve University, Cleveland, OH 44106
491. J. C. Williams, Chemistry Department, Memphis State University, Memphis, TN 38111
492. C. E. Winters, Washington Representative, Union Carbide Corporation, 1730 Pennsylvania Avenue, N.W., Washington, D.C. 20006
493. R. R. Winters, Department of Physics and Astronomy, Denison University, Granville, OH 43023
494. Alexander Xenoulis, Van de Graaff Laboratory, Nuclear Research Center Demokricos, Aghia Paraskevi Attikis, Athens, Greece
495. E. F. Zganjar, Louisiana State University, Department of Physics and Astronomy, Baton Rouge, LA 70803
- 496-624. Given distribution as shown in TID-4500 under Physics category (25 copies - NTIS)